

FRIB TRANSITION TO USER OPERATIONS, POWER RAMP UP, AND UPGRADE PERSPECTIVES*

J. Wei[†], H. Ao, B. Arend, S. Beher, G. Bollen, N. Bultman, F. Casagrande, W. Chang, Y. Choi, S. Cogan, C. Compton, M. Cortesi, J. Curtin, K. Davidson, X. Du, K. Elliott, B. Ewert, A. Facco¹, A. Fila, K. Fukushima, V. Ganni, A. Ganshyn, T. Ginter, T. Glasmacher, J. Guo, Y. Hao, W. Hartung, N. Hasan, M. Hausmann, K. Holland, H. C. Hseuh, M. Ikegami, D. Jager, S. Jones, N. Joseph, T. Kanemura, S. H. Kim, C. Knowles, T. Konomi, B. Kortum, E. Kwan, T. Lange, M. Larmann, T. Larter, K. Laturkar, R.E. Laxdal², J. LeTourneau, Z.-Y. Li, S. Lidia, G. Machicoane, C. Magsig, P. Manwiller, F. Marti, T. Maruta, E. Metzgar, S. Miller, Y. Momozaki³, M. Mugerian, D. Morris, I. Nesterenko, C. Nguyen, P. Ostroumov, M. Patil, A. Plastun, L. Popielarski, M. Portillo, J. Priller, X. Rao, M. Reaume, K. Saito, B. M. Sherrill, M. K. Smith, J. Song, M. Steiner, A. Stolz, O. Tarasov, B. Tousignant, R. Walker, X. Wang, J. Wenstrom, G. West, K. Witgen, M. Wright, T. Xu, Y. Yamazaki, T. Zhang, Q. Zhao, S. Zhao, Michigan State University, East Lansing, MI, USA
M. Wiseman, Thomas Jefferson National Laboratory, Newport News, VA, USA
M. Kelly, Argonne National Laboratory, Argonne, IL, USA
K. Hosoyama, KEK, Tsukuba, Japan
S. Prestemon, Lawrence Berkeley National Laboratory, Berkeley, CA, USA
P. Hurh, Fermi National Accelerator Laboratory, IL, USA
¹also at INFN - Laboratori Nazionali di Legnaro, Legnaro (Padova), Italy
²also at TRIUMF, Vancouver, Canada
³also at Argonne National Laboratory, Argonne, IL, USA

Abstract

After project completion on scope, on cost, and ahead of schedule, the Facility for Rare Isotope Beams began operations for scientific users in May of 2022. This paper reports on FRIB status and progress, emphasizing complexity, challenges, resolutions and lessons learned from construction to the power ramp-up, along with progress with accelerator improvements and R&D for the upgrades.

INTRODUCTION

The Facility for Rare Isotope Beam (FRIB) project was completed in April 2022, ahead of the baseline schedule established about 10 years ago (Table 1). In December 2021, the project commissioning was completed with acceleration of heavy ions to energies above 200 MeV/nucleon (MeV/u) using 324 superconducting radiofrequency resonators housed in 46 cryomodules, striking a target to produce rare isotope beams [1].

The scientific user program started in May 2022. During the first 12 months of user operations, the FRIB accelerator complex delivered 5250 beam hours, including 1528 hours to nine science experiments conducted with primary beams of ³⁶Ar, ⁴⁸Ca, ⁷⁰Zn, ⁸²Se, ¹²⁴Xe, and ¹⁹⁸Pt at beam energies >200 MeV/u; 2724 hours for beam developments, studies, and tuning; and 998 hours to industrial users and non-scientific programs using the FRIB Single Event Effect

*Work supported by the U.S. Department of Energy Office of Science under Cooperative Agreement DE-SC0000661, the State of Michigan, and Michigan State University.

[†]wei@frib.msu.edu

(FSEE) beam line. More than 200 rare isotope beams were produced by the FRIB target and delivered to user stations (Fig. 1). The facility availability is 92%.

Table 1: FRIB Project Major Milestones

Milestone	Date
DOE & MSU cooperative agreement	Jun. 2009
CD-1: preferred alternatives decided	Sep. 2010
CD-2: performance baseline	Aug. 2013
CD-3a: start of civil construction & long lead procurements	Aug. 2013
CD-3b: start of technical construction	Aug. 2014
CD-4: project completion	Apr. 2022
Start of user experiments at 1 kW	May 2022
User experiments at 5 kW primary beam	Feb. 2023

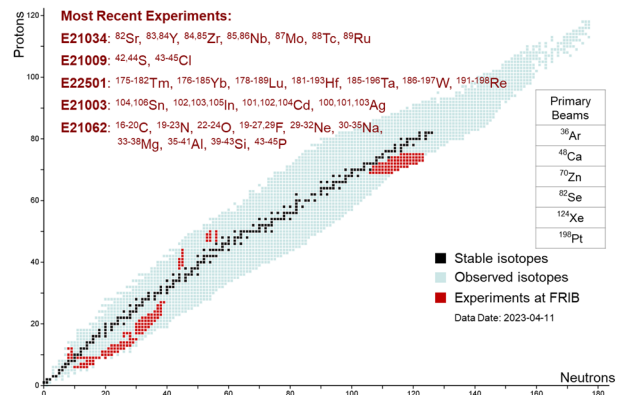


Figure 1: Rare isotopes delivered to FRIB scientific users.

PROGRESSES IN THE ESS SUPERCONDUCTING LINAC INSTALLATION

H. Przybilski[†], on behalf of the European Spallation Source ERIC (ESS), Lund, Sweden

Abstract

The ESS Linac is progressing into the technical commissioning phase. The normal conducting linac up to the first 4 tanks of the DTL is being commissioned with beam. All the 13 spoke cryomodules and the 9 elliptical modules (7 MB+2 HB) foreseen for the first operation at 570 MeV on the beam dump in summer 2024 are available in Lund and waiting for the completion of the cryogenic distribution system (CDS) commissioning. The test program of all the 30 elliptical cryomodules that will enable the 5 MW potential operation after the target commissioning is progressing well, as well as the installation of the RF power stations necessary up to the 2 MW stage of the first project phase. Pilot installation of one spoke and one elliptical cryomodule in the tunnel is in progress. The talk will cover the status of the component deliveries from the partners, the CM preparation and SRF activities at the ESS test stands, with the resolution of several non-conformities, and the experience of the pilot installations and technical commissioning activities in the accelerator tunnel.

INTRODUCTION

The European Spallation Source (ESS) [1], currently under construction in Lund, Sweden, will be the world's most powerful linear accelerator driven neutron spallation source. The normal and superconducting sections of the linac (NCL/SCL) will deliver an ultimate average beam power of 5 MW at 2 GeV. The superconducting linac uses three types of cryomodules: Spoke cryomodules, medium- β and high- β elliptical cryomodules. Figure 1 shows a schematic layout of the linac, and Table 1 lists the high-level parameters for the full facility design [1] and for the configuration of its initial operation [2].

Table 1: ESS Linac High Level Parameters for the Design and Initial Operations (InitOps)

Parameter	Unit	Value
Beam power (design)	MW	5
Beam energy (design)	GeV	2
Beam power (InitOps.)	MW	2
Beam energy (InitOps.)	GeV	0.8
Peak beam current	mA	62.5
Beam pulse length	ms	2.86
Beam pulse repetition rate	Hz	14
Duty factor	%	4
RF frequency	MHz	352.21/704.42
Availability	%	95

[†] henry.przybilski@ess.eu

The NCL of the ESS linac already went through several commissioning steps and the beam was successfully sent through all four DTL tanks during 2023. For the downstream part of the linac, components are being manufactured, installed and tested. This paper first provides a summary on the ESS linac project with a focus on the progresses in the klystron gallery, Cryogenic Distribution System (CDS) commissioning, spoke and elliptical test activities, and then presents a summary and highlights of the pilot installation of one spoke and one elliptical cryomodule in the ESS tunnel.

PROJECT STATUS

This section gives an overview of the ESS linac project. Previous progress reports can be found in [2-4].

Schedule and Linac Configurations

Similarly to other facilities, ESS is based on staged commissioning phases, summarized in Table 2. As shown in Fig. 1, the linac is composed of 13 spokes, 9 medium- β , and 21 high- β cryomodules. Spoke cryomodules contain two spoke cavities whereas medium- β and high- β cryomodules house four cavities. At the beginning of the project, no high- β cryomodule was supposed to be installed for the fifth and sixth commissioning steps in Table 2 [5], to operate at the design energy of the output of the medium- β section, 570 MeV. The current plan assumes a configuration with seven medium- β cryomodules (the blue coloured ones in Fig. 1) and two high- β cryomodules for those steps [2]. This change is due to some medium- β cavity production issues and a good progress with the production of high- β cryomodules. The maximum energy remains approximately 560 MeV. The remaining cryomodules (2 medium- β and 19 high- β cryomodules) will be installed later and only some of them will be powered in order to get the 800 MeV beam energy for the initial operations phase.

Currently, a temporary shielding wall is separating the NCL from the SCL to allow beam commissioning activities on one side and cryomodule installation on the other side

Table 2: ESS Linac High-Level Schedule

	Step	Start	Energy [MeV]
1	Commissioning to LEPT	2018-09	0.075
2	Commissioning to MEBT	2021-11	3.62
3	Commissioning to DTL1	2022-05	21
4	Commissioning to DTL4	2023-04	74
5	Beam on Dump (BOD)	2024	560
6	Beam on Target (BOT)	2025	560
7	Start Of User Operations	2026	800

COMMISSIONING OF THE SECOND JLab C75 CRYOMODULE & PERFORMANCE EVALUATION OF INSTALLED C75 CAVITIES*

M. McCaughan[†], G. Ciovati, G. Davis, M. Drury, T. Powers, A. Reilly
 Jefferson Lab, Newport News, VA, USA

Abstract

JLab has long been a hub of SRF technology with the CEBAF accelerator as one of its first large scale adopters. As SRF technology has advanced, the C50 and C100 programs have allowed for the extension of CEBAF's total energy to 6 GeV and nearly 12 GeV respectively. Along with the increase in energy reach, rates of accelerating gradient degradation have been extracted for these cryomodule designs. A plan to mitigate these losses & maintain robust gradient headroom to deliver the 12 GeV program - the CEBAF Performance Plan - established a multi-year effort of cryomodule refurbishments and replacements. Part of this plan included a cost optimization of the C50 program with more modern processing techniques and the replacement of existing cavities with larger grain boundary cavities produced from ingot Niobium (dubbed C75 for 75 MeV gain). Reports have been made on the prototype pair of C75 cavities installed in a C50 cryomodule and the first full C75 cryomodule installed in 2017 and 2021. This paper reports on the results from the qualification of the cavities for the second C75 module in both a vertical cryostat and the commissioning results of the cryomodule in the CEBAF tunnel.

BACKGROUND

The C75 program makes use of a cavity design and tooling previously designed and optimized for high current Free Electron Laser use while employing modern cavity processing techniques with the cost saving measure of using large grain medium-to-high purity ingot Niobium (supplied by CBMM, Brazil) in place of traditional fine grain sheet Niobium to form cavities. This process is described in [1, 2] and their associated references and will not be covered herein other than to note that cavity production continues to be performed by Research Instruments (RI) located in Germany. End groups are cut from the cavities of the extracted original CEBAF C20 cryomodule to be refurbished and shipped to the vendor for attachment to the newly fabricated cavities. Cavities are deep drawn, electron beam welded into dumbbells, and shape corrected via a fixture prior to assembly for field flatness. Assembled C75 cavities are 8mm shorter in length than C20 cavities. ($L_{C75}=0.492m$) Once fabrication is completed cavities are then returned to JLab for further cavity processing, testing, and assembly.

CAVITY PREPARATION & RECIPE

Following receipt and incoming RF and dimensional inspection, the cavities receive a 100 mm bulk removal from the inner surface, followed by annealing in a vacuum furnace at 800 °C/3 h with a 3 h hold at 450 °C prior to reaching 800 °C. A 30 mm layer is removed from the inner surface by electropolishing (EP) after annealing. Afterwards, the cavities are subjected to dimensional check and adjustments, RF tuning. Finally, all the Nb flanges are lapped and etched by buffered chemical polishing (BCP), followed by ultrasonic cleaning and high-pressure water rinsing with ultra-pure water.

The bulk removal consisted of 100 mm EP for 3 of the cavities for cryomodule C75-02, whereas it consisted of 60 mm removal by centrifugal barrel polishing and 40 mm EP for the other 5 cavities for C75-02.

VERTICAL TEST AREA (VTA) RESULTS

Following treatment each cavity undergoes assembly of supporting components in an ISO Class 4 cleanroom followed by a slow pump down and leak check on a vertical test stand. Test stands are craned into a vertical cryostat which is then cooled down and filled with 2 K liquid Helium for cavity testing. Table 1 shows the test results.

Table 1: Vertical Test Results (FE Onset in MV/m, Cav. 3 was Limited by Multipacting)

Cav.	Emax (MV/m)	Limit	Qo @ Emax	FE onset	FE max. (mRad/hr)
1	22.0	Admin	1.23e10	13.9	3.37
2	18.2	Quench	1.11e10	11.4	1.90
3	15.6	MP	7.94e09	17.5	251.0
4	20.8	Cable	6.74e09	10	98.9
5	19.6	Rad.	6.18e09	10.75	1000
6	20.7	Quench	8.69e09	15	3.61
7	20.3	Admin	9.21e09	20.3	-
8	20.2	Cable	8.51e09	14	12.60

* This material is based upon work supported by the U.S. Department of Energy, Office of Science, Office of Nuclear Physics under contract DE-AC05-06OR23177.

[†] michaelm@jlab.org

PIP-II PROJECT OVERVIEW AND STATUS*

R. Stanek[†], C. Boffo, S. Chandrasekaran, S. Dixon, E. Harms, L. Kokoska, I. Kourbanis, J. Leibfritz, O. Napoly, D. Passarelli, E. Pozdeyev, A. Rowe, Fermilab, Batavia, IL, USA

Abstract

The Proton Improvement Plan II (PIP-II) Project at Fermilab is constructing an 800 MeV H⁻ ion superconducting radio frequency linear accelerator (SRF Linac). Capitalizing on advances in superconducting radio frequency (SRF) technology, this new Linac will provide the initial acceleration chain to power the Fermilab accelerator complex throughout the next decade and beyond. In addition, upgrades to the existing Booster, Main Injector, and Recycler rings will enable them to operate at a 20 Hz repetition rate and will provide a 1.2 MW proton beam to drive neutrino research at the Deep Underground Neutrino Experiment (DUNE) in Lead, South Dakota.

The SRF Linac for PIP-II consists of twenty-three cryomodules (CM) with cavities of three different frequencies and five different shapes. PIP-II is the first U.S. accelerator project to be built with major international contributions, thus benefitting from their world-leading expertise and capabilities. U.S. National Laboratory Partners include Argonne National Lab, Lawrence Berkeley Lab, Jefferson Lab, and SLAC National Accelerator Lab. International Partner Countries include India, France, Italy, United Kingdom, and Poland. The PIP-II Project is one year into the execution phase and is making good progress, but as is the case in many big projects currently being executed, is facing challenges from inflationary pressures, and supply chain delays. These issues are being addressed in collaboration with Fermilab management, our Partners, and the U.S. Department of Energy.

INTRODUCTION

PIP-II will be a world-class SRF-based accelerator which will enhance performance and operational reliability of the Fermi National Accelerator Laboratory (FNAL) complex. It is the latest step to revitalization of the accelerators that power America's High Energy Physics Program. The science objective is to enable the accelerator complex to provide 1.2 MW proton beam on the LBNF target (upgradeable to multi-MW) and to provide a flexible, multi-user capability for a broader reaching physics program. The Linac output will be 800 MeV when injecting into the existing Booster. The machine will run in pulsed mode initially but will be fully continuous wave (CW) compatible. Performance Goals are tabulated in Table 1.

* Work supported by the U.S. Department of Energy, Office of Science, Office of High Energy Physics, under U.S. DOE Contract No. DE-AC02-07CH11359

[†] rstanek@fnal.gov FERMILAB-CONF-23-331-PIP2

Table 1: PIP-II Performance Goals

Performance Parameter	Value	Units
Delivered Beam Energy	800	MeV
Beam Particles	H ⁻	
Beam Pulse Length	0.54	ms
Particles per Pulse	6.7	10 ¹²
Pulse repetition Rate	20	Hz
Average Beam Current	2	mA
Maximum Bunch Intensity	1.9	10 ⁸
Maximum Bunch Rep Rate	162.5	MHz
Bunch Pattern	Prog and Arbitrary	
RF Frequency	162.5 harmonic	
Bunch Length (RMS)	< 4	ps
Transverse Emittance	≤ 0.3	mm-rad
Longitudinal Emittance (RMS)	≤ 0.3	mm-rad

The accelerator is being built in collaboration with several key International Partners including Bhabha Atomic Research Centre (BARC), Commissariat à l'énergie atomique (CEA), Centre National de la Recherche Scientifique/Institut national de physique nucléaire et de physique des particules (CNRS/IN2P3), Istituto Nazionale di Fisica Nucleare (INFN), Inter-University Accelerator Centre (IUAC), Raja Ramanna Centre for Advanced Technology (RRCAT), Science & Technology Facilities Council UK Research and Innovation (STFC UKRI), Lodz University of Technology (TUL), Variable Energy Cyclotron Centre (VECC), Wrocław University of Science and Technology (WUST), and Warsaw University of Technology (WUT). The collaboration is functioning very well, and Partners are committed to delivering their scope of work [1].

Additionally, FNAL is working with other Department of Energy (DOE) labs including Lawrence Berkeley National Lab (LBNL), Argonne National Lab (ANL), Thomas Jefferson National Lab (JLab) and SLAC National Accelerator Lab on various aspects of the machine.

The scope of the project includes extensive new civil construction, the SRF-based Linac, a 2.5 kW @2 K cryoplat housed in a new standalone building, all necessary power and auxiliary equipment, and the connection into the Booster to allow injection. The Linac begins with a Warm Front End followed by multiple cryomodules including a Half Wave Resonator (HWR), nine Single Spoke Resonators (two SSR1 and seven SSR2), and thirteen 650 MHz Elliptical units (nine LB650 and four HB650). The beam

PROTON POWER UPGRADE PROJECT PROGRESS AND PLANS AT THE SPALLATION NEUTRON SOURCE IN OAK RIDGE TENNESSEE*

J. Mammosser[†], J. Galambos, L. Pinion, S.-H. Kim, M. Howell, M. Champion, B. Robertson, S. Stewart, G. Hines, R. Afanador, D. J. Vandygriff, D. Vandygriff, B. Degraff, M. Doleans, C. McMahan, D. Kraft, D. Barnhart, P. Pizzol, S. Gold, R. Maekawa, M. Greenwood, M. Dayton
Spallation Neutron Source, Oak Ridge National Laboratory, Oak Ridge, TN, USA
E. F. Daly, K. M. Wilson, P. Dhakal, N. Huque, K. Davis, J. Fischer, D. Forehand
Jefferson Lab, Newport News, VA, USA
A. Navitski, L. Zweibaeumer, K. B. Bolz, A. Bitter, Research Instruments GmbH., Germany

Abstract

The Proton Power Upgrade project is well underway at the Spallation Neutron Source (SNS) facility in Oak Ridge, Tennessee. This project aims at increasing the proton beam power capability from 1.4 to 2.8 MW, by adding linac energy, increasing the beam current and implementing target developments to handle the increased beam power. This talk will cover the current status of increasing the beam energy, issues encountered along the way, operational experience with the new SRF cryomodules and target improvements and results from operation with beam so far.

INTRODUCTION

The Proton Power Upgrade (PPU) project currently underway at Oak Ridge National Laboratory, will increase the proton beam power from 1.4 MW to 2.8 MW to maximize the neutron flux at the experimental beam-lines and provide capability to drive a Second Target Station (STS) in the future [1], see Fig. 1. The increased neutron flux will increase the number of experiments conducted during each run as well as expand the scientific capabilities of SNS. From the beginning of SNS construction, additional space was provided for the increase of the linac energy with 10 additional cryomodule slots at the end of the installed High Beta cryomodules. The PPU project and STS project are currently at DOE critical decision 3 and 1 respectively. The scope of PPU project includes fabrication and installation of seven new 0.81 beta cryomodules; High Power RF klystrons and modulators; Low Level RF systems; vacuum and instrumentation controls; equipment racks; site utility upgrades; beam instrumentation; chicane magnets; new injection dump septum magnet; fabrication of 2 test targets; testing of the new targets; conventional facility modifications; utility upgrades and a stub-out added to the ring to target beam transport section to extend the tunnel towards the proposed STS target station location. The stub-out construction will reduce interruptions to beam operations during construction of the second target station tunnel. The scope of the STS project will include a second target hall housing a solid rotating target and additional beam-lines for experiments. For the First

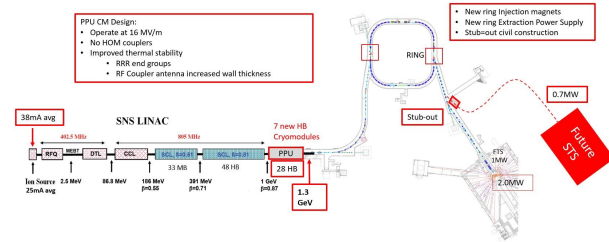


Figure 1: SNS layout and design parameters.

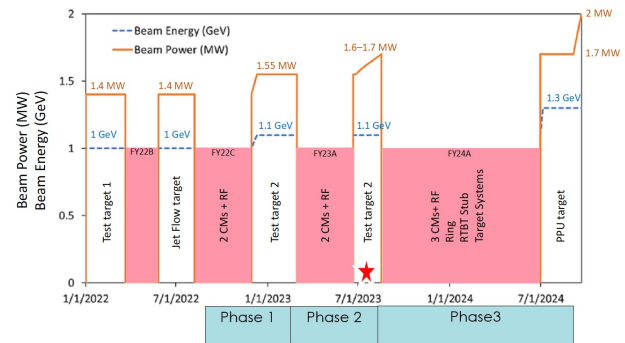


Figure 2: PPU planned outages.

Target Station (FTS) improvements to the target design were necessary for the full 2.0 MWs of beam power to increase their lifetime, a portion of the 2.8 MW beam (0.7 MWs) will be sent to the STS once it is complete [1].

Major Specification	Current operation	PPU full capability	PPU FTS operation
Beam power (MW)	1.4	2.8	2.0
Beam energy (GeV)	1.0	1.3	1.3
Beam current, macro-pulse average (mA)	25	38	27
Macro-pulse length (ms)	1	1	1
Energy per pulse (kJ)	24	47	33
Repetition rate (Hz)	60	60	60
Key Performance Parameter	Threshold	Objective	
Beam power on target (MW)	1.7	2.0	
Beam energy (GeV)	1.25	1.3	
Target operation without failure (hours)	1250 at 1.7 MW	1250 at 2.0 MW	
Stored beam intensity in ring (protons per pulse, ppp)	1.6×10^{14} ppp ¹	2.24×10^{14} ppp ²	

¹ corresponds to 1.92 MW at 1.25 GeV and 60 pps
² corresponds to 2.80 MW at 1.30 GeV and 60 pps

Figure 3: PPU key performance parameters.

* Work supported by UT-Battelle, LLC, under contract DE-AC05-00OR22725

[†] mammosserjd@ornl.gov

OPERATIONAL EXPERIENCE FOR RIKEN SUPERCONDUCTING LINEAR ACCELERATOR

K. Yamada*, M. Fujimaki, H. Imao, O. Kamigaito, M. Komiyama, K. Kumagai, T. Nagatomo, T. Nishi, H. Okuno, K. Ozeki, N. Sakamoto, K. Suda, A. Uchiyama, T. Watanabe, Y. Watanabe
RIKEN Nishina Center, Wako, Japan

Abstract

The RIKEN superconducting heavy-ion linac, SRILAC, has been successfully operating for almost four years and has stably delivered heavy-ion beams for super-heavy-element synthesis experiments. SRILAC consists of ten superconducting (SC) quarter-wavelength resonators made from pure Nb sheets that operate at 4.5 K. The effects of a broken coupler during the initial operation and after four years of operation resulted in increased X-ray emission levels in several superconducting cavities. Recently, we found that field emissions can be significantly reduced with high-voltage pulse conditioning. We are also preparing ten new couplers and two spare superconducting cavities to permanently solve this problem. This article shares the lessons learned from experiences in a four-year operation with low-beta SC cavities.

INTRODUCTION

The Radioactive Isotope Beam Factory (RIBF) [1, 2] at the RIKEN Nishina Center began operations in 2006. The aim was to pursue heavy-ion beam science through basic and applied research, such as determining the origin of the elements, establishing new nuclear models, synthesizing new elements and isotopes, researching nuclear transmutation, and supporting industrial applications, including the biological breeding and production of useful RIs. Figure 1 shows a schematic of the RIBF. The RIBF can provide an intense RI beam for all masses by accelerating heavy-ion beams up to 70% of light speed in cw mode, using a cascade of four separate-sector cyclotrons: the RIKEN ring cyclotron (RRC [3], $K = 540$ MeV), the fixed-frequency ring cyclotron (fRC [4–6], $K = 700$ MeV), the intermediate-stage ring cyclotron (IRC [7], $K = 980$ MeV), and the world’s first superconducting ring cyclotron (SRC [8], $K = 2600$ MeV). The cyclotron cascade is combined with different types of injectors: a variable-frequency heavy-ion linac (RILAC [9, 10]), fixed-frequency heavy-ion linac (RILAC2 [11, 12]), and K70-MeV AVF cyclotron (AVF [13]). RILAC is used as an injector for medium-mass ions such as ^{48}Ca , RILAC2 for very heavy ions such as xenon and uranium, and AVF for light-mass ions. RILAC and AVF were also operated in stand-alone mode. In particular, RILAC plays a crucial role in providing high-intensity beams for superheavy elements (SHEs) experiments. Nihonium, the first element discovered in Japan, was synthesized [14] using a beam supplied by RILAC.



Figure 1: Schematic of the RIBF at RIKEN Nishina Center. The linac facility described in this article is shown in the lower part of the figure.

After the discovery of nihonium in the old linac facility, the facility was upgraded [15] to increase the beam intensity and energy for synthesizing new SHEs above $Z = 118$ and to produce valuable RIs such as ^{211}At . For the upgrade, we constructed a new superconducting ECR ion source [16] to obtain a higher beam intensity and introduced a superconducting booster linac named SRILAC to increase the beam energy in a limited space, as shown in Fig. 2. The goal of the RILAC upgrade project was to accelerate ions with $m/q = 6$ to 6.5 MeV/u. The budget was approved in fiscal year 2016, and construction was completed in 2019.

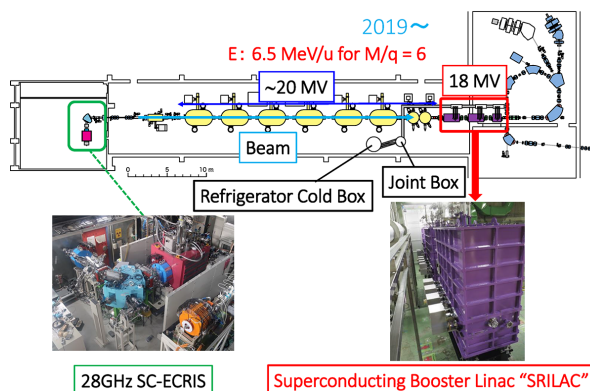


Figure 2: Schematic of the heavy-ion linac facility at RIKEN after the upgrade. The eight tanks shown in yellow are the existing room-temperature drift-tube linac, RILAC.

* nari-yamada@riken.jp

OPERATING EXPERIENCE OF SRF SYSTEM AT HIGH BEAM CURRENT IN SuperKEKB

M. Nishiwaki*¹, K. Akai, T. Furuya, S. Mitsunobu, Y. Morita, T. Okada¹
High Energy Accelerator Research Organization (KEK), Tsukuba, Japan
¹also at Accelerator Science Program, Tsukuba, Japan

Abstract

SuperKEKB aims for high luminosity on the order of 10^{35} /cm²/s with beam currents of 2.6 A for electron and 3.6 A for positron to search new physics beyond the Standard Model in the B meson regime. In recent operations, we achieved a new record of luminosity of 4.65×10^{34} /cm²/s with 1.1 A for electron and 1.3 A for positron. The SRF system that was designed for KEKB, the predecessor of SuperKEKB, is operating stably with the high beam currents owing to the measures against the large beam powers and the large higher-order-mode (HOM) powers. As a measure against the large beam powers, our SRF cavities have increased a coupling of high-power input couplers during the KEKB operation. As a measure against the large HOM power, newly developed SiC HOM dampers have been installed in the SuperKEKB ring. In addition, we have established the horizontal high-pressure rinse method to recover the cavity performance that has degraded due to vacuum works and accidents in the long-term operation. In this report, we will present our operation experience of SRF system under the high beam currents.

INTRODUCTION

The SuperKEKB accelerator that is an electron-positron asymmetric energy collider is an upgraded machine from KEKB accelerator aiming for a significant increase of luminosity. SuperKEKB main ring consists of a 7 GeV electron ring (high energy ring, HER) and a 4 GeV positron ring (low energy ring, LER). To achieve high luminosity, the designed beam currents are increased to 2.6 A for HER and 3.6 A for LER [1]. A full-scale collision experiment has been continued since 2019. In recent operation, the achieved beam currents are 1.14 A for HER and 1.46 A for LER, and the peak luminosity of 4.65×10^{34} /cm²/s was recorded [2, 3].

The RF system of SuperKEKB is operating stably at large beam current of higher than 1 A in 2022 operation [4]. The RF-related operation parameters in KEKB (achieved) and SuperKEKB (design) are shown in Table 1. The design beam current is nearly twice as high as the KEKB achieved, and the beam power becomes large accordingly [5–7]. The RF system of HER consisting both of eight superconducting cavities (SCC) [8,9] and normal-conducting cavities (ARES) [10–12] has been reused from KEKB with reinforcement to handle the high beam current and the large beam power.

Because the beam power can be shared with SCC and ARES by giving phase-offset, the load of the input coupler

of SCC will be almost the same as KEKB. On the other hand, the HOM power excited in the SCC module at the design current is estimated to be more than double the power achieved in KEKB, and to be unacceptable loads of the existing ferrite dampers. Then, additional SiC dampers are installed to reduce the load of ferrite dampers.

In this report, the operation status and experiences of SRF system under the high beam current are described.

SCC MODULE

A cross sectional view of the SCC module is shown in Fig. 1 [13]. The SCC module was designed for KEKB with HOM damped structure equipped with a pair of ferrite HOM dampers on both small beam pipe (SBP) and large beam pipe (LBP) [14]. The eight SCC modules are operating in HER. In the latest beam operation in 2022, each SCC provided an RF voltage of 1.35 MV and delivered the beam power of ~260 kW in the maximum beam current of 1.14 A so far. Figure 2 shows the power delivered to the beam by each SCC module as a function of the stored beam current.

Input Coupler

The coaxial antenna-type input coupler was also developed for KEKB based on the input coupler of SCC in TRISTAN. The features of the input coupler are summarized in Ref. [15, 16]. Figure 3 shows the input coupler designed

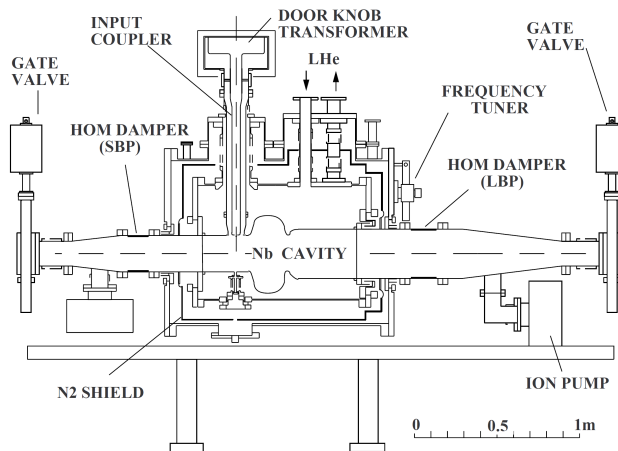


Figure 1: Cross-sectional view of HOM damped SCC designed for KEKB. This cavity is used for SuperKEKB. Ferrite HOM dampers are equipped on both SBP and LBP. The SBP and LBP diameters are 220 mm and 300 mm, respectively.

* michiru.nishiwaki@kek.jp

OPERATIONAL EXPERIENCE WITH THE EUROPEAN XFEL SRF LINAC

C. Schmidt*, J. Branlard, M. Bousonville, M. Diomedea, S. Göller,
D. Kostin, M. Scholz, V. Fogel, N. Walker
Deutsches Elektronen-Synchrotron DESY, Hamburg, Germany

Abstract

The European X-ray Free Electron laser (EuXFEL) is a 3.4 km long research facility which generates ultrashort X-ray flashes of outstanding brilliance since 2017. Up to 27000 electron bunches per second are accelerated in a 1.3 km long superconducting radio frequency (SRF) linac to a maximum energy of 17.6 GeV. Within this time, operational experience with a pulsed RF machine has been gained and new operation modes simultaneously delivering electron bunches to 3 different SASE undulator beamlines have been successfully implemented. Recent activities on increasing the linac availability, power efficiency and duty cycle are discussed.

INTRODUCTION

The European X-ray Free-Electron Laser (XFEL), operated at the Deutsches Elektronen-Synchrotron (DESY) is a research facility which provides its users ultrashort X-ray flashes of photon energies up to 30 keV by 3 different SASE beamlines. Centerpiece of this facility is the 1.3-km-long particle accelerator consisting of 776 Tesla-type superconducting RF cavities. The accelerator is divided into 4 accelerating sections which are the Injector (I1), two bunch compression sections L1 and L2 plus the main linac L3. The maximum achievable beam energy is 17.6 GeV at a 10 Hz repetition rate delivering up to 27000 bunches per second. A facility overview is presented in [1-2] and shown in Fig. 1. The individual RF stations in sections L1 to L3 are composed of 4 cryomodules, each housing 8 cavities. Each RF station is driven by a 10 MW multi-beam klystron. Within this architecture the vector sum voltage of 32 cavities is controlled by a Low-Level Radio Frequency (LLRF) control system, based on a Micro Telecommunications Computing Architecture (MicroTCA.4) [3]. High precision control of the accelerating fields inside the cavities is essential to achieve the required beam energy and arrival time stability. Furthermore, the system has to be flexible in order to cope with variations of bunch patterns, linac energy requirements and bunch compression settings. Overall, availability, parameter reproducibility, and long-term stability are key aspects in achieving the high demands from the photon users. Developments in the direction of improving operability and automation are continuously ongoing. An overview about past LLRF system developments can be found in Ref. [4], further investigations in order to reach the maximum gradients for individual cavities are described in Ref. [5].

This contribution summarizes the operational experience of the superconducting accelerator over the last two years.

* christian.schmidt@desy.de

Linac operation modes are described in the following section, reporting on the machine availability and experience in daily operation. The next section gives an outline in the machine performance and the attempts to foster and improve the operability and reliability. This is followed by new developments introduced to improve the flexibility of the machine operation as well as the efforts to reduce the energy consumption for the RF part of the machine. Finally this paper discusses the next steps in machine development towards the extension of the RF pulse to continuous wave (CW) operation.

LINAC OPERATION

Figure 2 presents the annual operation hours of the European XFEL since the beginning of regular user operation. Typically the machine runs for 7000 hours/year, and the user delivery has steadily ramped up to a planned 5000-hours/year in 2024. Improvements in automation and operational experience has resulted in requiring less time for machine setup and tuning. Figure 2 also shows the draft outlook for the upcoming 2 years, including a longer shutdown period in the second half of 2025.

Typical photon delivery operations run on a weekly cycle. Mondays are reserved for tuning and setup of the SASE parameters requested for the remainder of the week (agreed upon at the end of the last weekly cycle). This time is also used for routine adjustment of linac parameters which may have drifted during the previous weeks operations. If deemed necessary, access to the accelerator tunnel (where most of the accelerator systems are housed) is also scheduled during this time, typically for 2-4 hours, for more significant repairs and maintenance. Non-critical maintenance requests are collected until there are sufficient in number or criticality to schedule an access. Typically this happens every 3-4 weeks. In addition to these short maintenance periods, two longer shutdowns are scheduled per year (typically summer and winter). These are mandatory for the German safety authority for testing of the interlock systems, and are also used for more major works, routine maintenance and service tasks.

Depending on the requested photon energy, the machine is typically operated at three electron beam energy configurations of 11.5, 14 and 16.3 GeV. The final photon energy is tuned by variable gap undulators. The configuration of the injector sections including L1 and L2 usually remains the same for different final electron beam energies (2.4 GeV at the exit of L2). The final electron beam energy is achieved by the setup of the main linac L3. The two lower energies (11.4 and 14 GeV) are achieved by running the RF stations at a reduced RF voltage, whereas the 16.3 GeV beam energy is achieved by running the stations at their maximum voltage. In all cases, the RF stations are typically run at an

DEVELOPMENT AND TESTING OF SPLIT 6 GHz CAVITIES WITH NIOBIUM COATINGS*

N. Leicester^{†1}, G. Burt¹, H. Marks¹, D. Seal¹, J. Conlon¹, O.B. Malyshev², T. Sian², R. Valizadeh²
Cockcroft Institute, Daresbury Laboratory, Warrington, UK
E. Chyhyrynets, C. Pira, Legnaro National Laboratories INFN, Legnaro, Italy
¹also at Engineering Department, Lancaster University, Lancaster, UK
²also at ASTeC, STFC Daresbury Laboratory, Sci-Tech Daresbury, Warrington, UK

Abstract

Superconducting thin-films on a copper substrate are used in accelerator RF cavities as an alternative to bulk Nb due to the high thermal conductivity of copper and the lower production costs. Although thin-film coated RF cavities can match, or even exceed the performance of bulk Nb, there are some challenges around the deposition. The RF cavities are often produced as two half-cells with a weld across the centre where the RF surface current is highest, which could reduce cavity performance. To avoid this, a cavity can be produced in 2 longitudinally split halves, with the join parallel to the surface current. As the current doesn't cross the join a simpler weld can be performed far from the fields, simplifying the manufacturing process, and potentially improving the cavities performance. This additionally allows for different deposition techniques and coating materials to be used, as well as easier post-deposition quality control. This paper discusses the development and testing of 6 GHz cavities that have been designed and coated at the Cockcroft Institute, using low temperature RF techniques to characterise cavities with different substrate preparations and coating techniques.

INTRODUCTION

Niobium (Nb), which is commonly used for accelerating cavities, is expensive and has a low thermal conductivity at cryogenic temperatures. The low thermal conductivity can lead to localised heating, leading to a quench. In order to avoid this, a thin superconducting film can be deposited onto a copper (Cu) substrate, which utilises the high thermal conductivity of copper, while maintaining the benefits of a SRF cavity. Modern research is also beginning to reveal a number of other superconductors that would not be suitable for application as a bulk superconductor, due to physical properties, such as brittleness, but can match, or even exceed the performance of niobium when it is used in thin film applications. These include Nb₃Sn, NbTiN, and V₃Si [1].

Most commonly, RF cavities are produced as 2 half cells, known as cups, which are then e-beam welded together around the equator. This weld occurs across the region where the magnetic field and surface current is highest, which research on ISOLDE is showing may result in lowered performance[2]. In addition when using thin films, this weld is an

area where micro cracks can occur, which can also reduce the Q-factor of the cavity. One solution to this has been to produce a seamless cavity, however this is expensive and creates a more challenging deposition process as the target must be located on the inside of the cavity for deposition.

At the Cockcroft Institute, a novel longitudinally split cavity geometry has been developed, which is constructed from 2 half cells split longitudinally, rather than transversely, such that the surface current runs along, rather than across, the seam. As such the cavity may be operated with a gap between the two half-cells and so a any weld can be located far from the RF surface, and can hence be applied after coating. The open design also allows for planar thin film deposition techniques as well as surface characterisation prior to welding making research and development of thin-film superconductors much simpler [3, 4].

Simultaneously at CERN, a similar cavity known as a Slotted Waveguide Elliptical cavity is under development for potential use on the FCC. SWELL cavities are manufactured in 4 quadrants rather than 2 longitudinally split half-cells with HOM dampers placed in the gaps between sections [5].

This paper describes the process for designing and testing the cavities that have been produced at the Cockcroft Institute. The aim is to compare the RF surface resistance (R_s) for different Nb coatings, that were performed using various deposition parameters, and look at the effect of electropolishing (EP) on the cavity performance.

CAVITY DESIGN USING CST AND MANUFACTURE

The cavity was designed in CST [6]. It has an elliptical geometry, with a resonant frequency, $f_0 = 6$ GHz. The shape was chosen for this first iteration simply due to it being a standard cavity shape. The coupling pipe was made long to reduce any losses from the end plates. In the future an optimization process will be performed in order to improve the cavity for the longitudinal design. Figure 1 shows the E field for the current cavity geometry.

The present design has a coupling pipe radius = 14 mm, equator = 22.95 mm, and the length of the coupling pipes = 80 mm. Using these parameters, simulations predict a maximum magnetic field strength = 3.66 mT with 0.1 mJ of stored energy.

The cavity is formed from 2 Cu blocks, which can be accurately aligned with each other using 2 pins and then bolted together with 4 bolts. The cuboid shape provides good me-

* This work has been supported by: the IFAST collaboration which has received funding from the European Union's Horizon 2020 Research and Innovation programme under Grant Agreement No 101004730.

[†] nathan.leicester@cockcroft.ac.uk

FLUX EXPULSION LENS: CONCEPT AND MEASUREMENTS

D. A. Turner^{1,*}, I. González Díaz-Palacio², W. Hillert², T. Koettig¹, A. Macpherson¹,
G. Rosaz¹, N. Stapley¹, A. Gallifa Terricabras¹, M. Wenskat²

¹CERN, Geneva, Switzerland

²Institute of Nanostructures and Solid State Physics, Universität Hamburg, Germany

Abstract

A magnetic flux expulsion lens (MFEL) has been designed and built at CERN. This device uses closed topology conduction cooling of samples to quantify magnetic flux expulsion of superconductors, and allows for systematic measurements of the cooling dynamics and the magnetic response during the superconducting transition. Measurements for bulk Nb, cold worked Nb, sputtered Nb on Cu, and SIS multilayer structures are given. Preliminary results for both sample characterisation of expulsion dynamics, and observation of an enhanced flux expulsion in SIS samples are also reported.

INTRODUCTION

During the transition from the normal conducting (NC) state to the superconducting (SC) state, a perfect SC will expel all ambient magnetic field (B_a) from its volume, i.e. no B field is present within the volume of a SC whilst in the Meissner state. However, for imperfect SC's, impurities and defects within the sample impede flux expulsion, leaving magnetic flux trapped within the SC as vortices. For SRF cavities, the trapped vortices can result in localised heating on the RF surface, which then contributes to the surface resistance (R_s) and reduces the maximum Q_0 of the cavity.

It is well documented that cavity performance is affected by the cooling dynamics, with both the temperature gradient (dT) and the cooling rate as the SC transitions into the Meissner state at T_c [1] correlating with expelled magnetic flux. Within the literature, cool down versus cavity performance improvements have been detailed for slow cooling rates for cavities in a horizontal orientation [2, 3], and fast cooling (high dT) for cavities in a vertical orientation [4–6]. Interpreting flux expulsion efficiency of SRF cavities in terms of flux pinning dynamics is not necessarily straightforward, as an increased spatial thermal gradient (dT/dx) increases the de-pinning force on the flux line, and decreases the probability of a flux line interacting with a pinning site.

In order to establish an assessment of magnetic flux expulsion in materials used for SRF cavities, without the complications of cavity geometry and orientation on flux dynamics during the SC transition, a dedicated flux expulsion measurement system has been developed at CERN. This system, known as the Magnetic Flux Expulsion Lens or MFEL, measures the magnetic flux expulsion of macroscopic samples under controlled thermo-magnetic conditions.

* daniel.andrew.turner@cern.ch

MAGNETIC FLUX EXPULSION LENS

The MFEL, designed and built at CERN, is a simple laboratory device to quantify magnetic flux trapping in samples considered for SRF materials. The MFEL works by applying heat pulses to the sample such that it transitions out of and back to the Meissner state, with the key to the MFEL being the sample geometry, which is a flat annulus geometry (90 mm outer diameter with a 6 mm inner aperture). For this geometry, the outer edge of the sample is in contact with an isothermal cold source, whilst the heat pulse is applied at the inner radius of the annulus. This causes the sample to transition from the SC to the NC state, with the transition propagating radially through the sample. At the end of the heat pulse, the Meissner transition front is driven from the outer radius by the cold source to the centre aperture by the thermal gradient. The extent to which the magnetic flux is driven into the central aperture provides a quantitative measure of the associated flux pinning within the sample. Further, variation of deposited energy from the heat pulse permits measurement of flux expulsion efficiency as a function of thermal gradient, while the time structure of the observed magnetic response offers insight into the thermo-electric dynamics of the transition. The concept of the MFEL flux dynamics is shown in Figs. 1b-1e with the corresponding measurement observables given in Fig. 1a.

Realisation

The MFEL is an axially symmetric device based on an annulus sample that undergoes pulsed heating at the inner radius, while maintaining a thermal connection to a cold source at the outer radius. The magnetic response of the MFEL is measured by a flux gate (Bartington Mag-01H probe) positioned on axis, normal to the sample surface, such that it is sensitive to the flux density traversing the annulus aperture. In addition, thermometry (calibrated CERNOX CX-1050-SD-HT-1.4L with standard Lakeshore acquisition system) is installed at inner and outer edges of the sample and the cold source. Both the magnetic field probe and the temperature (T) sensor are read throughout the heat pulse cycle, with readout rates of 20 Hz and 10 Hz respectively. This readout rate is sufficient for accurate digitising of the thermo-magnetic transition. The heat pulse is provided by a pulsed resistor connected to the sample by a Cu nose cone. A labelled cross section is shown in Fig. 2, which also portrays the heat path through the facility.

For operation, the MFEL is mounted in a vacuum chamber with a Cu base plate that serves as the cooling interface between cold source and MFEL. The vacuum chamber is

MUON SPIN ROTATION STUDIES OF BILAYER SUPERCONDUCTORS AND LOW TEMPERATURE BAKED NIOBIUM

Md Asaduzzaman^{1,*}, Ryan M. L. McFadden¹, Edward Thoeng²,
Robert E. Laxdal, Tobias Junginger^{1,†}, TRIUMF, Vancouver, Canada

¹also at Department of Physics and Astronomy, University of Victoria, Victoria, Canada

²also at Department of Physics and Astronomy, University of British Columbia, Vancouver, Canada

Abstract

Muon spin rotation (μ SR) results have shown that the first vortex penetration field detected by muons ($H_{vp,\mu}$) into Nb can be delayed up to the superheating field, H_{sh} by coating a single layer of a material with larger London penetration depth, λ_L . For low-temperature baked (LTB) (i.e., 120 °C baked) Nb an increase in the $H_{vp,\mu}$ has also been observed. While clearly exceeding the lower critical field H_{c1} , $H_{vp,\mu}$ was found to remain significantly below H_{sh} for LTB Nb. Further, magnetometry experiments suggested that there is no interface barrier in LTB Nb and that the apparent $H_{vp,\mu}$ increase as observed by μ SR was due to surface pinning. By varying the implantation depth of muons of $E \sim 4.1$ MeV using moderating foils, new μ SR measurements confirm that the apparent $H_{vp,\mu}$ increase in LTB Nb is indeed due to surface pinning, while for a Nb₃Sn (2 μ m)/Nb bilayer we find that an interface energy barrier prevents flux penetration. These results confirm the potential of using superconducting bilayers to achieve a flux free Meissner state up to the H_{sh} of the substrate.

BACKGROUND

Superconducting radio frequency (SRF) cavities need to be operated in a flux free Meissner state to avoid strong dissipation from magnetic vortices. The maximum field that can be sustained by a superconductor in the Meissner state is proportional to the accelerating gradient (E_{acc}), which sets the ultimate limit of a cavity. The lower critical field H_{c1} defines the field at which it is energetically favorable for flux to be located inside the superconductor instead of being expelled by Meissner currents. The vortex penetration field (H_{vp}) can potentially exceed H_{c1} in case of a surface barrier with the ultimate limitation set by the superheating field H_{sh} . Nb is the preferred material for fabricating SRF cavities because it possesses the highest H_{c1} and critical temperature T_c among all elemental superconductors. For clean Nb, H_{c1} is about 170 mT [1] and $H_{sh} = 240$ mT [2] at a temperature of 2 K corresponding to E_{acc} of about 40 and 55 MV m⁻¹ for elliptical cavities. Some SRF cavities baked at 120 °C for 48 h in vacuum or low pressure gas atmosphere (i.e., LTB) have reached peak surface magnetic fields exceeding H_{c1} but for mass production operating E_{acc} values around 30 MV m⁻¹ or below are chosen [3].

In the context of LTB study, it is important to understand the underlying mechanisms that can influence the material

properties. The effect of LTB treatments can induce changes in the outermost nanoscale region of the material through diffusion processes. This results in the formation of a dirty layer with a larger London penetration depth (λ_L) compared to the bulk value of the material [4, 5]. This layer could potentially lead to a reduction of Meissner currents and the formation of a surface barrier at the interface between the outer dirty layer and the bulk material [6]. Consequently, this scenario can be viewed as the creation of a potential bilayer superconductor. In a bilayer superconductor when the top layer penetration depth is larger than the substrate's two effects occur. First, H_{vp} into the surface layer is increased due to strong suppression of Meissner current. Second, an interface energy barrier between the layers [6] similar to the Bean-Livingston barrier [7] at the vacuum-superconductor interface is created potentially prohibiting flux penetration into the substrate up to the substrate's H_{sh} .

μ SR experiments have reported evidence for an interface barrier in bilayer samples of different materials and thicknesses [8] and a slight increase of H_{vp} above H_{c1} for LTB samples. Magnetometry measurements could not confirm the enhancement for LTB samples [9] and we, therefore, hypothesize that the $H_{vp,\mu}$ for LTB was due to increased accumulation of vortices caused by vortex pinning in the near-surface region. Pinning centers can act as supplementary barriers, impeding the movement of vortices from the edges of the sample to the center [8]. As a result, they introduce additional resistance which leads to a delayed flux propagation towards the center of the samples compared to a scenario without pinning. Note that the implantation depth in so-called surface μ SR experiments using a ~ 4.1 MeV beam is on the order of 130 μ m for Nb. The aim of this study is to test whether flux could have been trapped in a thin layer comparable to this length scale before being detected by muons. In this case one would find $H_{vp,\mu} > H_{vp}$. Understanding the dominant mechanism at play is crucial for guiding further developments in materials and layered structures beyond conventional bulk Nb technology.

DESCRIPTION OF EXPERIMENT

Brief General Description of the Muon Spin Rotation Technique

μ SR is a powerful condensed matter technique for the direct measurement of the magnetic field inside the sample. In this experiment, 100% spin-polarized radioactive muons (μ^+) were implanted into the sample one at a time

* asadm@uvic.ca

† junginger@uvic.ca

SIMS CHARACTERIZATION OF NITROGEN DOPING OF LCLS-II-HE PRODUCTION CAVITIES*

C. E. Reece, E. M. Lechner[†], M. J. Kelley

Thomas Jefferson National Accelerator Facility, Newport News, VA, USA

J. W. Angle, Virginia Polytechnic & State University, Blacksburg VA, USA

Abstract

The thermal diffusion of nitrogen into the surface of niobium has been shown to yield superior low-loss SRF performance. An effective solution was identified and promptly employed in the production of cryomodules for LCLS-II. With added experience and R&D, a modified process was chosen for use in the upgrade for LCLS-II-HE. Largely motivated by this circumstance, supporting research has significantly refined the technique for making calibrated secondary ion mass spectrometry (SIMS) measurements of the N concentration depth profiles produced by production processes. Standardized reference samples were included with four HE production cavities in their N-doping furnace runs. We report the calibrated dynamic SIMS depth profiles of N, C, and O for these samples, together with the cryogenic acceptance test performance of the associated cavities. Interpretation and comparison with similar samples acquired in other furnaces highlights the importance of intentional process quality control of furnace conditions.

SIMS ANALYSIS OF NIOBIUM

Sample Preparation

Over the past several years a standardized Nb sample preparation process has been developed at Jefferson Lab to facilitate high quality SIMS characterization of the surfaces produced by various candidate SRF cavity preparation methods. The key characteristics are: fabrication from cavity sheet stock, dimensions standardized for multiple loading in custom SIMS sample holder and custom electropolishing sample holder that assures only single face exposure to electrolyte, annealing of the samples to obtain grain sizes (~200 μm) to enable SIMS sampling of only single grains (since sputter rates vary with grain orientation), planarization of the sample face to ~5 nm via chemical/mechanical polishing and electropolishing, with minimum disturbance of the lattice of the surface grains. Such surface planarization is necessary in order to obtain uniform sputter depth and thus maximize the depth resolution during SIMS sputter profiling.

Development of SIMS Quantification Techniques

There having been no prior work refining dynamic SIMS technique on Nb matrix, this became the subject of the PhD dissertation efforts of J. Tuggle and J. Angle at the Nano

Characterization and Fabrication Lab (NCFL) of Virginia Tech. Method sensitivities and vulnerabilities were explored and refined such that measurement errors on contaminant species concentrations approaching 10% have been realized. [1-4]

SAMPLING PRODUCTION PROCESS

Having recognized a vulnerability to potential process variation with “tightness” of the cavity “caps” that can restrict N₂ flow into the cavity during doping [5], we arranged to have standard prepared samples included with the doping furnace run of four LCLS-II-HE cavities at RI Research Instruments GmbH. Our purpose was to sample the doping variability within the routine production process.

A single standard Nb sample was included inside each of two cavity envelopes during each of two routine N-doping production furnace runs. The samples experienced the same N₂ pressure and temperature profile as that cavity's interior surface. The standard protocol for N-doping for the LCLS-II-HE project is heating at 800 °C for 3 hours under high vacuum conditions followed by 2 min exposure to ~33 mbar N₂ gas while sustaining 800 °C. Then the nitrogen gas is evacuated and the furnace heat is removed, and contents are allowed to cool down under vacuum. Between preparation at Jefferson Lab and placement in cavity, and then also between removal from cavity and transport to analysis, the samples were stored in concave base sample holders to protect the key surface. The HE production cavities sampled were CAVR076, CAVR142, CAVR144, and CAVR151.

SIMS CHARACTERIZATION

The four samples were shipped to the NCFL for analysis with a Cameca 7f dynamic SIMS system. Depth concentration profiles were measured on three randomly selected niobium grains on each sample. Secondary ion yields indicating atomic N, O, and C concentrations within each Nb grain were calibrated against a similar standard sample ion-implanted by Kroko. The obtained concentration profiles are presented in Fig. 1.

The sputter times and current were the same for all sampled grains. The grain orientation dependence of sputter rates produces the variation in sampled depths. With these samples we were seeking to acquire profiles to a depth of at least 10 μm .

* Work supported by the U.S. Department of Energy, Office of Science, Office of Nuclear Physics under contract DE-AC05-06OR23177.

[†] lechner@jlab.org

IN-SITU QUALITY FACTOR MEASUREMENTS OF SRF CAVITIES AT S-DALINAC*

M. Arnold, A. Brauch, M. Dutine, R. Grewe[†], L. Jürgensen, N. Pietralla, F. Schließmann, D. Schneider, Institute for Nuclear Physics, Technische Universität Darmstadt, Darmstadt, Germany

Abstract

The Superconducting Darmstadt Linear Accelerator (S-DALINAC) is a thrice recirculating electron accelerator which can be operated in a multi-turn energy recovery mode. The design parameters for kinetic energy and beam current are up to 130 MeV and up to 20 μA respectively. The injector consists of a six-cell capture cavity and two 20-cell srf cavities. The main linac consists of eight 20-cell cavities. The cavities are operated at a temperature of 2 K with a frequency of 2.9972(1) GHz. Monitoring of the srf cavities is important for the overall performance of the accelerator. A key parameter for the rating of the srf cavity performance is the intrinsic quality factor Q . At the S-DALINAC it is measured for selected cavities during the yearly maintenance procedures. The unique design of the rf input coupler allows for a wide tuning range for the input coupling strength. This makes in-situ quality factor measurements using the decay time measurement method possible. The contribution illustrates the principal design of the input couplers and the benefits it yields for Q measurements. Recent results including the progression of the quality factors over time will be presented.

INTRODUCTION

The thrice recirculating S-DALINAC (Superconducting Darmstadt Linear Accelerator) is in operation since 1991 (Fig. 1). To reach its design energy of 130 MeV within the limited space available at the Institute for Nuclear Physics at TU Darmstadt, the S-DALINAC utilizes the high energy gain and low power losses of superconducting radio-frequency (srf) cavities [1]. At the time the S-DALINAC has been built, 3 GHz 20-cell cavities were figured to be the best compromise of size, dissipated power P_d and accelerating field gradient E_{acc} [2]. Measurement of the performance parameters *intrinsic quality factor* Q_0 and *maximum accelerating gradient* E_{max} of each cavity allows optimization of the energy gain distribution by Q_0 , and thus maximizing the total energy gain of the accelerator with respect to total loss $\sum P_d$.

S-DALINAC CRYOMODULES AND INPUT COUPLER

The 20-cell srf cavities of the S-DALINAC are mounted in a frequency tuning frame resting in a liquid helium bath at a temperature of 2 K. A schematic view of the important parts of the S-DALINAC cryomodule is shown in Fig. 2.

* Work supported by DFG (GRK 2128) and the State of Hesse within the Research Cluster ELEMENTS (Project ID 500/10.006)

[†] rgrewe@ikp.tu-darmstadt.de

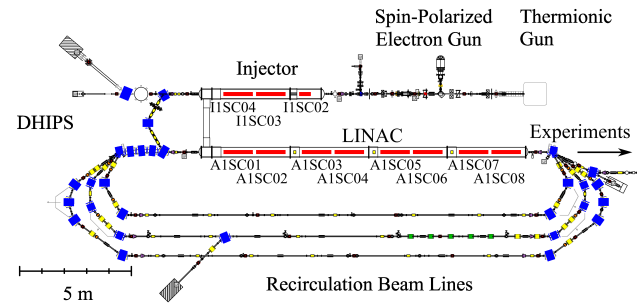


Figure 1: Floorplan of the S-DALINAC accelerator hall. Two electron sources create an electron current of up to 60 μA with an energy of up to 250 keV which is prepared for srf acceleration in a normalconducting section. A single 5-cell cavity and two 20-cell cavities (red) are used to capture and accelerate the beam to 10 MeV to be used for nuclear fluorescence experiments or further acceleration in the main LINAC. The main LINAC consists of eight 20-cell cavities, which add up to 30 MeV to the beam energy in each of up to four passes.

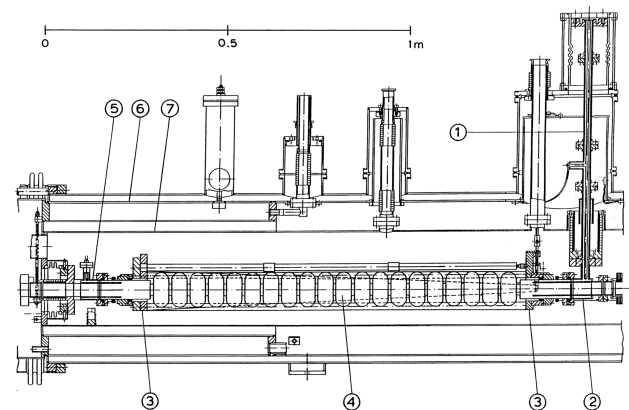


Figure 2: Sectional view of a cut in half cryomodule of the S-DALINAC. (1) Coaxial rf transmission line, (2) Coaxial input coupler, (3) Cavity tuning frame, (4) 20-cell elliptical cavity, (5) rf output coupler, (6) 80 K shielding, (7) 2 K helium vessel [3].

To optimize the operation of the Low Level RF control (LLRF) [4] for each cavity, the rf transmission line allows variation of the penetration depth of the rf input antenna into the coaxial input coupler by means of a bellow in the outer conductor of the transmission line. A detailed schematic of the input coupler layout is shown in Fig. 3. By variation of the penetration depth the external quality factor Q_{ex} can be adjusted in the range $3 \cdot 10^6 < Q_{ex} < 3 \cdot 10^9$ [3], covering the design quality factor $Q_0 = 3 \cdot 10^9$ of the srf cavities.

PLASMA ELECTROLYTIC POLISHING TECHNOLOGY PROGRESS DEVELOPMENT FOR Nb AND Cu SUBSTRATES PREPARATION*

E. Chyhyrynets[†], O. Azzolini, R. Caforio¹, D. Fonnesu, D. Ford, G. Keppel, C. Pira, A. Salmaso, F. Stivanello, G. Marconato¹

INFN Laboratori Nazionali di Legnaro, viale dell'Università 2, Legnaro (PD), Italy

¹ also Università degli Studi di Padova, Padova, Italy

Abstract

Superconducting radio frequency (SRF) cavity performance is highly dependent on surface preparation. Conventionally, electropolishing (EP) is used to achieve a clean surface and low roughness for both Nb and Cu substrates (in thin films SRF cavities), but it requires harsh and corrosive solutions like concentrated acids. Plasma Electrolytic Polishing (PEP) is a promising alternative that uses only diluted salt solutions and has several advantages over EP. PEP can replace intermediate steps like mechanical or chemical polishing, thanks to its superior removal rate of up to 2-8 $\mu\text{m}/\text{min}$ of Nb and 3-30 $\mu\text{m}/\text{min}$ of Cu. It achieves Ra roughness of 100 nm for both substrates and has a higher smoothing effect than EP. PEP is also suitable for normal conducting cavities and other accelerator components, including couplers. We demonstrate the effectiveness of PEP on SRF substrates and analyse substrate defect evaluation. We demonstrate the application of PEP onto SRF substrates: Cu QPR sample and 6 GHz cavity.

INTRODUCTION

The PEP process is a non-conventional method used to treat various types of metal and alloy surfaces. It is a powerful and fast process that does not require any preparation of the treated surface. However, ensuring scalability and application of PEP can be a complex endeavour. The application of PEP onto Cu and Nb surfaces for SRF has already been discussed and published [1]. In this study, we discuss further advancements in scalability and present a new setup designed for treating larger samples.

THE NEW SET-UP

All experiments were conducted in the chemical laboratory of the Superconductivity and Surface Treatment Service at Legnaro National Laboratories (LNL) of INFN. Two DC power supplies were connected in series to deliver a high voltage (300 V) and high currents (up to 150 A) output. Various samples with different geometries and dimensions were subjected to treatment. The experiments conducted on the 18 cm² samples demonstrated a current density ranging from 0.2 to 0.8 A/cm². The process for these samples was carried out using a 3 L solution.

* Work supported by the INFN CSNV experiment SAMARA. This project has received funding from the European Union's Horizon 2020 Research and Innovation programme under Grant Agreement No 101004730. Financial support from: PNRR MUR project PE0000023-NQSTI.

[†] eduard.chyhyrynets@lnl.infn.it

Considering the constant value of the experimented current density, the larger samples treated in subsequent experiments could easily reach currents approaching 150 A. Consequently, an increase in heat production is expected. The high temperatures generated during the process may decrease the stability of the treatment and potentially lead to oxidation or corrosion effects. During the initial stages of the process, current spikes were observed, reaching values 2-5 times higher than the working currents. These current values exceed the maximum sustainable limits of the currently employed power supplies, indicating the need for improvements to the setup.

Design and Production

A new facility was designed and developed specifically for the treatment process of larger area samples such as QPRs [1], and 6 GHz cavities. The design of the facility took into consideration several fundamental characteristics, including:

- The ratio of bath volume to anode area, which needed to be greater than 0.2 L/cm².
- The material of the bath had to be an insulator.
- The capability to accommodate a large surface cathode, with an anode to cathode ratio of 10:1.

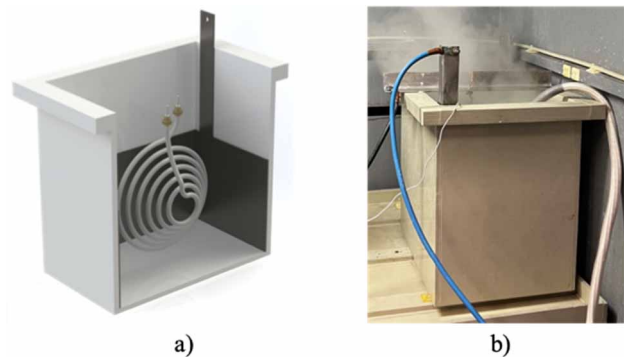


Figure 1: a) A schematic render of the plastic bath used for PEP; b) Photo view during PEP process.

Figure 1a illustrates the polymeric bath made of PVC that was designed and fabricated for this purpose. The experimental setup consisted of an Nb cathode, a resistance element, and a thermocouple to ensure precise temperature control. The treated sample (anode) was connected positively and suspended in the bath, as shown in Fig. 1b. The bath had a capacity of approximately 30 L of solution, with a total volume of 50 L. Such system provided better temperature control and a more stable polishing process.

ANALYSIS OF SEMICONDUCTOR COMPONENTS AS TEMPERATURE SENSORS FOR CRYOGENIC INVESTIGATION OF SRF MATERIALS

A. Cierpka*, S. Keckert, F. Kramer, O. Kugeler, J. Knobloch¹
Helmholtz-Zentrum Berlin, Berlin, Germany
¹also at Universität Siegen, Siegen, Germany

Abstract

Temperature mapping systems have been used for many years to detect local heating in an SRF cavity surface or materials sample. They require a large number of temperature sensors. Most often, low-cost Allen-Bradley resistors are used for this purpose. Since they have poor sensitivity and reproducibility above 4 K, sensor alternatives that combine the precision of Cernox¹ sensors with the low-cost of Allen-Bradley resistors would be highly desirable. In this work various semiconductor components that exhibit a temperature dependent electrical response, such as diodes and LEDs were analyzed with respect to sensitivity, reproducibility and response speed in a temperature range between 6.5 K and 22 K. In this range, many diodes and LEDs were found to be more sensitive than Cernox sensors. However, in some components the response time was slow – possibly due to poor thermal contact.

INTRODUCTION

Since many years, temperature mapping systems have been valuable tools for SRF cavity R&D, for example, to detect local heating in the surface of cavities [1].

As most niobium cavities are operated at 1.8 K to 2 K a large number of high-precision temperature sensors optimized for this temperature range is needed. If the temperature is only measured at a few points, commercial Cernox sensors can be used, offering great accuracy. For large T mapping systems, mainly 100 Allen-Bradley carbon resistors are used since their low-cost allows for affordable scaling of the mapping systems.

Although Allen-Bradley resistors are applicable for temperatures below 4 K their sensitivity drops for temperatures above 4 K [2]. This is unfavorable for the analysis of cavities made of Nb₃Sn, which is a promising material for future SRF cavities as it allows the operation at 4.4 K [3]. In addition, Allen-Bradley resistors exhibit systematic temperature deviations after performing several temperature cycles [2]. Thus, it reduces their suitability for use in experiments studying effects during transition to the superconducting phase, in which several temperature cycles are often performed.

In this paper, the search for advanced temperature sensors that combine the high-precision of Cernox sensors and low-cost of Allen-Bradley resistors is presented. Building on the results of [4], various commercially available semiconductor components are studied. The components are analyzed with respect to the following parameters: In order to achieve high

sensitivity, a strong dependence of the electrical response on temperature is needed. Additionally, a high response speed is required in order to detect quick effects. Also, high reproducibility is desired.

EXPERIMENTAL SETUP

For the analysis of the mentioned properties at cryogenic temperatures, a two-stage cryo-cooler is used. In an isolation vacuum it can reach temperatures down to about 6 K. A round copper plate is mounted onto the cryo-cooler, on which a Cernox sensor for calibration and two semiconductor components to be tested are screwed. A heater foil glued to the cryo-cooler and driven by a PID controller allows for precise temperature control (see Fig. 1).

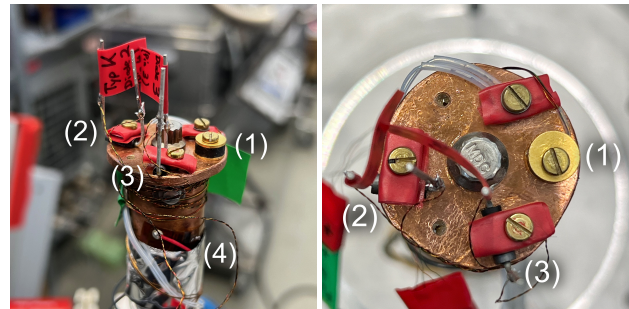


Figure 1: Photographs of the experimental setup. A copper plate is mounted onto the cryo-cooler on which the Cernox sensor (1) and semiconductor components (2)&(3) are screwed. The heater foil (4) is glued onto the cryo-cooler below the plate.

The following commercial semiconductor components have been tested (see Table 1). Among them are both LEDs and diodes.

All tested components have an insulating casing (i.e. the casing of LEDs or the cylindrical housing of wired diodes), which lowers the thermal conductivity between the copper plate and sensor and thus could have an impact on response speed. Therefore, the wired diodes are polished until the semiconducting material has direct contact with the surface. In order to avoid a short between the diode and the copper plate, the diode is insulated with a thin layer of varnish. This grinding process is not possible for LEDs, as the wirebonds inside the insulation will be damaged immediately.

* alexander.cierpka@helmholtz-berlin.de

¹ Temperature sensors from the manufacturer LakeShore.

DEPOSITION AND CHARACTERISATION OF V₃Si FILMS FOR SRF APPLICATIONS*

C. Benjamin^{1†}, L. Smith¹, J. Conlon¹, O. B. Malyshev¹, R. Valizadeh¹,
D. Seal², N. Leicester², H. Marks², G. Burt²

Cockcroft Institute of Accelerator Science, Daresbury, United Kingdom

¹also at ASTeC, STFC Daresbury Laboratory, United Kingdom

²also at Lancaster University, Lancaster, United Kingdom

Abstract

A15 superconducting materials, like V₃Si and Nb₃Sn, are potential alternatives to Nb for next generation thin film SRF cavities when operated at 4 K. Their relatively high T_c and superconducting properties could allow for higher accelerating gradients and elevated operating temperatures. We present work on the deposition of V₃Si thin films on planar Cu substrates and an open structure 6 GHz cavity, using physical vapour deposition (PVD) and a V₃Si single target. The surface structure, composition and DC superconducting properties of two planar samples were characterised via secondary electron microscopy (SEM), energy dispersive x-ray spectroscopy (EDX) and in a magnetic field penetration facility. Furthermore, the first deposition using PVD of a V₃Si film on a 6 GHz split cavity and the RF performance is presented.

INTRODUCTION

As bulk and thin film niobium (Nb) superconducting RF (SRF) cavities approach their theoretical limit, the requirement for alternative superconducting materials is increased. Thin film A15 superconductors such as: V₃Si and Nb₃Sn are promising candidates due to their relatively high critical temperatures of T_c = 18 and 17 K, and upper critical fields (H_{c2}) of 28 and 24.5 T respectively [1]. These properties may allow for operation of SRF cavities at higher temperatures (≥4 K instead of ≈2 K), potentially reducing cost of cryogenics and may allow increased accelerating gradients, simplifying infrastructure of the particle accelerator [2].

Previous production of thin V₃Si films have implemented a variety of methods: thermal diffusion, co-sputtering and single alloy target magnetron sputtering, with varying levels of success. In the thermal diffusion method, Si is either deposited on a vanadium substrate or introduced via SiH₄ gas. The substrate is then annealed (850 °C) forming the correct A15 phase. This method resulted in a successful superconducting cavity, however it suffers from surface Si and performance lower than a typical Nb cavity [3]. Co-sputtered magnetron methods have produced successful V₃Si thin films on Cu, they also observed that the high deposition and annealing temperatures produces Cu-Si phases and Cu inclusions [4]. Further magnetron sputtered films on a stripline

resonator formed on a thin sapphire substrates show an RF response inline with weak coupling BCS theory predictions with surface resistances significantly lower than Nb [5].

This paper focuses on the current progress of V₃Si thin films using pulsed DC magnetron sputtering deposition using a single target. The surface structure, composition and DC superconducting properties of two planar samples were characterised via secondary electron microscopy (SEM), Energy-dispersive X-ray spectroscopy (EDX) and in a magnetic field penetration facility [6]. The latter section of this report presents the first deposition of a V₃Si film on a split 6 GHz cavity with surface resistance measured in the RF characterisation facility [7, 8].

THIN FILM V₃Si ON PLANAR Cu SUBSTRATES

Sample Preparation and Deposition

Two V₃Si thin films were deposited on polycrystalline oxygen-free, high conductivity (OFHC) Cu substrates (Labelled S1 and S2). Both substrates underwent *ex situ* chemical treatment with BPS-172 solution, etching any surface oxide formation and atmospheric contamination. Once loaded into the vacuum system they were both heated to 500 °C for 24 hours to remove any residual contamination from the loading process.

V₃Si deposition was performed in a stainless steel vacuum chamber, with a base pressure 5 × 10⁻⁹ mbar, equipped with a single planar magnetron source. The source was equipped with a commercially bought V₃Si target. The sample stage is positioned 100 mm away from the magnetron source, with sample heating up to 800 °C. Deposition was conducted using a Pulsed DC magnetron power supply using the deposition parameters shown in Table 1. During deposition Kr is admitted into chamber as the process gas to a pressure of 5 × 10⁻³ mbar. Substrate temperature between S1 and S2 were 670 °C and 710 °C respectively.

Characterisation and Performance

Figure 1 displays two SEM images of the surface topography of V₃Si thin films on (a): S1 and (b): S2 samples. The surface topography of S1 is a dense structure of small grains that are a few hundred nanometers in size. S2 shows a similar structure, however, the grain size is much larger approaching micrometer in size. Further analysis using EDX showed a difference in composition between the two samples:

* This work has been supported by: the IFAST collaboration which has received funding from the European Union's Horizon 2020 Research and Innovation programme under Grant Agreement No 101004730.

† Christopher.Benjamin@stfc.ac.uk

INVESTIGATION, USING Nb FOILS TO CHARACTERISE THE OPTIMAL DIMENSIONS OF SAMPLES MEASURED BY THE MAGNETIC FIELD PENETRATION FACILITY*

L. Smith^{1†}, D. Turner², G. Burt², T. Junginger², O.B. Malyshev¹

Cockcroft Institute, UKRI/STFC Daresbury Laboratory, Daresbury, Warrington, UK

¹also at ASTeC, UKRI/STFC Daresbury Laboratory, Daresbury, Warrington, UK

²also at Engineering Department, Lancaster University, Lancaster, UK

Abstract

At Daresbury Laboratory, in depth Research and Development is attempting to push the maximum accelerating gradient (E_{acc}) forward through its Thin Films SRF programme, by increasing the maximum magnetic field (B) that can be applied to an SRF cavity wall whilst maintaining the Meissner effect. Nb is the best performing single element as it has both the highest T_c and highest lower critical field (B_{c1}) allowing the cavity to maintain the Meissner effect longer and improve efficiency. At Daresbury Lab, the Magnetic Field Penetration Facility (MFPPF) tests flat samples by applying a DC magnetic field parallel to sample, replicating the conditions of the cavity wall. The field of full flux penetration (B_{fp}) is determined by two Hall probes (HP1 and HP2), situated on either side of the sample. The facility can measure samples no larger than 50 mm diameter, but it is important to know how sample size can affect results due to field leakage around the sample. This paper shows results of a study that measured the effects of sample size (from 50 x 50 – 10 x 10 mm²) and sample thickness in the range of 1 - 100 μ m to determine the ideal geometry for field penetration measurements using MFPPF. Nb foil samples were used to allow easy alteration of size.

INTRODUCTION

Charged particles are accelerated in particle accelerators by using radio frequency (RF) cavities. Superconducting Radio Frequency (SRF) cavities are used to enhance power and prevent energy loss through a resistive heat into the cavity walls, improving efficiency, whilst lowering operating costs. Superconducting materials are used to coat the cavities as they have unique properties, meaning they can remain in the Meissner state at higher acceleration field E_{acc} than other materials and therefore limit power loss [1]. In the Meissner state, DC resistance is equal to zero and all external magnetic fields are expelled, as long as the material remains below the critical temperature T_c . Therefore, it is important to develop new materials that can push the T_c higher and allow greater cavity performance. Nb is currently the leading, single element material used for cavity coating, as it has the highest critical temperature $T_c = 9.25$ K and

the largest, lower critical field (H_{C1}) [2]. However, a new approach to sample structure using thin films which incorporate a thin Nb film, more than 1 micron on top of a Cu substrate to improve thermal conduction and multi-layers that use multi structures in the sample: Superconducting – insulation – superconducting (SIS) make it possible to push the boundaries of bulk Nb further, increasing T_c and H_{c1} [3, 4].

EXPERIMENTAL

Magnetic Field Penetration Facility

The Magnetic Field Penetration Facility (MFPPF), built at Daresbury Laboratory, is described in details in Ref. [1]. It allows a practical and time efficient alternative to testing SRF cavity layers for their SC properties. Quicker turnaround times of sample testing, allows the optimal material composition to be identified without the need to coat the cavity beforehand thus, improving operational costs and time efficiency. The MFPPF schematically shown in Fig. 1 operates by applying a DC magnetic field, through a 2 mm gap in a carbon based, steel, yoke magnet, parallel to the surface of a flat sample, to replicate the conditions met by the cavity wall. B_{fp} is defined using two Hall probes, HP1 and HP2. HP1 is situated between the yoke dipoles, directly above the sample, and measures the maximum applied magnetic field (B_1) [1], while HP2 sits in a carved out trench, directly below the sample. The MFPPF operates within the temperature range of 2.6 and 30 K and can apply an optimal magnetic field of 600 mT. The facility operates by reducing the temperature below the T_c of the sample to induce the Meissner effect. Once the sample is in a SC state, a magnetic field is applied until the SC state is overcome and B_{fp} is defined as the point the field fully penetrates the sample. This operation is then repeated at different temperature set points to provide an overall picture of how the material is performing. With these applications in mind, it is sensible to determine a good understanding of the MFPPF's limitations as a function of sample size and thickness in order to ensure the correct sample geometry is used and in turn provides the best results. An investigation was performed earlier [1], using a type one SC (Pb) to correctly identify the size limitations of a sample before leakage around the edges becomes an issue. Pb was used as it demonstrates a sharp transition and is malleable, making it simple to manipulate to different sizes. The MFPPF

* This work has been supported by: the IFAST collaboration which has received funding from the European Union's Horizon 2020 Research and Innovation programme under Grant Agreement No 101004730.

† liam.smith@stfc.ac.uk

INFLUENCE OF THE COATING PARAMETERS ON THE T_c OF Nb_3Sn THIN FILMS ON COPPER DEPOSITED VIA DC MAGNETRON SPUTTERING*

D. Fonnesu[†], O. Azzolini, R. Caforio¹, E. Chyhrynets, D. Ford, V. A. Garcia Diaz, G. Keppel,
G. Marconato¹, C. Pira, A. Salmaso, F. Stivanello

National Institute for Nuclear Physics - Legnaro National Laboratories (INFN-LNL) Legnaro, Italy
¹also at University of Padua, Padova, Italy

Abstract

The IFAST collaboration aims at pushing the performance of particle accelerators by developing sustainable innovative technologies. Among its goals, the development of thin film-coated copper elliptical accelerating cavities covers both the optimization of the manufacturing of seamless substrates and the development of functional coatings able to conform to the 3D cavity geometry while delivering the needed performance. For the latter, the optimization of the deposition recipe is central to a successful outcome. The work presented here focuses on the deposition of Nb_3Sn films on flat, small copper samples. The films are deposited via DCMS from a planar stoichiometric Nb_3Sn commercial target. The results of the film characterization are presented here. The observed dependencies between the critical temperature T_c of the films and the deposition parameters are discussed and, in particular, $T_c^{90\%-10\%} = (17.9 \pm 0.1)$ K is reported for Nb_3Sn on sapphire and $T_c^{90\%-10\%} = (16.9 \pm 0.2)$ K for Nb_3Sn on copper with a 30 μ m thick niobium buffer layer.

INTRODUCTION

In the pursuit for sustainability, one goal is to make possible the operation of the SRF cavities at 4.5 K to reduce the amount of cryopower needed for the operation [1]. To this aim, the A15 compound Nb_3Sn , with a higher critical temperature of 18.3 K compared to niobium's 9.2 K, has the potential to provide at 4.5 K quality factors comparable to the ones obtained with bulk niobium ($Q_0 \approx 10^{10}$) at 2 K. Coating copper SRF cavities with a superconducting thin layer is a well-established technique, primarily using niobium coatings. However, the high temperatures required to form the A15 phase of Nb_3Sn (≈ 930 °C) [2] introduce a major challenge when using copper as a substrate, so that optimizing the coating parameters becomes crucial to compensate for the limitations in reaching those high temperatures. Standardized procedures with high control and reproducibility are essential to identify factors influencing film quality and refine the R&D feedback process. The experimental methods adopted here, obtained results and future plans are detailed in the following sections.

* The IFAST project has received funding from the European Union's Horizon 2020 Research and Innovation programme under Grant Agreement No 101004730. Work supported by the INFN CSNV experiment SAMARA and by the INFN CSN1 experiment RD FCC.

[†] dorothea.fonnesu@lnl.infn.it

EXPERIMENTAL METHODS

Each Nb_3Sn film deposition process is performed on three different substrate types: sapphire, OFHC copper and OFHC copper pre-coated with a niobium buffer layer. Prior to the deposition of the Nb_3Sn film, the substrates are prepared according to a standard procedure: the sapphire substrates are cleaned with ethanol in an ultrasound bath; the copper substrates are first cleaned in a detergent solution (GP17.40) in an ultrasound bath, then treated with SUBU [3] for 2-3 minutes. A 1 μ m thick niobium buffer layer is then deposited via DC Magnetron Sputtering (DCMS) on the prepared copper substrate. For the later tests presented in this study some copper substrates with a thicker 30 μ m niobium buffer layer were also prepared and included in the deposition run, in addition to the ones prepared with the 1 μ m niobium buffer layer. These were coated via DCMS as multi-layers [4]. The copper substrates pre-coated with the buffer layer are stored in vacuum until the Nb_3Sn coating process takes place, to minimize the chances of oxidation. In preparation to the coating, the substrates are then fixed on a custom plate, as shown in Fig. 1. Inside the ultra-high vacuum coating

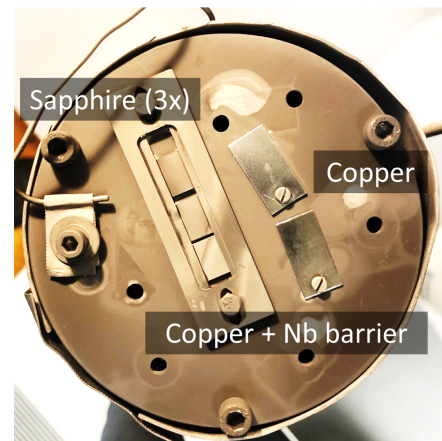


Figure 1: Flat samples right after the coating process, still mounted on the sample holder.

chamber, the plate is placed in front of a commercial 4'' planar stoichiometric Nb_3Sn target. The distance between the target and the samples is 9 cm. The process takes place in three main phases: the baking, the coating phase and the annealing. The baking of the vacuum system is performed by heating the system for 48 h while pumping the vacuum. After the baking, the coating of the Nb_3Sn films

NbTi THIN FILM SRF CAVITIES FOR DARK MATTER SEARCH*

G. Marconato^{†1}, O. Azzolini, R. Caforio, E. Chyhyrynets, D. Fonnesu, D. Ford, V. Garcia,
G. Keppel, C. Pira, A. Salmaso, F. Stivanello

INFN, Laboratori Nazionali di Legnaro, Legnaro (Padova), Italy

C. Braggio², INFN, Sezione di Padova, Padova, Italy

D. Alesini, C. Gatti, A. D'Elia, D. Di Gioacchino, C. Ligi, G. Maccarrone, A. Rettaroli, S. Tocci
INFN, Laboratori Nazionali di Frascati, Frascati (Rome), Italy

U. Gambardella, D. D'Agostino, Gruppo Collegato di Salerno,
INFN Sezione di Napoli, Salerno, Italy

S. Posen, Fermi National Accelerator Laboratory, Batavia, Illinois, USA

¹Also at Dipartimento di Scieze Chimiche, Università degli Studi di Padova, Padova, Italy

²Also at Dipartimento di Fisica, Università degli Studi di Padova, Padova, Italy

Abstract

The search for dark matter is now looking at ALPs (axion-like particles) as a very promising candidate to understand our universe. Within this framework, we explore the possibility to use NbTi thin film coatings on Cu resonating cavities to investigate the presence of axions in the range of 35-45 μeV mass by coupling the axion to a very strong magnetic field inside the cavity, causing its conversion to a photon which is subsequently detected. In this work the chemical treatments and DC magnetron sputtering details of the preparation of 9 GHz, 7 GHz, and 3.9 GHz resonant cavities and their quality factor measurements at different applied magnetic fields are presented.

INTRODUCTION

An outstanding result of modern cosmology is that a significant fraction of the universe is made of dark matter. However, the nature of such component is still unknown, besides its gravitational interaction with ordinary baryonic matter. A favored candidate for dark matter is the axion: a new particle introduced by Peccei and Quinn to solve the strong CP problem [1]. Axions and axion-like particles (ALPs) have extremely small coupling to normal matter and radiation.

The QUAX (QUaerere AXion) proposal [2] explores the possibility to study the interaction of the cosmological axion with the spin of fermions (electrons or nucleons). In fact, due to the motion of the Solar System through the galactic halo, the Earth is effectively moving through the cold dark matter cloud surrounding the Galaxy and an observer on Earth would see such axions as a wind. In particular, the effect of the axion wind on a magnetized material can be described as an effective oscillating RF field with frequency determined by axion mass. Thus, a possible detector for the axion wind could be a magnetized sample placed inside a microwave resonant cavity, both cooled down at

ultra-cryogenic temperature to avoid the noise due to thermal photons. This setup will be called haloscope hereafter. Since the mass of the ALPs is unknown, many cavities have been fabricated to explore different frequencies within the calculated range of existence of the axions.

The work presented hereby focuses on the superconductive coating of 3 copper microwave cavities (6 half-cells) made in collaboration with different laboratories. The coatings were performed via DC magnetron sputtering (DCMS) by means of a 4 inches NbTi planar target. The first NbTi on Cu haloscope realized, was a 9 GHz cavity coated by DCMS using a Nb_{0.38}Ti_{0.62} target in 2019 [3, 4]. The goal of this research was to improve the performance of this previous haloscope by changing the sputtering target from the Nb_{0.38}Ti_{0.62} to a Nb_{0.31}Ti_{0.69} since this particular composition of NbTi had been proven to have higher pinning for flux vortices due to precipitations of titanium particles, leading to theoretical better performances of the superconductive cavity, in particular higher quality factor in presence of high magnetic field [5]. We also studied the effect of introducing a Nb barrier layer between the copper substrate and the NbTi layer to prevent diffusion at the interfaces. This barrier layer is commonly used in NbTi superconducting magnets production [6].

EXPERIMENTAL PROCEDURE

After mechanical fabrication each cavity semi-cell needed to be chemically treated, in order to have a polished substrate for the deposition process (Fig. 1 A). The recipe for copper polishing involved several steps as follows:

1. Ultrasonic degreasing in GP17.40 soap at 40 °C for approximately 1 hour;
2. Ultrasonic in deionized water;
3. Electropolishing in H₃PO₄ (85 %): Butanol (99,9 %) at 3:2 volume ratio at room temperature with applied voltage 2-3 V for different times depending on the cavity shape and dimensions;
4. Ultrasonic, ethanol rinsing and drying with nitrogen.

* This project received resources from U.S. DOE, Office of Science, NQISRC, SQMS contract No DE-AC02-07CH11359 and from EU's Horizon 2020 Research and Innovation programme, Grant Agreement No 101004730. It also received funding from INFN CSNV experiment SAMARA. Acknowledge financial support also from: PNRR MUR project PE0000023-NQSTI

[†] giovanni.marconato@lnl.infn.it

DEVELOPMENT OF A PLASMA-ENHANCED CHEMICAL VAPOR DEPOSITION SYSTEM FOR HIGH-PERFORMANCE SRF CAVITIES*

G. Gaitan[†], A. Holic, W.I. Howes, G. Kulina, M. Liepe, P. Quigley, J. Sears, Z. Sun, B. Wendland
Cornell Laboratory for Accelerator-Based Sciences and Education (CLASSE) Ithaca, NY, USA

Abstract

Next-generation, thin-film surfaces employing Nb₃Sn, NbN, NbTiN, or other compound superconductors are essential for reaching enhanced RF performance levels in SRF cavities. However, optimized, advanced deposition processes are required to enable high-quality films of such materials on large and complex-shaped cavities. For this purpose, Cornell University is developing a plasma-enhanced chemical vapor deposition (CVD) system that facilitates coating on complicated geometries with a high deposition rate. This system is based on a high-temperature tube furnace with a high-vacuum, gas, and precursor delivery system, and uses plasma to significantly reduce the required processing temperature and promote precursor decomposition. Here we present an update on the development of this system, including final system design, safety considerations, assembly, and commissioning.

INTRODUCTION

Niobium-3 tin (Nb₃Sn) is the most promising alternative material to niobium for next-generation SRF accelerator cavities. The material has the potential to double accelerating gradients and operating temperature of SRF cavities, decreasing costs and increasing efficiency of future accelerators, [1–5]. The dominant process currently used at Cornell University and elsewhere to grow Nb₃Sn films is based on vaporizing tin in a vacuum furnace and allowing the tin to diffuse to the surface of a Nb substrate cavity to form Nb₃Sn. The vapor diffusion growth process creates films of good quality, and there have been major improvements recently [4], leading to quench fields of up to 24 MV/m. Defects and surface roughness have been to hinder the performance of these films well below the ultimate potential of this material [3] and the improved vapor diffusion process in Refs. [4, 6] tries to address these concerns. Exploring alternative Nb₃Sn growth methods is important as some offer more control over the growth process and allow for more flexibility in the growth mechanism. Superconductors like Nb₃Sn, NbN, NbTiN, or depositing a thin film such as Zr in Ref. [7] could lead to superior RF performance levels in SRF cavities. Growing very thin films or compound superconductors will require advanced deposition processes to achieve high-quality, uniform films of such materials on large and complex shaped cavity surfaces. Remote Plasma-Enhanced Chemical Vapor Deposition (RPECVD) is a vacuum deposition method that allows for the deposition of a broad range

of materials with good uniformity even on complex shapes, see Fig. 1.3 in Ref. [8]. The remote part of RPECVD refers to the fact that the plasma generation region and the area of the reactor where the substrate is located are spatially separated [9]. This leads to better performance compared to having both the substrate and the plasma generation in the same region. PECVD uses various chemical precursors to deposit films and plasma reduces the temperature at which the deposition can take place. Furthermore, plasma can help with reducing contamination and with depositing a film on more temperature sensitive substrates, such as copper cavities that have a lower melting point. A broad range of chemical precursors allows for exploration of many materials under diverse growth conditions. The initial work to develop a dedicated cavity CVD system at Cornell can be found in Refs. [10, 11]. The design evolved from the initial stages and we will present here the current status.

REMOTE PLASMA-ENHANCED CHEMICAL VAPOR DEPOSITION (RPECVD) SYSTEM

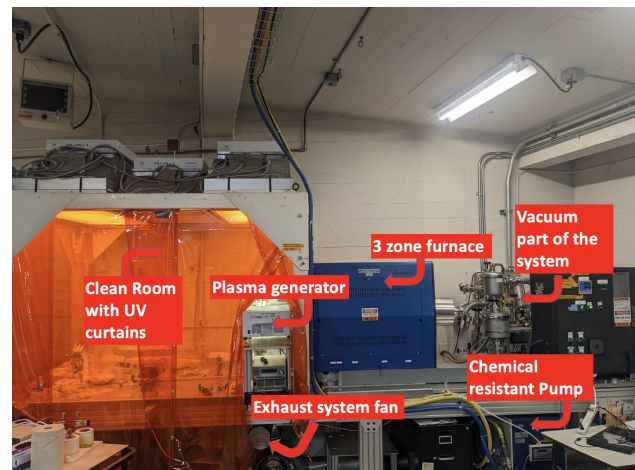


Figure 1: Overview of CVD system.

Figure 1 shows an overview for part of the CVD system and Fig. 2 shows the schematic for the whole system.

The precursor and gas delivery part of our system that are currently being installed are shown in Fig. 2. We use UHP gasses (Ar and Ar/H₂ mixtures) that carry the precursors from the bubblers to the reaction chamber. The H₂ gas plays a role in the reaction while Ar as an inert gas carries the precursors and forms the plasma. The solenoid pneumatic valves are designed to close as a protective measure in case the quartz tube breaks and the precursors are exposed to air.

* This work was supported by the U.S. National Science Foundation under Award PHY-1549132, the Center for Bright Beams.

[†] gg465@cornell.edu

SUCCESSFUL Al_2O_3 COATING OF SUPERCONDUCTING NIOBIUM CAVITIES WITH THERMAL ALD

Getnet Kacha Deyu*, M. Wenskat, I. Gonzales, R. Blick, R. Zierold, W. Hillert
Universität Hamburg, Hamburg, Germany

Abstract

Surface modification of superconducting radiofrequency (SRF) cavities is mandatory to further push the limits in future accelerators. One strategy is the deposition of a multilayer of superconducting and insulating materials on top of the inner surface of a SRF cavity. Here we report on a successful low-temperature coating of a SRF cavities with insulating Al_2O_3 by thermal atomic layer deposition (ALD) without mitigating their maximum achievable accelerating field of more than 40 MV/m. Furthermore, an improvement of the surface resistance above 30 MV/m has been observed. Our results show that ALD is perfectly suited to conformally coat the interior of the cavity and to even modify and improve the properties of such devices.

INTRODUCTION

To achieve significant advancements in superconducting radio frequency (SRF) technology, it is crucial to explore new concepts that can enhance accelerating fields and improve cavity performance. These developments are necessary to address the demanding requirements posed by upgrades to existing accelerators or the construction of future ones [1, 2]. Our research focuses on a particularly promising direction known as the superconductor-insulator-superconductor (SIS) or multilayer approach. This approach involves coating the inner surface of Nb cavities with alternating layers of superconducting and insulating materials. The concept of this structuring was initially proposed by Gurevich in 2006 [3], and it has been further refined through theoretical studies to determine the optimal layer thickness for improved RF performance [4, 5].

In order to surpass the performance of Nb cavities, a promising approach involves coating the inner surface with thin films or multilayers of superconductors that have higher critical temperatures than niobium, such as NbN or NbTiN. These composite accelerator cavities are anticipated to exhibit lower RF losses and achieve higher accelerating gradients, potentially surpassing 100 MV/m [3].

To achieve this objective, it is important to tailor the deposited superconducting film. Specifically, the thickness of the superconducting layer, denoted as d_S , should be smaller than the London penetration depth (λ_L) of the coated superconductor, and d_S should be less than 100 nm. Moreover, the higher critical magnetic field (H_{c1}) of these multilayers should exceed the superheating field (H_{sh}) of niobium. This characteristic allows for the application of higher accelerating fields compared to niobium. The presence of the thin higher- H_c layers acts as a magnetic shield, preventing the

penetration of vortices into the bulk superconducting cavity. This magnetic screening effect is further enhanced by the insulating layer, which typically has a thickness (d_I) ranging from approximately 5 to 20 nm.

In this work, we conducted a comprehensive study to examine the effects of introducing an insulating layer of Al_2O_3 on the inner surface of SRF cavities using thermal atomic layer deposition (ALD). The purpose of depositing insulating layers on the RF surface was to gain insight into the overall impact of the coating process on the RF performance. Achieving a uniform coating with an insulating layer, while maintaining or improving cavity performance, is a significant milestone on the path towards coating cavities with a multilayer structure. This investigation aimed to understand the influence of the insulating layer and ensure that it does not adversely affect the performance of the cavity.

EXPERIMENTAL DETAIL

The main part of the experiments and results summarized herein have been recently published in Wenskat et al., SUST [6]. The work was divided into three phases: first the recipe development on samples, then the transfer of the optimized recipe to a test (dummy) cavity, and finally coating of actual cavities. It is important to note that the cavity is not within a larger ALD chamber, but rather resembles the ALD chamber itself, and only the inner surface is coated.

The ALD processes for depositing Al_2O_3 coatings were carried out on an in-house developed thermal ALD system. The system maintained a base pressure of 10^{-3} mbar and utilized trimethylaluminum (TMA) and purified water (H_2O) as precursors.

To prepare the cavity for the coating process, it was initially evacuated until reaching the base pressure of 10^{-3} mbar. Following that, a constant flow of nitrogen 6.0 at a rate of 20 SCCM was introduced into the system as a carrier/purge gas. As a result, the working base pressure increased to approximately 1 mbar. This controlled environment provided the necessary conditions for the ALD process to occur effectively, ensuring proper deposition of Al_2O_3 coatings on the cavity's inner surface.

In the initial stages of recipe development, we utilized $\text{SiO}_2/(100)\text{Si}$ wafer substrates. These substrates allowed us to fine-tune the deposition parameters and optimize the process. Later on, we extended the recipe development to conical-shaped fine-grain Nb substrates. The deposition temperature during the optimization process ranged from 50 – 200 °C, with a focus on achieving target film thicknesses below 20 nm. These thicknesses align with the proposed insulator thicknesses for SIS structures. Detailed in-

* getnet.kacha.deyu@desy.de

DEVELOPMENT OF A THERMAL CONDUCTANCE INSTRUMENT FOR NIOBIUM AT CRYOGENIC TEMPERATURES

Cem Saribal*, C. Martens, M. Wenskat, W. Hillert
Universität Hamburg, Hamburg, Germany

Abstract

Particle accelerators form an important tool in a variety of research fields. In an effort to reduce operation costs while maintaining high energies, their accelerating structures are steadily improved towards higher accelerating fields and lower RF losses. Stable operation of such a cavity generally requires Joule-heating, generated in its walls, to be conducted to an outer helium bath. Therefore, it is of interest to experimentally evaluate how present and future cavity treatments affect thermal characteristics. We present an instrument for measuring the thermal performance of SRF cavity materials at cryogenic temperatures. Pairs of niobium disks are placed inside of a liquid helium bath and a temperature gradient is generated across them to obtain total thermal resistance for temperatures below 2 K. To get an idea of the instruments sensitivity and how standard cavity treatments influence thermal resistance, samples are tested post fabrication, polishing and 800 °C baking. The first tests show the commissioning of our newly set up system and if it is feasible to observe relevant changes and evaluate new and promising cavity treatments such as SIS structures.

INTRODUCTION

The thermal performance of accelerating structures not only influences achievable accelerating fields, but also affects operation costs, which for the most part are given by the cryoplant. As the rf field interacts with normal conducting electrons on the inner surface of the cavity walls, heat is generated due to surface resistance. This undesirable power dissipation in form of so-called Joule-heating increases surface temperature and reduces quality factor. At sufficiently large fields heat cannot be conducted to the outer helium bath effectively anymore, leading to a sudden decrease of cavity performance.

In order to push breakdown towards its theoretical maximum field it is mandatory to avoid thermal feedback, deteriorating the rf performance before its inherent limitations. The thermal resistance of a cavity, which determines the cavities response to surface heating, is comprised of two components. First the resistance of the bulk material determines how freely heat flows from the inner surface, where it is created, through the metal and to the outer surface. For a homogeneous bulk this resistance linearly depends on thickness. The second component is given by the resistance at the interface between cavity wall and liquid helium bath. In typical cavities at cryogenic temperatures these resistances often are comparable to each other in magnitude and their sum makes up the total thermal resistance.

* cem.saribal@studium.uni-hamburg.de

Here, we present the current development status of our Niobium Thermal Conductance Instrument (NTCI), a thermal conduction instrument for niobium at cryogenic temperatures. Its design is based on a similar device, which was first introduced and utilized by J. Amrit, M.X. François and C.Z. Antoine over two decades ago [1, 2]. In comparison to standard thermal conduction instruments, which most of the time are limited to thermal characteristics of the bulk, this design additionally allows taking interface resistance into account, which makes results better applicable to the real world thermal behaviour of cavities. Therefore, NTCI also allows to study the impact of 10 – 100 nm thin layers, effectively representing only a fraction of the whole volume, on total thermal resistance.

EXPERIMENTAL SETUP

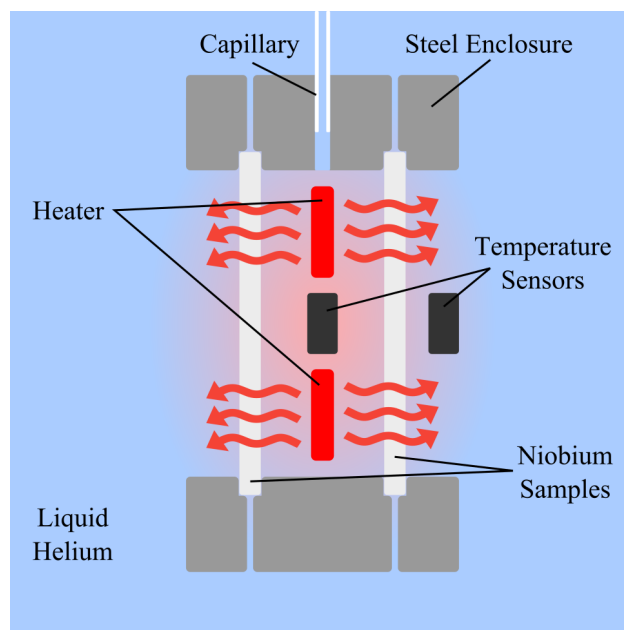


Figure 1: Cross-sectional view of NTCI.

The fundamental working principle of NTCI can be understood by looking at its cross-section shown in Fig. 1. A pair of identically treated disc-shaped niobium samples with a diameter of 45 mm is mounted to a ring-shaped steel enclosure with a wall thickness of 20 mm, creating a 16 mm deep cylindrical cavity with a diameter of 40 mm in-between the samples. Inside of this cavity a heating element, consisting of a 1 m long Manganin wire with 0.1 mm diameter is symmetrically wound in a 3D-printed fixture, resulting in an electrical resistance of about 50 Ω. In its center this fixture houses a Cernox CU-HT temperature sensor (see

NUMERICAL CALCULATIONS OF SUPERHEATING FIELD IN SUPERCONDUCTORS WITH NANOSTRUCTURED SURFACES*

W. P. M. R. Pathirana^{1†}, A. Gurevich^{2‡}

¹Department of Physics and Astronomy, Virginia Military Institute, Lexington, VA, USA,

²Department of Physics and Center for Accelerator Science, Old Dominion University, Norfolk, USA

Abstract

We report calculations of a dc superheating field H_{sh} in superconductors with nanostructured surfaces. Particularly, numerical simulations of the Ginzburg-Landau (GL) equations were performed for a superconductor with an inhomogeneous impurity concentration, a thin superconducting layer on top of another superconductor, and S-I-S multilayers. The superheating field was calculated taking into account the instability of the Meissner state with a nonzero wavelength along the surface, which is essential for realistic values of the GL parameter κ . Simulations were done for the materials parameters of Nb and Nb₃Sn at different values of κ and the mean free paths. We show that the impurity concentration profile at the surface and thicknesses of S-I-S multilayers can be optimized to reach H_{sh} exceeding the bulk superheating fields of both Nb and Nb₃Sn. For example, a S-I-S structure with 90 nm thick Nb₃Sn layer on Nb can boost the superheating field up to ≈ 500 mT, while protecting the SRF cavity from dendritic thermomagnetic avalanches caused by local penetration of vortices.

INTRODUCTION

The superconducting radio-frequency (SRF) resonant cavities are crucial components of particle accelerators enabling high accelerating gradients with minimal power consumption. The best Nb cavities can have high quality factors $Q \sim 10^{10} - 10^{11}$ and sustain accelerating fields up to 50 MV/m at $T = 1.5 - 2$ K and 1.3 - 2 GHz [1, 2]. The peak fields $B_0 \approx 200$ mT at the equatorial surface of Nb cavities approach the thermodynamic critical field $B_c \approx 200$ mT at which the screening rf current density flowing at the inner cavity surface is close to the depairing current density $J_c \approx B_c / \mu_0 \lambda$ - the maximum dc current density a superconductor can carry in the Meissner state [3], where λ is the London penetration depth. Thus, the breakdown fields of the best Nb cavities have nearly reached the dc superheating field $B_{sh} \approx B_c$ [4-7]. The Q factors can be increased by materials treatments such as high temperature annealing followed by low temperature baking which not only increase $Q(B_0)$ and the breakdown field but also reduce deterioration of Q at high fields [8, 9]. High temperature treatments combined with the infusion of nitrogen, titanium or oxygen can

produce an anomalous increase of $Q(B_0)$ with B_0 [10-13]. These advances raise the question about the fundamental limit of the breakdown fields of SRF cavities and the extent to which it can be pushed by surface nano-structuring and impurity management [2, 14].

Several ways of increasing dc superheating field by surface nanostructuring without detrimental reduction of the field onset of dissipative penetration of vortices have been proposed, including high- T_c superconducting multilayers with thin dielectric layers [15-19] or a dirty overlayer with a higher concentration of nonmagnetic impurities at the surface [20]. Dc superheating field of such structures has been evaluated using the London, Ginzburg-Landau and Usadel equations in the limit of $\kappa \rightarrow \infty$ in which the breakdown of the Meissner state at $H = H_{sh}$ occurs uniformly along the planar surface. Yet it has been well established that the breakdown of the Meissner state at $H = H_{sh}$ occurs via a periodic modulation of the order parameter with a wavelength $\sim (\xi^3 \lambda)^{1/4}$ along the surface [5, 6]. The effect of such periodic instability on H_{sh} can be particularly important for Nb cavities with $\kappa \sim 1$. Addressing the effect of κ (which in turn depends on the mean free path l) on H_{sh} in superconductors with a nanostructured surface is the goal of this work.

We present results of numerical calculations of H_{sh} for different superconducting geometries in materials with finite κ , and determine the optimal surface nanostructure that can withstand the maximum magnetic field. In particular we consider a bulk superconductor with a thin impurity diffusion layer, a clean superconducting overlayer separated by an insulating layer from the bulk (e.g., Nb₃Sn-I-Nb₃Sn), a thin dirty superconducting layer on top of the same superconductor (e.g., dirty Nb₃Sn-I-clean Nb₃Sn), and a thin high- T_c superconducting layer on top of a low- T_c superconductor (e.g., Nb₃Sn-I-Nb). We calculate H_{sh} and determine the optimal layer thickness for each geometry by numerically solving the Ginzburg-Landau (GL) equations using COMSOL [21].

GINZBURG-LANDAU THEORY AND NUMERICAL CALCULATION OF H_{sh}

We first consider a semi-infinite uniform superconductor in a magnetic field H_0 applied along the z axis, parallel to the planar surface. In this case the GL equations can be reduced to two coupled partial differential equations for the amplitude $\Delta(x, y, t)$ of the complex order parameter $\psi = \Delta e^{i\theta}$ and the z -component of the magnetic field $H(x, y, t)$. It is convenient

* This work was supported by DOE under Grant DE-SC 100387-020 and by Virginia Military Institute (VMI) under Jackson-Hope Grant for faculty travel and Jackson-Hope Funds for New Directions in Teaching and Research Grants (Quantum Initiative in Undergraduate Education at VMI).

† walivepathiranagemr@vmi.edu

‡ gurevich@odu.edu

A COMPREHENSIVE PICTURE OF HYDRIDE FORMATION AND DISSIPATION*

N. S. Sitaraman[†], T. A. Arias, M. U. Liepe
Department of Physics, Cornell University, Ithaca, NY, USA

A. Harbick[‡], M. Transtrum
Department of Physics and Astronomy, Brigham Young University, Provo, UT, USA

Abstract

Research linking surface hydrides to Q-disease, and the subsequent development of methods to eliminate surface hydrides, is one of the great successes of SRF cavity R&D. We use time-dependent Ginzburg-Landau to extend the theory of hydride dissipation to sub-surface hydrides. Just as surface hydrides cause Q-disease behavior, we show that sub-surface hydrides cause high-field Q-slope (HFQS) behavior. We find that the abrupt onset of HFQS is due to a transition from a vortex-free state to a vortex-penetration state. We show that controlling hydride size and depth through impurity doping can eliminate HFQS.

INTRODUCTION

Hydride formation occurs at cryogenic temperatures in a process analogous to familiar water vapor condensation, where the high-entropy “gas” of interstitial hydrogen minimizes its free energy by organizing into “droplets,” i.e. hydride crystals. These crystals can accurately be described as low-energy ordered configurations of interstitial hydrogen with some accompanying distortion of the niobium lattice [1]. In general, the physics of droplet formation is not trivial because there is a surface energy associated with the droplets which competes with the volume energy associated with the bulk phase transition. The volume energy grows with the cube of hydride radius while the surface energy grows with the square of hydride radius. Thus, for given conditions of hydrogen chemical potential and temperature, there is a “critical” droplet radius above which hydride crystals are stable and below which they are unstable [2]. The fact that sub-critical droplets are unstable means that the hydrogen atoms must form a super-critical droplet purely by statistical chance, so that there is a free energy barrier to hydride precipitation which is potentially much larger than the thermal energy scale. The rate of droplet nucleation depends exponentially on this ratio and so can potentially be many orders of magnitude slower than the hopping rate of impurities.

The free energy barrier to hydride precipitation depends on the size of the critical droplet, which generally varies throughout a macroscopic sample. Of particular interest are the places where the critical droplet size and corresponding free energy barrier are small enough that hydrides can form quickly relative to the typical timescale (minutes) of

cavity cooldown—we will call these places “nucleation sites.” Many material defects can potentially affect critical droplet size, including interstitial impurities, as well as more complex defects, such as impurity-vacancy complexes, dislocations and grain boundaries, that we will not describe in detail here. Impurities are of particular interest because their near-surface concentrations can be altered through low-temperature baking, and because first-principles calculations have previously shown that they create low-energy trap sites for hydrogen, potentially encouraging hydride nucleation [3]

We present a new theory for the important physical effects of low-temperature bakes, how they improve cavity performance, and what can be done to further improve high-field quality factors. We use time-dependent Ginzburg-Landau theory to calculate dissipation from sub-surface nanohydrides, finding excellent agreement with experimentally-observed high-field Q-slope (HFQS) behavior [4] and a clear relationship between hydride size and position and HFQS onset field. We argue that increasing the concentration of hydride nucleation sites by impurity doping effectively decreases the typical size of hydrides, delaying the onset of HFQS and improving cavity performance. Our results lend additional credibility to the idea that low-temperature bakes affect high-field cavity behavior by controlling nanohydride formation.

METHODS

The Time-Dependent Ginzburg-Landau Equations

Ginzburg-Landau (GL) theory is one of the oldest theories of superconductivity, and it remains relevant today owing to its relative simplicity and direct physical insights into the electrodynamic response of superconductors under static applied fields and currents[5]. The *time-dependent* Ginzburg-Landau (TDGL) equations were originally proposed by Schmid[6] in 1966 and Gor’kov and Eliashberg[7] derived them rigorously from BCS theory later in 1968. The TDGL equations (in Gaussian units) are given by:

* This work was supported by the U.S. National Science Foundation under Award PHY-1549132, the Center for Bright Beams.

[†] nss87@cornell.edu, these authors contributed equally

[‡] aidenharbick@gmail.com, these authors contributed equally

CORRELATING LAMBDA SHIFT MEASUREMENTS WITH RF PERFORMANCE IN MID-T HEAT TREATED CAVITIES

R. Ghanbari*, M. Wenskat, R. Monroy-Villa, G. Kacha Deyu, W. Hillert

Institute of Experimental Physics, University of Hamburg, Hamburg, Germany

J. Wolff, C. Bate, L. Steder, D. Reschke, Deutsches Elektronen-Synchrotron DESY, Germany

Abstract

Heat treatment procedures have been identified as crucial for the performance of niobium SRF cavities, which are the key technology of modern accelerators. The so called “mid-T heat treatments”, invert the dependence of losses on the applied accelerating field (anti-Q slope) and significantly reduce the absolute value of losses. The mechanism behind these improvements is still under investigation, and further research is needed to fully understand the principle processes involved. Anomalies in the frequency shift near the transition temperature (T_c), known as “dip” can provide insight into fundamental material properties and allow us to study the relationship of frequency response with surface treatments. Therefore, we have measured the frequency versus temperature of multiple mid-T heat treated cavities with different recipes and studied the correlation of SRF properties with frequency shift features. The maximum quality factor correlates with two such shift features, namely the dip magnitude per temperature width and the total frequency shift.

INTRODUCTION

Superconducting radio-frequency (SRF) cavity research opens doors to fascinating discoveries and technological advancements in modern accelerators field. Understanding the role of impurities in the RF layer, which is approximately the first 200 nm of the cavity surface, is crucial for optimizing the RF performance [1, 2]. Mid-T heat treatment, a surface treatment which is defined as heating for 3-20 hours (h) at 200-400 °C in Ultra High Vacuum (UHV), utilizes the diffusion of oxygen from the native niobium oxide and increases the concentration of oxygen impurities into the RF layer [3–6]. It enhances high quality factor (Q_0) values of up to 4.2×10^{10} at 20 MV/m with showing anti-Q slope, along with an average maximum accelerating field around 24-30 MV/m, where few cavities achieved more than 30 MV/m [7–10]. Previous reports have explored main characteristic of mid-T heat treated cavities, particularly focusing on the Q_0 in relation to the E_{acc} to study the principals responsible for their exceptional performance [1, 2, 11–14]. While much attention has been given to Q_0 and surface resistance (R_s), fewer studies have explored the behavior of frequency shift of cavities as a function of temperature (df vs. T), which holds valuable insights into the surface reactance (X_s) and the behavior of superconducting carriers. Recent theoretical studies have started to model the frequency response of SRF cavities,

and have sparked ongoing studies to identify the underlying processes [15]. Remarkably, dip features show variations based on the surface treatment, and correlations with cavity performance are found [1, 2]. Despite the recent progress achieved, several questions remain, such as how the impurity concentrations [16–19], especially the oxygen profile, relate to the observed changes in RF performance. The potential application of these findings extends across multiple applications, from accelerator technology to dark matter detection and quantum information technology, propelling scientific and technological progress in diverse fields with reducing BCS resistance (R_{BCS}) and residual resistance (R_{res}) [1–10]. Here, we aim to investigate the features of dip phenomenon resulting from the mid-T heat treatment on the surface of SRF cavities and correlate them with RF performance and oxygen diffusion.

EXPERIMENTAL

The most commonly employed method, also used in this study, is the S21 measurement, which measures the transmitted signal at the pick-up through the cavity, after exciting it at the input. From this measurement, the resonance frequency can be easily obtained. To ensure accurate results, it is crucial to maintain a constant ambient pressure within the cryostat during this measurement, thereby preventing any frequency changes due to mechanical deformations. The cavities are initially parked at a specific starting temperature and pressure. A slow, non-adiabatic warm-up process is then initiated. Temperature data for this measurement is acquired from a Cernox[®] sensor attached to the outer surface of the cavity at the equator. Additionally, the temperature at the top and bottom of the cavity, along with the helium pressure, is continuously monitored and recorded during the warm-up process to assess the experimental procedure and ensure data quality. After RF tests, liquid helium is removed and df vs. T are measured during the warm-up process, in temperature range between 4.5 K and 12 K at a controlled rate of 0.5-1.5 K/h, while maintaining a stable pressure of 1111 mBar. During the measurement process, the resonance frequency is monitored using a Vector Network Analyzer (VNA). Adjusting the RF setup for the highest signal-to-noise ratio and a Lorentz distribution is fitted to obtain the resonance frequency. The entire spectrum at each temperature is recorded. Through the use of these techniques and data analysis methods, we can achieve precise and reliable df vs. T curve.

In our study, we have focused on investigating TESLA-shaped 1.3 GHz bulk niobium (Nb) single-cell SRF cavi-

* rezvan.ghanbari@desy.de

RECENT MID-T SINGLE-CELL TREATMENTS R&D AT DESY*

C. Bate[†], D. Reschke, J. Schaffran, L. Steder, L. Trelle, H. Weise
Deutsches Elektronen-Synchrotron DESY, Hamburg, Germany

Abstract

The challenge of improving the performance of SRF cavities is being faced worldwide. One approach is to modify the superconducting surface properties through certain baking procedures. Recently a niobium retort furnace placed directly under an ISO4 clean room has been refurbished at DESY. Thanks to an inter-vacuum chamber and cryopumps, with high purity values in the mass spectrum it is working in the UHV range of 2×10^{-8} mbar. The medium temperature (mid-T) heat treatments around 300 °C are promising and successfully deliver reproducible very high Q_0 values of $2 - 5 \times 10^{10}$ at medium field strengths of 16 MV/m. Since the first DESY and Zanon Research & Innovation Srl (Zanon) mid-T campaign yielded promising results, further results of 1.3 GHz single-cell cavities are presented here after several modified treatments of the mid-T recipe.

In addition, samples were added to each treatment, the RRR value change was examined, and surface analyses were subsequently performed. The main focus of the sample study is the precise role of the changes in the concentration of impurities on the surface. In particular, the change in oxygen content due to diffusion processes is suspected to be the cause of enhancing the performance.

MID-T HEAT TREATMENTS AT DESY

In-situ medium temperature bake experiments conducted at approximately 300 °C [1] demonstrated remarkable high quality-factors. Subsequently, two studies [2, 3] performed mid-T heat treatments using commercially available ultra-high vacuum (UHV) furnaces, followed by sequential cleaning and assembly procedures of the cavities in an air environment. DESY has also investigated this treatment as part of its R&D programs, which was presented in Ref. [4]. This approach shows great potential for future applications in accelerator projects. The performance characteristics of the cavities, as depicted by the quality factor Q_0 versus the accelerating gradient E_{acc} ($Q(E)$), closely resemble those observed for nitrogen-doped cavities [5, 6]. Notably, there is an increase in Q_0 , reaching its peak at an E_{acc} of approximately 16 MV/m, commonly called the "anti-Q-slope." Further investigation is required to determine whether the mid-T heat treatment exhibits comparable limitations on the gradient, similar to specific doping techniques [5, 7], or whether it can provide high gradients surpassing 30 MV/m. A major advantage of the mid-T heat treatment approach compared to other recipes that achieve similar performances is its significantly shorter baking time and absence of the need for

additional gases such as nitrogen in the furnace. In addition, no chemical surface treatment is required afterwards.

NIOBIUM-RETORT FURNACE

In late 2021, the newly refurbished all-niobium furnace at DESY enabled the application of heat treatments. The furnace, located in the ISO 4 area of the cavity assembly clean room, comprises a niobium retort with a separate vacuum enclosure that houses the heaters. It has a usable diameter of 0.3 m and a depth of 1.3 m, allowing for the treatment of a 1.3 GHz nine-cell cavity or one or two single-cell cavities simultaneously, all positioned vertically as depicted in Fig. 1. The heat ramping of the furnace is regulated by temperature sensors located near the heating zone outside of the separate vacuum. Additional temperature sensors installed near the cavity equators on the insert are monitored and utilized for analysis. The furnace can reach a maximum temperature of

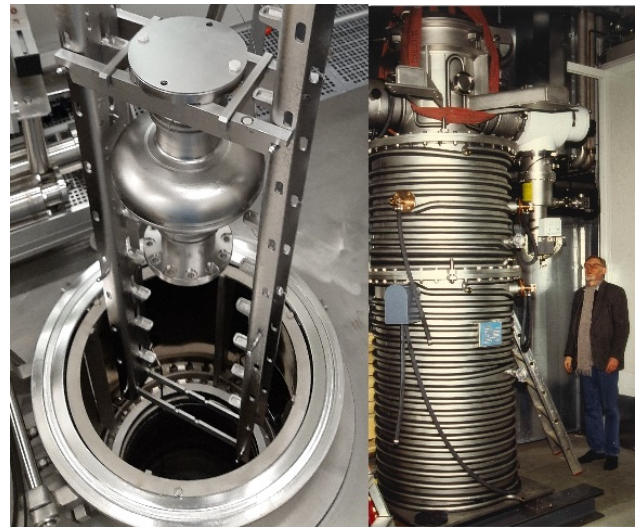


Figure 1: Single-cell Cavity inserted in the niobium-retort furnace (left side). External view of the niobium retort furnace during the initial assembly at DESY (right side).

1200 °C. The complete refurbishment involved the renewal of the entire vacuum, cooling, and control system, as well as the implementation of partial pressure control and a mass spectrometry system. The cryo pumping system is oil-free and maintains a base pressure of 2×10^{-8} mbar at room temperature. During cavity treatment at 800 °C, the pressure steadily increases to approximately $3 - 4 \times 10^{-7}$ mbar. After the furnace qualification, two successful treatments were conducted at 800 °C. While the commissioning of the furnace is complete, ongoing efforts focus on improving control features and establishing reproducible treatment protocols. Additionally, it is planned to conduct a tandem run,

* This work was supported by the Helmholtz Association within the topic Accelerator Research and Development (ARD) of the Matter and Technologies (MT) Program.

[†] christopher.bate@desy.de

MAGNETIC FLUX EXPULSION IN TRIUMF'S MULTI-MODE COAXIAL CAVITIES

R. Gregory^{*1}, T. Junginger¹, P. Kolb, R. Laxdal, M. McMullin¹, Z. Yao
TRIUMF, Vancouver, Canada
¹also at University of Victoria, Victoria, Canada

Abstract

The external magnetic flux sensitivity of SRF cavities is an important characteristic of SRF accelerator design. Previous studies have shown that n-doped elliptical cavities are very sensitive to external fields, resulting in stringent requirements for residual field and cavity cool-down speed. Few such studies have been done on HWRs and QWRs. The impact of applied field direction and cool-down speed of flux expulsion for these cavities is poorly understood. This study explores the effect of these cool-down characteristics on TRIUMF's QWR using COMSOL[®] simulations and experimental results.

This study seeks to maximize the flux expulsion that occurs when a cavity is cooled down through its superconducting temperature. Flux expulsion is affected by the cool-down speed, temperature gradient, and orientation of the cavity relative to an applied magnetic field. It was found that for a vertically applied magnetic field the cool-down speed and temperature gradient did not have a significant effect on flux expulsion. Contrarily, a horizontal magnetic field can be nearly completely expelled by a fast, high temperature gradient cool-down.

INTRODUCTION

The effects of cool-down speeds [1], temperature gradients [2, 3], and applied magnetic field orientations [4] on flux expulsion have been studied for 1.3 GHz elliptical cavities. It was found that for elliptical cavities fast cool-downs and large temperature gradients lead to more flux expulsion. A previous study on the effects of magnetic sensitivity on field orientation for a quarter wave resonator (QWR) cavity was performed by Lounguevergne and Miyazaki [5]. The influence of cool-down speeds and temperature gradients have not been previously evaluated for TEM mode coaxial cavities.

Two possible interpretations of the role of temperature gradient and cool-down speed have been proposed by Romanenko [1]. One is that in a fast cool-down, the superconducting phase front efficiently sweeps out magnetic flux, whereas as slow cool-down leads to normal conducting "islands" in the cavity and it is not energetically favorable for the flux in these islands to be expelled. Another hypothesis is that the superconducting phase front created by fast cool-downs with large temperature gradients is able to de-pin magnetic flux vortices. This paper examines the impact of cavity cool-down speed, temperature gradient, and magnetic

field orientation on flux trapping in a QWR as informed by COMSOL simulations.

METHODOLOGY

The cavity used in this study is the TRIUMF QWR [6]. A unique feature of this cavity is that it lacks beam ports because it is intended for use as a test cavity [7]. This QWR is made entirely of niobium. There are four ports on one end of the QWR which can be seen in Fig. 1. These ports are used for vacuum connections, rinsing, and mounting to the pick up antenna and variable RF coupler. RF is coupled to the electric field. The frequencies of interest for the TEM resonant modes of the QWR are 217 and 648 MHz. The field distribution for these modes is shown in Fig. 2.

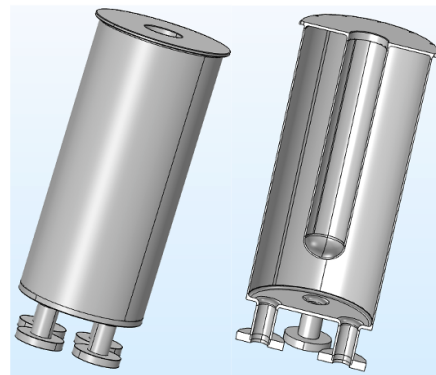


Figure 1: 3-Dimensional computer model of the QWR: Full cavity (left) and cut out (right). This model was generated using COMSOL Multiphysics[®].

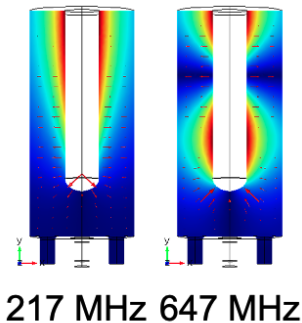


Figure 2: Field distributions for the QWR. Image courtesy of Ref. [6].

In order to perform experiments, the QWR is lowered into a cryostat along with Helmholtz coils, fluxgate probes,

* rgregory@triumf.ca

FLUX EXPULSION STUDIES OF NIOBIUM MATERIAL FOR 650 MHz CAVITIES FOR PIP-II

K. McGee, G. Wu, F. Furuta, M. Martinello, O. Melnychuk, A. Netepenko, Y. Xie
 Fermilab, Batavia, IL, USA

Abstract

Two different vendors supplied the niobium sheet material for prototype and pre-production PIP-II 5-cell 650 MHz cavities, of both low- β ($\beta = 0.61$) and high- β ($\beta = 0.92$) types. The ASTM sizes of this sheet material were found to differ both by lot and by manufacturer. These cavities were then heat-treated at various temperatures, and their flux expulsion performance was measured. Cavities fabricated from Vendor O material initially trapped most magnetic flux despite being cooled through a high thermal gradient, however, 900°C heat treatment subsequently improved the flux expulsion to an acceptable level. In contrast, Vendor A materials expelled flux very well initially, and 900°C annealing imparted no significant improvement. Understanding and characterizing these materials' flux expulsion properties and responses to heat treatment in detail will be critical to upcoming projects employing these two vendors' niobium.

INTRODUCTION

The Proton Improvement Plan-II (PIP-II) linear accelerator under development at Fermilab (FNAL) is a continuous-wave (CW)-compatible machine, which necessitates the usage of superconducting niobium cavities with field-leading quality factors (Q_0) [1]. Advanced RF surface processing techniques such as N-doping [2] and furnace-baking [3] have been explored mostly in the context of 1.3 GHz TESLA-type cavities, delivering very high quality factors. In the case of N-doping, the strength of these results lead to the industrialization of the technique for application in the Linear Coherent Light Source-II (LCLS-II) production cavities [4].

The PIP-II specifications for Q_0 in their 650 MHz cavities ($Q_0 = 2.4 \times 10^{10}$ at 15.9 MV/m for the $\beta = 0.61$ cavities and $Q_0 = 3.3 \times 10^{10}$ at 17.8 MV/m $\beta = 0.92$) have motivated study of the adaptation of these advanced RF surface processing techniques to lower frequency ranges, with promising initial results [5,6]. Unfortunately, while both recipes can produce cavities with very high Q_0 , they also significantly increase a cavity's sensitivity to trapped magnetic flux.

Magnetic flux sensitivity, S , is a measure of the increase in cavity RF surface resistance per unit of trapped flux, measured in n Ω /mG. Even in a low-Gauss environment, cavities can be expected to experience a few mG of background field, and with measured N-doping and furnace baking sensitivities being on the order of 3-4 n Ω /mG, the temperature-independent RF surface resistance arising from flux trapping can easily become the dominant contribution to the cavity's total RF surface resistance, and thus the primary Q_0 -limiting factor.

It is thus desirable to keep flux trapping in these cavities to an absolute minimum. While it is always practical to use active and passive magnetic shielding techniques in vertical test dewars, or passive shielding and good magnetic hygiene practices in cryomodules, to minimize the presence of trappable magnetic flux in the first place, it is still useful to study the means by which whatever residual field escapes these measures can be expelled from the cavities most efficiently during cooldown.

It has been shown that increasing the spatial cooldown gradient can promote flux expulsion [7], however practical experience has shown that this technique is not equally effective across all cavities [8]. Previous studies have shown that the ability of the cavity to expel magnetic flux does not correlate with grain size [9], but could be more strongly related to the dislocation density, increased during the coldworking processes, which can be unique to vendor, or even lot, of niobium [10].

Thus, when approaching a production project such as PIP-II, it is critical to understand in detail the specific flux expulsion properties of the niobium from the vendor with which the project intends to work. Moreover, one must also understand the treatments most likely to produce the best flux-expelling results so that they may be planned for, and implemented in production runs.

NIOBIUM SOURCES

Prototype and pre-production versions of the $\beta = 0.61$ and $\beta = 0.92$ 650 MHz 5-cell elliptical cavities were fabricated from niobium material from two different vendors, whom we shall refer to as "Vendor A" and "Vendor O." Table 1 lists each of these vendors, subdivided by niobium lot, and ASTM measurements.

Table 1: Niobium Material Sources

Niobium version	ASTM size	Hardness (HV10)	Elongation (%)	Specification	Notes
Vendor O v1	~7	≤ 60	≥ 30	XFEL	Used in LCLS-II
Vendor O v2	~6	≤ 60	≥ 30	XFEL	Used in PIP-II LB650 prototype (EZ-001, EZ-002, and 1-cell)
Vendor O v3	~5	≤ 50	≥ 50	PIP-II	Used in PIP-II LB650 Pre-production
Vendor O v4	~4.5	≤ 50	≥ 50	PIP-II	Used in LB650 Pre-production
Vendor A	~5	≤ 50	≥ 50	PIP-II	Used in PIP-II HB650 prototype

CAVITY FLUX EXPULSION SIMULATION

In order to quantify the flux expulsion properties of the cavities the cryomodule and vertical testing contexts, magnetic field strength measurements are taken with fluxgate magnetic probes mounted at the cavity equators before

DEVELOPMENT OF TRANSFORMATIVE CAVITY PROCESSING – SUPERIORITY OF ELECTROPOLISHING ON HIGH GRADIENT PERFORMANCE OVER BUFFERED CHEMICAL POLISHING AT LOW FREQUENCY (322 MHz)*

K. Saito[†], C. Compton, W. Chang, K. Elliott, T. Konomi, S-H. Kim, W. Hartung, E. Metzgar, S. Miller, L. Popielarski, A. Taylor, T. Xu
MSU, FRIB, East Lansing, MI, USA

Abstract

A DOE grant R&D titled “Development of Transformative Preparation Technology to Push up High Q/G Performance of FRIB Spare HWR Cryomodule Cavities” is ongoing at FRIB. This R&D is for 2 years since September 2022, until August 2024. This project focusses to develop the preparation for the high Q&G 0.53 half wave resonators to build high gradient spare cryomodule. This project proposes four objectives: 1) demonstration of superiority on high gradient performance of electropolishing (EP) over buffered chemical polishing on medium beta half-wave cavities at 322 MHz, 2) high Q_0 performance by the local magnetic shield, 3) Development of HFQS-free BCP, and 4) Wet N-doping method. This paper will report the result of first object, and some magnetic shield design for the object 2.

INTRODUCTION

FRIB has switched to user operation from the commissioning phase. In this stage, the reliability of the machine operation is the first priority. This proposal focuses on the FRIB machine maintenance strategy. Some FRIB cavities may have degrade the performance during a long machine operation, and the cryomodule(s) including the degraded cavity(s) would be replaced by spare cryomodule (s). So far, of the six FRIB cryomodule families, three have certified spares that were fabricated as part of the project.

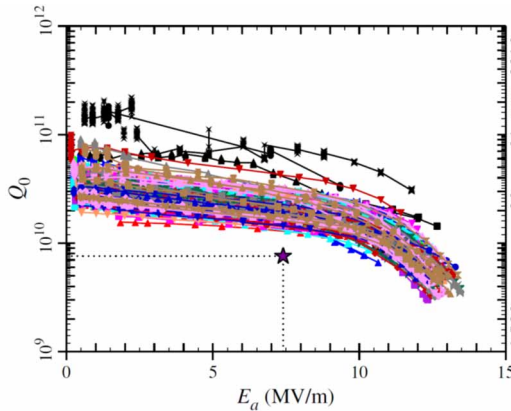


Figure 1: VTA cavity performance with FRIB beta 0.53 half wave resonator (HWRs).

* Work supported by the U.S. Department of Energy Office Science DE-SR114424

[†] email address: saito@frib.msu.edu

line. The spare beta 0.29 and 0.53 cryomodules were not included in the baseline, and are being planned as future scope of FRIB machine maintenance strategy. These spare cryomodules will utilize existing cavities that had been fabricated as part of production contracts. These spare cryomodules or cavities must have an enough performance margin against the degradation, for machine operation.

The goal of this proposal is to produce 0.53 HWRs operateable at acceleration gradients > 10 MV/m, keeping a high $Q_0 > 1 E + 10$ for the restoring or construction of FRIB spare cryomodules. The FRIB production cavities were all treated with BCP, as the result the usable gradient was limited by field emission or high field Q-slope (HFQS) in many cases. At first we will develop transformative processing technique for medium beta cavities, in order to mitigate or eliminate these issues.

PROBLEM STATEMENT/ CURRENT OF THE FIELD

Field limitation of FRIB Cavities

VTA cavity performance of all FRIB beta 0.53 HWRs are shown in Fig. 1 as an example. Note that FRIB cavities were treated by bulk BCP (120 μ m), hydrogen degassing (600 $^{\circ}$ C 10 hr), light BCP (20 μ m), high pressure rinsing (HWR) and cavity clean assembled in a class 100 cleanroom. A detailed FRIB VTA cavity data analysis summarized in Table 1 with the FRIB cavity performance limitation [1]. The dominant limitations are field emission (35% in average over four cavity families), and HFQS (54% in average over four cavity families).

Table 1: Statistics of Field Limitation of FRIB Cavities

Type	QWR-0.041	QWR-0.085	HWR-0.29	HWR-0.53
Total number of certificated cavities	16	106	72	148
1. Quench $< B_p=85$ mT	1 (0.6%)	0 (0%)	13 (18%)	2 (0.1%)
2. Field emission X-ray below $B_p=85$ mT	3 (19%)	41(39%)	21 (29%)	109 (74%)
3. Pure HFQS, including quench $> B_p=85$ mT	9 (56%)	26 (25%)	32 (44%)	21 (14%)
4. Suspicious HFQS X-ray onset $> B_p=85$ mT	3 (19%)	39 (37%)	6 (8%)	16 (11%)
HFQS total (3+4)	12 (75%)	65 (61%)	38 (53%)	37 (25%)

Proposed Solution

Objective 1: EP or EP+LTB Electropolishing provide a smooth surface finishing, which can make it easier to remove particle contamination by HPR. This could mitigated the field emission. As well established in the ILC cavity development, the post EP low temperature bake (LTB) can eliminate the HFQS [2]. So the first solution

SUCCESSFUL SUPERHEATING FIELD FORMULAS FROM AN INTUITIVE MODEL*

K. Saito[†] and T. Konomi, FRIB, East Lansing, MI, USA

Abstract

To date, many theoretical formulas for superheating field on SRF cavity have been proposed based rather complicated calculations. This paper proposes the formulas of superheating field a very intuitive and simple model led from energy balance between RF magnetic energy and superconducting condensed one, and a condition of vanishing the mirror vortex line image. The penetration of a single vortex determines the superheating field for a type II superconductor. On the other hand, for type I superconductors, the surface flux penetration determines it. The formula fits very well quantitatively the results of niobium cavity and Nb3Sn one. In addition, it gives a nice guideline for new material beyond niobium.

SUPERHEATING OF SRF

The RF critical field of superconducting cavity is determined by the superheating field (Bsh), which is higher than the H_c (Type-I) or H_{c1} (Type-II). So far, many models have been proposed for it [1-5]. In this paper, a plane flux penetration for Type-I SRF surface, and a vortex line penetration for Type-II SRF are assumed as the models [6]. By these models, the super-heating field is determined by an energy balance between the flux energy just before entering into SRF surface and the superconducting condensation energy. Combining to Abrikosov's theory, the temperature (T) dependence of superheating field are formalized, which are described by only the measurable characteristic parameters critical field H_c (T), and Landau-Ginsburg parameter κ (T). The forms derived here can estimate the number of vortex flux line per unit area, which gives a very intuitive understanding.

ABRIKOSOV'S EQUATIONS AND THE TEMPERATURE DEPENDENCIES

Abrikosov has derived relational expressions among H_c, H_{c2}, λ, and ξ, here λ is a field penetration depth, and ξ coherent length of a superconductor [5, 7, 8].

$$H_c = \frac{\phi_0}{2\pi\sqrt{2}\lambda\xi}, \quad (1)$$

$$H_{c2} = \frac{\phi_0}{2\pi\xi^2}, \quad (2)$$

from these equations, λ and ξ are expressed by H_c and H_{c2} as follows:

$$\lambda = \sqrt{\frac{\phi_0 H_{c2}}{4\pi H_c^2}}, \quad (3)$$

[†] saito@frib.msu.edu

*Work supported by the U.S. Department of Energy Office Science of under Cooperative Agreement DE-S0000661 and the National Science Foundation under Cooperative Agreement PHY-1102511

$$\xi = \sqrt{\frac{\phi_0}{2\pi H_c^2}}. \quad (4)$$

From the theory and experimental data, the temperature dependence of λ(T) and H_c(T) are given as:

$$\lambda(T) = \frac{\lambda_0}{\sqrt{1 - \left(\frac{T}{T_c}\right)^4}} \quad (5)$$

$$H_c(T) = H_c(0) \left[1 - \left(\frac{T}{T_c}\right)^2\right]. \quad (6)$$

From these expressions, the temperature dependence of H_{c2} (T), ξ (T), and κ (T) can be driven as:

$$H_{c2}(T) = H_{c2}(0) \frac{1 - \left(\frac{T}{T_c}\right)^2}{1 + \left(\frac{T}{T_c}\right)^2}, \quad (7)$$

$$\xi(T) = \xi(0) \sqrt{\frac{1 + \left(\frac{T}{T_c}\right)^2}{1 - \left(\frac{T}{T_c}\right)^2}}, \quad (8)$$

$$\kappa(T) \equiv \frac{\lambda(T)}{\xi(T)} = \frac{\kappa(0)}{1 + \left(\frac{T}{T_c}\right)^2}. \quad (9)$$

Figure 1 shows the temperature dependence H_c with niobium. H_c (0) is 1934.2 Gauss with very high purity Nb (RRR > 2000). Figure 2 shows the temperature dependence of κ with high purity niobium. T² dependence well hits the experimental data. κ (0) is 1.508 for high pure niobium.

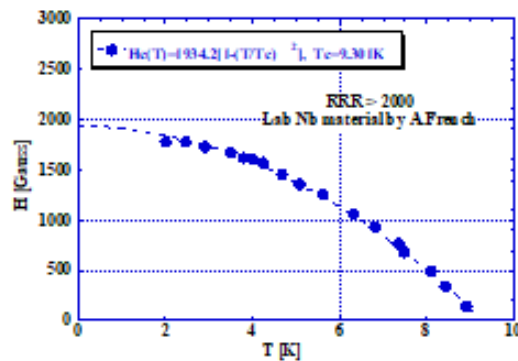


Figure 1: Temperature dependence of H_c with high purity niobium. The experimental data is from [9]. The T² dependence fits the experimental data. H_c (0) is 1900 Gauss.

EXPLORING THE DYNAMICS OF TRANSVERSE INTER-PLANAR COUPLING IN THE SUPERCONDUCTING SECTION OF THE PIP-II LINAC*

Abhishek Pathak[†], Fermi National Accelerator Laboratory, Batavia, IL, USA
Eduard Pozdeyev, Thomas Jefferson National Accelerator Facility, Newport News, VA, USA

Abstract

This study investigates the crucial role that an accurate understanding of inter-planar coupling in the transverse plane plays in regulating charged particle dynamics in a high-intensity linear accelerator and minimizing foil/septum impacts during injection from the linac to a ring. We performed an in-depth analysis for the emergence and evolution of transverse inter-planar coupling through multiple active lattice elements, taking into account space charge and field nonlinearities in the superconducting section of the PIP-II linac. The article compares various analytical, numerical, and experimental techniques for measuring transverse coupling using beam and lattice matrices and provides insight into effective strategies for its mitigation prior to ring injection

INTRODUCTION

The Fermilab PIP-II [1] upgrade aims to support the Deep Underground Neutrino Experiment (DUNE) at LBNF by accelerating a high-intensity H^- CW beam to 800 MeV, with 1.6 MW power output. Ensuring optimal performance involves careful control of emittance blow-up, halo growth, and transmission loss. Among various challenges, transverse inter-planar coupling [2] can cause significant emittance blow-up and beam loss through the creation of ellipticity [3] in the transverse particle density distribution.

This article delves into factors such as space charge non-linearity and off-diagonal terms in the lattice elements that contribute to the transverse inter-planar coupling. It subsequently juxtaposes different measurement techniques for quantifying the extent of inter-planar coupling in the high beta section of the linac beam. Lastly, it advocates for potential techniques to abate the coupling terms from the beam matrix prior to injection into the booster.

SPACE CHARGE AND INTER-PLANAR COUPLING

In the study of non-relativistic charged particle beams' dynamics in high-intensity accelerators, the nonlinear space-charge forces are pivotal as they degrade the beam's quality and introduce inter-planar coupling. Our Particle-in-Cell simulations via the TraceWin code, employing Gaussian, parabolic, water-bag, and KV particle density distributions, were performed to analyze the impact of these forces on

transverse beam coupling. We utilized a drift of 1.5 m, devoid of any external fields, to measure the inter-planar coupling, and introduced a coupling parameter Σ defined as $\sqrt{\sigma_{1,3}^2 + \sigma_{1,4}^2 + \sigma_{2,3}^2 + \sigma_{2,4}^2}$, where $\sigma_{i,j}$ are off-diagonal terms in the beam's sigma matrix.

The study reveals a non-linear rise in the coupling parameter,

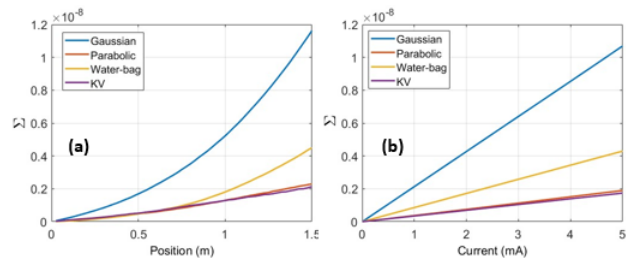


Figure 1: (a) Depiction of the variation in the inter-planar coupling term along a drift, stemming from initial particle density distributions with varying degrees of space charge nonlinearity. (b) Display of the fluctuation in the inter-planar coupling term in relation to beam current, associated with initial particle density distributions subject to various levels of space charge nonlinearity.

Σ , as the beam propagates through the drift space, influenced by the non-linearity in the space-charge field. Moreover, Σ linearly grows with the beam current, independent of space-charge non-linearity, yet the growth rate is influenced by the initial particle distribution. Figures 1(a) and 2(b) illustrate the variation of Σ across a 1.5 m drift space and its relation to the beam current, highlighting the significant role of space-charge effects in high-intensity accelerators. The correlation of Σ with beam radius was explored using an 800 MeV, 5 mA H^- beam. We computed Σ for particles within varying transverse radii from the core to the tail. Figure 2(a) shows y-integrated density along x, while Fig. 2(b) displays Σ variation from the beam's core to the tail. Within a 2 mm radius, Σ remains fairly constant. However, moving outwards, Σ nonlinearly decreases - most steeply for the KV distribution and least for Gaussian. Thus, tail region particles in a non-linear density distribution significantly influence x-y beam coupling.

LATTICE ELEMENTS AND INTRA-PLANAR COUPLING

Utilizing field maps across the PIP-II lattice, we linearized the motion equations of charged particles in RF fields to derive transfer matrices. This included the consideration of

* This manuscript has been authored by Fermi Research Alliance, LLC under Contract No. DE-AC02-07CH11359 with the US Department of Energy, Office of Science, Office of High Energy Physics.

[†] abhishek@fnal.gov

MEDIUM TEMPERATURE FURNACE BAKING OF LOW-BETA 650 MHz FIVE-CELL CAVITIES*

G. Wu[†], S. Posen, V. Chouhan, A. Netepenko, F. Furuta, G. Ereemeev, K. McGee, H. Park,
 S. K. Chandrasekaran, J. Ozelis, A. Murthy, Fermilab, Batavia, USA

Abstract

Medium Temperature baking of low beta 650 MHz cavities was conducted in a UHV furnace. A systematic study of cavity surface resistance components, residual and BCS, was conducted, including analyzing surface resistance due to trapped magnetic flux. Cavities showed an average 4.5 nano-ohm surface resistance at 17 MV/m under 2 K, which meets PIP-II specifications with a 40% margin. The results provided helpful information for the PIP-II project to optimize the cavity processing recipe for cryomodule application. The results were compared to the 1.3 GHz cavity that received a similar furnace baking.

INTRODUCTION

Mid-T baking of superconducting radio-frequency (SRF) cavities is a technique that aims to improve the quality factor (Q_0) of these cavities by dissolving the oxides on the niobium surface. SRF cavities are widely used in particle accelerators and require high Q_0 values to reduce the cryogenic cost and increase the beam energy. Mid-T baking involves heating the cavity at a temperature range of 250–400 °C under an ultra-high vacuum for several hours. It was conducted in situ, where the 1.3 GHz cavity was fitted with testing hardware and was actively evacuated during the baking process resulting in higher Q_0 values and anti-Q-slope behavior [1]. A carefully cleaned and protected cavity can be placed in a UHV furnace without testing hardware. A naturally formed oxide layer provided the source of oxygen to diffuse into the niobium bulk. As the cavity is re-exposed to air after the furnace baking, a new oxide layer is formed. The cavity can then be cleanly prepared for a cold test without the need for chemical processing. The cavity performance was similar to that of the in-situ baked cavities [2]. Similar baking was conducted for 650 MHz cavities [3]. Mid-T baking in a furnace is more convenient and easier than other techniques, such as nitrogen doping [4] or infusion [5], and can also simplify the surface processing of SRF cavities.

The PIP-II linac is a high-power proton accelerator under construction, enabling the world's most intense neutrino beam for the DUNE experiment [6]. It consists of an 833 MeV superconducting linear accelerator. An important linac section includes 23 cryomodules operating at 2 K with continuous wave (CW) mode [7]. Nine cryomodules use the 650 MHz 5-cell cavities with β values of 0.61, known as LB650.

* Work supported by Fermi Research Alliance, LLC, under Contract No. DE-AC02-07CH11359 with the U.S. Department of Energy, Office of Science, Office of High Energy Physics

[†] genfa@fnal.gov

The LB650 cavities will be operated at a comparatively higher E_{acc} of 16.9 MV/m and a high $Q_0 = 2.4 \times 10^{10}$. To achieve such high-performance specifications, high Q processing of N-doping [4], N-infusion [5], and Mid-T baking [1] were evaluated. With the successful electropolishing (EP) optimization [8], the mid-T baked cavity showed promising results during the LB650 preproduction cavity qualification. Two different baking temperatures were studied. The impact of the temperature on the flux trapping was evaluated and could guide further studies of the temperature dependence of cavity Q_0 in a real-world cryomodule.

In addition, some benefits of mid-T baking related to cavity testing will be discussed.

EXPERIMENT

Cavity Processing

Bare cavities were fabricated by a commercial vendor, who used the niobium and NbTi material procured by Fermilab. The cavity's inner surface received 40 μm BCP before the final welding during bare cavity fabrication. There were no following chemistry or heat treatments after the final welding at the vendor's facilities.

Once the cavity arrived at Fermilab, the incoming inspection was conducted, and cavity wall thickness was measured. Cavities received 120 μm bulk EP, followed by UHV furnace treatment to reduce hydrogen concentration in niobium bulk. The heat treatment temperature was either 800 °C or 900 °C for three hours. Cavities then were tuned to achieve 98% field flatness before 40 μm EP, where the final 20 μm was performed at a cold temperature (12 °C). The cavities were high-pressure water rinsed and assembled in a clean room for cold tests.

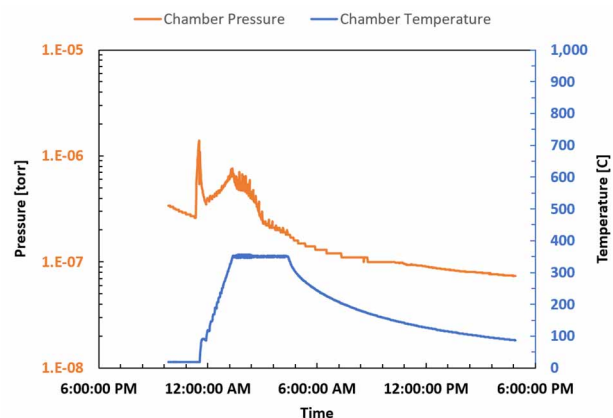


Figure 1: Cavity temperature and furnace pressure during the mid-T baking.

Content from this work may be used under the terms of the CC BY 4.0 licence (© 2023). Any distribution of this work must maintain attribution to the author(s), title of the work, publisher, and DOI

THE COLLABORATIVE EFFECTS OF INTRINSIC AND EXTRINSIC IMPURITIES IN LOW RRR SRF CAVITIES*

K. Howard[†], Y.-K. Kim, University of Chicago, Chicago, IL, USA

D. Bafia, A. Grassellino, Fermi National Accelerator Laboratory, Batavia, IL, USA

Abstract

The SRF community has shown that introducing certain impurities into high-purity niobium can improve quality factors and accelerating gradients. We question why some impurities improve RF performance while others hinder it. The purpose of this study is to characterize the impurity profile of niobium coupons with a low residual resistance ratio (RRR) and correlate these impurities with the RF performance of low RRR cavities so that the mechanism of impurity-based improvements can be better understood and improved upon. The combination of RF testing and material analysis reveals a microscopic picture of why low RRR cavities experience low BCS resistance behavior more prominently than their high RRR counterparts. We performed surface treatments, low temperature baking and nitrogen-doping, on low RRR cavities to evaluate how the intentional addition of oxygen and nitrogen to the RF layer further improves performance through changes in the mean free path and impurity profile. The results of this study have the potential to unlock a new understanding on SRF materials and enable the next generation of high Q /high gradient surface treatments.

INTRODUCTION

As we approach the theoretical limit of niobium for superconducting radio-frequency (SRF) cavities, the last decade has brought immense improvements in quality factor (Q_0) and accelerating gradients though intentionally added impurities into the niobium surface [1, 2]. Many SRF studies follow a “clean bulk dirty surface” technique to optimize the BCS resistance (R_{BCS}) by adding extrinsic impurities to the surface layer of high purity niobium [3–5]. Advancements have been made with nitrogen through N-doping, where cavities experience an anti- Q_0 slope and record breaking Q_0 's at mid fields [6–8]. Oxygen added through a low temperature bake (LTB) has also provided high Q_0 's and mitigation of the high field Q_0 slope typically seen in electropolished (EP) niobium cavities [9, 10]. The performance of these surface treatments is shown in Fig. 1.

The success of intentionally added impurities to the niobium surface has drawn deeper questions about how these impurities affect cavity behavior, and has prompted an investigation of cavities with a low residual resistance ratio (RRR). Low purity niobium has been studied in the past for the purpose of cost reduction and possible high Q_0 [11].

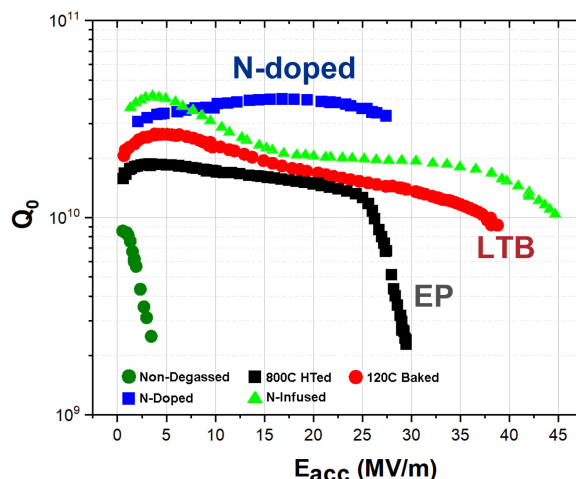


Figure 1: Comparison of quality factor versus gradient for surface treatments, adapted from Ref. [6].

In this study, we look to use the intrinsic impurities as a resource to optimize the R_{BCS} and understand the mechanism of impurity-based improvements. RRR and mean free path (mfp) have a direct relationship, so we might expect experience low R_{BCS} behavior at low RRR, as seen in Fig. 2. We ask if the intrinsic impurities can improve performance, as we observe in extrinsic impurities.

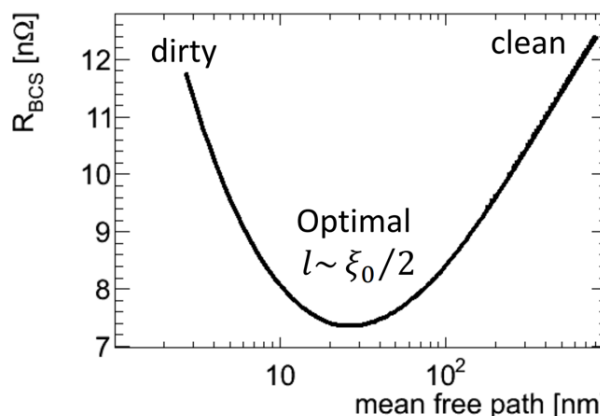


Figure 2: BCS resistance versus mean free path shows an optimization in BCS resistance for moderately dirty surface, adapted from Ref. [12].

In this study, we investigate a single-cell TESLA-shaped 1.3 GHz cavity with RRR 61. First, the cavity receives EP treatment to make the surface layer and bulk uniform [13]. We measure Q_0 versus gradient at 2 K and low temperature (< 1.5 K) in the vertical test stand [2]. The surface resis-

* This manuscript has been authored by Fermi Research Alliance, LLC under Contract No. DE-AC02-07CH11359 with the U.S. Department of Energy, Office of Science, Office of High Energy Physics. This work was supported by the University of Chicago.

[†] khoward99@uchicago.edu

EFFORTS TO SUPPRESS FIELD EMISSION IN SRF CAVITIES AT KEK

Mathieu Omet[†], Hayato Araki, Takeshi Dohmae, Hayato Ito, Ryo Katayama,
Kensei Umemori, Yasuchika Yamamoto
High Energy Accelerator Research Organization, Tsukuba, Japan

Abstract

Our main objective is to achieve as high as possible quality factors Q_0 and maximal accelerating voltages E_{acc} within superconducting radio frequency (SRF) cavities. Beside an adequate surface treatment, key to achieve good performance is a proper assembly in the clean room prior cavity testing or operation. In this contribution we present the methods and results of our efforts to get a better understanding of our clean room environment and the particulate generation caused during the assembly work. Furthermore, we present the measures taken to suppress filed emission, followed by an analysis of vertical test results of the last six years.

INTRODUCTION

Superconducting radio frequency (SRF) cavities [1] are state-of-the-art technological components utilized in accelerators worldwide. The primary parameters that determine their performance are the unloaded quality factor Q_0 and the acceleration gradient E_{acc} . Field emission (FE) [2] can have detrimental effects on both parameters. Particulate contaminations can act as potent field emitters. Therefore, it is imperative to prevent the deposition of particulates on the inner surface of the cavity. Particulate contaminations can originate from two sources: the environment, such as particulates present in the clean room, and the generation during the assembly process. Understanding the cleanliness of the environment is crucial to identify areas for improvement. Similarly, comprehending the mechanisms of particulate generation and their movement during the assembly process is essential. In this proceeding, we discuss the efforts undertaken to address these issues. We also provide information on additional measures employed to suppress FE, as well as statistics on FE over the last six years.

CAVITY PREPARATION AND TEST CYCLE

Upon the production or receipt of a new cavity, the initial action involves conducting an optical examination of the inner surface using the Kyoto camera [3]. Subsequently, bulk electro polishing (EP), known as EP1, is applied, where a 100 μm layer is removed from the cavity's surface [4]. Afterwards, a high-pressure rinsing (HPR) with ultra-pure water is carried out. This is succeeded by annealing, e.g. at a temperature of 900 $^{\circ}\text{C}$ for a duration of 3 hours.

The typical cycle for cavity preparation and testing proceeds as follows: The cavity undergoes optical inspection using the Kyoto camera. If any defects are detected, localized grinding is performed. The cavity is

then transferred to the tuning machine, where frequency, field flatness, and straightness are measured and, if necessary, adjusted. In the subsequent step, EP2 and HPR processes are employed. After the HPR, the cavity is directly transferred to the clean room for assembly. Subsequently, the cavity is connected to a pumping station and leak checked. If the cavity passes this test, it is baked, e.g. at a temperature of 120 $^{\circ}\text{C}$ for 48 hours [5]. Finally, the cavity is moved to the vertical test (VT) stand, where it is tested at temperatures of 4 K and 2 K.

CLEAN ROOM SURVEY

To assess the level of cleanliness within a clean room, commonly a particle counter is set up at various positions and heights. Particle counts are then recorded over specific time intervals. However, in the studies detailed below, a novel approach was adopted by utilizing two different light sources (spot light and ViEST D Light Type F, provided by Shin Nippon Air Technologies (SNK) [6]), enabling the inspection of surfaces. In preparation for the subsequent studies, the ambient lights within the clean room were turned off. Due to the presence of large windows in most of the clean room walls, a certain amount of ambient light persisted.

In the direct comparison of the spot light and the D Light the latter one proved to be more versatile. With its light spectrum primarily centered around violet, extending into the ultraviolet range, it enables the observation of contaminants and stains containing fluorescent components.

Using the D Light we investigated a total of 564 different surfaces within the following areas were investigated: changing room at the Center of Innovation (COI), COI class 1000 clean room, COI class 10 clean room, the changing room at the Superconducting RF Test Facility (STF), STF class 1000 clean room, and STF class 10 clean room.

In the changing rooms at both facilities, a substantial amount of dust and stains were discovered. Additionally, the walls of the air locks equipped with air showers exhibited dust accumulation. Furthermore, dust particles were visible on the majority of surfaces in both clean rooms, with notable areas of concern being tools and tool trays. Beside this, dust particulates were present on surfaces where items were stored on shelves, as well as on devices such as pumping stations and ultrasonic baths.

Based on the findings of this study, it was concluded that cleaning of certain surfaces was necessary. Following the cleaning procedures involving alcohol wiping and dry blowing, windows within the STF class 1000 clean room exhibited no visible dust particles.

[†] mathieu.omet@kek.jp

MAGNETIC FIELD MAPPING OF A LARGE-GRAIN 1.3 GHz SINGLE-CELL CAVITY*

I. P. Parajuli[†], G. Ciovati¹, J. Delayen, A. Gurevich, Old Dominion University, Norfolk, VA, USA
¹also at Jefferson Lab, Newport News, VA, USA

Abstract

A new magnetic field mapping system for 1.3 GHz single-cell cavities was developed in order to reveal the impact of ambient magnetic field and temperature gradients during cool-down on the flux trapping phenomenon. Measurements were done at 2 K for different cool-down conditions of a large-grain cavity before and after 120 °C bake. The fraction of applied magnetic field trapped in the cavity walls was ~ 50% after slow cool-down and ~ 20% after fast cool-down. The results showed a weak correlation between trapped flux locations and hot-spots causing the high-field Q-slope. The results also showed an increase of the trapped flux at the quench location, after quenching, and a local redistribution of trapped flux with increasing RF field.

INTRODUCTION

Pinning of magnetic vortices in superconducting radio-frequency (SRF) cavities upon cooling below the critical temperature is a well-known cause of residual RF losses [1]. The quest towards ever increasing quality factor, Q_0 , of bulk Nb cavities at 2 K requires achieving residual resistance values of the order of 1 n Ω .

As a result, understanding the flux trapping mechanisms in Nb cavities has become a growing research topic in recent years [2–18]. The ability to measure the magnitude and distribution of trapped vortices in an SRF cavity is particularly challenging due to the size and shape of a typical cavity. We have developed a magnetic field scanning system (MFSS) which allows mapping of the local magnetic field at the surface of 1.3 GHz single-cell cavities in liquid He (LHe) [19]. Initial results were reported in Ref. [20]. In this contribution we report the results of a systematic study of trapped flux in a 1.3 GHz single-cell cavity before and after baking at 120 °C for 48 h. The location of hot-spots on the cavity outer surface caused by excessive RF heating of the inner surface during the high-power RF test at 2 K was also determined by a temperature mapping system.

EXPERIMENTAL RESULTS

Experimental Setup and Test Procedure

The 1.3 GHz single-cell cavity used for this study, labeled PJ1-1, was fabricated from high-purity, large-grain Nb from OTIC, China, and it had the same shape as that of the TESLA/XFEL cavity [21].

* This work was supported by the National Science Foundation under Grant No. PHY 100614-010. G. C. is supported by Jefferson Science Associates, LLC under U.S. DOE Contract No. DE-AC05-06OR21377.
[†] ipara001@odu.edu

The MFSS has two arms, 180° apart, matching the contour of the cavity. One arm has 8 cryogenic Hall probes, measuring the magnetic field component perpendicular to the cavity surface, B_r , whereas the other arm has 8 pairs of anisotropic magnetoresistance (AMR) sensors. The first AMR sensor in a pair measures the B_r -component while the second sensor measures the magnetic field component tangential to the cavity surface, B_t , within ~ 3 mm of the first one. Details of the characteristics of the two type of sensors can be found in Ref. [22]. The sensors are pushed in contact with the cavity outer surface by soft springs. The two arms with the magnetic field sensors are mounted on a large gear, driven by a stepper motor on the top plate of the cryogenic vertical test stand, allowing a full rotation of the arms around the cavity. Further details about the MFSS and the data acquisition system can be found in Ref. [19].

A static temperature mapping system consisting of 576 thermometers based on 100 Ω carbon resistors was also used to measure the local temperature of the outer surface of the cavity, during the high-power RF test in LHe [23]. The test procedure with the thermometry system assembled onto the cavity consists of:

- cooldown below 9.2 K in a fixed axial dc magnetic field, B_a , while applying a temperature gradient along the cavity axis.
- Fill the cryostat with LHe at 4.3 K and measure $Q_0(T)$ at low RF field as well as the resistance of each thermometer during LHe pump-down to 1.6 K.
- Measure Q_0 as a function of the peak surface RF magnetic field, B_p , at 2 K up to the cavity limit and back to $B_p \sim 10$ mT, acquiring temperature maps.

After a sequence of tests with the T-mapping system, the cavity was disassembled, high-pressure rinsed (HPRed) with ultra-pure water, re-assembled, evacuated, leak checked and hang on the test stand under static vacuum. The MFSS is assembled onto the cavity and the entire setup is inserted into a vertical cryostat. The typical test procedure of the cavity with the MFSS can be summarized as follows:

- reset of the AMR sensors' magnetization by applying a current pulse at room temperature, in low ambient field, $B_a \sim 0.5$ μ T.
- Cooldown to ~ 10 K and measure the offset voltages of the magnetic field sensors.
- Set B_a and the cooldown rate as the cavity is cooled below T_c .
- Fill the cryostat with LHe at 4.3 K, reduce B_a to ~ 0.1 μ T and measure $Q_0(T)$ at low RF field during LHe pump-down to 1.6 K.

EXPLORATION OF PARAMETERS THAT AFFECT HIGH FIELD Q-SLOPE*

K. Howard[†], Y.-K. Kim, University of Chicago, Chicago, IL, USA

D. Bafia, A. Grassellino, Fermi National Accelerator Laboratory, Batavia, IL, USA

Abstract

The onset of high field Q-slope (HFQS) around 25 MV/m prevents cavities in electropolished (EP) condition from reaching high quality factors at high gradients due to the precipitation of niobium hydrides during cooldown. These hydrides are non-superconducting at 2 K, and contribute to losses such as Q disease and HFQS. We are interested in exploring the parameters that affect the behavior of HFQS. We study a high RRR cavity that received an 800 °C by 3 hour bake and EP treatment to observe HFQS. First, we explore the effect of trapped magnetic flux. The cavity is tested after cooling slowly through T_c while applying various levels of ambient field. We observe the onset of the HFQS and correlate this behavior with the amount of trapped flux. Next, we investigate the effect of the size/concentration of hydrides. The cavity is tested after holding the temperature at 100 K for 14 hours during the cooldown to promote the growth of hydrides. We can correlate the behavior of the HFQS with the increased hydride concentration. Our results will help further the understanding of the mechanism of HFQS.

INTRODUCTION

The high field Q-slope (HFQS) observed in electropolished (EP) cavities has a typical onset around 25 MV/m. This effect is from the precipitation of niobium hydrides during cooldown and prevents EP cavities from reaching high Q_0 's at high gradients [1, 2]. Hydrogen is an unavoidable impurity, even in high RRR niobium. Niobium hydrides are non-superconducting at 2 K, and contribute to losses such as "Q disease" and HFQS. A 800 °C bake mitigates the Q disease, and LTB mitigates the growth of hydrides, preventing the HFQS.

In this study, we investigate a high RRR single-cell TESLA-shaped 1.3 GHz cavity. The cavity receives a 800 °C by 3 hour bake to isolate the HFQS without Q disease. Then, the cavity receives EP treatment to make the surface layer and bulk uniform [3]. Before testing, we hold the cavity at 100 K to promote the growth of hydrides. Then we perform a fast cooldown. During RF testing, we observe the behavior of the HFQS. Because the morphology of hydrides grown at these temperatures is understood [2], we can correlate the behavior of the HFQS to the hydride size/concentration.

During cavity testing, a fast cooldown is typically performed to prevent trapped magnetic flux, which is known to

harm performance by increasing the residual resistance [4–9]. By not following the fast cooldown procedure, flux may be trapped through the incomplete Meissner effect, where there are normal conducting vortices within the superconducting lattice [10]. The oscillation of such normal conducting vortices in niobium during RF operation introduces significant dissipation, limiting the Q_0 [11, 12]. The sensitivity to trapped flux of surface treatments such as LTB and N-doping has been studied [6, 7, 9], but its effect, if any, on hydrides is not well understood. The cavity will be tested after cooling slowly through the superconducting transition while applying various levels of ambient field. Then, we observe the onset and slope of the HFQS and correlate this behavior with the amount of flux trapped.

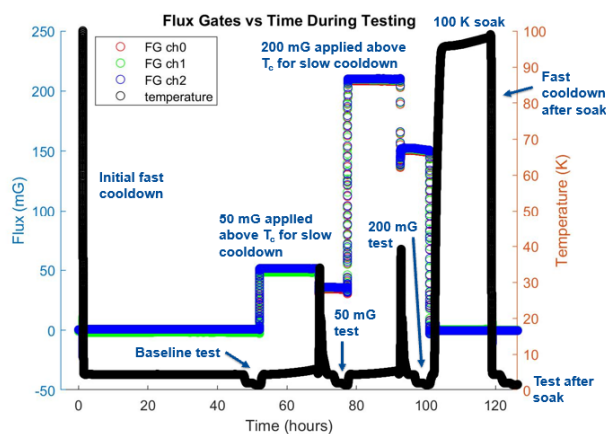


Figure 1: Measurements from flux gates and temperature sensors during testing.

The test procedure is shown in Fig. 1. In real time, the flux testing occurred before the hydride testing so that we could complete the testing in one session. We started with a fast cooldown followed by the baseline test. We measure Q_0 versus gradient at 2 K and low temperature (< 1.5 K) in the vertical test stand [13]. We measure the Q_0 at a given gradient by maintaining the cavity at its resonant frequency, inputting power via antenna, and then measuring the reflected and transmitted power [14]. The Q_0 is the ratio of the energy gain per RF period and dissipated power. The surface resistance is the geometry factor of the cavity divided by the Q_0 ; this can be broken down into the residual resistance (R_{res}) and R_{BCS} . The residual resistance (R_{res}) taken at low temperature is temperature-independent, and comes from impurities in the superconducting lattice as well as any trapped flux from cooldown or quench. The R_{BCS} is calculated by taking the difference between the total surface resistance at 2 K and low T. This temperature-dependent

* This manuscript has been authored by Fermi Research Alliance, LLC under Contract No. DE-AC02-07CH11359 with the U.S. Department of Energy, Office of Science, Office of High Energy Physics. This work was supported by the University of Chicago.

[†] khoward99@uchicago.edu

TEMPERATURE MAPPING FOR COAXIAL CAVITIES AT TRIUMF

P. Kolb*, B. Matheson, J. Keir, R.E. Laxdal, Z. Yao, TRIUMF, Vancouver, BC, Canada
 H. Al Hassini, T. Junginger, University of Victoria, Victoria, BC, Canada,
 L. Fearn, University of Waterloo, Waterloo, ON, Canada

Abstract

Temperature mapping (T-map) on superconducting radio-frequency (SRF) cavities has been shown as a useful tool to identify defects and other abnormal sources of losses. So far T-map systems have only been realized for elliptical cavities that have an easily accessible outer surfaces. TEM mode cavities such as quarterwave and halfwave resonators (QWR, HWR) dissipate most of their power on the inner conductor of the coaxial structure. The limited access and constrained space are a challenge for the design of a temperature mapping system. This paper describes the mechanical and electrical design including the data acquisition of a T-map system for the TRIUMF multi-mode coaxial cavities, and prototyping of the system will be shown.

INTRODUCTION

Temperature mapping has been a reliable tool to detect defects in SRF cavities since the late 90s [1]. Defects or other sources of abnormal power dissipation have a strong negative effect on the unloaded quality factor:

$$Q_0 = \frac{\omega U}{P} \quad (1)$$

with ω as resonant frequency, U as stored energy in the RF fields and P as dissipated power in the cavity walls. A decrease in Q_0 results in a higher power requirement for the cryoplant.

Temperature-mapping systems have been developed in the past for elliptical cavities operating in a TM010 mode. Elliptical cavities are a widely used cavity and dissipate their heat in easily accessible areas of the cavity body. Coaxial cavities such as QWRs and HWRs on the other hand have the majority of their magnetic field distributed on the inner conductor of the coaxial structure as can be seen in Fig. 1. This poses a challenge for the T-map system as space and access is limited to the relevant surface of the cavity. The T-Map system described here is designed to fit into the TRIUMF Coaxial Multi-mode cavities [2]. In the discussed design, eight boards are used with each board hosting 19 sensors in a vertical array down the inner conductor shown in Fig. 2. The goal for the Data Acquisition (DAQ) is a sampling frequency for all 152 sensors of 1 Hz or lower.

MECHANICAL DESIGN

The QWR and HWR share a large number of dimensions. This includes the inner diameter of the inner conductor. This allows the design of a common Tmap system used for both cavities. An early design choice was to make one T-map

* kolb@triumf.ca

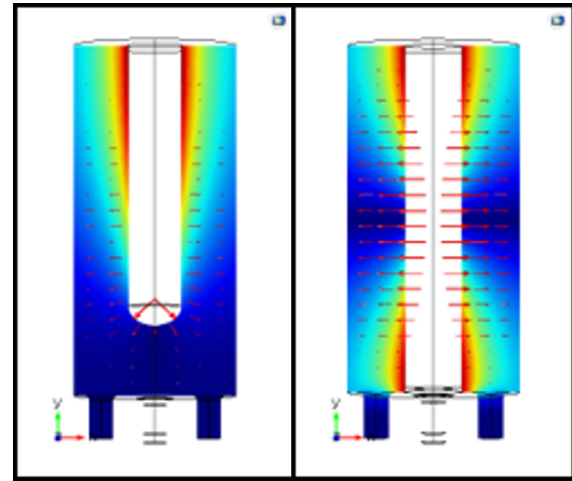


Figure 1: Field Distribution of QWR and HWR.

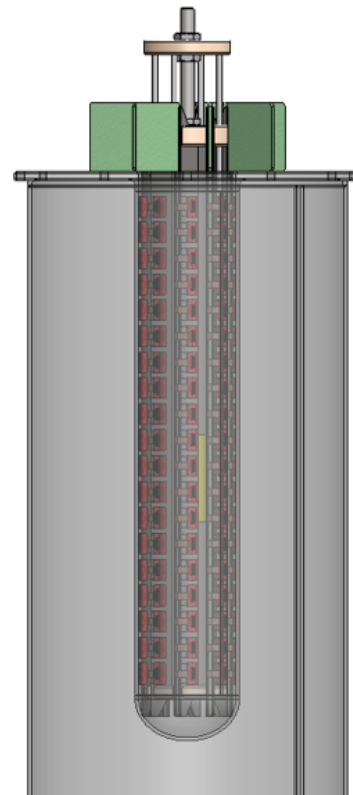


Figure 2: Conceptual setup of the coaxial Tmap system: 8 boards with each 19 sensors are arranged in a 45deg pattern to cover the inner conductor surface of the QWR. An actuation mechanism expands the system and presses the sensors against the cavity wall.

COMPARING THE EFFECTIVENESS OF LOW TEMPERATURE BAKE IN EP AND BCP CAVITIES*

H. Hu[†], Y.-K. Kim, University of Chicago, Chicago, IL, USA
D. Bafia, Fermi National Accelerator Laboratory, Batavia, IL, USA

Abstract

Electropolishing (EP) and buffered chemical polishing (BCP) are conventional surface preparation techniques for superconducting radiofrequency (SRF) cavities. Both EP and BCP treated SRF cavities display high field Q-slope (HFQS) which degrades performance at high gradients. While high gradient performance in EP cavities can be improved by introducing oxygen via a low temperature bake (LTB) of 120°C by 48 hours, LTB does not consistently remove HFQS in BCP cavities. There is no consensus as to why LTB is not effective on BCP prepared cavities. We examine quench in EP, BCP, EP+LTB, and BCP+LTB treated 1.3 GHz single-cell Nb cavities by studying the heating behavior with field using a temperature mapping system. Cavity performance is correlated to characterizations of surface impurity profile obtained via time of flight secondary ion mass spectrometry studies. We observe a difference in near surface hydrogen concentration following BCP compared to EP that may suggest that the causes of quench in EP and BCP cavities are different.

INTRODUCTION

Superconducting radiofrequency (SRF) cavities are resonators with extremely low resistivity that enable high performance accelerators. For the realization of the next generation SRF accelerator, we need to push the limits of achievable quality factor (Q_0) and quench field. Recent work has demonstrated the importance of the profile of impurities in the first 100 nm of the surface in achieving high Q_0 and high accelerating gradients (E_{acc}). Introducing a uniform concentration of nitrogen via nitrogen doping has yielded high Q_0 of $> 4 \times 10^{10}$ [1]. Introducing oxygen via *in-situ* baking has been shown to achieve similar effects as nitrogen in the high Q_0 regime [2, 3]. However, the path to reliably reaching high E_{acc} is less clear. Nitrogen infusion, which introduces a sharp inhomogeneous surface disorder, has repeatedly displayed E_{acc} of 45 MV/m, but other cavity treatments have not had much success with consistently reaching such high quench fields [4–7]. The 75/120°C modified LTB has achieved record high quench fields of 50 MV/m, but this treatment has displayed a bifurcation in performance that is not fully understood [7].

There are two main types of limiting factors to achieving high quench fields. First, the thermal breakdown of

superconductivity may occur when inclusions or defects in the cavity drive significant heating and raise the local temperature above the transition temperature. An example of this is the precipitation of dissolved hydrogen within the niobium surface as non-superconducting niobium hydrides [8]. These hydrides cause the proximity breakdown of superconductivity, leading to the phenomena of high field Q-slope (HFQS) [8, 9]. Secondly, quenches of magnetic origin occur when the intrinsic superheating field of Nb is reached [10]. Surface defects and impurities may drive local magnetic field enhancement above the superheating field and cause premature breakdown of superconductivity [10, 11]. Increased surface roughness and the precipitation of impurities at grain boundaries have also been shown to lower quench fields through local field enhancements [4, 11, 12].

In this work, we will be exploring these limiting factors by studying the two conventional surface preparation techniques: electropolishing (EP) and buffered chemical polishing (BCP). In the late 1990s, EP replaced BCP for its superiority at reaching high gradients > 30 MV/m [12–14]. More recent studies have proven that introducing oxygen via low temperature baking (LTB) reliably cures HFQS by suppressing the precipitation of hydrides in EP cavities [15, 16]. However, LTB is not effective at curing HFQS for BCP treated cavities [12, 13]. We study the role of impurities and surface roughness in the performance of EP, BCP, EP+LTB and BCP+LTB treated SRF cavities to better understand the origins of and limiting factors to quench for these treatments.

EXPERIMENTAL METHOD

Two single-cell TESLA shaped Nb cavities with resonant frequency of 1.3 GHz were first degassed at 800°C for 3 hours. The first cavity received 40 μm EP removal while the second cavity received 40 μm BCP removal with the parameters described in Ref. [17]. Both cavities were then low temperature baked at 120°C for 48 hours. The BCP cavity underwent an additional 200°C × 1 hour *in-situ* bake to further diffuse oxygen into the surface. After the initial EP and BCP, the cavities were fully assembled and never reopened to maintain vacuum in between and during treatments.

Following each treatment set, the two cavities were tested at the Fermilab vertical test stand (VTS) to find Q_0 vs. E_{acc} at both 2 K and low T (< 1.5 K) in continuous wave (CW) operation for the decomposition of surface resistance into BCS and residual resistances [18]. Cooling followed the fast cool down protocol to minimize the possibility of trapping magnetic flux [2]. We also investigated how the cavity heated with increasing fields with temperature mapping (TMAP) [7]. 576 carbon resistance temperature detectors (RTDs) were

* Work supported by the Fermi National Accelerator Laboratory, managed and operated by Fermi Research Alliance, LLC under Contract No. DE-AC02-07CH11359 with the U.S. Department of Energy; the University of Chicago

[†] hannahhu@uchicago.edu

MICROSTRUCTURE DEVELOPMENT IN A COLD WORKED SRF NIOBIUM SHEET AFTER HEAT TREATMENTS*

S. Balachandran^{1,†}, P. Dhakal¹, S. Chetri², P. J. Lee², Z. Thune³,
T. R. Bieler³, A. M. Valente-Feliciano¹

¹Thomas Jefferson National Accelerator Facility, Newport News, VA, USA

²National High Magnetic Field Laboratory, ASC, FSU, Tallahassee, FL, USA

³Department of Chemical Engineering and Material Science, MSU, East Lansing, MI, USA

Abstract

Bulk Nb for TESLA shaped SRF cavities is a mature technology, with high gradient (>35 MV/m) and high Q_0 cavities (10^9 - 10^{10} , $T=2$ K) routinely fabricated. Significant advances are necessary to push Q_0 's to 10^{10-11} ($T=2$ K), and involve modifications to the sub-surface Nb layers by impurity doping. In order to achieve the lowest surface resistance any trapped flux needs to be expelled for cavities to reach high Q_0 's. There is clear evidence that cavities fabricated from polycrystalline sheets meeting current specifications require higher temperatures beyond 800°C for better flux expulsion. Recently, cavities fabricated with a non-traditional Nb sheet with initial cold work due to cold rolling expelled flux better after $800^\circ\text{C}/3$ h heat treatment than cavities fabricated using fine-grain polycrystalline Nb sheets. Here, we analyze the microstructural development of Nb from the vendor supplied cold work non-annealed sheet that was fabricated into an SRF cavity as a function of heat treatment building upon the methodology development to analyze microstructure being developed by the FSU-MSU-UT, Austin-JLAB collaboration. The results indicate correlation between full recrystallization and better flux expulsion.

INTRODUCTION

Superconducting radio frequency (SRF) Nb cavities have been the workhorse for delivering high-quality, high energy beams for high-energy physics, nuclear physics, and microscopy applications [1]. The main driver for current Nb cavity technology is to decrease the footprint by pushing towards the maximum possible gradients and high efficiency defined by high quality factor ($Q_0 > 10^{10}$, $T=2$ K) [2]. Interstitial additions through surface diffusion of N [3,4], O [5-7] have shown that carefully tuning the surface layers leads to high Q_0 's, presently in the gradient range of 10-20 MV/m. The pursuit of high Q_0 has led to uncovering the influence of trapped flux on the surface resistance which scales linearly in the range of 1-2 n Ω /mG [8,9] in Nb cavities thus limiting the highest Q_0 attainable. It is widely accepted that the trapped flux, and flux expulsion is a bulk phenomena and dominated by bulk Nb microstructure [10, 11], whereas surface modifications increase the propensity to trap flux [12, 13]. Work

around to improve flux expulsion have typically involved increase in final heat treatment temperatures in the range of 900 - 1000°C [14] and faster cool-down by using a higher temperature differential through the superconducting transition of Nb ($T_c=9.2$ K) [15].

Improved flux expulsion with increase in heat treatment temperature has led us to the following driving questions: Would an improved recrystallized microstructure lead to better flux expulsion? Can we promote full recrystallization by adopting a newer fabrication strategy of starting with a cold-worked sheet and fabricating a cavity and then performing an $800^\circ\text{C}/3$ h heat treatment? Our preliminary results indicate that a sheet with initial cold work can be fabricated into an SRF Nb cavity, and heat treatment at $800^\circ\text{C}/3$ h shows a much improved flux expulsion performance than a traditionally fabricated SRF Nb cavity as shown in Fig. 1 [16] [and this conference]. In a traditionally fabricated Nb cavity with fine grain size sheet or large grain Nb, surface damage, strain path and location in SRF Nb cavities have an influence on recrystallization and temperatures as high as 1000°C may not be sufficient to remove all defects contributing to flux trapping [17, 18]. Hence, changes in processing path applied to SRF Nb sheets fabricated into cavities need to be evaluated in terms of microstructure development with respect to heat treatments.

In the following paper we track the microstructure development in the cold work/non-annealed (NA) sheet as supplied from Vendor A, that was used to make the cavity that expels flux better than a standard cavity even after $800^\circ\text{C}/3$ h. To track the recrystallization behavior we use cross-sectional micro-texture data collected from heat treated SRF Nb sheet at $700^\circ\text{C}/3$ h - $900^\circ\text{C}/3$ h and extend the approach of determining recrystallization through the analysis of geometrically necessary dislocations (GND) that is being currently developed for Nb [19, 20]. Our results indicate high levels of recrystallization at $800^\circ\text{C}/3$ h in the sheet that was used in the fabrication of the better flux expelling SRF Nb cavity.

MATERIALS AND METHODS

The starting material is the as-received sheet from an SRF Nb supplier, Vendor A, with unknown percent cold work and no heat treatments. Since the sheet was requested in an off-specification condition (without a final anneal), the residual resistivity ratio (RRR), hardness and mechanical strength is not certified. However, the initial composition

* Work supported by U.S. DOE, Office of Science, Office of HEP under Award No. DE-SC0009960. NMF- NSF Cooperative Agreement No. NSF DMR-1644779 (-2022) DMR-2128556 (2023-), the State of Florida, and JSA, LLC U.S. DOE Contract No. DE-AC05-06OR23177.

[†] shreyas@jlab.org

EVALUATION OF FLUX EXPULSION AND FLUX TRAPPING SENSITIVITY OF SRF CAVITIES FABRICATED FROM COLD WORK NB SHEET WITH SUCCESSIVE HEAT TREATMENT*

B. D. Khanal^{1,†}, P. Dhakal²

¹Department of Physics, Old Dominion University, Norfolk, VA, USA

²Thomas Jefferson National Accelerator Facility, Newport News, VA, USA

Abstract

The main source of RF losses leading to lower quality factor of superconducting radio-frequency cavities is due to the residual magnetic flux trapped during cool-down. The loss due to flux trapping is more pronounced for cavities subjected to impurities doping. The flux trapping and its sensitivity to rf losses are related to several intrinsic and extrinsic phenomena. To elucidate the effect of re-crystallization by high temperature heat treatment on the flux trapping sensitivity, we have fabricated two 1.3 GHz single cell cavities from cold-worked Nb sheets and compared with cavities made from standard fine-grain Nb. Flux expulsion ratio and flux trapping sensitivity were measured after successive high temperature heat treatments. The cavity made from cold worked Nb showed better flux expulsion after 800 °C/3 h heat treatment and similar behavior when heat treated with additional 900 °C/3 h and 1000 °C/3 h. In this contribution, we present the summary of flux expulsion, trapping sensitivity, and RF results.

INTRODUCTION

Niobium has been the material of choice for superconducting radio-frequency (SRF) cavities not only because of low power loss at the inner surface of the cavities' inner wall but also its high ductility which makes easier to fabricate the complex structures [1]. The niobium is elemental superconductor with highest critical temperature, $T_c \sim 9.25$ K and highest critical field, $H_c \sim 200$ mT. The performance is measured in terms of the quality factor (Q_0) which defined as the ratio of stored energy inside the cavities to the power dissipation on the inner wall of the cavities per radio frequency (RF) cycle as a function of accelerating gradient (E_{acc}). The ambient magnetic flux trapping during the cooldown is one of the prominent factors causing the degradation of quality factor in cavities. The trapped flux in the form of vortices oscillates in the presence of RF field and dissipate energy. The field dependence of RF losses due to trapped vortices is much stronger than the ohmic-type loss [2, 3]. The ambient flux trapping and the flux trapping sensitivity to rf losses are related to several extrinsic and intrinsic phenomena. The primary host sites of flux trapping are the materials defects, dislocations, impurities, normal

conducting precipitates. For instance, the RF loss due to flux trapping can be minimized by maximizing the flux expulsion when the cavity transition to the superconducting state from normal conducting during the cavity cool-down by creating a large thermal gradient across the cavity surface. Intrinsically, we can minimize the flux trapping by minimizing the defects, dislocations, impurities with different temperature heat treatments followed by chemical and mechanical polishing and by high pressure rinse with de-ionized water. It has been demonstrated that several different pinning mechanism plays a role to the rf losses due to vortices [4]. Studies showed that doped cavities are more vulnerable to the vortex dissipation loss due to the presence of the dopant on cavities rf surface [5-7]. The flux expulsion can be maximized by increasing the annealing temperature [8]. The increase in annealing temperature minimizes the pinning centers by removing the clusters of dislocations and impurities. In addition, the metallurgical state with larger grain size is expected as the annealing temperature is increased. Fine-grain recrystallized microstructure with an average grain size of 10-50 μm leads to flux trapping even with a lack of dislocation structures in grain interiors [9]. Thus, it is important to consider the crystallize structure of the niobium before the fabrications and during the cavity processing [10]. In this contribution, we have fabricated two single cell cavity, one from cavity grade SRF Nb with grain size specified to ASTM 4-6 and other from the cold worked sheet with no specified grain size. The cavity were processed together for chemical polishing with electropolishing and successive annealing at 800, 900 and 1000 °C/3 h heat treatment. The flux expulsion ratio, flux trapping sensitivity and $Q_0(B_p)$ at 2.0 K were measured.

FABRICATION AND SURFACE PREPARATION

The SRF grade and cold-worked Nb sheets with residual resistivity ratio ≥ 300 were purchased from Ningxia OTIC, China and 1.3 GHz TESLA shaped cavities were fabricated at Zanon Research & Innovation Srl, Italy using standard practice of deep drawing to half cells, trimming, machining of the iris and equator of the half-cells, electron beam welding of the beam tubes (made from low purity niobium). The cavity labeled TE1-05 was made from SRF grade Nb and TE1-06 was made from cold-worked sheet. The cavities' inner surface of ~ 150 μm was removed in horizontal electropolishing setup using a mixture of electronic grade

* Work supported by the U.S. Department of Energy, Office of Science, Office of Nuclear Physics under contract DE-AC05-06OR23177 and U.S. Department of Energy, Office of Science, Office of High Energy Physics under Awards No. DE-SC 0009960.

† bkhan001@odu.edu

CHARACTERIZATION OF DISSIPATIVE REGIONS OF AN N-DOPED SRF CAVITY*

E. M. Lechner^{1,†}, B. D. Oli, M. Iavarone, Temple University, Philadelphia, PA, USA
 J. Makita, A. Gurevich, Old Dominion University, Norfolk, VA, USA
 G. Ciovati², Thomas Jefferson National Accelerator Facility, Newport News, VA, USA
¹also at Thomas Jefferson National Accelerator Facility, Newport News, VA, USA
²also at Old Dominion University, Norfolk, VA, USA

Abstract

We report scanning tunneling microscopy measurements on N-doped cavity hot and cold spot cutouts. Analysis of the electron tunneling spectra using a proximity effect theory shows that hot spots have a reduced superconducting gap and a wider distribution of the contact resistance. Alone, these degraded superconducting properties account for a much weaker excess dissipation as compared with the vortex contribution. Based on the correlation between the quasiparticle density of states and temperature mapping, we suggest that degraded superconducting properties may facilitate vortex nucleation or settling of trapped flux during cooling the cavity through the critical temperature.

INTRODUCTION

Doping SRF cavities with impurities has been an effective method of producing Nb resonators with very high quality factors at moderate accelerating fields [1–8]. Performance of SRF cavities is inherently multifaceted. Towards gaining a deeper understanding of the mechanisms by which N-doping affects RF performance, accessing the quasiparticle density of states (DOS) is of great interest [9]. The DOS of surface of a superconductor can be examined in a straightforward manner by measuring the differential conductance via electron tunneling, dI/dV . In tunneling experiments that utilize a normal metal counter electrode the differential conductance reflects the DOS of the sample by Eq. (1) [10]

$$\frac{dI}{dV} \propto - \int_{-\infty}^{\infty} \frac{\partial f(\epsilon + eV)}{\partial V} N(\epsilon) d\epsilon, \quad (1)$$

where f is the Fermi-Dirac distribution function, ϵ is the quasiparticle energy, V is the electric potential and N is the DOS of the sample. In the low temperature limit the differential conductance probes directly the density of states in the material of interest. Point contact spectroscopy and low temperature scanning tunneling microscopy and spectroscopy (STM/STS) have been used recently to investigate Nb cavity cutouts [11, 12]. These studies have revealed changes in $N(\epsilon)$ in the first few nm at the surface of Nb cavities after N-doping [11, 12]. It was shown that N-doping shrinks the metallic suboxide layer and reduces lateral inhomogeneities of the superconducting gap Δ and the contact resistance R_B between the suboxide and the Nb matrix, making R_B closer

to an optimum value which minimizes R_s [12, 13]. At the same time, N-doping slightly reduces Δ at the surface [11, 12]. Here we identify hot and cold spots via temperature mapping of an SRF cavity and study their DOS via scanning tunneling microscopy.

EXPERIMENTAL

The cavity measured in this work was fabricated from ingot Nb from Tokyo Denkai, Japan, with residual resistivity ratio (RRR) of ~ 300 and large grains with size of a few cm^2 . The cavity shape is that of the center cell of TESLA/EXFEL cavities [14]. Prior to N-doping, the cavity underwent standard buffered chemical polishing (BCP) and high pressure rinsing (HPR) with ultra-pure water. The cavity was N-doped by heating to 800°C and exposing the cavity to a 25 mTorr nitrogen atmosphere for 30 minutes. After, the nitrogen was pumped-out and the cavity remained at 800°C for 30 minutes, after which the furnace cooled naturally back to room temperature. Ultimately, $\sim 10\ \mu\text{m}$ were removed from the cavity's inner surface by electropolishing, followed by HPR, assembly in a clean room and evacuation on a vertical test stand. The temperature mapping system was attached to the outer cavity surface prior to insertion into a vertical test cryostat at Jefferson Lab [15].

The cavity performance, shown in Fig. 1, was limited in both tests by a quench at $B_p \sim 88\ \text{mT}$, without any field emission. The first test was performed after cooling with liquid He with a cool-down rate of $\sim 1.5\ \text{K/min}$ when the temperature at the bottom of the cavity crossed the critical temperature. The second test was performed after warming up the cavity to 80 K followed by a cool-down at a faster rate of $\sim 5\ \text{K/min}$. The higher Q_0 in Test 2 compared to that of Test 1 is due to a lower residual resistance, decreasing from $3.4\ \text{n}\Omega$ to $2.4\ \text{n}\Omega$. This reduction of R_i resulting from a faster cooling rate is related to better expulsion of the residual ambient magnetic field inside the cryostat [16], B_a , which was $\sim 0.2\ \mu\text{T}$ during the experiments. Taking the difference of $1/Q(B_a)$ curves for these two tests we extract the additional surface resistance ΔR caused by the slower cooling rate. As shown in the inset in Fig. 1, ΔR_s is practically independent of B_a , thus extra vortices trapped at a lower cooling rate do not produce additional nonlinearity in $R_s(B_a)$ in this field range. $Q_0(T_0)$ was also measured between $1.6 - 2.1\ \text{K}$ and $1 - 15\ \text{mT}$ after the second cool-down. The temperature maps measured just below the quench field are shown in Fig. 2. The quench location was the same in

* Work supported by DE-AC05-06OR23177

† lechner@jlab.org

TOPOGRAPHIC EVOLUTION OF NITROGEN DOPED Nb SUBJECTED TO ELECTROPOLISHING*

E. M. Lechner^{1,†}, J. W. Angle², C. Baxley¹, M. J. Kelley^{1,2}, C. E. Reece¹

¹Thomas Jefferson National Accelerator Facility, Newport News, VA, USA

²Virginia Polytechnic Institute and State University, Blacksburg, VA, USA

Abstract

Surface quality is paramount in facilitating high performance SRF cavity operation. Here, we investigate the topographic evolution of samples subjected to N-doping and 600 °C vacuum anneal. We show that in N-doped Nb, niobium nitrides may grow continuously along grain boundaries. Upon electropolishing high slope angle grooves are revealed which sets up a condition that may facilitate a suppression of the superheating field.

INTRODUCTION

The N doping process [1] of thermally diffusing N at 800 °C in a low pressure N₂ environment has resulted in substantial decreases of the surface resistance at moderate accelerating gradients. Based on the reproducibility of the intended performance N doping was chosen for production cavities in the LCLS-II and LCLS-II HE upgrades. The LCLS-II HE research and development program investigated the performance of three N doping protocols [2]. It was shown that the process of N doping Nb cavities at 800 °C for two minutes in an N₂ atmosphere with no post-dope anneal (referred to as “2N0”) was superior to cavities doped for 2 minutes and annealed for 6 minutes or doped for 3 minutes and annealed for 60 minutes. After N doping, a 7 μm electropolish is performed to recover performance. The N doping process is known to leave behind topographic defects due to the removal of nitrides during the electropolishing process [3]. Topographic defects are one vector that may reduce superheating fields either by magnetic field enhancement [4-6] or by nanoscale defects [7, 8]. Another source of degradation may be from impurities [9]. To investigate the possible topographic contribution we examine the topographic evolution of 2N0 N-doped and vacuum annealed Nb samples subjected to electropolishing using an atomic force microscope (AFM).

RESULTS

Here, we examine nitrogen doped and vacuum annealed (600 °C/10 hr) samples using atomic force microscopy after sequential electropolishing. Electropolishing (EP) was performed using a 1 to 10 by volume mixture of HF(49%) to H₂SO₄(98%). Samples of 6 × 10 × ~3 mm³ were wrapped in PTFE tape, mounted in a sample holder and immersed in the EP electrolyte allowing only the polished face to be exposed to the electrolyte. Samples were electropolished at 13 °C and 9 V. Tapping-mode AFM topographies were made using a Digital Instruments Nanoscope IV

atomic force microscope. The AFM probe tip used was a Si tip with a tip radius less than 10 nm.

The N doping process precipitates nitrides within grains and can precipitate nitrides along grain boundaries. During the electropolishing process nitrides are preferentially removed as shown in Fig. 1. Smaller holes are formed within grains while relatively deep grooves may be produced along grain boundaries. Electropolishing leaves behind long grooves along grain boundaries and reveals high slope angle areas. To study the evolution of topographic features we examined two 2N0 N doped samples and

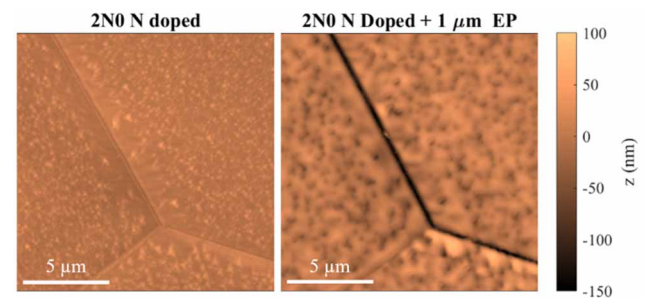


Figure 1: Before (left) and after (right) electropolishing at a triple-junction.

two electropolished samples for comparison. Representative intragrain tapping-mode atomic force microscope topographies are shown in Fig. 2 which shows the evolution of surface upon electropolishing. Some holes of approximately 1 μm in width are introduced into the 600 °C heat treated samples which are suspected to be due to growth of an unidentified Nb compound. With increasing electropolishing depth the holes tend to become more rounded and shallower. The evolution of average surface roughness S_a is shown in Fig. 3 for the 2N0 samples compared with 600 °C, 10 hour vacuum annealed samples.

Along some grain boundaries, grooves are present which also become more rounded and shallower with electropolishing depth. The evolution of topography at triple junctions is shown in Fig. 4. A common defect observed at the grain boundary is a deeper removal of material around the triple-junction likely due to enhanced diffusion between grains. The geometry of the groove topographic defect is reminiscent of the triangular groove defect studied by Kubo [8]. Kubo’s model predicts a superheating field suppression from nanoscale features of the surface and the superconductor’s coherence length. The suppression of the superheating field is dependent on the triangular groove

* Work supported by U.S. DOE contract DE-AC05-06OR23177

† lechner@jlab.org

QUENCH DETECTION IN A SUPERCONDUCTING RADIO FREQUENCY CAVITY WITH COMBINED TEMPERATURE AND MAGNETIC FIELD MAPPING*

B. D. Khanal^{1,†}, P. Dhakal², G. Ciovati^{1,2}

¹Department of Physics, Old Dominion University, Norfolk, VA, USA

²Thomas Jefferson National Accelerator Facility, Newport News, VA, USA

Abstract

Local dissipation of RF power in superconducting radio frequency cavities create so called “hot-spots”, primary precursors of cavity quench driven by either thermal or magnetic instability. These hot-spots are detected by a temperature mapping system, and a large increase in temperature on the outer surface is detected during cavity quench events. Here, we have used combined magnetic and temperature mapping systems using anisotropic magneto-resistance (AMR) sensors and carbon resistors to locate the hot spots and areas with high trapped flux on a 3.0 GHz single-cell Nb cavity during the RF tests at 2.0 K. The quench location and hot spots were detected near the equator when the residual magnetic field in the Dewar is kept < 1 mG. The hot spots and quench locations moved when the magnetic field is trapped locally, as detected by T-mapping system. No significant dynamics of trapped flux is detected by AMR sensors, however change in magnetic flux during cavity quench is detected by a flux gate magnetometer, close to the quench location. The result provide the direct evidence of hot spots and quench events due to localized trapped vortices.

INTRODUCTION

Superconducting radio frequency (SRF) cavities made from elemental niobium are the building blocks of modern particle accelerators, superconducting electronics and quantum computers because of their formability in complex structures and lithographic thin films. Recent advances in surface engineering by doping and annealing led to an unprecedented quality factor [1–3], however the process is vulnerable to residual flux trapping when the cavity transitions to superconducting state during cooldown [4]. The trapped vortices within the RF penetration depth oscillates under the RF field and lowers the quality factor with additional RF dissipation.

The temperature mapping technique is able to detect the regions of large RF power dissipation, referred as “hot-spots” [5]. The source of hot-spots could be due to the normal conducting inclusion or segregation of impurities in dislocations sites or grain boundaries. If the origin of hot spot is due to trapped vortices, those could be moved

or change their intensity an application of a thermal gradient [6, 7]. The combined temperature and magnetic field mapping system used in 1.3 GHz cavity showed an enhancement of magnetic field trapping due to quench events either by trapping of thermo current induced flux or trapping to additional residual flux [8,9]. Here, we present the results of RF measurements done on a 3.0 GHz single cell cavity with combined temperature and magnetic field mapping where the hot-spots are created on the cavity surface by trapping magnetic field locally.

EXPERIMENTAL SETUP

The 3 GHz single cell cavity used in this study was made from high purity large grain Nb and scaled down from the TESLA end-cell cavity shape [10, 11]. After previous measurements reported in Ref. [12] the cavity was subjected to ~ 25 μm electropolishing followed by high pressure rinse with deionized water. The cavity was assembled with input and pick up antennas. A cavity vacuum of < 10⁻⁸ mbar was maintained with active pumping during the cooldown and RF tests.

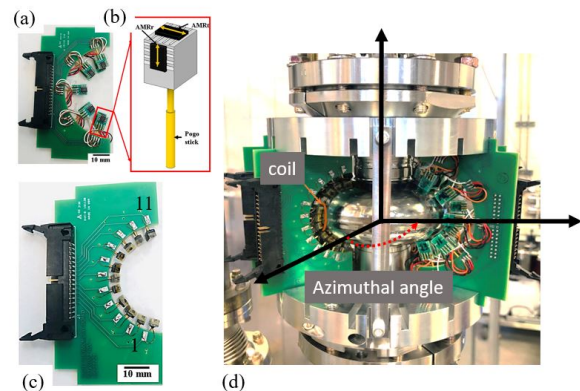


Figure 1: (a) and (b) AMR sensors and (c) temperature sensors board, (d) assembled on the surface of cavity [13].

The combined temperature and magnetic field mapping system relies on 100 Ω Allen-Bradley carbon resistors to measure the temperature and AMR sensors to measure the magnetic field. The details of set up, sensors calibration, sensitivity and measurement can be found in Refs. [13–15]. The AMR sensors boards and temperature sensors boards are place alternatively on every 22.5° around the cavity. There are 10 AMR sensors on each board measure the radial and tangential component of the magnetic field in the vicinity of

* The work is partially supported by the U.S. Department of Energy, Office of Science, Office of High Energy Physics under Awards No. DE-SC 0009960, NSF Grant 100614-010, and by the U.S. Department of Energy, Office of Science, Office of Nuclear Physics under contract DE-AC05-06OR23177.

† bkhan001@odu.edu

COMMISSIONING OF DEDICATED FURNACE FOR Nb₃Sn COATINGS OF 2.6 GHz SINGLE CELL CAVITIES

P. A. Kulyavtsev^{1,2}, G. Ereemeev^{1,*}, S. Posen¹, B. Tennis¹, J. Zasadzinski²

¹Fermi National Accelerator Laboratory, Batavia, IL, USA

²Illinois Institute of Technology, Chicago, IL, USA

Abstract

We present the results of commissioning a dedicated furnace for Nb₃Sn coatings of 2.6 GHz single cell cavities. Nb₃Sn is a desired coating due to its high critical temperature and smaller surface resistance compared to bulk Nb. Usage of Nb₃Sn coated cavities will greatly reduce operating costs due to decreased dependence on cryo cooling. Tin is deposited by use of a tin chloride nucleation agent and tin vapor diffusion. Analysis of the resultant coating was performed using SEM/EDS to verify successful formation of Nb₃Sn. Witness samples in line of sight of the source were used in order to understand the coating efficacy.

INTRODUCTION

Nb₃Sn-coated cavities achieve accelerating gradients E_{acc} above 10 MV/m and quality factors in excess of 10^{10} at 4 K [1–5]. High quality factors of Nb₃Sn-coated cavities at 4 K are the enabling technology for compact cryomodules for industrial accelerators [6]. Several projects look to exploit this technology for various industrial applications [7,8]. Given that the superheating critical field and superconducting transition temperature of Nb₃Sn is higher than that of niobium, Nb₃Sn superconducting material has the potential to sustain accelerating gradients twice that of niobium cavities and quality factors close to $5 \cdot 10^{10}$, which will significantly reduce the operating and capital cost of future accelerators. Research and development efforts are ongoing to understand and improve vapor diffusion deposition techniques to realize their potential of Nb₃Sn material.

Several institutions are pursuing Nb₃Sn coatings and research is ongoing to understand material limitations and to optimize coating process [9–12]. Nb₃Sn coatings at Fermilab are done in the large coating system designed to coat multicell cavities. The coating system is constantly used to coat cavities for various projects. In order to enable Nb₃Sn coating research on small cavities and samples in parallel with multicell cavity coating, we refurbish and commission for Nb₃Sn coating an old furnace. Unlike the larger Nb₃Sn system, which is routinely used for coating of Nb₃Sn films on single and multi-cell cavities [4], the new system will be used to coat smaller single-cell cavities and for samples studies. This contribution presents the results from the commissioning of the new coating system.

* grigory@fnal.gov

EXPERIMENTAL SETUP

For these Nb₃Sn studies, the old IVI Model 3312-1212-120V furnace was adopted. This is the horizontal front loading furnace that features 12" x 12" x 15" hot zone. The furnace heaters as well as the inner shields are made out of molybdenum. The furnace is controlled by PLC connected to a computer and can reach up to 1200 °C. The furnace is evacuated with an oil-free mechanical pump and a cryopump and can reach down to 10^{-8} Torr range cold. The temperature is monitored with four molybdenum-sheathed type C thermocouples.

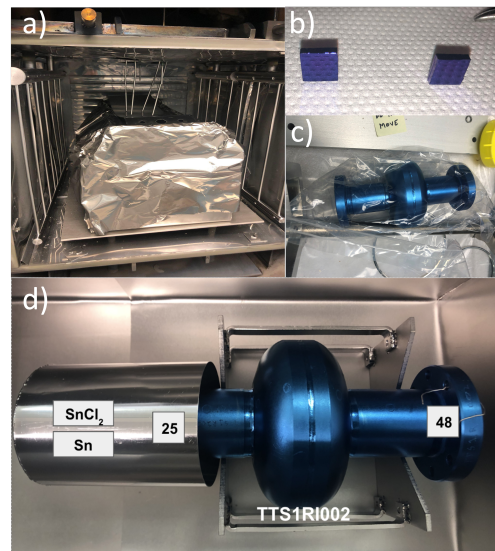


Figure 1: Experimental setup for Nb₃Sn coating. [a] Assembled experimental setup in the hot zone of the furnace. Note niobium foil covering the assembly and thermocouples at the top. [b,c] Niobium samples (b) and niobium cavity (c) prepared for the coating. Note that the blue color is due to 30 V anodizing. [d] Niobium cavity assembled for the coating inside niobium box on the niobium support fixture.

For Nb₃Sn coating, a cavity is placed inside a niobium box onto niobium supports, fig. 1. Two samples, one on each end of the cavity, are mounted with niobium wires. One end of the cavity is then assembled with a molybdenum cup, which holds Sn and SnCl₂. The other end is left open. For the first coating of 2.6 GHz cavity, 2 g of Sn and 0.5 g of SnCl₂ were used. The assembly is then covered with niobium foil. As part of the preparation for the first Nb₃Sn coating on SRF cavity, both the cavity and the samples were anodized for 30 V. The coating was done at 1150 °C for 3 hours preceded by the nucleation step at 500 °C. 1.6 g of Sn was consumed in the coating.

IN-SITU PLASMA PROCESSING ON A 172 MHz HWR CAVITY AT THE ARGONNE TANDEM LINAC ACCELERATOR SYSTEM

M. McIntyre, K. Villafania, Z. Wei, M. Kelly, J. McLain, G. Zinkann, B. Blomberg
Physics Division, Argonne National Laboratory, Lemont, IL, USA

Abstract

Maintenance and cleaning of superconducting rf cavities is labor intensive task that involves disassembling the cryostat holding the resonators and removing them to be cleaned. At the Argonne Tandem Linac Accelerator System (ATLAS) at Argonne National Laboratory, a project is underway to research cleaning the cavities in-situ by plasma processing. Previous plasma processing research by SNS, MSU, FNAL, IJCLab, and JLab has been successful in improving field emissions post processing. It is advantageous to pursue research in this method, allowing for possible use on modern ATLAS cryomodules, A-tank and G-tank quarter-wave resonators (QWR). The results presented show initial plasma ignition testing and plasma simulations for the coupled E and B fields, both done on a 172 MHz HWR cavity previously designed as early R&D for FRIB. Future plans are also included, laying out next steps to test plasma processing on the same HWR cavity and eventually a QWR.

INTRODUCTION

The first rf superconducting accelerator for heavy ion acceleration, ATLAS, has been in operation since the 1970's with the first successful acceleration of an ion beam in 1978 [1]. Significant upgrades have occurred over the years, including installing and upgrading quarter-wave resonator cavities (QWR) to replace the original split-ring resonator design. In 2009 a major upgrade took place, installing G-Tank, a cryostat containing seven 109 MHz $\beta = 0.15$ QWR cavities, increasing the deliverable energy of ATLAS by providing 15 MV additional voltage [2]. These were removed, upgraded, and re-installed in 2022 (Fig. 1). In 2014, A-Tank, a cryostat containing seven 72 MHz QWR $\beta = 0.077$ cavities, was installed, further increasing the accelerating potential of ATLAS [3]. A-tank has since yet to be removed for cleaning.



Figure 1: G-Tank upgrade work performed in clean room.

The design of G-tank and A-tank QWR resonators included specific attention to reducing the particulates on

the rf surfaces, therefore reducing field emissions from the resonators and improving their efficiency [2]. For these resonators to be of peak performance, the rf surface must remain clean, only allowing a low number of particulates. At this point (i.e., 2023), the A-tank resonators are showing a degradation in performance characterized by higher field emissions and an increased heat load on the cryogenics system. Investigations are underway to identify where the particulates have developed inside the cryostat indicating which resonators have been contaminated and possibly the cause. Unfortunately, pulse conditioning and thermal cycling are no longer adequate to reduce field emissions and recover performance. Cleaning these resonators and returning them to their prior performance, would require removal for six months to a year to be Electropolished (EP), rinsed, baked, and re-installed. This would severely impact the facility's current yearly goal of delivering ~6000 beam hours.



Figure 2: A-Tank cryostat in ATLAS beamline.

Cavity removal is not only time consuming and cumbersome but also exposes equipment to the risk of damage, owing to the cramped quarters in which the cryostats sit (Fig. 2) [4]. In recent years, a solution has been investigated in a collaborative effort by FNAL, SLAC, MSU/FRIB, JLab, and IJCLab for plasma processing of the resonators in-situ of the cryomodules. Proven to reduce field emissions (FE), this process could be applied to A-tank and possibly future work on G-tank [5, 6]. This technique utilizes the vacuum and rf coupling system already installed to the cryomodule in addition to the cavity's fundamental and higher order modes (HOM), so no additional upgrades or significant installation of new equipment is required. The plasma is created by injecting a Ne-O₂ or Ar-O₂ gas mixture into the cavity, maintaining around 100-200 mTorr pressure and 10% O₂, and then delivering rf power via the fundamental coupler [5, 7]. Results have found this method effective for removing hydrocarbons from the internal surface of the cavity, thereby reducing FE. Hydrocarbon removal is observed via a Residual Gas Analyzer (RGA) showing the peak material removed. This process is cycled in specific time intervals

THERMAL FEEDBACK IN COAXIAL SRF CAVITIES*

M. W. McMullin^{†1}, T. Junginger¹, P. Kolb, R. E. Laxdal, Z. Yao, TRIUMF, Vancouver, BC, Canada
¹also at Department of Physics & Astronomy, University of Victoria, Victoria, BC, Canada

Abstract

The phenomenon of Q -slope in SRF cavities is caused by a combination of thermal feedback and field-dependent surface resistance. There is currently no commonly accepted model of field-dependent surface resistance, and studies of Q -slope generally treat thermal feedback as a correction to whichever surface resistance model is being used. In the present study, we treat thermal feedback as a distinct physical effect whose effect on Q -slope is calculated using a novel finite-element code. We performed direct measurements of liquid helium pool boiling from niobium surfaces to obtain input parameters for the finite-element code. This code was used to analyze data from TRIUMF's coaxial test cavity program, which has provided a rich dataset of Q -curves at temperatures between 1.7 K and 4.4 K at five different frequencies. Preliminary results show that thermal feedback makes only a small contribution to Q -slope at temperatures near 4.2 K, but has stronger effects as the bath temperature is lowered.

THERMAL FEEDBACK (TFB) ABOVE T_λ

During operation, the walls of an SRF cavity are constantly heated by the RF power density

$$q = \frac{1}{2} R_s H^2$$

on the inner surface of the cavity. Because of the finite thermal conductivity of niobium and imperfect cooling by the helium bath, the RF surface of the cavity is always warmer than the helium bath, and the difference in temperature increases with q (see Fig. 1). This heating in turn increases the temperature-dependent part of the surface resistance, further increasing q to create a feedback loop. The feedback loop results either in unbounded heating, quenching the cavity, or in steady-state operation with an increased dynamic heat load.

Because of thermal feedback (TFB), the total power P dissipated in the cavity increases faster than the square of the field strength, quantified by the peak surface magnetic field B_p . Since the energy U stored in the cavity fields is proportional to B_p^2 , the quality factor

$$Q_0 = \frac{\omega U}{P} \quad (1)$$

decreases with an increase in B_p . Therefore, TFB impacts measured Q -slope whether or not R_s is itself dependent on the applied field. The thermal conductivity of the cavity

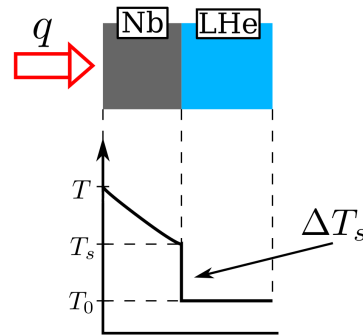


Figure 1: Cross section showing the temperature gradient across the wall of an SRF cavity.

walls and efficiency of heat transfer to the helium bath determine the amount of Q -slope that comes from TFB as opposed to intrinsic field dependence of R_s .

Measurements on a quarter-wave and half-wave resonator (QWR and HWR) in TRIUMF's coaxial test cavity program (detailed in Ref. [1], HWR shown in Fig. 2) show signs that TFB is a non-negligible effect. These measurements are separated into sets of Q_0 vs. B_p curves taken repeatedly in a single cavity mode while cooling the helium bath from about 4.4 K to 2.0-1.7 K. Below $T_\lambda = 2.177$ K, the surface resistance drops abruptly, as shown in Fig. 3, and the size of the drop grows with B_p . This drop is believed to occur because the helium bath enters a superfluid state and cooling is significantly enhanced, mitigating TFB. Measurements of niobium cooling in superfluid helium have previously been conducted and integrated into studies of Q -slope [2-4], but TFB above T_λ has not been extensively studied because of the lack of data on cooling at the niobium-helium interface in the normal fluid regime.

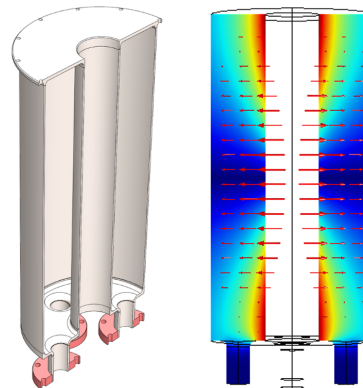


Figure 2: Model (left) and field distribution in the fundamental 389 MHz mode (right) for the HWR in Ref. [1].

* Work supported by the National Research Council Canada

[†] mmcmullin@triumf.ca

THEORETICAL STUDY OF THIN NOBLE-METAL FILMS ON THE NIOBIUM SURFACE*

C. A. Méndez[†], N. S. Sitaraman, M. U. Liepe, T. A. Arias
 Cornell University Department of Physics, Ithaca, NY, USA

Abstract

Recent experiments suggest that noble-metal deposition on niobium metal surfaces can remove the surface oxide and ultimately improve superconducting radio-frequency (SRF) cavities performance. In this preliminary study, we use density-functional theory to investigate the potential for noble-metal passivation of realistic, polycrystalline niobium surfaces for SRF. Specifically, we investigate the stability of gold and palladium monolayers on niobium surfaces with different crystal orientations and evaluate the impact of these impurities on superconducting properties. In particular, our results suggest that gold can grow in thin layers on the niobium surface, whereas palladium rather tends to dissolve into the niobium cavity. These results will help inform ongoing experimental efforts to passivate niobium surfaces of SRF cavities.

INTRODUCTION

Recent experiments suggest that modifications to the niobium native oxide can substantially improve RF performance by reducing the thickness of the oxide. In particular, it has been found that noble-metal deposition can passivate the surface and completely remove the oxide. However, experiments on noble-metal layers have only been performed so far on small single-crystal samples under highly controlled conditions [1]. To shed further light on the potential for noble-metal layers, here we use first principles density-functional theory electronic structure software [2] to investigate the potential for noble-metal passivation of realistic, polycrystalline niobium surfaces for SRF. Specifically, we investigate the stability of gold and palladium monolayers on niobium surfaces with the most common, low-index crystal orientations. The preliminary results that we present here help inform and extend ongoing experimental efforts, which so far have shown a modest but significant benefit from sub-monolayer gold deposition on niobium.

BACKGROUND

Density-Functional Theory

Density Functional Theory (DFT) is a highly adaptable tool that can compute and predict a diverse array of fundamental material properties, ranging from electronic structures to formation energies to superconducting characteristics, with an accuracy within a few percent and without the necessity of experimental input. This positions DFT as an

immensely beneficial complement to experimental investigations of advanced materials, like those utilized in SRF cavities. In this paper, we employ DFT to predict the effects of thin noble-metal films of Au and Pd on the Nb surface. In particular, we estimate the number of monolayers that can form a coherent interface, study the stability of these atoms on the surface, and calculate the effects of impurities on the superconducting transition temperature T_c [2].

Coherent Interfaces with Nb

In nature, niobium forms a body-centered cubic structure (bcc), with a lattice constant of approximately $a_{\text{Nb}} = 3.30 \text{ \AA}$, whereas Au and Pd typically form face-centered cubic structures (fcc), with lattice constants $a_{\text{Au}} = 4.16 \text{ \AA}$ and $a_{\text{Pd}} = 3.95 \text{ \AA}$ respectively (values obtained from our *ab initio* relaxation calculations). Nevertheless, for a small number of monolayers (ML), we expect the noble metal to occupy bcc lattice sites. As the number of MLs grows, we expect the formation of misfit dislocations, and finally a transition of the material to its preferred fcc geometry. Our goal is to estimate how many MLs it is possible to deposit on the Nb surface before this final phase transition occurs.

It is not straightforward to directly predict the lattice constant of an element in its bcc phase given its lattice constant in the fcc phase, as the change in the structure can involve physical changes due to different atomic packing, bonding characteristics, and potential energy minima. We can roughly estimate the lattice constant by relating it to the atomic radius r through the equations $a_{\text{fcc}} = \sqrt{2} \cdot 2r$ and $a_{\text{bcc}} = \sqrt{3} \cdot 2r$. Using these relations and the above fcc lattice constants, we estimate $a_{\text{Au,bcc}} \approx 3.39 \text{ \AA}$ and $a_{\text{Pd,bcc}} \approx 3.22 \text{ \AA}$. The proximity of these values to the niobium lattice constant of $a_{\text{Nb}} = 3.30 \text{ \AA}$ make Au and Pd potential candidates for having a smooth coherent interface with Nb.

Given that the above lattice constants are not perfect matches, to compensate for the resulting interfacial strain energy, the material must lower the total energy by replacing the surface energy of niobium with an energetically favorable interface. We call this energy difference E_{gain} , and it is given by the sum of the energy of the interface and the surface of the film, minus the energy of the original niobium surface,

$$E_{\text{gain}} = E_{\text{interface}} + E_{\text{surface film}} - E_{\text{surface Nb}} \quad (1)$$

On the other hand, for a coherent interface (which we assume for a low number of MLs), there is a strain energy cost per atom per ML due to the lattice-constant mismatch, of

$$E_{\text{strain}} = E_{\text{bcc}} - E_{\text{fcc}}, \quad (2)$$

* This work was supported by the US National Science Foundation under award PHY-1549132, the Center for Bright Beams.

[†] cam559@cornell.edu

CEA CONTRIBUTION TO THE PIP-II LINEAR ACCELERATOR

N. Bazin[†], J. Belorgey, S. Berry, Q. Bertrand, P. Bredy, E. Cenni, C. Cloue, R. Cubizolles, J. Drant, M. Fontaine, P. Garin, H. Jenhani, S. Ladegaillerie, A. Le Baut, A. Moreau, O. Piquet, J. Plouin, A. Raut, P. Sahuquet, C. Simon, Université Paris-Saclay, CEA, Département des Accélérateurs, de la Cryogénie et du Magnétisme, Gif-sur-Yvette, France.

Abstract

The Proton Improvement Plan II (PIP-II) that will be in-stalled at Fermilab is the first U.S. accelerator project that will have significant contributions from international part-ners. CEA joined the international collaboration in 2018, and will deliver 10 low-beta cryomodules as In-Kind Con-tributions to the PIP-II project, with cavities supplied by LASA-INFN (Italy) and VECC-DAE (India) and power couplers and tuning systems supplied by Fermilab. An im-portant milestone was reach in April 2023 with the Final Design Review of the cryomodule, launching the pre-pro-duction phase. This paper presents the status of CEA activ-ities that includes the design, manufacturing, assembly and tests of the cryomodules and the upgrade of the existing infrastructures to the PIP-II requirements.

INTRODUCTION

The PIP-II project is an upgrade of the accelerator complex of Fermilab to enable the world's most intense neu-trino beam for the Long Baseline Neutrino Facility (LBNF) and the Deep-Underground Neutrino Experiment (DUNE) located in South Dakota, 1200 km from the neutrino pro-duction in Illinois.

PIP-II will deliver 1.2 MW of proton beam power from the injector, upgradeable to multi-MW capability. The cen-tral element of PIP-II is an 800 MeV linear accelerator, which comprises a room temperature front end followed by a superconducting section. The superconducting section consists of five different types of cavities and cryomodules, including Half Wave Resonators (HWR), Single Spoke and elliptical resonators operating at state-of-the-art parameters.

PIP-II is the first U.S. accelerator project that will be constructed with significant contributions from interna-tional partners, including India, Italy, France, United King-dom and Poland [1, 2].

OVERVIEW OF THE CEA CONTRIBUTION TO THE PIP-II PROJECT

CEA is designing, building, testing, installing and com-missioning superconducting linear accelerators (or part of them) for others labs since 20 years. It includes the devel-opment of a wide range of cryomodules with different fre-quencies, different types of cavities (low beta ones – half-wave and quarter-wave resonators – and high beta ones – elliptical cavities), different types of

supports and insertion modes of the cold mass:

352 MHz cryomodule for SO-LEIL, 88 MHz QWR cryomodules for Spiral2, 1.3 GHz cryomodules for XFEL, 175 MHz HWR cryomodules for IFMIF/EVEDA, IFMIF-DONES and SARAF, 704 MHz cryomodules for ESS [3, 4].

Thanks to this expertise, CEA joined the PIP-II collabo-ration in 2018. The involvement of CEA in the PIP-II Linac construction was formally approved by the French Minis-try of Research in July 2020 with the definition of the scope of work and the budget envelope.

CEA contribution focuses on the 650 MHz supercon-ducting accelerating section, with the design, fabrication, assembly and test of 1 pre-production and 9 production low-beta 650 MHz cryomodules (called “LB650” hereaf-ter) according to the PIP-II project specified requirements. This includes:

- The design of the LB650 cryomodule.
- The procurement of most of the components of the cryostat (i.e. the cryomodule without the cavities, the tuning systems, the power couplers and some standard components provided by the PIP-II collaboration).
- The assembly and cold RF tests of the 10 LB650 cryomodules.
- The design of the transport frame for the LB650 cryomodules, fabrication of 3 units and road test of the pre-production cryomodule.
- The preparation for shipment before the transfer title from CEA to the U.S Department of Energy (DOE) and the overseas transportation from France to the USA.

DESIGN OF THE LB650 CRYOMODULE

The LB650 cryomodule houses four 5-cell $\beta=0.61$ cavi-ties (developed by Fermilab, INFN, and VECC for the pre-production cryomodule and series cryomodules). The fre-quency tuning systems and the power couplers for the low beta and high beta cavities are identical. They are under the responsibility of Fermilab, with CEA contribution on the design studies of the power couplers. Each cavity is con-nected to the a supporting system that stays at room tem-perature , the strongback, using two support posts made of low thermal conductivity material to limit the thermal load between the room temperature strongback and the helium temperature devices. The posts have two thermal inter-cepts, one connected to the thermal shield (cooled around 40 K) and the 5 K line where liquid helium flows inside.

[†] nicolas.bazin@cea.fr

SARAF-PHASE II: TEST OF THE SRF CAVITIES WITH THE FIRST CRYOMODULE*

Guillaume Ferrand[†], Stéphane Berry, David Darde, Gabriel Desmarchelier, Florian Hassane, Tom Joannem, Sébastien Monneré, Nicolas Pichoff, Olivier Piquet, Thomas Plaisant
Commissariat à l’Energie Atomique et aux Energies Alternatives (CEA-Irfu) Institut de Recherche sur les lois Fondamentales de l’Univers, Gif-sur-Yvette, France

Abstract

CEA is committed to delivering a Medium Energy Beam Transfer line and a superconducting linac (SCL) for SARAF accelerator in order to accelerate 5 mA beam of either protons from 1.3 MeV to 35 MeV or deuterons from 2.6 MeV to 40 MeV. The SCL consists in four cryomodules. The first cryomodule hosts 6 half-wave resonator (HWR) low beta cavities ($\beta=0.09$) at 176 MHz. The low-beta cavities were qualified in 2021, as well as the power couplers and frequency tuners. The Low-Level RF (LLRF) system was qualified in 2022 with a dedicated test stand. This contribution will present the results of the RF tests of the first SARAF cryomodule at Saclay.

INTRODUCTION

In 2014, CEA (Commissariat à l’Energie Atomique et aux Energies Alternatives, Saclay, France) was committed to delivering a Medium Energy Beam Transfer line and a superconducting linac (SCL) for SNRC (Soreq Nuclear Research Center, Yavne, Israel), on the SARAF (Soreq Applied Research Accelerator Facility) site. CEA is currently driving the manufacturing of this new accelerator [1]. CEA planned the end of the commissioning of the last cryomodule for 2023.

The frequency of the entire accelerator was fixed to 176 MHz. The beam dynamics fixed the optimal “geometric betas” to 0.09 and 0.18. The SARAF-Phase II accelerator contains 13 superconducting cavities with $\beta_{opt} = 0.09$, called low-beta (LB) cavities, and 14 superconducting cavities for $\beta_{opt} = 0.18$, called high-beta (HB) cavities [2]. The first two cryomodules contain the LB cavities (6 and 7 cavities each), and the last two cryomodule the HB cavities (7 cavities each).

A full description and details about the design and the tests of the LB cavities can be found in [3]. All of them were successfully tested up to an accelerating gradient of 10 MV/m, the requirement being 7 MV/m. Considering the accelerating length of 155 mm @ $\beta = 0.091$, this corresponds to an accelerating voltage of 1.085 MV.

The couplers were already conditioned and tested with a dedicated test stand in 2019 and 2020. See [4] for more details about the coupler design and the test stand.

The equipped cavity, with couplers and tuners was tested with a dedicated test stand, called ECTS [5].

* Work supported by the Commissariat à l’Energie Atomique et aux Energies Alternatives (CEA, France) and by Soreq Nuclear Research Center (SNRC, Israel)

[†] Guillaume.ferrand@cea.fr

The qualification of the electronics included the Low-Level RF (LLRF) systems and the detection of arcs with photomultipliers and electron pick-up. The LLRF and most of the electronics were already tested with the ECTS test stand [6]. However, they were never tested in “operation” mode, that is, at the nominal frequency, with tuners compensating variations of He bath pressure and Lorentz detuning.

The first cryomodule was prepared for test in December 2022 (see Figure 1), and tests began in February 2023. This paper presents the RF tests of the first cryomodule, including warm and cold conditioning, tests at nominal field and in operation mode. These tests concluded the Saclay acceptance tests of the equipped cavities before shipment to SNRC and tests with beam in Israel.



Figure 1: Preparation of the first cryomodule for tests.

REQUIREMENTS

1. Warm conditioning

The first step was the warm conditioning of the RF couplers. All of them were conditioned on the cryomodule again after having been stored under vacuum during 3 years.

The pressure inside of the coupler is measured with a cold cathode gauge. The target (software threshold) was 2.10^{-6} mbar at room temperature for input power from 0 to 1 kW. Most of the multipactor effect is observed from 150 to 400 W. Conditioning was done with a repetition frequency of 1 Hz, with pulses from 20 μ s to 1 s by factor 2 steps. The RF signal is increased by steps of 10 mV on the

IMPLEMENTATION OF THE TEST BENCH FOR THE PIP-II LB650 CRYOMODULES AT CEA

H. Jenhani[†], N. Bazin, Q. Bertrand, P. Bredy, L. Maurice, O. Piquet, P. Sahuquet, C. Simon
Université Paris-Saclay, CEA, IRFU, Gif-sur-Yvette, France

Abstract

The Proton Improvement Plan II at Fermilab is the first U.S. accelerator project that will have significant contributions from international partners. As a part of the French In-Kind Contributions to this project, CEA will provide ten 650 MHz low-beta cryomodules (LB650) equipped with LASA-INFN (Italy), Fermilab (USA) and VECC-DAE (India) cavities and Fermilab power couplers and RF tuning systems. CEA is accordingly in charge of the design, manufacturing, assembly and testing of these cryomodules. This paper presents the future implementation of the test stand dedicated to the cryogenic and RF power testing of the LB650 cryomodules. The choice of the equipment and the current status will be detailed, as well.

INTRODUCTION

The Proton Improvement Plan II (PIP-II) project is an upgrade of the accelerator complex of Fermilab, in Illinois, with significant in-kind contributions from international partners. It will enable the world's most intense neutrino beam for the Long Baseline Neutrino Facility (LBNF) and the Deep-Underground Neutrino Experiment (DUNE) located in South Dakota. The central element of PIP-II is an 800 MeV linear accelerator that will deliver 1.2 MW of proton beam power from the main injector. The superconducting Linac section consists of five different types of cavities and cryomodules, including Half-Wave Resonators, Single Spoke and Elliptical Resonators operating at state-of-the-art parameters [1].

The CEA major contribution is the design [2], fabrication, assembly [3], and cryogenic and RF performances testing of one preproduction and nine production LB650 cryomodules. The scope of the CEA covers other collaboration aspects related to the design harmonisation efforts and the collaborative design activities such as for the 650 MHz power couplers [4] and the HB650 cryomodules [5]. An overview of the CEA contribution to the PIP-II project is given in references [6].

Each LB650 cryomodule will undergo a comprehensive cryogenic and RF test at CEA in order to compare its performances with respect to a defined Acceptance Criteria List (ACL). The cryomodules are expected to be directly operational on accelerator after their validation. Only the first three LB650 cryomodules will be retested after their transportation to Fermilab.

Details about the expected tests for the LB650 cryomodules at CEA, the Test Bench status and the equipment choices will be presented in this paper.

[†] hassen.jenhani@cea.fr

LB650 CRYOMODULE

The LB650 cryomodule activities at CEA use lessons learned from the cryomodules previously developed for the PIP-II project as a result of the design standardization choice adopted by the PIP-II project [7]. The HB650 prototype cryomodule [5], currently under the cold RF testing and validation process at Fermilab, has the most similar design to the LB650 cryomodule [8]. HB650 cryomodules house six 5-cells high-beta cavities [9], while the LB650 cryomodules only include four 5-cells low-beta cavities [10]. Furthermore, the power couplers [11] and the frequency tuning systems [12] are identical for both cryomodule types. The procurement of these three main cryomodule subparts are under Fermilab responsibilities.

The design of the LB650 is detailed in the [2] and partially presented on Figs. 1 and 2.

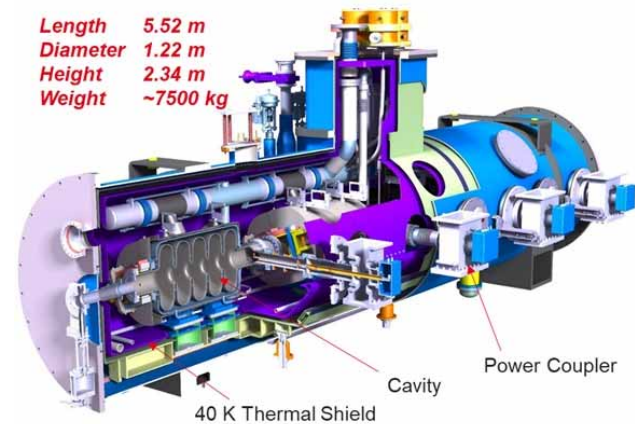


Figure 1: LB650 cryomodule layout.

Figure 2 shows schematics of the cryogenic lines of the LB650 cryomodules. It has a High Temperature Thermal Shield (HTTS) and a Low Temperature Thermal Source (LTTS) both cooled using pressurised GHe at ~ 40 K and ~ 5 K, respectively. The cool down piping shall balance the He flow to each cavity so that it is within 5% of the average cavity flow during the 175 to 90 K and the 45 to 4.5 K phases of the cool down. The cryocircuits associated with cavity cool down must support a “fast cool down” (FCD) of the cavities, at a rate of 20 K/min from 45 K to 4.5 K. This typically requires a LHe flowrate of 50 g/sec. To implement this operation mode, new cryogenic equipment are procured by CEA. Their main technical requirements are detailed later in this paper.

SUMMARY OF THE SUPERCONDUCTING RF MEASUREMENTS IN AMTF HALL AT DESY

M. Wiencek, K. Kasprzak, D. Kostin, D. Reschke, L. Steder
 Deutsches Elektronen-Synchrotron, Hamburg, Germany

Abstract

The AMTF (Accelerator Module Test Facility) at DESY was built for the tests of all superconducting cavities and cryomodules for the EuXFEL linac. After successful commissioning of the EuXFEL, the AMTF has been adapted in order to perform SRF (superconducting radio frequency) measurements of cavities and accelerating modules for different projects. Several SRF cavities related projects are still ongoing, while others were just finished. Some of those projects are dedicated to test components for the infrastructure of accelerators which are under construction, while other ones are devoted to new R&D paths aiming for cavities and modules with high performance which are under investigation at DESY. This paper describes present activities performed at AMTF with special emphasis on performing SRF measurements for the ongoing cavity productions. Most of the presented data is related to vertical cryostat cavity testing. However, some data about cryomodules and a new coupler test stand will be shown as well. Detailed statistics about the number of vertical tests performed within the last two years are also presented.

INTRODUCTION

After successful commissioning of EuXFEL, several modifications of the AMTF test stands and inserts were introduced. Currently, AMTF consists of the following test benches (cf. Fig. 1):

- Vertical test stand with possibility of changing the operating frequencies (424 MHz, 704 MHz, 852 MHz, 1.3 GHz)
- Vertical test stand for 1.3 GHz elliptical cavity tests
- Horizontal test stand for tests of 3.9 GHz cryomodules
- Horizontal test stand for tests of 1.3 GHz cryomodules
- Coupler test stand

Six vertical cryostats inserts are available in AMTF preparation area. For the EuXFEL purposes all of them could house up to four 1.3 GHz cavities. Nowadays, after rebuilding, following insert configurations are available:

- 2 x R&D inserts with different instrumentation, both for a single 1.3 GHz cavity (single or nine cell)
- 2 x 704 MHz inserts for two ESS cavities at once (shown in Fig 2)
- 1 insert for up to four 1.3 GHz cavities
- 1 insert for up to three 1.3 GHz cavities and one QPR (quadrupole resonator) cavity (cf. Fig 3)

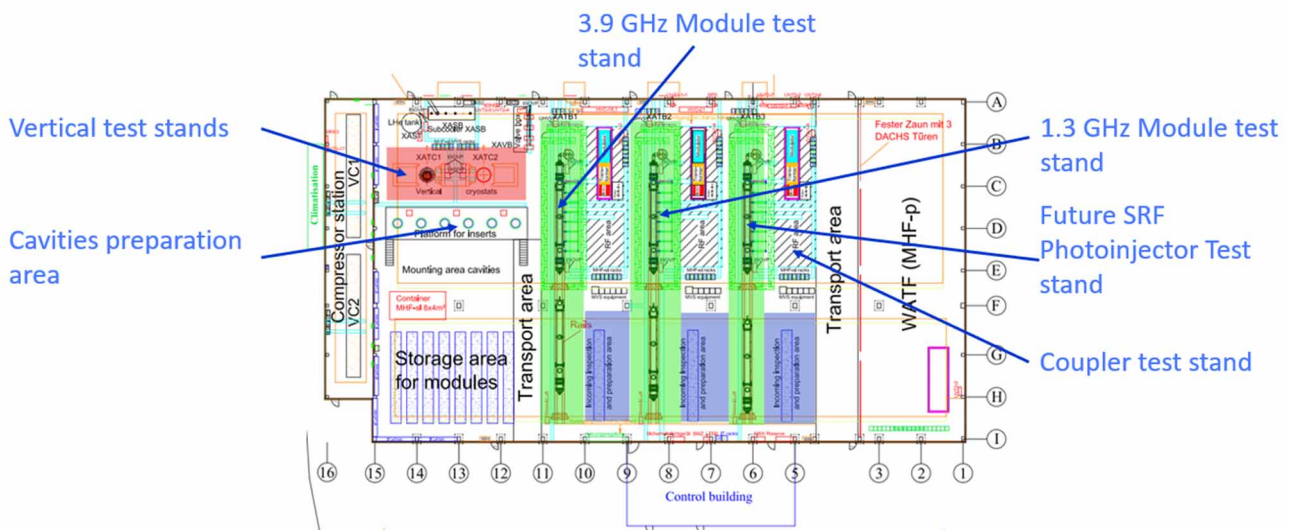


Figure 1: Diagram of the AMTF.

Content from this work may be used under the terms of the CC BY 4.0 licence (© 2023). Any distribution of this work must maintain attribution to the author(s), title of the work, publisher, and DOI

OPTIMISATION OF NIOBIUM THIN FILM DEPOSITION PARAMETERS FOR SRF CAVITIES *

D. Seal^{1†}, G. Burt¹, J. Conlon², O.B. Malyshev², K. Morrow², R. Valizadeh²
Cockcroft Institute, UKRI/STFC Daresbury Laboratory, Daresbury, Warrington, UK

¹also at Engineering Department, Lancaster University, Lancaster, UK

²also at ASTeC, UKRI/STFC Daresbury Laboratory, Daresbury, Warrington, UK

Abstract

In order to accelerate the progression of thin film (TF) development for future SRF cavities, it is desirable to optimise material properties on small flat samples. Most importantly, this requires the ability to measure their superconducting properties. At Daresbury Laboratory, it has been possible for many years to characterise these films under DC conditions; however, it is not yet fully understood whether this correlates with RF measurements. Recently, a high-throughput RF facility was commissioned that uses a novel 7.8 GHz choke cavity. The facility is able to evaluate the RF performance of planar-coated TF samples at low peak magnetic fields with a high throughput rate of 2-3 samples per week. Using this facility, an optimisation study of the deposition parameters of TF Nb samples deposited by HiPIMS has begun. The ultimate aim is to optimise TF Nb as a base layer for multi-layer studies and replicate planar magnetron depositions on split 6 GHz cavities. The initial focus of this study was to investigate the effect of substrate temperature during deposition. A review of the RF facility used and results of this study will be presented.

INTRODUCTION

Superconducting radio frequency (SRF) cavities are typically made from niobium (Nb) because it has the highest critical temperature (T_c) and the highest superheating field (H_{sh}) of any element. These cavities are usually made of bulk Nb. However, given the increasing cost of liquid helium (LHe), electricity and accelerator infrastructure, copper (Cu) cavities coated with thin film (TF) superconductors (SC) is an area of growing attention for the SRF community. One focus of this research is on Nb TFs, because they provide an attractive and economical alternative to bulk Nb cavities. Nb on Cu in comparison to bulk Nb benefits from improved thermal stability as a result of a higher thermal conductivity of Cu. It is also less sensitive to trapped magnetic flux during cooldown, and allows for operation at 4.2 K with lower BCS resistance (R_{BCS}) than bulk Nb.

Nb TF cavities have been used successfully at CERN since the early 1980s having first been installed in the Large Electron-Positron (LEP) collider [1] and most recently on the High Intensity and Energy Isotope mass Separator On-Line facility (HIE-ISOLDE) [2]. Typically, these cavities

have exhibited high quality (Q) factors at low fields comparable with bulk Nb, however they have suffered from high RF losses in medium to high field operation, known as Q -slope. Recent improvements to deposition techniques have produced Nb TFs with RF properties comparable to bulk Nb [3], resulting in improved accelerating gradients (E_{acc}) and significant reduction of the Q -slope. However, more studies are needed to understand the relationship between deposition parameters and RF performance to achieve Q factors comparable to bulk Nb at high field. This demonstrates the importance of mastering TF Nb depositions if Nb on Cu cavities are to be used in facilities requiring high E_{acc} .

The simplest way to develop coating technology is to begin with planar samples prior to full cavity depositions. This allows the use of simple deposition facilities, a low-cost sample design, easy visual inspections before and after, and analysis with surface characterisation instruments. After deposition, the samples have mainly been used for DC superconducting property evaluation. At Daresbury Laboratory, facilities for quick DC analysis of TF samples have existed for many years [4]. These are used to measure, T_c , the residual resistance ratio (RRR), [5] and the field of full flux penetration (B_{fp}) [6, 7]. However, these facilities are unable to analyse the behaviour of films under RF conditions, which is arguably the most important measurement. As a result, a custom facility was developed to measure the average RF surface resistance (R_s) of TF SC samples. Most importantly, the facility has a very high sample throughput of up to 3 per week, allowing for quick optimisation of RF performance [8, 9].

With an RF facility now available for quick sample analysis, optimisation studies of the deposition parameters of Nb TFs can be performed. The coating technique for these TFs has been high-power impulse magnetron sputtering (HiPIMS). This technique can produce higher density plasmas and denser films compared with conventional pulsed DC magnetron sputtering [10]. The ultimate aim is to develop the best parameters to be used as a Nb TF baseline for multi-layer studies. After planar sample deposition, these parameters can be repeated on split 6 GHz, also designed and tested in-house, to analyse TF performance on a cavity-like geometry [11, 12].

The first step to Nb TF optimisation has been the effect of substrate temperature during deposition on RF performance. Previous studies have shown effects on DC properties [10, 13], however limited RF measurements were possible. Ex-

* This work has been supported by: the IFAST collaboration which has received funding from the European Union's Horizon 2020 Research and Innovation programme under Grant Agreement No 101004730.

† daniel.seal@cockcroft.ac.uk

MULTIPACTING PROCESSING IN CRYOMODULES FOR LCLS-II AND LCLS-II-HE*

A. Cravatta[†], T. Arkan, D. Bafia, J. Kaluzny, S. Posen
Fermi National Accelerator Laboratory, Batavia, IL, USA

J. Vennekate, M. Drury, Thomas Jefferson National Accelerator Facility, Newport News, VA, USA
S. Aderhold, M. Checchin, D. Gonnella, J. Hogan, J. Maniscalco, J. Nelson, R. Porter, L. Zacarias
SLAC National Accelerator Laboratory, Menlo Park, CA, USA

Abstract

Multipacting (MP) is a phenomenon which can affect stability in particle accelerators and limit performance in superconducting radio frequency cavities. In the TESLA shaped, 1.3 GHz, 9-cell cavities used in the LCLS-II (L2) and LCLS-II-HE (HE) projects, the MP-band (~ 17 -24 MV/m) lies within the required accelerating gradients. For HE, the operating gradient of 20.8 MV/m lies well within the MP-band and cryomodule testing has confirmed that this is an issue. As such, MP processing for the HE cryomodule test program will be discussed. Early results on MP processing in cryomodules installed in the L2 linac will also be presented, demonstrating that the methods used in cryomodule acceptance testing are also successful at conditioning MP in the accelerator and that this processing is preserved in the mid-term.

MULTIPACTING IN LCSL-II AND LCLS-II-HE CAVITIES

The phenomenon of multipacting (MP) in SRF cavities has been described in many places and one such treatment can be found in Ref. [1]

In the TESLA shaped, 1.3 GHz, 9-cell cavities of the type used in LCSL-II (L2) and LCSL-II-HE (HE) cryomodules (CM), the MP-band is in the range of 17-24 MV/m. This poses a particular challenge to the two projects as cavities will operate at gradients within the MP-band. For HE in particular, the nominal gradient of 20.8 MV/m lies well within this range.

Fermilab has built, tested, and delivered 22 CM for the L2 project and 14 CM are slated for HE. As of this conference, 5 CM, including a prototype, the vCM, have been successfully tested. Details of the vCM testing and the Fermilab CM testing scheme can be found in Ref. [2, 3].

MP IN THE FERMILAB TEST STAND

Of the 40 cavities within the 5 HE CM tested at the Fermilab Cryomodule Test Facility so far, 35 have exhibited MP. It should be noted that of the 5 cavities which did not exhibit MP, 1 of these was limited to well below the MP-band due to field emission (FE). Table 1 shows any occurrence of MP in the 5 CM tested so far: the vCM, the first article CM (F21), and the 3 production CM tested to so far (F22-F24).

*This manuscript has been authored by Fermi Research Alliance, LLC under Contract No. DE-AC02-07CH11359 with the U.S. Department of Energy, Office of Science, Office of High Energy Physics.

[†] cravatta@fnal.gov

Table 1: Occurrence of MP During HE CM Testing

Cavity #	vCM	F21	F22	F23	F24
1	YES	YES	YES	YES	YES
2	YES	NO	YES	YES	YES
3	YES	YES	YES	YES	YES
4	YES	NO	NO	YES	YES
5	YES	YES	YES	YES	YES
6	YES	YES	NO	YES	NO*
7	YES	YES	YES	YES	YES
8	YES	YES	YES	YES	YES

A common signature of MP in the test stand is sporadic quenching in the MP-band and associated radiation spikes as seen in Fig. 3. A quench interlock in the EPICS controls system inhibits RF and produces a fault waveform, with traces of the forward (red), reverse (orange), and transmitted powers (blue) along with a trace of the calculated decay of the transmitted power signal (light blue) to verify a ‘true’ quench (Fig. 1) and not a false signal (Fig. 2).

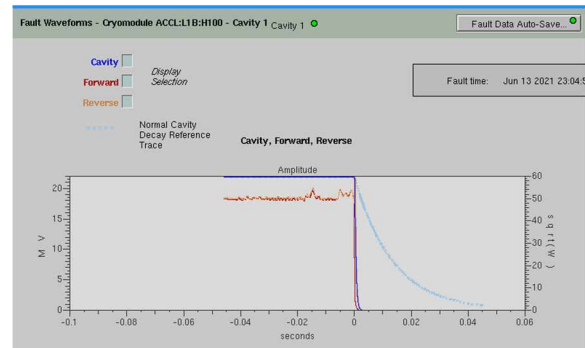


Figure 1: Waveforms showing a ‘true’ quench.

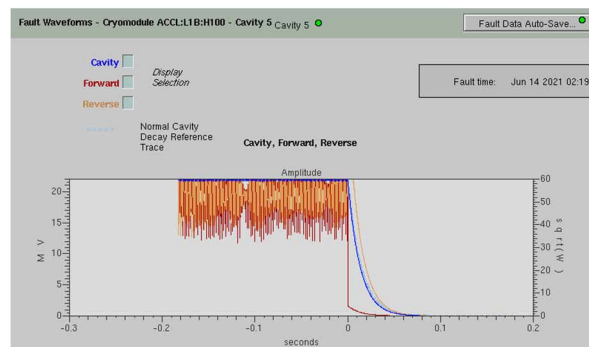


Figure 2: Waveforms showing a ‘false’ quench.

DESIGN STATUS OF BCC CRYOMODULE FOR LCLS-II HE*

C. Narug, T. Arkan, S. Cheban, M. Chen, B. Hartsell, J. Kaluzny, Y. Orlov, V. Kashikhin
Fermi National Accelerator Laboratory, Batavia, IL, USA

Abstract

A Buncher or Capture Cavity (BCC) Cryomodule is currently in development at Fermilab for use in a second injector for LCLS-II-HE. The BCC Cryomodule is designed to contain one 1.3 GHz cavity and one solenoid magnet as part of a 100 MeV low emittance injector. The design considerations for the Cryomodule are similar to the LCLS-II cryomodule with additional requirements to account for additional vacuum loading at the end of this vessel due to the termination of the insulating vacuum. To accomplish this design, the cryomodule is being developed using the experience gained during the development of the LCLS-II cryomodule. The design, analysis, and status of the Cryomodule will be discussed.

PROJECT OVERVIEW

A Buncher or Capture Cavity (BCC) Cryomodule is currently in development at Fermilab for use in a second injector for the High Energy upgrade of the Linac Coherent Light Source (LCLS-II HE). The BCC Cryomodule is designed to contain one 1.3 GHz cavity and one solenoid magnet as part of a 100 MeV low emittance injector. The current design of the vessel can be seen in Fig. 1 and a cross sectional view can be seen in Fig. 2. There are five general regions of the design of the assembly; the cavity, the magnet, internal piping, cryostat shell, and the support stands. The cavity will be the same 1.3 GHz cavity that is used in the LCLS-II HE cryomodules. The magnet that will be used is a combined solenoid, dipole, and quadrupole design. The internal piping, cryostat shell, and support stands will all be designed to be compatible and reuse design aspects of the other LCLS-II HE Cryomodules. The BCC Cryomodule is located at the end of the assembly, it will be required to adapt to some additional loading/design requirements. The piping system is required to be terminated or be recirculated at the end of the vessel. Due to the insulating vacuum, a pressure load will be present at the end of the assembly which will require additional strength in the supports and consideration of load paths. The Cryomodule will also need to be supported on a adjustable stand to for alignment.

SAFTEY REQUIREMENTS

The BCC cryomodule will be installed and be designed to be the safety requirements of Stanford Linear Accelerator Center [1, 2]. Equipment built and tested at Fermilab are also required to meet the Fermilab Environment, Safety and Health Manual [3]. The safety requirements for both laboratories require components to be designed using design codes. The internal piping system will be designed to meet

* Work supported by Fermi Research Alliance, CONF-

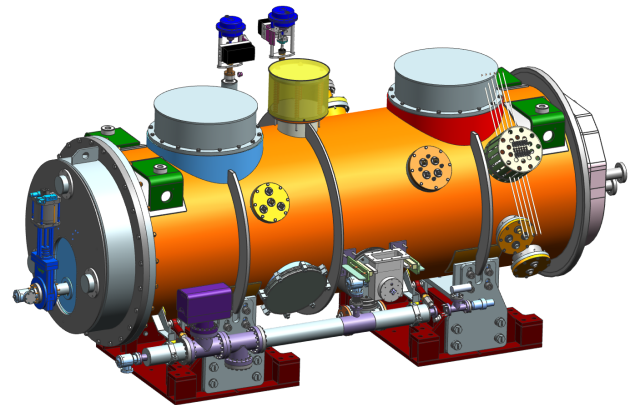


Figure 1: BCC cryomodule.

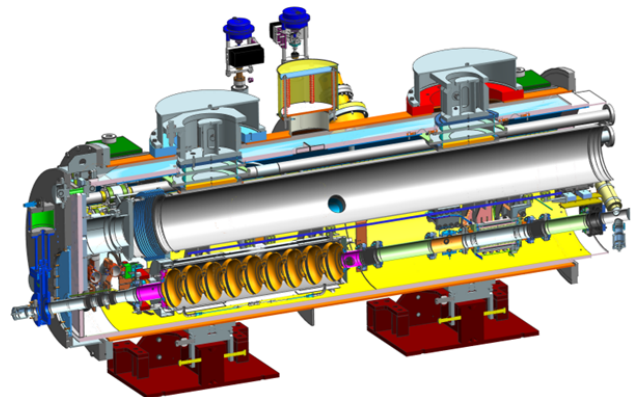


Figure 2: BCC cryomodule cross sectional view.

the requirements of the American Society of Mechanical Engineers (ASME) B31.9 Piping requirements. The main components of the Cryomodule will be designed to meet the ASME Boiler and Pressure Vessel Code (BPVC) Section VIII Division 1 [4] with additional methods used from the ASME BPVC Section VIII Division 2 [5]. The cryomodule stand is be designed to meet American Institute of Steel Construction (AISC) Specification for Structural Steel Buildings [6] while using design by analysis methods to verify components that are outside of the scope of the specification. The cryomodule will also meet the requirements of the American Society of Civil Engineers (ASCE) Minimum Design Loads and Associated Criteria for Buildings and Other Structures [7].

ANALYSIS PERFORMED

In the design of the BCC Cryomodule four sets of analysis that have been performed; a magnet design, a piping analysis for the cryogenic system, a transportation analysis, and structural analysis for the shell and supporting components.

DESIGN OF A CATHODE INSERTION AND TRANSFER SYSTEM FOR LCLS-II-HE SRF GUN*

R. Xiang[†], A. Arnold, S. Gatzmaga, A. Hoffmann, P. Murcek, R. Steinbrueck, J. Teichert
Helmholtz-Zentrum Dresden-Rossendorf, Dresden, Germany

T. Xu, W. Hartung, S-H. Kim, T. Konomi, S. J. Miller, L. Popielarski, K. Saito

Facility for Rare Isotope Beams, Michigan State University, East Lansing, MI, USA

J. Smedley, C. Adolphsen, SLAC National Accelerator Laboratory, Menlo Park, CA, USA

M. Kelly, T. Petersen, Argonne National Laboratory, Lemont, USA

J. W. Lewellen, Los Alamos National Laboratory, Los Alamos, NM, USA

Abstract

Superconducting radio frequency photo injectors (SRF gun) offer advantages for operating in continuous wave (CW) mode and generating high-brightness and high-current beams. A new SRF gun is designed as a low emittance photo injector for LCLS-II-HE and a prototype gun is currently being developed under collaboration between SLAC, FRIB, HZDR and ANL. The aim is to demonstrate stable CW operation at a cathode gradient of 30 MV/m.

One of the crucial components for successful SRF gun operation is the photocathode system. The new SRF gun will adopt the HZDR-type cathode, which includes a cathode holder fixture (cathode stalk) developed by FRIB and a cathode exchange system designed by HZDR. This innovative cathode insertion system ensures accurate, particle-free and warm cathode exchanges. A novel alignment process targets the cathode to the stalk axis without touching cathode plug itself.

To commission the prototype gun, metallic cathodes will be used. A specifically designed vacuum system ensures vacuum pressure of 10^{-9} mbar for transport of a single cathode from the cleanroom to the gun.

INTRODUCTION

The LCLS-II high-energy upgrade aims to enhance the capabilities of the existing LCLS-II by increasing the energy of the electron beam. This upgrade will result in the production of X-rays with higher energy and brightness at the end of the superconducting linac [1]. To achieve this goal, one of the key technologies being employed is a new low-emittance injector [2].

The preferred solution for the low-emittance injector is a low-frequency SRF-Gun (Superconducting Radio-Frequency Gun) [3]. This system enables continuous wave (CW) operation with a high accelerating field and a quasi-DC field across the bunch. Currently, a collaborative project involving FRIB, HZDR, ANL and SLAC is underway to design and prototype a high-field SRF-Gun [4, 5]. The project incorporates a 185.7 MHz Quarter-Wave Resonator (QWR) [6] and a cathode system [7]. This new cathode system will be compatible with high-performance photocathodes operating at either cryogenic temperature

(55-80 K) or warm temperature (300 K). Additionally, the prototype cryomodule will undergo testing with a metal photocathode.

The design requirements for this SRF-Gun are technically demanding. The operation of a QWR SRF-Gun with a cathode field at the 30 MV/m level has not been demonstrated before. Therefore, this project represents a significant challenge in achieving these objectives.

To facilitate precise, particle-free, and warm cathode exchanges, an ingenious cathode insertion system should be designed. We will utilize HZDR's well-established operational expertise with ELBE SRF-Gun [8] and modify the cathode insertion and load-lock system we have developed.

Furthermore, an ultra-high vacuum (UHV) transfer chamber is designed to securely transfer a singular cathode from the clean room to the gun, maintaining optimal cleanliness throughout the process.

The cathode insertion system must fulfill the following requirements: (1) safely and reliably insert a warm cathode into a cold cavity; (2) prevent the introduction of particles into the superconducting cavity; (3) maintain a high-quality vacuum level of less than 10^{-9} Torr ; (3) operate in a safe and reliable manner.

CATHODE AND MANIPULATION

The cathode plug incorporates the HZDR-type cathode shape, featuring a stem diameter of 10 mm and a bayonet structure for easy manipulation. This design offers the advantage of compatibility with various materials and surfaces. Additionally, the bayonet mechanism ensures that the cathode plug can be handled without direct contact with the plug.

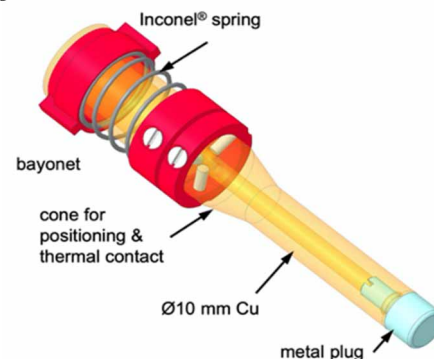


Figure 1: Cathode plug with plug tip, Cu body and bayonet structure.

* Work supported by the US Department of Energy under Contract DE-AC02-76SF00515.

[†] email address r.xiang@hzdr.de

LOADING TEST OF HOM DAMPERS FOR SUPERCONDUCTING CAVITIES FOR HIGH CURRENT AT SuperKEKB

T. Okada*, K. Akai, T. Furuya, S. Mitsunobu, Y. Morita, M. Nishiwaki, KEK, Tsukuba, Japan

Abstract

The design storage current of the electron ring for SuperKEKB is 2.6A which is around twice KEKB achievement. The HOM power of the superconducting cavity is estimated to increase over 35 kW from 14 kW, that is the achievement value at KEKB. The large load is unacceptable for the ferrite HOM dampers mounted on both sides of the cavity. As a countermeasure, the duct-type SiC HOM dampers are installed between the cavities. The load of the downstream ferrite HOM damper decreased because the HOM power is absorbed by the upstream SiC damper. The filling pattern of the beam affects the HOM power. The dependence is caused by the build-up factor of trapped mode that propagates to the LBP side.

INTRODUCTION

SuperKEKB is an energy asymmetric electron-positron collider for the particle physics [1]. SuperKEKB consists of two rings for positron and electron, named as low energy ring (LER) and high energy ring (HER), respectively. Superconducting cavities installed in HER. The design beam currents for LER and HER are 3.6 A and 2.6 A, which are over twice KEKB the typical operating current of 1.6 A and 1.2 A, respectively [2]. The main purpose of accelerator ring for particle physics is to push up the luminosity. SuperKEKB adopts the nano-beam scheme and very high current storage beam towards the goal. The luminosity archived the highest value of 4.65×10^{34} in June 2022 [3,4]. SuperKEKB continues to be upgraded and increase beam current to design value.

The loading power by beam is proportional to the loss factor, beam current, and bunch charge. Bunch charge is not changed from KEKB. On the other hand, the loss factor and beam current are higher than KEKB. The design bunch length of SuperKEKB is 5 mm, which is shorter than KEKB operation value of 6 mm [1,5]. The expected loading higher order mode (HOM) power at SuperKEKB design parameter of 37 kW is over twice of achieved value at KEKB era [1]. This power consumption is as the heat of the HOM damper. Additional power absorbers are installed between the cavities to address this enormous load.

This study shows the two experiments. The first confirms the validity of the SiC damper located between the cavities to increase the beam current [6–9]. The second result shows the fill pattern dependence of HOM power evaluated using an equivalent loss factor.

SUPERCONDUCTING RF CAVITIES AT SuperKEKB

HOM Damped Cavity for SuperKEKB

Electron in HER is accelerated by eight superconducting cavities, and eight ARES cavities that are normal conducting cavities [1, 5]. The superconducting cavity was designed for KEKB, which is the previous high current accelerator project of SuperKEKB. The cavity parameters are shown in Table 1 [10, 11].

Table 1: Superconducting cavity parameters of SuperKEKB. RF Parameters not specified are those for TM010 mode.

Parameters	Unit	Value
Cavity type		single-cell
Material		Niobium (RRR)
Operating temp. (LHe)	K	4.4
Frequency	MHz	508.9
Gap length	mm	243
R_{sh}/Q_0		93
Geometrical factor		251
E_{sp}/E_{acc}		1.84
H_{sp}/E_{acc}	mT/MV/m	4.03
Q_0 at 1.5 MV (6.2 MV/m)		$> 1 \times 10^9$
Operating Q_L $\approx Q_{ext}$ of input coupler		$5.3 - 7.7 \times 10^4$

This cavity focuses on the damping HOM caused by a high beam current and small beam size. Beam pipes of different large diameters are attached to the ends of the cavity and are called a small beam pipe (SBP) and a large beam pipe (LBP), respectively. SBP diameter is 220 mm, the same as the iris diameter of the cavity to propagate the parasitic monopole mode [10]. The diameter of the LBP is 300 mm to propagate the lowest parasitic dipole mode. The propagated HOMs are absorbed by the ferrite damper located outside the cryostat [11, 12]. Feature of superconducting HOM damped cavity at KEKB have already been explained in many past papers such as [7, 10, 11, 13–15].

SiC HOM Damper

Superconducting cavities are located at one straight section of the HER named the Nikko section. Figure 1 shows the layout of the cavities and the additional SiC HOM damper between the cavities [6, 8, 9]. Currently, two additional SiC HOM dampers have been installed to ring.

The cut-off frequencies of 150 mm diameter beam pipe are 1.17 GHz and 1.53 GHz for TE11 mode and TM01 mode, respectively. Therefore, if the frequency of HOM power is

* takafumi.okada@kek.jp

DEVELOPMENT OF A NON-INTRUSIVE LEAK DETECTION METHOD FOR SRF LINACS

P. Pizzol†, V. Morozov, R. Afanador, J. D. Mammosser, D. Vandygriff
Oak Ridge National Laboratory, Oak Ridge, TN, USA
R. Geng, Jefferson Laboratory, Newport News, VA, USA

Abstract

The SNS accelerator has been vital in delivering high-impact research for the world scientific community since 2006, with an availability of 99%. This high availability rate is crucial to the success of the facility, and after 16 years of operations, the aging of the components could start to impact this parameter. To mitigate this, condition-based maintenance can be applied to areas of the LINAC to reduce or nullify the possibility of unwanted events that may damage the accelerator functionality. In this work, we describe the development of a non-intrusive leak detection methodology that verifies the health condition of the cryomodule isolation gate valve seals. In case of a sudden vacuum leak in a warm section between the cryomodules, these valves act as a final line of defense to protect the SRF cavities from atmosphere gases contamination, hence knowing their sealing integrity condition is paramount. Data taken from the machine during different maintenance periods will be presented, together with the analysis done, to verify the robustness of the numerical method vs. the experimental findings.

INTRODUCTION

Particle accelerators have revolutionized scientific research by enabling the investigation of fundamental particles and their interactions at increasingly higher energies. These sophisticated machines, such as the SNS accelerator, have been crucial in delivering high-impact research to the global scientific community since its inception in 2006.

However, as with any complex technological system, particle accelerators are subject to aging, impacting their performance and reliability over time [1, 2].

The aging of particle accelerators can be attributed to several factors. These machines intense and repetitive operation exposes their components to extreme conditions, including high temperatures, intense electromagnetic fields, and mechanical stresses. These conditions can lead to material fatigue, degradation, and wear, affecting the overall functionality of the accelerator. Furthermore, the accumulation of radiation damage in critical components, such as magnets and vacuum systems, can decrease efficiency and increase failure rates.

Predictive-based maintenance strategies are gaining prominence to mitigate aging's impact on accelerator performance. Traditional maintenance approaches, such as time-based or reactive maintenance, are often inefficient and costly, as they rely on fixed intervals or the occurrence of failures. In contrast, predictive-based maintenance aims to optimize maintenance activities by utilizing real-time

data and advanced analytics to predict equipment health and anticipate maintenance needs.

Predictive-based maintenance offers several advantages over traditional approaches [3]. Monitoring the condition of critical components allows for the early detection of potential issues and the implementation of proactive maintenance actions [4]. This approach minimizes the likelihood of unexpected failures, reduces unplanned downtime, and extends the operational lifespan of the accelerator [5-7]. Moreover, predictive-based maintenance can optimize resource allocation by enabling targeted interventions on components that are at higher risk of failure, thus maximizing the efficiency and cost-effectiveness of maintenance activities.

Elastomers used for O-rings in vacuum isolation valves are amongst the more damage-sensitive accelerator components. Isolation valves play a crucial role in preserving the performance of the SRF cavities during maintenance operations or in case of sudden pressure spike events. Radiation encountered during accelerator operation can cause detrimental effects on the o-rings, leading to embrittlement that causes both decay in the seal integrity and the creation of particulate that, if deposited inside the surface of the SRF cavities, can stimulate field emission or arcing, damaging the cavities [8-11].

Assessing the quality of these seals is not an easy task: accessing them requires the warm-up to room temperature of the neighbouring cryomodules and the opening of the beamline, potentially exposing the inner SRF surfaces to more contamination than warranted, so unless deemed extremely necessary, it is not a routine maintenance activity.

The need to be able to evaluate the seals without intrusive actions is what has driven our work presented here. Taking advantage of the scheduled SNS maintenance operations, a numerical analysis is being developed to verify if it is possible to predict which o-rings may be underperforming due to radiation damage.

EXPERIMENTAL SETUP

LINAC Side

We took advantage of the first day of maintenance to perform our study. The methodology was kept the same as the study conducted in August 2022. The vacuum isolation valves that separate the cryomodules from the warm sections between them were closed simultaneously at 8:00 AM. Subsequently, the LINAC SRF cavities temper-

LCLS-II-HE CAVITY QUALIFICATION TESTING

J. T. Maniscalco^{1,2,*}, S. Aderhold¹, T. T. Arkan³, D. Bafia³, M. E. Bevins²,
M. Checchin¹, A. Cravatta³, D. Gonnella¹, A. Grabowski², J. Hogan¹,
J. Kaluzny³, R. D. Porter¹, S. Posen³, C. E. Reece², J. Vennekate²

¹SLAC National Accelerator Laboratory, Menlo Park, CA, USA

²Thomas Jefferson National Accelerator Facility, Newport News, VA, USA

³Fermi National Accelerator Laboratory, Batavia, IL, USA

Abstract

Acceptance testing of the LCLS-II-HE production cavities is approximately 65% complete. In this report, we present details of the test results, including summaries of the quench fields, intrinsic quality factors, and experience with field emission. We also offer an outlook on the remaining tests to be performed.

INTRODUCTION

LCLS-II-HE is an ongoing project to upgrade LCLS-SC, the superconducting part of the X-ray free electron laser at SLAC National Accelerator Laboratory. Among other improvements, the project will extend the linac with 23 additional cryomodules, increasing the target beam energy to 8 GeV. To fill the cryomodules, the project has procured 192 new nine-cell cavities from an industrial supplier in Europe, following the “2N0” nitrogen doping recipe developed during the project’s R&D phase.

The cavity supplier mechanically fabricates the cavities from niobium sheets, processes the surface (including high-temperature furnace treatments, electropolishing, and high-pressure rinsing), installs the liquid helium jacket, and mounts all antennas and accessories required for vertical test. The cavities are shipped under vacuum to the partner laboratories, Fermilab and Jefferson Lab, where they undergo acceptance testing.

Additionally, the project has engaged in an effort to recover spare cavities from the earlier LCLS-II project and remediate them to the LCLS-II-HE performance requirements. The remediation procedures have varied depending on the cavity, with some receiving only high pressure rinse (HPR) and others undergoing electropolishing (EP) or other chemical surface treatments.

The cavities are tested vertically at the partner laboratories at 2.0 K, under static beamline vacuum. The full test procedure and qualification criteria have been reported previously [1]. Key requirements include a peak accelerating gradient $E_{\text{acc}} \geq 23$ MV/m and intrinsic quality factor $Q_0(E_{\text{acc}} = 21 \text{ MV/m}) \geq 2.5 \times 10^{10}$, with no detectable field emission radiation present.

At time of writing, 156 new cavities have been received from the supplier. Of these, 115 have been qualified for assembly into cryomodules, 16 are disqualified, 19 are undergoing HPR, 1 is “on hold” with marginal Q_0 performance,

* jamesm@slac.stanford.edu

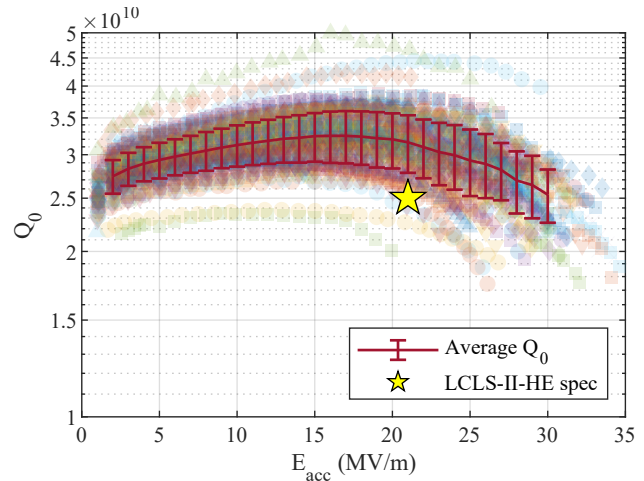


Figure 1: Intrinsic quality factor Q_0 as a function of accelerating gradient E_{acc} for all production LCLS-II-HE cavities without field emission in vertical test (131 cavities). Red error bars show the average Q_0 with a $\pm 1\sigma$ interval, up to an arbitrary limit of 30 MV/m.

and the remainder are awaiting first test. The remediation effort has yielded 12 qualified cavities. In addition, 12 of the disqualified cavities will be reprocessed at the cavity supplier.

VERTICAL TEST RESULTS

The cavities have generally shown strong performance, with a large majority exceeding the qualification requirements. While field emission radiation has been a recurring issue (discussed in further detail below), nearly all unaffected cavities exceed the performance specifications. Figure 1 illustrates the Q_0 vs. E_{acc} results for all cavities without field emission. This includes cavities that had previously exhibited field emission but which were recovered by HPR or otherwise. In total, 120 cavities out of 131 without field emission met all performance requirements; five additional cavities were accepted with accelerating gradient below the nominal threshold for vertical test but above the threshold for cryomodule performance (20.8 MV/m) since they could be matched with high-gradient cavities in cryomodule strings. Four cavities were disqualified due to low quench fields and one was disqualified due to low Q_0 . As mentioned above, one cavity has been temporarily set aside due to its “marginal” $Q_0 = 2.25 \times 10^{10}$: this is below the nominal ac-

CRYOMODULE STORAGE FOR LCLS-II HE*

D. White[†], M. Checchin, D. Gonnella, J. Hogan, J. T. Maniscalco, R. D. Porter
SLAC National Accelerator Laboratory, Menlo Park, CA, USA

Abstract

The Linac Coherent Light Source-II High Energy (LCLS-II HE) project will upgrade the superconducting LCLS-II with 23 additional cryomodules, increasing the beam energy from 4 GeV to 8 GeV. Due to the user schedule of the existing linac, Cryomodules arriving at SLAC cannot immediately be installed in the linac. They are scheduled to be stored for up to three years before the 12 month installation window. During this storage period, the risk of damage to Cryomodules prior to installation will be mitigated with procedures and best practices incorporating experience from LCLS-II.

STORAGE AREA ACTIVITIES

While the LCLS-II HE project plans to install similar equipment used on LCLS-II, the installation window will be much shorter to accommodate SLAC's user schedule. To prepare for this timeline, several changes to the receipt of Cryomodules have been made. Instead of inspecting, preparing, and then immediately installing Cryomodules as they arrive on site, Cryomodules will be delivered to various storage areas where inspection and preparation for final installation will be performed (Figure 1). Cryomodules will be stored in these locations for up to three years.



Figure 1: Cryomodule unload in storage area.

After being shipped from Fermi National Accelerator Laboratory (FNAL) or Thomas Jefferson National Laboratory (JLab), newly arrived Cryomodules have their systems inspected for damage from being shipped across the country. Results are compared to measurements the partner labs made before shipment. Once arrived, the Cryomodule is immediately connected to a vacuum monitor to confirm the beamline vacuum is still intact. Then, a complete physical inspection is performed to check couplers, cryo valve

stems, and sealing surfaces of the outer vacuum flange are all in good condition. Data from shock loggers is analyzed for any shocks above 1.5 g during shipment. Transport fixtures are removed, then an alignment team confirms key fiducials. Cavity tuners, instrumentation, and magnets are all tested to verify correct wiring and functionality. The gauges on the coupler vacuum manifold are connected to a local controller to ensure it remains at an acceptable pressure. Lastly, the insulating vacuum system is tested by installing caps on either end of the Cryomodule, and helium leak checking all joints. The insulating vacuum test is performed last in case electrical connectors may have damaged electronics feedthroughs on instrumentation flanges.

After inspection is finished, the Cryomodule is prepared for installation by removing remaining transportation fixtures (Figure 2) and installing missing heat shield parts behind the tuner access ports. Helium process pipes are cut to their correct lengths for welding as shown in Fig. 3 and actuators are mounted on the cryo valves. The gauge tree and right-angle valve adapter on the beamline are kept on the Cryomodule for the entire length of storage.



Figure 2: Removal of transport fixtures in storage.



Figure 3: Cutting helium process pipes to length.

* Work supported by the United States Department of Energy through the LCLS-II project.

[†] dwhite@slac.stanford.edu

PROVISION OF HIGH BETA CAVITIES FOR EUROPEAN SPALLATION SOURCE BY UKRI-STFC DARESBUURY LABORATORY

A. E. Wheelhouse[†], A. E. T. Akintola, A. J. Blackett-May, M. Ellis, S. Hitchen, P. C. Hornickel,
C. Jenkins, M. Lowe, D. A. Mason, P. McIntosh, K. Middleman, G. Miller, J. Mutch, A. Oates,
S. Pattalwar, M.D. Pendleton, J. O. W. Poynton, I. Skachko, P. A. Smith, N. Templeton,
S. Wilde, J. T. G. Wilson, UKRI-STFC, Daresbury Laboratory, UK
D. Reschke, L. Steder, M. Wiencek, Deutsches Elektronen-Synchrotron, Hamburg, Germany

Abstract

As part of the requirement for the European Spallation Source (ESS) facility in Lund, Sweden, a project has been undertaken by Accelerator Science and Technology Centre (ASTeC) as part of a UK In Kind Contribution to provide 84 704 MHz High-Beta superconducting RF cavities. The project has included the procurement of niobium and the testing of cavities at Daresbury Laboratory and Deutsches Elektronen-Synchrotron, in preparation for integration into the cryomodules which is being performed at Commissariat à l’Energie Atomique et aux Energies Alternatives, Saclay, France. To date all the cavities have been manufactured in industry apart from the final cavity and 3 cavities remain to be tested. An overview of the experiences for the provision of these cavities is described.

INTRODUCTION

Testing of 704 MHz high-beta superconducting RF cavities for the European Spallation Source (ESS) [1] facility in Lund, Sweden started in 2019 with the aim to deliver 84 cavities to Commissariat à l’Energie Atomique et aux Energies Alternatives (CEA) Saclay, France for their integration into 21 cryomodules. The requirements for the cavity have an accelerating gradient of 19.9 MV/m at a quality factor (Q₀) of 5 x 10⁹ (see Table 1).

Table 1: ESS High-beta 704 MHz Cavity

Parameter	Value
Geometrical β	0.86
Frequency (MHz)	704.42
No. of cryomodules	21
No. of cavities per cryomodule	4
Cryomodule length (m)	6.584
Nominal accelerating gradient (MV/m)	19.9
Nominal accelerating voltage (MV)	18.2
Q ₀ at nominal gradient	5 x 10 ⁹

At the beginning of the project for the testing of the ESS high-beta cavities it was estimated that the failure rate of cavities undergoing test would be of the order of 30% and

as such that between 115 and 120 cavity tests would be required. To date 88 out of 89 ESS high-beta cavities (Figure 1) have been fabricated in industry by Research Instruments (RI) in Germany and have been delivered to Daresbury Laboratory and Deutsches Elektronen-Synchrotron (DESY) for qualification testing.

The cavity test set-ups at the 2 facilities are different; DESY test system uses the conventional complete bath immersion and is able to test two 704 MHz cavities in a single run. Whereas in the STFC system the cavities are tested horizontally [2] with the cavities cooled by filling the liquid helium jackets, with the capability of testing three cavities in a single run. Additionally, the setups for the measurement of radiation from the cavities are different; DESY’s facility has monitors positioned at the top and bottom of the test bunker approximately 2 m from the cavities on the vertical centre line, whereas at Daresbury Laboratory radiation detectors are located at either end of each cavity along the beam axis of the cavity approximately 25 – 30 cm from the cavity. As such the radiation measurements at Daresbury Laboratory are much more sensitive, around a factor of 300.



Figure 1: ESS high-beta 704 MHz cavity.

[†] Alan.Wheelhouse@stfc.ac.uk

SURFACE CHARACTERIZATION STUDIES OF GOLD-PLATED NIOBIUM*

S. Seddon-Stettler[†], M. Liepe, T. Oseroff, N. Sitaraman, Z. Sun
 Cornell University (CLASSE), Ithaca, NY, USA

Abstract

The native niobium oxide layer present on niobium has been shown to affect the performance of superconducting RF cavities. Extremely thin layers of gold on the surface of niobium have the potential to suppress surface oxidation and improve cavity performance. However, depositing uniform layers of gold at the desired thickness (sub-nm) is difficult, and different deposition methods may have different effects on the gold surface, on the niobium surface, and on the interface between the two. In particular, the question of whether gold deposition actually passivates the niobium oxide is extremely relevant for assessing the potential of gold deposition to improve RF performance. This work builds on previous research studying the RF performance of gold/niobium bilayers with different gold layer thicknesses. We here consider alternative methods to characterize the composition and chemical properties of gold/niobium bilayers to supplement the previous RF study.

INTRODUCTION

Niobium is a standard choice of superconducting metal for the construction of superconducting radio frequency (SRF) cavities. As cavity fabrication and preparation procedures have improved, resulting in corresponding improvement in cavity performance, the surface properties of the niobium used have become a focus of research and development. Since an RF field excited in a cavity interacts with the cavity most strongly at the surface (within the first few tens of nanometers [1]), changes to the surface can dramatically impact performance of the cavity [2].

The native niobium oxide is the outermost layer present on niobium, and its properties are relevant to RF applications and research. The oxide is thin (less than 10 nm in total) and is dominated by an Nb₂O₅ layer, followed by a layer of NbO₂, then NbO_x ($x \leq 1$) phases [3]. A diagram of the oxide layers, taken from [4], is shown in Fig. 1.

This work is an extension of previous work carried out at Cornell which uses thin gold layers to study changes to surface resistance as a result of replacing the native niobium oxide with a non-oxidizing normal conducting layer. The full extent of that work can be found in [4] and [5]. The goal of the previous work was to study the effect of changes to surface resistance on cavity performance. Rather than trying to manipulate the properties of the niobium oxide directly (a time-consuming and challenging process, owing to the many subtle ways that the oxide can be manipulated through procedures such as heat treatments, chemical treatments,

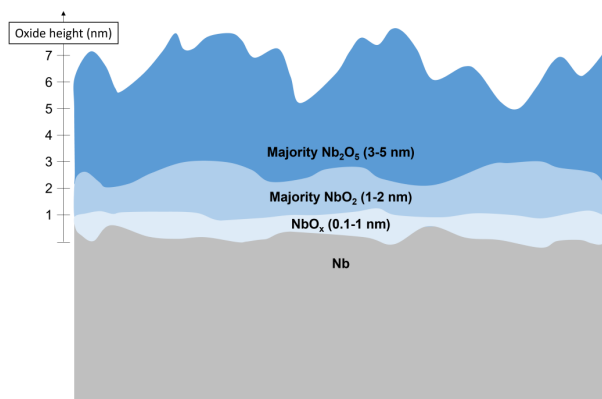


Figure 1: Cartoon of the native niobium oxide structure, taken from [4].

atmospheric environment, and more), the authors aimed to replace the native oxide with a thin layer of gold. Since gold is a non-oxidizing normal conductor that adheres well to niobium even at thin layers, this effectively allows for the isolation of the oxide as an experimental variable. RF performance and surface resistance could then be directly analyzed without concern for the intervening oxide.

In this study, we introduce two main extensions to the original work. The first is the use of X-Ray Photoelectron Spectroscopy (XPS) to study the composition of the surface of the niobium directly. The second is the development of alternative deposition methods for gold on niobium. The use of XPS is explained fully in the **Analysis and Results** section, and the development of alternative deposition methods is explained fully in the **Gold Deposition** section, specifically the *Electroplating* subsection.

GOLD DEPOSITION

Sample Preparation

The samples utilized for this study were 1 cm by 1 cm by 2 mm high-RRR (Residual-Resistance Ratio) niobium samples, which are shown in Fig. 2. The samples were prepared using a standard niobium preparation procedure, consisting of an approximately 75 μ m electropolish, followed by a five-hour ultra high-vacuum bake at 800 $^{\circ}$ C, then a short electropolish of approximately 2 μ m. Following the short electropolish, the samples were loaded into an inert-atmosphere glovebox with a nitrogen atmosphere with less than 3 ppm of oxygen content and less than 5 ppm of water content. The samples were submerged in 1-2% hydrofluoric acid for 30 minutes, then were rinsed with methanol and allowed to dry. Unfortunately, it should be noted that due to technical issues with the glovebox, the oxygen content did fluctuate up to 15-20 ppm of oxygen during the procedure. As this is still superior to atmospheric oxygen content by a

* This work is supported by the National Science Foundation under Grant No. PHY-1549132 (the Center for Bright Beams).

[†] sgs238@cornell.edu

DESIGN AND PROTOTYPING OF THE ELECTRON ION COLLIDER ELECTRON STORAGE RING SRF CAVITY*

J. Guo[†], E. Daly, E. Drachuk, R. Fernandes, J. Henry, J. Matalevich, G. Park,
R. A. Rimmer, D. Savransky, JLAB, Newport News, VA, USA
D. Holmes, K. Smith, W. Xu, A. Zaltsman, BNL, Upton, NY, USA

Abstract

Among the numerous RF subsystems in the Electron Ion Collider (EIC), the electron storage ring's (ESR) 591 MHz fundamental RF system is one of the most challenging. Each cavity in the system will handle up to 2.5 A of beam current and supply up to 600 kW beam power under a wide range of voltage. The EIC R&D plan includes the design, fabrication and testing of such a cavity. In this paper, we will report the latest status and findings of the ongoing design and prototyping of this cavity, including the RF and mechanical/thermal design, fabrication design, and the progress of fabrication.

EIC ESR RF SYSTEM REQUIREMENTS

EIC ESR is a high current electron storage ring required to operate at a wide range of beam energy (5-18 GeV) and beam current (0.23-2.5 A average, with one abort gap) [1, 2]. The project plans to build and install 17 SRF elliptical single cell cavities of 591 MHz in the ESR in a single phase before operation starts, providing up to 10 MW beam power for the electron beam. Although the RF/SRF systems for the B factories (such as KEKB/SuperKEKB and PEP-II [3, 4]) have demonstrated this level of beam power in their High Energy Rings (HERs) and the beam current of 2-3 A in their Low Energy Rings (LERs), the EIC ESR will combine both challenges in one ring, imposing more stringent HOM impedance budget per cavity. The wide range of operation voltage, beam current and synchrotron phase requires a factor of 10-20 variation in Qext to minimize the reflected RF power and suppress the Robinson instability of the beam, if all cavities are operating at the same synchrotron phase.

One possibility is to operate some cavities in reversed or defocusing phase (RPO) for low energy cases. This operation mode can increase the single cavity voltage while keeping the vector sum of voltage the same, reducing the required range of Qext variation. Transient beam loading effects induced by the abort gap in the ring can also be mitigated by the higher stored energy in the RPO, in combination with a low R/Q design. This concept has been demonstrated at SuperKEKB [5], although long term operation has not been proven yet. Table 1 shows that with RPO, it's possible to operate the ESR cavities at fixed Qext of $\sim 2 \times 10^5$ with tolerable reflected RF power. The RF power values in Table 1 are analytically calculated based on CW beam loading using the peak values.

* Authored by Jefferson Science Associates, LLC under U.S. DOE Contract No. DE-AC05-06OR23177, with additional support from U.S. DOE Award Number DE-SC-0019287

[†]jguo@jlab.org

Simulation by T. Mastoridis with the actual beam time structure and direct feedback showed that the peak forward RF power for the 18 GeV case is about the same as the analytical result; for the 10 GeV case the simulated peak is also similar to the analytical CW value with optimum coupling, and a few percent higher than analytical if we double the Qext; for the 5 GeV 2.5 A all focusing case, the simulated peak is about 10% higher when the Qext is close to optimum, but the peak may increase quickly for higher Qext. With the RPO, the extra RF power needed to compensate the transient is significantly reduced in all cases.

The ESR cavity will have two fundamental power couplers (FPC), each powered by a 200 kW SSA will be installed in the initial phase but will upgrade to 400 kW later to provide the full power. Currently we assume that the cavity will have the capability to operate with full beam power under the all focusing mode, so Qext tuning is required in the full power phase.

The baseline of the cryomodule design contains a single symmetric cavity, with beampipes tapered to 75 mm radius to match the largest available gate valve possible to fit in the space available for the ESR. Two single-cavity cryomodules will be arranged in one straight between two quadrupole magnets. We are also studying the possibility to taper the beampipes to 36 mm radius, making it possible to reuse quadrupole magnets retired from APS, which are also more efficient due to the smaller aperture.

The nominal maximum voltage of each ESR cavity is 4 MV, and the gradient is 15.8 MV/m.

Table 1: Estimate of ESR Cavity Power and Qext for Different Operation Cases, Assuming 17 Cavities in Total

Beam energy (GeV)		18	10	5
Beam current (A, exc gap)		0.272	2.72	2.72
Beam current (A, average)		0.25	2.5	2.5
Beam power/cav (kW, pk)		593	628	218
V total (MV)		61.5	21.7	9.84
All Focusing	Vcav (MV)	3.62	1.28	0.58
	Qext per cav	2.0E5	6E4	2.5E4
	Pfwd/cav, kW	614	680	221
RPO, Focus Cav	Vcav (MV)		3.7	2.0
	Qext		2E5	2E5
RPO, Defocus Cav	Pfwd/cav (kW)		650	212
	Vcav (MV)		3.22	2.0
RPO, Defocus Cav	Qext		2E5	2E5
	Pfwd/cav, (kW)		629	212
# of def cav			6	6

Beam power includes synchrotron radiation and HOM losses

DEDICATE SRF CRYOMODULE TEST FACILITIES FOR S³FEL

H. Li[†], C. F. He, W. M. Yue, X.L. Wang, W. Q. Zhang
 Institute of Advanced Science Facilities (IASF), Shenzhen, China

Abstract

Shenzhen Superconducting Soft-X-Ray Free Electron Laser (S³FEL) has been proposed to build a continuous wave (CW) superconducting linear accelerator and produce FEL in the soft X-ray wavelength region. The proposed S³FEL LINAC consists of twenty-eight SRF cryomodules to accelerate beam energy up to 2.5 GeV. Prior to the cryomodules installed in the tunnel, SRF cavities and cryomodules will be conditioned and tested at a dedicate SRF Cryomodule Test Facility (SMTF). The SMTF for S³FEL is currently under design which equipped with two vertical cryostats and three horizontal test benches. R&D work for the SMTF and its corresponding cryomodule assembly procedure is now on going. This paper describes the full set of layout design and implementation of the SMTF for S³FEL project as well as its latest status.

INTRODUCTION

Institute of Advanced Science Facilities, Shenzhen (IASF) is a multi-disciplinary research institute responsible for Shenzhen's large-scale science facilities' whole life cycle planning, construction, operation, and maintenance [1]. So far, one of two active infrastructure projects proposed by IASF, Shenzhen Superconducting Soft-X-Ray Free Electron Laser (S³FEL) is officially approved and is in the stage of designing and construction. S³FEL is a 6-year-construction-period project which will locates in Guangming science city, Shenzhen, China.

S³FEL is a high repetition rate soft-X-ray free-electron laser facility that consists of a CW superconducting linear accelerator, four FEL amplifiers, four beamlines, and eight end stations at the first stage. More beamlines and end stations will add on at next step. Bright electron pulses will be generated efficiently on a photocathode, through the photoelectron effect, using a high-repetition laser. The electron pulses are then accelerated to 2.5 GeV by a superconducting linear accelerator. The high brightness electron pulses are then split and injected into long undulator FEL amplifiers to generate soft X-ray light from 0.5 to 30 nm with extremely high brightness. Figure 1 shows the layout of S³FEL facility.

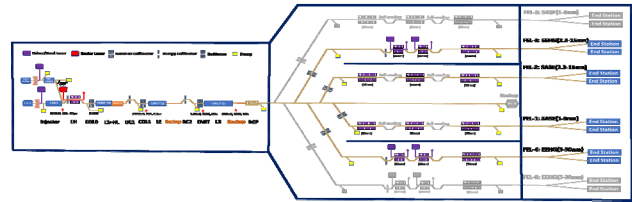


Figure 1: The layout of S³FEL facility.

The photon energy of S³FEL ranges from 40 eV to 1 keV, which covers wavelengths from EUV to soft X-ray with pulse energy up to 500 μJ. The key performance parameters of S³FEL are listed in Table 1.

Table 1: Key Parameters of S³FEL

Parameters	Design Value
Electron beam energy	2,5 GeV
Charge per bunch	200 pC
Bunch Repetition rate	1 MHz
Photon energy	40 eV-1 keV
Pulse energy	500 μJ @1 keV

The development of multiple FEL beamlines will provide abundant opportunities for future scientific research in numerous diverse and important fields, such as quantum materials, energy research, dynamics of biological systems, combustion, atmospheric and interstellar chemistry, frontiers in atomic and molecular physics, as well as new developments in technology. The application of the FEL capabilities towards research and development efforts in these fields will significantly enhance the competitive edge of both academic and industrial institutions in Shenzhen and the greater bay area, and facilitate the development of top research universities, as well as high tech companies.

S³FEL LINAC

S³FEL will use a total of 224 TESLA-type elliptical cavities operating in a CW mode in its superconducting LINAC section, which will be installed in twenty-six 1.3 GHz and two 3.9 GHz cryomodules (with 8 cavities integrated into one cryomodule), in order to accelerate the electron beam up to 2.5 GeV. The overall design of S³FEL LINAC is similar to LCLS II and SHINE facility, which are also CW FEL [2, 3]. Figure 2 shows the layout of the main LINAC.

[†] email address: lihan@mail.iasf.ac.cn

MICROPHONICS IN THE LCLS-II SUPERCONDUCTING LINAC*

R. D. Porter[†], S. Aderhold, L. E. Alsberg, D. Gonnella, J. Nelson, N. R. Neveu, L. M. Zacarias
SLAC National Accelerator Laboratory, Menlo Park, CA, USA
G. Gaitan, N. A. Stilin, Cornell University (CLASSE), Ithaca, NY, USA
A. T. Cravatta, J. P. Holzbauer, S. Posen, Fermilab, Batavia, IL, USA
M. A. Drury, M. D. McCaughan, C. M. Wilson, JLab, Newport News, VA, USA

Abstract

The LCLS-II project has installed a new superconducting linac at SLAC that consists of 35 1.3 GHz cryomodules and 2 3.9 GHz cryomodules. The linac will provide a 4 GeV electron beam for generating soft and hard X-ray pulses. Cavity detuning induced by microphonics was a significant design challenge for the LCLS-II cryomodules. Cryomodules were produced that were within the detuning specification (10 Hz for 1.3 GHz cryomodules) on test stands. Here we present first measurements of the microphonics in the installed LCLS-II superconducting linac. Overall, the microphonics in the linac are manageable with 94% of cavities coming within the detune specification. Only two cavities are gradient limited due to microphonics. We identify a leaking cool down valve as the source of microphonics limiting those two cavities.

INTRODUCTION

The LCLS-II project has recently installed and commissioned 35 1.3 GHz cryomodules (CMs) and 2 3.9 GHz cryomodules at SLAC National Accelerator Laboratory to create a new superconducting linac for the Linear Coherent Light Source (LCLS) [1, 2]. The new superconducting linac will provide 4 GeV electrons for generation of soft and hard X-rays. Each cryomodule contains 8 9-cell TESLA-style elliptical cavities that operate at a nominal accelerating gradient of 16 MV/m.

Microphonics can be a serious issue for superconducting cavities. Small vibrations can cause the cavities to detune (shift the resonance frequency) and if microphonics are large enough there may be insufficient power available to keep the cavity at gradient or the RF controller may not be able to cope with the detuning and lose control of the cavity. Considerable research and development was invested into the LCLS-II cryomodule design to minimize microphonics and ensure a functional linac [3–6]. The design specification for the cryomodules requires that the peak detuning (the largest detune observed during regular operation) be less than 10 Hz for the 1.3 GHz cavities and 30 Hz for the 3.9 GHz cavities. Specifications were met during cryomodule testing, but microphonics have the potential to be worse in the final installed machine. Here we show preliminary microphonics/detuning measurements from the installed LCLS-II cryomodules.

Cryomodule Details

Some details of the cryomodule design are needed to understand the microphonics seen in the cryomodules. The liquid helium vessel and the helium supply circuit are of particular interest to us.

Each cavity in the cryomodule has an individual helium vessel around it. The helium vessel is attached to the “two-phase pipe” via a chimney. The two-phase pipe runs the length of the cryomodule and connects to all 8 cavities. The two-phase pipe does not connect to neighboring cryomodules. The accelerator tunnel has a 0.5% grade, resulting in each cavity having a different “height” of helium above it. Acoustic resonant modes can be excited in these liquid helium vessels.

Liquid helium is supplied to the cryomodule through two main circuits: the Joule-Thomson (JT) valve/line and the Cool Down (CD) valve/line. The JT line and CD line both connect to the helium supply line: a supercritical helium gas line. The JT valve is the helium supply during regular operations and connects to the two-phase pipe. The JT valve is a pneumatic valve and actuates to keep the helium level constant (within tolerances) in the two-phase pipe. Gas (called, “flash”) is produced by the JT valve and can drive microphonics. The CD valve/line is used during fast cool down operations of the linac and connects directly to the bottom of each cavity’s helium vessel. The CD valve should be closed during normal operations of the linac, but due to the position of the line, leaks through the CD valve could produce significant microphonics. JT valve actuation, flash from the JT valve/line, and leaks through the CD line could produce significant microphonics. We find that CD valve leaks are responsible for unmanageable microphonics in some of our cavities.

Machine Layout

Figure 1 shows detuning of the cavities for the entire linac and a schematic layout of the linac. The superconducting linac is divided into 4 sections: L0B, L1B, L2B, and L3B. L1B contains the 2 3.9 GHz modules (HL’s). There are warm beam line sections between each of the superconducting linac sections which contain a variety of equipment which may generate vibrations. In particular, the connection to the cryoplant is located between L2B and L3B, and highway 280 crosses over the accelerator tunnel \approx 1 km past L3B. Nine insulation vacuum pumps are connected to the cryomodules at locations indicated in Fig. 1.

* Work supported by the LCLS-II project.

[†] rdporter@slac.stanford.edu

SRF ACCELERATING MODULES UPGRADE FOR FLASH LINAC AT DESY

D. Kostin[†], S. Barbanotti, J. Eschke, B.v.d. Horst, K. Jensch, N. Krupka, A. Muhs, D. Reschke, S. Saegbarth, J. Schaffran, P. Schilling, M. Schmoekel, L. Steder, N. Steinhau-Kuehl, A. Sulimov, E. Vogel, H. Weise, M. Wiencek, Deutsches Elektronen-Synchrotron DESY, Hamburg, Germany

Abstract

SRF accelerating modules with 8 TESLA-type 1.3 GHz SRF cavities are the main part of the linear accelerators currently in user operation at DESY, FLASH and the European XFEL. For the FLASH upgrade in 2022 two accelerating modules have been exchanged in order to enhance the beam energy to 1.3 GeV. The two modules have been prototype modules for the European XFEL. After reassembly both modules were successfully tested and installed in the FLASH linac. Data taken during the commissioning at the end of 2022 did confirm the test results. This paper presents described efforts and their conclusions since last two years and continues the presentation given at SRF 2021.

INTRODUCTION

The FLASH [1, 2], as well as European XFEL [3, 4] linacs are based on the TESLA SRF technology and are built with accelerating Cryo-Modules (CM) with 8 SRF cavities each. Currently 97 CMs are installed in the European XFEL linac and 7 CMs in FLASH. Before the CM assembly all SRF cavities were tested in the Vertical Cryostat Test (VT) in the Accelerating Module Test Facility (AMTF) at DESY [5]. After the assembly each CM was also tested in AMTF [6, 7]. During the FLASH upgrade in 2022 [8] two old CMs were replaced by new ones – PXM2.1 and PXM3.1.

CM RF TEST RESULTS

The CMs under discussion started as the European XFEL CM prototypes, called PXFEL2 and PXFEL3, went through re-assembly and test sequence as PXM2 and PXM3, with rather disappointing results and were re-assembled again as PXM2.1 (Fig. 1) and PXM3.1 [9]. The CMs SRF cavities are listed in Table 1. The cavities of PXM2.1 belong to an earlier production of FLASH-type cavities, while the PXM3.1 cavities are a part of the European XFEL production.

Table 1: CMs PXM2.1 and PXM3.1 SRF Cavities

Position	PXM2.1 cavity	PXM3.1 cavity
1	AC115	CAV00277
2	AC128	CAV00351
3	AC122	CAV00761
4	Z139	CAV00177
5	Z108	CAV00071
6	AC150	CAV00791
7	Z134	CAV00247
8	AC124	CAV00208

Unexpectedly, both CMs required additional repair after their test at the AMTF: PXM2.1 – cavity 7 probe cable short, fixed with further re-assembly; PXM3.1 – cavity 6 Fundamental Power Coupler (FPC) cold part issue [9], cold part was exchanged in a local clean room in AMTF in June 2021, see Fig. 2, showing the procedure.



Figure 1: Module PXM2.1 in AMTF (March 2022).

[†] denis.kostin@desy.de

INVESTIGATION OF THE MULTILAYER SHIELDING EFFECT THROUGH NbTiN-ALN COATED BULK NIOBIUM *

I. H. Senevirathne^{1,2,†}, D. R. Beverstock^{2,3}, A-M Valente-Feliciano², A. Gurevich¹, J. R. Delayen^{1,2}, Center for Accelerator Science, Old Dominion University, Norfolk, VA, USA

²Thomas Jefferson National Accelerator Facility, Newport News, VA, USA

³Applied Science Department, William & Mary, Williamsburg, VA, USA

Abstract

We report measurements of the dc field onset B_p of magnetic flux penetration through NbTiN-ALN coating on bulk niobium using the Hall probe experimental setup. The measurements of B_p reveal the multilayer shielding effect on bulk niobium under high magnetic fields at cryogenic temperatures. We observed a significant enhancement in B_p for the NbTiN-ALN coated Nb samples as compared to bare Nb samples. The observed dependence of B_p on the coating thickness is consistent with theoretical predictions.

INTRODUCTION

Improving the performance of superconducting radio frequency (SRF) cavities, reducing their high-field Q-slope and increasing the maximum RF breakdown field are key goals of current SRF accelerator R&D. The breakdown field and the high-field Q-slope of Nb cavities is eventually limited by dissipative penetration of superconducting vortices. The high-field performance of Nb cavities can be improved by depositing Superconducting-Insulating-Superconducting (SIS) multilayers [1] which act as barriers for penetration of vortices, allowing the bulk Nb to sustain higher magnetic fields. As a result, SIS structures can increase the accelerating gradients in SRF cavities.

The field of flux penetration, B_p through the SIS structure is an important parameter of merit of the multilayer shielding effect on bulk niobium under high magnetic fields. Recently a dc magnetic Hall probe technique [2] has been developed to measure the penetration field in various materials, including bulk, thin films, and specifically SIS structures. In this work we use this dc Hall probe technique to investigate the effectiveness of NbTiN-ALN coatings on bulk niobium.

SIS MULTILAYER SYSTEM

The SIS multilayer structure consists of alternating thin layers of superconducting and insulating materials deposited on the inner surface of the niobium cavity as shown in Fig. 1.

The SIS structure provides a barrier for penetration of vortices into the bulk superconducting material. The superconducting layers are typically high-transition-temperature (high- T_c) superconductors such as niobium titanium nitride (NbTiN), niobium nitride (NbN) or

niobium tin (Nb₃Sn). Thin superconducting overlayers are separated from a bulk superconductor by thin (a few nm thick) insulator layers which suppress tunnelling of Cooper pairs between superconductors.

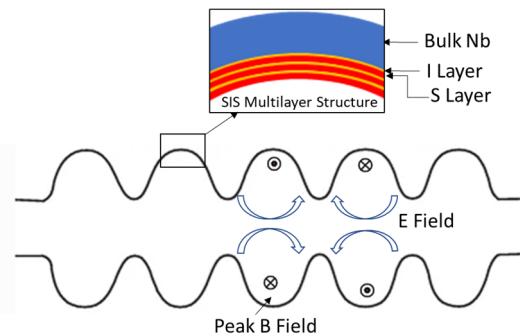


Figure 1: SIS multilayers deposited on the inner surface of the bulk Nb cavity to enhance the peak surface magnetic field and delay the vortex penetration into the cavity wall.

CANDIDATE MATERIALS

The multilayer structures comprising NbTiN and ALN as superconducting and insulating materials are promising candidates for the SIS coating of Nb cavities. Bulk NbTiN has a higher T_c as compared to Nb, and the T_c of NbTiN films can be varied from 8 to 17.3 K by tuning the stoichiometry and the film thickness. In terms of material characteristics, NbTiN offers excellent mechanical properties and robustness. NbTiN has been found to exhibit a particularly low surface resistance at RF frequencies [3], making it a desirable SRF material. Another significant advantage of NbTiN is its compatibility with established fabrication techniques. It can be deposited as a thin film using various deposition methods such as Chemical Vapor Deposition (CVD) like Atomic Layer Deposition (ALD) or Physical Vapor Deposition (PVD) like Direct Current Magnetron Sputtering (DCMS) and High-Power Impulse Magnetron Sputtering (HiPIMS).

Furthermore, ALN is a good insulator with a relatively high thermal conductivity (as compared to Al₂O₃, MgO), which helps transferring the RF heat dissipated in high- T_c overlayers through the Nb cavity wall.

THEORETICAL PREDICTIONS

The magnetic shielding of bulk Nb by SIS structures depends on the thickness of the superconducting overlayers [4, 5]. It was shown that the maximum superheating field $H_{sh}(d)$ of the SIS structure on Nb has a maximum as a function of the overlayer thickness d due to the current

*Work supported by NSF Grants PHY-1734075 and PHY-1416051, and DOE Awards DE-SC0010081 and DE-SC0019399.

† isene001@odu.edu

FRIB DRIVER LINAC INTEGRATION TO SUPPORT OPERATIONS AND PROTECT SRF CRYOMODULES*

H. Ao[†], K. Elliott, D. Jager, S.-H. Kim, L. Popielarski

Facility for Rare Isotope Beams, Michigan State University, East Lansing, MI, USA

Abstract

The driver linac for the Facility for Rare Isotope Beams (FRIB) at Michigan State University includes 324 superconducting radio-frequency (SRF) cavities, and the SRF particle-free beamline spans approximately 300 meters. Protecting the beamlines against contamination is critical to FRIB operations, and thus, various administrative and engineered controls have been put in place to protect the SRF cryomodules and beamlines. These controls include local vacuum interlocks for cryomodule isolation, accelerator-wide interlocks, and software controls to safeguard the cryomodules and beamlines. Meanwhile, efforts are being made to provide training and development programs with the goal of preventing critical failures during maintenance. This paper discusses the measures and approaches used for both system integration to support operations and SRF beamline protection.

INTRODUCTION

The Rare Isotope Beams (FRIB) at Michigan State University (MSU) is a scientific user facility for the Office of Nuclear Physics in the U.S. Department of Energy Office of Science (DOE-SC) and will provide access to rare isotopes based on a high-power superconducting linac. The FRIB driver linac will accelerate stable ion beams (from protons to uranium) to > 200 MeV/u, and at continuous wave beam power up to 400 kW. The primary beam is introduced to a rotating carbon target, the produced secondary fragments are separated by the Advanced Rare Isotope Separator, and the selected isotope is transported to experimental vaults (see Fig.1). The FRIB construction was complete, and user operations has begun since May 2022 [1].

Protecting the beamlines against contamination is critical to FRIB operations, and thus, various administrative and engineered controls have been put in place to protect the SRF cryomodules and beamlines. The locations of beamline gate valves and fast acting valves were defined at the early design phase. During the construction we detailed a local vacuum interlock configuration, started a beamline management program and trained employees according to the progress of the FRIB beamline installation. We have also integrated accelerator-wide interlocks and software controls with operational requirements in keeping with beam commissioning and user operations. This paper discusses the above-mentioned measures and approaches used for both system integration to support operations and SRF beamline protection.

*Work supported by the U.S. Department of Energy (DOE) Office of Science under Cooperative Agreement DE-SC0000661

[†]ao@frib.msu.edu

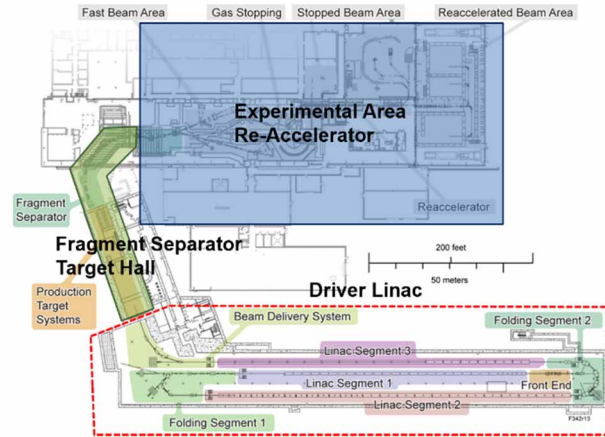


Figure 1: Facility for Rare Isotope Beams at Michigan State University.

ROLES AND RESPONSIBILITIES

In the FRIB laboratory organization, Accelerating Systems Division (ASD) owns and maintains accelerator systems. The ASD Division Director assigns the Segment Manager for each beamline segment (see Fig. 1), and they are responsible for integrated operation. Currently an SRF scientist leads Linac Segments 1, 2 and 3 (LS1, 2, and 3) as the Segment Manager. Two accelerator physics scientists are matrixed and in charge of Front End, Folding Segments 1 and 2 (FS1 and 2), Beam Delivery System taking into preparation for power ramp up.

System Owners and the System Owning Department are assigned to beamline devices. The System Owning Department is responsible to provide operational support. The Linac Vacuum Group within the SRF & Superconducting Magnet Department maintains all the vacuum systems in the driver linac. The group members are experts on SRF particle-free beamline and qualified to operate and maintain all SRF and ultra-high vacuum (UHV) beamlines in the driver linac. Another vacuum group within the Rare Isotope Operations Department separately owns and maintains the beamline vacuum systems downstream in the Target Hall, because the hardware designs and requirements are quite different from the driver linac.

PROTECTION OF SRF CRYOMODULES AND BEAMLINES

Engineered Controls

Cold Cathode Gauges (CCG) monitor vacuum pressures in the cryomodules and the warm boxes. Beamline gate valves are interlocked closed when any CCG reports a pressure higher than $5E-7$ Torr by Programmable Logic

DEVELOPMENT OF NON-DESTRUCTIVE BEAM ENVELOPE MEASUREMENTS IN SRILAC WITH LOW BETA HEAVY ION BEAMS USING BPMs

T. Nishi*, T. Adachi, O. Kamigaito, N. Sakamoto, T. Watanabe, K. Yamada
RIKEN Nishina Center, Wako, Saitama, Japan

Abstract

The Superconducting RIKEN Linear accelerator (SRILAC) has been providing heavy ion beams of a few $p\mu\text{A}$ for the synthesis of new superheavy elements since June 2020, utilizing ten superconducting quarter-wavelength resonators. Although the beam supply has been stable, measurement and control of the beam dynamics in the SRILAC are critical to increasing the beam intensity up to 10 $p\mu\text{A}$. However, destructive monitors cannot be used to avoid generating dust particles and outgassing. So far, the beam has been tuned by monitoring the beam center using Beam Energy Position Monitors (BEPMs) and vacuum monitors. In order to improve the beam control, we are developing a method for estimating the beam envelope by combining the quadrupole moments deduced from BEPMs, which consist of four cosine-shape electrodes, with calculations of the transfer matrix. While this method has been applied to electron and proton beams, it has not been practically demonstrated for heavy ion beams in beta \sim 0.1 regions. By combining BEPM simulations, we are making progress toward reproducing experimental results, overcoming specific issues associated with low beta beams. We will report on the current status of our developments.

INTRODUCTION: SRILAC AND PHASE ELLIPSE MEASUREMENT

SRILAC started the operation in 2020, and it has been providing a stable supply of heavy ion beam with intensity of a few $p\mu\text{A}$ and beam energy of about 6 MeV/u [1, 2]. In the future, the intensity is planned to increase up to 10 $p\mu\text{A}$. SRILAC is also planned for medical isotope production and as an injector for the RI beam factory, where higher beam intensities are required. Precise measurement and control of the beam dynamics are essential to achieve stable operation in high-intensity conditions. However, there are no destructive monitors, such as wire scanners between SRF cavities to suppress dust production and outgassing. The only option to optimize the beam envelope inside the cavities is currently to minimize the vacuum levels between cavities. To estimate the beam dynamics in these sections, we perform Q scan measurement downstream, changing the magnetic field of quadrupole magnets several times and measure the beam profile for each magnetic field to reconstruct the phase ellipse. Based on the estimated phase ellipse downstream of SRF cavities, we can estimate the beam envelope with transfer matrices from the cavity sections to downstream

sections. The disadvantage of the Q-scan method is that we cannot perform the measurement frequently during beam supply to the users because it takes at least 30 minutes and we need temporary to change the magnetic fields. Another restriction of the method is to decrease the beam intensity to \approx 100 enA to avoid melting the wire and generating dust.

Therefore, we started to develop a new phase ellipse measurement method using non-destructive monitors, which can be applied to high-intensity beams and utilized for continuous measurements.

PRINCIPLE OF METHOD

In the new method, the beam envelopes are derived from the beam quadrupole moment $Q \equiv \sigma_x^2 - \sigma_y^2$ at several points in the beamline, which are measured by Beam Energy Profile Monitors (BEPMs), with the transfer matrices between the BEPMs [3]. Figure 1 shows the layout of SRILAC and beamline with 8 BEPMs in between SRF cavities. There are two types of BEPMs: type-A (numbers 1 to 6) with a longitudinal length of 50 mm and type-B (numbers 7 and 8) with a longitudinal length of 60 mm. These detectors were originally introduced to measure beam position and energy and have contributed significantly to the stable beam operation of SRILAC. The beam energy is calculated by measuring the time of flight from the time difference between signals in pairs of each section. Figure 2 shows the CAD model of type-A BEPMs on CST simulation. These BEPMs have cosine-like shape electrodes. This shape realizes the ideal response of the quadrupole moment while maintaining good linear position sensitivity [4]. The value of Q at each of the BEPMs is connected with the phase ellipses upstream using transfer matrices as

$$\begin{pmatrix} Q_1 \\ Q_2 \\ \vdots \\ Q_8 \end{pmatrix} = (\mathbf{H}, \mathbf{V}) \begin{pmatrix} \sigma_{xx}(0) \\ \sigma_{xx'}(0) \\ \sigma_{x'x'}(0) \\ \sigma_{yy}(0) \\ \sigma_{yy'}(0) \\ \sigma_{y'y'}(0) \end{pmatrix} \quad (1)$$

where

$$\mathbf{H} \equiv \begin{pmatrix} (M_{11}^{01})^2, 2M_{11}^{01}M_{12}^{01}, (M_{12}^{01})^2 \\ \vdots \\ (M_{11}^{08})^2, 2M_{11}^{08}M_{12}^{08}, (M_{12}^{08})^2 \end{pmatrix}, \quad (2)$$

$$\mathbf{V} \equiv \begin{pmatrix} -(M_{33}^{01})^2, -2M_{33}^{01}M_{34}^{01}, -(M_{34}^{01})^2 \\ \vdots \\ -(M_{33}^{08})^2, -2M_{33}^{08}M_{34}^{08}, -(M_{34}^{08})^2 \end{pmatrix}. \quad (3)$$

The quadrupole moment can be calculated based on the asymmetry of signal strength of four electrodes reflecting the flatness of

* takahiro.nishi@riken.jp

INSTALLATION OF LCLS-II CRYOMODULES*

D. White[†], S. Aderhold, R. Coy, D. Gonnella
SLAC National Accelerator Laboratory, Menlo Park, CA, USA

Abstract

The Linac Coherent Light Source II (LCLS-II) superconducting accelerator is fully installed and operational. Cryomodules were designed and manufactured by Fermi National Accelerator Laboratory (FNAL) and Thomas Jefferson National Laboratory (JLab) during 2017-2020. From November 2018 through March 2021, SLAC National Accelerator Laboratory installed 37 Cryomodules. Full system cooldown was completed in March 2022.

Installation processes were optimized at SLAC for best quality, especially during particle-free and UHV assembly. These processes and successful Cavity and Cryomodule manufacturing resulted in installed gradient exceeding design requirements by more than 20%. No statistical variation in field emission onsets or magnitudes were observed between manufacturing and site testing. This paper summarizes SLAC experience during installation, and relevant testing results.

CRYOMODULE INSTALLATION PROCESS OVERVIEW

Following delivery to SLAC and acceptance testing, the Cryomodule installation sequence consisted of first rigging Cryomodules onto stands in the SLAC tunnel. Custom dollies were used, which were pulled by an electric tugger at low speeds. To protect sensitive components from tight tunnel clearances during transit, guide rollers kept the Cryomodule couplers at a safe distance from the accelerator tunnel wall. Cryomodules were then rigged onto their stands and aligned to the proper position (Figure 1).



Figure 1: Cryomodule installed in the SLAC tunnel.

Once in place, Cryomodules were then connected, starting with joining helium process pipes together using orbital welding. The joints were verified with visual examination, ultrasonic examination, and helium mass spectrometer leak

check. Once all helium lines were connected and inspected, a pressure test of the entire line served as a final validation of joints. For the pressure test, lines were filled with a mixture of air and helium at a closure weld prior to connecting the Cryomodule string to the Cryo Plant. This allowed the team to stay well away from pressure piping during testing.

Next the particle-free and UHV beamline connection was made with flanges. This was left until validation of helium process pipes was complete to avoid removing components in the event weld repair was needed in an interconnect. This also reduced the risk of work above the beamline causing dents or an uncontrolled vent to the Cryomodule string. After beamline interconnect pieces were installed, helium process pipes are wrapped in several layers of MLI. Lastly, heat shields and a final MLI blanket were installed before the vacuum vessel is closed over the interconnect.

After all Cryomodules in a string were connected, the insulating vacuum was prepared for cooldown with three cycles of pumping and purging with dry nitrogen. After the final purge, turbo pumps were installed to reduce insulating vacuum pressure to meet spec for cooldown.

While all installation steps required cautious handling due to shock sensitivity and exposed parts, the particle-free installation of beamline components was developed with the most care under SLAC's enhanced rigor policy. As the cavity string of the Cryomodules are critical to accelerator performance, beamline installation practices will be looked at in more detail. See Fig. 2 for full process flow diagram.

PARTICLE-FREE TOOLING

Cryomodules were connected to each other and surrounding beamlines with either Beamline Absorbers (BLA) or spool pieces. All particle-free connections of vacuum components must take place in an ISO Class 5 Cleanroom (FED-STD Class 100) or Clean Zone per ISO 14644-1, in the operational state, for 0.5 micron and 5.0 micron particles. Custom tools were developed to manage these conditions and to create a successful installation environment.

Custom Installation Clean Zones

The small amount of space between the Cryomodules and wall of the accelerator housing made an overhead cleanroom impractical for installation. Instead, a custom clean zone was designed to fit underneath the helium process pipes to keep the working area clear of debris and unexpected air currents (Figure 3). With no space to place an air filter above the beamline, the air filter provided laminar air flow from the bottom to the top of the zone. Curtains on either end allowed technicians to reach in from the two sides of the working area. Airborne particle counters were continuously used when beamline components were

* Work supported by the United States Department of Energy through the LCLS-II project.

[†] dwhite@slac.stanford.edu

MEASURING Q_0 IN LCLS-II CRYOMODULES USING HELIUM LIQUID LEVEL

Lisa Zacarias*, S. Aderhold, D. Gonnella, J. Maniscalco, J. Nelson, R. D. Porter
SLAC National Accelerator Laboratory, Menlo Park, CA, USA
A. Cravatta, J. Holzbauer, S. Posen
Fermi National Accelerator Laboratory, Batavia, IL, USA
M. Drury, M. McCaughan, C. Wilson
Thomas Jefferson National Accelerator Facility, Newport News, VA, USA

Abstract

The nitrogen-doped cavities used in the Linac Coherent Light Source II (LCLS-II) cryomodels have shown an unprecedented high Q_0 in vertical and cryomodel testing compared with cavities prepared with standard methods. While demonstration of high Q_0 in the test stand has been achieved, maintaining that performance in the linac is critical to the success of LCLS-II and future accelerator projects. The LCLS-II cryomodels required a novel method of measuring Q_0 , due to hardware incompatibilities with existing procedures. Initially developed at Jefferson Lab during cryomodel acceptance testing before being used in the tunnel at SLAC, we use helium liquid level data to estimate the heat generated by cavities. We first establish the relationship between the rate of helium evaporation from known heat loads using electric heaters, and then use that relationship to determine heat from an RF load. Here we present the full procedure along with the development process, lessons learned, and reproducibility while demonstrating for the first time that world record Q_0 can be maintained within the real accelerator environment.

BACKGROUND

Design and Specifications

Commissioned in 2022, LCLS-II has seen the installation of 37 cryomodels into a part of the tunnel at SLAC that previously housed a decommissioned part of the normal conducting accelerator. Each cryomodel was built with eight nitrogen-doped cavities, each of which has both its own electric heater and helium jacket. Each helium jacket connects via a "chimney" to a two-phase pipe that spans the length of the cryomodel. That two-phase pipe has one liquid level sensor on its upstream end, and one on its downstream end. Because the linac was built on a 0.5% grade, the downstream liquid level sensor always reads higher than the upstream liquid level sensor. Both liquid level sensors read out as % full, from 0 to 100.

Standard LCLS-II operation mandates cryogenic support for rapid changes in total linac amplitude, seen by the cryoplant as drastic swings in RF heat load. This support is only possible when the cryoplant can use cavity Q_0 s to accurately estimate the power being dissipated by the cavities in

order to offset the changes in amplitude by using the cavity heaters. This reliance on Q_0 for our cryogenic control loops, along with potential for Q_0 degradation from trapped flux caused by nitrogen doping, means that we require the ability to measure Q_0 whenever we suspect a change in thermal performance.

Existing Methodology

One of the standard ways to measure Q_0 is to measure the loaded Q (Q_L) and make the approximation that the external Q (Q_{ext}) $\approx Q_0$ in order to use Eq. (1). We are unable to use this method due to the fact that our cavities are very strongly coupled with Q_0 on the order of 10^{10} and Q_L on the order of 10^7 , which instead yields the relationship $Q_L \approx Q_{ext}$ [1].

$$\frac{1}{Q_L} = \frac{1}{Q_0} + \frac{1}{Q_{ext}} \quad (1)$$

Another standard method correlates the rate of helium flow in g/s to cavity heat load, but our cryomodel design did not include the mass flow meters necessary for that measurement [2]. Similarly, the fact that cryomodels cannot be isolated due to shared cryo piping means that we cannot use the method that correlates helium pressure to heat load [3].

Instead, Ed Daly from Jefferson Lab proposed trying to correlate rate of helium *evaporation* to cavity heat load during cryomodel acceptance testing at the Low Energy Recirculator Facility (LERF) in 2019 [4].

DEVELOPING THE PROCEDURE

Our new method relies on the following premise: if the heat load stays constant in a cryomodel, the liquid helium should settle into a steady state where its rate of refill equals its rate of evaporation. The system is built such that the Joule-Thomson (JT) valve maintains the downstream liquid level at a steady value; if the heat load stays constant, the JT should eventually reach a steady position. If we were to find that steady state and then manually set the JT valve to that position so that it is only maintaining the liquid level steady for that one very specific heat load, changing the heat load in any way should cause the liquid level to either rise (if the heat load is lowered) or fall (if the heat load is increased).

If the JT can no longer regulate, the helium should evaporate faster with higher heat loads from the cavity. Given that assumption, the proposal was to use the heaters to introduce known heat loads and see if there was a robust relationship

* zacarias@slac.stanford.edu

PERFORMANCE OF CONTAMINATED SUPERCONDUCTING LINAC AFTER VACUUM EXCURSION*

Z. Yao[†], R.E. Laxdal, TRIUMF, Vancouver, Canada

Abstract

ISAC-II superconducting heavy ion linac is the high energy section of TRIUMF ISAC facility to accelerate rare isotopes with $A/q \leq 6$ from 1.5 MeV/u to above the Coulomb barrier for experiments. There was a vacuum excursion caused by an operational error and the failure of the fast protection system in summer 2022. The beamline downstream to the SC linac was vented with atmosphere air from the experimental hall resulting in pollution of the linac. This paper reports the RF performance of the contaminated linac. The typical cavity performance changes, the average magnitude of degradation, the impact range in the SC linac, the observations in the recovery processes and the analyses on the most distinct cavity are discussed. The cavity refurbishment in the recent winter shutdown with the observations and outcomes is also reported. The ISAC-II event provided a unique data set for the SRF community.

INTRODUCTION

The Isotope Separator and ACcelerator (ISAC) at TRIUMF (see Fig. 1) uses the Isotope Separation On-Line (ISOL) technique to produce rare-isotope beams (RIB) for studies in astrophysics, nuclear structure and reactions, electroweak interactions and material science [1]. RIB production consists of a 500 MeV cyclotron producing a proton driver beam of up to 100 μ A onto one of two thick production targets, an on-line ion source and a mass-separator. The radioactive ions are accelerated in a chain of linear accelerators (linac) consisting of a room temperature RFQ and DTL to an energy of 1.5 MeV/u and a superconducting (SC) linac that adds a further 40 MV to the beam for nuclear physics investigations near the Coulomb barrier.

ISAC-II is the SC section downstream of the normal conducting linac and a S-bend beamline. It accepts RIBs at an energy of 1.5 MeV/u and further accelerates to > 6.5 MeV/u for $A/q = 6$ isotopes or > 16 MeV/u for $A/q = 2$ ions. The SC linac was built in two stages. Phase-I (SCB) consists of five cryomodules. Each cryomodule has four SC quarter-wave resonators (QWR). SCB cavities operate at 106.08 MHz with two optimized beam velocities (β) at 5.7% and 7.1% of the speed of light. Phase-II (SCC) consists of three cryomodules. The first two modules have six QWRs, while the last one has eight QWRs. SCC cavities operate at 141.44 MHz with geometry β at 11%. The operating temperature is 4 K. Cryomodules use a single vacuum design where the RF spaces and the thermal isolation space

share the same vacuum. There are no beam pipe connections between cavities or between the cavity and the vacuum tank.

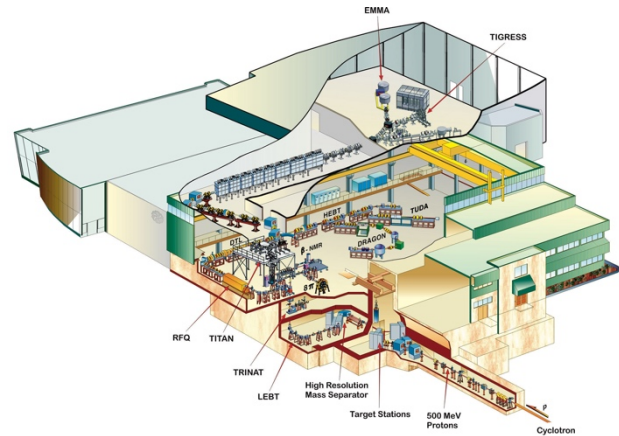


Figure 1: ISAC facility at TRIUMF. The top left corner is ISAC-II accelerator vault with the beam accelerating from left to right. The 8 grey boxes represent the 8 cryomodules. The upstream 5 boxes are SCBs while the downstream 3 boxes are SCCs. The top right corner is the ISAC-II experimental hall.

ISAC-II has been in operation since 2006 [2]. Cavities are specified to provide 1 MV effective voltage each. In the past 5 years, around 37 cavities were available for beam deliveries. The unavailable ones are due to the internal ancillaries' failures with either mechanical or RF reason. The total effective voltage had been improved to 39 MV gradually. The downtime of the beam delivery caused by the RF system and cryomodule failures has been reduced and maintained below 10 hours/year [3].

VACUUM EXCURSION

In June 2022, there was an accidental vacuum excursion caused by an inadvertent opening of a wrong valve such that atmospheric air was sucked into the beamline that was operating at vacuum. The valve location is 19.6 metres downstream of the ISAC-II linac. [4, 5].

Prior to the event, the ISAC-II linac was under vacuum with all isolation valves opened up to the first valve (SEBT1:IV0) on one beamline in ISAC-II experimental hall. IV0 was closed and interlocked. The beamline downstream of IV0 was open to atmosphere for an experimental chamber alignment. When experimenter requested for the line of sight, the interlock of IV0 was bypassed and the valve was opened in error. The beamlines upstream of IV0 was exposed to atmosphere air from the experimental hall.

There is a fast valve on the beamline at about 5 m downstream of the last SCC cryomodule (SCC3) in the accelerator vault, whose purpose is to quickly close to protect cry-

* TRIUMF receives funding via a contribution through the National Research Council Canada

[†] zyyao@triumf.ca

OPTIMIZING GROWTH OF NIOBIUM-3 TIN THROUGH PRE-NUCLEATION CHEMICAL TREATMENTS

S. Arnold*, L. Shpani[†], G. Gaitan, M. Liepe, N. Sitaraman, Z. Sun

Cornell Laboratory for Accelerator-Based ScienceS and Education (CLASSE), Ithaca, NY, USA

T. Arias, Cornell University, Ithaca, NY, USA

Abstract

Niobium-3 tin is a promising alternative material for SRF cavities that is close to reaching practical applications. To date, one of the most effective growth methods for this material is vapor diffusion, yet further improvement is needed for Nb₃Sn to reach its full potential. The major issues faced by vapor diffusion are tin depleted regions and surface roughness, both of which lead to impaired performance. Literature has shown that the niobium surface oxide plays an important role in the binding of tin to niobium. In this study, we performed various chemical treatments on niobium samples pre-nucleation to enhance tin nucleation. We quantify the effect that these various treatments had through scanning electron microscopy and energy dispersive spectroscopy. These methods reveal information on tin nucleation density and uniformity, and a thin tin film present on most samples, even in the absence of nucleation sites. We present our findings from these surface characterization methods and introduce a framework for quantitatively comparing the samples. We plan to apply the most effective treatment to a cavity and conduct an RF test soon.

INTRODUCTION

Niobium-3 tin has great promise for applications in SRF cavities, with a higher critical temperature and the potential for more powerful acceleration in comparison to conventional niobium utilized in SRF particle accelerators. [1–11]. The state-of-the-art growth method of Nb₃Sn in SRF cavities is thermal vapor diffusion, which involves exposing a niobium cavity to vaporized tin and SnCl₂ to high temperatures in a high-temperature vacuum furnace. SnCl₂ has a higher vapor pressure than tin and is used as a nucleation agent at lower temperatures. While tin diffusion-based growth is the only method to date has consistently yielded high-performing Nb₃Sn cavities, there is still much room for improvement for this material to reach its theoretical limits. One key obstacle is achieving a consistently smooth and uniformly thick layer of stoichiometric Nb₃Sn, which is essential for high-performance, reliable cavities [2]. To address this challenge, this research focuses on optimizing the initial stage of this growth process, which involves the nucleation of tin-rich droplets on the oxide surface of the niobium substrate.

Past literature has shown the oxide present on the surface of niobium to be an active catalyst for various chemical processes, with some structures better suited to the binding of

tin than others [12, 13]. Studies have shown that anodizing the niobium substrate prior to coating results in a more dense and uniform nucleation, as well as a smoother final Nb₃Sn film with smaller grains [2, 4]. This further confirms that oxygen plays a crucial role in the diffusion process. Additionally, DFT calculations suggest that acidic solutions which remove OH groups will generate more SnCl₂ binding sites, encouraging a more uniform nucleation [3, 14].

The goal of this study is to alter the niobium oxide through various chemical treatments with varying pH values, aiming to find an optimal treatment which will promote a uniform and dense distribution of tin nucleation sites on the niobium substrate, and thereby minimize the potential for surface roughness and tin depleted regions. This study presents a framework for and results of quantitatively comparing the impact of surface chemistry on the nucleation of tin and thin tin film formation on a niobium substrate.

EXPERIMENTAL METHOD

All samples were electropolished at room temperature and anodized prior to the application of the chemical treatments. Then, each sample, aside from the control, was soaked in prepared solutions for 30 minutes in a nitrogen atmosphere. The control sample had no additional chemical treatment applied after the anodization step. A photo of the samples (except the control) after soaking with labeled chemical treatments and respective pH value is shown in Fig. 1. After soaking, the samples were put in the vapor diffusion furnace for nucleation. For more details on the sample preparation, see Ref. [9]. The coating of the samples was halted after the nucleation step and samples were extracted for surface imaging and characterization.

The surface characterization techniques used are Scanning Electron Microscopy (SEM), and Energy Dispersive Spectroscopy (EDS). We analyzed the SEM images to characterize the formation of nucleation sites, also referenced to as droplets in this paper. EDS analysis of the samples was used to determine the atomic composition of the surface of the samples and to get information on the composition of the droplets, as well as to confirm thin tin film growth on each sample. For all EDS spectra, we used an accelerating voltage of 10 kV. By maintaining a constant accelerating voltage, we can obtain a relative comparison of the ratio of atomic compositions of Sn and Nb among our samples.

We used two types of EDS scans to attain the elemental composition of the samples: point analysis, and area scans. In point scans, the electron beam is focused on a chosen point on the sample, while in the area scans, the beam probes

* sga46@cornell.edu

[†] ls936@cornell.edu

DESIGN OF A 1.3 GHz HIGH-POWER RF COUPLER FOR CONDUCTION-COOLED SYSTEMS*

N.A. Stilin[†], A. Holic, M. Liepe, T. O’Connell, P. Quigley, J. Sears, V. D. Shemelin, J. Turco
Cornell Laboratory for Accelerator-Based ScienceS and Education (CLASSE), Ithaca, NY, USA

Abstract

Cornell is designing a new standalone, compact SRF cryomodule which uses cryocoolers in place of liquid helium for cooling. One of the biggest challenges in implementing such a system is designing a high-power input coupler which is able to be cooled by the cryocoolers without any additional liquid cryogenics. Due to the limited heat load capacity of the cryocoolers at 4.2 K, this requires very careful thermal isolation of the 4.2 K portion of the coupler and thorough optimization of the RF behavior to minimize losses. This paper will present the various design considerations which enabled the creating of a conduction-cooled 1.3 GHz input coupler capable of delivering up to 100 kW CW RF power.

INTRODUCTION

While many particle physics experiments seek high-energy collisions up to the TeV range, there are also important applications for small-scale accelerators operating between 1 and 10 MeV. These applications cover various fields such as environmental sustainability, medicine, national security and industry [1, 2]. Many of these operations would benefit from higher throughput and thus high average beam power (up to 1 MW), which superconducting radio-frequency (SRF) technology is well-suited for. However, established SRF accelerators require liquid helium to cool the cavities during operation. The use of helium requires additional complex and expensive infrastructure which becomes prohibitive for small-scale operations.

New research is examining the feasibility of using cryocoolers in place of liquid helium for cooling Nb₃Sn-coated SRF cavities. Currently available commercial cryocoolers are capable of extracting up to 2.5 W of heat at 4.2 K [3], and improvements in Nb₃Sn cavity performance has resulted in cavities which only dissipate about 1 W of heat while operating continuously at 10 MV/m and 4.2 K [4–10]. Proof-of-principle studies have already been completed at laboratories such as Cornell [11, 12], Fermilab [13] and Jefferson Lab [14], demonstrating the ability to operate conduction-cooled Nb₃Sn cavities at fields relevant to small-scale operations.

To further develop this technology, Cornell is designing a new, cryogen-free standalone cryomodule which only uses two cryocoolers as a cooling source [15]. The combined cooling capacity of the cryocoolers (PT-420RM and PT-425-RM) are 100 W at 45 K and 4.15 W at 4.2 K [3]. The primary

operating parameters of this cryomodule are listed in Table 1. This paper will focus on the recently completed design of the RF input couplers which will be installed in the system. Due to the limited cooling capacity of the cryocoolers, careful attention must be paid to the coupler heat loads at 4.2 K. Here we will discuss how such challenges were addressed and examine the resulting RF and thermal behavior of the couplers.

Table 1: Cryomodule Operating Specifications

Property	Value	Units
Frequency	1.3	GHz
Energy Gain	1	MeV
Max Current	100	mA
Max Power	100	kW

DESIGN CHALLENGES

The design process for the couplers began using the injector couplers from Cornell’s Energy Recovery Linac (ERL) as a baseline. The ERL injector couplers were designed to handle high average power (target 75 kW) with strong coupling to deliver power to a beam with a current up to 100 mA [16]. These properties match very closely to those desired for the new couplers, and thus the design provided an appealing starting point. However, many modifications were required for the couplers to be usable in the new conduction-cooled cryomodule. These can be summarized by the following challenges which were used to guide the design process:

1. Enable up to 100 kW operation (per coupler) while reducing 4.2 K heat load to ~1 W.
2. Remove all fluid cryogenic cooling and replace with conduction-cooling capabilities.
3. Reduce cost by simplifying overall design while maintaining necessary functionality.

The first challenge presented the most significant obstacle to overcome. This restriction indicates that the heat load at 4.2 K must be a factor of about 10⁵ smaller than the targeted forward power. Achieving this required significant optimization of the coupler’s RF design in order to minimize reflections and improve heat load distribution. One implemented solution was the addition of a quarter-wave transformer to each side of the inner bellows. The geometry of this transformer was optimized in order to minimize

* This work was supported by U.S. DOE award DE-SC0021038 “Next Steps in the Development of Turn-Key SRF Technology,” which supports the full development of a conduction cooling based cryomodule.

[†] nas97@cornell.edu

TWENTY YEARS OF CRYOGENIC OPERATION OF THE FLASH SUPERCONDUCTING LINAC

S. Barbanotti[†], E. Abassi, Y. Bozhko, A. Wagner, D. Kostin, K. Honkavaara, K. Jensch, S. Lederer, T. Schnautz, S. Schreiber, H. Weise, Deutsches Elektronen-Synchrotron DESY, Germany
J. Rossbach, University of Hamburg, Hamburg, Germany
J. Zajac, Linde Kryotechnik AG, Pfungen, Switzerland

Abstract

The FLASH superconducting linac is in operation at DESY since more than 20 years. Many changes and upgrades took place to transform a test stand for single cryomodules to a successful free electron laser.

We summarize here the main steps of the FLASH history from the cryogenic point of view including the latest major upgrade that took place in 2022.

We also give an overview of cryomodule performances like cavity gradient and heat load measurements and their evolution over the time.

INTRODUCTION

FLASH [1, 2, 3, 4] is DESY's free-electron laser (FEL) user facility providing ultra-short femtosecond laser pulses in the XUV and soft-X ray wavelength range with unprecedented brilliance. FLASH is a high-gain FEL which achieves laser amplification and saturation within a single pass of a bunch of electrons through a long undulator.

The electron bunches are produced in a laser-driven photoinjector and accelerated by a superconducting linear accelerator. The superconducting techniques allows to accelerate thousands of bunches per second, which is not easily possible with other technologies.

At intermediate energies of 150 and 550 MeV the electron bunches are longitudinally compressed, thereby increasing the peak current from initially 50-80 A to 1-2 kA, as required for the lasing process in the undulator. The beam is then accelerated to 1.35 GeV, passing through a collimation section to scrape of unwanted beam halo.

The beam then enters the undulators. The FEL radiation is produced by SASE (self-amplified spontaneous emission) process. The electrons interact with the undulator field in such a way, that so-called micro bunches are developed. These micro bunches radiate coherently and produce intense X-ray pulses. Finally, a dipole magnet deflects the electron beam into a dump, while the FEL radiation propagates to the experimental halls.

A SHORT HISTORY OF FLASH

FLASH emerged from the TESLA Test Facility (TTF) [5], an international effort to develop superconducting cavities and increase their deliverable accelerating gradient. In February 2000 for the first time worldwide, lasing has been achieved with a SASE FEL at a VUV wavelength of 109 nm. The facility has been substantially upgraded in 2002/2003 and became FLASH.

The commissioning of FLASH started in 2004 and the first lasing (32 nm) was achieved in January 2005. The FEL user operation started in summer 2005. In 2006, FLASH was operated with electron beam energies up to 700 MeV, providing photon wavelengths down to 13 nm. In 2007, the sixth accelerating module was installed, which increased the electron beam energy to 1 GeV, and decreased the achievable photon wavelength down to 6.5 nm. In 2009/2010, the accelerator has again been significantly upgraded being extended by a seventh accelerating module and by four superconducting cavities operating at 3.9 GHz to linearize the longitudinal electron beam phase space. The new configuration pushes the electron beam energy up to 1.25 GeV allowing lasing at 4.1 nm and thus entering into the water window.

In 2012, the construction of a second undulator beamline, FLASH2 has started and finished early 2014. The long trains of electron bunches of FLASH are split in two - such that one part serves the original FLASH1 beamline, the other part the new FLASH2 beamline, both with the 10 Hz repetition rate of the accelerator. This allows to almost double the test time available for scientific experiments.

During a nine-month shutdown in 2021/22, first part of a major upgrade of the overall facility, the FLASH linac was upgraded by replacing two accelerator modules by modern prototype modules of the type used in the European XFEL. They add features already present in most FLASH modules like double row piezo tuning, modern RF couplers, and a waveguide system optimized for better performance and highest energy gain. The new modules increase the energy gain by 100 MeV. A laser heater system has been set-up to reduce micro-instabilities in the electron beam. The second bunch compressor has now a new C-chicane design with a new matching section. The shutdown was also used for refurbishment work, especially for the cryogenic system.

OVERVIEW OF THE FLASH SUPER- CONDUCTING LINAC IN 2023

The SC linac consists of one 3.9 GHz cryomodule with four cavities and seven 1.3 GHz modules with eight TESLA type 9-cell cavities each, in red and yellow respectively in Figure 1. The linac is divided in three sections, injector (one accelerating module and the 3.9 GHz module), a first accelerating section with two 1.3 GHz cryomodules and a second section with the remaining 4 cryomodules; bunch compressors are installed between the different linac sections.

[†] serena.ba rbanotti@desy.de

THE FLASH 2020+ UPGRADE PROJECT

M. Vogt*, E. Ferrari, Ch. Gerth, K. Honkavaara, J. Rönsch-Schulenburg, L. Schaper,
S. Schreiber, J. Zemella, Deutsches Elektronen-Synchrotron DESY, Germany

Abstract

FLASH, the Soft X-Ray and Extreme-UV Free Electron Laser at DESY, is undergoing a substantial upgrade and refurbishment project, called FLASH2020+. The project will finally enable externally seeded and SASE FEL operation for a wavelength range down to 4 nm with the EEHG method. A key ingredient of the upgrade was replacing two early TTF-type L-band RF cryo accelerator modules by modern, high-gradient XFEL-type ones. The beam energy range of the injector has been increased by 100 MeV. This was achieved in the first of two long shutdowns from November 2021 to August 2022. The energy increase together with an afterburner APLE III type undulator for variable circular polarization in the FLASH2 beamline will make it possible to reach the oxygen K-edge (530 eV). This talk will report on the project and the first shutdown with emphasis on the upgraded modules.

FLASH

FLASH [1–7] is a superconducting high-gain vacuum-ultraviolet (VUV) / soft X-ray free-electron laser (FEL), operated mainly as a photon user facility with up to two beamlines operated simultaneously. FLASH is segmented into three functional beamlines: the common injector and linac FLASH0, preparing and accelerating bunch trains suitable for the FEL process, and the two FEL beamlines FLASH1 and FLASH2 which finalize and diagnose the bunch preparation, house the FEL process each in their own internal undulator beamline, and finally dispose of the spent beam in a beam dump. Figure 1 shows a schematic layout of FLASH before the first upgrade shutdown 2021/22. FLASH2 can be disconnected from FLASH0 in a radiation-safety compliant way, so that maintenance on FLASH2 is possible while the FLASH0/1 complex is operated with beam. FLASH1 on the other hand shares the tunnel building with FLASH0 so that FLASH0 and FLASH1 are operationally permanently connected. There is in fact a third experimental beamline (FLASH3) which is extracted from FLASH2 and is placed in the FLASH2 tunnel. The FLASH3 beamline is used by the plasma wake field acceleration experiment FLASHForward [8] which can be activated *alternatively* to FLASH2 by powering a DC dipole. The FLASH accelerating RF is based on L-band (1.3 GHz). The L-band systems except for the RF-gun are superconducting modules of 8 nine-cell niobium cavities. They were designed and built in various stages of the TESLA/TTF/FLASH/XFEL SRF development process [9]. Apart from the L-band modules FLASH includes four more RF systems. The superconducting 3.9 GHz third harmonic linearizer, and three normalconducting RF systems

operated at 2.856 GHz (American S-band) for the transverse deflecting structure (TDS) LOLA [10, 11], 3.0 GHz (S-band) for the beam arrival time compensation cavity BACCA [12], and 12.0 GHz (X-band) for the PolariX TDS [13–16].

At the moment FLASH is undergoing a substantial upgrade and refurbishment project, called FLASH2020+ (see next section). Some sub-projects of FLASH2020+ have already been accomplished 2019-2020, but the major remodeling phases are two long (> 1/2 year) shutdowns. The first shutdown started November 2021 and ended August 2022 successfully and the next, scheduled to start June 2024 and to end August 2025, is being prepared now.

The original FLASH injector (before the upgrade) consisted of a normal-conducting photo-cathode 1.6-cell RF-gun (1.3 GHz), an accelerating superconducting TTF-type L-band module (ACC1), the third harmonic linearizer (ACC39) which contains 4 Tesla-type but scaled down nine-cell niobium cavities operated at 3.9 GHz, the BACCA longitudinal feedback cavity, the first bunch compression chicane, two more TTF-type L-band modules (ACC2, ACC3), and the second bunch compression chicane — at that time an S-type 6-dipole chicane.

The bunches are produced in up to three trains mapped to the three injector lasers. The two “standard lasers” are in operation since almost 15 years and still constitute the backbone of the low-energy part of the injector system concerning stability and reliability. However, it is feared that at some stage they will become non-maintainable. The two standard lasers produce pulses with a Gaussian longitudinal profile with about 4.5 ps and 6.5 ps rms duration. The third “short pulse” laser produces pulses of between 0.8 ps and 1.6 ps rms duration. The beam spots on the CS₂Te cathode are approximately flat circular spots with a typical diameters in operation of 0.7 mm to 2.0 mm for laser 1 and 2 and 0.5 mm to 1.5 mm. The two standard laser are operated in burst mode and each can produce pulse trains of up to 800 μs at 10 Hz with variable pulse repetition rates between 40 kHz and 1 MHz while the third laser is operated in continuous mode and allows to extract arbitrary bunch patterns from a 1 MHz raster.

In its standard setting, the RF-gun is operated with approximately 5 MW and produces a 600 μs flat top. The bunch at the exit of the gun then has a momentum of 5.6 MeV/c¹. It can therefore generate up to 6000 bunches per second (in 10 trains) at 1 MHz bunch repetition frequency and 10 Hz pulse repetition frequency. If the RF pulse is split between two sub-trains (for FLASH1 and FLASH2), a minimum of 70 μs has to be subtracted for transient effect of the extraction kicker and interpolating between the RF parameters of the two flat tops which are (within certain ranges) independent.

* vogtm@mail.desy.de

¹ we know of course that $c \equiv 1$:-)

A THREE-FLUID MODEL OF DISSIPATION AT SURFACES IN SUPERCONDUCTING RADIOFREQUENCY CAVITIES

Michelle M. Kelley, Sean Deyo, Nathan Sitaraman, Danilo B. Liarte, Tomás Arias, James P. Sethna
Laboratory of Atomic and Solid State Physics, Cornell University, NY, USA

Thomas Oseroff, Matthias Liepe

Cornell Laboratory for Accelerator-Based Sciences and Education, Cornell University, NY, USA

Abstract

Experiments on superconducting cavities have found that under large RF fields the quality factor can improve with increasing field amplitude, a so-called “anti- Q slope.” We numerically solve the Bogoliubov-de Gennes equations at a superconducting surface in a parallel magnetic field, finding at large fields there are surface quasiparticle states with energies below the bulk superconducting gap that emerge and disappear as the field cycles. Modifying the standard two-fluid model, we introduce a “three”-fluid model where we partition the normal fluid to consider continuum and surface quasiparticle states separately. We compute dissipation in a semi-classical theory of conductivity, where we provide physical estimates of elastic scattering times of Bogoliubov quasiparticles with point-like impurities having potential strengths informed from complementary *ab initio* calculations of impurities in bulk niobium. We show, in this simple yet effective framework, how the relative scattering rates of surface and continuum quasiparticle states can play a role in producing an anti- Q slope while demonstrating how this model naturally includes a mechanism for turning the anti- Q slope on and off.

INTRODUCTION

Superconducting radio-frequency (SRF) cavities are useful in a variety of modern applications, such as free-electron lasers and particle accelerators [1]. The primary advantage of using superconducting materials over their normal-conducting alternatives is a lower surface resistance, which comes with the benefits of lower operating costs and a lower energy footprint [2]. Despite decades of steady improvements, leading to quality factors in the neighborhood of 10^{10} [1] and accelerating fields up to 25–45 MV/m [2], some open research questions remain. As the accelerating field increases there is often what is referred to as a “ Q slope,” meaning a quality factor that decreases—or, equivalently, a surface resistance that increases—as the accelerating field increases. However, recently some cavities, in particular niobium cavities doped with nitrogen, have been observed to produce a so-called “anti- Q slope,” referring to a quality factor that perplexingly increases with the accelerating field [1]. Further observations of this phenomenon include stronger anti- Q slopes when increasing the resonant frequency of the cavity [3], yet, definitive theoretical explanations for the anti- Q slope remain elusive.

Conventional theories of AC dissipation in superconductors predict quality factors that remain constant as the acceler-

ating field increases, i.e. no Q slope. Mattis and Bardeen [4] applied linear response methods to BCS theory [5] to yield an expression for the complex conductivity of a superconductor subject to a magnetic field. (Here we ignore other sources of dissipation such as trapped magnetic vortices oscillating near the cavity surface [6–8] and within grain boundaries [9, 10].) The result they found was a surface resistance that roughly goes as $\omega^2 \exp(-\Delta/k_B T)$ at low temperatures, where Δ is the superconducting gap and ω is the angular frequency of the oscillating field. Central to these calculations is the idea that a quasiparticle in a state with energy E_1 transitions to a state of energy $E_2 = E_1 + \hbar\omega$ upon absorbing a photon of energy $\hbar\omega$. In order for the photon energy to be well defined the absorption must happen coherently over many cycles of the AC perturbation.

Extensions of the linear-response theory of Ref. [4] have been routinely implemented in order to interpret experimental data exhibiting anti- Q slopes. Applying the Keldysh formalism in the context of non-equilibrium Green’s functions, Gurevich rederived the expression for the conductivity to evaluate the surface resistance at low frequencies, low mean free paths, and high magnetic fields [11]. There, the anti- Q slope originates from the smearing of the quasiparticle density of states in the presence of an oscillating superflow. At high enough fields, the superconducting gap decreases and the density of states smears to weaken the zero-frequency singularity from the Mattis-Bardeen expression, which eventually leads to a field dependent surface resistance. This calculation involves an approximate nonequilibrium quasiparticle distribution function, a key quantity that is difficult to find when working with fundamental theories. Goldie and Withington obtained non-linear solutions to the kinetic equations for the coupled quasiparticle and phonon systems [12]. Later, their solutions for the non-thermal quasiparticle distribution function were combined with the Mattis-Bardeen theory when by de Visser et al. proposed a mechanism for microwave suppression on superconducting aluminum resonators [13].

Though some of these extensions can be used in the regimes of strong fields [11, 14], they conceptualize the notion of $E_1 \rightarrow E_2 = E_1 + \hbar\omega$. At large enough fields, however, we shall see that there are quasiparticle surface-states with energies that change dramatically during each cycle of the AC field. The situation we introduce here is reminiscent of the smeared density of states in Ref. [11], except we include explicitly the depth and time dependence of both the superconducting gap and the quasiparticle states. In

MEASUREMENTS OF THE AMPLITUDE-DEPENDENT MICROWAVE SURFACE RESISTANCE OF A PROXIMITY-COUPLED Au/Nb BILAYER*

T. Oseroff[†], M. Liepe, Z. Sun, CLASSE, Cornell University, Ithaca, NY, USA

Abstract

A sample host cavity is used to measure the surface resistance of a niobium substrate with a gold film deposited in place of its surface oxide. The film thickness of the gold layer was increased from 0.1 nm to 2.0 nm in five steps to study the impact of the normal layer thickness. The 0.1 nm film was found to reduce the surface resistance below its value with the surface oxide present and to enhance the quench field. The magnitude of the surface resistance increased substantially with gold film thickness. The surface resistance field-dependence appeared to be independent from the normal layer thickness. The observations reported in this work have profound implications for both low-field and high-field S.C. microwave devices. By controlling or eliminating the niobium oxide using a gold layer to passivate the niobium surface, it may be possible to improve the performance of SRF cavities used for particle acceleration. This method to reduce surface oxidation while maintaining low surface resistance could also be relevant for minimizing dissipation due to two-level systems observed in low-field low-temperature devices.

INTRODUCTION

The work presented at this conference is detailed in a paper for which we are currently seeking publication [1]. To avoid duplication, this paper will focus on a supplemental analysis regarding the expected thermal quench fields. As discussed in the main paper, the results of this analysis act as a crucial support for some of the work's main conclusions. As this is a supplementary writing, no attempt is made to introduce the details of the main work and the reader is assumed to be familiar with the information in [1].

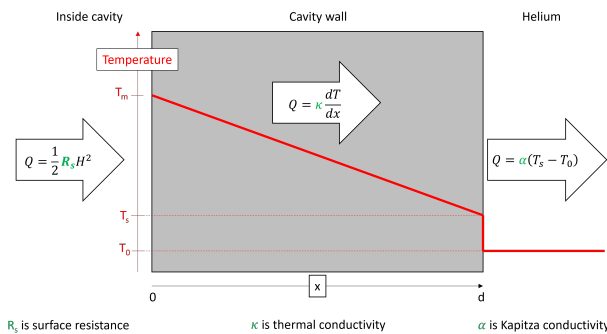


Figure 1: Diagram depicting system considered for model and defining relevant parameters and dimensions.

* Work supported by Center of Bright Beams from the National Science Foundation under Grant No. PHY-1549132

[†] teo26@cornell.edu

MODEL

A thermal quench occurs when the liquid helium surrounding the cavity is unable to adequately remove heating from the inner surface [2]. The physical situation consists of a 3 mm thick niobium bulk with a steady state heat flux, Q , created by an RF field, H , incident on one side and liquid helium cooling on the other. This scenario is demonstrated and relevant dimensions are defined in Fig. 1.

The analysis presented here closely follows that of Ref. [2] to obtain a steady-state estimate of the thermal quench field. Here it is assumed that the inner and outer surface temperatures are not increased substantially beyond that of the bath such that the thermal conductivity and Kapitza conductivity are approximately constant. This is likely not an ideal assumption for the frequencies considered in this work, but is sufficient for an initial consideration. From the steady-state heat flow at the metal-helium interface,

$$\kappa \frac{dT}{dx} = (T_s - T_0) \alpha.$$

All parameters included are defined in Fig. 1. Integrating both sides with respect to x from 0 to d yields an expression for T_s in terms of T_m

$$T_s = \frac{\alpha d T_0 + \kappa T_m}{\alpha d + \kappa}.$$

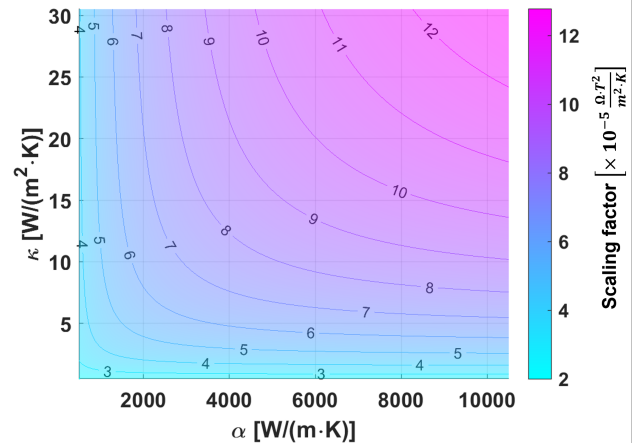


Figure 2: Scaling factor produced for a given combination of Kapitza conductivity and bulk thermal conductivity. Expected values include $\alpha = 1000 - 3000 \text{ W}/(\text{m}^2 \cdot \text{K})$ and $\kappa = 5 - 40 \text{ W}/(\text{m} \cdot \text{K})$ [3–5].

In the steady state, the heat flux into and out of the niobium will be equivalent:

$$\frac{1}{2\mu_0^2} R_s(T_m, B) |B|^2 = (T_s - T_0) \alpha.$$

FIRST RESULTS FROM β -SRF— TESTING SRF SAMPLES AT HIGH PARALLEL FIELD

Edward Thoeng^{1,2,*}, Md Asaduzzaman^{1,3}, R. M. L. McFadden^{1,3}, J. O. Ticknor^{1,4}, P. Kolb¹,
Gerald D. Morris¹, S. R. Dunsiger^{1,6}, D. Fujimoto¹, V. L. Karner¹, R. Li¹, M. Stachura¹,
T. Junginger^{1,3}, R. F. Kiefl^{1,2,5}, W. Andrew MacFarlane^{1,4,5}, R. E. Laxdal^{1,†}

¹TRIUMF, Vancouver, Canada,

²Department of Physics & Astronomy, University of British Columbia, Vancouver, Canada

³Department of Physics & Astronomy, University of Victoria, Victoria, Canada

⁴Department of Chemistry, University of British Columbia, Vancouver, Canada

⁵Stewart Blusson Quantum Matter Institute, University of British Columbia, Vancouver, Canada

⁶Department of Physics, Simon Fraser University, Burnaby, Canada

Abstract

The new β -SRF facility at TRIUMF has recently been commissioned. A new 1 m extension has been added to an existing β -NMR beamline with a large Helmholtz coil to produce fields up to 200 mT parallel to sample surfaces. The β -NMR technique allows depth dependent characterization of the local magnetic field in the first 100 nm of the sample surface making the probe ideal for studying Meissner screening in heat treated Niobium or layered SRF materials. First measurements of Meissner screening at fields up to 200 mT have been analyzed. The results show clear differences in the Meissner screening of baseline treatments compared to mid-T baked (O-doped) Niobium.

INTRODUCTION

The SRF community has been successful at improving the high gradient and high quality factor (Q_0) performance of Niobium through empirically developed heat treatments in vacuum or with small concentrations of doping agents. The most successful recipes have been repeatable at multiple labs and also in industry. Future projects like the ILC require performance at high gradient to reduce costs. The development of robust recipes and processes is a critical goal of the present development. Researchers are also pursuing thin films and layered structures [1, 2] in order to either reduce the cost of Nb or increase the performance or operating temperature.

Niobium is a marginal Type-II superconductor. Raising the applied field past a critical value, B_{c1} leads to a mixed state in which an increasing amount of magnetic flux penetrates the material in quantized flux vortices. At a second critical field strength, B_{c2} superconductivity is destroyed. However, above B_{c1} a metastable state persists up to the superheating field, B_{sh} allowed by a surface energy barrier that inhibits vortex nucleation. As RF fields increase in amplitude, magnetic vortices with normal cores can nucleate in the near surface and RF losses, hence surface heating, occurs. For high gradient performance we need a material that

can withstand vortex penetration up to a high peak magnetic field.

The intrinsic performance of SRF cavities is determined by the first 100 nm of the inner cavity surface, where RF currents flow with a length scale characterized by the London Penetration Depth. Cavity treatments impact the near-surface nanostructure in the first hundreds (or less) nanometers of the Niobium surface to improve Q_0 or gradient or both. The strategy moving forward will be to engineer a surface layer on bulk Nb to reproducibly optimize the performance beyond pure Nb. Thin film research and theory are continuing in parallel with work on NbN, Nb₃Sn, MgB₂ and Superconductor-Insulator-Superconductor (SIS) [1, 2] layers.

Investigations of new treatments and new materials would benefit from a diagnostic that provides details of the magnetic screening within the near surface. Ideally the probe should be able to diagnose the detailed magnetic screening near the critical fields which for Niobium is in the range of 200 mT. DC magnetic fields applied both perpendicular and parallel to the sample surface have been used as analogues of cavity operating conditions to characterize SRF materials with respect to the field of first flux penetration [3].

Perpendicular fields result in highly non-uniform surface fields when the sample is in the Meissner state, with flux accentuated at sample edges. Parallel fields on flat samples or ellipsoid samples provide near uniform surface fields up to the field of first flux penetration. Measurements typically record the maximum local surface field (based on the applied field and the sample geometry) that can be reached before flux is detected in the bulk. Such measurements do not provide local details of the role of the surface layer(s) in the field of first flux entry. Given the interest in layered structures and their precise role in enhancing the field of first flux entry, a diagnostic that provides the depth-resolved information of field attenuation through the London layer would provide new insight.

Facilities like β -NMR [4–6] (TRIUMF) and LE-muSR [7] (PSI) that use ⁸Li⁺ ions or low energy muons respectively have been limited to <30 mT parallel field on the sample as the transverse fringe field from the applied

* ethoeng@triumf.ca

† lax@triumf.ca

STUDY OF THE DYNAMICS OF FLUX TRAPPING IN DIFFERENT SRF MATERIALS

F. Kramer*, S. Keckert, O. Kugeler, J. Knobloch¹, Helmholtz-Zentrum Berlin, Berlin, Germany
T. Kubo², High Energy Accelerator Research Organization (KEK), Tsukuba, Japan
¹also at Universität Siegen, Siegen, Germany
²also at The Graduate University for Advanced Studies (Sokendai), Hayama, Japan

Abstract

A dedicated experimental setup to measure magnetic flux dynamics and trapped flux in samples is used to precisely map out how trapped flux is influenced by different parameters. The setup allows for rapid thermal cycling of the sample so that effects of cooldown parameters can be investigated in detail. We show how temperature gradient, cooldown rate, and the magnitude of external field influence trapped flux in large-grain, fine-grain and coated niobium samples. The detailed measurements show unexpected results, namely that too fast cooldowns increase trapped flux, large-grain material traps flux only when the external field is larger than a temperature gradient dependent threshold field, and the measured dependence of trapped flux on temperature gradient does not agree with an existing model. Therefore, a new model is presented which agrees better with the measured results.

INTRODUCTION

When type-I superconductors are cooled below their transition temperature a fraction of the surrounding magnetic field can be trapped in the form of quantized magnetic flux lines. The radio frequency (RF) field induced in superconducting radio frequency (SRF) cavities cause these flux lines to oscillate back and forth which dissipates power. This limits the performance of modern SRF cavities which is why they are operated in permalloy shields to reduce the earth's magnetic field. However, it is impossible to completely shield of all magnetic fields. Therefore, research is ongoing on how to improve flux expulsion in SRF cavities.

Experiments investigating trapped flux are done using either cavities or samples. Experiments using cavities have the advantage that cooldown parameters like temperature gradient during cooldown and cooldown rate can be influenced in certain limits and the increased surface resistance due to trapped flux can be measured. They have the disadvantage that experiments are very time consuming so only few data points can be recorded and they have a complex geometry which makes applying treatments more difficult compared to samples [1]. Experiments using samples like magneto optical imaging (MOI) make use of smaller samples but the experiments, so far, are limited in the adjustability of the cooldown parameters. Additionally, the magnetic flux

density required for MOI is in the range of mT, whereas the earth's magnetic field is $\approx 50 \mu\text{T}$.

Therefore, an experimental setup was designed at HZB which measures trapped flux in flat, rectangular samples. It allows for fast thermal cycles (≈ 300 per day) and independent control of the cooldown parameters of temperature gradient across the sample during cooldown, cooldown rate, and external magnetic field. This enables the dependencies of trapped flux on these parameters to be mapped out in more detail compared to cavity measurements. Additionally, the geometry of the samples is simpler so different materials and treatments can be tested more easily, and the impact of geometry is easier to understand.

Besides the developed setup we present data gathered with different samples showing how trapped flux is influenced by temperature gradient during cooldown, cooldown rate, and external magnetic field. Finally, a phenomenological model is developed describing the dependency of trapped flux on temperature gradient and external magnetic field.

EXPERIMENTAL SETUP

Experimental Infrastructure

The experiments are conducted in a small glass cryostat which is filled via a transfer line from a helium dewar. Figure 1 shows a picture of the cryostat with two rectangular Helmholtz-coil pairs attached to the holding frame and a solenoid wrapped around the aluminum housing of the cryostat. Since the cryostat has no permalloy shielding these coils are necessary to compensate the surrounding magnetic field. With these coils and an iterative compensation scheme the flux density at the position of the reference sensors is compensated below 15 nT. COMSOL Multiphysics [2] simulations suggest a field flatness in the sample volume of 0.8% for the solenoid coil and $<0.1\%$ for the Helmholtz-coil pairs. With the current power supplies a maximum field of $180 \mu\text{T}$ can be achieved in each direction.

Setup to Measure Flux Trapping in Flat Samples

The design of the setup follows two main goals: The first is to control the cooldown parameters of temperature gradient, and cooldown rate independently of each other. The second is to perform temperature cycles through the critical temperature quickly, so many data points can be recorded. Additionally, the sample geometry should be simple, so that geometric effects are easier to isolate and treatments are easy to apply. Furthermore, the sample should be large enough so that the measurements are not

* f.kramer@helmholtz-berlin.de

DEMONSTRATION OF NIOBIUM TIN IN 218 MHz LOW-BETA QUARTER WAVE ACCELERATOR CAVITY*

T. B. Petersen[†], M. P. Kelly, T. Reid, M. Kedzie, B. Guilfoyle, G. Chen
 Argonne National Laboratory, Lemont, IL, USA

S. Posen, B. Tennis, G. Ereemeev, Fermi National Accelerator Laboratory, Batavia, IL, USA

Abstract

A 218 MHz quarter wave niobium cavity has been fabricated for the purpose of demonstrating Nb₃Sn technology on a low-beta accelerator cavity. Niobium-tin has been established as a promising next generation SRF material, but development has focused primarily in high-beta elliptical cell cavities. This material has a significantly higher T_C than niobium, allowing for design of higher frequency quarter wave cavities (that are subsequently smaller) as well as for significantly lowered cooling requirements (possibly leading to cryocooler based designs). The fabrication, initial cold testing, and Nb₃Sn coating are discussed as well as test plans and details of future applications.

INTRODUCTION

Niobium-tin (Nb₃Sn) has been identified as the most promising next-generation superconducting material for accelerator cavities. The main reason for this choice is the higher critical temperature (T_C = 18.3 K compared to 9.2 K for pure niobium), which corresponds to a significantly lower surface resistance for a given temperature and frequency. This is a consequence of the dependence of the Bardeen-Cooper-Schrieffer (BCS) resistance on material characteristics like critical temperature T_C among others [1]. The relationship between frequency, critical temperature, operating temperature, and R_{BCS} (which is inversely proportional to RF power losses/cryogenic load) is illustrated in Figure 1 below (generated using SRIMP code) [2].

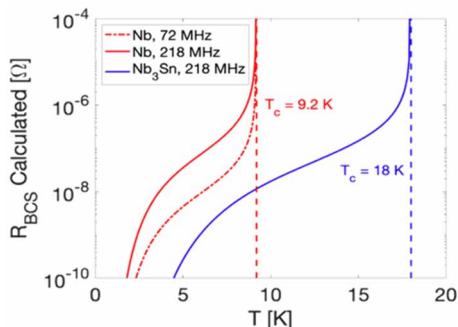


Figure 1: Predicted BCS surface resistance of Nb and Nb₃Sn vs operating temperature for two frequencies.

*This material is based upon work supported by the U.S. Department of Energy, Office of Science, Office of Nuclear Physics, under contract number DE-AC02-06CH11357, and the Office of High Energy Physics, under contract number DE-AC02-76CH03000. This research used resources of ANL's ATLAS facility, which is a DOE Office of Science User Facility.

[†]tpetersen@anl.gov

The incentive for utilizing Nb₃Sn is two-fold: drastically reduce the size of low-beta cavities for fabrication as well as the operational cooling requirements. This could lead to cryo-cooler based stand-alone cryomodules a fraction of the physical size of previous generations, with the cavity scale shown in Figure 2.

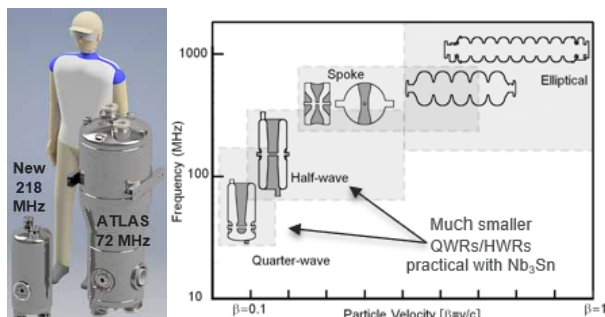


Figure 2: Physical scale of 218 MHz cavity compared to similar geometry 72 MHz cavity in ATLAS. This technology could expand the useful range of different cavity geometries.

CAVITY DESIGN AND FABRICATION

The cavity design was aimed at demonstrating a useful low-beta cavity near 200 MHz and with a peak magnetic field of 60 mT. The frequency was chosen as a multiple of the ATLAS clock, with the goal of installing two of these 218 MHz cavities in ATLAS. Cavity EM parameters are shown below in Figure 3 [3].

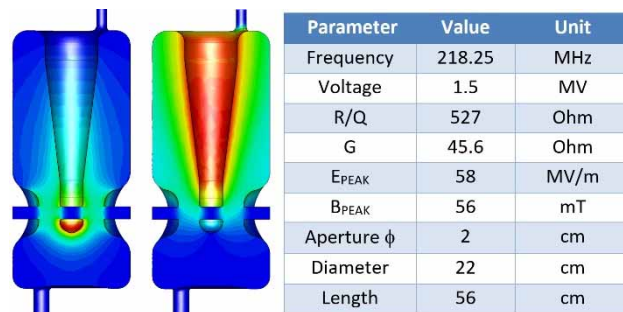


Figure 3: Cavity field distributions and EM parameters.

MODELLING TRAPPED FLUX IN NIOBIUM

F. Kramer*, S. Keckert, O. Kugeler, J. Knobloch¹, Helmholtz-Zentrum Berlin, Berlin, Germany
 T. Kubo², High Energy Accelerator Research Organization (KEK), Tsukuba, Japan
¹also at Universität Siegen, Siegen, Germany
²also at The Graduate University for Advanced Studies (Sokendai), Hayama, Japan

Abstract

Detailed measurements of magnetic flux dynamics and trapped magnetic flux in niobium samples were conducted with a new experimental setup that permits precise control of the cooldown parameters. With this setup the dependency of trapped flux on the temperature gradient, external magnetic field, and cooldown rate can be mapped out in more detail compared to cavity measurements. We have obtained unexpected results, and an existing model describing trapped flux in dependence of temperature gradient does not agree with the measured data. Therefore, a new model is developed which describes the magnitude of trapped flux in dependence of the temperature gradient across the sample during cooldown. The model describes the amount of trapped flux lines with help of a density distribution function of the pinning forces of pinning centers and the thermal force which can de-pin flux lines from pinning centers. The model shows good agreement with the measured data and correctly predicts trapped flux at different external flux densities.

INTRODUCTION

When superconductors transition to the Meissner state all magnetic flux is expelled in an ideal case. However, in experiments it is observed that some fraction of the external magnetic field gets trapped inside the superconductor in form of quantized magnetic flux lines. For the application of superconducting radio frequency (SRF) cavities this trapped flux increases the losses in the cavity wall. For this reason cavities are operated in shielded cryostat which reduce the earth's magnetic field. It is, however, impossible to completely shield off all magnetic field. For this reason research on how to reduce trapped flux is ongoing.

At this point the mechanism of flux trapping is not yet fully understood which makes it difficult to find treatments which effectively reduce flux trapping. To help understand the mechanism we conducted dedicated flux trapping experiments using samples. The experimental setup and the key findings are presented in these proceedings under TUCXA01. In this work the focus lies on a theoretical model which is developed on the basis of the data gathered during these experiments.

The model describes the magnitude of trapped flux with help of a density distribution function $n(f_p)$ which describes the probability of a flux line to interact with a pinning center with pinning force f_p . Whether a flux line gets trapped depends on the thermal force [1] which acts on the flux line. If it is larger than the pinning force the flux line gets pushed

over the pinning center and is expelled. If it is smaller than the pinning force the flux line gets pinned and is trapped inside the superconductor.

In the course of this work the gathered data is first compared to an existing model [2] which does not show good agreement. Then the idea of the new model is introduced which is then refined in a next step. Finally, the refined model is applied to the data, and the resulting prediction of trapped flux is compared with measurements.

APPLYING THE EXISTING MODEL

Figure 1 depicts measurement results of trapped flux versus temperature gradient during cooldown (∇T). To measure this curve an external magnetic flux density of $100 \mu\text{T}$ is set perpendicular to the samples surface during all cooldowns. The cooldown rate is kept constant as well, and only the temperature gradient is changed for each cooldown. The results shown here are recorded with a large grain sample. This sample consists of only two niobium grains (RRR=300) with a grain boundary running through the middle of the sample. The dimensions are $(100 \times 60 \times 3) \text{ mm}^3$. A model describing the flux trapping mechanism is developed by T. Kubo in Ref. [2]. This model predicts a dependency of trapped flux on the temperature gradient during cooldown that is proportional to $(\nabla T)^{-1}$. Therefore, a fit according to $a/\nabla T + b$ is performed with the data in Fig. 1. The result is also depicted in Fig. 1 in red.

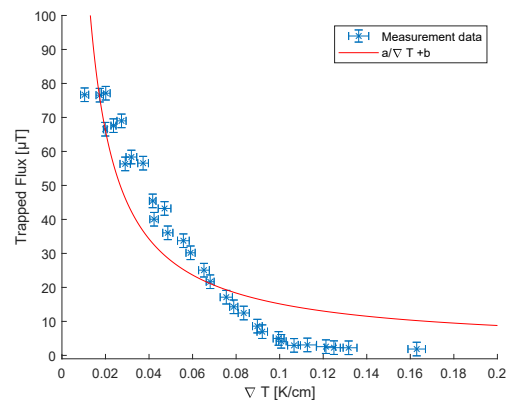


Figure 1: Measurement data of trapped flux versus temperature gradient during cooldown. The data is obtained using a large grain sample consisting only of two grains (sample dimension: $(100 \times 60 \times 3) \text{ mm}^3$). Additionally, a fit according to the prediction in Ref. [2] is performed and the result is depicted in red.

* f.kramer@helmholtz-berlin.de

PROGRESS ON ZIRCONIUM-DOPED NIOBIUM SURFACES*

N. S. Sitaraman[†], G. Gaitan, T. Oseroff, Z. Baraissov, Z. Sun, D. Muller, T. A. Arias, M. U. Liepe

Department of Physics, Cornell University, NY, USA

Abstract

The first experimental studies of zirconium-doped surfaces verified that zirconium can enhance the critical temperature of the surface, resulting in a lower BCS resistance than standard-recipe niobium. However, they also produced a disordered oxide layer, resulting in a higher residual resistance than standard-recipe niobium. Here, we show that zirconium-doped surfaces can grow well-behaved thin oxide layers, with a very thin ternary suboxide capped by a passivating ZrO₂ surface. The elimination of niobium pentoxide may allow zirconium-doped surfaces to achieve low residual resistance.

INTRODUCTION

Work on niobium-zirconium alloys as SRF materials began very recently as of this writing. Researchers in the Hennig group at the University of Florida and in the Arias group at Cornell independently identified the Nb-Zr system as a promising candidate material, which then helped motivate the development of the first niobium-zirconium surface alloy recipes at Cornell by Dr. Zeming Sun. The research quickly became even more interesting when experimental results not only showed the anticipated elimination of niobium oxide and formation of a bcc alloy, but also higher T_c 's than had previously been measured for this system. Specifically, multiple samples exhibited a T_c in the 13-16 K range, compared to the maximum of just under 11 K in reported literature [1].

There is much still to understand about the superconductivity of zirconium-doped niobium. In particular, ongoing theory work has explored the potential effects of alloy ordering and carbon contamination on T_c in the Nb-Zr system [2, 3]. In this short proceeding, however, we will focus on the effects of zirconium doping on the oxide surface. The first zirconium-doped sample to undergo RF testing utilized an electrochemical process, which resulted in a thick, disordered surface oxide and a relatively high residual surface resistance [1]. Here we show that sputter deposition of very thin zirconium layers on niobium followed by vacuum baking can produce a thin, zirconium-rich surface oxide. Notably, we show that it is possible to completely eliminate the niobium pentoxide from the surface. The result is a niobium surface terminated by a passivating zirconium oxide

of similar thickness to the usual niobium native oxide. The usefulness of this approach was first demonstrated with a passivating Al₂O₃ layer [4].

The niobium pentoxide is believed to cause significant losses that could hinder qubit and other low-field applications. Therefore, the demonstration of a practical method to eliminate this oxide from a niobium superconducting surface could be of considerable interest for low-field applications. In contrast to the niobium oxide, the zirconium oxide exists almost entirely in the inert, fully oxidized ZrO₂ state which should not contribute to RF dissipation [5, 6]. Our results are in agreement with previous XPS studies of atomic-layer-deposition zirconium nitride on niobium, which also produced a ZrO₂ surface with no niobium pentoxide after annealing [7].

METHODS

We use an AJA sputter deposition tool to deposit zirconium on niobium sample coupons. Prior to deposition, coupons received a standard pre-preparation consisting of a 60-micron electropolish, a 5-hour 800 °C vacuum bake, and a 2-micron electropolish. The sputter deposition tool first removed the niobium native oxide by argon plasma sputtering, and then deposited approximately 2, 3.75, 7.5, and 10 nm of zirconium on four different samples. The deposition rate was based on the rate for similar metals and has not yet been directly calibrated. The samples then received another 800 °C vacuum bake in order to fully dissolve any remaining niobium oxide and establish a uniform interface between the niobium metal and the protective zirconium oxide layer.

XPS allows identification of various elements present near a sample surface as well as analysis of different phases or oxidation states of an element. This allows for discrimination between different oxides of niobium and zirconium, and allows for at least an approximate understanding of the relative thicknesses of different oxide layers if we assume that sensitivity decreases exponentially with depth. The XPS system used for sample analysis in this study was a Thermo Scientific Nexsa G2 X-Ray Photoelectron Spectrometer System; this paper focuses on element-specific scans for niobium and zirconium. We then use CasaXPS analysis software to fit the data to a combination of elemental and oxide phases.

RESULTS

For increasing zirconium deposition thickness in the range of 0-3.75 nm, we find that the oxide rapidly becomes more zirconium-rich; in particular, by 3.75 nm thickness, there is no detectable niobium component in the primary oxide (Fig. 1). Additionally, the combined intensity of the

* This work was supported by the U.S. National Science Foundation under Award PHY-1549132, the Center for Bright Beams

This work was performed in part at the Cornell NanoScale Facility, an NNCI member supported by NSF Grant NNCI-2025233

This research was partially supported through the Cornell University Materials Research Science and Engineering Center DMR-1719875

[†] nss87@cornell.edu

MATERIALS DESIGN FOR SUPERCONDUCTING RF CAVITIES: ELECTROPLATING Sn, Zr, AND Au ONTO Nb AND CHEMICAL VAPOR DEPOSITION*

Z. Sun[†], M. U. Liepe, T. Oseroff

Cornell Laboratory for Accelerator-Based Sciences and Education, Ithaca, NY, USA

Z. Baraissov, D. A. Muller

Applied and Engineering Physics, Cornell University, Ithaca, NY, USA

M. O. Thompson

Materials Science and Engineering, Cornell University, Ithaca, NY, USA

Abstract

Materials scientists seek to contribute to the development of next-generation superconducting radio-frequency (SRF) accelerating cavities. Here, we summarize our achievements and learnings, in designing advanced SRF materials and surfaces. Our efforts involve electrochemical synthesis, phase transformation, and surface chemistry, which are closely coupled with superconducting properties, SRF performance, and engineering considerations. We develop electrochemical processes for Sn, Zr, and Au on the Nb surface, an essential step in our investigation for producing high-quality Nb₃Sn, ZrNb(CO), and Au/Nb structures. Additionally, we design a custom chemical vapor deposition system to offer additional growth options. Notably, we find the second-phase NbC formation in ZrNb(CO) and in ultra-high-vacuum baked or nitrogen-processed Nb. We also identify low-dielectric-loss ZrO₂ on Nb and NbZr(CO) surfaces. These advancements provide materials science approaches dealing with fundamental and technical challenges to build high-performance, multi-scale, robust SRF cavities for particle accelerators and quantum applications.

INTRODUCTION

Materials science becomes an integral part of multiple efforts in the development of next-generation superconducting radio-frequency (SRF) cavities, in designing advanced SRF materials and surfaces, including Nb₃Sn [1–3], ZrNb(CO) [4, 5], and Au/Nb surface design [6, 7], aiming to enable “bright beams” while reducing the size and cost of SRF systems [8–10]. We design advanced materials and surfaces guided by SRF performance metrics, which involve (i) achieving a suitably high critical temperature (T_c) to improve cryogenic cost and complexity, (ii) minimizing surface resistance (R_s) and maximizing quality factors (Q_0) to reduce power dissipation, and (iii) attaining a large superheating field (H_{sh}) and accelerating gradient (E_{acc}).

To explore and optimize SRF materials and surfaces, we employ a range of traditional strategies, including substitutional doping, light impurity processing and second-phase generation, surface passivation, and surface alloying. We

have investigated Nb₃Sn [1–3], ZrNb(CO) [4, 5], Au/Nb [6], NbTiN/AlN/Nb [11, 12], V₃Si [13], thick-film Nb [14], and impurity-processed Nb [7]. We aim to bridge the gap between fundamental study and practical cavity production.

Electrochemical and chemical vapor depositions are our primary approaches and offer distinct advantages for SRF investigations due to their low cost, versatility, and reactivity. We have developed recipes and processes on the Nb surface for electroplating Sn for Nb₃Sn alloying, electroplating Zr for substitutional doping of Nb, and electroplating Au for fabricating Au/Nb surface structures.

Here, we review our progress and highlight the key findings. Further details can be accessed in other publications [1, 4, 6, 7]. We outline the fundamental and technical challenges associated with cavity production, with the aim of facilitating broader application and improved manufacturing of SRF cavities.

ELECTROPLATING Au ON Nb

Surface nanostructures on Nb, which involve native oxides, are crucial according to theoretical calculations [15, 16]. We have pursued two main directions. First, we have, to date, precisely established the structural profiles of the oxide regions at various depths, taking into account different baking and processing conditions [7]. Our findings indicate that the Nb surface region, comprising a combination of amorphous oxides and metallic components, is most likely normal conducting and impacts the superconducting bulk.

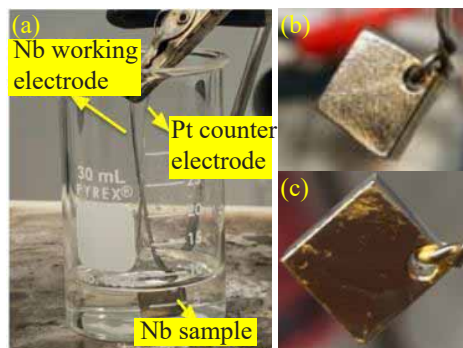


Figure 1: (a) Au electroplating setup. (b,c) Images showing Au film deposition on a Nb surface after different plating durations: (b) 60 s and (c) 600 s.

* Work supported by the U.S. National Science Foundation under Award PHY-1549132, the Center for Bright Beams.

[†] zs253@cornell.edu

PRESERVATION OF THE HIGH QUALITY FACTOR AND ACCELERATING GRADIENT OF Nb₃Sn-COATED CAVITY DURING PAIR ASSEMBLY

G. Ereemeev^{1,*}, U. Pudasaini², S. Cheban¹, J. Fischer², D. Forehand²,
 S. Posen¹, A. Reilly², R. Rimmer², B. Tennis¹

¹Fermi National Accelerator Laboratory, Batavia, IL, USA

²Thomas Jefferson National Accelerator Facility, Newport News, VA, USA

Abstract

Two CEBAF 5-cell accelerator cavities have been coated with Nb₃Sn film using the vapor diffusion technique. One cavity was coated in the Jefferson Lab Nb₃Sn cavity coating system, and the other in the Fermilab Nb₃Sn coating system. Both cavities were measured at 4 K and 2 K in the vertical dewar test in each lab and then assembled into a cavity pair at Jefferson Lab. Previous attempts to assemble Nb₃Sn cavities into a cavity pair degraded the superconducting properties of Nb₃Sn-coated cavities. This contribution discusses the efforts to identify and mitigate the pair assembly challenges and will present the results of the vertical tests before and after pair assembly. Notably, one of the cavities reached the highest gradient above 80 mT in the vertical test after the pair assembly.

INTRODUCTION

As the part of the development of Nb₃Sn for SRF applications in 2018, two Nb₃Sn-coated CEBAF cavities were assembled into a cavity pair, the standard step during CEBAF cryomodule assembly process. As a part of the pair qualification process, both Nb₃Sn-coated cavities assembled into the cavity pair were measured in the vertical dewar and were found to degrade significantly from their pre-pair assembly qualification tests, Fig. 1. The pair was taken apart and each cavity was measured in the vertical dewar separately. These tests confirmed that superconducting RF properties of both Nb₃Sn-coated cavities degraded [1].

Subsequent studies revealed that Nb₃Sn-coated SRF cavities are unexpectedly very sensitive to mechanical tuning at room temperature, which is a part of the standard process to qualify an SRF cavity for cryomodule integration. In the vertical dewar tests of Nb₃Sn-coated cavities the low-field surface resistance was observed to increase by about 100 nΩ and exhibit strong field dependence after room temperature mechanical tuning of a few hundred kilohertz. It must be noted that, in a different study by Posen et al., it was found that mechanical tuning done at cryogenic temperatures does not impact coated cavity performance significantly [2].

In order to mitigate the performance degradation after the room temperature tuning, the mechanical tuning step was eliminated from the next Nb₃Sn-coated cavity pair assembly. In addition to eliminating room temperature tuning, several improvements were made to the cavity preparation

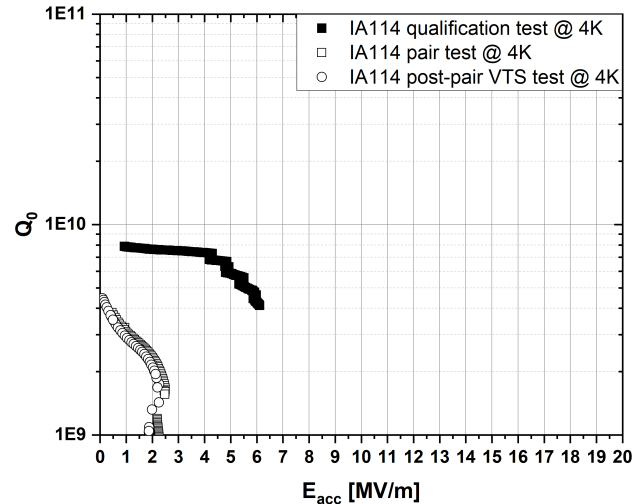


Figure 1: Nb₃Sn-coated cavity performance before and after the first Nb₃Sn-coated cavity pair assembly. Note the increase in the low-field surface resistance and strong field dependence in the pair test and the test after the pair assembly.

process, e.g., a special procedure and tooling was developed to shield the inner surface of cavities during chemical etching of niobium flanges in order to reduce the exposure of the coated inner surface to BCP vapor during treatment. Two new CEBAF 5-cell cavities of C75 shape [3] were procured from a commercial vendor, baselined in the vertical dewar tests, coated with Nb₃Sn film in Jefferson Lab Nb₃Sn coating system, and qualified for the pair assembly at Jefferson Lab.

With the adopted changes in the assembly process the coated cavity were assembled into the cavity pair and tested in the vertical dewar. The low-field surface resistance of the coated cavities was largely unchanged from the qualification tests: one cavity did not exhibit any degradation up to $E_{acc} = 3$ MV/m, Fig. 2, and the low-field surface resistance in the other cavity increased by about 10 mΩ. However, both cavities showed strong Q-slope above few MV/m of accelerating gradient, which limited field reach to below $E_{acc} = 10$ MV/m in both cavities.

The strong Q-slope degradation showed similarity in both cavities after the pair assembly. It was noticed that the resonant frequency of one of the cavities shifted by about 300 kHz from its value before the pair assembly. Although the other cavity showed little shift in the fundamental fre-

* grigory@fnal.gov

COMMISSIONING OF A NEW SAMPLE TEST CAVITY FOR RAPID RF CHARACTERIZATION OF SRF MATERIALS

S. Keckert*, F. Kramer, O. Kugeler, J. Knobloch¹, Helmholtz-Zentrum Berlin, Berlin, Germany
¹ also at University of Siegen, Siegen, Germany

Abstract

RaSTA, the Rapid Superconductor Test Apparatus, is a new sample test cavity that is currently being commissioned at HZB. It uses the established QPR sample geometry but with a much smaller cylindrical cavity operating in the TM_{020} mode at 4.8 GHz. Its compact design allows for smaller cryogenic test stands and reduced turnaround time, enabling iterative measurement campaigns for thin film R&D. Using the same calorimetric measurement technique as known from the QPR allows direct measurements of the residual resistance. We report first prototype results obtained from a niobium sample that demonstrate the capabilities of the system.

INTRODUCTION

Characterizing the RF properties of samples – especially by measuring the surface resistance (R_S) – is essential for systematic R&D on superconducting thin films and multilayer structures for SRF applications. The quadrupole resonators (QPR) at CERN [1] and HZB [2] are well suited for this and allow for high-precision measurements of R_S as a function of temperature and RF field at three frequencies. The effort for each measurement run is quite high: A quick test with only few days of cold testing requires at minimum two weeks including sample preparation, mounting and warmup of the cryostat. This is acceptable for characterizing samples in-depth from optimized preparation techniques. However, most of the time procedures and coating recipes have to be developed or optimized iteratively with a large number of samples. In that case, ‘yes/no’ statements or a monitoring of relative changes are more relevant. For that, a sample test cavity with higher throughput at reduced capabilities is highly desirable. The Rapid Superconductor Test Apparatus (RaSTA) is meant to be exactly this device. Its main features are:

- Full compatibility to the HZB QPR by using the same sample geometry, allowing pre-selection of samples, cross-calibration and direct comparison of both setups.
- Calorimetric measurement of R_S as a function of temperature at a frequency that is low enough to allow for a direct analysis of the residual resistance (R_{res}).
- Reduced turnaround time, aiming at testing more than one sample per week

The last point of reduced turnaround time is closely connected to the entire infrastructure and not (only) a property of the cavity itself. In our case, this goal can be achieved by

* sebastian.keckert@helmholtz-berlin.de

- Operation without radiation protection measures by limiting the maximum RF voltage in the cavity to few kV.
- Reduced size of the cavity to fit into a small and stand-alone cryostat with fast cycling times.

In the following, we introduce the design of RaSTA and discuss first results from the commissioning of a prototype cavity. The design is patented under DE 10 2021 123 261 [3].

DESIGN

For a calorimetric measurement of R_S on QPR samples a cavity has been found such, that (a) a sufficiently strong RF magnetic field is present on the sample surface but not on its cylindrical sidewalls and (b) the sample can be mounted into the cavity with sufficient thermal decoupling. Geometric boundary conditions are the sample diameter of 75 mm and its height of 85.5 mm when mounted into a CF100 flange. For further details of QPR samples see Ref. [2].

RF Design

Inspired by the mode spectrum of a pillbox cavity, the TM_{020} mode was chosen as the operating mode for the RaSTA cavity. This mode features a zero-crossing of the magnetic field which allows for a coaxial gap to insert a QPR sample into the cavity. The resonant frequency (i.e. the cavity radius) is chosen such, that the zero-crossing fits to the sample diameter of 75 mm. The obtained value of 4.8 GHz leads to much higher R_{BCS} compared to QPR measurements but when operating at 1.5 K, R_{BCS} of approx. 10 n Ω for niobium still allows for direct measurements of R_{res} . For higher- T_c materials the situation is more relaxed.

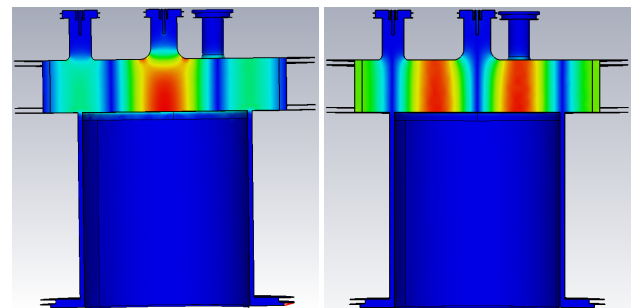


Figure 1: Simulated maps of electric (left) and magnetic (right) RF field for the operational TM_{020} mode at 4.8 GHz.

Given by the TM_{020} mode’s symmetry the height of the cavity can be made very small, for technical reasons a value of 23.7 mm was chosen. This comes with the advantages

DEVELOPMENT OF Nb₃Sn COATING SYSTEM AND RF MEASUREMENT RESULTS AT KEK

H. Ito^{1,*}, H. Sakai¹, K. Umemori¹, T. Yamada¹, KEK, Tsukuba, Ibaraki, Japan
K. Takahashi, SOKENDAI, Tsukuba, Ibaraki, Japan
¹ also at SOKENDAI, Tsukuba, Ibaraki, Japan

Abstract

We have constructed an Nb₃Sn cavity coating system based on the Sn vapor diffusion method. After the construction, our coating system and environment have been improved through sample and cavity coating tests. Our cavity achieves a Q_0 above 1×10^{10} at 4 K after improvement. We will report on the detail of improvement on our coating system and RF measurement results of single-cell Nb₃Sn cavities.

INTRODUCTION

Nb₃Sn is one of the leading candidates for SRF cavity materials because it has the potential to operate cavities at higher temperatures with a higher Q_0 and achieve a higher accelerating gradient [1]. Focusing on the operating temperature, since the transition temperature of Nb₃Sn is twice that of Nb, Nb₃Sn cavities can achieve Q_0 comparable to conventional Nb cavities at 4.2 K. In other words, the Nb₃Sn cavity has an attractive future potential to operate without liquid helium and with conduction cooling by cryocoolers and research for this purpose is actively underway [2–6]. Development of Nb₃Sn cavities has been actively carried out using a variety of methods [1], among which the thermal diffusion method is more advanced than others in terms of practical application [7–12]. We also started the development of Nb₃Sn cavities based on the thermal diffusion method in 2019 [13, 14]. Through furnace heating tests and sample Nb₃Sn coating tests, we have understood the characteristics of our furnace and have performed Nb₃Sn coating on single-cell cavities a total of four times so far.

FIRST Nb₃Sn COATING ON SINGLE-CELL CAVITY

After establishing the capability to form Nb₃Sn films on Nb substrates through sample coating tests, the first Nb₃Sn coating test was performed on a 1.3 GHz single-cell cavity, as shown in Fig. 1. The coating furnace has two heating systems, one that heats the entire furnace and one that heats the Sn crucible independently. During coating, the Sn crucible is heated to a higher temperature than the furnace to actively evaporate Sn. The surface of the cavity after the coating is visually darker gray than niobium and matte.

Figure 2 shows the $Q - E$ curves measured at 4.2 K for the single-cell cavity before and after the first coating. The first-coated cavity shows a Q_0 of 3.9×10^9 at 4.2 K and at low field which is 5 times higher than that of the Nb cavity.

* hayato.ito@kek.jp

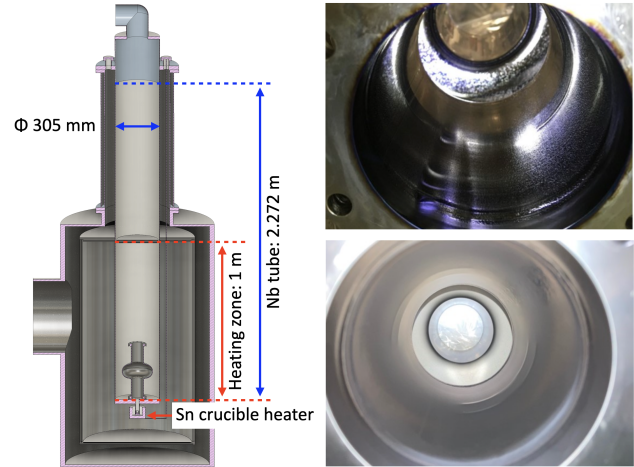


Figure 1: Cross-section of coating furnace (left), inside of cavity before (top right), and after first coating (bottom right).

However, this Q_0 is lower than the expected value of 1×10^{10} and shows a significant Q-slope.

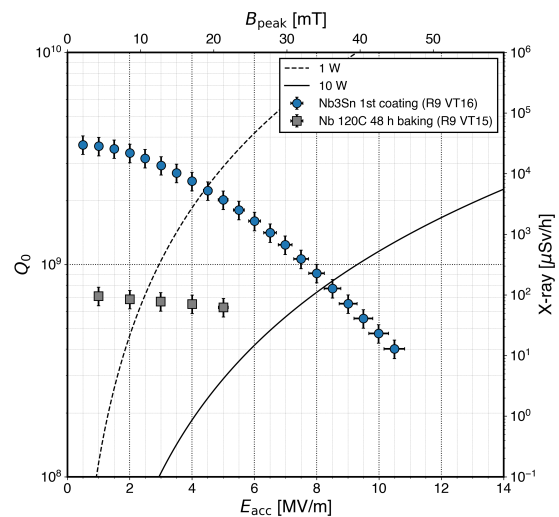


Figure 2: $Q - E$ curves measured at 4.2 K for the single-cell cavity before and after first coating.

SECOND AND THIRD Nb₃Sn COATING

After the RF measurement for the first-coated cavity, we found several points that need to be changed and began to modify them for the next coating on the cavity.

SUMMARY OF THE FRIB ELECTROPOLISHING FACILITY DESIGN AND COMMISSIONING, CAVITY PROCESSING, AND CAVITY TEST RESULTS*

E. Metzgar[†], B. Barker, K. Elliott, J. Hulbert, C. Knowles, L. Nguyen, A. Nunham, L. Popielarski, A. Taylor, T. Xu, Facility for Rare Isotope Beams (FRIB), Michigan State University, East Lansing, MI, USA

Abstract

Recently, a new Electropolishing (EP) facility was constructed and commissioned at the Facility for Rare Isotope Beam (FRIB) with the purpose of supporting advanced surface processing techniques for SRF R&D activities. The FRIB production cavities opted for a Buffered Chemical Polish (BCP) method due to its cost effectiveness and was supported by successful outcomes in other facilities with low beta cavities in a similar frequency range. All 324 cavities used in FRIB Linac were processed in-house at MSU using BCP and exhibited satisfactory performance during testing. As part of the FRIB energy upgrade R&D, 5-cell 644 MHz elliptical resonators will be employed, desiring the use of EP and advanced techniques such as nitrogen doping and medium-T baking. The EP facility is designed to accommodate all types of cavities used in FRIB and possesses the capability for performing EP at low temperatures. Here we report the details of design and commissioning of the EP facility, highlights of encountered issues and subsequent improvements, and preliminary results from vertical tests conducted on the cavities.

INTRODUCTION

As the production run of cavities for the FRIB accelerator reached completion, work began on planning for the future. An energy upgrade utilizing 644 MHz elliptical style $\beta=0.65$ cavities was already being planned for the FRIB accelerator. R&D work of advanced cavity processing techniques such as nitrogen doping and medium temperature baking were also being considered. These projects require the ability to chemically process cavities by EP.

FRIB worked with an outside contractors to design and build a processing room and accompanying ventilation scrubber similar to the existing chemical etching facility described previously [1]. The processing room and scrubber provide a negative pressure area to house and operate the EP system while mitigating potential hazard exposure outside the EP facility.

With the processing room in place, work began on building out the EP process. Mechanical design work was split into four design packages:

- **EP Hood:** Fume hood used to contain process, including cavity, acid tanks, and plumbing while

providing connections to scrubber ducting to ventilate area

- **EP Tool:** Included the end groups and support frame used for installing cavities to while providing interfaces to process plumbing, rotation mechanism, DC power supply, cooling water loop etc.
- **Cathode Installation and Rinse Area:** provided area for cathode and end group installation as well as rinse area to clean and neutralize cavities post-EP processing
- **Cooling Shower Enclosure:** provided means to connect to cooling water loop and contain spray inside EP hood

All design and fabrication work was performed/coordinated by the FRIB Mechanical Design Department. The primary driver for the design of the mechanical structure was to accommodate the largest planned cavities at the time shown in Table 1.

Table 1: Summary of Physical Cavity Processes Forming Mechanical Design Basis

Characteristic	Value	Cavity Type
Length	129 cm	SNS $\beta=0.80$ six-cell elliptical
Diameter	84 cm	Jacketed FRIB $\beta=0.65$ five-cell elliptical
Weight (plus volume full of acid)	320 kg	Jacketed FRIB $\beta=0.65$ five-cell elliptical

Installation was performed by FRIB processing personnel with close support from mechanical designers.

After mechanical infrastructure was installed, work on other sub-systems could take place:

- **Process plumbing:** storage tanks, pumps, valves, motors, and plumbing used for handling of chemicals, acidic rinse water, and external cavity cooling loop
- **Controls system:** developed for operator control of system, process and safety monitoring, process interlocks, etc.
- **DC Power Supply:** infrastructure for supplying direct current to cavities required to drive electropolishing reaction
- **Conventional Utilities:** connecting system to power, compressed air, dry nitrogen, ultra-pure water, and sanitary sewer

*This material is based on work supported by the U.S. Department of Energy Office of Science under Cooperative Agreement DE-SC0000661, the State of Michigan, and Michigan State University.

[†]metzgar@frib.msu.edu

MgB₂ COATING PARAMETER OPTIMIZATION USING A 1.3-GHz 1-CELL CAVITY

T. Tajima[†], T. P. Grumstrup, J. D. Thompson
Los Alamos National Laboratory, Los Alamos, NM, USA
H. Sakai, H. Ito, E. Kako, T. Okada, K. Umemori, KEK, Tsukuba, Japan

Abstract

We started performing the tests to react B-coated samples with Mg vapor using a full-size 1.3-GHz elliptical cavity with coupon holes. So far, we have tested 7 times and we started to see superconductivity on samples from the 4th test. The highest transition temperature (T_c) has been ~ 32 K so far. Comparing to the results with small furnace, new samples show wide superconducting transitions suggesting some contaminations. This paper describes the tests and their results. The B coating system has been under construction in parallel with this effort.

INTRODUCTION

MgB₂ has been studied for applications to SRF cavities due to its favorable properties such as significantly higher T_c of ~ 40 K compared to other promising superconductors for SRF cavities such as Nb₃Sn whose T_c is ~ 18 K [1]. We are constructing a system to coat a full-size cavity with MgB₂ at LANL [2]. Figure 1 shows a schematic of the new system. Elliptical cavities of ~ 1 GHz or higher can fit in the new furnace pipe. The method we chose for the MgB₂ coating is a 2-step technique, i.e., coat B layer with CVD using B₂H₆ gas in the first step and react it with Mg vapor in the 2nd step [3]. We were able to obtain samples with a T_c of >35 K with experiments using a small tube heater [3, 4]. Our effort has been to re-create the same conditions with the newly built large system. This paper presents the results of the reaction tests using existing flat B-coated samples (6 mm x 6 mm, on Nb or sapphire) attached at the coupon holes on beam pipes and cell on a 1.3-GHz 1-cell Nb elliptical cavity.

TEST PROCEDURE

The B-coated substrates being used were obtained during a project that ended in 2015 [5]. In that project we were able to coat B layer on the surface of a 1.3-GHz cavity but were unsuccessful in producing MgB₂. Nearly the end of that project, we tested this 2-step technique using a small tube heater and successfully obtained MgB₂ with a T_c of >35 K as shown in Fig. 2. After further studies of the parameters, we purchased a large furnace to apply this technique to full-size cavities. We started to follow the same process as we took with the small tube heater, i.e., (1) bake out the furnace at 50-100 °C higher than the B-Mg reaction temperature without including Mg pellets under vacuum using a 70-L/s turbo pump, (2) cool it down naturally and let up the furnace with nitrogen gas, (3) remove all the parts

out of the furnace, (4) install samples at the 3 locations (inlet and outlet beam pipes and cell equator as show in Fig. 3) and Mg pellets in the Nb tray in the Mo boat located in the smaller diameter pipe, (5) re-install all the parts back into the furnace, (6) make a gap between the cavity and Mg section and pump down the furnace including the cavity, (7) raise the temperature to ~ 150 °C and hold it for ~ 12 hours to degas the surfaces, (8) let up the furnace including the cavity with Ultra High Purity (UHP) Ar gas to slightly higher than 1 atm using a 1/3 psi check valve, (9) close the gap between the beam pipe and Mg section and raise the temperature to the planned temperature and hold it for ~ 6 hours, (10) cool down the furnace with slowly flowing UHP Ar gas to prevent the pressure from negative to avoid oxidation of the cavity in case of air leak during this cool down and (11) remove the parts out of the furnace at $< \sim 50$ °C and retrieve samples and Mg pellets.

RESULTS

So far, we have performed 7 tests. First 3 tests did not produce any superconductor probably because the temperature was too low at the MgB₂ section as shown in Fig. 4. We started to see superconducting transitions from the 4th test. Figures 5 through 8 show the temperature profiles and magnetometer test results of the samples taken from inlet beam pipe (BP), cell and outlet BP for each test from the 4th to 7th tests. The T_c 's were measured by the Quantum Design Model MPMS3.

Our goal was to create the same conditions as the tests with small tube heater, but the temperature control has been the most challenging issue with the large system. First, we found actual temperatures on the cavity was ~ 50 °C lower than those shown on the furnace controller. We installed thermocouples at the locations where the samples are located, on the Mg section pipe and on the end flanges, and controlled the temperatures based on these actual temperatures.

We have not been able to do detailed systematic studies, but the following summarizes the facts we found so far.

- The cell temperature tends to be higher than beam pipes.
- Mg pellets temperature seem to be lower than the pipe temperature since they did not melt much at 700 °C at the pipe. (Mg melting temperature is 650 °C.)
- The reaction at ~ 750 °C seems to be best so far.
- It is difficult to keep Mg temperature higher than the cell temperature without independent heater.
- The main reason for lower-than-expected T_c seems to be insufficient Mg vapor pressure.

[†] tajima@lanl.gov

FIRST RESULTS FROM Nb₃Sn COATINGS OF 2.6 GHz Nb SRF CAVITIES USING DC CYLINDRICAL MAGNETRON SPUTTERING SYSTEM*

M. S. Shakel[†], H. E. Elsayed-Ali, Old Dominion University, Norfolk, VA, USA
G. Ereemeev, Fermi National Accelerator Laboratory, Batavia, IL, USA
U. Pudasaini, A. M. Valente-Feliciano
Thomas Jefferson National Accelerator Facility, Newport News, VA, USA

Abstract

A DC cylindrical magnetron sputtering system has been commissioned and operated to deposit Nb₃Sn onto 2.6 GHz Nb SRF cavities. After optimizing the deposition conditions in a mock-up cavity, Nb-Sn films are deposited first on flat samples by multilayer sequential sputtering of Nb and Sn, and later annealed at 950 °C for 3 hours. X-ray diffraction of the films showed multiple peaks for the Nb₃Sn phase and Nb (substrate). No peaks from any Nb-Sn compound other than Nb₃Sn were detected. Later three 2.6 GHz Nb SRF cavities are coated with ~1 μm thick Nb₃Sn. The first Nb₃Sn coated cavity reached close to $E_{acc} = 8$ MV/m, demonstrating a quality factor Q_0 of 3.2×10^8 at $T_{bath} = 4.4$ K and $E_{acc} = 5$ MV/m, about a factor of three higher than that of Nb at this temperature. Q_0 was close to 1.1×10^9 , dominated by the residual resistance, at 2 K and $E_{acc} = 5$ MV/m. The Nb₃Sn coated cavities demonstrated T_c in the range of 17.9 – 18 K. Here we present the commissioning experience, system optimization, and the first results from the Nb₃Sn fabrication on flat samples and SRF cavities.

INTRODUCTION

In comparison to bulk Nb SRF cavities, Nb cavities coated with Nb₃Sn demonstrate superior performance in terms of quality factors at 4 K and have the potential to replace bulk Nb cavities operated at 2 K [1-3]. Various processes have been applied for Nb₃Sn coating onto SRF cavities including Sn vapor diffusion, bronze routes, co-deposition of Nb and Sn by thermal evaporation, electrochemical synthesis, Nb dipping into Sn liquid followed by thermal diffusion, and magnetron sputtering [4-11]. Until now the vapor diffusion method has demonstrated the most promising radiofrequency (RF) outcomes for Nb₃Sn-coated cavities, whereas magnetron sputtering offers improved control over stoichiometry [12-13]. Magnetron sputtering can be employed in multiple techniques to grow Nb₃Sn, such as depositing multilayers of Nb-Sn followed by annealing, depositing from a single stoichiometric Nb₃Sn target, or co-sputtering of Nb and Sn [14-16].

Recently we commissioned a DC cylindrical magnetron sputtering system and developed methods for coating

Nb₃Sn onto a 2.6 GHz Nb SRF cavity [17]. Our approach involves multilayer sequential sputtering using two identical cylindrical magnetrons to deposit Nb-Sn layers, which are subsequently annealed to promote the growth of Nb₃Sn. Initially, three Nb samples are positioned to mimic the beam tubes and the equator location of a 2.6 GHz Nb cavity. A deposition recipe is established to produce Nb₃Sn on the Nb samples and later the first Nb cavity (TTS1RI001) is coated following this recipe. Subsequently, optimization of the deposition conditions is carried out using a mock-up cavity and uniform thickness of Nb₃Sn is deposited on the beam tubes and the equator regions. Based on the refined conditions, two more 2.6 GHz Nb cavities (TTS1RI002 and TTS1RI003) are coated with Nb₃Sn following the multilayer sequential sputtering procedure.

OPERATING CYLINDRICAL DC MAGNETRON SPUTTER COATER

The cylindrical magnetron sputtering setup comprises a custom-designed high-vacuum deposition chamber that houses a 2.6 GHz cavity with shape scaled from the TESLA center-cell shape and two identical cylindrical magnetrons [17]. The operating conditions of the magnetron discharge are optimized to achieve stable and symmetrical plasma formation for the Nb and Sn targets, installed on the top magnetron and the bottom magnetron, respectively, as shown in Fig. 1. With a baseline pressure of $\sim 2 \times 10^{-9}$ Torr, 30 W DC power is used for Nb discharge, and 8 W DC power is used for Sn discharge at 10 mTorr pressure with an Ar flow rate of 50 SCCM. To control the cylindrical sputter system and the associated devices, custom software was developed that is capable of running the operation of the deposition program and storing relevant data such as current, voltage, power, and water flow rate during the discharge process.

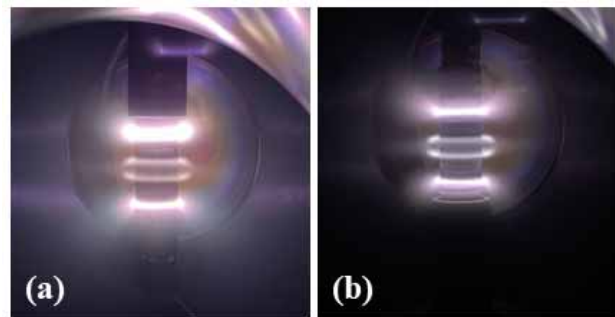


Figure 1: Photograph of stable plasma discharge at 10 mTorr using DC power (a) 30 W for Nb, (b) 8 W for Sn.

* Supported by DOE, Office of Accelerator R&D and Production, Contact No. DE-SC0022284, with partial support by DOE, Office of Nuclear Physics DE-AC05-06OR23177, Early Career Award to G. Ereemeev.

[†] mshak001@odu.edu

SURFACE PROPERTIES AND RF PERFORMANCE OF VAPOR DIFFUSED Nb₃Sn ON Nb AFTER SEQUENTIAL ANNEALS BELOW 1000 °C*

J. K. Tiskumara[†], J. R. Delayen

Center for Accelerator Science, Old Dominion University, Norfolk, VA, USA

U. Pudasaini, Thomas Jefferson National Accelerator Facility, Newport News, VA, USA

G. Ereemeev, Fermi National Accelerator Laboratory, Batavia, IL, USA

Abstract

Nb₃Sn is a next-generation superconducting material that can be used for future superconducting radiofrequency (SRF) accelerator cavities, promising better performance, cost reduction, and higher operating temperature than Nb. The Sn vapor diffusion method is currently the most preferred and successful technique to coat niobium cavities with Nb₃Sn. Among post-coating treatments to optimize the coating quality, higher temperature annealing without Sn is known to degrade Nb₃Sn because of Sn loss. We have investigated Nb₃Sn/Nb samples briefly annealed at 800-1000 °C for 10 and 20 minutes to potentially improve the surface to enhance the performance of Nb₃Sn-coated cavities. Following the sample studies, a coated single-cell cavity was sequentially annealed at 900 °C and tested its performance each time, improving the cavity's quality factor relatively. This paper summarizes the sample studies and discusses the RF test results from sequentially annealed SRF Nb₃Sn/Nb cavity.

INTRODUCTION

With a higher critical temperature $T_c \sim 18.3$ K and a superheating field $H_{sh} \sim 400$ mT (both twice that of Nb), Nb₃Sn is a potential alternative material to replace Nb in SRF cavities. Therefore, Nb₃Sn has the potential to exhibit lower dissipation compared to niobium at any given temperature due to its reduced surface resistance. Nb₃Sn cavities have demonstrated the ability to operate at 4 K while delivering performance similar to Nb cavities at 2 K. This offers a promising opportunity to reduce the operational cost of SRF accelerators. Furthermore, Nb₃Sn's superheating field indicates a higher breakdown field, enabling higher accelerating gradients and potentially reducing the initial cost of constructing SRF accelerators [1, 2]. However, Nb₃Sn is typically deposited as a thin film on already-built RF structures due to its brittleness and lower thermal conductivity. Among the various methods available, several laboratories have successfully pursued the Sn vapor diffusion technique to coat Nb SRF cavities with different shapes and frequencies. [3-7]. In this process, the Sn is evaporated and transported as a vapor to the substrate Nb

at temperatures exceeding 930°C to form the Nb₃Sn phase. In Jefferson Lab, we have utilized the Nb₃Sn coating facility to coat various Nb cavities using the vapor diffusion technique. Most coatings have been grown on elliptical-shaped single-cell and multi-cell SRF cavities with a single beamline. Additionally, for the first time, we successfully coated and tested a twin-axis cavity with a complex geometry housing two beamlines [8]. This twin-axis cavity has been proposed for applications in Energy Recovery Linacs (ERL) [8].

After conducting the initial coating and RF testing on the twin-axis cavity, we encountered specific issues unique to this cavity coating and some common challenges observed in other cavity coatings. Among the major problems we identified were potential non-uniformity caused by hard-to-reach areas, the mechanical stability of the cavity after the high-temperature Nb₃Sn coating, and the surface quality of the deposited thin film. We noticed recurring roughness and Sn residues, similar to those in other cavity coatings. Previous studies have attempted various chemical treatments to enhance the surface quality of the coated surface [9], but an optimal process has yet to be developed.

In order to customize the coating process for the twin-axis cavity, we conducted extensive studies on different coating parameters. Based on these studies, we updated the coating parameters and implemented various treatments to improve the quality of the coated surface. This process included optimizing the Sn supply by reducing the amount of Sn used, adjusting the size of the crucible, and modifying the temperature profile to minimize the accumulation of Sn residues during and at the end of the coating process [1].

Sn residues on the coated surface posed a persistent challenge, but the updated coating parameters involved multi-step coating temperatures and gradual cooling below 900 °C helped reduce the size of Sn residues. One potential approach to mitigate Sn residues is to anneal the coated surface without Sn, thereby evaporating the remaining Sn residue. But with the Potential of Sn loss when annealed at temperatures higher than 1000 °C or lower temperatures for more than 45 minutes [1, 10], we limited our study to temperatures below 1000 °C (950 °C, 900 °C and 850 °C) for shorter time periods (10 and 20 minutes) which has not been studied earlier. In this paper, we will present the results from systematic studies conducted on Nb₃Sn samples that were annealed at temperatures below 1000 °C and the RF performance from sequentially annealed Nb₃Sn coated cavity.

* Research supported by DOE Office of Science Accelerator Stewardship Program Award DE-SC0019399 and DOE Award DE-SC0010081. Partially authored by Jefferson Science Associates under contract no. DEAC0506OR23177. This material is based upon work supported by the U.S. Department of Energy, Office of Science, Office of Nuclear Physics and Office of High Energy Physics

[†] jtisk001@odu.edu

COBOTISATION OF ESS CRYOMODULE ASSEMBLY AT CEA

S. Berry*, A. Bouygues, J. Drant, C. Madec, A. Gonzalez-Moreau, C. Servouin
Université Paris-Saclay, CEA, Département des Accélérateurs, de la Cryogénie et du Magnétisme,
Gif-sur-Yvette, France

Abstract

The assembly of cavity string in the clean room is a tedious work that has noisy and painful steps such as cleaning the taped holes of a part. CEA together with the company INGELIANCE has developed a cobot: a collaborative robot operated by a technician one time and repeating the action without the operator. The cobot can work anytime without any operators: therefore it is working at night, reducing the assembly duration by some hours. The cobot consists of a FANUC CRX10 a 6-axis arm on an Arvis cart. At CEA, the cobot is used to blow the flange holes of the cavities and bellows. This allows to reduce the noisy steps that the technicians are exposed to. The process is also more reproducible since the cobot always does the same steps. The cobot is used on ESS cavity string to clean the coupler and cavity flanges. The development of this new tool is presented.

INTRODUCTION

The use of cobots (COLlaborative roBOTS) in activities linked to the SRF accelerators domain appears more and more as a solution to ease the preparation and assembly steps. Most developments have focused on component inspection operations and cleanroom activities, in particular all activities related to component assembly (cavities, valves, etc.) and preparation (high-pressure rinsing, handling, cleaning, etc.). There are two main reasons for this choice. The first one is the criticality of cleanroom operations, induced by particulate contamination due to the numerous movements and operations carried out by operators. The second one is the painful nature of certain cleanroom operations, which can adversely affect the repeatability. In addition to the CEA activities, other laboratories are developing robotization or cobotisation for clean room operations. Among these are KEK (Japan), which has developed a solution for cleaning cavities and assembling components on these cavities [1] or MSU (USA), which has developed a robotized high-pressure rinsing system that optimizes the cleaning process according to cavity geometry [2].

Among the wide range of cleanroom operations, the CEA team chose to focus, as a first step, on the use of the cobot for cleaning activities, due to the painful nature of these tasks. This choice was also motivated by the fact that most of the cleaning steps can be carried out in masked time during lunch or at night, to save time on cavity string assembly. This paper presents the steps involved in deploying cobotisation in the cleanroom assembly phases of the ESS project. From the definition of the specifications, the development of the chosen solution, the commissioning to validate the use of

the cobot in the CEA ISO4 cleanroom, to the development and implementation of "cobotised" cleanroom phases. This development was performed in parallel with the assembly of the cryomodules for the ESS project, with the aim of integrating the successful "cobotised" steps into the ESS project's production.

DESCRIPTION

The experience of assembling 100 cryomodules for XFEL has led us to better optimize the assembly of cavity string in the clean room by reducing the number of painful operations for the operators and by gaining time on the overall assembly. The clean room assembly steps are tedious operations where the operators have to remain static (see Fig. 1) with their arms in the horizontal position, meanwhile they are holding the nitrogen gun to blow flange holes and a particle counter detector. Depending on the cleanliness of the flanges, the blowing and checking could last for two hours. Moreover, some flanges with taped and threaded holes could be harder and longer to clean, adding longer painful work.



Figure 1: Manual cleaning operation on coupler to cavity assembly workstation.

To assemble a coupler on a cavity, two flanges are cleaned and, to minimize the contamination, these should be cleaned far from each other and in parallel. The operations are performed in a clean room which has its constraints: low particle emission, close environment with limited space and restricted number of operators. In the industry, cobot are intended for direct human-robot interaction within a shared space, or where humans and cobots are in close proximity. CEA took advantage of the development of cobots as a solution to lower the painful work in a clean room, save time and work in parallel if needed. Cobot are built with lightweight

* stephane.berry@cea.fr

PREPARATION OF THE ASSEMBLY OF THE 650 MHz LOW BETA CRYOMODULES FOR THE PIP-II LINEAR ACCELERATOR

J. Drant*, N. Bazin, S. Berry, R. Cubizolles, A. Moreau, A. Raut
Université Paris-Saclay, CEA, Département des Accélérateurs,
de la Cryogénie et du Magnétisme, Gif-sur-Yvette, France

Abstract

The Proton Improvement Plan II (PIP-II) that is under construction at Fermilab is the first U.S. accelerator project that will have significant in-kind contributions from international partners. CEA's scope covers the supply of the 650 MHz low-beta cryomodule sections with the cavities provided by LASA-INFN (Italy) and VECC-DAE (India) as well as the power couplers supplied by Fermilab. This scope includes the assembly of the 650 MHz low-beta cryomodules. Assembly studies have been conducted based on CEA experience acquired on previous projects, as well as on the feedback of Fermilab on the assembly of the HB650 prototype cryomodule. This paper presents the organization of assembly phases from the cavity string in the clean room and the assembly of the cryostat to the preparation of the cryomodule before its shipment to Fermilab.

INTRODUCTION

The PIP-II project is an upgrade of the accelerator complex of Fermilab to enable the world's most intense neutrino beam for the Long Baseline Neutrino Facility (LBNF) and the Deep-Underground Neutrino Experiment (DUNE) located in South Dakota, 1200 km from neutrino production in Illinois [1]. CEA is in charge of the design [2], fabrication, assembly and cold RF tests [3] of the low-beta 650MHz cryomodules (called "LB650" hereafter). The CEA contribution will consist of one pre-production cryomodule [4], whose assembly will start in 2024, and nine series cryomodules, whose assembly will start in 2026. The assembly studies have been conducted in parallel with the design of the cryomodule to allow for potential minor design changes to facilitate assembly steps or to allow for the addition of link interfaces to assembly tooling. The development of assembly tooling is also carried out in parallel with the assembly studies because it is directly impacted by the choice of assembly workflow. Thanks to the CEA experience on cryomodules assembly, the assembly studies are based on feedback from assembly teams who have participated in previous projects. In particular, the similarities between the LB650 cryomodules and the cryomodules of the ESS project (currently still in the assembly phase) allow a simplified transfer of knowledge. The choice to involve the CEA teams from the design of the high-beta cryomodules has resulted in high similarities between the two types of cryomodules [5]. These design similarities are reflected in the transposition of some assembly processes from Fermilab to CEA. This transposition is

facilitated by the numerous exchanges with the assembly team at Fermilab (reports, CEA visits, regular meetings).

ASSEMBLY GENERAL WORKFLOW

Based on the feedback from the ESS project teams and the experience from previous projects, it is possible to define the general workflow of the assembly process (see Fig. 1). This process extends from the preparation of the components before their entry in the clean room to the preparation of the cryomodule before shipping to Fermilab.

The first workstation (WAS/PRE) allows the preparation of all the elements assembled in the clean room. This preparation includes inspections, tests and washing operations to limit the risk of non-conformities that are more detrimental to clean room operations. The two following workstations (CAP & BLA) correspond to the assembly, in clean room, of all the elements to obtain the cavity string. The three following workstations (ABE & PAV & PAS) detailed the assembly of the three main component groups of the cryomodule: the beam line, the vacuum vessel and the strongback. The two following workstations (COS & CRY) allow the assembly of the main component groups. The beam line is assembled with the strongback in order to form the cold mass. This set is then inserted into the vacuum vessel to initiate the final assembly steps of cryomodule. The following workstation (CLO) allows, with the last assembly steps, the finalization of the cryomodule before the cold RF test phase (BUN). After the cold RF test, the cryomodule is prepared for shipping to Fermilab. This workstation (EXP) includes the disassembly of some elements for shipping and the assembly of transportation tooling. The disassembly phase has two objectives: to approach the final configuration of the cryomodule (operating configuration of the cryomodule in the accelerator tunnel) and to remove the elements not compatible with the available space for air transport of the LB650 cryomodule. An overview of the cryomodule assembly state after each workstation is presented in Fig. 2.

GEOGRAPHICAL LOCATION OF THE ASSEMBLY WORKSTATIONS

The previous cryomodule assembly projects have enabled the CEA to optimize the available infrastructure. Thus, the assembly of the LB650 cryomodules will be performed in the so-called "ESS Village" at CEA Saclay (former "XFEL Village"). The main objective of the LB650 assembly studies is the adaptation of these infrastructures to the specificities of the assembly of these cryomodules. The organization of the future "PIP-II Village" is presented in Fig. 3. The two main

* julien.drant@cea.fr

MEASUREMENTS OF HIGH VALUES OF DIELECTRIC PERMITTIVITY USING TRANSMISSION LINES

V. Shemelin*, M. Liepe

LEPP, Physics Department, Newman Laboratory, Cornell University, Ithaca, NY, USA

Abstract

Usage of lossy materials is necessary for absorption of higher order modes excited in the RF cavities. Presently, measurements of lossy materials with usage of transmission lines give errors rapidly increasing with increase of the dielectric permittivity. A method is presented for measurements of high values of dielectric permittivity epsilon in a waveguide at high frequencies with lower errors. This method supplements the method of measurements evolved for low values of epsilon and is close to resonant methods, when a sample is placed into a cavity and the measurement is done at one only frequency. The new approach with use of Microwave Studio simulations makes possible to measure this value in several frequency points at one measurement.

INTRODUCTION

The method to compute complex ϵ and μ with help of analytical formulas from the measured complex reflection (S_{11}) and transmission (S_{21}), when a sample of a material is placed into a transmission line, was proposed by W. Weir [1] and has been detailed in other publications [2 - 4].

The sample geometry for measurements with waveguides is a rectangular plate with two dimensions close to dimensions of the waveguide cross-section and with a thickness that can be different.

In [4] it was shown that measurement of high values of ϵ requires very high accuracy of measurement of the S-parameters. The commonly used Network Analyzers cannot guarantee this accuracy better than 0.01. Such an error leads to errors in $\text{Re } \epsilon$ about 20 % if ϵ is about 30, and +200/-20 % if ϵ is 80.

Moreover, these errors increase dramatically if there are gaps between the sample and the waveguide where this sample is inserted. In the theoretical approach no transformation into higher order modes were considered because their excitation needs a coupling with these modes. This coupling can be done by the gaps.

Measurements are performed with the wave TE₁₀ in a rectangular waveguide. In this case the electric field in the gap is ϵ times higher than in the sample, so the most part of power leaks through this gap if the gap is along the broader side of the waveguide, the size of the gap is bigger than 1 % of the waveguide size, and ϵ is bigger than 10.

It is impossible to insert a sample into the holder – a part of the line where the sample is placed - if there are no gaps between them. So, the situation seems hopeless and this method can only be used for ϵ about 10 or less.

However, real measurements give us a hint, how to improve measurement accuracy, at least partly.

HALF-WAVE RESONANCE

In Fig. 1 results of measurements of a sample of ZrO₂ are shown. The sample, 3 mm thick, was measured in a WR90 waveguide (22.86 × 10.16 mm) in the frequency range from 8.2 to 12.4 GHz. We can see two big resonances; their frequencies are $f_1 = 8.956$ and $f_2 = 10.33$ GHz. There are also several peaks above 10 GHz.

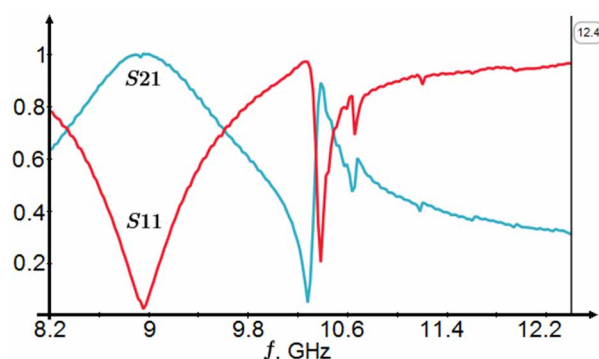


Figure 1: Measured S-parameters of a ZrO₂ sample.

Values of ϵ and μ , corresponding to the measured S-parameters, calculated by formulas from [1 - 4], are presented in Fig. 2. We can see that the theory doesn't work in this example near the resonances, and only at the higher frequencies the values become having some physical sense, though the imaginary part of ϵ should be negative in this case to correspond to losses in the material.

We simulated this example with help of CST Microwave Studio. The model used for the simulation is shown in Fig. 3.

In Fig. 4 one can see a resonance at 9.2 GHz like in Fig. 1, but no more resonances appear. The resonance at 9.2 GHz is a so-called half-wave-length resonance. The half-wave ceramic windows are used in RF technique in transitions between vacuum and air-filled waveguides. They make possible to transfer RF power in these waveguides without reflection if the thickness of the window $d = \Lambda/2$, where Λ is the wave length in the waveguide filled with the dielectric.

For a rectangular waveguide with cross-section $a \times b$

$$\Lambda = \frac{\lambda}{\sqrt{\epsilon - (\lambda/2a)^2}},$$

$$\text{then } \epsilon = \frac{\lambda}{4} \left(\frac{1}{a^2} + \frac{4}{\Lambda^2} \right) = \frac{c}{4f} \left(\frac{1}{a^2} + \frac{1}{d^2} \right), \quad (1)$$

where f is frequency, λ and c are the wave length and speed of light in free space.

* vs65@cornell.edu

CLEANROOM ASSEMBLY OF THE LIPAc CRYOMODULE

J. K. Chambrillon[†], P. Cara, Y. Carin¹, D. Duglué, H. Dzitko, D. Gex¹, G. Phillips, F. Scantamburlo¹
F4E, Garching, Germany
T. Ebisawa, K. Hasegawa, K. Kondo, K. Masuda¹, M. Sugimoto¹, T. Yanagimachi
QST, Rokkasho, Japan
N. Bazin, N. Chauvin, CEA, Saclay, France
D. Jimenez, J. Molla, I. Podadera, CIEMAT, Madrid, Spain
E. Kako, H. Sakai, KEK, Tsukuba, Japan
W-D. Moeller, F4E Expert, Hamburg, Germany
¹IFMIF/EVEDA Project Team, Rokkasho, Japan

Abstract

In complement to the development activities for fusion reactors (JT-60SA & ITER), Fusion for Energy contributes to the R&D for material characterisation facilities. The LIPAc is the technical demonstrator for the production and acceleration of a D⁺ beam that will be used for neutron production by nuclear stripping reaction on a liquid Li target. Since its first beam in 2014 [1, 2], the LIPAc construction and commissioning continues and will be concluded with the cryomodule installation, aiming for beam validation at nominal power.

The cryomodule assembly, started in March 2019, was paused due to welding issues on the solenoid bellows. The slow pumping group used for the cleanroom assembly also needed improvement to overcome helium contamination. Two and half years were devoted to the pumping improvement and, repair, cold tests and high pressure rinsing of the solenoids.

In August 2022, the cleanroom assembly resumed with the mounting of all power couplers to the SRF cavities. Despite good progress, the assembly had to be paused again to fix leaks on different vacuum components and a solenoid BPM port.

This paper presents the issues faced and their solutions along the cold mass assembly.

INTRODUCTION

The Linear IFMIF Prototype Accelerator (LIPAc) is the technical demonstrator for the production and acceleration of a Deuteron beam that will be used for neutron production by nuclear stripping reaction on a liquid lithium target.

The assembly of the accelerator will reach its conclusion with the addition of the SRF cryomodule, aiming for beam validation toward nominal power (125 mA D⁺, 9 MeV, CW).

Started in March 2019, the assembly of the cryomodule had to be paused to manage technical issues on the superconducting solenoids sitting between the cavities and a strong helium background on the slow pumping system used for the cleanroom assembly.

Two and half years later, the assembly could restart after the end of travel ban in Japan.

The different issues encountered during the different assembly periods and their solutions as well as the different

progress done on the cleanroom assembly are hereinafter presented.

THE SUPERCONDUCTING SOLENOIDS PACKAGES

The SRF cryomodule of the LIPAc contains eight superconducting solenoids to focus the beam before each acceleration by the SRF cavities. Provided by CIEMAT as part of the Spanish contribution to the LIPAc, each of them is equipped with a Beam Position Monitor (BPM) similar to the ones used in LHC and were delivered with their current lead interface. The strong fields produced by the inner coils necessary to focus the high intensity beam are actively shielded by bucking outer coils to minimize the fringe fields and avoid remnant magnetization of material inside the passive magnetic shield [3]. The final solenoid configuration therefore consists of two concentric coils and four steering coils to correct the beam orbit.

Material and Welding Issue

During a first High Pressure Rinsing (HPR) some solenoids presented different aspect defects that can be categorised as follow: rust dots, weld quality issue, material trapped in bellows, external surface finishing, Figure 1.



Figure 1: From top right to bottom, rust dots on bellow, oversized weld seam, trapped material in bellow.

These defects were considered as critical knowing the sensitivity of the SRF cavities with metallic particulate

MEASUREMENT OF PARTICULATES UNDER SLOW PUMPING AFTER HIGH PRESSURE RINSING OF SUPERCONDUCTING CAVITY BY USING MODIFIED SLOW PUMPING SYSTEM

Hiroshi Sakai[†], Kensei Umemori, Eiji Kako, Ryo Katayama
 High Energy Accelerator Research Organization (KEK), Tsukuba, Japan

Abstract

Slow pumping system was used for particle free vacuum pumping in Superconducting rf accelerator. In KEK, recently slow pumping system was developed for the cryomodule assembly work with STF 9-cell cavities and worked well to reduce the particulates movements under pumping. However, this slow pumping system also wants to be used for preparation of vertical test. Before assembly work in clean room for vertical test, we normally apply high pressure rinsing (HPR). There are many waters on the cavity surface after HPR. Therefore, we keep one night to dry inside cavity in clean room. Unfortunately, some waters still remain in the cavity even though we keep drying in clean room for one night. This water might make some icing under pumping and stop flow in mass flow meter, which is used for slow pumping to control the flow. Therefore, we modified the slow pumping system to be robust under slow pumping even when water exists in the cavity. In this paper, we present the modified slow pumping system in KEK and the results of the vacuum trend through slow pumping of 9-cell superconducting cavity. We also measured the particulates under slow pumping after HPR by using vacuum particle monitor.

INTRODUCTION OF SLOW PUMPING & VENTING SYSTEM AT KEK

In general, the dusts or particulates in the superconducting (SC) cavity can produce field emission from the inner surface of cavity, and generate large amounts of radiation and cause the degradation of SC cavity performance. For examples, STF-2 cryomodules in KEK, which was constructed to establish the fundamental technology for Superconducting RF cavities with beam operation for the ILC [1], met the heavy field emission after cryomodule assembly work in 2014 [2]. During cavity string assembly in a local clean booth at STF tunnel, the sudden venting was done when the gate valve opened. We did not control the pumping and venting speed and we understood that it is necessary to establish a pumping system that does not allow contamination of dusts. Slow pumping is very effective to suppress the particulates moving under pumping and venting and recently used for cryomodule assembly on big SC accelerators [3]. This situation led us to develop new slow pumping and venting system in KEK at this time.

Figure 1 shows the schematic diagram of slow pumping and venting system of our first prototype [4]. The pumping system is similar to the pumping system which was used

on EURO-XFEL construction [3]. The vacuum particle monitor [5] was equipped to measure the particulates under pumping and venting in our system. Furthermore, we controlled to slowly move all gate valves. This is necessary not to produce particulate by moving the gate valve [6]. Slow pumping and venting speed were controlled by mass flow meter. Under slow pumping, the mass flow meter controlled the flow via the bypass line with small pipe. When the pressure reached to less than 100 Pa, the pumping line changed to the main pumping line with large diameter of 40 mm to obtain sufficient conductance and finally the cavity vacuum was pumped by Turbo Molecular Pump (TMP). Nitrogen gas was used for slow venting and the diffusers were set on the slow venting line. The pressure was measured by an ion crystal gauge. Dynamic range of the vacuum particle monitor is from 0.3 μm to 3.6 μm of particle size. The slow pumping speed is typically 0.6 l/min and venting speed is 0.2 l/min. No particulate moving was observed during slow pumping and venting with the above conditions [6]. We could suppress the particle movements by using this prototype.

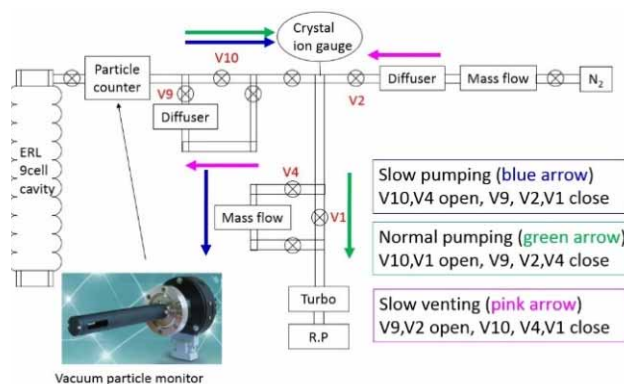


Figure 1: Schematic diagram of slow pumping & venting system of our first prototype with 9 cell cavity and valve assign (red).

After developing the first prototype slow pumping and venting system, we built slower pumping and venting systems that all valves were controlled automatically to slowly move the gate valve and its configuration was changed as shown in Fig. 2, for STF-2 cryomodule re-assembly work. Thanks to these slow pumping and venting system, we could keep the good pumping performance after STF cryomodule re-assembly work and satisfy the stable beam operation of 33 MV/m in STF-2 cryomodule [7]. Our developed slow pumping and venting system in KEK was also recently applied to other SRF laboratory in Japan [8].

[†] hiroshi.sakai.phys@kek.jp

Content from this work may be used under the terms of the CC BY 4.0 licence (© 2023). Any distribution of this work must maintain attribution to the author(s), title of the work, publisher, and DOI

DEVELOPMENT OF AUTOMATIC CLEANING AND ASSEMBLY SYSTEMS IN CLEAN ROOM AT KEK

Yasuchika Yamamoto, Masahiko Hiraki, Hiroshi Sakai, Kensei Umemori,
Takeshi Dohmae, Tomohiro Yamada, KEK, Tsukuba, Japan

Abstract

At KEK, new clean work systems including vertical auto cleaning system, replacement system between blank flange and bellows, and robot arm have been developed and installed since 2020 under the collaboration between Japan and France. The main purpose is unmanned and dust-free operation in clean room to avoid performance degradation with field emission in vertical test and cryomodule test. The vertical auto cleaning system and the replacement system between blank flange and bellows have been operated successfully in 2021-2022. Currently, clean work studies related to auto cleaning and assembly is under progress by combining the blank-bellows replacement system and a robot arm. In this report, the recent status of clean works at KEK will be presented.

INTRODUCTION

In recent years, as superconducting accelerators have become larger and larger, assembly work in clean rooms has become increasingly important. A typical clean room operation is the cleaning of cavities, input power couplers and vacuum components using an ionized gun. The cleaned parts are installed into the cavity one after another, and finally the cavity string assembly is completed and taken out of the clean room to finish. This cleaning work using the ionized gun is quite hard work, depending on the degree of contamination of the object, and requires high quality, as care must be taken to prevent dust from entering the cavity. Therefore, it makes sense to automate these tasks, which are difficult to maintain quality when performed by humans, using a robot arm.

Since 2020, KEK has been developing an automatic cleaning and assembly system for use in clean room operations under Japan-France cooperation. IRFU/CEA has already started their activities on the use of robotics in their clean room several years ago [1, 2].

The following three items have been developed: 1) a vertical automatic cleaning system for vertical test, 2) a replacement system between blanks and bellows for cavity string assembly, and 3) a robot arm system for automation. Of these, 1) is a prototype and fits only for cavity assembly for vertical test, while 2) and 3) are to be used in combination and are intended for cavity string assembly to install into cryomodule. We are currently conducting studies for each of these situations, which will be described in turn in the following chapters.

A VERTICAL AUTOMATIC CLEANING SYSTEM FOR VERTICAL TEST

The automatic vertical cleaning system was developed as a prototype automatic cleaning system to reduce the burden of the cleaning process during the assembly of the vertical test of the cavity. Instead of using a robot arm, the system uses a manipulator to enable horizontal and vertical swing oscillation in addition to R, θ , and Z-direction movements. However, only two patterns of simultaneous movement are possible: R- θ and R-Z planes. The typical speed is about several centimeters per second for safety. In the case of movement in the R- θ plane, the dust monitoring system counts the number of dusts as it moves in a circle, then returns to the origin along the same trajectory, and so on. The dust diameters that can be detected are 0.1 mm and 0.3 mm. R-Z plane operation is basically the same, although since it cannot move simultaneously in the θ direction, it must continue to clean the same angular location.

After various improvements and trajectory development since the commissioning test in March 2021, the system is now available as an automatic cleaning system. However, the ionized gun itself, which was selected for the first time at KEK, turned out to be a dust source, and in the end, 0.1 mm of dust was never eliminated. Figure 1 shows the vertical automatic cleaning system with an installed cavity. Figure 2 shows the developed trajectory on CAD and the dust trend during automatic cleaning.

A REPLACEMENT SYSTEM BETWEEN BLANKS AND BELLOWS FOR CAVITY STRING ASSEMBLY

The blank and bellows replacement auxiliary system is designed to replace the blank and bellows beam pipe attached to the flange of the cavity without direct hand contact, which is done during cavity string assembly. It can also be used as a training kit for practicing cavity string assembly procedures, consisting of two dummy cavities and three dummy bellows, with filters on the flanges at both ends for gas introduction. The dummy bellows also has a dust monitoring port, which leads to a dust monitoring system. The dust monitor used in this case is a SO-LAIR1100LD, which can detect simultaneously six dust diameters from 0.1 mm to 1.0 mm. During cavity string assembly, 0.1 MPa nitrogen gas through pneumatic lines is introduced as backflow from both ends of the cavity. However, in this study, the gas pressure through pneumatic line was increased as a trial. The results showed that there was no problem at 0.15 MPa, although many dusts penetrated through the filter when the pressure exceeded 0.2 MPa.

† yasuchika.yamamoto@kek.jp

OPERATIONAL CONSIDERATION IN THE LIPAc SRF WITH POTENTIAL SOLENOID FAILURE MODES

T. Ebisawa, K. Kondo, K. Masuda, A. Kasugai, K. Hasegawa, QST, Rokkasho, Japan
E. Kako, H. Sakai, KEK, Tsukuba, Japan

N. Chauvin, CEA Paris-Saclay, Gif-sur-Yvette, France

J. Chambrillon, G. Phillips, D. Gex, H. Dzitko, Y. Carin, Fusion for Energy, Garching, Germany

Abstract

The commissioning of LIPAc (Linear IFMIF Prototype Accelerator) is ongoing for the engineering validation of the high intensity deuteron beam accelerator system. The prototype Superconducting Radio-Frequency linac (SRF) cryomodule has been manufactured and will be assembled and tested on the LIPAc. During the cleaning process for the superconducting solenoid of SRF linac, some concerns appeared about two solenoids. As these two solenoids may not be used at nominal characteristics for the beam operation, the optimum positions of the suspicious solenoids and the condition of the beam transport were estimated as a mitigation action. By beam dynamics study, we concluded the position and condition for the beam operation without some solenoids. In this paper, the details of the beam dynamics simulation with solenoid failure modes will be presented.

INTRODUCTION

The International Fusion Materials Irradiation Facility (IFMIF) is an accelerator driven neutron source by D-Li reaction, which will produce high-energy neutrons at high intensity for the irradiation of the candidate materials for the nuclear fusion reactors [1]. One of the major technological challenges of the IFMIF accelerator is the handling the 125 mA deuteron beam at Continuous Wave (CW). Several SRF cryomodules are required for IFMIF to accelerate deuterons from 5 MeV to 40 MeV. In the EVEDA phase, the validation of the low energy section of the IFMIF accelerator up to 9 MeV is a prerequisite. The construction and commissioning of the Linear IFMIF Prototype Accelerator (LIPAc) is being conducted at Rokkasho Institute of QST, Japan in collaboration with EU. The LIPAc consists of the injector with ECR ion source and Low Energy Beam Transport (LEBT), Radio-Frequency Quadrupole accelerator (RFQ), Medium Energy Beam Transport (MEBT), one Superconducting Radio-Frequency Linac (SRF) cryomodule, High Energy Beam Transport (HEBT) and Beam Dump (BD) as shown in Fig 1. The first of these cryomodules is being assembled and will be subsequently installed and tested [2]. In 2019, the deuteron beam operation test of RFQ for 125 mA / 5 MeV at low duty cycle was successful. After the beam operation of the RFQ, a new beam transport line, MEBT Extension Line (MEL), was installed in place of the SRF Linac. It ensure the continuity between the MEBT and the HEBT, allowing their commissioning with the Beam Dump. The high duty beam operation test of the RFQ and

newly installed components have been started since 2021 and ongoing [3].

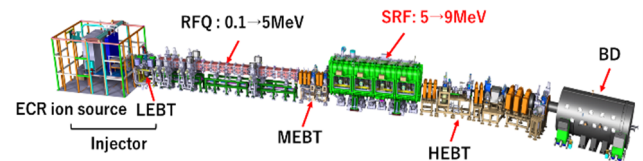


Figure 1: The schematic of the LIPAc.

As shown in Fig 2, the LIPAc SRF cryomodule consists of 8 superconducting Half Wave Resonator (HWR) working at 4.45 K, 175 MHz and RF power couplers for accelerating the beam. In addition, 8 superconducting solenoid magnet packages allow the focusing of the beam [4]. Table 1 shows the main specification of the LIPAc SRF cryomodule. The assembly of the cryomodule was started at QST, Rokkasho in 2019.

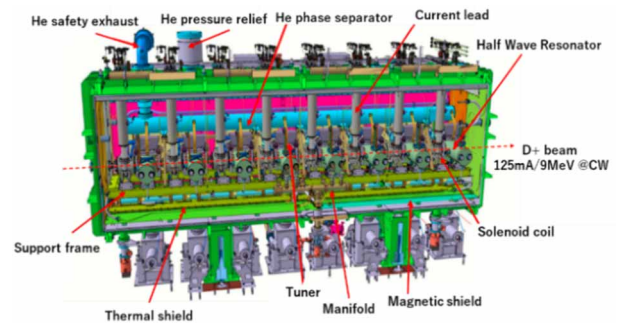


Figure 2: The schematic of the LIPAc SRF cryomodule.

Table 1: Main Specification of the LIPAc SRF

Parameter	Value
Frequency	175 MHz
Relativistic β	~ 0.1
Temperature	4.45 K
Average accelerating field	4.5 MV/m
Maximum solenoid field	6.0 T

After the fabrication and the tests of the superconducting solenoid packages in 2021, they were delivered to Japan and processed by High Pressure Rinsing (HPR) in clean room. By the completion of the solenoid HPR in 2022, the assembly was resumed. The detail of the progress is summarized in Ref. [5].

During the solenoid cleaning process, some concerns appeared about two solenoids having internal screws and pins disassembled [5]. After careful assessment of the

ON THE WAY TO A 10 MeV, CONDUCTION-COOLED COMPACT SRF ACCELERATOR

J. Vennekate*, A. Castilla, G. Cheng, G. Ciovati, J. Guo, K. Harding,
J. Henry, U. Pudasaini, R. Rimmer, JLab, Newport News, VA, USA
F. Hannon, Phase Space Tech, Bjärred, Sweden
D. Packard, General Atomics, San Diego, CA, USA
J. Rathke, JW Rathke Engineering Services, Centerport, NY, USA
T. Schultheiss, TJS Technologies LLC, Commack, NY, USA

Abstract

After the success of designing a compact 1 MeV, 1 MW accelerator based on conduction-cooled SRF, Jefferson Lab is now pursuing a concept to provide a tenfold increase of the beam energy. The obvious challenge for SRF is to move from a single-cell to a multicell cavity while maintaining high efficiency and the ability to operate the machine without a complex cryogenic plant. This paper summarizes the current state of this effort with respect to the design of a Nb₃Sn coated five-cell cavity and the corresponding RF components, especially the fundamental power coupler (FPC), as well as first thermal analysis of the cryocooler-based cooling setup.

MOTIVATION

The combination of Nb₃Sn coated SRF cavities and commercially available cryocoolers allows to envision accelerator designs which do not require a costly and complex cryogenic plant. Especially in the US, a variety of R&D efforts targeted at this technology transfer have been started [1–3]. As of now, these developments mostly aim at compact, single cavity systems yielding a beam energy of 1 to 10 MeV. Potential applications for such machines can be found in compact irradiation facilities for medical device sterilization, chemical industrial processes, as well as for many environmental applications, such as flue gas or wastewater treatment [4, 5]. The significant advantage of SRF compared to normal conducting (NC) technology in this field is the much higher efficiency of RF to beam power conversion. While existing NC solutions are therefore typically limited to few tens of kW in continuous wave mode (CW), the SRF design concepts mentioned above target the MW regime. Independent of the actual application, this allows for either much higher throughput or much larger dose application.

Recent studies at Jefferson Lab have successfully demonstrated the operation of multi-metallic, single-cell SRF cavity by conduction cooling in a horizontal test cryostat [6]. Together with this hardware demonstration, a concept design for a 1 MeV compact accelerator has been developed. In parallel, a new research effort aiming at a compact 10 MeV accelerator design has been initiated. A key element of the latter is advancing from a single to a multicell cavity.

* corresponding author – vennekate@jlab.org

915 MHz FIVE-CELL CAVITY

The first step for designing a multicell cavity is to pick the resonant frequency and the geometry with respect to the relative particle speed, i.e. $\beta = v/v_c$, with v_c the vacuum speed of light. As the operational cost of a compact SRF machine is dominated by the RF source, compare [1], the technology chosen here has a significant impact on the overall economical appeal of any derived application. Analyzing the available technology landscape, magnetrons stand out with an efficiency beyond 85%. Although there are certain disadvantages when compared to other available sources, namely phase stability and lifetime, significant progress has been made tackling these issues in dedicated research for compact machines [7]. The underlying technology is based upon industrial magnetrons used for heating processes. Their operation frequency is also within an acceptable range for SRF cavity design, i.e. 915 MHz, and was hence chosen for the multicell concept of this project. Table 1 gives the corresponding design parameters while Fig. 1 shows a 3D model of a 915 MHz five-cell cavity. A $\beta = 1$ has been chosen to reduce manufacturing and treatment complexity compared to a graded- β design while the actual geometry has been optimized to increase the accelerating field while minimizing the surface field.

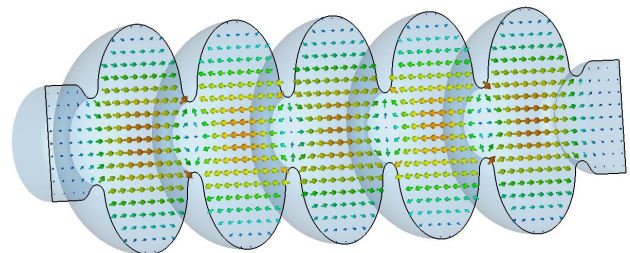


Figure 1: CST model of the 915 MHz five-cell cavity design, the arrows indicated the electrical field in π mode.

Multipacting Analysis

To analyze the generated resonator design for potential multipacting barriers, the code FISHPACT was utilized [8] with the secondary emission parameters for Nb₃Sn from [9]. The analysis is conducted by taking a field file computed with SUPERFISH [10] and examining the trajectories of electrons and secondary electrons emitted from the cavity surface. Fig-

DESIGN, FABRICATION, AND TEST OF A 175 MHz, BETA = 0.18, HALF WAVE RESONATOR FOR THE IFMIF-DONES SRF-LINAC*

J. Plouin[†], S. Chel, G. Devanz, N. Bazin, A. Madur, G. Jullien, C. Servouin, L. Maurice, M. Baudrier, Université Paris-Saclay, CEA, Département des Accélérateurs, de Cryogénie et du Magnétisme, Gif-sur-Yvette, France

Abstract

The IFMIF-DONES facility will serve as a fusion-like neutron source for the assessment of materials damage in future fusion reactors. The neutron flux will be generated by the interaction between the lithium curtain and the deuteron beam from an RF linear accelerator at 40 MeV and nominal CW current of 125 mA. The last accelerating stage is a superconducting (SRF) Linac hosting five cryomodules.

This SRF-Linac is equipped of two types of 175 MHz half wave superconducting cavities (HWRs). The first type of cavities (cryomodules 1 and 2), characterized by beta equal to 0.11, have been studied and qualified in the frame of IFMIF/EVEDA project. The development of the second type of cavities (cryomodules 3, 4, and 5), with higher beta of 0.18 is presented in this paper.

A prototype has been designed, fabricated and tested in a vertical cryostat at CEA. The measured quality factor at nominal accelerating field (4.5 MV/m) is $2.3 \cdot 10^9$, above the target in accelerator configuration (10^9). Moreover the quality factor stays above 10^9 up to 10 MV/m.

The next step is the fabrication of a helium vessel to be welded on the prototype, and the development of a dedicated frequency tuning system.

RF DESIGN

The SRF-Linac for IFMIF-DONES [1], represented in Fig. 1, hosts two cryomodules with low beta (LB) HWR cavities and three cryomodules with high beta (HB) HWR cavities, all the cavities working at 175 MHz [2, 3].

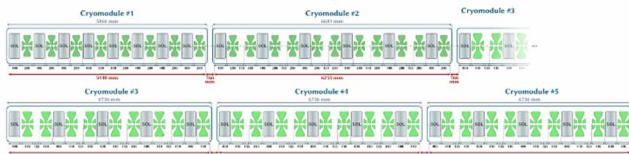


Figure 1: Layout of the 5-cryomodules SRF-Linac. Cavities are in green and solenoids in grey.

The design and qualification of the LB accelerating unit (low beta cavity equipped with its tuning system and power coupler) have been developed in the frame of IFMIF/EVEDA [4].

*This work has been carried out within the framework of the EUROfusion Consortium, funded by the European Union via the Euratom Research and Training Programme (Grant Agreement No 101052200 — EUROfusion). Views and opinions expressed are however those of the author(s) only and do not necessarily reflect those of the European Union or the European Commission. Neither the European Union nor the European Commission can be held responsible for them.

[†] juliette.plouin@cea.fr

Table 1: RF Design Requirements

Frequency	175 MHz
Beam current	125 mA
Beam aperture	50 mm
Nominal gradient, Eacc_nom	4.5 MV/m
Optimal beta	0.18
Quality factor @ Eacc_nom	10^9

The HB cavity, with a beta equal to 0.18, is aimed to reach a nominal gradient of 4.5 MV/m with a quality factor at least equal to 10^9 (see Table 1). The RF design has been optimized to reach all requirements, while limiting the peak field (see Fig. 2), and allowing RF power transfer to the beam. Both electric and magnetic peak fields at nominal gradient remain under the ones of the low-beta cavity (see Table 2). The external coupling range for the optimization of the RF power transfer to the beam is given in Table 2. For the nominal beam current and gradient, this range corresponds to an amount of RF input power between 100 and 140 kW. Moreover, it has been checked that this external coupling range could be reached with an antenna penetrating the 100 mm coupler port.

Table 2: RF Design Parameters

Max E field @ Eacc_nom	21 MV/m
Max B field @ Eacc_nom	36 mT
External coupling	$4.5 \cdot 10^5$ - $6 \cdot 10^5$

The high power RF couplers were validated up to 100 kW in the IFMIF/EVEDA project [5]. In order to fulfill the needs with margin, we plan some upgrades of the couplers to reach RF power as close as possible to 200 kW.

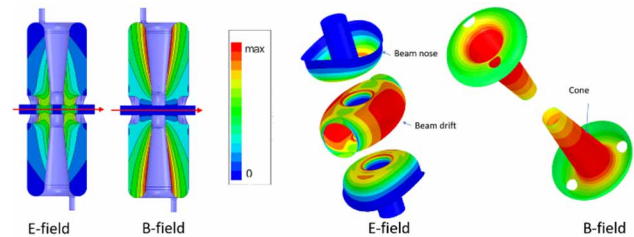


Figure 2: E and B field patterns in the DONES HB cavity: on cut planes (left) and on inner surfaces (right).

MECHANICAL DESIGN

The cavity body is made of bulk niobium (Nb), while the flanges are made of niobium/titanium (Nb/Ti) (Fig. 3). The

EQUIDISTANT OPTIMIZATION OF ELLIPTICAL SRF STANDING WAVE CAVITIES

V. Shemelin*, LEPP, Physics Dept., Newman Laboratory, Cornell University, Ithaca, NY, USA
 V. Yakovlev, Fermi National Accelerator Laboratory, Batavia, IL, USA

Abstract

A record accelerating rate was achieved earlier in standing wave (SW) SRF cavities when their shape was optimized for lower peak surface magnetic field. In view of new materials with higher limiting magnetic fields, expected for SRF cavities, in the first line Nb₃Sn, the approach to optimization of cavity shape should be revised. A method of equidistant optimization, offered earlier for traveling wave cavities is applied to SW cavities. It is shown here that without limitation by magnetic field, the maximal accelerating rate is defined to a significant degree by the cavity shape. For example, for a cavity with the aperture radius $R_a = 35$ mm the minimal ratio of the peak surface electric field to the accelerating rate is about $E_{pk}/E_{acc} = 1.54$. So, with the maximal surface field experimentally achieved $E_{pk} = 125$ MV/m, the maximal achievable accelerating rate is about 80 MeV/m even if there are no restrictions by the magnetic field. Another opportunity δ optimization for a low magnetic field, is opening for the same material, Nb₃Sn, with the purpose to have a high quality factor and increased accelerating rate that can be used for industrial linacs.

INTRODUCTION

A record accelerating rate was achieved earlier with elliptical SRF cavities [1] when their shape was optimized [2] so that the peak surface magnetic field B_{pk} was decreased by 10%, and the peak surface electric field E_{pk} was increased by 20% compared to the TESLA cavity with the same accelerating field E_{acc} on the cavity axis. This change of shape was done due to understanding that the superheating field B_{sh} (250 mT for Niobium [3]), the fac-

tual limit is about 210 mT) is the fundamental limit to acceleration in SRF cavities and decreasing the value B_{pk}/E_{acc} we can increase the accelerating rate E_{acc} . New materials, and first of all Nb₃Sn, are promised that they could be run at twice the magnetic field of Nb [3]. Does this mean that the accelerating rate can be twice the rate achieved in the Nb cavities? It seems that the surface electric field can become the next limit to the highest achievable accelerating rate. The surface electric field up to 12 MV/m has been demonstrated [1, 4, 5] in single-cell cavities. So, if this field is a limit, we need to decrease E_{pk}/E_{acc} to achieve maximal acceleration rate. For better results, as can be supposed, we should stay at equal distances from both limits. A method of equidistant optimization was offered earlier for TW cavities [6]. Now we apply this method to the SW elliptic cavities which are better studied than the TW SRF cavities and are easier in production than the TW ones.

GEOMETRY OF AN ELLIPTIC CAVITY

For easier explanation of the following, let us remind the geometry of the cavities under consideration.

Contemporary superconducting rf cavities for high energy particle accelerators consist of a row of cells coupled together as shown in Fig. 1. The contour of a half-cell consists of two elliptical arcs and a straight segment tangential to both. The contour can be described by several geometrical parameters shown in Fig. 1(b). Three of these parameters, length of the half-cell L , aperture R_a , and equatorial radius R_{eq} are defined by physical requirements: $L = \lambda/4$ (for π -mode), where λ is the RF wave length; the aperture is defined by requirements for coupling between cells and by the level of wakefields that can be allowed for a given

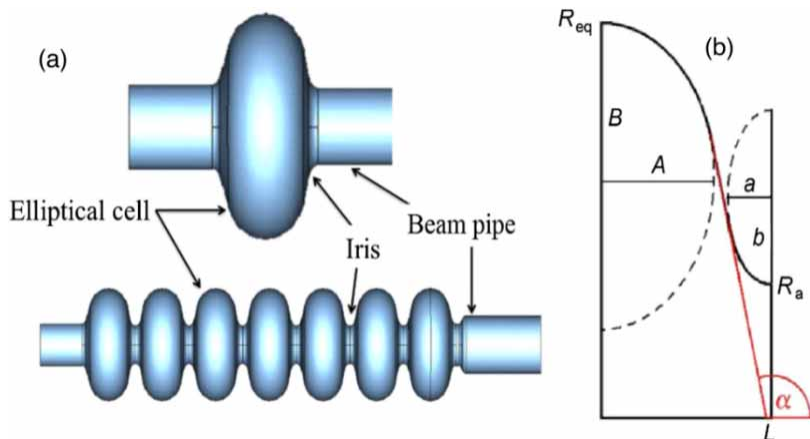


Figure 1: (a) Single-cell and multicell elliptical cavities; (b) geometry of the half-cell.

*vs65@cornell.edu

REFURBISHMENT AND REACTIVATION OF A NIOBIUM RETORT FURNACE AT DESY*

L. Trelle[†], C. Bate, H. Remde, D. Reschke, J. Schaffran, L. Steder, H. Weise
Deutsches Elektronen-Synchrotron DESY, Germany

Abstract

For research in the field of heat treatments of superconducting cavities, a niobium ultra-high vacuum furnace built in 1992 – originally used for the titanization of 1.3 GHz nine-cell cavities – and later shut down has recently been refurbished and reactivated. A significant upgrade is the ability to run the furnace in partial pressure mode with nitrogen. The furnace is connected directly to the ISO4 area of the clean room for cavity handling. At room temperature vacuum values of around 3×10^{-8} mbar are achieved. The revision included the replacement of the complete control system and a partial renewal of the pump technology. The internal mounting structures are optimized for single-cell operation including tandem operation (two single-cell cavities at once) and corresponding accessories such as witness-samples and caps for the cavities. The installation of additional thermocouples for a detailed monitoring of the temperature curves is also possible at the mounting structure. Due to the furnace design, its location and the strict routines in handling, very high purity levels are achieved in comparison to similar set-ups and hence provide a mighty tool for SRF cavity R&D at DESY.

THE FURNACE ARCHITECTURE

The furnace, designed for a vertical loading of 1.3 GHz nine-cell cavities, was originally built in 1992 for titanization purposes. After about 20 years of inactivity the furnace was reactivated in the context of research of new cavity temperature treatments.

The inner cylindrical recipient provides a diameter of 350 mm and is made entirely out of niobium. Also the removable furnace frame including the upper thermal shield consists completely of niobium. Loading and unloading takes place from above using a hand-operated crane. The recipient is surrounded by a second vessel which provides an additional vacuum for the heaters and the thermal shield. The structure is shown in Fig. 1.

Heating System

The heating capacity is dimensioned in such a way that temperatures of up to 1400 °C can be reached. The two tungsten heating coils, separated in upper and lower section, are located in the heater vacuum along with the thermal shielding.

Pump Infrastructure

The furnace has three different pump systems.

- **Support vacuum**
Volume: 1000 l
Target pressure: $p < 1 \times 10^{-6}$ mbar
Tubo pump: Leybold Turbovac 1000C
Scroll pump: Edwards nXDS10i
- **Recipient vacuum**
Volume: 330 l
Target pressure: depends on recipe
Cryo pumps: 2x Leybold COOLVAC 2000
Compressor: Leybold COOLPAK 6000H
Tubo pump: Edwards NEXT85D
Roots pump: Edwards EH250EU
Scroll pump: Edwards XDS35i
- **Intermediate suction (lid)**
Target pressure: $p < 2$ mbar
Membrane pump: Welch Iilmvac MP 201 T

Cooling System

The cooling system consists mainly of two separate water-cooling circuits.

- **Jacket cooling**
Net cooling capacity: 90 kW
Work pressure: 4 – 6 bar
Flow rate: 125 l/min
- **Cryo chiller**
Net cooling capacity: 0.97 kW
Work pressure: 1.5 – 2.5 bar
Flow rate: 20-30 l/min

The outer surface of the furnace and components that are particularly exposed to thermal loads, such as the flanges and electrical connections of the heaters, are connected to a circumferential pipe system for active water cooling. The system consists of a closed circuit that transfers the thermal energy to the nearby cooling water circuit via a heat exchanger. The system can be filled via a bypass to the well water network and can be fed directly from the well network in case of emergency.

The compressor of the cryo pump system possesses a dedicated cooling circuit connected to the well water network. The chiller itself works with an air-cooled cooling medium. It is located in the neighbouring hall section. The output water temperature is set to 16 – 17 °C to avoid condensation.

* This work was supported by the Helmholtz Association within the topic Accelerator Research and Development (ARD) of the Matter and Technologies (MT) Program.

[†] lennart.trelle@desy.de

NOVEL APPROACHES IN CHARACTERIZATION AND MODELLING OF FABRICATION PROCESSES FOR SRF COMPONENTS*

J. S. Swieszek^{1,†}, A. Gallifa-Terricabras, M. Garlasché, D. Smakulska, CERN, Geneva, Switzerland
¹also at Kraftanlagen Nukleartechnik GmbH, Heidelberg, Germany

Abstract

In the past years, Finite Element Methods have been increasingly applied at CERN, with the aim of modelling fabrication processes for SRF components. Currently, many large deformation processes such as deep drawing, forging, hydroforming, and spinning, are being simulated. Taking the initial trials out of the workshop via simulation has proven very efficient for steering fabrication strategy, avoiding unnecessary trials, and helping to reduce time and costs. This contribution will present a novel approach for studying fabrication process feasibility and failure prediction using numerical tools, based on the Forming Limit Diagram method, developed for OFE copper sheets. This contribution will show the application of the mentioned method on the study of tubular hydroforming, as an alternative way to produce seamless elliptical RF cavities. Analysis of past hydroforming trials is also discussed, together with the comparison of different fabrication strategies.

INTRODUCTION

The manufacturing of SRF cavities, as key components for particle accelerators, poses many challenges due to opposing requirements such as large ratio deformations, tight tolerances, and low surface roughness. In view of the current study for CERN's Future Circular Collider (FCC), seamless cavities are of interest, since they would allow to elude circular welds in correspondence of the cavity equator; the latter allowing to improve RF performance. Current R&D activities at CERN are focused on production of seamless OFE copper substrates for niobium coating, with hydroforming being one of the suitable processes. Nowadays, the presence of more reliable fabrication techniques, advanced calculation methods, and novel material characterization techniques, allows Hydroforming (HF) process to be better understood and optimized, providing a fast and repetitive fabrication method [1]. In this article the novel approach of characterization and modelling methods are being presented in the context of HF. The study focuses on 1.3 GHz OFE copper substrates, used as proof of principle, in view of production of the larger 400 MHz cavities, needed for FCC.

FAILURE MODELS

To properly assess the feasibility of a given process through FEM, an appropriate failure criterion needs to be defined. A commonly used failure criterion is maximal principal strain, which is based on the material elongation at break. However, this method proves conservative and inaccurate when modelling of large deformation behavior is

needed. Other measures can be maximal equivalent plastic strain or maximal allowable thinning. These failure criteria, if calibrated based on uniaxial tensile (UA), are equivalent with respect to the simple UA deformation conditions but are significantly different when considering three directional forming conditions. To obtain more accurate material' formability limits for sheet-like products, the Forming Limit Diagram (FLD) approach was thus adopted.

Forming Limit Diagram

FLD is a standard approach to predict ductile failure in metal sheet forming, being valid for proportional loading conditions. FLD correlates the minor vs major principal true strains (ϵ_2 and ϵ_1) for every volume in the formed piece. The Forming Limit Curve (FLC) indicates the onset of necking for different strain paths (i.e., uniaxial (UA), pure shear, plane strain (PS), ...) [2]. The preferable forming area is on the left branch of the graph, in between pure shear, and UA. The lowest point of the FLC, representing lowest formability, corresponds to the PS condition ($\epsilon_2=0$). FLD can also indicate failure by rupture thanks to the implementation of the Fracture Forming Limit (FFL) and of the Shear Fracture Forming Limit (SFFL). Figure 1 shows a part of FLD developed at CERN for Cu OFE 4 mm thick sheet [3].

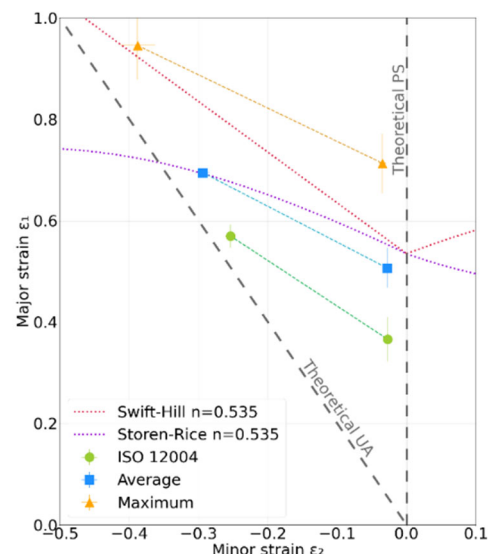


Figure 1: FLC for OFE-copper, 4 mm thick sheet [3].

Material Characterization

To build a complete FLD, Nakashima or Marciniak sets of tests need to be done. The material characterization campaign at CERN, was firstly focused on the left side of the FLD plot ($\epsilon_2 \leq 0$) since this region is of interest for HF simulations [1]. For such region, tensile tests were performed

* Work supported by FCC SRF WP2

† joanna.sylwia.swieszek@cern.ch

SIMULATION OF HIGH PRESSURE RINSE IN SUPERCONDUCTING RADIO FREQUENCY CAVITIES*

B. Gower[†], K. Elliott, E. Metzgar, T. Xu, FRIB, East Lansing, MI, USA

Abstract

The finish of radio frequency (RF) surfaces inside superconducting RF (SRF) cavities is of utmost importance as it dictates ultimate cavity performance. After the cavity surfaces have undergone chemical etching, polishing, and hydrogen degassing, the final step in surface preparation involves cleaning using a high pressure rinse (HPR) with ultra-high purity water (UPW) to remove any residue from the previous chemical processes. The complex surface geometry of cavities poses difficulties in achieving effective and thorough HPR cleaning. This study introduces a versatile simulation tool created in MATLAB, which has the potential to be applied to various SRF cavities. The detail of the algorithm used and nozzle and motion setup will be described using an FRIB $\beta = 0.53$ half wave resonator (HWR) cavity as an example.

INTRODUCTION

Using a high pressure rinse (HPR) to clean radio frequency (RF) surfaces inside superconducting RF (SRF) cavities is commonplace for removing chemical residues and particulates left behind from processing procedures. Introduced here is a simulation tool to determine HPR coverage a priori based on cavity geometry, nozzle geometry, and nozzle motion. Simulation using these geometries and parameters determines cleaning accessibility, cleaning intensity, and any areas of missed coverage. The FRIB $\beta = 0.53$ half wave resonator (HWR) [1-3] geometry is used here for illustration.

METHOD

At the heart of the HPR simulation tool is a ray casting algorithm created in MATLAB. Cavity interior surface geometry is imported from a stereolithography (STL) file consisting of a mesh of triangular elements. The jet exit plane(s) on an HPR nozzle are then used as the basis for the ray origin point and ray cast direction towards the mesh. Intersection of an individual ray with an individual triangular element is then determined.

Ray-Triangle Intersection

Figure 1 shows the geometrical considerations required to determine the intersection of a ray with a triangle [4]. Ray \mathbf{r} emanates from point P in the direction \mathbf{d} towards a triangle with vertices A , B , and C in three-dimensional (3D) space. An intersection, if it occurs, will be at point Q . The

algorithm determines the location of point Q , and the length, l , of the ray PQ .

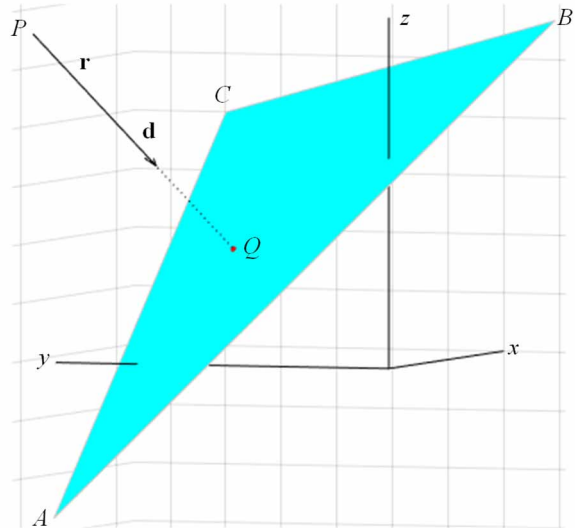


Figure 1: Ray-triangle intersection geometry.

The supporting plane of triangle ABC is described by the equation

$$ax + by + cz = d \quad (1)$$

The coefficients a , b , c form the vector normal to the plane in Eq. (1), i.e. $\mathbf{n} = [a \ b \ c]^T$, which is found by constructing vectors out of any two legs of the triangle and taking their cross product. Any vertex of triangle ABC can be substituted into Eq. (1) along with \mathbf{n} to determine d , thereby fully describing the supporting plane for ABC .

Prior to finding the length of PQ , the possibility of Q existing at infinity must first be ruled out, which is determined by taking the dot product of \mathbf{n} and \mathbf{d} . If this dot product is (deemed very close to) zero (i.e. \mathbf{n} and \mathbf{d} are perpendicular), the cast direction is said to be parallel with the supporting plane, and hence no intersection occurs.

In the case of a finite intersection point, substituting $\mathbf{r} = PQ = P + l\mathbf{d}$ for \mathbf{x} into $\mathbf{n} \cdot \mathbf{x} = d$ where $\mathbf{x} = [x \ y \ z]^T$ yields

$$l = \frac{d - P \cdot \mathbf{n}}{\mathbf{n} \cdot \mathbf{d}} \quad (2)$$

With the origin, direction, and length of the cast ray known, all that remains is to determine whether the intersection point lies on the interior of ABC . This is done by checking on which side of each edge point Q resides. Constructing a vector out of a leg and crossing it with a vector constructed from Q to the same base vertex determines whether or not e.g. QA is counter-clockwise from BA ; from the right hand rule, this cross product will be positive if so.

* Work is supported by the U.S. Department of Energy, Office of Science, Office of Nuclear Physics and used resources of the Facility for Rare Isotope Beams (FRIB), which is a DOE Office of Science User Facility, under Award Number DE-SC0000661.

[†] gower@frib.msu.edu

MECHANICAL DESIGN AND ANALYSIS OF SRF GUN CAVITY USING ASME BPVC SECTION VIII, DIVISION-2, DESIGN BY ANALYSIS REQUIREMENT*

M. Patil[†], S. Miller, T. Xu, S. H. Kim, C. Compton
Facility for Rare Isotope Beams, Michigan State University, East Lansing, MI, USA

Abstract

A prototype SRF gun is currently being designed at FRIB, MSU for the Low Emittance Injector of the Linac Coherent Light Source high energy upgrade at SLAC. This employs a 185.7 MHz superconducting quarter-wave resonator (QWR). The mechanical design of this cavity has been optimized for performance and to comply with ASME Section VIII, Div 2, Design by analysis requirements. This paper presents the various design by analysis procedures and how they have been adopted for the SRF gun cavity design.

INTRODUCTION

At the FRIB facility, MSU, there is an ongoing design and fabrication process for a cryomodule prototype intended for the high-energy upgrade of LCLS-II [1].

Figure 1, illustrates the SRF Gun cavity, which serves as the main element of the cryomodule. The cavity consists of a niobium resonator cavity encompassed by a titanium vessel. Operating at 4K, the titanium vessel holds superfluid helium gas. In addition to providing mechanical support to the cavity, the vessel plays a role in its tuning. Further information regarding the tuner and its mechanical analysis can be found in a separate reference [2]. The vessel is designated as a Pressure Vessel due to its capability to withstand pressures exceeding atmospheric pressure. While the exterior of the niobium RF resonator cavity is cooled by the helium gas, its interior remains in a vacuum state during beam line operation.

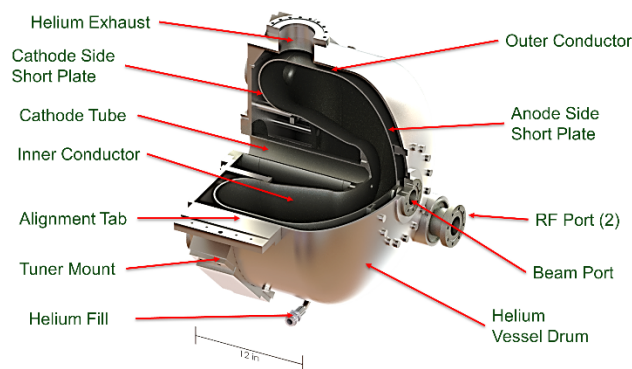


Figure 1: SRF Gun Cavity with key components.

MATERIALS

The SRF Gun Cavity assembly is constructed of four materials: Pure niobium, Ti-45Nb alloy, Grade 2 titanium, and 316L Stainless Steel. Of these materials, only Stainless Steel and Grade 2 Ti are approved by the Code [3], and hence has properties and allowable stresses available from Section II, Part D.

The room temperature material properties and allowable stresses for this analysis are identical to those established before for FRIB cavities.

At cryogenic temperatures, the yield and ultimate stress of Nb, Ti, and SS increase. The properties for these materials at cryogenic temperature were determined through previous work. However, no low-temperature data was available for Ti-45Nb alloy, so its room temperature properties were used for all temperatures. It is expected that, like the other materials, Ti-45Nb alloy would exhibit a significant increase in strength at cryogenic temperatures.

The most critical mechanical property for Niobium is its room temperature yield strength. As Niobium is the weakest material at room temperature and would be the first to yield in a hypothetical pressure scenario, we specify a minimum yield strength of 60 MPa for fine-grain Niobium to our vendors. Tensile tests conducted on Nb samples confirmed this minimum value, showing consistent yield strengths of around 60 MPa or more at room temperature [4]. The yield strength of these samples did not significantly change after baking at 600°C for 10 hours. Previous studies [5] aimed to determine the temperature at which niobium retains its mechanical properties while expelling most of the hydrogen present. They found that baking at 600°C is suitable, and a sharp decline in yield strength occurs at temperatures starting from around 650°C and above, as acknowledged by the authors of [6].

Based on this information, a yield strength of 60 MPa is used for BPVC calculations, which is consistent with all FRIB cavities designed and analyzed for a 60 MPa yield at room temperature

Table 1 presents the material properties employed for the SRF Gun Cavity analysis. Non-pressure boundary components such as the nose and stiffening rings utilize coarse-grain niobium for ease of fabrication and manufacturing. A yield strength of 30 MPa is assumed for these coarse-grain niobium components.

* Work supported by the Department of Energy under Contract DE-AC02-76SF00515

[†] patil@frib.msu.edu

VISUAL, OPTICAL AND REPLICA INSPECTIONS: SURFACE PREPARATION OF 650 MHz NB CAVITY FOR PIP-II LINAC*

V. Chouhan[†], D. Bice, D. Burk, M. K. Ng, G. Wu
Fermi National Accelerator Laboratory, Batavia, IL, USA

Abstract

Surface preparation of niobium superconducting RF cavities is a critical step for achieving good RF performance under the superconducting state. Surface defect, roughness, and contamination affect the accelerating gradient and quality factor of the cavities. We report surface inspection methods used to control the surface processing of 650 MHz cavities designated for the pre-production and prototype cryomodules for PIP-II linac. The cavity surface was routinely inspected visually, with an optical camera, and by microscopic scanning of surface replicas. This article covers details on the surface inspection methods and surface polishing process used to repair the surface.

INTRODUCTION

Proton Improvement Plan II (PIP-II) program is an essential upgrade to the Fermilab's accelerator complex. This includes a superconducting RF (SRF) linear accelerator (linac) to accelerate a proton beam to 800 MeV. The PIP-II linac includes normal and superconducting sections. The superconducting section will incorporate different types of cavities including two types of 650 MHz 5-cell elliptical cavities called low- β (0.61) and high- β (0.92) 650 MHz cavities. The cavity surface is processed with the state-of-the-art techniques including electropolishing (EP), heat treatment at 800 or 900 °C, and final light EP for the baseline test performed in a vertical cryostat.

Surface defects have a detrimental effect on the performance of the cavities. The common defects found earlier were deep pits appeared as cat-eye feature, non-conformality of weld zone, rough surface etc. Optical inspection is typically employed to detect these defects. Previous studies have involved surface study of 1.3 GHz cavities using an optical camera developed at Kyoto University [1], which has proven effective in identifying surface features and defects [2]. To capture surface features, surface replicas are created using a molding process using a silicone liquid gel [2]. These replicas enable high-resolution microscopic study of small surface features present on the cavity surface [2, 3].

This manuscript focuses on the challenges encountered during the surface processing steps involved in the preparation of low- β (LB650) and high- β (HB650) elliptical cavities. Furthermore, it presents the crucial roles played by surface inspection techniques, such as visual inspection, optical inspection, and surface replica examination, in aiding the decision-making process for surface treatment.

* This work was supported by the United States Department of Energy, Offices of High Energy Physics and Basic Energy Sciences under contract No. DE-AC02-07CH11359 with Fermi Research Alliance.

[†] vchouhan@fnal.gov

VISUAL AND CAMERA INSPECTIONS

Visual inspection of as-received cavity surface was performed to find any damage on the cavity surface. The visual inspection is performed to check the flanges, beam tube and the visible cell-wall through the beam tubes. Since the inner walls of the cells were not in line-of-sight through the beam tube, a small digital camera was inserted manually into the cavity to capture the images of the cell walls. Figure 1 shows a schematic of a digital camera inside the cavity. Each photograph covered a part of the half-cell. Multiple images were taken by rotating the camera along the cavity axis at every 45° angle. These images covered entire surface of the half-cell. The field of view of the camera covered the surface from the equator to iris of the half-cell. Photographs of another half-cell were captured when the camera angle was changed by 90° to face another half-cell. Figure 2 shows one of the captured photographs of the HB650 cavity before the EP process, providing sufficient clarity to detect any deep scratches, dents, or mechanical grinding marks. Except some minor scratches and mechanical polishing marks, no large defect was seen on the cavity surface. All the cavities qualified for the next step that was a detailed inspection of the equator surface with the optical camera.

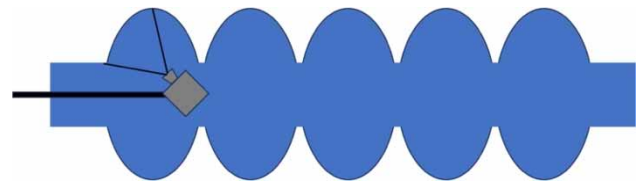


Figure 1: Schematic of a camera positioned inside the cavity.

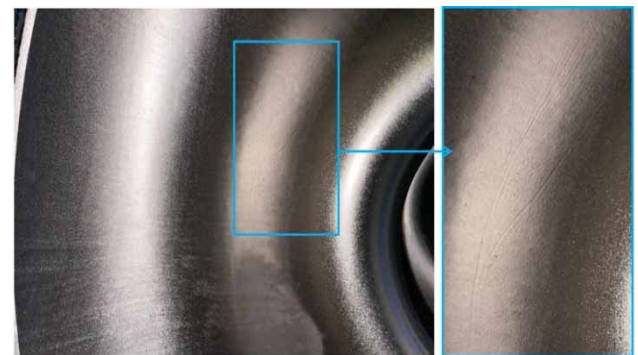


Figure 2: A part of the half-cell of an as-received HB650 cavity: Photograph captured with a digital camera inserted manually inside the cavity (left). Zoom-in image showing minor scratches (right).

LATEST DEVELOPMENT OF ELECTROPOLISHING OPTIMIZATION FOR 650 MHz NIOBIUM CAVITY*

V. Chouhan[†], D. Bice, D. Burk, S. Chandrasekaran, A. Cravatta, P. Dubiel, G. V. Ereemeev,
F. Furuta, O. Melnychuk, A. Netepencko, M. K. Ng, J. Ozelis, H. Park, T. Ring, G. Wu
Fermi National Accelerator Laboratory, Batavia, IL, USA
B. Guilfoyle, M. P. Kelly, T. Reid, Argonne National Laboratory, Lemont, IL, USA

Abstract

Electropolishing (EP) of 1.3 GHz niobium superconducting RF cavities is conducted to achieve a desired smooth and contaminant-free surface that yields good RF performance. Achieving a smooth surface of a large-sized elliptical cavity with the standard EP conditions was found to be challenging. This work aimed to conduct a systematic parametric EP study to understand the effects of various EP parameters on the surface of 650 MHz cavities used in Proton Improvement Plan-II (PIP-II) linear accelerator. Parameters optimized in this study provided a smooth surface of the cavities. The electropolished cavities met the baseline requirement of electric field gradient and qualified for further surface treatment to improve the cavity quality factor.

INTRODUCTION

Electropolishing (EP) is a widely utilized technique for treating metal surfaces. It is commonly employed to process niobium made superconducting radiofrequency (SRF) cavities [1–3], which are key components in particle accelerators. These cavities are operated at high frequencies, typically ranging from several hundred megahertz to a few gigahertz, in order to accelerate charged particles. The Proton Improvement Plan-II (PIP-II) linear accelerator (linac), with a target energy of 800 MeV, will incorporate various types of cavities, including low- β (0.61) and high- β (0.92) 650 MHz elliptical 5-cell cavities. These cavities are known as LB650 and HB650, respectively.

To meet the field gradient specification, the PIP-II elliptical cavities will undergo electropolishing to achieve a smooth interior surface. In a previous study, we emphasized the significance of cathode surface area by comparing the surface morphology of LB650 cavities. The larger cathode surface area provided required conditions including current plateau for electropolishing, as determined by I - V measurements [4]. It was previously established that the standard voltage of 18 V was insufficient for performing electropolishing of the LB650 cavities, particularly with a cathode surface area of approximately 5% of the cavity surface area. Increasing the cathode surface area to approximately 10% significantly reduced the required EP voltage. However, it was still higher than the standard 18 V

when the cavity temperature was 22 °C set in bulk EP process [4].

In this study, we present a new cathode specifically designed for electropolishing the HB650 elliptical cavities. The results include the cavity's surface and SRF performance, which are also compared to those obtained with LB650 cavities.

SETUP

EP Setup

The EP process for the 650 MHz cavities was conducted using a horizontal EP tool located at Argonne National Lab. Figure 1 displays a photograph of the EP setup, featuring a horizontally mounted 650 MHz 5-cell cavity.

For the standard EP procedure, a power supply with variable voltage from 0 to 80 V and the rated current of 500 A was used. Throughout the EP process, the temperature of the cavity was regulated by spraying temperature-controlled water onto the exterior surface of the cavity. The system utilized in this study was identical to the one used for EP of LB650 cavities. Further information about the system and data logging can be found elsewhere. [4, 5].

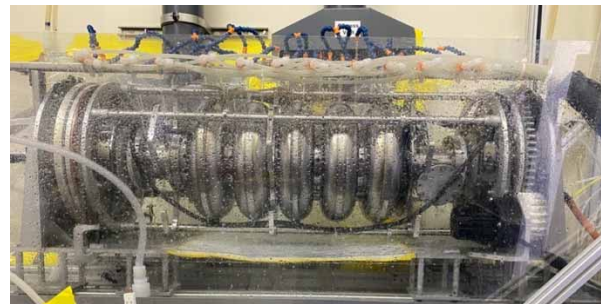


Figure 1: EP tool with a 650 MHz 5-cell cavity.

Cathode Structure

A novel cathode with an enhanced surface area was developed for EP of HB650 cavities. The surface area of HB650 cavity was 1.951 m². Figure 2 illustrates the design of the patented cathode [6]. There was no tape masking applied to the iris and beam tube regions. Instead, a floating mask that was set over the cathode pipe in the iris and beam tube regions was used. The entire cathode surface area was exposed to the acid to maximize the surface area of the cathode. This new design improved the ratio of cathode to anode surface area to approximately 3:10. Additionally, the cathode incorporated a spacious cross-sectional opening,

* This work was supported by the United States Department of Energy, Offices of High Energy Physics and Basic Energy Sciences under contract No. DE-AC02-07CH11359 with Fermi Research Alliance.

[†] vchouhan@fnal.gov

DEVELOPMENT OF 3-CELL TRAVELING WAVE SRF CAVITY*

F. Furuta[†], V. Yakovlev, T. Khabiboulline, K. McGee, Fermi National Accelerator Laboratory, Batavia, USA
R. Kostin, P. Avrakhov, Euclid Techlabs, Bolingbrook, IL, USA

Abstract

Traveling wave SRF cavity is a new technology and requires a multi-stage process for development. Conceptual designs have been proposed to adopt TW resonance in an SRF cavity. The early stages of developments have been funded by several SBIR grants to Euclid Techlabs which were completed in collaboration with Fermilab. A 3-cell proof-of-principle TW cavity was fabricated as part of that and demonstrated the TW resonance excitation at room temperature. A TW resonance control tuner for the 3-cell was also fabricated and the preliminary tests were performed. Now, the 3-cell cavity is being processed and prepared for the first cryogenic testing.

INTRODUCTION

Niobium SRF cavities have a theoretical peak magnetic field which limits the accelerating field to 50 - 60 MV/m using standard available designs. Presently all SRF cavities operate in a standing wave (SW) resonance field in which particles experience an accelerating force alternating from zero to peak. Changing to a travelling wave (TW) mode operation can improve the efficiency of acceleration per cell defined as the transit time factor T ($T = E_{acc}/E_{ave}$, E_{acc} : accelerating gradient, E_{ave} : average field gradient over the cell gap) since a TW resonance field propagate along with a TW structure and particles in such resonance field can experience a constant acceleration force. A TW structure proposed in the early study showed a T of 0.9 and the study suggested it could effectively increase the acceleration per cell more than 20% compared with a SW cavity [1]. Thereby, TW mode operation allows higher accelerating fields with niobium SRF cavities beyond the maximum gradient of 50 - 60 MV/m in a SW mode for the same peak surface magnetic field condition. This approach explores the path to 70 MV/m and higher using standard Niobium materials and processing technology. Increased cavity gradients can dramatically reduce the cost of SRF accelerators.

3-CELL TRAVELING WAVE CAVITY

Early Achievements

Traveling wave (TW) SRF cavity is a new technology and requires a multi-stage process for development. Conceptual designs have been proposed to adopt TW resonance in an SRF cavity [1, 2]. The early stages of developments have been funded by several SBIR grants to Euclid Techlabs which were completed in collaboration with Fermilab through a 1-cell prototype and 3-cell TW

cavity fabrication and testing. It demonstrated the feasibility of the fabrication and processing of multi-cell TW structure [3] and achieved the TW resonance excitation in the 3-cell TW cavity at room temperature [4, 5].

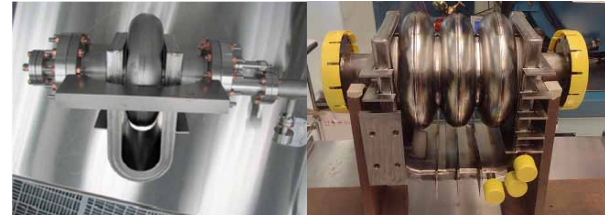


Figure 1: 1-cell prototype (left) [3] and 3-cell TW cavity (right).

TW Resonance Control in the 3-cell Cavity

To achieve TW resonance at 2 K in the 3-cell cavity, the following technical concepts were investigated and demonstrated during the early R&Ds; 1) the stiffened cavity design, 2) RF control using two input power couplers, and 3) a special tuner device [4, 5].

The loaded quality factor Q_{load} at 2 K in VTS will be around 10^8 , making the cavity bandwidth very narrow and sensitive to microphonics. The stiffening ribs were welded on the waveguide to reinforce the resonator (Fig. 1 right). Based on the simulations, the stiffened cavity design and fine tuning of RF input signals would be enough to withstand microphonics detuning.

The waveguide of the 3-cell cavity has two RF input couplers and three RF pick-up probes. During the study at room temperature, “clockwise” and “anti-clockwise” traveling waves inside the cavity and waveguide loop were mathematically extracted from the pick-up probe signals. The “anti-clockwise” traveling wave was suppressed by RF power redistribution and phase control between the two input signals. Thus, the desired “clockwise” traveling wave was established in the 3-cell cavity at room temperature. Figure 2 shows RF feed and measurement scheme at room temperature for the 3-Cell TW cavity by Euclid [4].

Lorentz force compensation was also considered to maintain the TW resonance at 2 K VTS conditions. A special tuner device (the matcher) for the 3-cell cavity was designed and fabricated to attach on the cavity. A matcher will deform the waveguide wall and decouple partial modes to compensate the Lorentz force [5]. The preliminary test on the matcher test assembly (Fig. 3) at room and liquid nitrogen temperatures indicated the feasibility of achieving TW resonance in 2 K. Figure 4 shows 3D model of the 3-cell prototype and the matcher.

*Fermilab is managed by Fermi Research Alliance, LLC (FRA), acting under Contract No. DE-AC02-07CH11359.

[†] ffuruta@fnal.gov

COMPACT MULTICELL SUPERCONDUCTING CRAB CAVITY FOR ILC*

A. Lunin[†], S. Belomestnykh, I. Gonin, T. Khabiboulline, Y. Orlov, V. Poloubotko, V. Yakovlev
FNAL, Batavia, IL, USA

Abstract

We propose a novel design of a crab cavity for the ILC project with low parasitic High Order Modes (HOM) losses and preserving the beam emittance, which is critical for operation with high beam current intensity. Multiple electrodes immersed in the hollow waveguide form a trapped-mode resonator. The transverse components of the electromagnetic field of the trapped dipole mode induce a transverse kick and efficiently deflect charged particles passing through the cavity. We present a scalable design of a superconducting Quasi-waveguide Multicell Resonator (QMIR) seamlessly connected with a beam vacuum chamber. The cavity is completely open at both ends, which significantly reduces the maximum loaded quality factor of the higher order modes, avoids complex HOM couplers, and thus simplifies the mechanical design of the cavity. The same port is used to feed RF power to the operating mode and to extract the same order modes. Finally, we estimate the expected cryogenic losses, HOM impedance limits, RF input power required, and frequency tuning for a QMIR cavity designed to operate at 2.6 GHz.

INTRODUCTION

International Linear Collider (ILC), a proposed linear electron-positron collider, plans to utilize crab cavities to enhance its luminosity. By introducing a transverse kick to the beams, the crab cavities (CCs) rotate the beam bunches, allowing for increased overlap at the interaction points. High intensity of the beam current and limited transverse space along the beam pipe near the interaction point resulted in choosing superconducting technology for the ILC/CC. There are numerous approaches on the design of the SRF deflecting cavities including elliptical multi-cell resonator, the Double Quarter Wave (DQW) resonator and the RF Dipole (RFD) crab cavity [1]. While all the designs can provide a necessary transverse kick voltage, one the biggest problem is dumping the spectrum of HOM excitation below given threshold to preserve a beam emittance. The conventional HOM couplers complicate the cavity geometry and increase the outer space occupied by the cavity. In this paper we present a novel scalable design of the Quasi-waveguide Multicell Resonator (QMIR) deflecting cavity originally developed for Short Pulse X-Ray operation of the ANL APS Upgrade project [2]. The cavity is fully open at both ends and connected with the beam vacuum chamber. Proposed solution significantly reduces the loaded quality factor of trapped modes, eliminates the need

of dedicated HOM couplers, and thus simplifies the mechanical design of the cavity. The prototype of QMIR cavity was build and successfully tested at 2 K in a vertical cryostat and demonstrated a record transverse kick of 2.6 MV [3]. We have re-optimized the cavity shape to comply with the requirements for the ILC crab cavity. The key specification parameters are listed in Table 1 for the baseline beam collision energy of 250 GeV (Higgs Factory) and for the ILC upgrade option of 1 TeV [4]. The cavity geometry with overall dimensions is illustrated in Fig. 1.

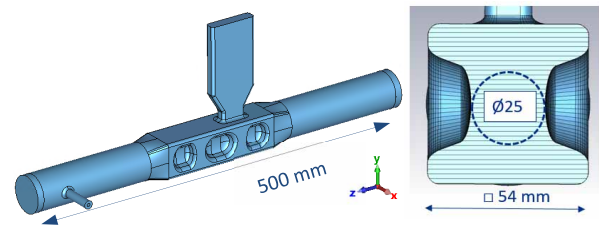


Figure 1: Geometry of the QMiR CC for ILC (left) and its cross-section showing the distance between opposite electrodes (right).

Table 1: Specifications for the ILC Crab Cavity

Parameter	250 GeV	1 TeV
Beam Energy (GeV)	125	500
Number of bunches	1312	2450
Repetition Rate (Hz)	5	4
Bunch Train Length (ms)	727	897
Bunch Spacing (ns)	554	366
Beam Current (mA)	5.8	7.6
Beam Size @CC (μm)	66, 300 (X,Y)	
Beta Function @CC (km)	23.2, 15,4 (X,Y)	
Cavity Frequency (GHz)	2.6	
Total Kick Voltage (MV)	0.92	3.7
Max surface E-field (MV/m)	45	
Max surface B-field (mT)	80	
Max Kick Factor (kV/pC/m)	1.6, 0.12 (X,Y)	
Max Impedance ($\text{M}\Omega/\text{m}$)	49, 62 (X,Y)	
Min CC aperture (mm)	25	
Beam lines separation (mm)	200 (at center)	
Max installation length (m)	3.8	

The cavity frequency was chosen to be 2.6 GHz, the operating mode second harmonic, as good compromise to provide the necessary kick and fit into the available transverse and longitudinal installation space. In this paper, we present the results of the cavity RF design, wakefield simulation, and statistical analysis of the HOM excitation. The

* This work was produced by Fermi Research Alliance, LLC under Contract No. DE-AC02-07CH11359 with the U.S. Department of Energy. Publisher acknowledges the U.S. Government license to provide public access under the DOE Public Access Plan

[†] lunin@fnal.gov

PIP-II SSR2 CAVITIES FABRICATION AND PROCESSING EXPERIENCE*

M. Parise[†], D. Passarelli, P. Berrutti

Fermi National Accelerator Laboratory (Fermilab), Batavia, IL, USA

D. Longuevergne, P. Duchesne

Irène Joliot-Curie Laboratoire (IJCLab), CNRS-IN2P3, Orsay, France

Abstract

The Proton Improvement Plan-II (PIP-II) linac will include 35 Single Spoke Resonators type 2 (SSR2). A pre-production SSR2 cryomodule will contain 5 jacketed cavities. Several units are already manufactured and prepared for cold testing. In this work, data collected from the fabrication, processing and preparation of the cavities will be presented and the improvements implemented after the completion of the first unit will be highlighted.

INTRODUCTION

The Radio-Frequency (RF) design and the mechanical design of the pre-production SSR2 [1] cavities was presented [2, 3]. The acquisition of the jacketed cavities, which were set to be produced by the industrial sector, was launched in early 2021, resulting in the first bare unit being finished by the year's end. Following a bulk Buffered Chemical Polishing (BCP), a thorough High Pressure Rinse (HPR) of the RF space, and a High Temperature Heat Treatment (HTHT), the jacketing process and testing at room temperature of the first cavity were finalized in July 2022. By September 2022 the first unit also received light BCP, HPR, the RF volume was sealed with flanges (2 of which included the antennas for the unity coupler and the field probe) in a cleanroom environment and 120 °C bake was the last step before shipping the unit. Other 2 units were manufactured by the same supplier and went through the same processing recipe since then. Moreover, the bare cavities' components for the next set of 3 units were formed and welded and they are waiting for the final Electron Beam (EB) welds to complete other 3 bare cavities. Some of the main parameters used for the design of the SSR2 cavities and that will be recalled in this work are reported in Table 1.

Table 1: Parameters of the SSR2 Cavity

Parameter	Value
Nominal Frequency, MHz	325
df/dp , $\frac{\text{Hz}}{\text{mbar}}$	<25
Target Frequency Allowable Error, kHz	+/-50
Maximum Allowable Working Pressure (MAWP) RT / 2 K, bar	2.05 / 4.1

* Work supported by Fermi Research Alliance, LLC under Contract No. DEAC02-07CH11359 with the United States Department of Energy

[†] mparise@fnal.gov

NIOBIUM FORMING

The crucial components to be fabricated include the endwalls, spokes, and spoke collars. In order to test the capabilities of the forming technique and equipment in producing components within the required mechanical tolerances, copper sheets are used as a substitute for precious niobium. Once the process is verified to yield the expected outcomes, the same procedures are followed to acquire the final components.

Metal spinning is employed to fabricate the endwalls, while deep drawing is utilized to obtain the spokes and spoke collars. The endwalls undergo the most significant reduction in thickness during the spinning process.

The thickness post spinning or forming is measured at (see Fig. 1):

- 36 different locations: 9 points spaced by 90 degrees for the endwalls;
- 30 different locations for the half spokes;
- 16 different locations: 4 points spaced by 90 degrees for the collars.

and the results are reported in Figs. 2, 3, and 4 as an average percentage thickness reduction at each location.

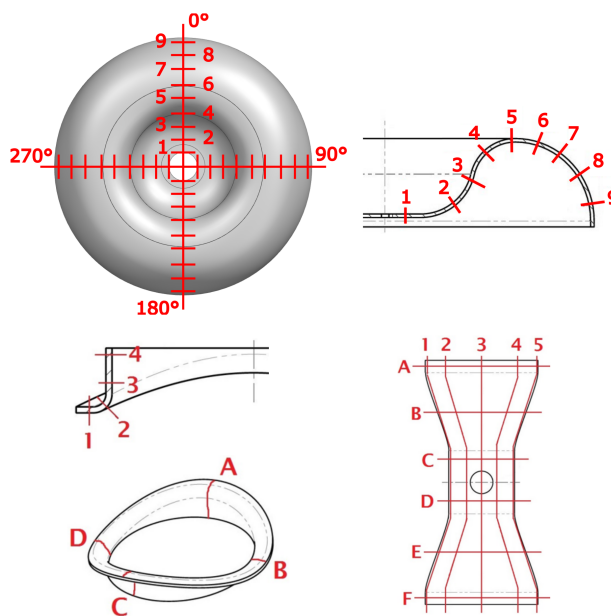


Figure 1: Points' location where the thickness is measured.

Content from this work may be used under the terms of the CC BY 4.0 licence (© 2023). Any distribution of this work must maintain attribution to the author(s), title of the work, publisher, and DOI

DEVELOPMENT AND PERFORMANCE OF RFD CRAB CAVITY PROTOTYPES FOR HL-LHC AUP*

L. Ristori[†], P. Berrutti, M. Narduzzi, Fermilab, USA
 J. Delayen, S. De Silva, Old Dominion University, USA
 Z. Li, A. Ratti, SLAC, USA; N. Huque, A. Castilla, JLab, USA

Abstract

The US will be contributing to the High Luminosity Large Hadron Collider (HL-LHC) upgrade at (Conseil Européen pour la Recherche Nucléaire) CERN with the fabrication and qualification of Radio-Frequency Dipole (RFD) crabbing cavities in the framework of the HL-LHC Accelerator Upgrade Project (AUP) managed by Fermilab. AUP received Critical Decision 3 (CD-3) approval by DOE in December 2020 launching the project into the production phase. The electro-magnetic design of the cavity was inherited from the LHC Accelerator Research Program (LARP) but needed to be revised to meet new project requirements and to prevent issues encountered during beam tests performed at CERN in the R&D phase. Two prototype cavities were manufactured in industry and cold tested. Challenges specific to the RFD cavity were the stringent interface tolerances, the pole symmetry, and the higher-order mode impedance spectrum. Chemical processing and heat treatments were performed initially at Fermilab (FNAL) and Argonne National Lab (ANL) and are now being transferred to industry for the production phase. Higher-Order Mode (HOM) dampers are manufactured and validated by Jefferson Laboratory (JLab). A summary of cold test results with and without HOM dampers is presented.

RF DESIGN

The RFD cavity utilizes the TE-11-like dipole mode to achieve crabbing of particle bunches. The cavity comprises two ridged deflecting poles housed within a square-shaped tank. The transverse shape was optimized to fit into the limited space available at the LHC beam line as shown in Fig. 1.

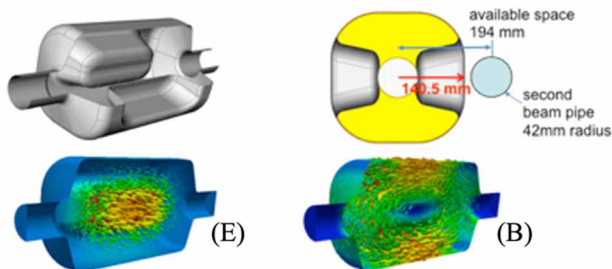


Figure 1: RFD cavity geometry (above left and right) and the electric and magnetic field patterns of its TE11-like deflecting mode (below left and below right).

* Work supported by Fermi Research Alliance, LLC under Contract No. DEAC02-07CH11359 with the United States Department of Energy
[†] leoristo@fnal.gov

With the transverse dimension being constrained, the cavity length and the rounding radius of the outer perimeter are the main parameters used to tune the cavity to the 400 MHz of design frequency. The pole length and the end gap are optimized to achieve a maximal shunt impedance. Elliptical rounding around the side corners of the poles and at around the pole tips were employed to minimize the peak surface fields. A curved profile is introduced to the gap surface to compensate the higher multipole fields due to the 3D geometry, especially the dominant sextupole term b_3 . Design parameters of the RFD cavity are shown in Table 1.

Table1: RFD Cavity Parameters, Including Higher-Order Modes (HOM)

Operating Mode	TE11
Frequency (MHz)	400.79
Lowest dipole HOM (MHz)	636
Lowest acc HOM	699
High R/Q acc HOM	752.2
Iris aperture (diameter) (mm)	84
Transverse dimension (mm)	281
Vertical dimension (mm)	281
R_T (ohm/cavity)	431
V_T (MV/cavity)	3.34
B_s (mT)	55.1
E_s (MV/m)	35.0
Multipole component b_3 (mT/m ² /10MV)	429

Higher-Order Mode Couplers

In the RFD design, there is no lower order mode. The deflecting mode is the lowest mode of the cavity. The lowest HOM frequency is more than 230 MHz above the operating mode. This makes it straight forward to utilize a high-pass filter approach in the HOM coupler design for wakefield damping. Figure 2 shows the RFD cavity with the HOM and FPC couplers.

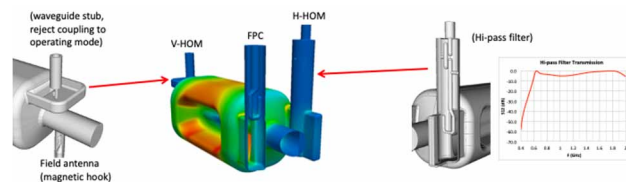


Figure 2: RFD cavity with HOM and FPC couplers. The H-HOM high-pass filter transmission curve is shown on the right.

THE EVALUATION OF MECHANICAL PROPERTIES OF LB650 CAVITIES*

J. Holzbauer, G. Wu[†], H. Park, K. McGee, A. Wixson, T. Khabiboulline, G. Romanov, S. Adams, D. Bice, S. K. Chandrasekaran, J. Ozelis, I. Gonin, C. Narug, R. Thiede, R. Treece, C. Grimm
 Fermilab, Batavia, IL, USA

Abstract

The PIP-II project's LB650 cavities could potentially be vulnerable to mechanical deformation because of the geometric shape of the cavity due to reduced beta. The mechanical property of the niobium half-cell was measured following various heat treatments. The 5-cell cavities were tested in a controlled drop test fashion and the real-world road test. The result showed that the 900 °C heat treatment was compatible with cavity handling and transportation during production. The test provides the bases of the transportation specification and shipping container design guidelines.

INTRODUCTION

The PIP-II linac consists of several types of cryomodules made of HWR, SSR1, SSR2, LB650, and HB650 cavities [1]. The dynamic heat load of the cavities in cryomodules is primarily of SSR2, LB650, and HB650 cryomodules, as shown in Figure 1 [2].

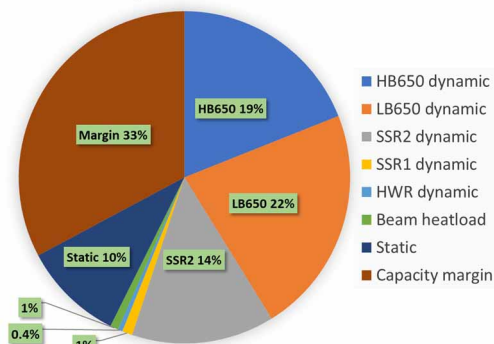


Figure 1: PIP-II linac total heat load includes the static, dynamic, beam, and static heat loads.

The 650 MHz cavities have high Q_0 processing procedures to minimize the total heat load. The high Q_0 processing includes nitrogen doping or medium-temperature furnace baking (Mid-T furnace baking). As a result, cavities receiving the high Q_0 processing have a higher surface resistance sensitivity to the trapped magnetic field [3], as seen in Table 1.

It has been demonstrated that a successful magnetic shielding design and magnetic hygiene implementation can reduce the residual magnetic field seen by cavities in a cryomodule to ~ 1.5 mG [4].

However, thermoelectric current could flow through cavities during the cryomodule cooldown, generating up to 8 mG residual magnetic fields [5]. If trapped during the superconducting transition, those residual magnetic fields could dramatically increase the cavity dynamic heat load regardless of the processing method.

Table 1: Surface Resistance Sensitivity of Magnetic Field Trapping

Processing	Surface Resistance Sensitivity [nΩ/mG]
EP only	0.4
N-doped	1.4
Mid-T furnace baking (350 °C)	1.0

The fast cooldown has been demonstrated in LCLS-II cryomodules that can effectively expel the thermoelectric current-induced magnetic field [6]. In addition, the heat treatment of niobium cavities at 900 °C for 3 hours has been confirmed for several LB650 cavities that can expel much of the residual magnetic field, while the cavities treated at 800 °C for 3 hours resulted in the field mainly being trapped [7].

The geometry of the PIP-II projects' 650 MHz cavities, particularly the LB650 cavities, indicated that the cavity's effective mechanical strength might be weaker than that of ILC 1.3 GHz cavities. A 900 °C treatment may decrease the niobium yield strength to a level that could deform the cavity during handling, transportation, and pressure testing. Therefore, a validation plan was developed to verify the cavity's mechanical strength. The plan included the following tests:

- Sample mechanical tests
- Transportation tests on local highways
- Controlled drop tests
- Pressure tests of a jacketed cavity.

EXPERIMENT

Sample Preparation

Niobium samples were made from the same niobium sheets used to fabricate LB650 Cavities. They were the corner material during the cavity sheet preparation. The material has a 4.5 mm thickness. The samples were prepared as full-size dog bones according to the ASTM standard. The

* Work supported by Fermi Research Alliance, LLC, under Contract No. DE-AC02-07CH11359 with the U.S. Department of Energy, Office of Science, Office of High Energy Physics

[†] genfa@fnal.gov

HORIZONTAL TEST RESULTS OF 1.3 GHz SUPERCONDUCTING RF GUN #2 AT KEK

T. Konomi^{#,†}, H. Inoue, X. Wang, R. Ueki, K. Umemori, E. Kako, Y. Kondo, K. Tsuchiya, T. Takatomi, A. Terashima, K. Hara, K. Hosoyama, Y. Honda, M. Masuzawa, M. Omet
KEK, Tsukuba, Japan

Abstract

Superconducting radio-frequency (SRF) electron guns are attractive for delivery of beams at a high bunch repetition rate with a high accelerating field. The SRF gun with 1.5 cell has been developing at KEK to demonstrate fundamental performance. The SRF gun consists of 1.3 GHz SRF gun cavity and multi-alkali photocathode coated on 2 K cathode plug. In the vertical test of the gun cavity, the surface peak electric field and the surface peak magnetic field reached to 75 MV/m and 170 mT, respectively. The SRF gun was installed into the horizontal multipurpose cryostat equipped with a superconducting solenoid, photocathode preparation chamber and beam diagnostic line. The peak surface gradient dropped to 42 MV/m. This was probably due to particulate issued that entered the cavity during assembly. The results in the horizontal test are presented in this paper.

INTRODUCTION

The design of a superconducting RF gun has been started at KEK for demonstration of fundamental performance based on the beam parameters of the KEK ERL project [1]. The gun consists of a 1.3 GHz, 1.5-cell niobium SRF cavity and a niobium cathode plug cooled down to 2 K. A prototype cavity (gun #1) was developed for demonstrate high gradient performance in vertical test. Optimized surface treatment methods for gun cavity shape were developed. a maximum surface electric field of 75 MV/m and a maximum surface magnetic field of 170 mT were achieved [2]. The KEK SRF gun #2 is designed to demonstrate high gradient performance with small current beam operation. RF design of gun #2 is same as gun #1. A helium jacket with frequency tuner, a superconducting magnet, and a 90-degree bending magnet were designed and fabricated. A beam line was designed to measure beam emittance and beam energy.

DESIGN OF KEK SRF GUN #2

Figure 1 shows the structure of the superconducting RF electron gun, which consists of a 1.3 GHz, 1.5-cell niobium superconducting RF accelerating cavity, a niobium cathode plug, and a choke cell to stop RF leakage from the cathode plug side. The cathode plug is removable and cooled by conduction cooling from the holder in 2 K helium bath of the cavity. The helium jacket covers the cavity and the cathode plug holder. The jacket has a bellows to tune the

cavity frequency and inside double bellows to adjust the position of the cathode plug. The frequency tuner is attached to the helium jacket.

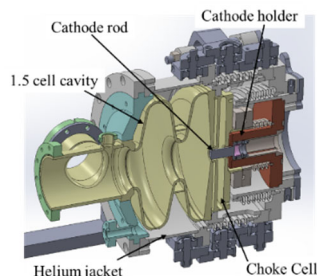


Figure 1: Structure of the KEK SRF gun #2.

Figure 2 shows the electromagnetic field distribution on the axis and surface of the superconducting RF electron gun. Because static magnetic field cannot penetrate superconducting wall, the beam is focused by the accelerating electric field distribution. In addition, the cell length of the second cell is shortened to prevent deceleration due to the RF leakage electric field. The acceleration voltage of the second cell is set low to achieve an acceleration voltage of 2 MV.

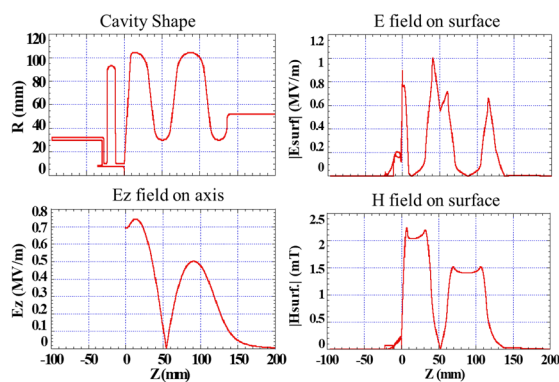


Figure 2: RF field distribution of the KEK SRF gun #2.

Table 1: RF Parameters of KEK SRF Gun #2

Parameter	Value
RF frequency	1.3 GHz
Accelerating Voltage (Vc)	2 MV
Geometrical Factor	133.1 W
Surface Peak Electric Field (E_{sp}) @Vc=2MV	41.9 MV/m
Surface Peak Magnetic Field (H_{sp}) @Vc=2MV	92.4 mT
H_{sp}/E_{sp}	2.2 mT/(MV/m)
Z_{ESP}^*	241.3

$$*E_{sp} = Z_{ESP} \sqrt{Q_0 P_{loss}}$$

SRF Technology

Cavity design/fabrication/preparation/tuning

Content from this work may be used under the terms of the CC BY 4.0 licence (© 2023). Any distribution of this work must maintain attribution to the author(s), title of the work, publisher, and DOI

[#] Current Affiliation is Michigan State University (MSU)/ Facility for Rare Isotope Beams (FRIB).

[†] konomi@frib.msu.edu

A NOVEL MANUFACTURE OF NIOBIUM SRF CAVITIES BY COLD SPRAY

M. Yamanaka[†], K. Shimada¹, KEK, Tsukuba, Japan

¹currently at College of Engineering, Nihon University, Koriyama, Japan

Abstract

Niobium coating technology has been developed for superconducting radiofrequency (SRF) cavities to reduce material costs. Cold spray (CS), a film formation method that feeds solid-state particles onto a target to form a thick film in a short time, is the focus of this study, with the aim of reducing the cost. To verify the feasibility of manufacturing an entire structure of SRF cavities using CS, an additive lathe method with CS was performed. Niobium particles were supplied through a CS gun manipulated by a robot arm to consistently orient the blast direction to the normal direction of an aluminum alloy sacrificial mandrel. Nb-made cavities were successfully fabricated by dissolving the mandrel in hydrochloric acid.

INTRODUCTION

Superconducting radiofrequency (SRF) cavities are a key component of particle accelerators, and they are mainly made of niobium (Nb) because they possess the highest transition temperature (T_c) of all pure materials [1, 2]. There are higher- T_c compounds such as NbN and Nb₃Sn, but at present, they do not match Nb in terms of their performance with increasing RF fields or ease of use for accelerator applications. In other words, Nb is still the best option for SRF cavities [2]. However, Nb is a rare metal and its material cost is a problem. Thus, Nb coating on copper (Nb/Cu; hereafter, a layer structure consisting of the outermost layer X₁, second layer X₂, third layer X₃, ..., and substrate Y is denoted as X₁/X₂/X₃.../Y) technology has been researched to reduce the raw material cost [3]. Additionally, Nb/Cu technology provides more advantages, such as thermal stability, insensitivity to earth magnetic field trapping, and freedom from undissolved inclusions [2, 3]. Sputter coating was developed at CERN for Nb/Cu coating in 1980 [4], and research has been conducted to overcome problems such as the theoretical limit of bulk Nb and the Q -slope [5]. As a unique alternative, Fonnesu et al. [6] developed a reverse coating that employed a sacrificial Al mandrel to form a Cu/Nb/Al structure, which was subsequently etched to obtain the Cu/Nb structure. They also reported that the Cu/Nb/Cu/Al structure was better for the Nb layer because the Cu layer between Nb and Al protected Nb from the final etching.

Because the London penetration depth λ_L of Nb is as short as ~ 40 nm and the SRF properties are determined only on the surface, a couple of micrometers is sufficient for the thickness of the deposition film in theory [2]; however, in practice, the thickness affects the technical difficulties of the pre- and post-process. For example, the surface roughness prior to a sputtering process strongly influences the quality of the deposition film [3]; thus, a

mirror finish of several nanometers is required on the entire internal surface of the cavity. In addition, a shallow deposition thickness does not allow post-processing to correct the shape defects of the film.

Cold spray (CS) is a film formation method; different from conventional thermal spraying techniques, CS feeds solid-state particles with supersonic speed to form thick films on the target [7]. Because the particles remain in a solid state throughout the process, CS can suppress oxidation, thermal stress, and high temperatures [8]. Additionally, the main advantage of CS over other film formation methods for SRF cavities, such as high-power impulse magnetron sputtering (HiPIMS) [5] and electron cyclotron resonance (ECR) [9], is its deposition rate; in our preliminary research, the deposition rate of the CS reached 300 mm³/min, which was several digits greater than that of the sputter method.

Kumar et al. [10] reported that CS successfully deposited a superconducting Nb film on a Cu substrate and confirmed that the film transitioned to the superconducting state. CS was also applied to form a thick copper layer on Nb SRF cavities, hoping to enhance the conduction cooling ability [11]. However, the fabrication of the entire structure of Nb SRF cavities has yet to be reported. Therefore, we attempted to manufacture models of seamless SRF cavities using CS to confirm their feasibility. In addition, superconducting tests were performed to confirm the superconducting performances of the test pieces.

EXPERIMENTAL

Cold Spray

The niobium powder employed in the CS experiment was manufactured by Taniobis GmbH, Germany (Ampertec® TS niobium metal powder 10–30 μ m), and its microphotography is illustrated in Fig. 1. The chemical compositions are listed in Table 1.

Cold spray was performed using a commercially available device (PCS-1000, Plasma Giken Co., Ltd., Japan [12]), and it was manipulated by a robot arm with six degrees of freedom (Motoman MS80, Yaskawa Electric Corp., Japan). The experimental conditions for the CS

Table 1: Chemical Compositions of the Niobium Powder Measured by Manufacturer (unit: wt. ppm)

C	H	N	O	Fe	Cr	Ni	Mn
<10	<10	57	526	<2	<2	<2	<1
Na	K	Mg	Ca	Si	Mo	Ta	W
<1	<1	97	<3	<3	<4	73	<5

INFN LASA EXPERIMENTAL ACTIVITIES FOR THE PIP-II PROJECT

M. Bertucci*, M. Bonezzi, A. Bosotti, D. Cardelli, E. Del Core, F. Fiorina, A. T. Grimaldi,
L. Monaco, C. Pagani, R. Paparella, D. Sertore, M. Zaggia
INFN Milano - LASA, Segrate, Italy

Abstract

INFN LASA is upgrading its vertical test facility to allow high-Q measurements of the PIP-II LB650 SRF cavities. Such facility is equipped with a wide set of diagnostics for quench, field emission and magnetic flux expulsion studies and will offer a better understanding of cavity performance. At the same time, R&D on LB650 cavity prototypes is ongoing, in order to optimize the overall processing as well as the cavity Jacketing in view of the forthcoming series production with industry. This paper reports on the overall status of these experimental activities.

INTRODUCTION

The Fermilab Proton Improvement Plan II (PIP-II) Linac [1] is designed to provide an 800 MeV H- beam. This beam will then undergo injection into the Booster Ring and subsequently be transferred to the Main Injector ring, ultimately enabling the generation of a powerful 1.2 MW beam. This high beam power is crucial for conducting the LBNF and DUNE neutrino physics experiments, which hold significant implications for scientific research.

A vital aspect of the PIP-II linac is the low-beta (LB) section, for which INFN LASA has taken responsibility. The task involves the production of 40 superconducting cavities operating at 650 MHz with a β value of 0.61 [2]. To ensure optimal performance within the machine, these cavities must meet specific requirements, including an E_{acc} of 16.9 MV m^{-1} and a Q_0 value of at least $2.4 \cdot 10^{10}$ at the operating field. Achieving these high-performance standards necessitates the development of a “high-Q” surface recipe. Extended research has been conducted to explore various recipes in order to identify the most optimal solution in terms of cavity performance and mechanical stability. It is for instance crucial to ensure that target values for Q_0 and E_{acc} are maintained throughout the entire production process, from before the Helium tank Jacketing to the installation in the cryostat. Any significant drifts in the operating frequency and cavity field flatness must be minimized. Meeting these stringent requirements has prompted the development of an optimized cavity processing sequence that is suitable in the context of a large-scale series production.

CURRENT STATUS OF PIP-II LB650 CAVITY PROTOTYPES

INFN, in collaboration with the company Zanon Research & Innovation Srl., manufactured a total of 7 PIP-II LB650 prototypes. Among them, 5 are single-cell cavities, while

* michele.bertucci@mi.infn.it

the remaining 2 are multicell cavities. As part of the collaboration, 2 cavities were shared with FNAL [3]. One of the single cell cavities, named B61S-EZ-001, underwent a high-Q recipe based on N-doping. The process included a $160 \mu\text{m}$ bulk EP, followed by a 900°C HT for 3 hours + $2/0$ N-doping at 800°C . The cavity was then subjected to a final EP. The second shared cavity, the multicell cavity named B61-EZ-001, underwent a baseline treatment. This involved a $160 \mu\text{m}$ bulk EP, a 800°C HT for 2 h, a final EP and a 120°C 48 h bake. Eventually the cavity was jacketed with helium tank. In both cases, the project goals were successfully met.

Single cell cavity B61S-EZ-002 and multicell cavity B61-EZ-002 were surface-treated at the company under the supervision of INFN, with the goal of optimizing the already operating infrastructures to the specific case of LB650 cavities, and then to demonstrate the feasibility of high-Q treatments of LB650 cavities in the industrial context. Two other single cell cavities will be surface processed in the future with high-Q recipes which are still under definition.

Cavity B61S-EZ-002

The single cell cavity B61S-EZ-002 played a crucial role in adapting the Electropolishing plant to the different size and geometry of PIP-II LB650 cavities. The treatment parameters were carefully optimized to enhance smoothness, removal rate and iris/equator removal ratio [4]. To increase the removal rate at the equators, aluminum cathode enlargements were installed in correspondence of the center of cells. Subsequently, the same cavity was then utilized to test a baseline treatment sequence that will serve as a reference for future high-Q treatments. This sequence involved a $150 \mu\text{m}$ bulk EP, a 800°C HT for 2 h, a $25 \mu\text{m}$ cold final EP and a 120°C 48 h bake. In the final EP treatment the “cold” regime was employed. The average temperature on cavity surface is maintained below 12°C , ensuring a smoother surface finishing at the end of the treatment. The vertical test results at 2 K are affected by poor flux expulsion regime due to the slow cooldown rate of LASA-INFN cryostat (approximately 1 K min^{-1} at the transition temperature corresponding to a 82% measured trapped flux efficiency). Despite this, a $Q_0 = 2 \times 10^{10}$ was achieved at the target $E_{acc}=16.9 \text{ MV m}^{-1}$ [5]

Cavity B61-EZ-002

The multicell cavity B61-EZ-002 underwent the mid-T bake recipe. The treatment involved a $150 \mu\text{m}$ bulk EP, followed by a 800°C HT for 2 h, a $5 \mu\text{m}$ cold final EP and a 300°C 3 h bake. This last step took place in the same

RECONSTRUCTION OF FIELD EMISSION PATTERN FOR PIP-II LB650 CAVITY

E. Del Core, M. Bertucci, A. Bosotti, A. T. Grimaldi, L. Monaco, C. Pagani¹,
R. Paparella, D. Sertore, INFN Milano - LASA, Segrate, Italy
¹ also at Università degli Studi di Milano, Segrate, Italy

Abstract

Field emission (FE) is a key limiting phenomenon in SRF cavities. An algorithm exploiting a self-consistent model of cavity FE has been developed. This method exploits experimental observables (such as Q value, X-ray endpoint, and dose rate) to reconstruct emitter position and size as well as the field enhancement factor. To demonstrate the model's self-consistency, the algorithm has been applied to the test results of a PIP-II LB650 prototype cavity. The results of the procedure are here described.

INTRODUCTION

One of the most limiting factor to the accelerating gradient in superconducting radio-frequency (SRF) cavities is Field Emission (FE). This phenomenon is associated with the surface electric field and refers to the emission of electrons from regions of high electric field on the cavity surface [1,2]. These emitted electrons, originating from the *emitters* sites, are accelerated by the RF field until they impact the cavity surface. As a result of this impact, X-ray radiation can be generated. The power deposited by the impacting electron depends both on the trajectory of the particle and on the intrinsic properties of the emitter. In SRF cavities, FE scales exponentially with the electric field and contributes to the consume of RF power. Consequently, it may correspond to an undesirable and unavoidable degradation of the Q-value, leading to an increase in cryogenic consumption [3].

Physical Description

In a metal, electrons are typically confined by a potential barrier that cannot be escaped in normal conditions. This gap between the Fermi level in the metal and the vacuum level, referred to as the metal work function and having a value of 4-5 eV, can be overcome when electron acquires energy through thermionic emission or photoemission phenomena. Under the influence of an applied electric field, the potential barrier assumes a triangular shape and its width diminishes as the field strength increases. Consequently, when the barrier becomes sufficiently thin, there exists a non negligible probability for electrons to tunnel it and escape from the surface [4] (see Fig. 1).

The tunnel probability and then the current I emitted by one site is described by the Fowler-Nordheim (FN) relation [5]:

$$I = S \frac{A_{FN} E^2 \beta^2}{\phi} \exp\left(-\frac{B_{FN} \phi^{3/2}}{\beta E}\right), \quad (1)$$

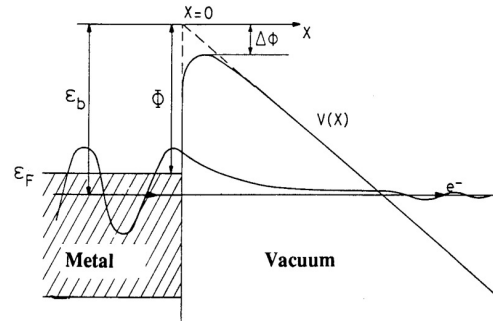


Figure 1: Potential barrier of metals with an applied E field to the surface [5].

where $A_{FN} = 1.54 \times 10^6$, $B_{FN} = 6.83 \times 10^3$, β is the field enhancement factor, ϕ is the work function eV and $E_s(t) = E_{s0} \sin(2\pi f t)$, measured in MV/m, is the instantaneous value of the surface electric field.

THEORETICAL APPROACH

Experimental Setup

What we currently use to analyze field emission in superconducting cavities, from a practical point of view, is:

- External radiation detectors: a portion of the impact electron energy is converted into X ray Bremsstrahlung radiation. The maximum X-ray energy (endpoint) corresponds to kinetic energy of the electrons at the impact point. To monitor the dose rate and partially simulate the power drained by electron dark current, a proportional counter¹ has been employed in the available setup. Additionally, a scintillator (NaI(Tl)) is utilized to capture the X-ray spectrum, enabling the evaluation of the endpoint, except in case of severe pile-up events determined by the poor shielding offered by the cryogenic structure (lead shielding brick are sometimes used (see Fig. 2)).
- Inner diagnostic devices, such as electron pick-up probe and an array of photodiodes.
- Cavity Q drop measurement: it offers a means to evaluate the overall power of field emission if it is the dominant factor limiting the performance.

¹ Gas-filled (Xe) proportional counter. Measurement range from 100 nSv/h to 1 Sv/h; continuous acquisition every 1 s; energy range from 45 keV to 1 MeV, so poor sensitivity for higher energies.

STATUS OF THE ESS MEDIUM BETA CAVITIES AT INFN LASA

D. Sertore*, M. Bertucci, M. Bonezzi, A. Bosotti, D. Cardelli, A. D'Ambros, E. Del Core, F. Fiorina, A. T. Grimaldi, L. Monaco, C. Pagani, R. Paparella, M. Zaggia
INFN Milano - LASA, Segrate, Italy

Abstract

The INFN LASA's contribution to the ESS Medium Beta Superconducting Linac consists of 36 cavities that raise the proton beam energy from 216 MeV to 571 MeV. Out of the 36 cavities, 28 have been successfully qualified and delivered for assembly into a cryomodule at CEA Saclay. The remaining cavities have been reprocessed in order to bring them up to ESS specifications. To mitigate further delays in the delivery of the cavities, four new ones are currently under construction. We are reporting on the current status of both the recovery actions we have developed so far and the performance of the newly produced resonators.

INTRODUCTION

INFN Milano - LASA is responsible for the Italian In-Kind contribution to the European Spallation Source (ESS) ERIC of the Superconducting (SC) Medium Beta Cavities. For these cavities, we developed the electromagnetic design and the we optimized it taking into account mechanical requirements, their feasibility in industry and their compliance to the ESS interface requests. This last point has been proven to be of critical importance to ensure the smooth assembly of the cavities in their cryomodule at CEA Saclay. Table 1 summarizes the key parameters of the INFN Medium Beta cavities.

Once operated in the SC linac, the Medium Beta ($\beta=0.67$) cavities will capture the 62.5 mA proton beam from the Spoke section (256 MeV) and accelerate it up to 571 MeV for its further injection in the High Beta cryomodules that will bring the beam to its final energy of 2 GeV.

The 5 MW average power proton beam will be pulsed at 14 Hz, each pulse being 2.86 ms long. This long beam pulses operation has been one of the driving reasons for using superconducting cavities. This choice allows achieving the project parameters while preserving in cost. Moreover, there is the additional need to operate the cavities at high accelerating gradient to reach the needed energy in the foreseen accelerator footprint.

The proton beam will then be delivered to the target station for producing the neutron beam by the spallation process [1]. The European Spallation Source (ESS) ERIC will be, once in operation, the most intense neutron source in the world [2].

This paper presents an update on the cavity production status with dedicated emphasis on the recovery actions we have performed so far to qualify low performance cavities. Moreover, to mitigate possible delay in completing our In-Kind contribution we are providing new resonators with

updated surface treatments as learnt during the recovery activity.

Table 1: ESS Medium Beta Cavities Main Parameters

Parameter	Value
R_{iris}	50 mm
Geometrical β	0.67
π -mode Frequency	704.42 MHz
Acc. length	0.855 m
Cell-to-cell coupling k	1.55%
π - $5\pi/6$ mode sep.	0.70 MHz
Geometrical factor G	198.8 Ω
Optimum beta, β_{opt}	0.705
Max R/Q at β_{opt}	374 Ω
E_{acc} at β_{opt}	16.7 MV/m
$E_{\text{peak}}/E_{\text{acc}}$	2.55
E_{peak}	42.6 MV/m
$B_{\text{peak}}/E_{\text{acc}}$	4.95 $\frac{\text{mT}}{\text{MV/m}}$
Q_0 at nominal gradient	$>5 \times 10^9$
Q_{ext}	7.8×10^5

ESS MEDIUM BETA CAVITIES STATUS

The production of ESS Medium Beta cavities is based on a scheme inherited from our previous work in industrial production of European XFEL SRF cavities. To ensure high quality, INFN has developed strict guidelines for cavity production and implemented a comprehensive Quality Control and Quality Assurance plan that encompasses the entire cavity production process [3].

In line with the objectives of the ESS project, we have chosen to treat the cavities using a Buffered Chemical Polishing (BCP) process, both in bulk and as a final treatment. The final treatment, known as the "Final BCP", is part of the cavity preparation necessary to assemble the cavity before the Vertical Test at cryogenic temperatures, required for cavity qualification. To accommodate the high cavity delivery rate required by the project, most of the qualification tests were conducted at DESY, utilizing the AMTF infrastructure [4].

However, for specific cavities, we utilized the LASA infrastructure, which is not able to sustain the series test rate but is equipped with advanced diagnostic tools capable of identifying quench and field emission sources that could potentially limit the cavity performance.

A total of twenty-eight cavities successfully met the ESS specifications and were subsequently assembled into cryomodules at CEA Saclay and, few of the, there tested. These cryomodules were then transferred to ESS for further testing

* daniele.sertore@mi.infn.it

RF MEASUREMENTS OF THE 3RD HARMONIC SUPERCONDUCTING CAVITY FOR A BUNCH LENGTHENING

Junyoung Yoon, Jun-ho Han, Hee-Su Park, Yeo-dong Yoon
Kiswire Advanced Technology Co., Ltd, Daejeon, Korea

Eiji Kako, High Energy Accelerator Research Organization (KEK), Tsukuba, Japan
Eun-San Kim*, Dept. of Accelerator Science, Korea University, Sejong, Korea

Abstract

The brightness can be increased by minimizing the emittance in the light source, but the reduced emittance also increases the number of collisions of electrons in the beam bunch. Therefore, the bunch lengthening by using the 3rd harmonic cavity reduces the collisions of electrons and increases the Touschek lifetime. Since the resonant frequency of the main RF cavity is 500 MHz, the resonant frequency of 3rd harmonic cavity is selected as 1500 MHz. The prototype cavity is a passive type in which a power coupler is not used, and power is supplied from the beam. The operating temperature is 4.5 K, which is a superconducting cavity. The elliptical double-cell geometry was selected to increase the accelerating voltage of the cavity and reduce power losses. Based on this design, three niobium cavities are fabricated and tested. In this paper, we present the RF measurement results of the 3rd harmonic cavity at room temperature.

INTRODUCTION



Figure 1: Fabricated niobium double-cell cavities.

The 3rd harmonic superconducting cavity is designed to improve the performance of the 4th generation storage ring. The fabricated niobium cavities are shown in Fig. 1. An elliptical double-cell geometry and a passive type were chosen for the basic geometry of the cavity. The double cell geometry can reach the required accelerating voltage ($V_{acc} = 800$ kV) at a lower accelerating gradient ($E_{acc} = 8$ MV/m \rightarrow 4 MV/m) [1]. The passive type cavity has a simple shape compared to the active type due to the absence of power couplers. We fabricate two niobium cavities by following the typical process of the elliptical cavity except for CBP and EP process [2-4]. For the improvement of the quality of the cavity, we measure every part of the niobium cavities.

* eskim1@korea.ac.kr

RF MEASUREMENTS

Half-Cell

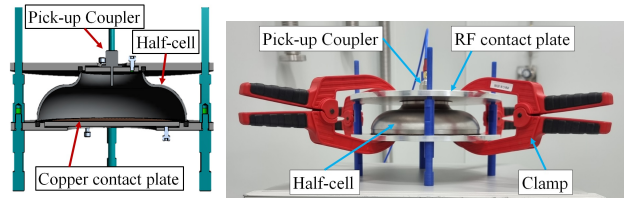


Figure 2: The set-up status of the RF measurement for the half-cell.

Figure 2 shows the RF measurement set-up for a niobium half-cell. A half-cell is a basic part of the cell of cavities. Copper contact plate and clamp are used to increase the RF contact surface [5]. Eighteen half-cells are fabricated by the deep drawing method. The resonant frequency is measured after trimming and fine machining. If we do not perform the trimming at the edge of a half-cell, we can not measure the resonant frequency due to poor RF contact at the copper plate. Before fine machining, we measure the average frequency sensitivity of niobium half-cells and the result is -6.39 MHz/mm.

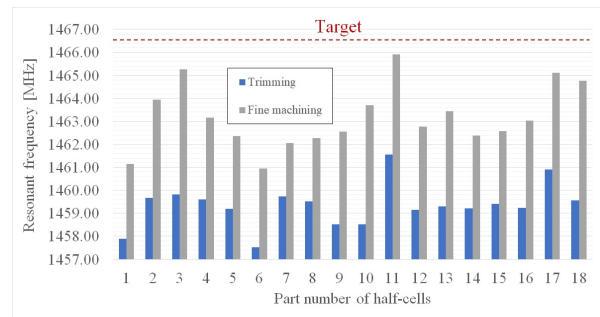


Figure 3: Resonant frequency distribution of niobium half-cells.

The distribution of the resonant frequency of each half-cell is shown in Fig. 3. The target frequency of a half-cell is 1466.42 MHz, but most half-cells are lower than the target frequency. After trimming the edge of half-cells, the maximum error is 7.89 MHz, but reduced to 4.5 MHz by fine machining. The error of half-cell numbers 1 and 6 is bigger than other half-cells due to trimming and chemical etching tests. We select four half-cells, which have the lowest error, to fabricate the dumbbell.

FABRICATION EFFORTS TOWARD A SUPERCONDUCTING RF PHOTO-INFECTOR QUARTER-WAVE CAVITY FOR USE IN LOW EMITTANCE INJECTOR APPLICATIONS*

C. Compton[†], K. Elliott, W. Hartung, J. Hulbert, J.W. Lewellen², M. Kedzie¹,
M. Kelly¹, S.-H. Kim, T. Konomi, E. Metzgar, S. Miller, M. Patil,
T. Petersen¹, J. Popielarski, L. Popielarski, K. Saito, J. Smedley², K. Witgen, T. Xu
Facility for Rare Isotope Beams, Michigan State University, East Lansing, MI, USA
¹Argonne National Laboratory, Lemont, IL, USA
²SLAC National Accelerator Laboratory, Menlo Park, CA, USA

Abstract

The Facility for Rare Isotope Beams (FRIB), in collaboration with Argonne National Laboratory and Helmholtz-Zentrum Dresden-Rossendorf, is working on the design and fabrication of a photo-injector cryomodule; suitable for operation as part of the Linac Coherent Light Source II High Energy accelerator systems at SLAC National Accelerator Laboratory. Project scope requires the fabrication of two 185.7 MHz superconducting, quarter-wave resonators-based injector cavities. Cavity fabrication will be completed at FRIB with contracted vendors supporting sub-component fabrication and electron-beam welding. Fabrication will use poly-crystal and large grain RRR niobium materials. The current status of cavity fabrication will be presented including material procurement, prototype forming, and electron-beam welding development.

INTRODUCTION

A research collaboration was formed in 2022 with the goal to design and fabricate a low-emittance superconducting injector cryomodule for potential use as part of the Linac Coherent Light Source II High Energy (LCLS-II-HE) project. The collaboration group is made up of research teams from The Facility for Rare Isotope Beams (FRIB), Argonne National Accelerator Laboratory (ANL), and The Helmholtz-Zentrum Dresden-Rossendorf (HZDR). The research is in support of the LCLS-II project at SLAC [1].

The project will conclude with the demonstration of a fully operational cryomodule; housing one 185.7 MHz quarter-wave superconducting radio frequency (SRF) gun cavity, shown in Figure 1, an emittance compensation solenoid [2], cathode stalk and plug system, power coupler, and cavity tuning system. The cryomodule is designed for 4 K operation and complete integration into the SLAC accelerator facility.

For the cavity construction phase of the project, a decision was made to fabricate two gun cavities. The first cavity will be used to prove out manufacturing methods, such as component forming and electron-beam (EB) welding, and document frequency change for each fabrication step.

This information is critical in predicting the final frequency of the second cavity; built into the cryomodule for operational use. The only mechanical difference between the two cavities is the first cavity will not have the beam aperture in the Nose component to easy processing. This feature will be added to the second cavity for injector operation. The fabrication steps, and related development, in the construction of the first SRF gun cavity will be presented.

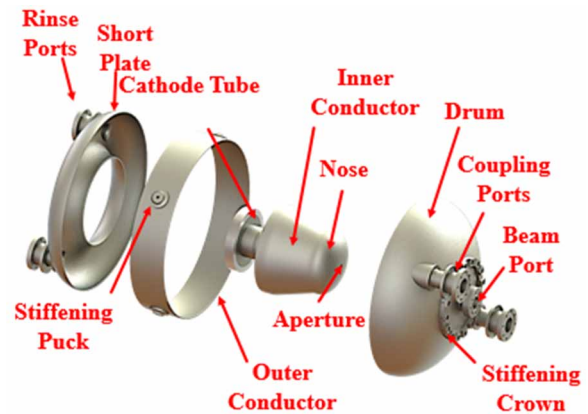


Figure 1: SRF gun cavity with key components.

CAVITY DESIGN

The cavity design is a collaborative effort among the three institutes; FRIB, ANL, HZDR. The design parameters and space envelope were directed by SLAC's Accelerator team. A mechanical drawing was established and used as the basis to begin optimizing the cavity shape using electro-magnetic simulation modelling.

Electro-Magnetic Design

The electro-magnetic modelling was a combined effort of FRIB, ANL, and SLAC. Superfish and CST Microwave Studio were used to model and optimize the cavity shape [3].

Mechanical Design

Upon completion of the electro-magnetic model, a full mechanical analysis was performed on the cavity structure using ANSYS WB for FEA [4]. ASME BPVC section VIII, Division-2 [5] was used as a basis for evaluation; looking closely at material thickness, weld joint design, and strategically placed stiffening elements.

* Work supported by the Department of Energy under Contract DE-AC02-76SF00515

[†]compton@frib.msu.edu

FABRICATION AND TESTING OF A PROTOTYPE RF-DIPOLE CRABBING CAVITY*

S. U. De Silva[†], J. R. Delayen, Old Dominion University, Norfolk VA, USA
H. Park¹, Thomas Jefferson National Accelerator Facility, Newport News VA, USA
¹currently at Fermi National Accelerator Laboratory, Batavia IL, USA

Abstract

Crabbing cavities are essential in particle colliders to compensate the luminosity degradation due to beam collision at a crossing angle. The 952.6 MHz 2-cell rf-dipole crabbing cavity system was proposed for the Jefferson Lab Electron-Ion Collider to restore the head-on collisions of electron and proton bunches at the interaction point. A prototype cavity was designed and developed to demonstrate the performance of multi-cell rf-dipole structures. This paper presents the fabrication process and cold test results of the first 2-cell rf-dipole prototype cavity.

INTRODUCTION

Advanced high energy particle colliders are currently being developed with high peak luminosities to study properties of particles in the Standard Model. These powerful colliders require higher rate of particle interactions between bunches to achieve the desired integrated luminosities over the duration of machine operation. The higher beam energies also require large crossing angles to minimize the beam interactions where the two beams share the same vacuum space. The reduction of luminosities due to large crossing angles are compensated by the implementation of crabbing systems at the interaction region [1]. The crabbing cavities provide a transverse kick to the head and tail of each bunch that will oscillate the bunches such that they overlap at the interaction point in maximizing the number of interactions between them.

Jefferson Lab Electron-Ion Collider

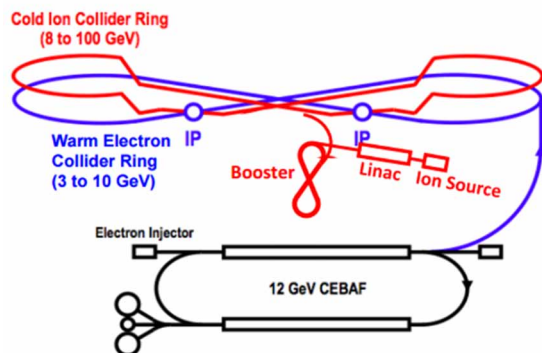


Figure 1: Schematic of Jefferson Lab Electron-Ion Collider.

* This material is based upon work supported by a grant from the Southeastern Universities Research Association (SURA). This research also used resources of the National Energy Research Scientific Computing Center (NERSC); a U.S. Department of Energy Office of Science User Facility operated under Contract No. DE-AC02-05CH11231.

[†] sdesilva@jlab.org

Jefferson Lab Electron-Ion Collider (JLEIC) was a next generation particle collider designed to be built at Jefferson Lab [2]. In parallel, another Electron-Ion Collider (EIC) was proposed by BNL [3]. JLEIC was designed to accelerate electrons in the existing CEBAF accelerator with a newly constructed figure-8 ring to accelerate protons and ions as shown in Fig. 1. The collider will consist of two interaction points with a luminosity goal in the range of low-to-mid 10^{33} cm⁻²sec⁻¹ per interaction point. The crab cavities are required to achieve the luminosity goal and are designed to operate at 952.6 MHz [4].

Following the site selection process in early 2020, BNL was selected as the site for the next EIC and JLEIC project was discontinued. This paper presents the details of the rf design, fabrication and rf testing of a prototype crabbing cavity that was designed and developed for the JLEIC.

RF DESIGN

The rf-dipole design is a compact crabbing cavity design that operates in a TE₁₁-like mode where the primary contribution to the transverse kick is provided by the transverse electric field across the pole gap [5,6]. Single cell rf-dipole cavities have been designed and developed for several deflecting and crabbing applications at 400 MHz, 499 MHz, 750 MHz [7]. Higher operating frequencies allow compact geometries as the cavity diameter is inversely proportional to the frequency. Multiple cavity geometries of squashed elliptical, 1-cell, 2-cell and 3-cell rf-dipole design options were evaluated at 952.6 MHz frequency and the 2-cell rf-dipole design was finalized as the crab cavity design for JLEIC [8,9].

Figure 2 shows the 2-cell rf-dipole cavity and cross section with the cavity dimensions. The cavity was designed with the beam aperture of 70 mm and center to center pole separation of 170 mm $> \lambda/2 = 157.4$ mm. The pole height and angle are optimized to reduce peak surface fields and to achieve a balance B_p/E_p ratio. Figure 3 shows the surface field profiles, and Table 1 lists the rf properties.

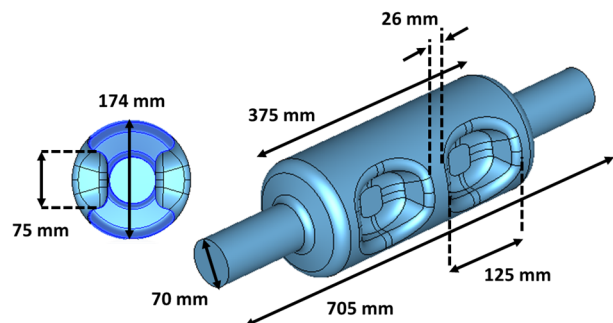


Figure 2: 952.6 MHz 2-cell rf-dipole cavity.

FABRICATION AND SURFACE TREATMENT OF SUPERCONDUCTING RF SINGLE SPOKE CAVITIES FOR THE MYRRHA PROJECT

M. Moretti[†], Y. N. Hoerstensmeyer, A. Navitski
RI Research Instruments GmbH, Bergisch Gladbach, Germany
F. Marhauser, SCK CEN, Mol, Belgium

Abstract

The MYRRHA project, based at SCK-CEN (Belgium), aims at coupling a 600 MeV proton accelerator to a sub-critical fission core operating at a thermal power of 60 MW. The first phase of the project, MINERVA, consists in realizing a 100 MeV superconducting linac in order to demonstrate the machine requirements in terms of reliability and fault tolerance. The MINERVA linac comprises several cryomodules, each containing two Single Spoke 352.2 MHz cavities made out of high RRR niobium and operating at 2 K. The fabrication and surface treatment of the Single Spoke RF Cavities have been completely undertaken by RI Research Instruments GmbH (Germany) and is currently ongoing; the first pre-series cavities were completed and delivered for cold testing. Main highlights of the fabrication include the deep-drawing of complex shapes, such as the central spokes and the outer caps of the cavities, which were successfully accomplished. As for the surface treatment, RI has commissioned, tested, and effectively started to use a new rotational buffered chemical polishing facility; this is required to polish the inner surface of the cavities, ensuring a uniform removal of material.

CAVITY FABRICATION

The Single Spoke RF cavity for MINERVA is a complete Electron-Beam (EB) welded structure made out of high RRR niobium, integrated into a helium tank in titanium grade 2 (Fig. 1). The main niobium parts of the bare cavity were fabricated starting from 3.4 mm thick sheets. The conceptual cavity design was performed by IJCLab [1].

The deep-drawing of the central half-spokes (Fig. 2) and the endcaps (Fig. 3) was entirely carried out at RI Research Instruments GmbH (RI) by means of a 100 tonnes hydraulic press. This represented a critical milestone for the fabrication and required a deep development effort due to the shape complexity. The conception and design of the deep-drawing process and tooling were supported by the FEM software AutoForm [2], focusing on the definition and the simulation of metal sheet forming processes. The accuracy of the numerical results as well as the functionality of the tooling were proven in parallel by performing trials on copper sheets. Finally, after the process validation, also the first niobium sheets were deep-drawn with satisfactory results. The so-validated processes were then extensively exploited for the serial production of the cavities.

Deep-Drawing of Central Half-Spokes

The spoke tooling design and the process definition were carried out according to RI's expertise and best practice. They were then supported and validated by means of numerical simulations and a test campaign on copper sheets.

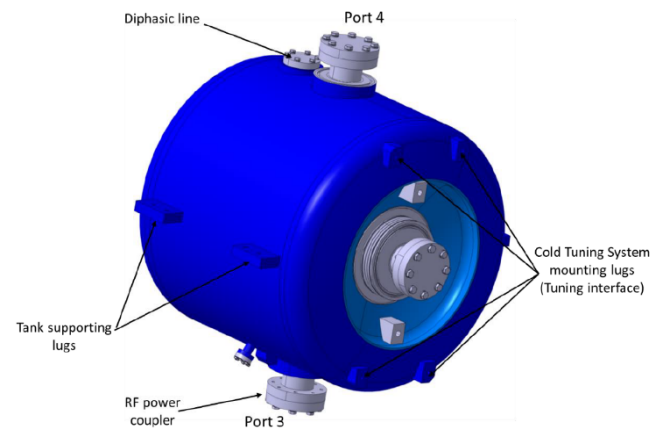
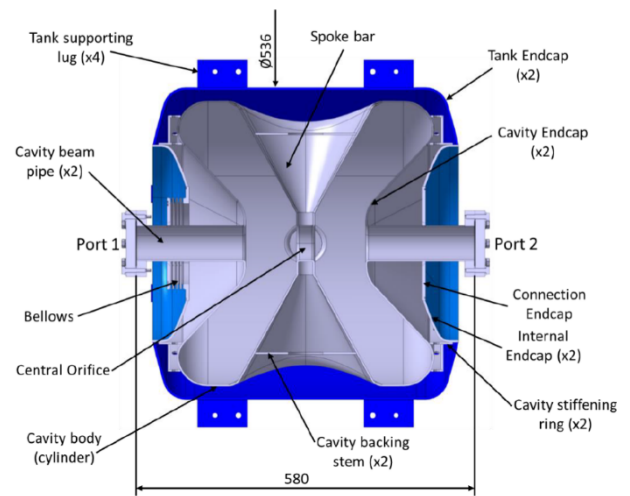


Figure 1: Cross-section and isometric overview of the Single Spoke RF Cavity for MINERVA; the niobium bare cavity is shown in grey, whilst the titanium helium tank is shown in light blue (Courtesy of IJCLab).

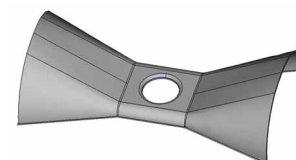


Figure 2: Central half-spoke.

[†] massimiliano.moretti@research-instruments.de

Content from this work may be used under the terms of the CC BY 4.0 licence (© 2023). Any distribution of this work must maintain attribution to the author(s), title of the work, publisher, and DOI

EIC 197 MHz CRAB CAVITY RF OPTIMIZATION*

Zenghai Li[†], SLAC, Menlo Park, CA, USA

Binping Xiao, Qiong Wu, Wencan Xu, BNL, Upton, NY, USA

J. R. Delayen, S. U. De Silva, Old Dominion University, Norfolk, VA, USA

R. Rimmer, JLab, Newport News, VA, USA.

Abstract

Crab cavities, operating at 197 MHz and 394 MHz respectively, will be used to compensate the loss of luminosity due to a 25 mrad crossing angle at the interaction point in the Electron Ion Collider (EIC). Both crab cavities are of the RF Dipole (RFD) shape. To meet the machine design requirements, there are a few important cavity design considerations that need to be addressed. First, to achieve stable cavity operation at the design voltages, cavity geometry details must be optimized to suppress potential multipacting. Incorporating strong HOM damping in the cavity design is required for the beam stability and quality. Furthermore, due to the finite pole width, the multipole fields, especially the sextupole and the decapole terms, need to be minimized to maintain an acceptable beam dynamic aperture. This paper will present the RF optimization details of the 197 MHz cavity.

INTRODUCTION

In the current EIC design, a large crossing angle of 25 mrad at the interaction region (IR) is required for fast separation of two colliding beams to minimize IR background and to ease the arrangements of IR beamline and detector components [1, 2]. Local crabbing scheme is adopted to recover the luminosity loss due to the crossing angle. A set of crab cavities with frequencies of 197 MHz and 394 MHz will be installed on each side of the detector. The RF dipole (RFD) [3], as shown in Fig. 1, is adopted for both the 197 MHz and 394 MHz crab cavities. The optimization of the 197 MHz cavity is required to meet the following design considerations. The beampipe aperture is 100 mm to accommodate the large beta function (1300 m) at the crab cavity region. The max peak surface fields are set to be 45 MV/m (E_{pk}) and 80 mT (B_{pk}) at the deflecting voltage of 11.5 MV. Strong HOM damping is essential to minimize the impedance contribution of the crab cavities. The deflecting field within the beam pipe aperture need to be highly uniform to maintain an acceptable beam dynamic aperture. Specifically, the field non-uniformity is dominated by the sextupole (b3) and decapole (b5) terms that need to be minimized. Further, the cavity geometry should be optimized to eliminate conditions of multipacting, especially around the operating voltage. In this paper, we present the results of the 197 MHz cavity optimization, focusing mostly on the multipacting and multipole field analysis and mitigations.

* Work supported by Brookhaven Science Associates, LLC under Contract No. DE-SC0012704 with the U.S. Department of Energy, and by DOE Contract No. DE-AC02-76SF00515. This work used computer resources at the National Energy Research Scientific Computing Center.

[†]lizh@slac.stanford.edu

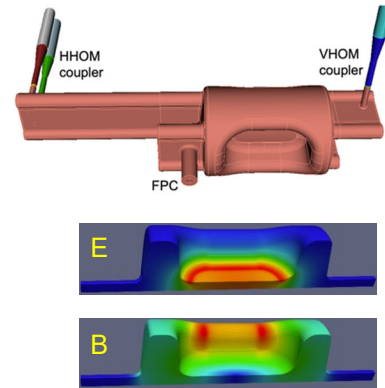


Figure 1: 197 MHz RFD cavity and field contour plots.

Table 1: 197 MHz RFD Cavity Parameters

Parameter	Value
Operating frequency [MHz]	197
1 st longitudinal HOM [MHz]	392
1 st transverse HOM [MHz]	342
R/Q [Ω] (with curved pole)	966
V_T (MV/cavity)	11.5
E_p (at $V_T=11.5$ MV) [MV]	45
B_p (at $V_T=11.5$ MV) [mT]	81
Beam pipe aperture [mm]	100
Transverse dimension [mm]	587
Longitudinal dimension [mm]	922

HOM DAMPING

The major RF parameters of the 197 MHz cavity is shown in Table 1. The operating mode in the RFD cavity is the fundamental mode. The lowest HOM mode is about 150 MHz higher in frequency which is advantageous for implementing the HOM damping. For impedance budget considerations [4], 2 IP are assumed in the hadron storage ring (HSR). Four 197 MHz crab cavities per side for IP-1 and five cavities per side for IP-2 (due to a larger crossing angle). That totals the number of 197 MHz cavities to twenty. The longitudinal impedance budget is 10.0 k Ω (circuit definition) per cavity. The transverse impedance budget per cavity are 0.132 M Ω /m and 0.66 M Ω /m respectively for the horizontal and vertical planes due to differences in beta functions. These impedance budget numbers were obtained by dividing the total impedance budgeted for the crab cavities by the number of cavities, which is a conservative assumption that all cavities are being identical. In reality, the HOM frequencies will deviate from cavity to cavity due to fabrication tolerances, which could loosen the impedance limit per cavity. Nevertheless, HOMs up to 2 GHz need to be adequately damped.

The HOM damping in the 197 MHz cavity is realized via two dogbone shaped waveguides that extract the HOM

DESIGN AND TESTS OF A CATHODE STALK FOR THE LCLS-II-HE LOW EMITTANCE INJECTOR SRF GUN*

T. Konomi[†], W. Hartung, S. Kim, S. Miller, D. Morris, K. Saito, A. Taylor, Z. Yin, T. Xu
 Facility for Rare Isotope Beams, Michigan State University, East Lansing, MI, USA

M. Kelly, T. Petersen, Argonne National Laboratory, Argonne, IL, USA

C. Adolphsen, J. Lewellen, J. Smedley, SLAC National Accelerator Laboratory, CA, USA

S. Gatzmanga, P. Murcek, R. Xiang, Helmholtz Zentrum Dresden Rossendorf, Dresden, Germany

Abstract

A superconducting radio-frequency photo-injector can in principle operate CW with a high cathode gradient and ultra-low vacuum for high-quantum efficiency, low MTE photocathodes, useful features for delivery of high-brightness, high-repetition-rate beams. For these reasons, an SRF based photoinjector was chosen for the proposed Low Emittance Injector (LEI) addition to the Linac Coherent Light Source II High-Energy Upgrade (LCLS-II-HE) facility, which will operate CW with bunch rates up to 1 MHz. For this injector, a prototype 185.7 MHz quarter-wave resonator gun is being developed in a collaborative effort among FRIB, HZDR, ANL and SLAC with the goal of achieving a photocathode gradient of at least 30 MV/m. The photocathode will be held by a coaxial fixture (“cathode stalk”) for thermal isolation from the cavity body. The system must allow for precise alignment of the photocathode, particle-free photocathode exchange, cryogenic (55-70 K) or warm (273-300 K) photocathode operating temperatures, and DC biasing to inhibit multipacting. A prototype cathode stalk has been built and bench tests are underway to validate the design. Measurements include RF power dissipation, DC bias hold-off, multipacting suppression and heat transfer effectiveness. This paper describes the cathode stalk design and the test results.

INTRODUCTION

The Linac Coherent Light Source II High Energy (LCLS-II-HE) Project at SLAC has designed a Low-Emittance Injector (LEI) that employs a quarter-wave resonator (QWR) type superconducting radio-frequency (SRF) cavity as the electron source [1, 2]. The cavity frequency is 185.7 MHz, one-seventh of the 1.3 GHz LCLS-II-HE linac frequency. The advantage of using a low frequency SRF cavity is that it can provide a quasi-DC field in the accelerator gap and operate efficiently at 4 K. A prototype gun cryomodule is being developed in a collaboration among FRIB, ANL, HZDR and SLAC [3-5]. One of the critical parameters to achieve high-brightness bunches is the cathode gradient. The goal of the gun R&D program is to demonstrate stable CW operation with a cathode gradient of at least 30 MV/m.

The cathode stalk that holds the cathode plug is shown in Fig. 1. The plug and its insertion mechanism, and the

stalk positioning mechanism, are based on those used in HZDR’s 1.3 GHz SRF gun [6]. The coaxial section between the outer stalk and the cavity cathode tube can be DC biased up to 5 kV for multipacting (MP) suppression. Cooling tubes that connect to the plug holder will allow the plug to be maintained at 300 K or 55 K [7, 8] during gun operation: helium gas will be used as the coolant.

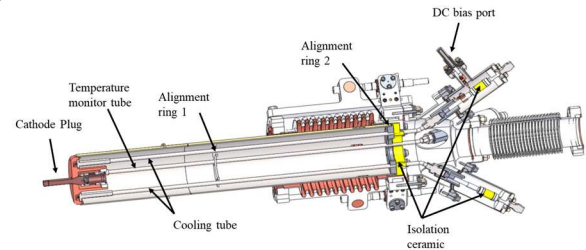


Figure 1: Cathode Stalk assembly [7].

RF/DC TEST SETUP

To demonstrate the cathode stalk temperature control and MP suppression, the RF/DC test setup shown in Fig. 2 was built [7]. The setup includes an RF-driven coaxial resonator that generates fields in the stalk coaxial region similar to those during gun operation. The resonator and stalk are installed into a vacuum chamber and pumped through slits on outer conductor and cathode stalk. The vacuum chamber has a monitor port to inset optical temperature sensors and a plug tip heater.

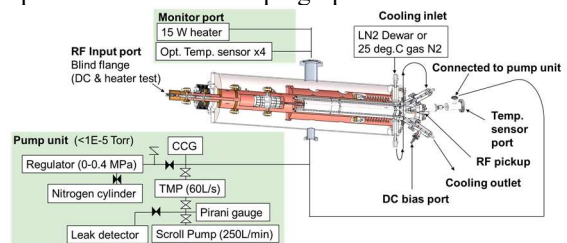


Figure 2: RF/DC test setup [7].

HEATER TEST

The thermal contact resistance between the plug and holder needs to be low to prevent the plug from overheating. A heater test was done to verify this. The resonator and RF input coupler were removed for this test and the input port was closed with a blank flange. The holder and upstream stalk flange were cooled with dry nitrogen gas or liquid nitrogen. The cathode plug was inserted into the cone-shaped socket in the plug holder and held in place by an Inconel spring mechanism, the same as in the HZDR

* Work supported by the Department of Energy under Contract DE-AC02-76SF00515

[†] konomi@frib.msu.edu

SURFACE ROUGHNESS REDUCTION AND PERFORMANCE OF Nb₃Sn FILM FOR SRF APPLICATIONS*

U. Pudasaini[†], C. E. Reece, M. J. Kelley, E. M. Lechner, A.-M. Valente-Feliciano, O. Trofimova
Thomas Jefferson National Accelerator Facility, Newport News, VA, USA

Abstract

Nb₃Sn offers better RF performance (Q and E_{acc}) than Nb at any given temperature because of its superior superconducting properties. The potential deployment of Nb₃Sn-coated SRF cavities at 4 K, delivering similar performance to that of Nb cavities at 2 K, will be a transformational technology to enable new classes of SRF accelerator applications. A clean and smooth surface can enhance the performance of the Nb₃Sn-coated cavity, typically, the attainable acceleration gradient. The reduction of surface roughness is often linked with a correlative reduction in average coating thickness and grain size. A new approach to enhance the nucleation centers using the pre-deposition of Sn on Nb is introduced for surface roughness reduction. Besides Sn supply's careful tuning, the temperature profiles were varied to engineer the coating surface with reduced roughness as low as ~40 nm in 20 $\mu\text{m} \times 20 \mu\text{m}$ AFM scans, one-third that of the typical coating. Electropolishing of coated sample shows surface a clear surface smoothening. A few sets of coating parameters were used to coat 1.3 GHz single-cell cavities to understand the effects of roughness variation on the RF performance. This presentation discusses ways to reduce surface roughness with results from a systematic analysis of the samples and Nb₃Sn-coated single-cell cavities.

INTRODUCTION

Superior superconducting properties, Nb₃Sn ($T_c \sim 18.33$ K, $H_{sh} \sim 425$ mT, and $\Delta \sim 3.1$ meV) promise better performance and a significant reduction in operational cost of SRF cavities compared to Nb ($T_c \sim 9.2$ K, $H_{sh} \sim 210$ mT, and $\Delta \sim 1.45$ meV) [1]. So, it promises a higher accelerating gradient, quality factor, and operation temperature than traditional bulk Nb. Nb₃Sn superconducting radio frequency (SRF) cavities at 4.3 K can deliver similar performance to Nb cavities at 2 K, resulting in enormous cost savings for future SRF accelerators by simplifying and reducing the cost of cryogenic facilities. The successful deployment of Nb₃Sn technology can start a new era by benefiting numerous SRF accelerators and enabling new classes of SRF accelerator applications.

Despite Nb₃Sn being considered the next-generation SRF material, Nb₃Sn is restricted to its use in a thin film form because it is prone to develop cracks under stress because of its brittleness and the lower thermal conductivity

that reduce the efficiency of dissipated heat removal from the cavity. Nb₃Sn thin films should be deposited or grown inside built-in metallic (e.g., Nb, Cu) cavity structures. Since SRF cavities typically have complicated geometries and demand uniformly coated surfaces, available thin film deposition techniques are limited to achieve them.

The Sn vapor diffusion coating is the most mature and, thus far, the only successful technique for growing quality Nb₃Sn on Nb cavities since the 1970s [2-4]. In general, the essence of the process is to create and transport Sn-vapor to the Sn surface at suitable temperature environments. This technique is adopted by most research institutions currently working to develop Nb₃Sn-coated cavities around the world [5-9]. Recent performance results of such cavities are promising, attaining high quality factors, with $> 10^{10}$ operating at 4.2 K at medium fields at ≥ 15 MV/m in several labs [5, 7, 10, 11]. The best-performing cavities have attained an accelerating gradient in excess of 20 MV/m. A typical cavity coating process consists of two steps: nucleation and growth. First, tin chloride is evaporated at about 500 °C, depositing a Sn film and particles on the niobium surface to mitigate potential non-uniformity in the coating by depositing Sn improving nucleation [12]. These tin deposits act as nucleation sites, which are assumed to facilitate Nb₃Sn growth with the influx of tin vapor during deposition at a higher temperature. The growth temperature should be above 930 °C to exclusively form the Nb₃Sn phase as dictated by the binary phase diagram of the Nb-Sn system. A temperature of about 1100-1200 °C is typical for Nb₃Sn growth at different labs.

The current understanding of performance limitations of Nb₃Sn-coated cavities is because of “extrinsic” factors such as localized defects. A few known issues that potentially contribute to performance limitations are forming very thin patchy regions, non-uniformity, accumulating Sn-residues, incorporating impurities, non-stoichiometric grain boundaries, surface topography, etc. It is needed to have pure Nb₃Sn with a clean and defect-free-smooth surface to enhance the performance. This contribution focuses on the roughness (or topography) of vapor-diffused Nb₃Sn and discusses ways to manage it with material analysis and RF test results.

VAPOR DIFFUSION COATING AND ROUGHNESS EVOLUTION

The quality of coated Nb₃Sn layers is mainly contingent on understanding the coating layer initiation and growth during the process. To understand the evolution of the Nb₃Sn thin film during the process, we ran a set of experi-

* Work supported by the U.S. Department of Energy, Office of Science, Office of Nuclear Physics under contract DE-AC05-06OR23177 with Jefferson Science Associates.

[†] uttar@jlab.org

DEVELOPMENT OF HIGH-PERFORMANCE NIOBIUM-3 TIN CAVITIES AT CORNELL UNIVERSITY

L. Shpani*, S. Arnold, G. Gaitan, M. Liepe, T. Oseroff, R. Porter,
N. Sitaraman, N. Stilin, Z. Sun, N. Verboncoeur
Cornell University (CLASSE), Ithaca, NY, USA

Abstract

Niobium-3 tin is a promising material for next-generation superconducting RF cavities due to its high critical temperature and high theoretical field limit. There is currently significant worldwide effort aiming to improve Nb₃Sn growth to push this material to its ultimate performance limits. This paper will present an overview of Nb₃Sn cavity development at Cornell University. One approach we are pursuing is to further advance the vapor diffusion process through reducing film thickness and optimizing the nucleation step to grow more uniform layers of stoichiometric Nb₃Sn. Additionally, we are exploring alternative growth methods, such as the development of a plasma-enhanced chemical vapor deposition (CVD) system, as well as Nb₃Sn growth via electrochemical synthesis.

INTRODUCTION

Niobium-3 tin (Nb₃Sn) has the potential to push the performance of next-generation SRF cavities beyond that of niobium due to its remarkable superconducting properties [1]. With twice the critical temperature of traditional Nb used in present-day SRF accelerator cavities, Nb₃Sn opens the possibility of higher operating temperatures, significantly reducing the cooling requirements and consequently having greater operational efficiency. Furthermore, this material can in theory withstand almost twice the RF fields than the typical Nb SRF cavity, hence doubling the maximum accelerating gradient achievable and allowing for shorter and more powerful accelerators [1, 2].

However, achieving optimal growth of this material remains an immensely challenging task. In fact, the development of Nb₃Sn SRF cavities has been a topic of significant research and progress since the 1970s. Early attempts by institutions like Siemens AG, Karlsruhe, and Wuppertal faced challenges such as the presence of a strong Q-slope at higher fields. Nevertheless, after a pause in research, Cornell University took the lead in resuming Nb₃Sn cavity development in 2009, through implementing an adapted Wuppertal growth method of this material [3, 4]. Cornell's efforts successfully tackled the Q-slope issue and showcased the material's potential for pushing the performance of SRF cavities to the next level [1, 3].

Thermal Vapor Diffusion

To this day, the state-of-the-art growth method for producing high quality Nb₃Sn cavities in a reproducible fashion

remains thermal vapor diffusion [2]. This technique involves exposing a niobium cavity to vaporized tin and tin chloride (which serves as a nucleating agent) in a high temperature vacuum furnace. Inspired by the Wuppertal method, at Cornell University we incorporate the use of a secondary heater for the tin source, and we impose a temperature gradient between the tin crucible and the cavity during coating. A temperature profile of a Nb₃Sn coating run at Cornell is shown in Fig. 1, and it consists of 3 main stages: nucleation, coating and annealing. During the nucleation stage, both the cavity and the Sn/SnCl₂ source are kept at 535 °C for 5 hours, during which tin-rich droplets start to form on the niobium oxide. Then, the temperature of the tin heater is ramped up to 1405 °C, while the cavity is kept at 1156 °C for 1.5 hours for coating. Lastly, we turn off the secondary (tin) heater and anneal the cavity at 1156 °C for one hour.

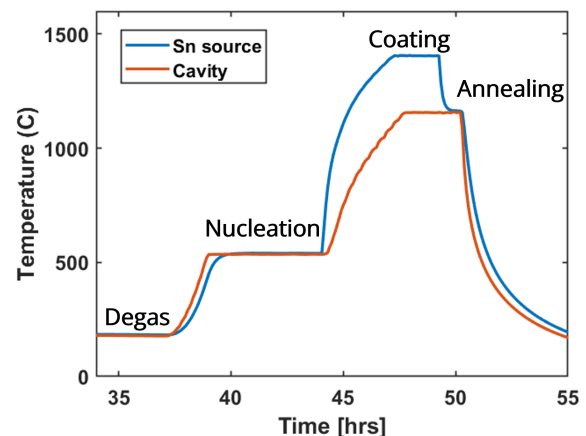


Figure 1: Vapor diffusion temperature profile at Cornell University showing the temperatures of the Sn/SnCl₂ source and Nb substrate (cavity) versus time. The main three stages of coating are nucleation, coating, and annealing.

Limitations

There are several practical limitations that stand in the way of Nb₃Sn cavities reaching the predicted fundamental limits of this material. It is very challenging to grow a smooth layer of stoichiometric Nb₃Sn with uniform thickness and composition. Deviating from the 3:1 atomic percent ratio of Nb to Sn in stoichiometric Nb₃Sn can result in drastic drop in both critical temperature and energy gap [5–7], which results in higher surface resistance and limits RF performance.

Not only does the layer composition need to be uniform, but so does the thickness. Due to this material's significantly lower thermal conductivity, a thicker layer will be thermally

* ls936@cornell.edu

PROGRESS IN EUROPEAN THIN FILM ACTIVITIES*

- C. Pira[†], O. Azzolini, R. Caforio, E. Chyhyrynets, D. Fomesu, D. Ford, V. Garcia, G. Keppel, G. Marconato, A. Salmaso, F. Stivanello, INFN Laboratori Nazionali di Legnaro, Legnaro (PD), Italy
M. Bertucci, R. Paparella, INFN LASA, Segrate (MI), Italy
M. Bonesso, S. Candela, V. Candela, R. Dima, G. Favero, A. Pepato, P. Rebesan, M. Romanato
INFN - section of Padova, Padova, Italy
C. Z. Antoine, S. Berry, Y. Kalboussi, T. Proslie, Université Paris-Saclay, CEA, Département des Accélérateurs, de la Cryogénie et du Magnétisme, Gif-sur-Yvette, France
D. Longuevergne, O. Hryhorenko, Université Paris-Saclay, CNRS/IN2P3, IJCLab, Orsay, France
E. Seiler, R. Ries, Institute of Electrical Engineering SAS, Bratislava, Slovakia
S. Keckert, O. Kugeler, J. Knobloch, Helmholtz Zentrum Berlin, Germany
S. Prucnal, S. Zhou, Helmholtz-Zentrum Dresden-Rossendorf, Institute of Ion Beam Physics and Materials Research, Dresden, Germany
X. Jiang, T. Staedler, A. Zubtsovskii, Institute of Materials Engineering, University of Siegen, Siegen, Germany
R. Berton, D. Piccoli, F. Piccoli, G. Squizzato, F. Telatin, Piccoli S.R.L., Noale (VE), Italy
A. Medvids, A. Mychko, P. Onufrievs, Laboratory of Semiconductor Physics, Riga Technical University, Riga, Latvia
C. Benjamin², O.B. Malyshev², T. Sian², L. Smith², R. Valizadeh², ASTeC, UKRI/STFC Daresbury Laboratory, Daresbury, Warrington, UK
G. Burt², N. Leicester², S. Marks², D. Seal², D. Turner²
Engineering Department, Lancaster University, Lancaster, UK
J. W. Bradley², S. Simon², Liverpool University, Liverpool, UK
A-M. Valente-Feliciano, Thomas Jefferson National Accelerator Facility, Newport News, VA, USA
¹also at Universität Siegen, Siegen, Germany
²also at Cockcroft Institute, UKRI/STFC, Daresbury, Warrington, UK

Abstract

Thin-film cavities with higher T_c superconductors (SC) than Nb promise to move the operating temperature from 2 to 4.5 K with savings 3 orders of magnitude in cryogenic power consumption. Several European labs are coordinating their efforts to obtain a first 1.3 GHz cavity prototype through the I.FAST collaboration and other informal collaborations with CERN and DESY. R&D covers the entire production chain. In particular, new production techniques of seamless Copper and Niobium elliptical cavities via additive manufacturing are studied and evaluated. New acid-free polishing techniques to reduce surface roughness in a more sustainable way such as plasma electropolishing and metallographic polishing have been tested. Optimization of coating parameters of higher T_c SC than Nb (Nb_3Sn , V_3Si , $NbTiN$) via PVD and multilayer via ALD are on the way. Finally, rapid heat treatments such as Flash Lamp Annealing and Laser Annealing are used to avoid or reduce Copper diffusion in the SC film. The development and characterization of superconducting coatings is done on planar samples, 6 GHz cavities, choke cavities, QPR and 1.3 GHz

cavities. This work presents the progress status of these coordinated efforts.

INTRODUCTION

The WP9 from IFAST, “Innovative superconducting cavities”, is focused on improving performance and reduce cost of SRF acceleration systems based mostly on the use of thin films. It comes after several European projects on the topics (WP12.2 within Eucard2, WP15 within Aries) that helped bringing together the teams working on that topic in Europe and keep in touch with the international community [1]. The European members are from France, Commissariat à l’Energie Atomique et aux Energies Alternatives (CEA), Centre National de la Recherche Scientifique (CNRS), from Germany, Helmholtz-Zentrum Berlin für Materialien und Energie (HZB), Helmholtz-Zentrum Dresden-Rossendorf (HZDR), Universität Siegen (USI), from Italy, Istituto Nazionale di Fisica Nucleare (INFN), PICCOLI SRL (PICCOLI), from Latvia, Rigas Tehniska Universitate (RTU), from Slovakia, Institute of Electrical Engineering, Slovak Academy of Sciences (IEE), and from the United Kingdom, United Kingdom Research And Innovation (UKRI) but we have also external collaborators, formal (JLAB); and informal (CERN, DESY).

* Work supported by the European Union’s IFAST collaboration H2020 Research and Innovation Programme under Grant Agreement no. 101004730

[†] cristian.pira@lnl.infn.it

SURFACE ENGINEERING BY ALD FOR SUPERCONDUCTING RF CAVITIES

Y. Kalboussi^{*1}, B. Delatte¹, F. Miserque², D. Drago³, M. Asaduzzaman^{4, 5}, L. Maurice¹,
M. Baudrier¹, G. Jullien¹, C. Boulch¹, T. Vacher¹, N. Lochet⁶, T. Pepin-Donat⁷, D. Longuevergne⁷,
F. Eozenou¹, P. Sahuquet¹, Q. Bertrand¹, T. Junginger^{4, 5}, C. Antoine¹, T. Proslie¹

¹IRFU, CEA Paris-Saclay University, Paris, France

²LECA, CEA Paris-Saclay University, Paris, France

³Plateforme ICMMO, Paris-Saclay University, Orsay, France

⁴University of Victoria, Dept. Physics and Astronomy, Victoria BC, Canada

⁵TRIUMF, Vancouver, BC, Canada

⁶DES, CEA Paris-Saclay University, Paris, France

⁷IJCLAB Paris-Saclay University, Orsay, France

Abstract

Atomic Layer Deposition is a synthesis method that enables a unique control of thin films chemical composition and thickness over complex shaped objects such as SRF cavities. This level of control opens the way to new surface treatments and to study their effect on RF cavity performances. We will present coupon and, in some cases, preliminary cavity results, from various surface engineering routes based on the deposition of thin oxides and nitrides films combined with post annealing treatments and study their interactions with the niobium. At CEA Saclay, three main research directions are under investigation:

1. Replacing the niobium oxides by other surface layers (Al_2O_3 , Y_2O_3 , MgO) and probe their effect on the low and high field performances,
2. Doping with N and combine approaches (1) and (2).
3. Optimizing the superconducting properties of NbTiN-AlN multilayers on Nb and Sapphire.

More details on the results presented in this paper can be found in the Phd. theses by the main author.

INTRODUCTION

For approximately five decades, bulk niobium resonators have been the backbone of superconducting particle accelerators. Thanks to the continuous research efforts made by the superconducting radio frequency (SRF) community, niobium cavities provide today reliably exceptional performances with accelerating gradient higher than 40 MV/m (TESLA shape — 1.3 GHz). Nonetheless, niobium cavities still witness performance degradation when exposed to high fields and are approaching their theoretical limits dictated by the Niobium's superheating field H_{sh} , the ultimate limit of the Meissner state. To keep up with future SRF facilities requirements in terms of quality factors and accelerating gradients as well as to improve their quality factor in the quantum regime, we aim at exploring a new technological pathway to enhance the performances of SRF cavities through functionalizing their inner surface with thin film

coatings. Due to its complex shape, coating an SRF cavity demands a fine tuning of the film's chemical and structural properties and a thickness uniformity down to the nanometric scale. One very promising deposition technique to achieve these requirements is atomic layer deposition (ALD). ALD is a chemical phase deposition technique based on sequential and self-saturating gas-surface reactions. Two or more chemical precursors are introduced to the surface separately, one at a time, following a cycle. An ALD cycle is typically composed of four steps:

- Pulse of precursor 1, allowing the first gas-surface reaction.
- Purge of precursor 1, allowing the evacuation of excess precursor 1 and the reaction products of the first gas-surface reaction.
- Pulse of precursor 2, allowing the second gas-surface reaction.
- Purge of precursor 2, allowing the evacuation of excess precursor 2 and the products of the gas-surface reaction.

Thus, after each pulse, a monolayer of precursor reacts with the surface and after each cycle, a monolayer of about 1 Å of the desired material is deposited, which guarantees atomic-level control of the thickness.

METHODS

In this study, we present the results of different ALD coatings performed on both samples and cavities using the two home-made thermal ALD systems. The coatings on coupons were performed using the research-scale ALD system which is a viscous-flow thermal ALD reactor with a 5 cm diameter deposition chamber. The reactor temperature was maintained between 60 °C and 450 °C by an external computer-monitored resistive heater system. Several K-type thermocouples were placed along the length of the flow tube to ensure the temperature homogeneity. A constant flow of ultrahigh-purity nitrogen (UHP, 99.999%) at 200 sccm with a pressure of 1.5 mbar was used to transport reactant to the substrate. The ALD system is also equipped with a residual gas analyser (RGA) device to help the control of the chemical reaction inside the deposition chamber. In order

* Yasmine.kalboussi@cea.fr

RESULTS OF THE R&D RF TESTING CAMPAIGN OF 1.3 GHz Nb/Cu CAVITIES

L. Vega Cid*, A. Bianchi, G. Bellini, L. A. Ferreira, S. Leith, C. P. Carlos¹, G. Rosaz,
W. Venturini Delsolaro, CERN, Geneva, Switzerland
¹also at University of Geneva, Geneva, Switzerland

Abstract

In the context of the R&D program on 1.3 GHz Nb/Cu carried out at CERN, a total of 25 tests have been performed since 2021. This talk will present these results. Three different manufacturing techniques have been used to produce the copper substrates, in order to investigate which is the most suitable in terms of quality and economy of scale. On one hand, the focus has been on optimizing the surface resistance at 4.2 K, as this will be the operating temperature of Future Circular Collider (FCC). The results at this temperature are encouraging, showing repeatable and optimized RF performance. On the other hand, RF tests have been done at 1.85 K too, aiming at deepening the knowledge of the mechanisms behind the Q slope. This is key to work on the mitigation of this phenomenon and ultimately to extend the application of this technology to high energy, high gradient accelerators. The influence of the thermal cycles has been thoroughly investigated. A systematic improvement has been observed of both the Q slope and the residual resistance with small thermal cycles.

INTRODUCTION

Historically, Nb has been the material of choice for Superconducting Radio Frequency (SRF) cavities. However, the development of niobium/copper (Nb/Cu) cavities introduced several advantages that made them an appealing alternative, such as improved thermal properties, easier fabrication and manufacturing and operation costs [1]. The latest is especially crucial for large-scale projects where the fabrication of numerous cavities is required. However, the degradation of performance at high fields, known as the Q-slope, has limited the use of Nb/Cu cavities to low-gradient machines such as LEP, LHC or HIE-ISOLDE [2].

Nb/Cu technology has been the selected baseline for the 400 MHz FCC SRF system [3]. However, there is a need of improvement to meet the stringent operational requirements imposed by the FCC project, which exceed the capabilities of the existing LHC SRF system. In response, CERN has undertaken significant efforts through an R&D campaign to address these challenges, focusing on advancements in various aspects such as substrate manufacturing, surface treatments prior to coating and deposition techniques [4]. The goal is to achieve high repeatability in terms of quality while maintaining cost-effectiveness on a large scale.

Furthermore, extensive efforts have been undertaken to comprehensively understand the underlying mechanisms be-

hind the Q-slope phenomenon. It is crucial to demonstrate that this issue is not intrinsic to the Nb/Cu technology and can be effectively overcome for its application on SRF systems of future high-gradient accelerators [5].

As part of the R&D campaign, a total of 25 cavities have been tested since 2021 [6]. Results will be reported and discussed in the following sections.

METHODOLOGY

The steps followed for fabricating the cavities and preparing them for finally proceeding to the RF testing are described in the following section:

Cavity Preparation

The first step in the cavity preparation is the production of the substrate. Three different techniques have been investigated:

- Machining a bulk copper billet (BM): Four seamless substrates have been produced by machining copper billets. The cut-offs are welded at the irises level [7].
- Electroforming (L): Two substrates were produced by growing a copper substrate on an aluminum mandrel. It is important to note that this is the only method that avoids welds in the entire cavity structure [8].
- E-beam welded at the equator (W): Two spun half cells were welded at the equator and also at the cut-offs from the inside using a deflector to improve the quality of the welded surface exposed to the RF fields [9].

It is important to note that out of the three techniques, only one (W) involves a weld at the equator. This is due to the observation at HIE-ISOLDE that seamless substrates showed significant improvement in performance compared to welded ones [10, 11]. Currently, the baseline for substrate production in the FCC project is spinning, similar to the LHC, with a strong effort dedicated to the investigation on hydroforming [9, 12]. Nevertheless, there is ongoing interest in exploring methods to produce high-quality welds, such as in the case of substrate W.

Before the coating process, the substrate undergoes several important steps. First, it is degreased to remove any hydrocarbon based contamination. Then, it is electropolished to remove any surface imperfections and contaminants. This step helps to achieve a smoother and cleaner surface, which is crucial for optimal RF performance. After electropolishing, the substrate is passivated to protect it from oxidation.

Next, a layer of niobium (Nb) is deposited on the substrate using High Power Impulse Magnetron Sputtering (HiPIMS).

* lorena.vega@cern.ch

OPTIMIZING THE MANUFACTURE OF HIGH-PURITY NIOBIUM SRF CAVITIES USING THE FORMING LIMIT DIAGRAM: A CASE STUDY OF THE HL-LHC CRAB CAVITIES RFD POLE*

Adrià Gallifa-Terricabras^{†,1}, Joanna Sylwia Świążek^{1,2}, Eduardo Cano-Pleite³, Marco Garlaschè¹, Simon Barrière¹, Laurent Prever-Loiri¹, Stephan Pfeiffer¹, Ignacio Avilés Santillana¹, Manuele Narduzzi⁴

¹European Organization for Nuclear Research (CERN), Geneva, Switzerland

²Kraftanlagen Nukleartechnik GmbH, Heidelberg, Germany

³Universidad Carlos III, Madrid, Spain

⁴Fermi National Accelerator Laboratory (Fermilab), Batavia, USA

Abstract

The Crab Cavities are key components of the High Luminosity Large Hadron Collider (HL-LHC) project at CERN, whose goal is to increase the integrated luminosity of the LHC, the world's largest particle accelerator, by a factor of ten. This paper explores the application of the Forming Limit Diagram (FLD) to enhance the manufacturing process of complex-shaped Nb-based crab cavities, with a focus on the formability challenges experienced with the pole of the RFD (Radio Frequency Dipole) Crab Cavities. The study includes the materials characterization of ultra-high-purity niobium (RRR300) sheets, namely mechanical tests and microstructural analysis; it also contains large-deformation Finite Element simulations of the pole deep drawing process, and the translation of the resulting strains in a FLD, together with several suggestions on how to improve the manufacturing process of such deep drawn parts. The results of this study can provide valuable insights for improving the design and fabrication of complex-shaped superconducting RF cavities made by large-deformation metal-sheet forming processes.

INTRODUCTION

The Crab Cavities are crucial devices to be installed in the High-Luminosity Large Hadron Collider (HL-LHC) at CERN, the upgraded version of the LHC. The goal of these complex-shaped cavities (see the RFD type in Fig. 1), which are made of 4 mm thickness sheets of ultra-high-purity niobium (RRR300), is to generate transverse electromagnetic fields that rotate the particle bunches longitudinally, such that they effectively collide head on, overlapping perfectly at the collision points (IR1 and IR5 of LHC) thus increasing the luminosity [1].



Figure 1: 3D View of bare RFD Crab Cavity. Courtesy R. Leuxe.

The cavities are operated at 1.9 K and are surrounded by a cold magnetic shield and a He tank, equipped with corresponding RF ancillaries, and hosted by a cryomodule containing the RF lines, cold and warm magnetic shield, thermal screen, cryogenic lines, tuning system, instrumentation for alignment and monitoring, among other devices [2].

Manufacturing Crab Cavities and RFD Pole

The manufacturing of Crab Cavities consists of a multi-technology process involving metal sheet forming (deep drawing, bending, extrusion), electron beam welding, vacuum brazing, machining, and surface processing such as Buffered Chemical Polishing (BCP).

The RFD Pole is one of the Crab Cavity sub-components experiencing the highest levels of deformation [3, 4], also along different strain paths, rendering it an object of study for pushing the understanding of Nb formability limits.

In the past, multiple studies have been conducted in order to understand the deep drawing of Niobium, including characterization of mechanical properties, FE simulations [3], friction studies [5], surface pollution studies, among others. Recent publications [6] introduce an experimental Forming Limit Curve (FLC) for 1 mm thickness RRR300 Nb sheets. However, the application of FE simulations incorporating the FLC for thicker Nb sheets (up to 4 mm thickness) for forming processes associated with SRF have not been studied before.

Challenges During Pole Forming

During the deep drawing of sub-components for RFD pre-series cavities at Zanon Research & Innovation (Zanon) -industrial partner of Fermilab within US HL-LHC AUP collaboration- some Poles manufactured using material from a specific batch (hereafter called Lot-2) exhibited orange peel appearance and experienced excessive thickness reduction in certain areas (minimum thickness around 2.3 mm), accompanied by the presence of wrinkles (as shown in Fig. 2).

*Work supported by CERN HL-LHC WP4

[†] adria.gallifa@cern.ch

DEVELOPMENT OF THE DIRECTLY-SLICED NIOBIUM MATERIAL FOR HIGH PERFORMANCE SRF CAVITIES

A. Kumar^{†1}, H. Ito¹, H. Araki, T. Saeki¹, T. Dohmae¹, K. Umemori¹, M. Yamanaka¹,
 A. Yamamoto, High Energy Accelerator Research Organization (KEK), Tsukuba, Japan
¹also at the Graduate University for Advanced Studies, Hayama, Japan

Abstract

For cost reduction studies for the ILC, KEK has been conducting R&D on direct sliced Nb materials such as large grain and medium grain Nb. 1-cell, 3-cell, and 9-cell cavities have been manufactured, and each has demonstrated a high-performance accelerating gradient exceeding 35 MV/m. The results of applying high-Q/high-G recipes, such as two-step baking and furnace baking to these cavities are also shown. Moreover, mechanical tests have been carried out for the beforementioned materials to evaluate their strength for application to the High-Pressure Gas Safety Law. The status of development of large grain and medium grain Nb will be presented.

INTRODUCTION

The International Linear Collider (ILC) is an electron-positron collider accelerator, that requires approximately 7800 1.3 GHz Niobium 9-cell cavities to attain 250 GeV centre-of-mass energy and is extendable up to 1 TeV [1, 2]. The ILC design update for the ILC-250 (GeV) has been already published [2] but the cost of its construction is a major hindrance. Cost reduction studies are being carried out at KEK and other facilities all over the world for the realization of ILC. A part of the cost-reduction studies at KEK is to research on various grades of Niobium, to reduce the manufacturing cost of the SRF cavity. Research on SRF cavities manufactured with fine grain Nb (FG Nb) has been carried out extensively but the cost of the material is high due to its manufacturing process. In this paper, we would like to introduce current progress regarding cost-effective alternative grades of Nb for the SRF cavity manufacturing.

The operational requirement for the ILC's 1.3 GHz 9-cell cavities is accelerating gradient (E_{acc}) > 31.5 MV/m with quality factor (Q_0) > 1E10, such specification generally requiring Niobium with high purity (RRR >300). However, the mechanical strength of Nb generally deteriorates with higher purity (Table 1). The Nb material in the SRF community is usually classified in two categories [1, 3, 4]:

1. Residual Resistivity Ratio (RRR) – Low (< 100), Medium (100 to 300) and High (> 300).
2. Grain Size – Fine Grain (< 50 μm), Medium Grain (MG) (200 - 300 μm with occasional grains as large as 1-2 mm) and large grain (LG) (few millimetres to centimetres) [1, 3, 4].

DIRECTLY-SLICED NIOBIUM

Large Grain (LG) Nb was developed as a clean and low-cost alternative, where the LG Nb Ingot is directly sliced

into disks, as shown in Fig. 1. Its grain size usually varies from a few mms to several cms, as seen in Fig. 2, due to which it has anisotropic mechanical properties causing its 0.2% Yield Strength (Y.S) and Tensile Strength (T.S) to sometimes fall short of the mechanical property requirement set for 9-Cell 1.3 GHz SRF cavities. W. Singer et al., Zhao et al., Enami et al., Yamanaka et al., has conducted in depth research on determining the mechanical properties of the LG Nb at various temperatures and strain rate ranges [5-8].

Medium Grain (MG) Niobium has an average grain size of 200 - 300 μm with occasional grains as large as 1-2 mm as a potential alternate to both FG and LG Nb, and potential cost reduction compared to FG Nb [1, 3, 4]. It is formed by forging and annealing of the LG Nb ingot to a billet to achieve smaller grain sizes. The forged billet is then directly sliced in disk forms, which lowers the number of manufacturing steps that are involved with FG Nb, such as rolling, etching, annealing etc., elimination of these steps having the potential to reduce material cost [1, 3, 4], as seen in Fig.1.

Table 1: Chemical Composition and Mechanical Properties Measured by ATI (Unit of Chemical Composition: wt ppm)

C	H	O	N	RRR	Hardness (HV10)
<20	<3	<50	<20	> 300	~ 41

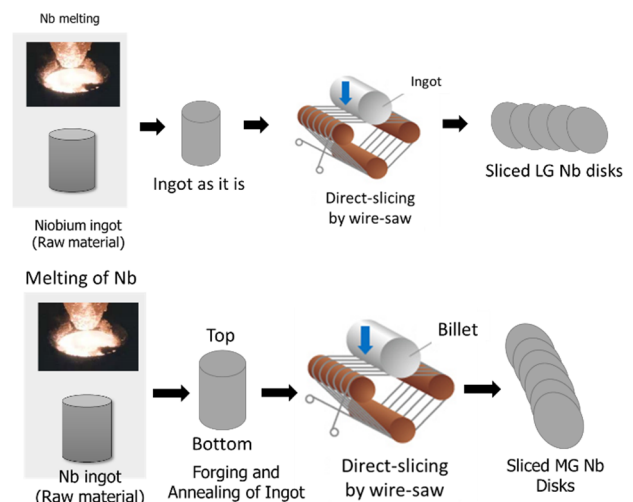


Figure 1: LG Nb manufacturing process (up) and ATI MG Nb manufacturing process (below) [3, 4].

Content from this work may be used under the terms of the CC BY 4.0 licence (© 2023). Any distribution of this work must maintain attribution to the author(s), title of the work, publisher, and DOI

ELECTROPOLISHING STUDY ON NITROGEN-DOPED NIOBIUM SURFACE*

V. Chouhan[†], T. Ring, E. Viklund, G. Wu, Fermi National Accelerator Laboratory, Batavia, IL, USA

Abstract

The nitrogen doping (N-doping) process is applied to niobium (Nb) superconducting cavities to enhance their quality factors. The N-doping is followed by an electropolishing process that provides the final surface of the cavities. A controlled EP process is necessary to get the benefit of N-doping and achieve a high accelerating gradient. We have performed electropolishing of N-doped Nb surface under various conditions to understand their impact on the surface. A modified EP process was developed to obtain a smooth pit-free surface.

INTRODUCTION

Niobium (Nb) made superconducting RF (SRF) cavities are used in particle accelerators. The performance of the accelerator machine obviously depends on the performance of individual cavity used to make the accelerator machine. The field gradient (E_{acc}) and quality factor (Q_0) of the cavity determines its performance. Higher Q_0 value reduces cryogenic power to run the machine. To improve Q_0 value of the cavities, nitrogen-doping (N-doping) was invented at Fermilab [1] and successfully implemented to prepare 1.3 GHz 9-cell cavities for Linac Coherent Light Source-II (LCLS-II) and LCLS-II HE. High- β (0.92) elliptical cavities for Proton Improvement Plan-II (PIP-II) are also processed with N-doping process [2].

The initial Nb surface is processed with electropolishing (EP) method to prepare a desired smooth surface. Optimum EP conditions are required to attain a smooth surface specially for 650 MHz cavities which have a large surface area, and EP parameters for these cavities deferred from the standard EP parameters applied to 1.3 GHz cavities. The surface is doped with nitrogen at a temperature of 800 °C. The N-doped surface is processed again with EP to remove the top 5–10 μm material. The top layer of the N-doped surface usually contains an undesired nitride layer. To reduce BCS resistance for Q_0 improvement, an adequate concentration of interstitial nitrogen atoms in the RF penetration depth without any nitride phase is required [3].

The N-doped surface in the EP process might show pitting. The pitting was attributed to a high temperature in the EP process [4]. Premature quench of the cavity at low field is attributed to the pit on the N-doped cavity surface. Cold EP, which was conducted at comparatively lower cavity temperature, improved the quench field of the cavities as confirmed with LCLS-II cavities.

* This work was supported by the United States Department of Energy, Offices of High Energy Physics and Basic Energy Sciences under contract No. DE-AC02-07CH11359 with Fermi Research Alliance.

[†] vchouhan@fnal.gov

This study aims to improve understanding on how different EP conditions impact the N-doped surface. This paper also proposes an EP process that reduces the risk of pit formation on the N-doped surface.

EXPERIMENT

EP Setup

The setup used for EP of the samples was a two-electrode system which employed an Nb sample as anode and aluminum as a counter electrode. The surface area of the aluminum cathode was chosen to be approximately 10% of the Nb surface area, similar to the cathode surface area used in cavity EP. Figure 1 shows a schematic of the setup. A power supply (40 V×12 A) was used for EP and an I - V measurement. To measure the I - V curve, the voltage was scanned from 0 to 20 V, and the corresponding current values were recorded. The temperature of samples during EP was regulated by a heat-sink coil immersed in the acid bath. Two thermocouples were used to measure acid and Nb sample temperatures. A LabView program was used to control the power supply and record a sample current, sample temperature, and acid temperature.

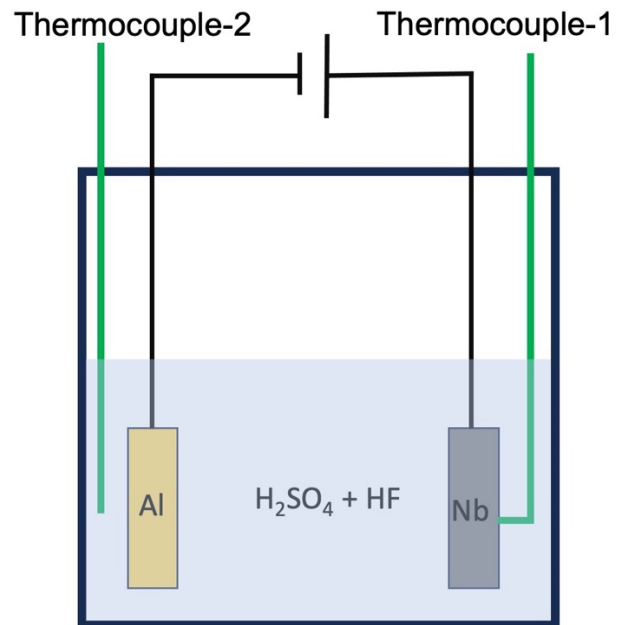


Figure 1: Schematic of the EP setup. Thermocouple-1 and -2 used to measure temperature of Nb sample and acid, respectively.

Sample Preparation

The samples, measuring 10×10 mm and 20×20 mm, were prepared from the same sheet of high RRR (relative resistivity ratio) Nb material. The samples experienced

RECENT ADVANCES IN METALLOGRAPHIC POLISHING FOR SRF APPLICATION

O. Hryhorenko*, Thomas Jefferson National Accelerator Facility (JLAB), Newport News, VA, USA
C. Z. Antoine, Université Paris-Saclay, CEA Département des Accélérateurs
de la Cryogénie et du Magnétisme (CEA-IRFU), Gif-sur-Yvette, France
T. Dohmae, High Energy Accelerator Research Organization (KEK), Tsukuba, Japan
S. Keckert, O. Kugeler, J. Knobloch, Helmholtz Zentrum Berlin (HZB), Berlin, Germany
D. Longuevergne, Université Paris-Saclay, CNRS/IN2P3, IJCLab, Orsay, France

Abstract

This paper is an overview of the metallographic polishing R&D program covering Niobium and Copper substrates treatment for thin film coating as an alternative fabrication pathway for 1.3 GHz elliptical cavities. The presented research is the result of a collaborative effort between IJCLab, CEA/Irfu, HZB, and KEK in order to develop innovative surface processing and cavity fabrication protocols capable of meeting stringent requirements for SRF surfaces, including the reduction of safety risks and ecological footprint, enhancing reliability, improving the surface roughness, and potentially allowing cost reduction. The research findings will be disclosed.

INTRODUCTION

The SRF cavities made of bulk Niobium are reaching their theoretical performance limits via different surface processing techniques (surface roughness decrease, interstitials engineering,...) [1–3]. The global strategy for future decades in the field of superconducting radiofrequency (SRF) technology is focused on the fabrication of novel superconducting cavities made of alternative superconductors and multilayer structures [4]. This approach aims to enhance performance beyond the theoretical limits of bulk Nb and improve the accelerator cost-efficiency using thin films with the ultimate goal of operation at 4.2K. A key aspect of this strategy involves optimizing and industrializing the substrate preparation (cavity), specifically focusing on materials such as Nb and Cu. This paper examines the protocols involved in the pursuit of substrate preparation via metallographic polishing (MP) technology for niobium and copper, highlighting the potential benefits of MP in the preparation of flat samples. In the framework of the IFAST project, RF disks and Quadrupole (QPR) resonator samples are used for superconducting RF evaluation of deposited thin films [5].

Samples were provided by STFC (Daresbury, UK) and HZB (Berlin, Germany) labs, were polished at IJCLab, and their surface quality was evaluated. The disclosed findings presented here contribute to the ongoing efforts in investigating an alternative cavity fabrication pathway, see related conference paper[6], in the framework of the FJPLP program. Moreover, in this work we show the first successful

results of the RF test achieved on the QPR sample after metallographic polishing.

EXPERIMENTAL SET-UP AND QUALITY CONTROL

RF disks and QPR samples were polished with a commercial metallographic polishing (MP) machine MASTERLAM 1.0 (LAM PLAN production) at IJCLab. The surfaces were studied and the achieved quality was controlled after each manipulation via visual inspection and roughness measurements using a laser confocal microscope Keyence VK-X 200. The roughness measurements were performed on 9 different spots with a scan area 290 μm X 215 μm . Two parameters as average roughness (S_a), and maximal height deviation (S_z) were monitored and recorded. To complete characterization of the MP influence on the SRF surface at a high magnetic field, a QPR sample was evaluated under RF at HZB.

RF Disks: Copper and Niobium Processing

Disks of the two types, see Fig. 1, are utilized at STFC for RF measurements with a choke cavity operated at 7.8 GHz, at a temperature of 4 K, and with surface magnetic fields up to 1 mT [7]. Type 1 (diameter of 100 mm), which can be made of copper (Cu) or Niobium (Nb), requires indium brazing between the sample and support holder, so indium removal after characterization is required. Type 2 (diameter of 110 mm), which is exclusively applied to copper, is based on a slightly complicated design as bolts are used to connect the sample with a choke cavity, resulting in the surface being drilled, but the step with indium removal is omitted.

The 5-step procedure described in Table 1 was used to MP polish RF disks made of copper. The recipe was applied on 3 disks of Type 1 and on one disk of Type 2. The first three steps are focused to planarize the surface. The last 2 steps are focused on removing the damage from the previous steps and creating a mirror-smooth and scratch-free surface. Considering prior experience with Nb (niobium), it was determined that the 5-step procedure could be replaced with a 2-step recipe [8]; however, this modification would significantly prolong the preparation time.

In addition to procedure steps, proper cleaning is required between steps. At the end of each step, the surface was rinsed with ultra-pure water, cleaned in the ultrasound bath (only de-ionized water), and dried with a Nitrogen gun. In order to improve the surface state, at the last polishing step,

* hryhoren@jlab.org

PREPARATION AND CHARACTERIZATION OF Nb FILMS DEPOSITED IN SRF CAVITY VIA HiPIMS*

H. C. Duan¹, Y. C. Yang, P. Zhang¹, P. He^{1†}, J. Dai, T. M. Xin¹, J. W. Kan¹, Y. S. Ma
Institute of High Energy Physics, Chinese Academy of Sciences, Beijing, China
¹also at University of Chinese Academy of Sciences, Beijing, China

Abstract

The RF performance of the niobium superconducting cavity has been continuously improved in recent 50 years. Since the maximum acceleration field (E_{acc}) has approached its theoretical limit, developing a more efficient and low-cost SRF cavity is one of the key challenges of the next generation particle accelerators. Niobium coated copper cavities are promising solutions because the SRF phenomenon occur within several hundred nanometers under the cavity surface. In literatures, the Nb coated Cu cavity prepared by direct current magnetron sputtering has serious Q-slope problem, which may be related to the low energy deposition. High power impulse magnetron sputtering (HiPIMS) can produce a high peak power and high ionization rate which may improve the thin film quality. Therefore, we prepared Nb coated Cu samples via HiPIMS on the 1.3 GHz dummy cavity at IHEP.

INTRODUCTION

RF superconducting accelerating cavity has been widely applied in various particle accelerator in the world due to its advantages of low surface loss, high gradient (E_{acc}), high quality factor (Q), and continuous wave mode adaptability. As a key component of accelerators, improving the performance of RF superconducting cavities has been widely studied by scholars. The performance of conventional bulk niobium cavities has approached their theoretical limit over decades of development, and there is little room for further improvement. Developing a more efficient and cost reduction SRF cavity is a key challenge of the next generation particle accelerator. Since the penetration depth of the RF magnetic field on the surface of the cavity is less than 1 μm , one layer of superconducting material coated on cavity of materials with good thermal conductivity is a solution for further improving the cavity performance. The superconducting thin film cavity was first proposed by Benvenuti[1] at CERN in the 1980s, which was several microns of niobium deposited on copper cavity via magnetron sputtering. In recent years Nb/Cu thin film cavity has been successfully applied in the Large Electron Positron Collider (LEP) and Large Hadron Collider (LHC) at CERN, and the Superconducting Linear Accelerator (ALPI) at Italian National Institute of Nuclear Physics (INFN) [2-4].

The Nb/Cu thin film cavity deposited by direct current magnetron sputtering (DCMS) has a good low field quality

factor Q , but the Q value decreases exponentially with RF injection power, which is called "Q-slope". This may due to the low energy deposition. HiPIMS is a high energy deposition technology, which has been applied in academia and industry in recent years. Because in HiPIMS the particles sputtered are ions, they have much higher deposition energy and can be further accelerated by substrate bias voltage. Compared to DCMS, HiPIMS has been proven to deposit Nb films with better microstructure, denser and better superconducting RF performance [5-8].

We have designed and constructed a deposition system at IHEP to conduct a series of research on preparing and characterizing 1.3 GHz Nb/Cu thin film cavity. Recently, this system has been used to deposit Nb films inside the 1.3 GHz Cu cavity via HiPIMS.

EXPERIMENTAL

Schematic diagram of the deposition system is shown in Figure 1. A 1.3 GHz dummy cavity made of stainless steel was mounted inside the cylindrical vacuum chamber. Copper plate samples treated by SUBU5 process[9] was fixed on the inner side of the dummy cavity at different positions. A cylindrical magnetron with a movable magnetic ring was mounted coaxial to the dummy cavity. The cylindrical Nb target was fixed outside the magnetron. The discharge was powered by a high pulse power supply (TruPlasma Highpulse 4002 G2). The dummy cavity was baked at 400 °C for 30 h by tantalum heater to obtain a base pressure of 8×10^{-7} Pa before the deposition. Krypton flow was set through a mass flow controller to obtain a working pressure of 0.6 Pa. The discharge was operated with a peak current of 110 A and a pulse voltage of 490 V. The pulse width was 30 μs with frequency of 800 Hz. The temperature of the samples was kept at 200 °C during deposition. The deposition duration was 6 h. The cathode target was a hollow cylindrical high-purity niobium target (RRR~300). The magnetic ring scans back and forth at a speed of 1 mm/s in the cavity.

SEM (HATACHI su8020) was used to investigate the surface morphology and cross-section. FIB was used to investigate the cross-section. The crystal structure and the size of crystallites are investigated by XRD (Bruker D8 Advance).

RESULTS AND DISCUSSIONS

The influence of the cavity shape on the morphology of Nb thin films was tested. SEM micrographs of the Nb thin films on copper plates at different positions of the dummy

* Work supported by High Energy Photon Source (HEPS).

† Email: heping@ihep.ac.cn

Nb₃Sn VAPOR DIFFUSION COATING SYSTEM AT SARI: DESIGN, CONSTRUCTION, AND COMMISSIONING

Q. Chen, Y. Zong

Shanghai Institute of Applied Physics, Chinese Academy of Sciences, Shanghai, China

J. Chen[†], S. Xing

Shanghai Advanced Research Institute, Chinese Academy of Sciences, Shanghai, China

J. Rong, Lanzhou University, Lanzhou, China

Abstract

This paper describes the design of a coating system for the preparation of a superconducting radio-frequency cavity with Nb₃Sn thin films. The device consists of a coating chamber made of pure niobium, a vacuum furnace for heating the coating chamber, a superconducting cavity bracket and two crucible heaters. The chamber is vacuum isolated from the furnace body to protect the superconducting cavity from contamination during the coating process. The device has been built and commissioned, which could be used for Nb₃Sn coating of a 1.3 GHz single-cell superconducting cavity in future.

INTRODUCTION

The Nb₃Sn coating superconducting cavity offers significant efficiency advantages compared to a standard niobium cavity. Its high operating temperature of 4.2 K simplifies the cooling requirements, resulting in reduced cooling costs [1, 2]. These advantages make the Nb₃Sn cavity a hot of research field. Several preparation methods are being investigated, and the vapor physical deposition method has shown the most promising results. Several laboratories have successfully coated high-quality Nb₃Sn films on niobium base cavities using this technique. Remarkably, the 1.3 GHz single cell Nb₃Sn cavity coated by Fermilab shows excellent performance in vertical test at 4.2 K, the Q-value reaches 3×10^{10} at low accelerating field and the maximum accelerating field reaches 22.5 MV/m [3].

In order to develop Nb₃Sn superconducting cavity, we have designed and built a new coating system. The main body of the coating system is a horizontal vacuum heat treatment furnace for vapor phase physical deposition. In addition, the furnace body is equipped with vacuum module, electric control module and water-cooling module. The coating system will be used for the studies of coating 1.3GHz single-cell cavities.

REQUIREMENT FOR COATING SYSTEM

The design of this coating system is based on Fermilab's 9-cell coating system [1]. Despite the object being treated is a single-cell cavity with shorter length, the dual-tin source design is chosen for its advantage in achieving coating uniformity compared with a single tin source [4]. Accordingly, a horizontal furnace with two evaporation sources was selected. Figure 1 depicts the overall design of

the furnace, including the furnace body, the Nb coating chamber, and the bracket and crucible heater.

In physical vapor deposition processes, maintaining cleanliness is extremely important. Environmental impurities, including those originating from the furnace body, may adhere to the cavity during the coating process or react to form undesirable products [5]. In order to reduce the contamination, a dedicated coating chamber has been constructed using pure Nb, effectively isolating the furnace and minimizing the possibility of pollution.

The reaction between niobium and Sn can result in the formation of multiple compounds, which is dependent on the reaction temperature and the ratio of niobium to tin content in the system [6]. Among the various potential products, Nb₃Sn exhibits a high transition temperature, aligning with our expectations. Specifically, in the niobium-tin system above 930 °C, only Nb₃Sn will form when the Sn component content ranges between 17% and 25%. Any excess tin or niobium will exist in the formation of simple substance within the system [7].

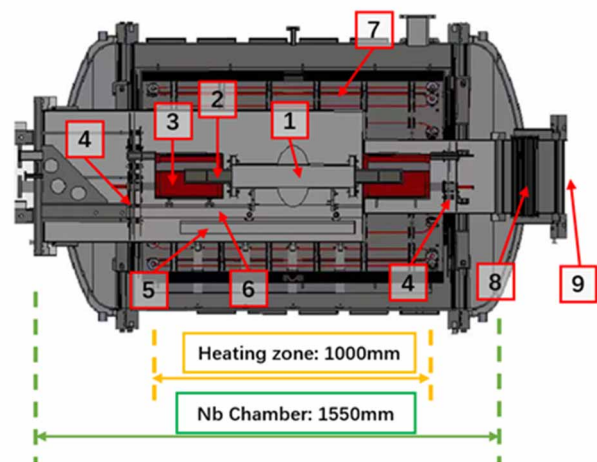


Figure 1: Overall design of the coating system at SARI: 1 Nb cavity, 2 Sn crucible, 3 Crucible heater, 4 Nb reflectors inside Nb chamber, 5 Bracket rails, 6 Cavity bracket, 7 Mo heater of furnace, 8 bellows, 9 Pumping port for Nb chamber.

DESIGN AND CONSTRUCTION

A photograph of the coating system's construction is depicted in Fig. 2. The photo provides a clear overview of the system's components, which have been built according to the description provided in the preceding section. The design parameters of the furnace are listed in Table 1.

[†] chenjinfang@sari.ac.cn

REALIZATION OF ACCELERATING GRADIENT LARGER THAN 25 MV/m ON HIGH-Q 1.3 GHz 9-CELL CAVITIES FOR SHINE*

Y. Zong, Q. X. Chen, X. Huang, Z. Wang, Shanghai Institute of Applied Physics, Shanghai, China
J. F. Chen[†], P. C. Dong, H. T. Hou, X. Y. Pu, J. Shi, S. Sun, D. Wang, J. N. Wu, S. Xing,
S. J. Zhao, Y. L. Zhao, Shanghai Advanced Research Institute, Shanghai, China
Y. W. Huang, ShanghaiTech University, Shanghai, China
X. W. Wu, Zhangjiang Lab, Shanghai, China

Abstract

We present our studies on the optimized nitrogen-doping and medium-temperature baking recipes applied on 1.3GHz SRF cavities, aiming at meeting the requirements of the SHINE project. The optimized nitrogen-doping process resulted in achieving a Q_0 of over 4.0×10^{10} at medium field and a maximum accelerating gradient exceeding 35 MV/m on single-cell cavities, and a Q_0 of over 2.8×10^{10} at medium field and a maximum accelerating gradient exceeding 26 MV/m in 9-cell cavities. For 1.3 GHz 9-cell cavities subjected to medium-temperature baking, Q_0 values exceeding 3.5×10^{10} at 16 MV/m and maximum accelerating gradients surpassing 25 MV/m were achieved. These studies provide two options of high-Q recipes for SHINE cavities. The treatment processes of cavities and their vertical test results are described in this paper.

INTRODUCTION

Shanghai High repetition rate XFEL and Extreme light facility (SHINE) is a new hard-XFEL facility under construction in China. This facility is designed to accelerate electron beams to 8 GeV by 600 1.3 GHz 9-cell cavities working in continuous wave mode with an intrinsic quality factor (Q_0) of 2.7×10^{10} at an accelerating gradient of 16 MV/m [1]. In recent years, two prominent approaches, nitrogen doping (N-doping) [2–6] and medium-temperature (mid-T) baking [7–11], have been extensively studied as key recipes for enhancing the Q_0 value of SRF cavities.

Starting from 2021, we have been conducting experimental cavity treatments utilizing the SHINE facilities for SRF cavity surface treatments on the platform located in Wuxi City, China (referred to as the Wuxi Platform, see Fig. 1). This paper presents the achievements obtained through the implementation of N-doping and mid-T baking treatments on 1.3 GHz SRF cavities.

OPTIMIZATION OF NITROGEN DOPING PROCESS

A single-cell cavity, TF63, was treated using the N-doping recipe [12] that we studied before at the Wuxi platform. The vertical test result at 2 K of TF63 after the first N-doping at the Wuxi Platform is shown in Fig. 2. TF63 reaches



Figure 1: Newly constructed SRF cavity surface treatment platform (main hall).

3.8×10^{10} at 16 MV/m but quenches at 18.9 MV/m. In order to improve its maximum accelerating gradient, an optimized N-doping process [13] was attempted on TF63. In this N-doping process, the furnace was heated to 800 °C and maintained for 30 min to stabilize the temperature. Then, nitrogen was injected directly for 3 min, and the cavity was annealed for 60 min in vacuum and cooled naturally. Thereafter, TF63 was tested at SARI and obtained interesting results, which are shown in Fig. 2. TF63 reaches 4.1×10^{10} at 16 MV/m, with a maximum accelerating gradient larger than 35 MV/m (admin limit to avoid quench), which is almost doubled compared with that at the first round N-doping. Another single-cell cavity S02 was processed as the same optimized N-doping recipe and realized the similar performance.

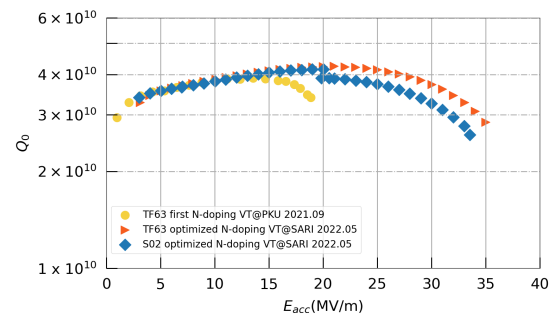


Figure 2: Vertical test results at 2 K of the two single-cell cavities, S02 and TF63.

Following the successful N-doping of single-cell cavities, two 9-cell cavities, HJ005 and HJ006, underwent subsequent treatment using the same recipe, as outlined in Table 1 for the second treatment of HJ005 and HJ006. Vertical test results at

* This work was supported by Shanghai Municipal Science and Technology Major Project (No. 2017SHZDZX02).

[†] chenjinfang@sari.ac.cn

THE OXIDIZING RESPONSES OF BAKED NIOBIUM EXPOSED TO VARIOUS GASES VIA IN-SITU NAXPS*

Zhitao Yang, Jiankui Hao[†], Shengwen Qaun, Kexin Liu, State Key Laboratory of Nuclear Physics and Technology & Institute of Heavy Ion Physics, Peking University, Beijing, China

Abstract

We carried out in-situ NAXPS (Near-atmospheric X-ray Photoelectron Spectroscopy) on SRF-cavity class niobium to observe its oxidizing responses when exposed to various gases. The niobium samples were baked at 800 °C until the peaks of niobium oxides disappeared in the spectrum. Then the revealed pure niobium samples were exposed to the air-proportion mixture of nitrogen and oxygen, pure oxygen, and pure water vapor respectively. And for the pure oxygen and water vapor group, we also carried out TOF-SIMS (Time-of-Flight Secondary Ion Mass Spectroscopy) measurements before and after the baking and oxidation experiments. We found that pure oxygen and water vapor could oxidize niobium at similar rate which was faster than the N₂/O₂ mixture. After re-oxidized by pure oxygen and water vapor, the niobium sample presented a significant increase of interstitial carbon and a moderate increase of interstitial oxygen in the magnetic penetration depth, while it showed a mild decrease of interstitial hydrogen.

INTRODUCTION

The tiny amounts of impurities in the magnetic penetration depth would influence the superconducting performance of SRF niobium cavities, including both non-magnetic impurities like carbon [1, 2], hydrogen [3-6], nitrogen [7-10] and oxygen [11-13], and magnetic impurities like iron, manganese, cobalt and titanium [14, 15]. The doping process of the impurities can hardly be completed without decomposing the niobium oxides layer at the surface, which serves as a safe guard for further intake of impurities [16, 17]. Among the impurities, oxygen and carbon released from the niobium oxides and the adventitious carbon at the surface during baking would diffuse into the deeper lattice and regulate the superconducting properties, while hydrogen from the environment could be actively absorbed into the niobium lattice when the oxide layer is removed by baking or polishing. One shall acknowledge that the more interstitial hydrogen inside the niobium lattice, the higher probability of niobium hydride precipitation with various sizes during cooling down, thus the lower the intrinsic quality and accelerating gradient of the cavities [18, 19].

High temperature baking around 800 – 1000 °C is usually used to degas hydrogen that results in less interstitial hydrogen in niobium lattice [20, 21], and baking above 200 °C has been enough for decomposing Nb₂O₅ [22, 23] which is the main component of the surface compounds.

However, after baking, the cavities with removal of surface oxide layer are usually exposed to air environment and go through high pressure rinsing afterwards, which are both highly possible for the hydrogen reabsorption by pure niobium before the oxide layer is completely reformed. Therefore, the pre-oxidization when niobium cavities are still in the baking furnace may suppress the reabsorption of hydrogen in the following industrial procedures effectively. So, we carried out in-situ near atmospheric X-ray photoelectron spectroscopy (NAXPS) to find out the oxidation responses of the pure niobium when exposed to mixed pure N₂/O₂, pure O₂, and pure H₂O vapor, which are available and economical supplies in laboratories and factories.

EXPERIMENT

We prepared 2 SRF-cavity class single crystal niobium samples with the size of around 1.5 mm × 5 mm × 8 mm with heavy buffered chemical polishing (BCP) and light electropolishing (EP) to obtain a flat and smooth surface of R_a = 10. We baked the first sample (Labeled as LGO22) at maximum temperature of 400 °C and then pumped in the air-proportion-mixed pure N₂/O₂ after cooling down to room temperature. The pressure inside the detection chamber was kept at about 200 Pa, which was the highest pressure the facility could withstand for in-situ observation, as shown in Fig. 1.

We baked the second sample (Labeled as LGO23) at the maximum temperature of 800 °C and used pure O₂ as oxidation gas at the same pressure, as presented in Fig. 2. In industrial production, the filtered air is pumped in when the cavities are about 70 °C to save waiting time. So, in the process of oxidization of this experiment, we raised the temperature from 25 °C to 70 °C to observe the difference. After exposing the second sample to air environment for 2 weeks, we re-baked it also at the maximum temperature of 800 °C but pumped in the pure H₂O vapor at the same pressure, as depicted in Fig. 3. We also carried out the time-of-flight secondary ion mass spectroscopy (TOF-SIMS) on the second sample before and after the oxidation experiments, and the relative concentration of C/O/H related impurities in depth are illustrated in Figs. 4, 5, and 6.

RESULTS

We focused on the Nb peaks during baking and oxidization during in-situ NAXPS experiments on both LGO22 and LGO23, and we compared the impurities of carbon, oxygen and hydrogen of LGO23 before and after the experiment. The results of the experiments and measurements are delivered as below.

* Work supported by National Natural Science Foundation of China National Key Programme for S&T Research and Development

[†] jkhao@pku.edu.cn

HIGHER ORDER MODE ANALYSIS OF A 915 MHz 2-CELL CAVITY FOR A PROTOTYPE INDUSTRIAL ACCELERATOR

A. Castilla*, G. Ciovati, J. Guo, G.-T. Park, R. Rimmer, J. Vennekate
Thomas Jefferson National Accelerator Facility, Newport News, VA, USA

Abstract

A possible solution to reduce the complexity posed by the cryogenic systems in a superconducting RF accelerator for industrial applications, is to capitalize on the advances achieved by the Nb₃Sn superconducting RF technology, as well as the feasibility of a reliable 4 K cooling system, based on commercial cryocoolers. Following this philosophy, the conceptual design for a prototype, conduction-cooled, 4 MeV, 20 kW SRF electron linac, is being developed at Jefferson Lab. Such design is based on a 915 MHz 2-cell Nb₃Sn cavity. In this contribution, we present the proposed cavity design, including the fundamental power coupler, and the preliminary analysis of the Higher Order Modes, using numerical simulations to estimate the potentially dangerous modes as a starting point to evaluate the requirements for damping for reliable operations with a cryocooler. Finally, different methods to calculate the Higher Order Modes' Impedances are briefly discussed.

INTRODUCTION

Recent advances in high-performance superconducting Nb₃Sn-coated superconducting radio-frequency cavities and commercial 4 K cryocoolers enabled the development of prototype SRF cavities operating at accelerating gradients up to ~12 MV/m, without the use of a liquid helium bath.

Such developments could facilitate transitioning the efficient SRF technology for use in industrial accelerators. One possible application is for environmental remediation such as the treatment of wastewater and flue gases, requiring an electron beam energy of ≤10 MeV but a high beam power, up to ~1 MW. The conceptual design for such type of accelerator, based on a 650 MHz 5-cell cavity, can be found in [1]. Jefferson Lab is developing the design for a similar type of accelerator [2], based on a 915 MHz 5-cell cavity. Low-cost, high efficiency, high-power magnetrons for industrial heating are commercially available at 915 MHz and using such devices as the accelerator's high-power RF source would lower both its capital and operating cost.

Most of the technical solutions related to the development of a compact, efficient, conduction-cooled SRF linac could be demonstrated in a demo accelerator, aiming at 4 MeV, 20 kW. Such an accelerator may represent a short path towards producing a working prototype that could attract the interest of potential users of the technology.

2-CELL CAVITY DESIGN

A 915 MHz 2-cell cavity has been designed to accelerate a 600 keV electron beam up to 4 MeV. The geometry of the 2-cell cavity is the same as that of the end-cells of the 5-cell cavity described in [3]. The cell length is 163.8 mm, the beam tube diameter is 110 mm, the diameter of the iris between the two cells is 90 mm and the equator diameter is 293.6 mm. To facilitate the interfacing of the demonstrator's module, a reduction in the beam pipe to 1.5 inches is proposed (similar to the CEBAF's C100 modules, see Fig. 1(a)). This modification increases the flange-to-flange length to approximately 1.5 m and results in a cutoff frequency of around 4.6 GHz for the TM₀₁₀ mode. This option can be revisited if it is deemed to introduce too many complications, an alternative could be to extend the 90 mm and place beam line absorbers (BLAs) in the warm section, prior to the beam pipe reduction. A fundamental power coupler (FPC) has been adapted from Oak Ridge's PPU design [4] to have a $Q_{\text{ext}} \approx 3.5 \times 10^6$ (see Fig. 1(b)). For a summary of the main parameters, refer to Table 1.

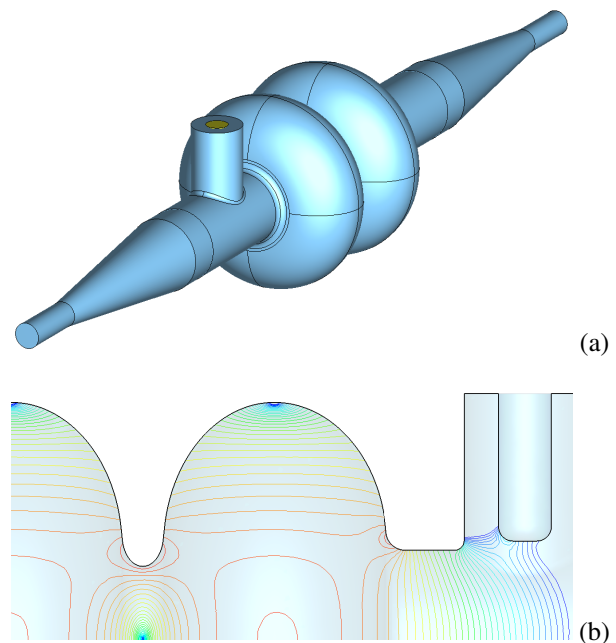


Figure 1: Schematic of the 2-cell cavity vacuum volume, including the FPC and beam-pipe tapers (a) and the equipotential lines of the operational mode including the FPC (b).

HOM CALCULATIONS

As part of the HOM analysis campaign, a comparison was conducted between two different methods of calculating HOM impedances using CST eigenmode solvers. The first

* acastill@jlab.org

GEOMETRY OPTIMIZATION FOR A QUADRUPOLE RESONATOR AT JEFFERSON LAB*

S. Bira, A-M. Valente-Feliciano, M. Ge

Thomas Jefferson National Accelerator Facility, Newport News, VA, USA

L. Vega Cid, W. Venturini Delsolaro, CERN, Geneva, Switzerland

Abstract

The quadrupole resonator (QPR) is a sample characterization tool to measure the RF properties of superconducting materials using the calorimetry method at different temperatures, magnetic fields, and frequencies. Such resonators are currently operating at CERN and HZB but suffer from Lorentz force detuning and modes overlapping, resulting in higher uncertainties in surface resistance measurement. Using the two CERN's QPR model iterations, the geometry was optimized via electromagnetic and mechanical simulations to eliminate these issues. The new QPR version was modeled for an increasing range of magnetic fields. The magnetic field is concentrated at the center of the sample to reduce the uncertainty in surface resistance measurements significantly. This paper discusses the QPR geometry optimization for the new version of QPR, which is now progressing toward fabrication.

INTRODUCTION

So far, almost all the superconducting accelerator cavities are generally made of bulk Niobium. High-performing Nb cavities have reached high accelerating gradients of ~50 MV/m on the beam axis, corresponding to a peak surface magnetic field of $B_c = 200$ mT, which is close to the fundamental limit of Niobium [1]. New materials such as Nb_3Sn , NbN , and MgB_2 that have higher critical temperatures and critical magnetic fields must be investigated to improve the performances of the accelerating cavities further. The deposition of elliptical cavities with these materials is often difficult and requires yet extensive development. Therefore, performing RF tests, specifically for the surface resistance measurement on flat samples, is essential. These tests must be realized with high-resolution surface resistance measurements in a large range of magnetic fields and operating temperatures. A quadrupole resonator is made to realize these measurements.

The schematic view of the resonator is shown in Fig. 1. It consists of four wire transmission lines related to a loop pair at the bottom end. All of these are fixed in the enclosed cylinder. The rod's top end is welded to the top of the cylinder. The length of the rods defines the fundamental frequency of the resonator. It is adjusted to $\lambda/2$ of the baseline operation frequency of 400 MHz. The sample is fixed at the bottom end of the cylinder, below the loops, where the

magnetic field is maximum. The sample is welded to a niobium cylinder from the measuring chamber of the quadrupole resonator [2, 3].

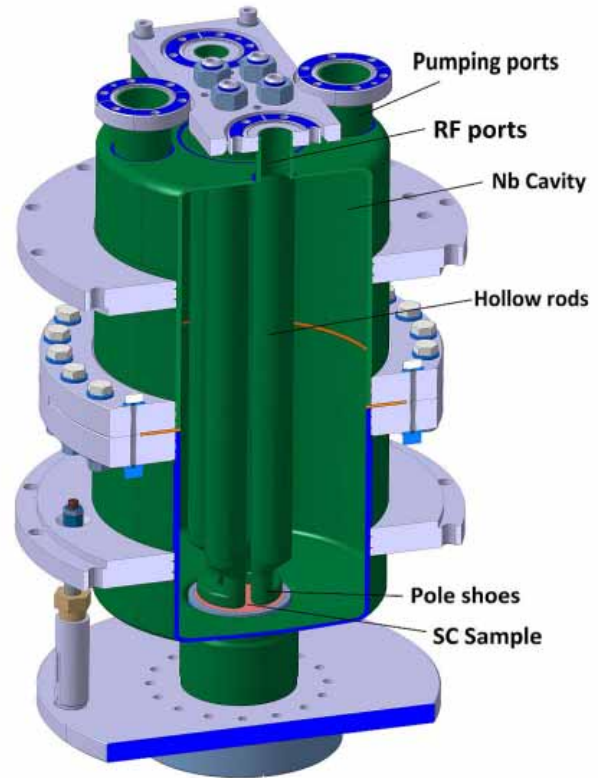


Figure 1: 3D view of the second quadrupole resonator at CERN [4].

The surface resistance is measured with a calorimetric compensation technique. Behind the sample, the heating element and thermocouples are fixed; the magnetic field is higher when heating at the center, and the thermocouples measure the temperatures (see Fig. 2). The measurement principle is straightforward; the sample is heated to a temperature of interest, $T_{interest}$. After the thermal equilibrium is established across the sample surface, RF power is applied, and the temperature of the sample increases. Decreasing the heating power to $T_{interest}$ allows us to determine the RF dissipated power on the sample. Assuming R_S is constant over the sample surface, it can be calculated with the following equation [5,6]:

$$R_S = \frac{2*(P_{DC1}-P_{DC2})}{\int_{sample} |H|^2 ds} \quad (1)$$

* work supported by the U.S. Department of Energy, Office of Science, Office of Nuclear Physics under contract DE-AC05-06OR23177 with Jefferson Science Associates.

† bira@jlab.org

MULTIPACTING IN C75 CAVITIES*

G. Ciovati[†], P. Dhakal, R. Rimmer, H. Wang, S. Wang, Jefferson Lab, Newport News, VA, USA

Abstract

Cavities for the C75 CEBAF cryomodule refurbishment program are currently being built, processed, tested and installed in the CEBAF accelerator at Jefferson Lab. They consist of 5-cell, 1497 MHz cavities with waveguide-type power coupler and for higher-order modes. Most of the cavities' RF tests in a vertical cryostat at 2.07 K were limited by strong multipacting at accelerating gradients in the range 18 – 23 MV/m. A softer multipacting barrier was sometimes encountered at 13 – 15 MV/m. An unusual feature of the multipacting was that the barrier often shifted to a lower gradient ~ 17 MV/m, after multiple quenches at ~ 20 MV/m. This phenomenon was reproduced in a single-cell cavity of the same shape. The cavity was tested after different amounts of mechanical tuning and different amounts of residual magnetic field, with no significant impact to the multipacting behavior. This contribution summarizes the experimental results from cavity RF tests, some of which were complemented by additional diagnostic instrumentation, such as oscillating superleak transducers, flux-gate magnetometers and temperature sensors. Results from 2D and 3D simulations are also presented, indicating favorable conditions for multipacting at the equator in the range 20 – 29 MV/m.

INTRODUCTION

One of the current cryomodule refurbishment programs at Jefferson Lab aims at replacing the lowest performing original cavities, installed in the CEBAF accelerator in the 1990s, with cells of a different shape with a target operational accelerating gradient, E_{acc} of 19.1 MV/m, with a quality factor $Q_0 \geq 8 \times 10^9$ at 2.07 K [1]. The 5-cell cavities are being fabricated by Research Instruments (RI), GmbH, Germany and 36 cavities have been fabricated since 2019. Eight 5-cell cavities are installed in each refurbished cryomodule which has a target energy gain of 75 MeV, hence the name "C75" to the cryomodule type. Two such cryomodules, C75-01 and -02, have been operating in CEBAF since June 2021 and the results are presented in Ref. [2].

The cell shape is the same as the one designed for a high-current free-electron laser [3, 4]. 2D multipacting (MP) simulations indicated that any MP barrier should occur at E_{acc} -values well above 20 MV/m [5]. Several single- and 5-cell prototype cavities were fabricated and tested as part of that project. No significant issues with MP was found, although two of the three 5-cell cavities were limited to $E_{acc} \sim 20$ MV/m [6–8].

The cavities' surface treatments are all done at Jefferson Lab and two options were pursued: the first option consisted of bulk removal (100 μ m) by electropolishing (EP) followed

by annealing at 800 °C for 3 h, followed by a final 30 μ m EP. The second option consisted of 60 μ m removal by centrifugal barrel polishing (CBP) and 40 μ m EP for bulk removal, 800 °C for 3 h, followed by a final 30 μ m EP.

The equator weld-prep for cells used for C75-01 cavities (with serial numbers 5C75-RI-001 to -008) was only 5.2 mm wide and resulted in sharp grain boundary steps intercepting the equatorial weld, which was a cause of concern for possible premature quenching due to local field enhancement. To eliminate such concern, the width of a cell's equator weld-prep was increased to 1.3 cm for all the remaining cavities.

The cryogenic RF tests of the cavities in a vertical dewar at Jefferson Lab showed that MP was the dominant limitation to the performance of the C75 cavities [9]. An unusual feature of the MP was that, after multiple MP-induced quenches, the barrier sometimes shifted to a lower gradient ~ 17 MV/m, and could not be rf processed quickly. The phenomenon could be reproduced by thermally cycling the cavity to ~ 20 K. It should be noted that two C75 cavities made of standard, high-purity, fine-grain Nb were also built by RI for Nb₃Sn coating studies and one achieved 23 MV/m while the other reached 28 MV/m [10].

Besides differences in the equator weld-prep geometries and surface preparation, we investigated the impact of changes in the cavity shape by mechanical tuning of a single-cell cavity. The following Sections described some of the experimental results and multipacting simulations.

EXPERIMENTAL RESULTS

Five-Cell Cavities

The results from the initial cryogenic RF test of cavity 5C75-RI-013 shown in Fig. 1 have been observed in many C75-type cavities: the cavity reached ~ 20.5 MV/m, then after several multipacting-induced breakdown events, the cavity broke-down at ~ 17 MV/m, with no improvement after ~ 30 min RF processing. The same behavior is reproduced after thermally cycling the cavity to ~ 20 K. Oscillating superleak transducers (OSTs) were mounted on the test stand to aid locating the breakdown location, which was found to be in the middle cell, ~ 5 cm away from the equator weld, for the barrier at ~ 17 MV/m. The cavity was processed by CBP.

The cavity was baked, while on the test stand, at 120 °C for 48 h and re-tested. The breakdown was now stable at ~ 20.5 MV/m and the location was at the equator of the middle cell. The test stand was equipped with a needle-valve and a high-purity He gas bottle and He processing for attempted to overcome the MP barrier. The maximum gradient increased by ~ 1.5 MV/m following He processing for ~ 1.5 h, as shown in Fig. 1. No radiation due to field-emitted electrons was detected on top of the test stand during any of the tests shown in Fig. 1

* This work was supported by Jefferson Science Associates, LLC under U.S. DOE Contract No. DE-AC05-06OR23177.

[†] gciovati@jlab.org

EXPLORING INNOVATIVE PATHWAY FOR SRF CAVITY FABRICATION

O. Hryhorenko^{*1}, C. Z. Antoine², T. Dohmae³, R. Valizadeh⁴, D. Longuevergne⁵

¹Thomas Jefferson National Accelerator Facility (JLAB), Newport News, VA, USA

²Université Paris-Saclay, CEA Département des Accélérateurs
de la Cryogénie et du Magnétisme (CEA-IRFU), Gif-sur-Yvette, France

³High Energy Accelerator Research Organization (KEK), Tsukuba, Japan

⁴Science and Technology Facilities Council (STFC/DL/ASTeC), Daresbury, Warrington, UK

⁵Université Paris-Saclay, CNRS/IN2P3, IJCLab, Orsay, France

Abstract

This article shows a study on an alternative pathway for the fabrication of a complete 1.3 GHz SRF cavity, aiming at improving production reliability, reducing the use of chemical polishing (EP or BCP) which is a costly and safety-critical step, and preserving surface quality after forming. Unlike the conventional pathway, the fabrication process is performed after polishing. This point is crucial as the used polishing technology could be applied only to flat geometries. The performed investigation demonstrates that damages during the fabrication process can be considered minor, localized, and limited to the near-surface. Moreover, these studies confirm that the damaged layer (100-200 μm) is mainly caused by the rolling process, and not by the subsequent fabrication steps. A laser confocal microscope and SEM-EBSD technique were used to compare samples before and after forming. The preliminary results are discussed and presented in this paper.

INTRODUCTION

Extensive chemical treatment for material removal around 100-200 μm is required after cavity fabrication to meet the needs of the SRF surface [1]. This step is focused on eliminating/reducing crystalline defects (high residual strain, dislocations, grain boundaries...), and impurities/contamination release from the surface [2]. Furthermore, as some cavities are almost reaching the physical limit of Niobium [3, 4], new superconductors are required to achieve higher performance levels [5, 6]. These superconductors are obtained in the form of thin films via different deposition techniques [5, 7], so surface roughness has gained even greater significance, as the film quality closely related to the substrate quality [8, 9]. This goal is one of the reasons to push the R&D efforts to explore alternative surface processing for preparing improved substrates [9-11], but not only. Moreover, the use of dangerous acids in conventional polishing methods poses risks for both personnel and environment. In order to overcome such safety concerns and potentially reduce the costs of surface processing, by using a more robust, eco-friendly, and reproducible technique, metallographic polishing (MP) is used as an alternative. This technique might find an application for large-scale facilities production (ILC, FCC), as this method can be easily industrialized, and create smoother

surfaces than conventional polishing, potentially improving the production yield, and preparing substrates for a thin-film deposition applicable not only to Nb, but to Cu also [12]. However, MP is performed only on flat geometries, so polishing has to be done before the cavity fabrication. Hence, the damages after fabrication have to be characterized and evaluated.

Recent studies by O. Hryhorenko et al. on Nb samples have highlighted that grain quality can be preserved after optimized deep-drawing and high residual strain regions are located only at the grain boundaries [13]. However, a systematic study that investigates the distribution and propagation of those damages into the bulk on the completed cavity has not yet been investigated.

In this article, we show the fabrication of a 1.3 GHz cavity using an alternative pathway (polishing before forming) and systematic studies of the internal surface quality to complete research.

NIOBIUM SURFACE PROCESSING

Metallographic Polishing

Mechanical polishing is a polishing technology, the principles of which are used in different fields [14, 15] to obtain a very smooth surface in a limited number of steps and time. However, additional requirements are necessary to consider for SRF applications, as the RF penetration into the bulk is of the order of 200 nm, where the material has to meet SRF requirements meaning a very low level of impurities and crystal damages. A specific 2 steps procedure was developed at IJCLAB and CEA-IRFU [12], to preserve the quality of the surface. Metallographic polishing (a subtype of mechanical polishing) was done on a standard lapping machine and performed at the company LAM PLAN (Gailard, France) [16]. For this project, large Nb disks with a diameter of 260 mm were used and were polished with 2 steps MP.

The following recipe is applied:

- Diamonds 9 μm on the New Lam M³M³ Green lapping disk (200 μm removal, approximately 2 hours).
- SiO₂ + H₂O₂ + a basic solution on the polyurethane cloth (2 hours cycle).

Figure 1 shows a final surface after the application of a 2 steps MP procedure. The resulting surface is considered

* hryhoren@jlab.org

DEVELOPMENT OF A PROTOTYPE 197 MHz CRAB CAVITY FOR THE ELECTRON-ION COLLIDER AT JLab

N. Huque, J. Henry, M. Marchlik, A. Castilla, E. Drachuk, E. F. Daly
Thomas Jefferson National Accelerator Facility, Newport News, VA, USA
S.U. De Silva, Old Dominion University, Norfolk, VA, USA
B. Xiao, Brookhaven National Laboratory, Upton, NY, USA

Abstract

Thomas Jefferson National Accelerator Facility (JLab) is currently developing a prototype 197 MHz Radio-Frequency Dipole (RFD) crab cavity as part of the Electron-Ion Collider (EIC) to be built at Brookhaven National Laboratory (BNL). Cryomodules containing these cavities will be part of the Hadron Storage Ring (HSR) of the EIC. The prototype cavity is constructed primarily of formed niobium sheets of thickness 4.17 mm, with machined niobium parts used as interfaces where tight tolerancing is required. The cavity's large size and complex features present several challenges in fabrication, tuning, and RF testing. Structural and forming analyses have been carried out to optimize the design and fabrication processes. An overview of the design phase and the current state of fabrication are presented in this paper.

INTRODUCTION

The EIC will be built at BNL and will be the newest accelerator under the US Department of Energy's Nuclear Physics program. The construction will be split between several US national labs, with the bulk of the scope under JLab and BNL; JLab's scope includes the design and fabrication of the superconducting Radio-Frequency (RF) systems for the collider.

Collisions between ions and electrons will occur in the Interaction Regions (IR) between the Hadron Storage Ring (HSR) and the Electron Storage Ring (ESR). The luminosity requirements ($10^{34} \text{ cm}^{-2}\text{s}^{-1}$) require that crabbing systems be used in the interaction region [1]. The RF-dipole design was chosen for the crab cavities in these regions. The HSR will have cryomodules containing 197 MHz crab cavities and second-harmonic 394 MHz cavities to linearize the kicks [2]. The shorter bunch lengths in the ESR mean that only 394 MHz cavities will be sufficient.

Eight 197 MHz cavities will be installed in four cryomodules in the HSR. Table 1 shows the deflecting voltage requirements for the HSR and ESR. As the 197 MHz crab cavity system is considered one of the critical components in the RF systems scope, a prototype will be fabricated at JLab.

Table 1: Crabbing Systems of EIC [1]

System	V_t [MV]		No. of cavities	
	HSR	ESR	HSR	ESR
197 MHz	33.83	–	8	–
394 MHz	4.75	2.90	4	2

RF DESIGN

The RF performance requirements for the cavity are listed below [3]:

- Nominal transverse voltage per cavity = 8.5 MV
- Maximum transverse voltage per cavity = 11.5 MV
- Peak fields at 11.5 MV: $E_p < 45 \text{ MV/m}$ and $B_p < 80 \text{ mT}$

Figure 1 shows the distribution of the surface electric and magnetic fields. Figure 2 shows the baseline crab cavity design, showing coaxial Higher-Order Mode (HOM) dampers.

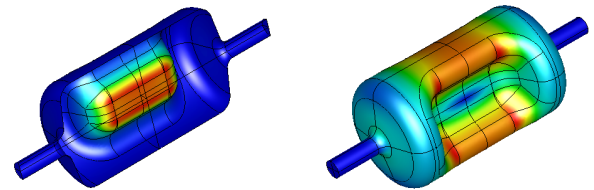


Figure 1: 197 MHz RFD cavity surface electric fields (left) and surface magnetic fields (right) [1]. The color scale from blue to red represents low to high amplitude, respectively.

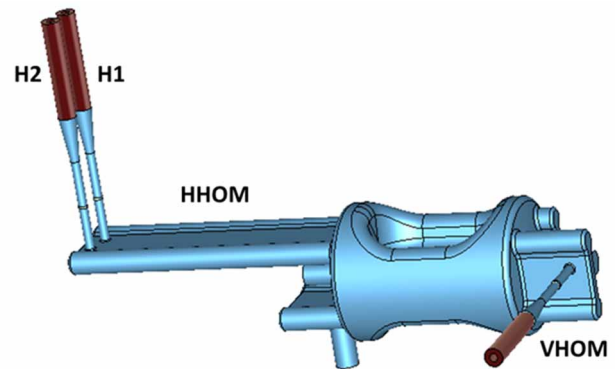


Figure 2: Coaxial HOM dampers and waveguides on the baseline 197 MHz cavity design [2].

In addition to the RF requirements, the already-built accelerator tunnel and other existing systems impart physical constraints on the cavities and cryomodules [3]:

- Beampipe aperture: 100 mm
- Cavity length (flange-to-flange): $< 1.5 \text{ m}$
- Cryomodule Length: $< 12.5 \text{ m}$

The waveguides for the horizontal and vertical HOM dampers have a novel 'dogbone' shape. The waveguides on

TEMPERATURE, RF FIELD, AND FREQUENCY DEPENDENCE PERFORMANCE EVALUATION OF SUPERCONDUCTING NIOBIUM HALF-WAVE COAXIAL CAVITY*

N. K. Raut^{1,†}, B. D. Khanal², J. K. Tiskumara², S. De Silva², P. Dhakal¹, G. Ciovati^{1,2}, J. R. Delayen^{1,2}

¹ Jefferson Lab, Newport News, VA, USA

² Center for Accelerator Science and Dept. of Physics, Old Dominion University, Norfolk, VA, USA

Abstract

Recent advancement in superconducting radio frequency cavity processing techniques, with diffusion of impurities within the RF penetration depth, resulted in high quality factor with increase in quality factor with increasing accelerating gradient. The increase in quality factor is the result of a decrease in the surface resistance as a result of nonmagnetic impurities doping and change in electronic density of states. The fundamental understanding of the dependence of surface resistance on frequency and surface preparation is still an active area of research. Here, we present the result of RF measurements of the TEM modes in a coaxial half-wave niobium cavity resonating at frequencies between 0.3 – 1.3 GHz. The temperature dependence of the surface resistance was measured between 4.2 K and 1.6 K. The field dependence of the surface resistance was measured at 2.0 K. The baseline measurements were made after standard surface preparation by buffered chemical polishing.

INTRODUCTION

Superconducting radio-frequency (SRF) cavities are the building blocks of modern particle accelerators that can store and transfer electromagnetic energy with very little dissipation [1]. High-quality factor in SRF cavities is not only limited to particle accelerators but also emerging as an application to quantum computing and quantum information science [2–4].

The performance of SRF cavities is measured in terms of the quality factor (Q_0) which is inversely proportional to the surface resistance (R_s) as a function of accelerating gradient (E_{acc}). Surface engineering with nonmagnetic impurity doping (Ti, N, O) has been shown to reduce surface resistance and improve the quality factor [5–7]. Nevertheless, the fundamental understanding of the dependence of surface resistance on frequency, surface preparations, and RF field is still an active area of research [8]. In this contribution, we have measured the frequency, temperature, and RF field dependence of surface resistance using a half-wave coaxial cavity. The benefit of using the same cavity for different modes will eliminate the variability that comes when using different cavities, although the same treatment is applied.

* Work supported by the U.S. Department of Energy, Office of Science, Office of Nuclear Physics under contract DE-AC05-06OR23177.

† raut@jlab.org

CAVITY DESIGN AND SURFACE PREPARATION

The quality factor is defined as the ratio of energy stored (U) to the energy dissipation (P_d) per rf cycle as:

$$Q_0 = \frac{\omega U}{P_d} = \frac{2\pi f \mu_0 \iiint_V |H|^2 dV}{R_s \iint_S |H|^2 dS} = \frac{G}{R_s}, \quad (1)$$

where,

$$G = \frac{2\pi f_0 \mu_0 \iiint_V |H|^2 dV}{\iint_S |H|^2 dS} \quad (2)$$

is geometric factor of the cavity and depends on the shape. Here, f_0 , μ_0 , and $|H|$ represent the frequency, vacuum permeability, and peak RF magnetic field. R_s represents the surface resistance of the cavity which is expressed as the sum of temperature independent R_i and temperature dependent R_{BCS} . The R_i arise due to several intrinsic and extrinsic factors and R_{BCS} is the result of RF dissipation by unpaired quasi-particles in superconductors and is explained by BCS theory of superconductivity [9]. A simplified expression for R_{BCS} valid in the dirty limit and $T \ll T_c$ is [10]:

$$R_{BCS}(T) \approx \frac{A}{T} f^2 e^{-\frac{\Delta}{k_B T_c} \frac{T_c}{T}} \quad (3)$$

where A depends on the material properties like penetration depth, coherence length, Fermi velocity, etc. Δ is the energy gap at 0 K, k_B is Boltzmann constant, and T_c is the transition temperature.

Accelerating elliptical cavities are excited in TM_{010} mode where the electric field is concentrated along the cavity axis with peak magnetic field on the surface of the cavity. The fundamental and higher-order transverse electromagnetic wave (TEM) modes of the half-wave coaxial cavity have a strong field on the center conductor that decays exponentially towards the outer conductor [11–13]. Such identical field distribution of the TEM modes on the center conductor makes it an ideal platform to study the frequency dependence of the surface resistance at different temperature, RF field and for different surface treatments [14].

The length of the half-wave coaxial cavity used in this experiment is $l = 457.55$ mm, which determines the fundamental mode frequency (f) by the relation $f = \frac{c}{2l}$. The TEM modes are sufficiently separated by other TM and TE modes. Our modes of interest are fundamental and three higher harmonics of the cavity. Figure 1 shows the E and B profile of the first four TEM modes. The CST Studio Suite

SIMULATION OF THE DYNAMICS OF GAS MIXTURES DURING PLASMA PROCESSING IN THE C75 CAVITY*

N. K. Raut[†], T. Ganey, P. Dhakal, T. Powers

Thomas Jefferson National Laboratory, Newport News, VA, USA

Abstract

Plasma processing using a mixture of noble gas and oxygen is a technique that is currently being used to reduce field emission and multipacting in accelerating cavities. Plasma is created inside the cavity when the gas mixture is exposed to an electromagnetic field that is generated by applying RF power through the fundamental power or higher-order mode couplers. Oxygen ions and atomic oxygen are created in the plasma which breaks down the hydrocarbons on the surface of the cavity and the residuals from this process are removed as part of the process gas flow. Removal of hydrocarbons from the surface increases the work function and reduces the secondary emission coefficient. This work describes the initial results of plasma simulation, which provides insight into the ignition process, distribution of different species, and interactions of free oxygen and oxygen ions with the cavity surfaces. The simulations have been done with an Ar/O₂ plasma using COMSOL® multiphysics. These simulations help in understanding the dynamics and control of plasma inside the cavity and the exploration of different gas mixtures.

INTRODUCTION

Field emission in superconducting radio-frequency (SRF) cavities leads to thermal instability and is one of the prime factors in limiting the performance of accelerating cavities [1]. Hydrocarbons (C_xH_y) build-up on the surface of the cavity enhance multipactors and field emission [2]. Particulate contamination is the major cause of field emission. Plasma helps to break down organic bonds (C=C, C-C, C-O, C-H) from the contamination [3] and increases the work function (ϕ) and secondary emission yield ($<SEY>$) of the niobium [4]. Recently, promising improvement on the onset of field emission and increase in usable accelerating gradient on SRF cavities [2, 5, 6].

In the plasma processing of the cavity, the reactive ions and species such as O⁻, O⁺, O, O₂⁺ play an essential role to crack the hydrocarbons from the surface of the cavity forming residual byproducts such as CO, H₂O, CO₂, and etc. In the experimental settings, it is challenging to get the information about plasma and other species' growth in a fraction of a second as well as the interaction between the species with the cavity's surface. Furthermore, the generation of plasma with the optimum proportion of the gases mixture (n% of

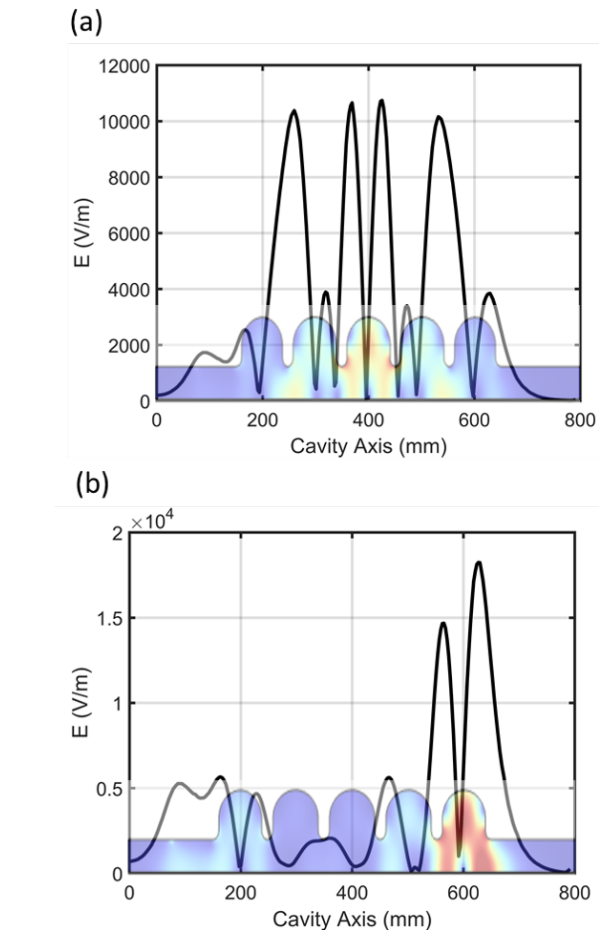


Figure 1: Electric field profile of two TE211 modes of interest on the axis of the C75 cavity, (a) 2656 MHz and (b) 2724 MHz.

inert gas & (100-n)% of oxygen) requires careful control of the gas mixture and plasma dynamics. Experimentally, optical camera attached on cavity opening is used to observe the plasma ignition and its evolution. Simulation of plasma ignition, dynamics with respect to the partial pressure of gas and rf power could be a useful tool to design the experimental setup in complex cryomodules where visual observations are not available.

COMPUTATIONAL MODEL

In this study, we have chosen two quadrupole mode resonating at 2656 MHz and 2724 MHz of the C75 cavity [7] to ignite plasma on the center and end cells of the cavity. COMSOL Multiphysics [8] has been implemented to study the interaction between the cavity's modes and the gaseous mix-

* This work is supported by SC Nuclear Physics Program through DOE SC Lab funding announcement Lab-20-2310 and by the U.S. Department of Energy, Office of Science, Office of Nuclear Physics under contract DE-AC05-06OR23177.

[†] raut@jlab.org

IN SITU PLASMA PROCESSING OF SUPERCONDUCTING CAVITIES AT JLab, 2023 UPDATE*

T. Powers[†], N. Brock, T. Ganey

Thomas Jefferson National Accelerator Facility, Newport News, VA, USA

Abstract

Jefferson Lab has an ongoing R&D program in plasma processing which just completed a round of production processing in the CEBAF accelerator. Plasma processing is a common technique for removing hydrocarbons from surfaces, which increases the work function and reduces the secondary emission coefficient. The initial focus of the effort was processing C100 cavities by injecting RF power into the higher order mode (HOM) coupler ports. Results from processing cryomodules in the CEBAF accelerator as well as vertical test results will be presented. The goal of in-situ processing is to improve the operational gradients and the energy margin of the linacs. This work will describe the systems and methods used at JLab for processing cavities using an argon-oxygen gas mixture as well as a helium-oxygen gas mixture. Before and after plasma processing results will also be presented.

METHODS

Plasma processing is being explored by a number of facilities that work with superconducting cavities [1]. Between 2015 and 2018 it was used to process 32 cavities in the SNS accelerator at ORNL where they achieved an average improvement in operational gradients of 2.5 MV/m [2, 3]. Unlike helium processing which relies on ion bombardment of the field emitters, plasma processing uses atomic oxygen produced in an RF plasma to break down the hydrocarbons on the surface of the cavity. Processing of SRF cavities is done using a mixture noble gas such as argon, neon or helium and oxygen. The discharge is operated at pressures between 50 and 300 mTorr. The current gas mixture used at Jefferson lab is 94% helium and 6% oxygen at 300 mTorr.

Gas Supply and Vacuum Systems

Process gas was supplied by a mobile cart that had a cylinder of 99.999% helium or argon and a cylinder of 20% oxygen with the remainder of the gas being helium or argon depending on the gas that was being used. The gas cart used in the vertical test area also has a cylinder of 95% argon and 5% methane which is used to “contaminate” a cavity with hydrocarbons so that we could experiment with different processing techniques. Using a series of valves and flow controllers we were able vary the percentage of oxygen in the process gas as well as to regulate the flow and pressure in the cavities. The pumping system consisted of two turbo molecular pumps, a 300 L/s primary pump and a 70 L/s secondary pump. The 70 L/s pump was used as part

of a differentially pumped RGA system. In addition to monitoring the argon to oxygen ratio, the RGA is used to monitor H₂, CO, CO₂ and H₂O, which are hydrocarbon fragments that are produced when the free oxygen interacts with the hydrocarbons.

RF System

Each channel of the RF system, which is described in [4], is capable of processing up to 2 cells in a cavity simultaneously. Four channels of RF system were prepared for use in the CEBAF tunnel. They were set up in pairs each of which shared a 4-port network analyzer and process control computer. The output of two RF sources and network analyzer are combined and applied to the input of a 100 W amplifier. The output of the amplifier is applied to the cavity via one of the HOM coupler antennas. The system monitors the incident and reflected power and the power that is emitted from the fundamental power coupler. The latter is effectively acting as a field probe for the electric field in the cell furthest away from the HOM couplers. Control over which cell or combination of cells is processed is accomplished by selecting one of the TE₁₁₁ modes that provided a peak electromagnetic field in the desired cells. Early on we determined through simulation and confirmed with bead pull measurements that there were two modes that were strongly tilted towards cells 1 and 7, where cell 1 is closest to the HOM couplers. There was a mode that had peak fields in cell 4 and two other modes that had peak fields symmetrically in cells 2/6 and 3/5 [5]. Using these 5 modes we were able to predictably establish a plasma in each of the cells by starting furthest away from the HOM couplers then turning on the second source. For example, if we started with cell 7 on and turned on the frequency for cells 2/6 we would establish a plasma in cells 6 and 7. When we turned off the mode for cell 7 the plasma remained in cell 6. The modes and methods are described more fully in Ref. [4, 5]. Figure 1(a) shows an image of an argon/oxygen plasma in each of the 7 cells of a cavity in a C100 cryomodule. Figure 1(b) shows an image of a helium/oxygen plasma in cells 7, 5 and 6, 4 and 3 as well as 2 and 1. The blue shift in the colors in the cell 7 mode is due to a reduction in oxygen content in the process gas coupled with an increase in the hydrocarbon residues.

C100 Cryomodule Issues

One of the issues with processing a C100 cryomodule is that both of the HOM coupler antennas are located on the same end of the cavity. Because of the geometry there is a relatively strong coupling between the antennas in the HOM frequency bands that provide a uniform plasma. Because of this strong coupling, RF power that is applied to one HOM coupler is picked up by the second coupler,

* Funding provided by SC Nuclear Physics Program through DOE SC Lab funding announcement DE-FOA-0002670

[†] powers@jlab.org

FIRST EXPERIENCE WITH LIQUID NITROGEN CLEANING

R. Ruber*, R. L. Geng, A. Eslinger, Jefferson Lab, Newport News, VA, USA

Abstract

Field emission caused by microscopic particulate contamination is a limiting factor for the performance of superconducting RF (SRF) cavities. In an SRF based accelerator, particulates may be transported over the surface of an operational SRF cavity, becoming field emitters and consequentially degrading the performance of the SRF cavity. The most commonly used method for removing particulates from cavity surfaces is high-pressure ultra-pure water rinsing. We are developing a novel high-pressure liquid nitrogen cleaning technique that may possibly enable superior cleaning power and particulate removal from cavities in a cryomodule without taking apart the cryomodule components. This technique provides cleaning mechanisms beyond what are accessible by its high-pressure water rinsing counterpart and leaves no residues on the cleaned surface.

INTRODUCTION

Performance degradation of SRF cavities due to field emission has become one of the major limiting factors in SRF accelerator technology. Field emission is observed to increase after assembling SRF cavities with auxiliary equipment and subsequent assembly in multiple cavity strings that are inserted in cryomodules and installed in accelerators. Additional performance degradation has also been observed during long-term operation in the CEBAF accelerator which has warm-to-cold transitions between each and every 8-cavity cryomodule. Observed performance degradation by increased field emission has been linked to surface pollution by particulates and hydrocarbons. Sources of surface pollution have been identified as both material defects and contaminants introduced during processing and assembly. These observations and associated studies have been richly published in conference proceedings and scientific journals

While some surface pollution is assumed to be introduced during initial fabrication, others are introduced during assembly, operation or maintenance. Combinations of cleaning processes are used to mitigate field emission. These are however not always successful and the established procedures are often impossible to apply after a cavity has been assembled into a cryomodule. No well defined final cleaning method does yet exist. Several specific cleaning processes have been developed or proposed over the years to help in this effort such as high-pressure ultra-pure water rinsing, helium processing, plasma processing, and dry-ice cleaning. We started a new effort based on the idea of liquid nitrogen jet cleaning.

* ruber@jlab.org

LIQUID NITROGEN CLEANING

The liquid nitrogen jet was developed as a technique for cutting materials [1] and industrial cleaning services [2]. The technique presented here was proposed for cleaning CEBAF cryomodules by removal of microscopic particulates [3]. In this process, filtered liquid nitrogen flows through a booster pump to increase the pressure and is then supplied to a lance inside the cavity. The liquid nitrogen exits through a small nozzle at the end of the lance, producing a high pressure liquid nitrogen jet as shown in Fig. 1.

The liquid nitrogen cleaning technique shares ideas and essence with both high pressure rinsing with ultra-pure water [4, 5] and dry-ice cleaning [6-9]. Both methods have shown to eliminate field emission or at least to increase the electric gradient at field emission onset. Liquid nitrogen cleaning combines the high velocity jet from high pressure water rinsing with the thermal impact of dry-ice cleaning. The liquid nitrogen jet is supposed to remove particulates from the cavity surface by multiple actions such as aerodynamic drag, impact, and thermal shock. As with dry-ice cleaning, the liquid nitrogen jet should not leave a residue when drying. An important aspect for future in-situ cleaning of cryomodules.

A moving fluid creates an aerodynamic drag on a particulate of which the force is proportional to the cross sectional area of the particulate. However, the fluid velocity becomes zero at the cavity surface area, resulting in a decreased aerodynamic force for tiny particulates stuck to the surface. Therefore the drag force on small micron-sized particulate can be less than the surface adhesion force. The typical cross-over point is suggested to be for particulates between 0.5 and 1.0 μm in diameter [7]. The evaporation of the liquid nitrogen fluid when touching the warm cavity

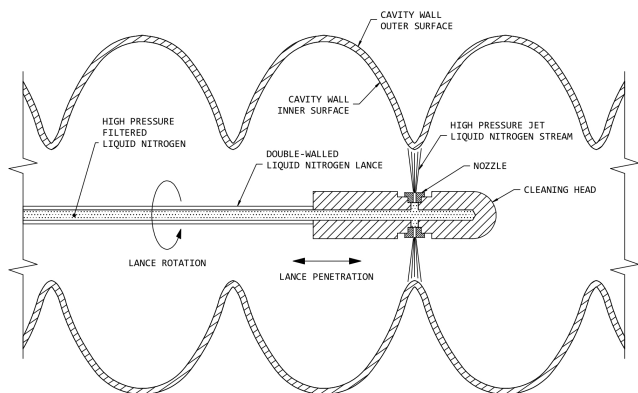


Figure 1: Concept of a high pressure liquid nitrogen jet stream cleaning a cavity surface [3].

REFURBISHMENT OF AN ELBE-TYPE CRYOMODULE FOR COATED HOM-ANTENNA TESTS FOR MESA*

P. S. Plattner[†], F. Hug, T. Stengler
Institut für Kernphysik der JGU Mainz, Mainz, Germany

Abstract

The Mainz Energy-Recovering Superconducting Accelerator (MESA), an energy-recovering (ER) LINAC, is currently under construction at the university Mainz. In the ER mode a continuous wave (CW) beam is accelerated from 5 MeV up to 105 MeV with a beam current of up to 1 mA. This current is accelerated and decelerated twice within a cavity. For future experiments, the beam current limit has to be pushed up to 10 mA. An analysis of the MESA cavities has shown that the HOM antennas quench at such high beam currents due to the extensive power deposition and the resulting heating of the HOM coupler. To avoid quenching it is necessary to use superconducting materials with higher critical temperature. For this purpose, the HOM antennas will be coated with NbTiN and Nb₃Sn and their properties will be investigated. For use in the accelerator, the HOM antennas will be installed in the cavities of a former ALICE cryomodule, kindly provided by STFC Daresbury. This paper will show both the status of the refurbishment of the ALICE module to suit MESA, and the coating of the HOM antennas.

INTRODUCTION

Research on the adequate damping of Higher Order Modes (HOMs) in superconducting radio-frequency (SRF) cavities is a fundamental aspect of advancing Energy Recovery Linacs (ERLs) in terms of beam currents and energy capabilities. To address these obstacles in the MESA project, the MESA Enhanced ELBE-type Cryomodules (MEEC) was developed [1]. The MEEC was designed that the two 9-cell TESLA cavities have a field gradient of 12.5 MV m⁻¹ at a $Q_0 = 1.25 \times 10^{11}$. To achieve the requirements the commercial available ELBE/Rossendorf-type cryomodules (CM) needed to be modified in three major parts: the tuner, HOM feedthrough and Helium supply. MESA is designed for 1 mA cw current in the beginning. But based on calculations considering MESA stage 2 beam currents as high as 10 mA, it has been determined that the power levels in the MEEC's HOM dampers will exceed their designed limits [2]. To address this issue, a cryomodule from the decommissioned ALICE ERL¹ [3] is currently undergoing refurbishment in Mainz. Once the cavities have been refurbished, they will be utilized to conduct tests on coated HOM antennas, aiming to enhance the cavities' performance under high beam currents. Table 1 presents

a comparison of the key parameters between the MESA and ALICE systems. Since both accelerators operate at the identical frequency, the goal of the refurbishment is first to achieve quality factor which are acceptable for MESA. The reassembled and modified ALICE cryomodule can be used as a platform for SRF-research and spare cryomodule for MESA.

Table 1: Comparison of the Key Parameters of ALICE and MESA

Parameter	MESA	ALICE
Q_0	1.25×10^{10}	5×10^9
Field gradient	12.5 MV m ⁻¹	12.9 MV m ⁻¹
Beam current (ERL)	1(10) mA	13 μ A
RF Frequency	1.3 GHz	1.3 GHz
Cavities	9-cell	9-cell
	XFEL/TESLA	XFEL/TESLA

MAINZ ENERGY-RECOVERING SUPERCONDUCTING ACCELERATOR

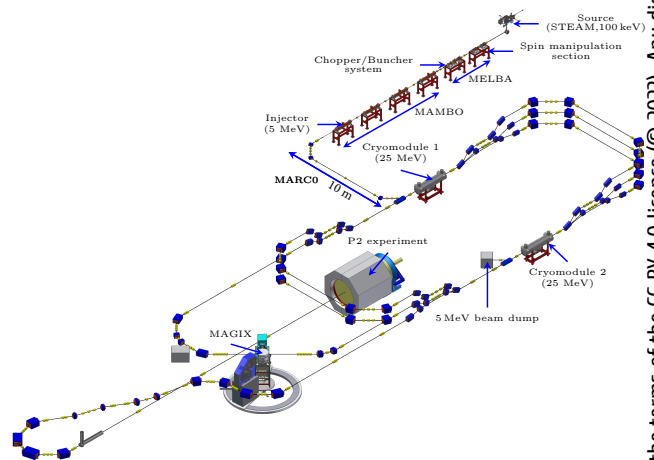


Figure 1: The MESA lattice.

In Fig. 1 is shown the lattice of MESA [4], which has an normal conduction pre-accelerator and a superconducting main accelerator. MESA is a continuous wave multiturn LINAC, which operates at a frequency of 1.3 GHz and can be operated in the Energy Recovering (ER)-mode or in the External Beam (EB) mode. For MESA are planned two electron sources: A Small Thermalised Electron Source at Mainz (STEAM) [5], which provides polarised electrons at a beam current of 150 μ A up to 1 mA and the

* The work received funding by BMBF through 05H21UMRB1.

[†] pplattne@uni-mainz.de

¹ The authors acknowledge the transfer of one cryomodule to Mainz by the STFC Daresbury.

CONTRIBUTION OF IN2P3 TO PIP-II PROJECT: PLANS AND PROGRESS*

D. Longuevergne, N. Bippus, P. Duchesne, N. Gandolfo, D. Le Dréan, G. Mavilla, T. Pépin-Donat, L. M. Vogt, S. Roset, S. Wallon, Université Paris-Saclay, CNRS/IN2P3, IJCLab, Orsay, France
P. Berrutti, S. Kazakov, J. Helsper, M. Parise, D. Passarelli, N. Solyak, A. I. Sukhanov
Fermi National Accelerator Laboratory (Fermilab), Batavia, IL, USA

Abstract

IJCLab is one of the labs of IN2P3 (National institute of nuclear and particle physics), one of the ten research institutes composing the French National Center for Scientific Research (CNRS). Since 2018, IJCLab has been involved in the PIP-II project, assisting with the design, development, and qualification of accelerator components for the SSR2 (Single Spoke Resonator type 2) section of the superconducting linac. The first pre-production components (cavity, coupler, and tuner) have been fabricated, and some of the first qualification tests have been performed at IJCLab. This paper will summarize the complete scope of IJCLab contributions to PIP-II and give updates on the performances of the first pre-production components.

INTRODUCTION

The Proton Improvement Plan-II (PIP-II) encompasses a set of upgrades and improvements to the Fermilab accelerator complex. In particular, PIP-II project is aiming at constructing a new superconducting linac for which Fermilab benefits from a strong commitment as in-kind contributions of international partners among which France is involved through CEA and CNRS/IN2P3 agencies. Since 2018, year of signature of a SoI (Statement of Interest), IJCLab [1, 2] is the only laboratory of CNRS/IN2P3 French research institute to be involved in this contribution. The scope of technical contribution and project schedule are captured in the Project Planning Document Part2 (Non legally binding document) that will be signed in a near future by IN2P3 institute and DOE.

A complete set of deliverables and associated milestones have been mutually built and agreed aiming at monitoring the progress during the project. Both International Milestones (linked to partner activities) and PIP-II project internal milestones (linked to PIP-II project activities) have been defined. These milestones are on both sides tracked and updated on a regular basis (monthly reporting) allowing each party to evaluate efficiently the impact of any delay on their own schedule and risk register. The definition of the complete list of milestones allowed the definition of early and late delivery dates for each deliverables. The early delivery dates are defined by partners whereas late delivery dates by PIP-II Project. This ensures partner schedule to be encapsulated in PIP-II Project schedule with defined margins. This proceeding aims at describing the In-

Kind contribution of CNRS/IN2P3 to PIP-II project and share the progress up to date.

TECHNICAL CONTRIBUTION

The technical contribution of CNRS/IN2P3 is limited to the second Spoke section (SSR2 cryomodules) of the superconducting linac [3] but covers from the preliminary design phase up to delivery phase of production components. The contribution focuses on the three main components composing the so-called SSR2 dressed cavity meaning the cavity, tuner and power coupler.

Preliminary Design Phase

This phase is completed since 2019 when Final Design Reviews (FDR) of the pre-production cavity, tuner and power coupler have been closed.

CNRS/IN2P3 involvement in this phase was limited as most of design work was already well advanced in 2018 for most of components. Based on IJCLab experience on the design, fabrication and integration of Spoke cryomodules for ESS project [4], several inputs in term of lessons learned served to consolidate the initial design performed at Fermilab.

- For SSR2 cavity, RF design [5] was fully accomplished by Fermilab but mechanical design was jointly achieved [6] benefitting from lessons learned from both SSR1 and ESS experiences.
- For SSR2 tuner, the system was fully designed already by Fermilab for the first Spoke section (SSR1) [7]. SSR2 mechanical design was limited to interface adaptation so as to optimize the number of standardized parts.
- For SSR2 power coupler, support has been provided to Fermilab team to optimize SSR1 coupler design and make it compatible with SSR2 requirements. This support consisted in performing thermal simulations and providing inputs based on IJCLab experience for XFEL [8].

Final Design Phase and Pre-production

This phase has started at the successful completion of the preliminary design phase and will end with the successful completion and close-out production SSR2 dressed cavities FDR. This phase is including the fabrication of pre-production components and the full experimental validation of one dressed cavity in horizontal cryostat at Fermilab.

* Work supported by IN2P3. Work supported, in part, by the U.S. Department of Energy, Office of Science, Office of High Energy Physics, under U.S. DOE Contract No. DE-AC02-07CH11359.

PRE-INSTALLATION PERFORMANCE OF THE RHIC 56 MHz SUPERCONDUCTING SYSTEM*

Z. A. Conway[#], R. C. Anderson, J. C. Brutus, K. M. Hernandez, D. S. Holmes, K. J. Mernick, G. Narayan, S. Polizzo, S. K. Seberg, F. F. Severino, M. P. Sowinski, R. Than, Q. Wu, B. Xiao, W. Xu, A. Zaltsman, Brookhaven National Laboratory, Upton, NY, USA

Abstract

Pre-installation test results for the RHIC 56 MHz superconducting RF system are presented here. The 56 MHz quarter-wave resonator achieved a stable accelerating potential of 1.1 MV with 13 W of RF loss at 4.5 K demonstrating its viability for increasing the luminosity of sPHENIX collisions. The new 120 kW travelling wave fundamental mode damper and dual 6 kW combined-function fundamental power couplers perform as expected at 3 kW but remain to be operated with the expected ~40 times greater power achievable with the RHIC sPHENIX beams.

INTRODUCTION

The 56 MHz superconducting quarter-wave resonator (QWR) cryomodule first demonstrated during the 2016 RHIC run RHIC [1, 2] has undergone upgrades to the fundamental power coupling and fundamental mode damping systems. These upgrades are needed for higher intensity RHIC beams. These systems were identified for upgrade to meet future sPHENIX experimental program requirements and ease manipulation of the cavity fields during operations [2, 3]. This paper will review relevant aspects of the cryomodule assembly, and several measurements related to coupler performance prior to installation in RHIC.

As of this writing the 56 MHz superconducting quarter-wave cryomodule is installed in RHIC where it is fully damped. Work is ongoing to make the system ready and it is expected to start operations later this year.

CRYOMODULE RESULTS

Assembly

The 56 MHz QWR design was undertaken to provide 2-2.5 MV [4]. This was accomplished with an advanced design using a bellows-like outer conductor to prevent multipacting with straight cylinder inner and outer conductors [1].

The cryomodule assembly incorporated one unique aspect not typically employed for SRF cryomodules, horizontal HPR of components on the assembly tooling. The beam-line cold mass is comprised of 3 distinct assemblies: 2 end groups each weighing more than 300 pounds and the ~1,000 pound SRF resonator located in between. These 3 assemblies are joined in the clean room

after alignment on the tooling and are very cumbersome to handle. While each of these components was high pressure rinsed with the rinse wand located beneath the device the 2 end-groups were also HPRed horizontally. Figure 1 shows a picture taken during this assembly. Due to the frequent “dirty” work ongoing around the end groups after the initial HPR and during alignment this extra HPR step was found to be necessary. After horizontal HPR water pooled inside the all metal RF gate valves and beam-line formed bellows which were subsequently dried with external radiant heaters.

Following clean assembly and leak check, no leaks found above a background of 1×10^{-11} mbar-l/s helium. The hermetic beam-line assembly was baked at 120 °C for 48 hours. The clean and baked assembly was then built into its cryomodule as was done in 2015. Minor changes were made to the system to improve cryogenic stability and will be discussed in a later paper.



Figure 1: 56 MHz quarter-wave resonator cryomodule immediately before final clean assembly in the BNL class 10 clean room.

Table 1: 56 MHz QWR RF Parameters

Parameter	Value
Frequency	56.3 MHz
Beam Aperture	3.937 in
β	1
Effective Length ($\beta\lambda/2$)	2.7 m
$E_{\text{peak}}/E_{\text{acc}}$	56
$B_{\text{peak}}/E_{\text{acc}}$	121 mT/(MV/m)
$G = R_s Q$	20.2 Ω
R_{sh}/Q	80.5 Ω

* Work supported by Brookhaven Science Associates, LLC under contract No. DE-SC0012704 with the U.S. Department of Energy.

[†] zconway@bnl.gov

FINAL DESIGN OF THE LB650 CRYOMODULE FOR THE PIP-II LINEAR ACCELERATOR

R. Cubizolles[†], N. Bazin, S. Berry, J. Drant, A. Moreau, A. Raut, P. Garin,
S. Ladegaillerie, C. Simon, Université Paris-Saclay, CEA, Université Paris-Saclay, CEA,
Département des Accélérateurs, de la Cryogénie et du Magnétisme, Gif-sur-Yvette, France
O. Napoly, V. Roger, S. Chandrasekaran, Fermilab, Batavia, IL, USA

Abstract

The Proton Improvement Plan II (PIP-II) that will be installed at Fermilab is the first U.S. accelerator project that will have significant contributions from international partners. CEA joined the international collaboration in 2018, and its scope covers the supply of the 650 MHz low-beta cryomodule section, with the design of the cryostat (i.e. the cryomodule without the cavities, the power couplers and the frequency tuning systems) and the manufacturing of its components, the assembly and tests of the pre-production cryomodule and 9 production modules. An important milestone was reached in April 2023 with the Final Design Review. This paper presents the design of the 650 MHz low-beta cryomodules.

INTRODUCTION

The PIP-II project is an upgrade of the accelerator complex of Fermilab to enable the world's most intense neutrino beam for the Long Baseline Neutrino Facility (LBNF) and the Deep-Underground Neutrino Experiment (DUNE) located in South Dakota, 1200 km from the neutrino production in Illinois.

PIP-II will deliver 1.2 MW of proton beam power from the injector, upgradeable to multi-MW capability. The central element of PIP-II is an 800 MeV linear accelerator, which comprises a room temperature front end followed by a superconducting section. The superconducting section consists of five different types of cavities and cryomodules, including Half Wave Resonators (HWR), Single Spoke and elliptical resonators operating at state-of-the-art parameters.

PIP-II is the first U.S. accelerator project that will be constructed with significant contributions from international partners, including India, Italy, France, United Kingdom and Poland [1]. As described in [2], the CEA contribution focuses on the 650 MHz superconducting accelerating section, with the design, fabrication, assembly and test of 1 pre-production and 9 production low-beta 650 MHz cryomodules (Figure 1 - called "LB650" hereafter) according to the PIP-II project specified requirements.

DESIGN OF THE LB650 CRYOMODULE

The LB650 cryomodule, that houses four 5-cell $\beta=0.61$ cavities (developed by Fermilab, INFN, and VECC for the pre-production cryomodule and series cryomodules), is similar to the HB650 cryomodule that was assembled and cold RF tested at Fermilab [3]. The frequency tuning

systems and the power couplers for the low beta and high beta cavities are identical and are procured by Fermilab.

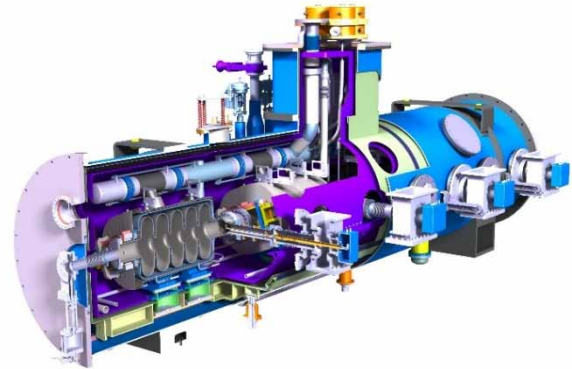


Figure 1: The LB650 cryomodule.

In order to benefit from the HB650 cryomodule design and to apply the same design concepts to the LB650 cryomodule, CEA was part of the integrated design team with Fermilab, UKRI-STFC and DAE. CEA was in charge of the mechanical and thermal design of the strongback and performed similar computations as the ones described in [4]. Moreover, the design strategy for the LB650 cryomodule was to reuse components designed for the HB650 cryomodule as much as possible and to do modifications whenever necessary.

Thanks to a close collaboration between CEA and Fermilab design teams, lessons learnt from the HB650 prototype cryomodule have been implemented in the design of the LB650 cryomodule. These lessons learnt were gathered either during visits of CEA personnel during the assembly phase and then the testing phase, or during several workshops organized by Fermilab to share experiences and solve problems.

The LB650 cryomodule is shown in Fig. 2. It is 5.52-meter long, 2.34-mm tall (distance between the feet and the helium guards at the top). The diameter of the main tube of the vacuum vessel is 1.22 m. The total weight is 7.5 tons.

Each cavity is connected to a supporting system that stays at room temperature, the strongback, using two support posts made of low thermal conductivity material to limit the thermal load between the room temperature strongback and the helium temperature devices. The posts have two thermal intercepts, one connected to the thermal shield (cooled around 40 K with pressurized helium gas) and the 5 K line where liquid helium flows inside.

[†] robin.cubizolles@cea.fr

PERFORMANCE ANALYSIS FROM ESS CRYOMODULE TESTING AT CEA

O. Piquet, C. Arcambal, P. Bosland, E. Cenni, G. Devanz, T. Hamelin, P. Sahuquet, Q. Bertrand
Université Paris-Saclay, CEA, IRFU, Gif-sur-Yvette, France

Abstract

CEA Saclay is in charge of the production of 30 elliptical cavities cryomodule as part of the in-kind contribution to the ESS superconducting. The two medium and high beta prototypes and the three first of each type of the series cryomodules have been tested at CEA in slightly different conditions than at ESS (both in terms of cryogenic operation as well as RF conditions). The goal of these tests was to validate the assembly procedure before the delivery of the series to ESS where the final acceptance tests are performed.

This paper summarizes the main results obtained during the tests at CEA with particular attention to the field emission behaviour.

INTRODUCTION

CEA is in charge of the production of 30 cryomodules of the ESS LINAC [1, 2, 3]. This is one of the main French in-kind contribution to the ESS accelerator construction. CEA is delivering 9 medium-beta cryomodules ($\beta=0.67$) and 21 high-beta cryomodules ($\beta=0.86$).

Previous papers presented the cryomodule design (Figure 1), which is similar to medium and high-beta cryomodules with four 704 MHz elliptical cavities [3]. The cryomodule design has been made in a collaboration with CEA and IJCLab where CEA was in charge of the cavity packages Medium and High Beta and IJCLab was in charge of the cryostat of the cryomodule.

For the series production, CEA provides all the components except the M-Beta cavities provided by LASA and the H-Beta cavities provided by STFC. The cryomodules are assembled at CEA Saclay by a private Company under the supervision of CEA.

CEA has tested the two prototype cryomodules and has also the three first cryomodules of the series of each type before sending them to ESS. They are tested a second time at ESS in nominal conditions for the final acceptance.

The main objectives of the tests at CEA are to:

- Check the quality of the assembly and procedures by measuring the cavities and couplers performances
- Verify the Qext of the power couplers
- Check that the performances of the tuners (stepper motor and piezo actuators) meet the requirements of ESS
- Measure cryogenic heat loads (static and dynamic)

A total of seven M-Beta cryomodules and eight H-Beta cryomodules have been delivered to ESS. All seven M-Beta cryomodules have passed the RF power tests performed at ESS for the acceptance. The first H-Beta has also been accepted but the second H-Beta presents a leak

between the LHe circuit and the insulating vacuum that is only visible at cold with superfluid helium. The acceptance tests are still in progress on the following cryomodules that have been delivered.

Nominal gradients are respectively 16.7 MV/m and 19.9 MV/m for medium and high-beta cavities and the maximum power transferred by the power couplers is 1.1 MW at 14 Hz, 3.6 ms pulse length.

This paper summarizes the results of the RF power tests performed at CEA on eight cryomodules.

CEA TEST STAND

The CEA test stand (see Fig. 1) is about 100 m from the cryomodule assembly hall. It is equipped with a liquefier that can deliver 90l/h of 4K LHe at 1.1 bar to the 2000 l Dewar close to the cryomodule. The experimental conditions are different between CEA and ESS: the thermal shield can be cooled only by N₂ to 80 K (@ESS, 50 K), the Liquid Helium (LHe) cooling is performed at 4 K – 1 bar whereas ESS cools with SHe at 3 bars. The cryomodule is equipped with an internal Hampson heat exchanger (HX) that is well adapted to the supercritical helium fluid used at ESS, but is not adapted for the helium boiling at 1 bar and containing a too high rate of GHe bubbles. This caused some difficulties in the first tests performed on the prototype CM00. We fixed this issue by adding a small phase separator to remove part of the GHe generated in the last 10 meters of the cryogenic line between the Dewar and the cryomodule. This small phase separator allows the HX to run and we obtain an easy regulation of the 2 K LHe level above the cavities.

The RF power source is a 704MHz klystron with a home-made modulator. It can generate 1.2MW RF pulses of 3.6 ms length at 14 Hz. 4P/P pulse is possible with our current setup. The RF distribution line is equipped with an RF switch that can send the RF power to one of the two branches at the entrance of the test stand. Each branch is equipped with a power divider that can distribute the power in one cavity or two cavities. We can test one cavity at a time, or two maximum together instead of 4 cavities @ ESS.

RF instrumentation (electron pick-up, arc detector, and RF measurements) used mainly for coupler protection are based on home-made electronics boards developed for projects where CEA is involved. These systems permit to acquire data and realize fast protection functions in order to switch RF off in less than 20 μ s.

IMPACT OF MEDIUM TEMPERATURE HEAT TREATMENTS ON THE MAGNETIC FLUX EXPULSION BEHAVIOR OF SRF CAVITIES*

J. C. Wolff^{1,†}, J. Eschke, A. Goessel, K. Kasprzak, D. Reschke, L. Steder, L. Trelle, M. Wiencek
Deutsches Elektronen-Synchrotron DESY, Hamburg, Germany
W. C. A. Hillert, University of Hamburg, Germany
¹also at University of Hamburg, Germany

Abstract

Medium temperature (mid-T) heat treatments at about 300 °C are used to enhance the intrinsic quality factor of superconducting radio frequency (SRF) cavities. Unfortunately, such treatments potentially increase the sensitivity to trapped magnetic flux and consequently the surface resistance of the cavity. For this reason, it is crucial to maximize the expulsion of magnetic flux during the cool down. The flux expulsion behavior is next to the heat treatment mainly determined by the geometry, the niobium grain size and the grain orientation. However, it is also affected by parameters of the cavity performance tests like the cool down velocity, the spatial temperature gradient along the cavity surface and the magnetic flux density during the transition of the critical temperature.

To improve the flux expulsion behavior and hence the efficiency of future accelerator facilities, the impact of these adjustable parameters as well as the mid-T heat treatment on 1.3 GHz TESLA-Type single-cell cavities is investigated by a new approach of a magnetometric mapping system. In this contribution first performance test results of cavities before and after mid-T heat treatment are presented.

INTRODUCTION

Close to the transition temperature T_c of a type II superconductor (e.g. niobium) the critical magnetic field is strongly suppressed and can fall below the ambient magnetic field [1]. In this case magnetic flux vortices penetrating the bulk are trapped in so-called pinning centers even if the Meissner region is reached. This effect is enhanced by imperfections of the crystal lattice like material impurities, dislocations and grain boundaries [2]. Since these pinning centers remain normal conducting in the Meissner region, they have a significant negative impact on the surface resistance R_s given by:

$$R_s = R_{BCS} + R_{res} + R_{flux} \quad (1)$$

and consequently on the intrinsic quality factor Q_0 [3]. Here R_{BCS} represents the temperature dependent contribution described by the Bardeen Cooper Schrieffer (BCS) theory, R_{res} the constant residual resistance and R_{flux} the impact by the normal conducting pinning centers with a linear dependence

of the ambient magnetic field [2, 3]. Studies by [1, 2, 4, 5] have shown that the amount of trapped magnetic flux is influenced by the cool down velocity and the spatial temperature gradient. At least at the first glance these works resulted in contradictory conclusions concerning these two cool down dynamics. Studies at Helmholtz Zentrum Berlin (HZB) presented in Ref. [2] observed the presence of thermoelectric fields and a related inherent trapping of magnetic flux for cavities dressed by a helium tank made of titanium. Since the responsible thermoelectric voltage (Seebeck effect) rises for larger spatial temperature gradients, an increased R_{flux} was observed during subsequent studies using a sample-based setup in an ambient field below 50 nT. During these studies a larger cool down velocity at the T_c transition led to a greater suppression of the Meissner effect.

A similar setup at HZB presented in Ref. [4] is operated in an ambient field of up to $\pm 200 \mu T$. At these fields a positive impact of larger spatial temperature gradients at the T_c transition could be shown and a temperature gradient dependent threshold which needs to be reached before any flux trapping could be measured was reported.

Contrary to these reports, colleagues at Fermi National Accelerator Laboratory (FNAL) observed a positive impact of a larger cool down velocity during cavity studies [5] which was explained by different cool down procedures. To achieve the high cool down velocity, the cryostat was filled with liquid helium resulting in a well defined T_c transition from the bottom of the cavity to the top. However, to perform the slow cool down a controlled mixture of warm- and liquid helium was used. This slow cool down method potentially resulted in the formation of normal conducting “islands” enclosed by superconducting material and consequently in an increase of trapped magnetic flux.

Based on these former investigations the impact of the cool down velocity and the temperature gradient can be summarized as follows. In general, a slower cool down velocity seems to be beneficial for a greater expulsion of magnetic flux. Indeed, the formation of normal conducting “islands” enclosed by superconducting material during the cool down should be avoided by choosing an appropriate cool down procedure.

The impact of the temperature gradient is strongly dependent on the ambient conditions. If the experimental setup enables the generation of thermoelectric currents, a larger temperature gradient potentially affects the cavity performance due to the related inherent trapping of magnetic flux. Exemplary this can be the case for a dressed cavity in a

* This work was supported by the Helmholtz Association within the topic Accelerator Research and Development (ARD) of the Matter and Technologies (MT) Program.

† Jonas.Wolff@desy.de

FINAL DESIGN OF THE PRODUCTION SSR1 CRYOMODULE FOR PIP-II PROJECT AT FERMILAB*

J. Bernardini[†], V. Roger, D. Passarelli, M. Parise, G. Romanov, J. Helsper, M. Chen, M. Kramp,
F. Lewis, B. Squires, T. Nicol, P. Neri¹, FNAL, Batavia, IL, USA
¹also at University of Pisa, Pisa, Italy

Abstract

This contribution reports the design of the production Single Spoke Resonator Type 1 Cryomodule (SSR1 CM) for the PIP-II project at Fermilab. The innovative design is based on a structure, the strongback, which supports the coldmass from the bottom, stays at room temperature during operations, and can slide longitudinally with respect to the vacuum vessel. The Fermilab style cryomodule developed for the prototype Single Spoke Resonator Type 1 (pSSR1), the prototype High Beta 650 MHz (pHB650), and preproduction Single Spoke Resonator Type 2 (ppSSR2) cryomodules is the baseline of the present design. The focus of this contribution is on the results of calculations and finite element analyses performed to optimize the critical components of the cryomodule: vacuum vessel, strongback, thermal shield, and magnetic shield.

INTRODUCTION

The PIP-II linac [1] will utilize a total of two production SSR1 cryomodules (CMs) to accelerate H⁻ ions from 10 MeV to 35 MeV. A prototype SSR1 CM has already been constructed, tested, and validated at Fermilab [2]. The valuable insights gained during testing have been incorporated into the design of the production CM. The design of the SSR1 CM is based on a groundbreaking concept developed at Fermilab known as the Fermilab style cryomodule [3, 4]. This design takes into consideration the standardization strategy established for the PIP-II CMs [5-7]. To streamline the process of assembly, and minimize movement of the beamline components and ancillaries during the cooldown, a full-length strongback is utilized to support the coldmass and the beamline components. The strongback is designed to slide into the vacuum vessel during the CM assembly process, and to be maintained at room temperature during operations. A High Temperature Thermal Shield (HTTS) and Low Temperature Thermal Source (LTTS), along with connections for intercepts are made available between the inner surface of the vacuum vessel and the 2 K helium to reduce radiation and conduction heat transfers. The current PIP-II beam optics design requires that each SSR1 cryomodule contains eight identical SSR1 cavities and four focusing lenses with beam position monitors. Each cavity is equipped with one high-power RF coupler, and one tuner.

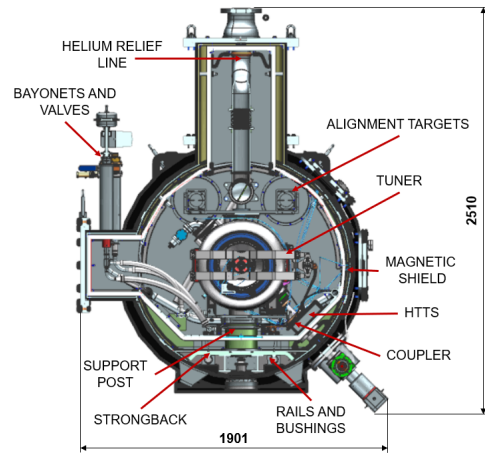


Figure 1: SSR1 CM transverse cross section showing the main components and subsystems (dimensions in mm).

Cavities and focusing lenses are supported by individual support posts, which are mounted on the strongback, situated between the vacuum vessel and the HTTS. Alignment plates are incorporated between cavities/solenoids and the support posts, and they allow for 5 degrees of freedom (DOF) which are needed to align beamline components during the CM assembly process. In addition, the cavities and solenoids are equipped with reference targets that serve the purpose of monitoring their movements throughout various stages of the CM assembly, transportation, pump-down, and cooldown processes. These reference targets play a crucial role in ensuring the accurate tracking and assessment of any displacements or shifts that may occur [8, 9]. A two-phase helium pipe runs the length of the cryomodule and is connected to the cavities via Ti-SS transition joints. The focusing lenses are connected to the two-phase pipe using thermal straps. The two-phase pipe is linked to the relief line through the top hat and to the pumping line through the bayonets on the lateral extension of the vessel. The heat exchanger, as well as the interfaces with the 2 K relief line and pressure transducers, are positioned on the top hat of the vacuum vessel. Inside the vessel, an inner frame supports a global magnetic shield, as displayed in Figs. 1 and 2.

MAIN CRYOMODULE COMPONENTS

Vacuum Vessel

The vacuum vessel is constructed with a carbon steel (ASTM A-516) cylindrical shell. It is securely anchored to alignment stands, bolted to the floor, using bottom sup-

* Work supported by Fermi Research Alliance, LLC under Contract No. DEAC02-07CH11359 with the United States Department of Energy, Office of Science, Office of High Energy Physics.

[†] jbernard@fnal.gov

HB650 CRYOMODULE DESIGN: FROM PROTOTYPE TO PRODUCTION*

V. Roger[†], S. Chandrasekaran, C. Grimm, J. Holzbauer, O. Napoly, J. Ozelis, D. Passarelli
Fermilab, Batavia, IL, USA

Abstract

In early 2023 the assembly of the prototype HB650 cryomodule (pHB650 CM) was completed and cold tests started to evaluate its performance. The lessons learned from the design, assembly and preliminary cold tests of this cryomodule, and from the design of the SSR2 pre-production cryomodule played a fundamental role during the design optimization process of the production HB650 cryomodule (HB650 CM). Several workshops have been organized to share experiences and solve problems. This paper presents the main design changes from pHB650 to the HB650 production cryomodules and their impact on the heat loads.

INTRODUCTION

This pHB650 CM has been designed by an integrated design team, consisting of Fermilab (USA), CEA (France), STFC-UKRI (UK), and RRCAT (India) [1]. This cryomodule is the second PIP-II cryomodule which has been assembled at Fermilab using a strong-back supporting the entire coldmass [2]. This cryomodule is also the first one for which a standardization among all PIP-II cryomodules was applied [3]. Therefore, its completion and the on-going cryogenic tests have an important impact on all other PIP-II cryomodules especially for the production HB650 cryomodules which will be assembled by STFC-UKRI and for the pre-production and production LB650 cryomodules which are designed and assembled by CEA [4].

LESSONS LEARNED

After the completion of the pHB650 CM assembly, the lessons learned from both cavity string assembly and cryomodule integration have been compiled and shared with Partners during workshops [3]. These lessons learned encompassed assembly process issues, design problems, component interferences, component QC, alignment issues, and opportunities for optimization.

Assembly Process & Design Issues

While checking the alignment of the cavities with the HBCAMs before and after the coldmass insertion and while preparing the cryomodule for on-site transportation, additional lessons learned have been identified.

- One of the goals of the monitoring cameras (HBCAMs) were to check the alignment of the cavities after the coldmass insertion [5]. To do this, the HBCAMs locations with regards to the coldmass need to be fixed. During the assembly process a support on

wheels was used, which didn't provide enough precision. For next cryomodules, the HBCAM support will be part of the beam pipe end assembly tooling. Thus, the HBCAM support will remain attached to the coldmass during the insertion (see Fig. 1).

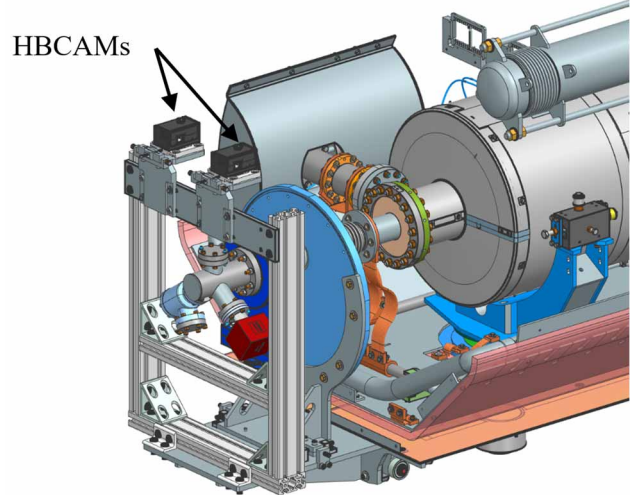


Figure 1: HBCAMs on the beam pipe end assembly tooling.

- The C-shape elements on each cavity lugs are used to keep the cavity aligned after cool-down [1] but also to constraint the cavity during transportation by using a cap. The plan was to use these caps only for transportation, but the latest calculations have shown that these caps can remain in place during the cold tests which will ease the assembly process. The Fig. 2 shows the design and location of these caps. Also, for production cryomodule the stiffness of the Belleville washers will be higher to make sure that the bearings are always in contact to the cavity.

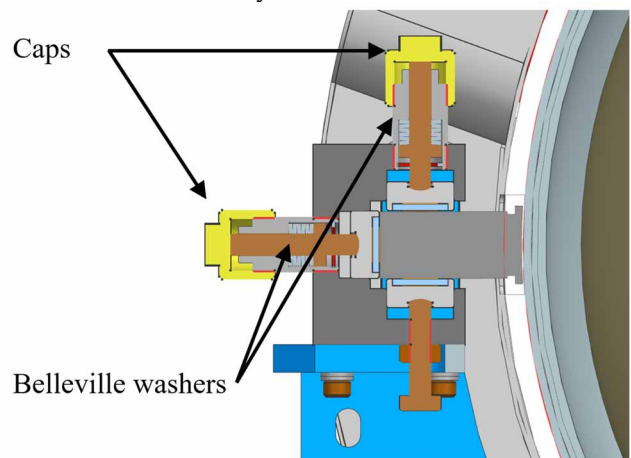


Figure 2: C-shape elements with caps.

* Work supported by Fermi Research Alliance, LLC under Contract No. DE AC02 07 CH11359 with the United States Department of Energy

[†] vroger@fnal.gov

CHARACTERIZATION OF ADDITIVE MANUFACTURING MATERIALS FOR STRING ASSEMBLY IN CLEANROOM*

J. Bernardini[†], M. Parise, D. Passarelli, FNAL, Batavia, IL, USA

Abstract

Beamline components, such as superconducting radio frequency cavities and focusing lenses, need to be assembled together in a string while in a cleanroom environment. The present contribution identifies and characterizes materials for additive manufacturing that can be used in a cleanroom. The well known advantages of additive manufacturing processes would highly benefit the design and development of tooling needed for the mechanical support and alignment of string components. Cleanliness, mechanical properties, and leak tightness of the chosen materials are the main focus of this contribution, which also paves the way for the integration of such materials in cryomodule assemblies. Results reported here were obtained in the framework of the PIP-II project at Fermilab.

INTRODUCTION

The cleanroom assembly [1] of beamline components requires precise connections that are free from particles and leaks [2]. Additionally, each beamline component needs to be individually supported and aligned in relation to the others. This necessitates the design and production of custom tooling that can handle, support, and align these components. For the development of such tooling, materials like stainless steel, aluminum, titanium, and silicone bronze are commonly chosen. After machining and welding, these materials should be electropolished or anodized to ensure smooth and easily cleanable surfaces.

To expedite the development of cleanroom assembly tooling and reduce associated lead time and cost, additive manufacturing techniques such as stereolithography (SLA), fused deposition modeling (FDM), and digital light processing (DLP) could be utilized. These techniques enable the customization of tooling designs according to the unique requirements of each project. However, before utilizing additive manufacturing techniques, it is necessary to qualify the associated materials for cleanroom use. This involves characterizing the mechanical properties and composition of the materials to be considered in the design. To this end, six different materials, including Accura 25 (SLA, 3D systems[®], solid density 1.19 g/cm³), Somos WaterShed (SLA, DSM[®], solid density 1.12 g/cm³) with and without clear coating, Somos WaterClear (SLA, DSM[®], solid density 1.13 g/cm³), Epoxy 82 (DLP, Carbon[®], solid density 1.16 g/cm³), and ABS M30i (FDM, Stratasys[®]), have been procured as equally sized flanges (as shown in Fig. 1) and test samples. After

conducting an initial visual inspection, the mechanical properties of Accura 25, Somos WaterShed with clear coating, and ABS M30i have been tested at three different temperatures: 293 K, 77 K (liquid nitrogen), and 4 K (liquid helium). Additionally, the cleanliness, ease of cleaning, and leak-tightness of ACCURA 25 and SOMOS WaterShed with clear coating have been assessed.



Figure 1: Flanges in ABS M30i, SOMOS watershed with clear coating, Accura 25.

VISUAL INSPECTION

The flanges underwent a visual inspection to assess their appearance and detect any surface defects or scratches. Flanges made of SOMOS WaterShed and SOMOS WaterClear materials are translucent. Among the samples, the clearest and smoothest surface was achieved through the clear coating applied to SOMOS WaterShed, as shown in Fig. 2. ACCURA 25 flanges consistently exhibit a smooth



Figure 2: Comparison between clear flanges.



Figure 3: Flanges in Epoxy 82, fractures are visible near corners and sharp edges.

* Work supported by Fermi Research Alliance, LLC under Contract No. DEAC02-07CH11359 with the United States Department of Energy, Office of Science, Office of High Energy Physics.

[†] jbernard@fnal.gov

TEST SHIPMENT OF THE PIP-II 650 MHz TRANSPORT FRAME BETWEEN FNAL TO STFC-UKRI*

J.P. Holzbauer[†], S. Chandrasekaran, C. Grimm, J. Ozelis, R. Thiede, A. Wixson
Fermi National Accelerator Laboratory, Batavia, IL, USA
M. Kane, STFC-UKRI, Warrington, UK

Abstract

The PIP-II Project will receive fully assembled cryomodules from CEA and STFC-UKRI as in-kind contributions. Damage to these cryomodules during transport is understood to be a significant risk to the project, so an extensive testing and validation program is in process to mitigate this risk. The centerpiece of this effort is the eventual shipment from FNAL to STFC-UKRI and back of a prototype HB650 cryomodule with cold testing before and after shipment to verify no functionality changes from shipment. Most recently, a test shipment was completed to the UK and back using a cryomodule analog using realistic logistics, handling, instrumentation, and planning. The process of executing this test shipment, lessons learned, and plan moving forward will be presented here.

INTRODUCTION

The PIP-II SRF linac is composed of five types of cryomodules at 3 sub-harmonics of 1.3 GHz (162.5, 325, and 650 MHz) [1]. The 650 MHz section of the linac is composed of two cryomodule types, Low-Beta (LB) and High-Beta (HB). The PIP-II Project has significant international contributions in almost every part of the machine, and the 650 section is no exception. The LB modules are being designed and produced by CEA in France while the HB modules are produced by STFC-UKRI in the UK as in-kind contributions to the project. The PIP-II project has adopted the design philosophy of convergent design, aligning the techniques and technologies between different modules as much as possible. This philosophy extends to transportation of the LB and HB modules from the partner labs in Europe to FNAL. Transportation experts at all three labs have worked closely to ensure that a consistent and systematic approach is used for assessing and mitigating the risks of these critical cryomodule transports.

TRANSPORT SYSTEM VALIDATION STRATEGY

A conservative approach to transportation and transport validation has been adopted by PIP-II driven by past experience with cryomodule shipping for LCLS-II [2]. This includes the choice to forego sea and rail, relying on air transport for the transatlantic segments. The following major stages are chosen to systematically validate the integrated

transport system design (cryomodule plus shipping frame) while minimizing risk to critical equipment.

1. Design, fabrication, and integration of HB650 transport frame with cryomodule analog (Dummy Load)
2. Local road testing with Dummy Load to validate isolation and handling performance
3. Realistic transport of Dummy Load from FNAL to STFC-UKRI to validate air transport and handling
4. Local road testing with a cold-tested and validated prototype HB650 (pHB650) to reverify isolation performance as well as any module-internal resonances
5. Realistic transport of the pHB650 module from FNAL to STFC-UKRI and back, concluding with second cold-test to assess impacts of transatlantic shipment on cavity performance.
6. Design optimization of HB650 and LB650 transport frames by the respective partner labs.
7. Integration tests and local road testing with first article modules produced by partners.
8. First shipment of production modules from partners to FNAL for the PIP-II Linac, proceeding to regular shipment of the remaining items.

The transportation scope of each partner is distributed based on many factors which are outside the scope of this document. The diversity of activities and design details of both transport systems and cryomodules means that it is critical that the transportation approaches are aligned and designs and lessons learned are shared strongly as early as possible within the project to minimize duplicated effort or increased risk.

TRANSPORT SYSTEM DESIGN

The transport system, designed by STFC-UKRI [3], is a tessellated steel frame meant to enclose the cryomodule during transport, isolating the CM during transport with wire-ropes sized for the weight and shocks/vibrations expected during transport. The model of the transport system (frame, isolators, and CM) can be seen in Fig. 1. The frame is covered in plywood panels during transport to prevent access and protect from weather. Access ports were added to allow instrumentation inspection during transport, viewing windows in case of customs inspections, and labeling for ease of assembly.

VALIDATION PROGRESS

The documentation and specification process used by the PIP-II project to manage this transportation work, especially across the international collaboration, is detailed in a previ-

* Work supported by Fermi Research Alliance, LLC under Contract No. DeAC02-07CH11359 with the United States Department of Energy.

[†] jeremiah@fnal.gov

PROTOTYPE HB650 CRYOMODULE HEAT LOADS SIMULATIONS*

G. Coladonato^{1,†}, D. Passarelli, V. Roger, Fermilab, Batavia, IL, USA
¹also at University of Illinois, Chicago, IL, USA

Abstract

During the design stages of the PIP-II cryomodules, many analytical calculations and FEA have been performed on simpler geometry in order to estimate the heat loads and also to optimize the design. To better analyse the cryomodule cold tests, simulations have been performed with MATLAB to determine the temperature of the main components during cool-down and to determine the heat loads of the cryomodule. These simulations have been applied to the High Beta 650 MHz prototype cryomodule design and compared to the cold tests performed on it.

INTRODUCTION

Over the last years, calculations have been done to estimate the heat loads of the PIP-II linac [1] in order to design the appropriate cryogenic plant and the cryogenic distribution system. Therefore, accurate estimations of these heat loads are crucial for the project. In early 2023, the assembly of the prototype HB650 cryomodule was completed [2] and the cold tests started to evaluate its performance [3]. This cool-down and heat analysis gave us a great opportunity to compare the estimation to the measurements and also to develop with MATLAB a reliable tool to estimate the cooling time and heat loads in an automatic way. While previous studies have explored this aspect [4], the novelty lies in validating the results using actual data from experimental testing, further enhancing the reliability and applicability of the heat load calculations to use later on the LB650, SSR1 and SSR2 cryomodules [5, 6, 7].

CRYOMODULE DESIGN AND FIRST COOL-DOWN

The PIP-II SSR and 650 cryomodules are designed adopting the Fermilab style cryomodule that uses a room temperature strongback as foundation. This design choice is part of a design strategy [8] that was defined by the project to standardize parts in between cryomodules [9].

The Figure 1 describes the cryomodule layout of the HB650 cryomodule. A High Temperature Thermal shield (HTTS) to shield the heat loads by radiation from the vacuum vessel and to intercept heats by conduction on several components such as the support posts, couplers, relief line, pressure transducer lines, bayonets and cryogenic valves. A Low Temperature thermal source (LTTS) is being used as a thermal intercept for the beam line, couplers, relief line and support posts. A cool-down valve is used to cool-down the cavities up to 4 K, then an heat exchanger, Joule Thomson valve and pumping line are used together to reach 2 K.

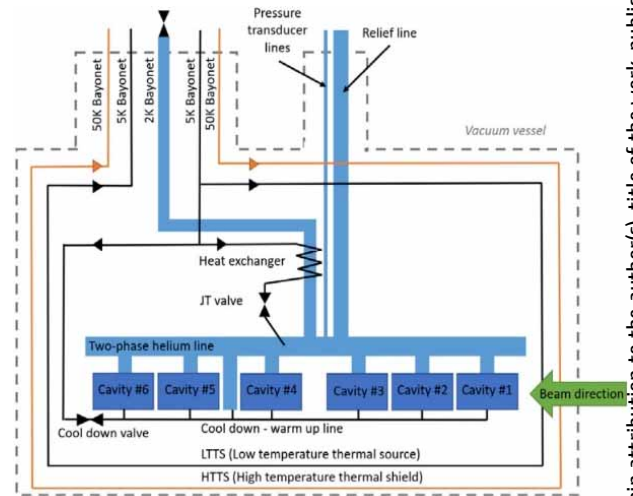


Figure 1: HB650 cryomodule layout.

The cool-down of the cryomodule is done using a detailed procedure to operate safely cryomodule and reach the appropriate performance. First only the thermal shield is cooled down from room temperature to 50 K by maintaining a maximum temperature difference of 100 K across the shield. While maintaining close the outlet of the LTTS and open the cool-down valve, the cavities are cooled to 4 K. The requirement is to go as fast as possible and to ensure a minimum rate of 20 K/hr between 175 K and 90 K. This step is critical to ensure a flux expulsion of the cavities required to reach a high Q_0 . The next step is to open the outlet of the LTTS cooling down many thermal intercepts and reducing the 2 K heat loads. Finally, the cool-down valve is closed, and the Joule Thomson valve is open to reach 2 K.

This cryomodule being a prototype, it has been decided to close the helium inlets during the night for safety reasons. That is why the curves on the Figure 2 shows two plateaus. It took 49 hours to cool-down the thermal shield before starting to cool-down the cavities until 4 K and finally to reach 2 K.

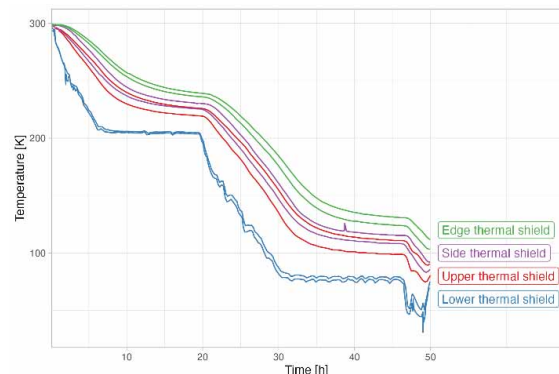


Figure 2: Cool-down of the HTTS.

Content from this work may be used under the terms of the CC BY 4.0 licence (© 2023). Any distribution of this work must maintain attribution to the author(s), title of the work, publisher, and DOI

* Work supported by Fermi Research Alliance, LLC under Contract No. DE AC02 07 CH11359 with the United States Department of Energy
 † gcolad2@uic.edu

IMPACT OF SOLENOID INDUCED RESIDUAL MAGNETIC FIELDS ON THE PROTOTYPE SSR1 CM PERFORMANCE*

D. Passarelli[†], J. Bernardini, C. Boffo, S. Chandrasekaran, A. Hogberg, T. Khabiboulline, J. Ozelis, M. Parise, V. Roger, G. Romanov, A. Sukhanov, G. Wu, V. Yakovlev, Y. Xie
FNAL, Batavia, IL, USA

Abstract

A prototype cryomodule containing eight Single Spoke Resonators type-1 (SSR1) operating at 325 MHz and four superconducting focusing lenses was successfully assembled, cold tested, and accelerated beam in the framework of the PIP-II project at Fermilab. The impact of induced residual magnetic fields from the solenoids on performance of cavities is presented in this contribution. In addition, design optimizations for the production cryomodules as a result of this impact are highlighted.

INTRODUCTION

The PIP-II project [1] has the scope to upgrade the existing Fermilab's accelerator complex to deliver the most intense high-energy beam of neutrinos for the international Deep Underground Neutrino Experiment (DUNE) at the Long Baseline Neutrino Facility (LBNF). It is based on a proton superconducting linac that comprises of five different Superconducting Radio Frequency (SRF) cavity types: 162.5 MHz half wave resonator (HWR), 325 MHz single spoke resonators type 1 and type 2 (SSR1, SSR2), low-beta and high-beta 650 MHz elliptical 5-cell cavities (LB650, HB650). International research institutions in India, the United Kingdom, Italy, France, and Poland are making significant contributions to the project, focused on accelerator technologies. Their contributions are playing a vital role in advancing and enhancing the project.

Positioned as the second cryomodule type in the linac, the two SSR1 cryomodules operate at a frequency of 325 MHz with continuous wave (CW) RF power and peak currents of 5 mA to accelerate H- beam from 10 MeV to 32 MeV. The PIP-II beam optics design requires that each SSR1 string assembly (see Fig. 1) contains four superconducting focusing lenses (solenoids) and eight identical SSR1 cavities [2, 3], where each cavity is equipped with one high-power RF coupler [4] and one frequency tuner [5].

The focusing lenses are combined superconducting magnets that include a solenoid with bucking coils and four corrector coils that can be power separately to provide both dipole and quadrupole steering. The focusing lenses are helium bath cooled and include resistive current leads optimized to minimize the heat load at 2 K. The design of the current leads feedthroughs was optimized to minimize potential frosting while avoiding the use of fans that could

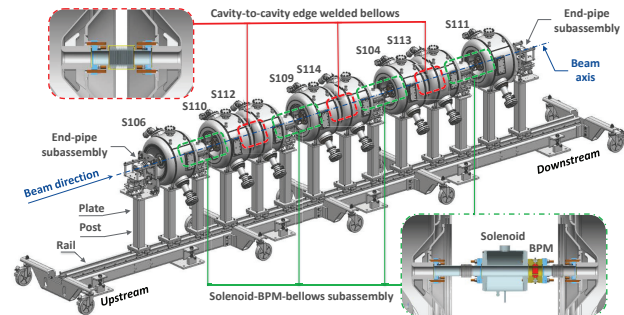


Figure 1: Layout of the string assembly for the prototype SSR1 cryomodule.

introduce microphonics issues. The geometry of the main and the bucking coils, the type and size of superconducting strand, and the number of turns in the winding packages were chosen to satisfy the minimum required integrated focusing strength of $4 T^2 m$. The bucking coils are wound concentrically to the main coil and are located at each end of the lens. The maximum magnetic field generated by lenses in the cryomodule in the area near the surface of the SSR1 superconducting cavities is such that it will not result in more than two-fold reduction of the intrinsic quality factor after quench event at any point on its surface. However, no specification was defined for the maximum residual magnetic field induced of parts magnetized during the operation of the focusing lenses that would be trapped into the niobium surface during subsequent warmup and cooldown of the cryomodule. Figure 2 illustrates the magnetic field distribution along the beam axis for the prototype SSR1 focusing lenses. It is evident that the fringe field extends significantly beyond the length of the focusing lens package, reaching magnitudes of thousands of Gauss outside the range of ± 82.5 mm as depicted in the plot.

The prototype SSR1 cryomodule [6, 7] was designed to include a global, room temperature, magnetic shield positioned near the inner wall of the carbon steel vacuum vessel. The design and manufacturing of the global magnetic shield were aimed at reducing the impact of Earth's magnetic field to a level below 15 mG at the surfaces of the cavities. After the installation of the global magnetic shield in the vacuum vessel and the completion of the now standard demagnetization procedures [8], rigorous measurements validated the effectiveness of the shield's design to ensure that the desired performance requirement of magnetic field less than 15 mG along the beam axis (center of the vessel) was met.

* This manuscript has been authored by Fermi Research Alliance, LLC, under Contract No. DE-AC02-07CH11359 with the U.S. Department of Energy, Office of Science, Office of High Energy Physics.

[†] donato@fnal.gov

LOW PARTICULATES NITROGEN PURGE AND BACKFILL DURING PROTOTYPE HB650 CRYOMODULE STRING ASSEMBLY*

T. Ring, M. Quinlan, G. Wu[†], Fermilab, Batavia, IL, USA

Abstract

A low particulate vacuum and purging system was developed to support PIP-II cryomodule string assembly. The overpressure can be controlled at a precision of 1 mbar above the atmospheric pressure regardless of the cavity or string assembly air volume. The system minimized the risk of uncontrolled nitrogen flow during the string assembly. Design features are presented.

INTRODUCTION

The PIP-II linac consists of several types of cryomodules made of HWR, SSR1, SSR2, LB650, and HB650 cavities [1]. A 6-cavity string assembly is shown in Figure 1. The beamline space volume of PIP-II cavities is considerably higher than a typical 8-cavity 1.3 GHz cryomodule. A string assembly requires the disassembly of cavity beamline flanges when the cavity beamline pressure is under a positive 50 mbar above the atmospheric pressure. This practice was used to purge the cavity beam pipe when the cavity end flanges were removed. This would prevent the particulates from migrating into the cavity.

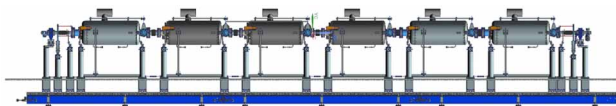


Figure 1: PIP-II 650 MHz string assembly sitting on clean-room tooling.

During the LCLS-II production [2], it was found that some cavity flange removal did not result in a slow pressure release when the cavity flange was loosened. Instead, a sudden pressure burst was seen. A potential pressure wave could draw the particulates back into the cavity. Unfortunately, it was difficult to reliably repeat this phenomenon to help measure the pressure wave and assess the risk of particulate migration. Nevertheless, this situation was considered an uncontrolled pressure change.

A much larger volume for the PIP-II string assembly means this potential risk could be much worse than that in the LCLS-II string assembly. A standard 50 millibar overpressure would cause high-speed flow when released during cavity flange removal. The mass flow increases when cavity volume increases. 650 MHz and spoke cavities have a substantial risk of uncontrolled pressure change. PIP-II SSR1 prototype string assembly chose to implement this

prototype low particulate purging system to avoid the potential pressure wave that could have moved the particulates in the string assembly [3].

A much lower overpressure, such as 5 mbar instead of 50 mbar, would reduce this risk significantly. A precise pressure measurement, controllable overpressure, and fast detection of pressure drops are required for a new system.

DESIGN OF THE SYSTEM

System Configuration

A brand new backfill and purging system was designed and being built for cavity coupler installation and string assembly, shown in Figure 2. Nine channels allow the system to build a string assembly with up to eight cavities, including end-group sub-assemblies.

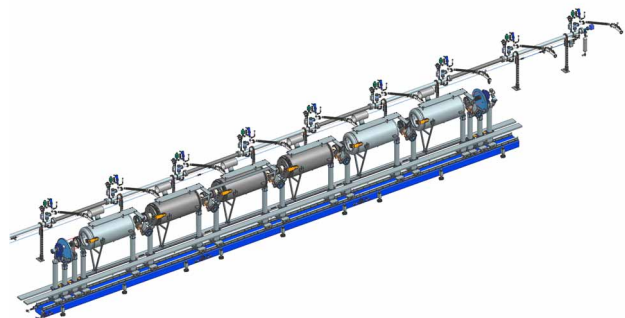


Figure 2: A 9-channel vacuum/purge system in a clean-room.

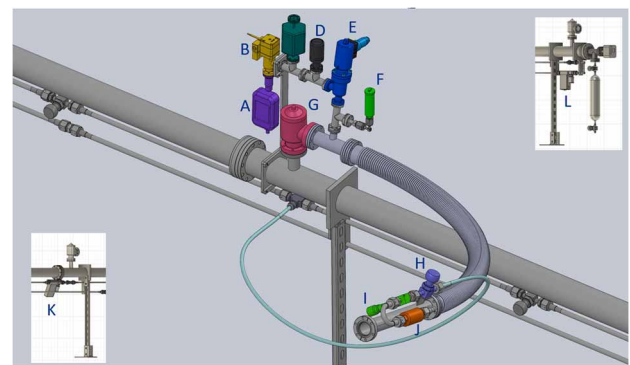


Figure 3: One channel of the purging line with the purging head assembly connected to the main vacuum line.

Two mass flow controllers are located at two ends that can precisely control the flow rate from 0.25 to 15 L/m. The system allows for a closed loop with feedback control or an open-vented system if needed, like the SSR1 prototype string used. The purging entry point is right at the cavity right angle valve (RAV). The venting flow goes through

* Work supported by Fermi Research Alliance, LLC, under Contract No. DE-AC02-07CH11359 with the U.S. Department of Energy, Office of Science, Office of High Energy Physics

[†] genfa@fnal.gov

OPERATIONAL EXPERIENCE WITH TURN-KEY SRF SYSTEMS FOR SMALL ACCELERATORS LIKE MESA*

T. Stengler[†], K. Aulenbacher, F. Hug, P.S. Plattner

Institute for Nuclear Physics, Johannes Gutenberg-Universität Mainz, Mainz, Germany

Abstract

New SRF-based accelerator development at sites without long-term experience in SRF development is a major challenge. Especially in-house development of cryomodules is an almost impossible obstacle to overcome for small projects. To minimize such obstacles, turn-key SRF systems provided by industry can be of great importance. For the multiturn ERL MESA, which is currently under construction at Johannes Gutenberg-Universität Mainz, two turnkey cryomodules have been purchased from industry and successfully tested. The specifications of a design gradient of 12.5 MV m^{-1} in CW operation with an unloaded Q of $1.25 \cdot 10^{10}$ at 1.8 K had to be met. Since the design of the modules had to be modified for high current CW operation, a close cooperation with the manufacturer was of great importance. By purchasing such a turn-key SRF system, the MESA project successfully established the SRF accelerator technology at the site within six years. This was achieved through close monitoring of the manufacturing process and close cooperation with the manufacturer. An overview of the experience with the successful technology transfer of a complete turn-key SRF system for small accelerators will be given.

INTRODUCTION

The development and operation of accelerators based on superconducting radio frequency (SRF) technologies is a major challenge. In particular, small institutes that want to develop smaller accelerator facilities for research and development often lack long-term experience and resources, which makes entry into the technology difficult. Especially in-house development of cryomodules is an almost impossible obstacle to overcome for small projects. Cryomodules play a crucial role in SRF-based accelerator systems, providing the necessary cooling and RF infrastructure for efficient operation. However, the design, fabrication, and integration of cryomodules require specialized expertise and significant financial investments. Small institutes often lack the necessary infrastructure, equipment, and technical know-how to undertake such complex endeavors independently. Consequently, they face significant barriers in realizing their ambitions for SRF-based accelerator development. Collaboration with established institutions, industry partners and research centres can provide a potential pathway for small projects to access the necessary expertise and facilities to

meet this challenge and contribute to the advancement of SRF technology.

To gain a better understanding of these challenges, this paper analyses the integration of SRF technology within the framework of the MESA project at the Institute for Nuclear Physics, Johannes Gutenberg University Mainz. The MESA project serves as a case study to examine the difficulties and successes encountered in implementing SRF-based accelerators within a small institute.

MAINZ ENERGY-RECOVERING SUPERCONDUCTING ACCELERATOR (MESA)

The Mainz Energy-recovering Superconducting Accelerator (MESA) is an electron accelerator designed as an Energy Recovering Linac (ERL) which is currently under construction at the Institute for Nuclear Physics, JGU Mainz [1].

MESA has been specifically designed to meet the requirements of experiments [2–4] aimed at verifying the Standard Model of particle physics. These experiments demanding moderate beam energies up to 155 MeV but high beam currents up to 1 mA (CW). Ongoing research efforts are focused on exploring additional modifications to push the beam current limit up to 10 mA [5].

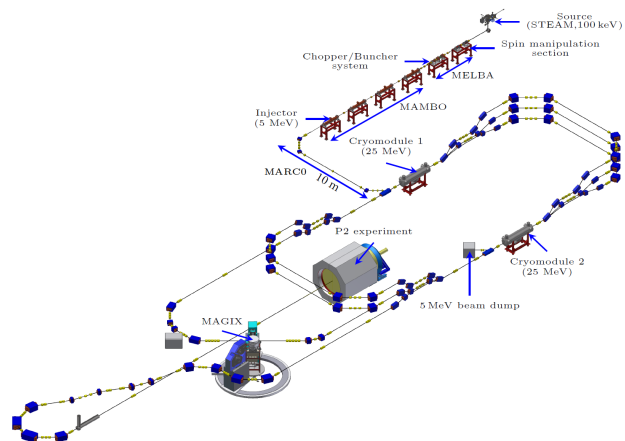


Figure 1: Layout of MESA. A normal-conducting pre-accelerator injects a 5 MeV CW beam into the recirculating main accelerator. Two cryomodules accelerate the beam. In external beam mode for the P2 experiment a 150 mA beam is recirculated thrice to a energy of 155 MeV and dumped afterwards. For the ERL experiment MAGIX 1 mA is recirculated twice up to 105 MeV. Afterwards the beam is decelerated in the main accelerator down to 5 MeV.

* The work is funded by the German Research Foundation (DFG) under the Cluster of Excellence "PRISMA+" EXC 2118/2019 and the Federal Ministry of Education and Research (BMBF) through project 05H21UMRB1
[†] stengler@kph.uni-mainz.de

BASIC DESIGN AND CONSIDERATION OF LI-VAPOR CONTAMINATION FOR A-FNS SRF

T. Ebisawa[†], QST, Rokkasho, Japan and KEK, Ibaraki, Japan
K. Hasegawa, A. Kasugai, M. Oyaizu, S. Sato, QST, Rokkasho, Japan
E. Kako, H. Sakai, K. Umemori, KEK, Ibaraki, Japan

Abstract

The Advanced Fusion Neutron Source (A-FNS) project is in progressing in Japan, QST Rokkasho institute. A-FNS will demonstrate a performance of the DEMO DT fusion reactor material. In order to perform the test, a high intensity deuteron beam accelerator will be used to produce a high flux neutron field which is similar to the 14 MeV DT neutron. The Superconducting Radio-Frequency linear accelerator (SRF) is one component of the A-FNS accelerator system. Although the A-FNS accelerator system design is based on the IFMIF design, the improvement of some subsystem has been considering by taking into account the lessons learnt from the LIPAc project. In order to keep a high stability and availability of the SRF performance, we plan to increase the number of SRF cavities and cryomodules considering the trouble or degradation of the cavity performance and modify the engineering design of some components. In addition, changing of the beam transport line design and Li vapor contamination study of SRF cavity are conducting. In this presentation, the progress of the SRF design and related activities for A-FNS in QST will be presented.

INTRODUCTION

The A-FNS project is in progressing at QST Rokkasho institute to conduct the fusion neutron irradiation tests of the materials for a fusion reactor by the accelerator driven neutron source system. The A-FNS accelerator will produce a Continuous Wave (CW) deuteron beam of 125 mA/40 MeV and inject to the Li target to generate neutrons with energy around 14 MeV which is similar to energy of the neutron generated by a DT fusion reactor [1].

As shown in Fig. 1, the A-FNS accelerator system consists of an injector system with ECR ion source and LEBT (Low Energy Beam Transport), Radio-Frequency Quadrupole accelerator (RFQ), Medium Energy Beam Transport (MEBT), multiple Superconducting Radio-Frequency linear accelerator (SRF linac) cryomodules (CM), High Energy Beam Transport (HEBT) and Beam Dump (BD). Table 1 shows the main specification of the A-FNS accelerator. The design is based on the International Fusion Materials Irradiation Facility (IFMIF) accelerator design [2]. In order to solve the concerns of the design and improve it, some components are to be improved by reflecting the outcomes of Linear IFMIF Prototype accelerator (LIPAc)

commissioning and design of the IFMIF/EVEDA (Engineering Validation and Engineering Design Activities) project [2].

There is the inadequate energy margin design of the SRF linac as the concern. In order to keep a stable operation for 40 MeV, we redesigned the SRF linac lattice design. In addition, we reviewed some SRF components with considering the mechanical issues in LIPAc SRF activity and design.

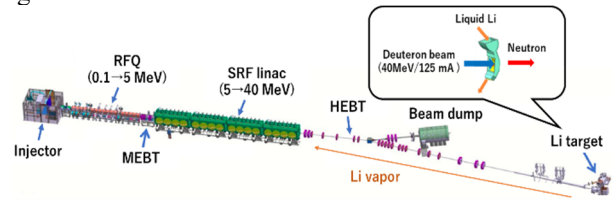


Figure 1: The schematic of the initial design of the A-FNS accelerator.

Table 1: Main Specification of the A-FNS Accelerator

Parameter	Value
Beam current	125 mA
Beam energy	40 MeV
Duty	CW
Beam profile at Li target	20 cm x 5 cm

There is the beam loss of the low energy particles which are not accelerated in the RFQ as another concern. From the results by beam dynamics simulation, the beam loss is too high so that thermal load is severe for the cooling system. To prevent the quench due to the thermal load, the energy filtering system is necessary to be installed in MEBT.

There is the unique issue of the A-FNS SRF which is the Li vapor contamination of the SRF cavity from the free surface liquid Li target. In order to minimize the Li vapor contamination, a concept of the dogleg HEBT has been introduced and its design is ongoing. Also, there are no information that the relation between the performance of the SRF cavity and the Li vapor contaminations. Therefore, we have investigated it to feedback for the design of the A-FNS accelerator system. For this study, we considered the Li vapor source apparatus to control the production of the nano scale mass vapor. The testing cavity for Li contamination study was prepared.

In this paper, the progress of the basic design of the A-FNS accelerator and the Li vapor contamination study are presented.

[†] ebisawa.takashi@qst.go.jp

THE INTERACTION AMONG INTERSTITIAL C/N/O/H AND VACANCY IN NIOBIUM VIA FIRST-PRINCIPLES CALCULATION

Hantian Liu, Zhitao Yang, Jiankui Hao[†], State Key Laboratory of Nuclear Physics and Technology
& Institute of Heavy Ion Physics, Peking University, Beijing, China

Abstract

We calculate the interaction among zero dimensional defects in niobium lattice through first-principles calculation. And we compare the trapping effect of hydrogen among carbon, nitrogen, and oxygen as well as the trapping effect of interstitial atoms by vacancy. We find that the interstitial C/N/O have similar effect of trapping interstitial hydrogen in niobium lattice, and the vacancy can trap interstitial C/N/O/H in adjacent protocells and strengthen their chemical bond with Nb. These calculations give some explanation for improving superconducting performance of niobium cavities through medium temperature baking.

INTRODUCTION

In bulk niobium, hydrogen is an active light impurity element that are highly diffusive in baking processes [1]. Insulating at room temperature, niobium hydride behaves as superconductor in bulk niobium below the critical temperature (1-2 K [2, 3]) owing to proximity effect. As SRF cavities are cooled down to liquid helium temperature during operations, niobium hydride form clusters of various sizes. Hundred-nanometer-scaled niobium hydride clusters are considered responsible for low field Q-slope in niobium cavities, while nanometer-scaled hydride clusters are the speculated causes of high field Q-slopes [4]. To reduce the precipitation of niobium hydrides during the cooling process of niobium cavities, various surface treatment methods, such as nitrogen doping [5, 6] and medium temperature baking [5, 6], have been employed. While the mechanisms of such treatments are not yet fully understood, it is speculated that the distribution of defects in niobium bulks may be altered owing to thermal effect and interactions among defects. Based on experiments and simulations, some existing works have demonstrated that both interstitial nitrogen [7, 8] and oxygen [9, 10] atoms trap interstitial hydrogen atoms and suppress the formation of niobium hydride clusters, while vacancies are able to trap the three kinds of interstitial atoms and regulate the superconducting properties of bulk niobium [11, 12]. It is also assumed that interstitial carbon atoms may trap interstitial hydrogen atoms [9]. In this work, we carry out first-principles calculations to better understand the interaction among interstitial carbon, vacancy, and hydrogen.

METHOD

Calculations are conducted in a supercell that consists of $3 \times 3 \times 3$ body-centered cubic (bcc) niobium cells.

Considered as zero-dimensional defects, interstitial atoms and vacancies are introduced into the supercell sequentially. We first introduce a single interstitial carbon atom or vacancy (by simply removing a niobium atom) and conduct geometry optimization [13] to relax the crystal. The interstitial carbon is located at an octahedral point as initial configuration, which was reported to be the lowest energy position for interstitial nitrogen and oxygen [10]. After the convergence of geometry optimization, we redefine the unit cell to put the defect at center (which does not alter any physical property of the crystal) and then introduce an interstitial hydrogen atom.

For hydrogen atom, two types of calculations are conducted, namely stable point energy calculation and two-dimension energy distribution calculation. For stable point energy calculation, hydrogen atoms are first placed at different points as initial configuration. Then, geometry optimizations are conducted with no constraint to relax the entire lattice. It is found that after relaxation, the introduction of the hydrogen atom causes displacements of other atoms by no more than 0.02 Å. The global lowest-energy configuration is found. Furthermore, we calculated the electron density difference and partial density of states (PDOS) of the lowest energy configuration to study the bonding between atoms. For two-dimension energy distribution calculation, the key idea is to ignore the displacement of niobium atoms and other impurity atoms caused by the introduction of the hydrogen atom at unstable points, which is inspired by the result of stable point geometry optimization. A hydrogen atom is placed at different points (not necessarily stable points) on a plane sized 9.9018×9.9018 Å in (0 0 1) direction.

Utilizing CASTEP module [14] of Materials Studio 2020, all first-principles calculations in this work are based on density function theory (DFT) [15, 16]. Perdew-Burke-Ernzerhof (PBE) functional under Generalized Gradient Approximation (GGA) [17] is used to estimate the exchange-correlation interaction. For high accuracy, norm-conserving pseudopotential is used. The cut-off energy of the plane wave basis set is set to 440 eV. For self-consistent field (SCF) calculations, the SCF tolerance is set to 5.0×10^{-7} eV/atom. Geometry optimization accuracy is set to ‘ultra-fine’ setup, the most accurate set of preset convergence parameters. To be specific, the energy tolerance is set to 5.0×10^{-6} eV/atom, atom force tolerance 0.01 eV/Å, maximum pressure 0.02 GPa, and single atom displacement 5.0×10^{-4} Å. To compare the C-H interaction with the O-H and N-H interaction, the carbon atom with interstitial nitrogen and oxygen atoms in the same niobium lattice configuration undergoes the same calculation procedure. In this work, carbon, nitrogen, and oxygen atoms are referred to as ‘heavy impurity atoms’ for being

Fundamental SRF research and development

High quality factors/high gradients

[†] jkhao@pku.edu.cn

DEGRADATION AND RECOVERY OF CAVITY PERFORMANCE IN SRILAC CRYOMODULES AT RIBF

N. Sakamoto*, O. Kamigaito, K. Ozeki, K. Suda, K. Yamada
RIKEN Nishina Center, Saitama, Japan

Abstract

The RIKEN superconducting (SC) heavy-ion linear accelerator (SRILAC) has been providing beam supply for super-heavy elements synthesis experiments [1] since its commissioning in January 2020 [2]. However, the long-term operation of SC radio-frequency (RF) cavities leads an increase in the X-ray levels caused by field emissions resulting from changes in the inner surface conditions. More than half of the ten SC 1/4 wavelength resonators (SC-QWRs) of SRILAC, operating at a frequency of 73 MHz, have experienced an increase in X-ray levels, thus, requiring adjustments to the acceleration voltage for continuous operation. While several conditioning methods have been employed for SC cavities, a fully established technique is yet to be determined. To address this situation, a relatively simple conditioning method was implemented at RIKEN. The proposed method uses high-voltage pulsed power and imposes a low load on the cavities.

INTRODUCTION

The mission of the RIKEN Radioactive Isotope Beam Factory (RIBF) [3] is to improve our understanding of the mechanism underlying the synthesis of elements by performing experiments using intense heavy-ion beams. At the RIBF, heavy-ion beams at various energies are available, from sub-coulomb energy levels employed for fusion reactions to intermediate energy levels for radioisotope beam production using fission reactions. Beams of ion species ranging from H to U are accelerated in accordance with experimental requirements. The RIBF accelerator complex consists of booster ring cyclotrons and three injectors, namely the azimuthally varying field (AVF) cyclotron, the RIKEN liner accelerator (RILAC), and a second linear accelerator (RILAC2), as shown in Fig. 1. The velocity change of heavy ions is moderate during acceleration. Therefore, various accelerator structures are combined. The frequency tunable accelerators of RIBF enable the usage of various ion species with different energies. To achieve an increasingly high beam power, several efforts have been made in terms of improving performance and reliability of each component of the accelerators. One of the injector linacs, RILAC, was upgraded to enable a new element synthesis experiment at the RIKEN RIBF.

In 2016, a new comprehensive superheavy element (SHE) research program commenced at the RIKEN Nishina Center (RNC). The main objective was to expand the periodic table of elements by synthesizing new superheavy elements. After the synthesis of oganesson ($Z = 118$), the aim of the SHE

project was to synthesize an element with $Z > 118$. Aiming to synthesize the element with $Z = 119$, at the RNC we adopted a ^{51}V as the beam and ^{248}Cm as the target. For this experiment, the required beam energy was higher than 6 MeV/u with an intensity of 2.5 pμA. Thus, the primary aim of this project was to upgrade of the accelerator by introducing a SC linear accelerator to increase the final beam energy from 5.5 to 6.5 MeV/u, and a SC electron-cyclotron-resonance ion source (ECRIS) to multiply the beam intensity by a factor of five.

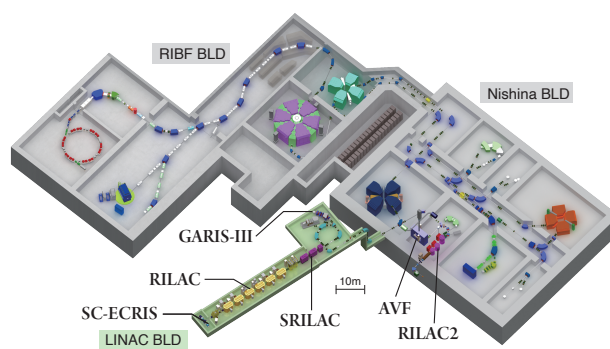


Figure 1: Birds-eye view of the RIBF accelerators.

After the beam commissioning, user beam service started subsequently. After elaborate tuning of the accelerator components, we successfully delivered a ^{51}V beam with an energy ranging from 4.2 to 6.3 MeV/u, thus, was accelerated and delivered proving the required energy and intensity.

For the synthesis of new elements, we expect a long bombarding time in the order of years owing to a small production cross section. Therefore, the reliability of the accelerator hardware is crucial for the success of this long-term project. As lessons learned by the long-term operation the degradation of the SC cavities might pose a significant problem for continuous long-term operations [4]. We observed a sudden increase of field emission (FE) and heavy multipacting (MP). Moreover, the maximum acceleration voltage decreases gradually year by year. In the following sections, we report our experiences collected from the SRILAC over a four-year operation period and provide insights on improving the degradation of the SC cavities.

SRILAC OVERVIEW

The RIKEN superconducting heavy-ion linac (SRILAC) comprises three cryomodules (CMs), CM1, CM2, and CM3,

* nsakamoto@ribf.riken.jp

COPPER PLATING QUALIFICATION PROCESS FOR THE FUNDAMENTAL POWER COUPLER WAVEGUIDES FOR CEBAF CRYOMODULES*

L. Zhao[#], G. Cheng, K. M. Wilson, G. Ciovati
Thomas Jefferson National Accelerator Facility, Newport News, VA, USA

Abstract

To provide sufficient energy for CEBAF operation, cryomodules and components are being refurbished yearly as necessary. Copper-plated fundamental power coupler waveguides are important components of the cryomodules. The integrity and quality of copper plating is critical to reduce the heat load from the waveguides into the He bath at 2.07 K. A search of copper plating resources is underway for plating or re-plating CEBAF-style waveguides. This effort ensures a continuous capability of copper plating on cryomodule components, especially on waveguides. To qualify plating vendors, the waveguide copper plating specifications were revisited, and a thorough plating evaluation process is being developed. The evaluation process ranges from coupon testing to sample waveguide qualification. Recent results are summarized and future work is planned.

BACKGROUND

The CEBAF cryomodules use a waveguide (WG) with rectangular cross-section as a fundamental power coupler (FPC) [1, 2] (Figure 1). In C100 cryomodules, the cold waveguide connects to the cavity flange directly [3]. In C20 and C75 style cryomodules, the FPC waveguide connects to the cold section at a flange on the helium vessel. The interiors of these waveguides are copper plated. It has been 30 years since the initial fabrication and installation of some of the C20 style waveguides.

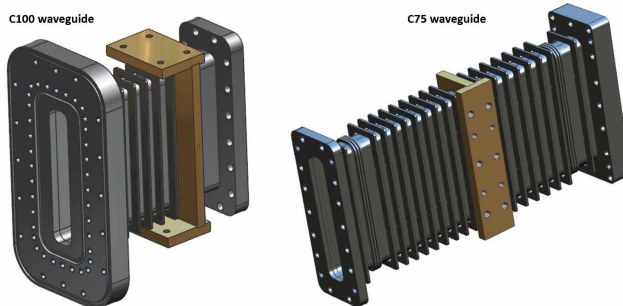


Figure 1: 3D models of C100 and C75 waveguide.

As an effort to maintain the beam energy in the CEBAF accelerator, selected cryomodules are being refurbished each year to recover their performance from degradation [4]. The components in these cryomodules are

being reused or replaced. Waveguides can be reused as long as critical features have not been compromised.

During cryomodule refurbishment, it was noticed that the copper plating on some of the waveguide has deteriorated. It is necessary to restore the copper plating on these WGs to ensure satisfactory performance. The original plating vendor is no longer available and new ones need to be found.

WAVEGUIDE COPPER PLATING SPECIFICATION CONSIDERATIONS

The original CEBAF waveguide (C20) plating thickness requirement was $1.5 +0.5/-0.3 \mu\text{m}$ from inner flange to heat transfer plate, and $3 \pm 1 \mu\text{m}$ from heat transfer plate to outer flange [5]. These values were based on theoretical analysis of static and dynamic heat load on the waveguide [6]. In practice, data from operation experiments and simulation indicates that the copper plating thickness is likely not uniform. An average of $0.2 \mu\text{m}$ is estimated from the simulation, much less than specified [7]. This can mean there may be areas missing copper plating.

The non-uniformity of plating thickness is difficult to avoid due to the nature of the traditional electro-plating process. During this process, the valleys in the convolutions of bellows are much harder for copper ions to reach, comparing with reaching flat surfaces. Therefore, inside the convolutions of the bellows the plating thickness could be significantly thinner than in other areas. A more realistic goal for plating thickness variation is about $5 \mu\text{m}$, based on feedback from industry practice and experience from other projects [8-10]. Taking this variation into consideration, the plating thickness requirement for C75 waveguide was changed to $10 \pm 5 \mu\text{m}$. This helps reduce the chance of having unplated areas when the required plating thickness is too thin.

To evaluate the impact of changing plating thickness requirement on the total heat load, a 2D numerical analysis of C75 WG total heat load was done for plating thickness ranging from $0.2 \mu\text{m}$ to $15 \mu\text{m}$. This range covers possible plating thickness scenarios using both the original requirement and the new requirement. This calculation adopted the same method as mentioned in reference [7], using a 2.78-inch wide thermal intercept plate to evaluate heat loads from 8 kW forward power. The results (Table 1) show that the $10 \pm 5 \mu\text{m}$ specification yields lower 2 K heat load as compared with the $0.2 \mu\text{m}$ case, indicating that the new coating thickness specification is acceptable.

* Work supported by Jefferson Science Associates, LLC, under U.S. DOE contract DE-AC05-06OR23177.
[#] lzhaoy@jlab.org

THEORETICAL MODEL OF EXTERNAL Q TUNING FOR AN SRF CAVITY WITH WAVEGUIDE TUNER*

Wencan Xu^{†,1}, Z.A. Conway¹, E. Daly², J. Guo², R.A. Rimmer², K. Smith¹, A. Zaltsman¹

¹Brookhaven National Laboratory, Upton, NY, USA

²Thomas Jefferson National Accelerator Facility, Newport News, VA, USA

Abstract

Brookhaven National Laboratory (BNL) and Thomas Jefferson National Accelerator Facility (TJNAF) are collaborating on the design and construction of the next Electron Ion Collider (EIC) to be built at BNL. The EIC is a unique high-energy, high-luminosity, polarized electron-proton/ion collider. A wide range of electron beam energies (5 – 18 GeV) and beam currents (0.2 – 2.5 A) are planned for the EIC Electron Storage Ring (ESR). The wide range of operating scenarios requires an adjustable coupling factor, ~20, for each of the 591 MHz Superconducting Radio Frequency (SRF) cavity. Each ESR cavity has two fundamental power couplers (FPC) delivering continuous wave (CW) 2 x 400 kW (800 kW total) RF power to the beam. Currently, adjusting external Q of an SRF cavity is done by varying protrusion of FPC's inner conductor in beam pipe or using three stub tuner to adjust external Q value, which either has limit on tuning range or limit on operating power. This paper presents a method of tuning the FPC external Q by a waveguide tuner, which allows for higher power, wide tuning range operations. A prototype of the waveguide tuner was tested up to CW 1 MW. Detail waveguide tuner design and the prototype test results will be presented.

INTRODUCTION

The EIC [1] to be built at BNL will be a discovery machine, providing answers to long-elusive mysteries of matter related to our understanding of the origin of mass, structure, and binding of atomic nuclei that make up the entire visible universe. The hadron beams in EIC will be provided by an upgraded version of the Relativistic Heavy Ion Collider [2] (RHIC) accelerator system at BNL. The electron beams in EIC will be provided by a new electron accelerator, including a pre-injector linac, a Rapid Cycling Synchrotron (RCS) and an ESR. Figure 1 shows the RF systems layout for the EIC. In the EIC ESR, there are 17 single-cell 591 MHz SRF cavities which must operate over a wide range of parameters to satisfy the various EIC operating scenarios. Each cavity has two high power FPCs to deliver up to CW 400 kW each to beam. Table 1 lists the EIC ESR SRF cavity operating scenarios. Notice that the cavity's external Q (Q_{ext}) varies by more than a factor of 15 from $2.6E4$ to $3.6E5$ reducing the total required RF power. Adjusting a Q_{ext} under such high power in CW operation is a challenge for the EIC. This paper proposes a high power large range Q_{ext} tuning mechanism based on a variable waveguide tuner.

* This work is supported by Brookhaven Science Associates, LLC under Contract No. DE-SC0012704 with the U.S. Department of Energy.

[†] wxu@bnl.gov

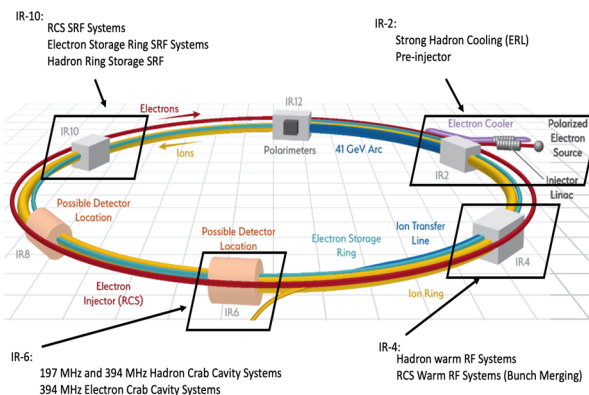


Figure 1: RF systems in EIC.

Table 1: EIC ESR Operation Scenarios

ESR RF Parameter	Unit	18 GeV	10 GeV	5 GeV
Number of Bunches		290	1160	1160
Average Beam Current	A	0.23	2.50	2.50
Energy Loss per Turn	MeV	37.0	3.52	0.95
Total Power to Beam	MW	8.4	10.7	2.9
Total Voltage	MV	61.5	21.6	9.8
PhiS	Deg	142.9	170.0	173.1
Power per FPC	kW	296	380	105
Optimal Cavity Q_{ext}		3.6×10^5	3.9×10^4	2.6×10^4

WAVEGUIDE TUNER DESIGN

System Matching Concept

The impedance presented by the beam-cavity system to the RF source determines the power transfer efficiency to the beam. The function of the waveguide tuner is to match the beam to the RF source impedance. Figure 2 (top) shows the simplified schematic diagram of the RF system with a tuner. In practice, the waveguide tuner acts like an additional current I_{tuner} , due to the RF reflection from the waveguide stub. I_{tuner} and I_g , the generator current comprise I_{load} , and I_{load} vector summed with I_b gives I_c , the cavity current. The phasor diagram of the RF system is shown in Fig. 2(bottom) for illustrational understanding. The system matches when the imaginary part of I_{load} and I_b cancel each other. If the waveguide tuner was not there $I_{load} = I_g$, i.e., the generator not only has to provide the resistive contribution to beam loading but also the additional reactive power necessary for cancelling the imaginary part of the beam loading, which is an obviously low efficiency system in spite of its unaffordability. Thus, an adjustable tuner is crucial. As illustrated in Table 1, the beam current in EIC ESR

Content from this work may be used under the terms of the CC BY 4.0 licence (© 2023). Any distribution of this work must maintain attribution to the author(s), title of the work, publisher, and DOI

TEST-STAND FOR CONDITIONING OF FUNDAMENTAL POWER COUPLERS AT DESY

K. Kasprzak[†], T. Buettner, A. Goessel, D. Klinke, D. Kostin, C. Mueller, E. Vogel, M. Wiencek
Deutsches Elektronen-Synchrotron DESY, Germany

Abstract

During the construction of the European-XFEL, activities related to Fundamental Power Couplers (FPCs) were outsourced to external partners and the former FPC test-stand area at DESY was given up due to infrastructure rearrangements. For the study of various European-XFEL upgrade scenarios a new test-stand for conditioning of FPCs at DESY is required. It will be used for evaluation of new coupler preparation methods with particular emphasis on Continuous Wave (CW) and long RF pulse operation. The new test-stand has been recently commissioned. Four FPCs have been prepared and tested. RF pulses were applied to the couplers, starting with the shortest possible pulse and increasing its power until maximum power was reached. The process was repeated with several pulse lengths until the maximum RF pulse length was reached. A review of the commissioning and first operation experience of the RF system are presented here.

INTRODUCTION

The European-XFEL utilizes a short flat-top pulse (0.65 ms) at 10 Hz repetition rate. In order to explore potential upgrades, such as continuous wave (CW) or long pulse (LP) modes, investigations are being conducted [1, 2]. The possible upgrade of the linear accelerator corresponds to the reduction of the operating

gradient of the 1.3 GHz cavities and increase of the heat loads [3]. These limitations will apply to the European-XFEL Fundamental Power Couplers (FPCs) as well.

FPCs consists of warm, cold and waveguide main parts (see Fig.1). FPC is used to deliver the energy carried by the radio frequency (RF) fields into the cavity, ultimately to the beam. To maintain the desired operating conditions of the cavities, which operate at a temperature of 2 K, it is necessary to isolate the cavity from the environment, particularly atmospheric temperature and pressure. The European-XFEL 1.3 GHz couplers achieve this isolation through two cylindrical RF windows and a vacuum. There are three separate vacuums related to FPCs: the beam vacuum (in the RF cavity), the isolation vacuum (surrounding the coupler in the cryomodule), and the coupler vacuum (between two RF windows).

The ceramic RF windows are coated with a thin titanium nitride (TiN) layer, which suppresses the secondary electron emission. Aside from ceramic windows and the antenna part on the cold side of the coupler (which is made out of oxygen free copper), the remaining components are made of stainless steel and are coated partially with a layer of copper. To overcome concerns about an overheating of the inner conductor bellow during CW and LP mode operations, the design of the new European-XFEL couplers has been updated [4].

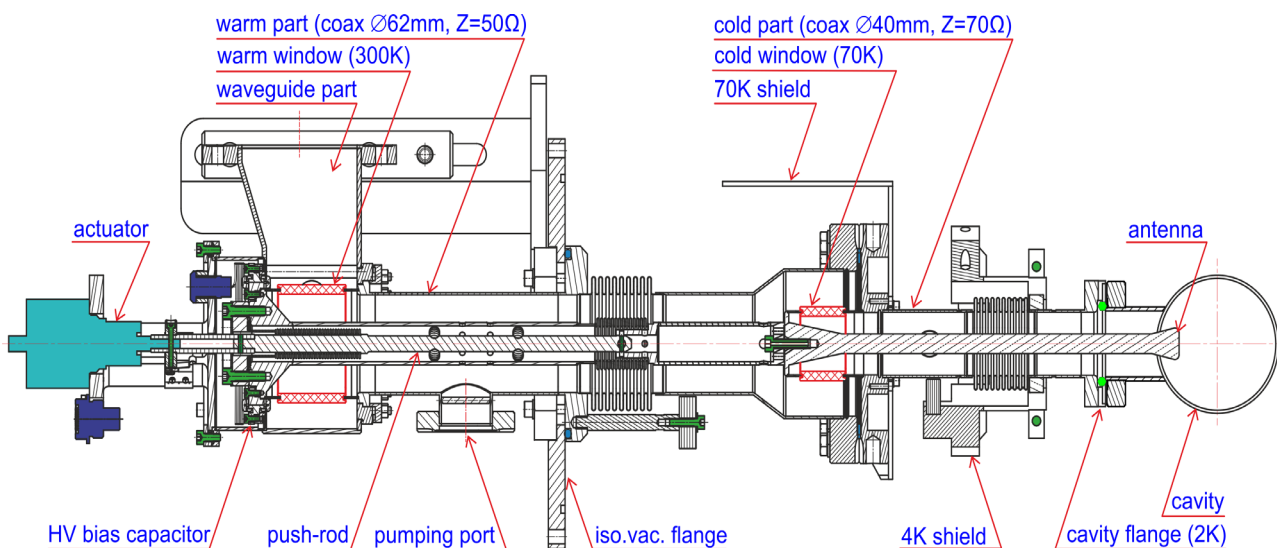


Figure 1: European-XFEL 1.3 GHz FPC.

[†] karol.kasprzak@desy.de

TRANSPORTATION FATIGUE TESTING OF THE pHB650 POWER COUPLER ANTENNA FOR THE PIP-II PROJECT AT FERMILAB*

J. Helsper[†], S. Chandrasekaran, J. Holzbauer, N. Solyak
FNAL, Batavia IL, USA

Abstract

The PIP-II Project will see international shipment of cryomodules from Europe to the United States, and as such, the shocks which can occur during shipment pose a risk to the internal components. Of particular concern is the coupler ceramic window and surrounding brazes, which will see stresses during an excitation event. Since the antenna design is new, and because of the setback failure would create, a cyclic stress test was devised for the antenna. This paper presents the experimental methods, setup, and results of the test.

INTRODUCTION

The Proton Improvement Plan II (PIP II) is a multinational project which will overhaul Fermi National Accelerator Laboratory's (FNAL) linear accelerator (linac) [1]. FNAL will receive overseas shipments via land and air of cryomodules (CM), individual linac sections, from both the Commissariat à l'Énergie Atomique et aux Énergies (CEA) of France and the Science and Technology Facilities Council as part of the UK Research Innovations (STFC-UKRI) of the United Kingdom. These shipments pose significant risk to the CMs if not carefully considered.

The first CM to ship will be the prototype high-beta 650 MHz (HB650) CM [2], which was evaluated for the rigors of transportation analytically [3], and for which the shipment frame [4] has been tested [5]. The low-beta 650 MHz (LB650) CM [6] will also be transported overseas to FNAL.

The RF couplers [7] used on these CMs are of a novel design, having a single ceramic window brazed to thin copper sleeves isolating the beamline vacuum from atmosphere. Given this, and that past CM shipments have seen failure occur at the couplers [8], a higher level of scrutiny has been applied to the design to ensure its readiness for transport as part of the CM shipments. The vacuum side coupler assembly is shown in Fig. 1.

METHODOLOGY

To validate the 650 MHz coupler design (used on both HB650 and LB650 CMs), first the dynamic behavior was checked. Measurement of the antenna's first resonant frequency and estimation of mechanical damping, coupled with information on the transportation itself, allowed for an estimation of the total number of stress-inducing oscillations the coupler can experience. With this number, the antenna was

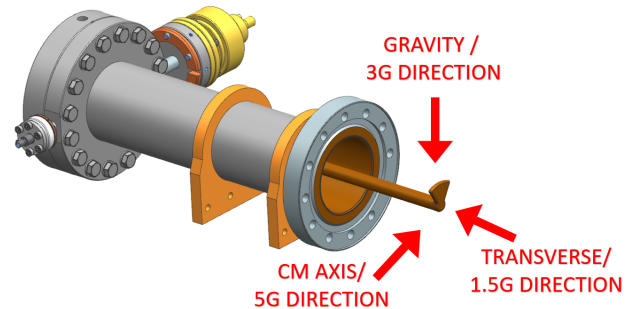


Figure 1: pHB650 coupler vacuum side assembly.

then forcibly displaced to simulate the shocks experienced during transportation, in fully reversed cycles. The deformation was applied slowly to prevent any dynamic effects, and the stress created as a result was considered quasi-static (i.e. equivalent to that of a static-structural finite element analysis). The resonance which followed any excitation was assumed to take the form of a similar stress state, as the fundamental resonant mode is that of a simple cantilevered beam.

While not identical to the true excitation scenario (large, sudden shocks), displacement of the antenna creates a near identical stress state. The effects of multiple shocks occurring within the mechanical decay period of the antenna are excluded by this method, but accounted for in the high factor of safety (FOS) in the final number of completed cycles.

A shaker test, while valuable for certain components, was not selected for the coupler antenna since the excitation of the antenna can be difficult to control accurately and the amplitude of movement could quickly exceed any realistic values, leading to lasting and unnecessary damage.

ANALYSIS

Mechanical/Stress Response

The shipping frame [4] of the HB650 CM is designed to limit shocks to 3 G vertical, 5 G axial, and 1.5 G transverse. The frame also isolates shocks above 10 Hz by at least 80%, relative to the input excitation. See Fig. 1 for the aforementioned directions. The 5 G axial shocks, coupled with the effects of gravity (5 G+1 G) are considered to be the worst case scenario.

To determine the required applied displacement to mimic 5 G+1 G, an ANSYS® model of the antenna was used. The boundary conditions account for vacuum, and are shown along with the mesh in Fig. 2. Only solid hexahedral mesh was used in the high stress areas, and all objects had a minimum of three elements through the thickness.

* Work supported, in part, by the U.S. Department of Energy, Office of Science, Office of High Energy Physics, under U.S. DOE Contract No. DE-AC02-07CH11359.

[†] jhelsper@fnal.gov

DESIGN, MANUFACTURING, ASSEMBLY, AND LESSONS LEARNED OF THE PRE-PRODUCTION 325 MHz COUPLERS FOR THE PIP-II PROJECT AT FERMILAB*

J. Helsper^{1,†}, S. Wallon², D. Passarelli¹, D. Longuevergne², S. Kazakov¹, N. Solyak¹

¹FNAL, Batavia, IL, USA

²Université Paris-Saclay, CNRS/IN2P3, IJCLAB, Orsay, France

Abstract

Five 325 MHz high-power couplers will be integrated into the pre-production Single Spoke Resonator Type-II (ppSSR2) cryomodule for the PIP-II project at Fermilab. Couplers were procured by both Fermilab and IJCLAB for this effort. The design of the coupler is described, including design optimizations from the previous generation. This paper then describes the coupler life cycle, including design, manufacturing, and assembly, along with the lessons learned at each stage.

INTRODUCTION

The pre-production Single Spoke Resonator Type-II (ppSSR2) couplers will provide radio frequency (RF) input to the superconducting accelerating cavities housed within the ppSSR2 cryomodule (CM) [1], which is part of the PIP-II Project [2]. Five ppSSR2 couplers will be used in the ppSSR2 CM string. Nine ppSSR2 couplers were procured; five being procured by FNAL, and four being procured and contributed in-kind by IJCLAB [3]. The ppSSR2 couplers are predated by the prototype Single Spoke Resonator Type-I (pSSR1) couplers [4], which were successfully used and tested on the pSSR1 CM [5]. The ppSSR2 couplers share many design details with the prototype High Beta 650 MHz (pHB650) couplers, which are also part of the PIP-II Project [6].

DESIGN

The critical design components of the ppSSR2 coupler are shown in Fig. 1.

A single alumina ceramic window separates the beam-line volume from atmosphere. The window is brazed to pliable copper sleeves which allow for thermal expansion without undue stress. The copper antenna contains an internal stainless steel (SS) tube which provides cooling air and additional stiffness necessary for transportation and handling. TiN coating was applied to several of the alumina windows, and the results are discussed separately [7]. A high voltage (HV) bias of 3.5 kV is maintained during operation between inner conductor/antenna and the outer conductor, resulting in suppressed multipacting activity. The antenna tip is symmetric and fixed, and so Qext is not adjustable.

* Work supported, in part, by the U.S. Department of Energy, Office of Science, Office of High Energy Physics, under U.S. DOE Contract No. DE-AC02-07CH11359.

† jhelsper@fnal.gov

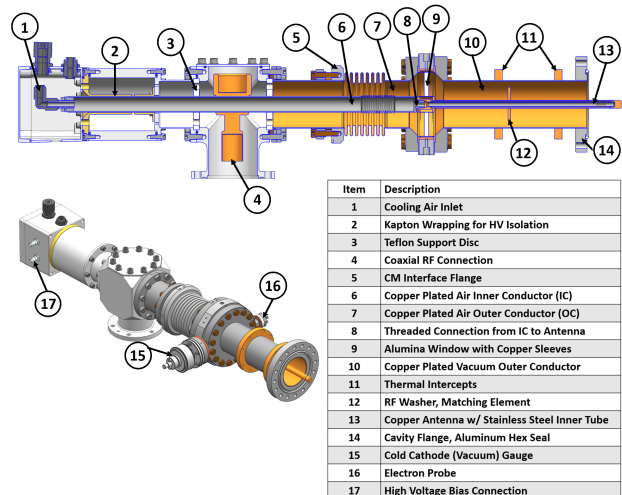


Figure 1: The full ppSSR2 coupler assembly.

The antenna assembly, cold outer conductor (OC), air inner conductor (IC), and air OC were all designed to be furnace brazed. The cold OC is plated with 12 microns of OFHC copper to reduce RF losses.

The DC Block, shown in Fig. 2, serves to isolate the coupler input and protect the RF amplifier from HV bias.

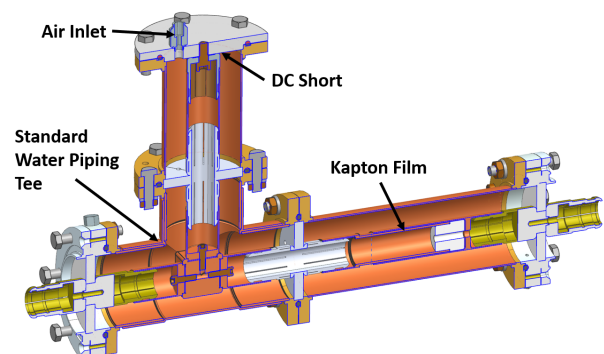


Figure 2: DC block design.

Changes from Previous Design

The pSSR1 coupler design [4] is shown in Fig. 3. The following is a summary of the major design changes implemented on the ppSSR2 couplers: air inlet tube changed from removable to fixed, air outer conductor has a single bellow and is copper plated, the ceramic disk stress relief sleeves

Content from this work may be used under the terms of the CC BY 4.0 licence (© 2023). Any distribution of this work must maintain attribution to the author(s), title of the work, publisher, and DOI

TESTING OF PIP-II PRE-PRODUCTION 650 MHz COUPLERS IN WARM TEST STAND AND CRYOMODULE

N. Solyak[†], S. K. Chandrasekaran, B. Hanna, J. Helsper, J. Holzbauer, S. Kazakov, A. Sukhanov
Fermilab, Batavia, USA

Abstract

650 MHz fundamental power couplers were developed for PIP-II project to deliver RF power for low-beta and high-beta elliptical cavities [1]. Few prototypes were built and tested and after some modification we built 8 pre-production couplers (with three spares for vacuum side) for ppHB650 cryomodule. All couplers were successfully tested in pulse mode (up to 100 kW) and in CW mode (up to 50 kW) in test stand at full reflection at 8 phases. In baseline configuration with DC bias we do not see any multipactoring activity after short processing. We also tested power processing without bias for uncoated and TiN coated ceramic window. Results of these studies presented in this paper. One of the coupler was assembled on LB650 cavity and tested at cryogenic environment in STC cryostat at ~30 kW power with full reflection at different reflection phase. We also demonstrated good result from power processing without bias for warm and cold cavity. Six couplers were assembled on HB650 cavities in pre-production cryomodule. Test results from cryomodule qualification is discussing in this paper.

INTRODUCTION

In PIP-II project both LB650 and HB650 cavities will use same design for 650 MHz fundamental power coupler. Mechanical model of pre-production coupler design is shown in Fig. 1 [2]. Coupler consist of few sub-assemblies: vacuum side, air side, wave-guide assembly and instrumentation box. Ceramic window is part of vacuum assembly and separate vacuum from the air. Antenna and all air side components are cooled by dry air.

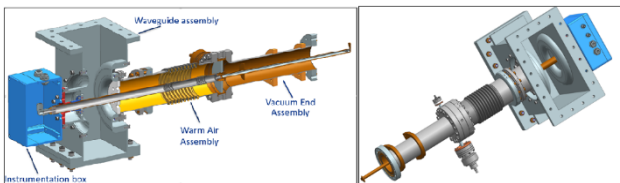


Figure 1: Mechanical design of the 650 MHz pre-production coupler. Cut-view on the left picture. Vacuum gauge and pickup antenna are located near the ceramic window.

Current design of the coupler is based on experience learnt from building and testing two coupler prototypes: one is conventional design and another is RF shielded design, details and test result was reported in paper [3, 4]. Two vacuum parts of each design were built by CPI, both

designs demonstrated good performances [3, 4]. For production we choose convention design which looks simpler in manufacturing and lighter which is beneficial to eliminate potential transportation problem. Several modifications were introduced in the pre-production design to compare with prototype [2]. Major modifications in pre-production couplers are the following:

- Thicker ceramic window: 7 mm vs. 6 mm.
- Conflat flanges for warm to cold connection and for connection antenna assembly to vacuum outer conductor to replace aluminum diamond seal flanges.
- Standard WR1150 waveguide (instead of narrow two steps waveguide) matched to coaxial coupler.
- Vacuum gauges located in vicinity of window.
- Pickup antenna is longer and moved closer to ceramic
- Modification of air cooling channel design
- Modification of instrumentation box.

As a result waveguide heating reduced, passband increased, added vacuum diagnostics, stresses on ceramic window decreased and assembly process improved.

For HB650 prototype cryomodule project built 8 pre-production couplers and extra 3 cold-end assemblies at Canon/Japan. All couplers were accepted and qualified in coupler test stand. We tested coupler pairs 1&2; 3&4; 5&6; 8&9 and 10&11 with DC bias at 50kW CW full reflection. Pair 10&11 was also tested without DC bias for coupler #11. Two couplers after tests received TiN coating of vacuum side of ceramic at CPI (#7 and #11) and currently assembled for testing performance with and without DC bias.

Additional to that coupler #7 was used for fatigue test and couplers #7 and #11 for the pressure tests.

Power Specification

Most strict power requirements for 650 MHz coupler comes from high-beta HB650 cavities. Maximum forward power in operation with 2 mA beam is ~43 kW with 20% reflection, but most of time linac will work in regime without beam at ~30 kW forward power. Total power (forward + reflection) in both cases more or less the same < 60 kW (Figure 2). Test stand power requirements for the coupler is higher: 50 kW CW at full reflection at arbitrary reflection phase. Power overhead allows cover cavity operation at higher gradient with high detuning from microphonics and tolerate higher coupling errors.

* Work supported, in part, by the U.S. Department of Energy, Office of Science, Office of High Energy Physics, Under U.S. DOE CONTRACT NO. DE-AC02-07CH11359.

[†]solyak@fnal.gov.

TESTING AND PROCESSING OF PRE-PRODUCTION 325 MHz SINGLE SPOKE RESONATOR POWER COUPLERS FOR PIP-II PROJECT

N. Solyak^{†,1}, B.Hanna¹, J.Helsper¹, S.Kazakov¹, D. Passarelli¹, S. Wallmon²
¹FNAL, Batavia IL, USA

²Université Paris-Saclay, SNRS/IN2P3, IJCLAB, Orsay, France

Abstract

Fundamental 325 MHz power couplers are designed, built and tested for SSR cavities in PIP-II project. Couplers should work in CW mode at power level 7.5 kW w/o beam and ~15 kW with the 2 mA beam. At pre-production stage we built and tested 6 couplers, produced by CPI (FNAL) and PMB (IJCLab) and 4 more couplers will be tested soon. Two of tested couplers had TiN coated ceramic window. In warm test stand two couplers were mounted on the coupling chamber and tested in SW regime at full reflection with phase controlled by position of short and reflection insert. Couplers were tested at pulse mode (up to 25 kW) and cw mode (12 kW) with HV bias or without bias. Test results demonstrated that 3.5 kV DC bias completely suppresses multipactor in coupler. Vacuum activity in coupler was controlled by e-pickups and build-in vacuum gauges, located near the vacuum side of window. Power processing without DC bias was done for several couplers with and without TiN coating on ceramic window. Test results are presented and discussing in paper.

INTRODUCTION

First generation of SSR couplers, called prototype, was built for pre-production SSR1 cryomodule (ppSSR1) [1-3]. Finally we tested around 10 couplers in warm test stand and in cold environment on STC (superconducting test cryomodule) with SSR1 cavities. Eight of them were then assembled on pre-production SSR1 cryomodule and successfully tested at full available power, 8 kW CW [4-6]. Based on experience with prototype coupler as well as experience with 650 coupler we modified design of SSR2 coupler taking into account higher power requirements for SSR2 cavities [7]. For example, design of the ceramic window brazed to flange is practically the same as for 650 pre-production coupler, which allow to use same proven brazing technology. General view of 325 MHz coupler is shown in Fig. 1.

It consist of vacuum end assembly, air side assembly and instrumentation box. Ceramic window separates vacuum from air side. Vacuum gauge and pick-up antenna (not visible here) are located on vacuum outer conductor flange near the window. More details on coupler design can be found in paper [7] presented in this conference. Same design of coupler are used for SSR1 and SSR2 couplers, required coupling is provided the appropriate geometry of the coupling port in cavity.

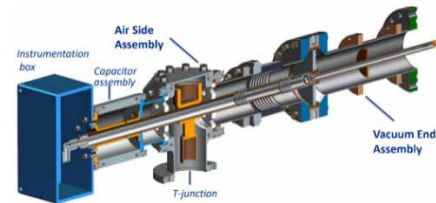


Figure 1: Cut view of the 325 MHz coupler.

At pre-production stage we built 5 full couplers and one antenna assembly in CPI. Additional to that PIP-II partner lab, IJCLAB, built 4 couplers in PMB, two cold parts were delivered to Fermilab for testing. Two vacuum end (one CPI, one PMB) have a problem with antenna (bent or damaged) and were not used in RF qualification tests. Other six couplers were successfully tested. Window on two couplers (one CPI and one PMB) were TiN coated from vacuum side. All couplers were tested with DC bias 3-3.5 kV (baseline regime of operation), but in test where we have TiN coated coupler we also did power processing without DC bias to clean coupler surfaces by MP discharge. 3 RF qualification tests were completed:

- coupler 1&4 (CPI, both no TiN coating) – with DC bias
- coupler 3&6 (both CPI, one TiN coated) with and without DC bias
- coupler 2&1' (CPI uncoated and PMB TiN coated) with and without DC bias

COUPLER TEST STAND

Two vacuum ends of the couplers are assembled on coupling cavity in clean room, pumped out and leak checked. After vacuum baking at 120°C for 48 hours with active pumping and RGA measurements. Subassembly then moves to the testing cave where air side of the couplers, DC blocks and other connections are assembled in warm test stand as shown schematically in Fig. 2.

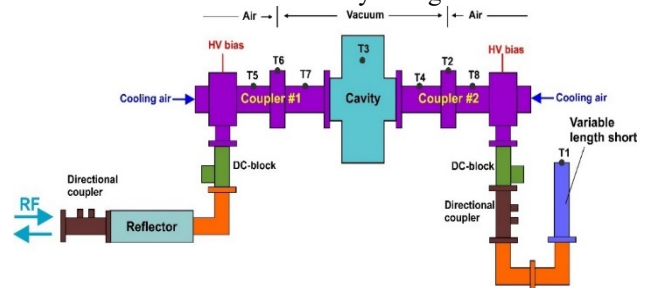


Figure 2: Schematic view of coupler test stand.

In this setup we have a resonance condition with standing wave between short and reflector, it allow amplify power by factor of 4-5 to get 30-40 kW using available 8 kW power source.

* Work supported, in part, by the U.S.Department of Energy, Office of Science, Office of High Energy Physics, Under U.S. DOE CONTRACT NO. DE-AC02-07CH11359.

[†]solyak@fnal.gov.

DEVELOPMENT AND EVALUATION OF STF-TYPE POWER COUPLER FOR COST REDUCTION AT THE HIGH ENERGY ACCELERATOR RESEARCH ORGANIZATION

Yasuchika Yamamoto[†], Shinichiro Michizono, Toshihiro Matsumoto
High Energy Accelerator Research Organization, Tsukuba, Japan

Abstract

At the High Energy Accelerator Research Organization, cost reduction study for STF-type input power coupler used in the STF-2 accelerator has been attempted since FY2015. In FY2019, one cold coupler was fabricated by some cost-effective and non-conventional methods including different alumina-ceramic material, copper plating and TiN coating. In high power RF test at room temperature, this coupler achieved 1 MW at 900 $\mu\text{sec}/5$ Hz, and 935 kW at 1.65 msec/5 Hz. After that, this coupler experienced 10 thermal cycle tests from room temperature to liquid nitrogen temperature without vacuum leakage. In this report, the detailed results will be presented.

INTRODUCTION

Since 2017, the High Energy Accelerator Research Organization (KEK) has been conducting a new research and development project to reduce the cost of superconducting cavities under the Japan-U.S. Science and Technology Cooperation. The main goal of this project is to find the best surface treatment for the cavities, on the other hand it also includes R&D on ancillaries such as input couplers, etc. The input couplers used in the STF cryomodules are of the STF type with two disc-washer ceramic pieces on the cold and warm sides. In order to reduce the cost of this input coupler, a new input power coupler was manufactured by changing the titanium nitride (TiN) coating applied to the ceramic and copper plating, and its performance was evaluated on a test bench at STF. At the same time, we selected ceramic materials because the ceramic manufacturer that had been used at KEK withdrew from the market a few years ago, and it became necessary to find a new manufacturer. In the following sections, each process will be described in detail. The previous studies on the STF-type power coupler are described in [1-3].

PRODUCTION OF STF-TYPE POWER COUPLER FOR COST REDUCTION

Mock-up Study for Copper Sulfate Plating

In this production, we decided to change the copper plating from pyrophosphate copper plating to copper sulfate plating. In our previous research, we had found that copper sulfate plating had a better yield and a higher RRR at low temperature. However, this was the first time copper sulfate plating had been applied to the STF-type input couplers, therefore a mock-up was manufactured first, and a

damage test was conducted after heat treatment and ultrasonic cleaning. The results were satisfactory, and we were able to proceed with the manufacturing of the real cold power coupler without any problems. Figure 1 shows this mock-up of the STF-type cold power coupler.



Figure 1: Mock-up of STF-type cold power coupler for the study of copper sulfate plating.

Titanium-Nitride Coating on Ceramics

In this production, the ceramic material was also changed from the conventional material. This is because the ceramics long used at KEK are no longer available due to the withdrawal of the manufacturer. Therefore, AL300 (Morgan Advanced Materials), which has been also used in E-XFEL, was selected as good candidate. The side planes (inner/outer) are metalized for brazing as shown in Figure 2.

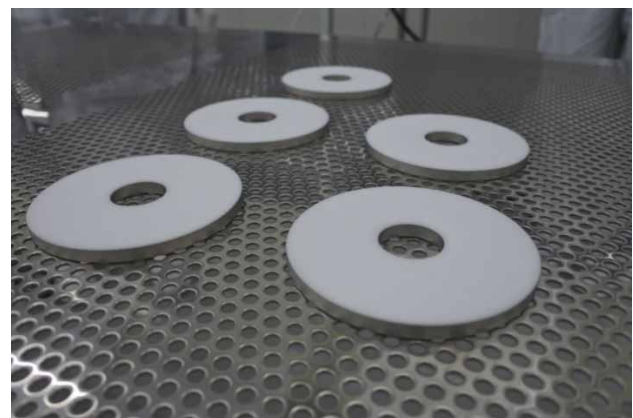


Figure 2: Five metalized disk-washer type ceramics for RF window.

[†] yasuchika.yamamoto@kek.jp

PRESENT STATUS OF RIKEN POWER COUPLERS FOR SRILAC

K. Ozeki[†], O. Kamigaito, N. Sakamoto, K. Suda, K. Yamada
RIKEN Nishina Center, Wako, Japan

Abstract

The heavy ion linac of the RIKEN, utilizing superconducting technology, began operations in September 2019. Over the following 13 months, two of the ten superconducting accelerating cavities experienced vacuum leaks from the vacuum windows of the fundamental power couplers (FPCs). Currently, additional vacuum windows are installed on all ten FPCs, and the beam supply continues without encountering any major issues with the FPCs. Additionally, the fabrication of ten replacement FPCs has been completed, addressing the underlying issues that led to the deterioration of the vacuum window strength. Currently, we are conducting radio frequency (RF) process of the new FPCs. In addition, we are designing a bias applying component to suppress multipacting in the FPCs. This paper reports the status of these issues related to the FPCs at the RIKEN.

INTRODUCTION

In RIKEN Nishina Center, the RIKEN Heavy Ion Linac (RILAC) [1] had been used to supply intense beams for the synthesis of super-heavy elements (SHEs) [2]. Additionally, it serves as an injector for the following radio isotope beam factory (RIBF) accelerator complex comprising four ring cyclotrons [3].

RILAC has been upgraded for the synthesis of new SHEs ($Z > 118$) and production of radioactive isotopes for medical use. As part of this upgrade, a superconducting linac (SRILAC) [4-10] was constructed and installed downstream of the RILAC (see Fig. 1) to enhance the acceleration voltage. The SRILAC consists of three cryomodules with ten superconducting quarter-wavelength resonators (SC-QWRs). The two upstream cryomodules have four SC-QWRs each, and the one downstream cryomodule has two SC-QWRs.

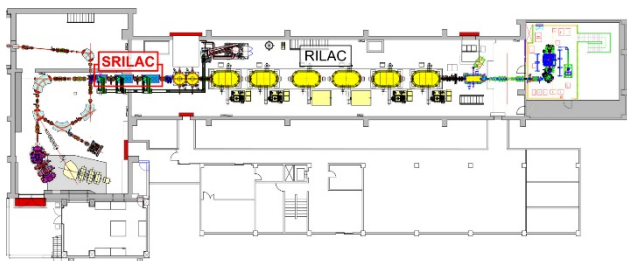


Figure 1: Overview of the RILAC and SRILAC.

Each SC-QWR was equipped with a fundamental power coupler (FPC) with a single-disc-type vacuum window. A schematic representation of the FPC is shown in Fig. 2. The inner conductor (IC) and outer conductor (OC) are com-

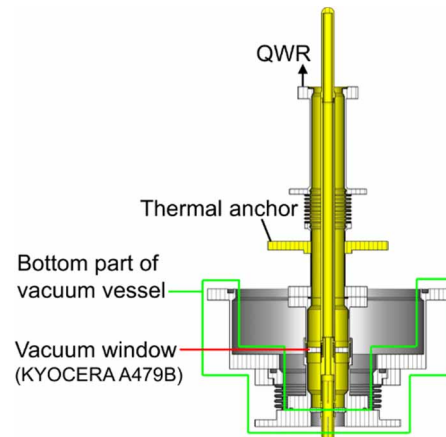


Figure 2: Schematic of the FPC.

posed of bulk copper and copper-plated stainless steel, respectively. A thermal anchor was connected to a thermal shield cooled using liquid nitrogen.

VACUUM LEAKS FROM FPCS

The installation of cryomodules on the beamline was completed in March 2019, and the cooling tests began in September 2019. In November, during repeated cooling tests, the first vacuum leak occurred in the vacuum window of an FPC. The vacuum leakage into the cavity was stopped via an evacuation from the atmospheric side of the vacuum window (the RF supply to that cavity was no longer available). Beam acceleration tests were conducted using the remaining nine SC-QWRs, and the beam supply for the new SHE synthesis experiments began in June 2020.

The second vacuum leak occurred at another FPC in October 2020. The condition of the atmospheric side of the vacuum window was examined for all FPCs, and the dew condensation and rust were observed. The metallization of alumina used for the vacuum window deteriorated owing to galvanic corrosion, and the strength of the vacuum window brazing was reduced. This deterioration may have led to the vacuum leak. The vacuum leakage was stopped using the same method employed during the initial incident. The beam supply was continued using the remaining eight SC-QWRs, while dry nitrogen was introduced around the vacuum windows of the remaining eight FPCs to prevent dew condensation. Simultaneously, additional vacuum windows (outer windows) were developed, described in the next section.

INSTALLATION OF OUTER WINDOWS

To enable radio frequency (RF) supply and restore the two SC-QWRs that were no longer available for beam acceleration, outer windows were developed. A schematic of

[†] k_ozeki@riken.jp

RECENT PROGRESS OF FUNDAMENTAL POWER COUPLERS FOR THE SHINE PROJECT

Zhen-Yu Ma, Jin-Fang Chen[†], Yu-Bin Zhao, Hong-Tao Hou, Shen-Jie Zhao, Sen Sun,
Xiang Zheng, Yi-Yong Liu, Meng Zhang, Bo Liu, Li-Xin Yin, Dong Wang, Zhen-Tang Zhao
Shanghai Advanced Research Institute, Chinese Academy of Sciences, Shanghai, China

Abstract

The superconducting radio-frequency electron linear accelerator of the Shanghai High repetition rate XFEL aNd Extreme light facility contains 610 1.3 GHz fundamental power couplers which are assembled in 77 superconducting cryomodules used for beam acceleration, and 16 3.9 GHz fundamental power couplers, which are assembled in two third harmonic superconducting cryomodules used for linearizing the longitudinal phase space. The first batch of 26 1.3 GHz coupler prototypes and two 3.9 GHz coupler prototypes have been manufactured from three domestic manufacturers for basic research. Several key manufacturing processes have been developed and qualified, including high residual resistivity ratio copper plating, vacuum brazing of ceramic windows, electron beam welding and titanium nitride coating. All the 1.3 GHz coupler prototypes have been power conditioned with 14 kW travelling wave (TW) and 7 kW standing wave (SW) RF in continuous-wave (CW) mode. Even higher power levels have been demonstrated with 20 kW TW and 10 kW SW RF, which indicates their robustness. Both 3.9 GHz coupler prototypes have been power conditioned with 2.2 kW TW and 2 kW SW RF in CW mode.

INTRODUCTION

The Shanghai High repetition rate XFEL aNd Extreme light facility (SHINE) is a new continuous-wave (CW)

hard X-ray free electron laser (FEL) currently under construction in China [1-2]. The SHINE facility includes an 8 GeV superconducting linear accelerator (Linac), three undulator lines, three FEL beamlines, and the first ten experimental stations. The total facility length is 3110 meters, and the tunnels are buried 29 meters underground. Its goal is to be become one of the most efficient and advanced FEL user facilities in the world, providing high-resolution imaging and other X-ray methods for cutting-edge research in diverse fields, including physics, chemistry, life science, materials science, and energy science.

The fundamental power coupler (FPC), which is used to transmit a high radio-frequency (RF) power to the beam and providing isolation between atmospheric pressure and ultrahigh vacuum in the superconducting cavity through ceramic windows, is a crucial component of the superconducting cryomodules in the superconducting Linac [3]. The SHINE Linac contains 610 1.3 GHz FPCs which are assembled in 77 1.3 GHz superconducting cryomodules used for beam acceleration, and 16 3.9 GHz FPCs, which are assembled in two third harmonic superconducting cryomodules used for linearizing the longitudinal phase space before bunch compression [4, 5]. The SHINE 1.3 GHz FPCs, which are used for CW operation, are modified, and optimized based on the TTF-III coupler design developed at DESY for high power pulsed operation [6, 7]. The main technical parameters of the SHINE 1.3 GHz FPC are listed in Table 1, and the mechanical design of the SHINE 1.3 GHz FPC is shown in Fig. 1a.

Table 1: Main Technical Parameters of the SHINE 1.3 GHz and 3.9 GHz FPC

Parameters	1.3 GHz FPC Specification	3.9 GHz FPC Specification
Operating Frequency (GHz)	1.3	3.9
Type	Coaxial, Double-RF-window	Coaxial, Double-RF-window
Ceramic RF Window type	Cylindrical (cold) + Cylindrical (warm)	Cylindrical (cold) + Planar (warm)
Maximum power (kW)	7	1.8
External quality factor, Q_{ext}	4.12×10^7	2.13×10^7
Q_{ext} adjustment range	$4.0 \times 10^6 \sim 1.1 \times 10^8$	$1.0 \times 10^7 \sim 5.0 \times 10^7$
Antenna adjustment range (mm)	± 7.5	± 3

[†] email: Jin-Fang Chen (corresponding) chenjinfang@sari.ac.cn

SIMULATIONS AND FIRST RF MEASUREMENTS OF COAXIAL HOM COUPLER PROTOTYPES FOR PERLE SRF CAVITIES

C. Barbagallo^{1,*}, P. Duchesne, W. Kaabi, G. Olivier, G. Olry, S. Roset, F. Zomer¹
Laboratoire de Physique des 2 Infinis Irène Joliot-Curie (IJCLab), Orsay, France

J. Henry, S. A. Overstreet, G.-T. Park, R. A. Rimmer, H. Wang, JLab, Newport News, VA, USA

S. Barrière, S. Clement, R. Gérard, F. Gerigk, P. Maurin, CERN, Geneva, Switzerland

¹also at The Paris-Saclay University, Gif-sur-Yvette, France

Abstract

Superconducting Radio-Frequency (SRF) linac cryomodules are foreseen for the high-current multi-turn energy recovery linac PERLE (Powerful Energy Recovery Linac for Experiments). Coaxial higher order mode (HOM) couplers are the primary design choice to absorb beam-induced power and avoid beam instabilities. We have used 3D-printed and copper-coated HOM couplers for the prototyping and bench RF measurements on the copper PERLE cavities. We have started a collaboration with JLab and CERN on this effort. This paper presents electromagnetic simulations of the cavity HOM-damping performance on those couplers. Bench RF measurements of the HOMs on an 801.58 MHz 2-cell copper cavity performed at JLab are detailed. The results are compared to eigenmode simulations in CST to confirm the design. RF-thermal simulations are conducted to investigate if the studied HOM couplers undergo quenching.

INTRODUCTION

The PERLE accelerator [1] is a multi-turn energy recovery linac (ERL) comprising two 82 MeV superconducting linacs, each hosting four 5-cell elliptical Nb cavities ($\beta=1$) operating at 801.58 MHz in continuous-wave mode [2]. The installation of coaxial-type HOM couplers is being considered for mitigating beam-induced HOM effects. After optimizing the RF transmission of the Probe, Hook, and Double Quarter Wave (DQW) couplers using the HOM spectrum of the 5-cell PERLE cavity [3], we fabricated prototypes of each coupler [4] for validating their performance on an 801.58 MHz 2-cell PERLE-type Oxygen-free High Thermal Conductivity OFHC copper cavity (see Fig. 1). In the following, we first present external quality factor (Q_{ext}) measurements for the fundamental mode (FM) and trapped high- R/Q HOMs. The measurements were compared with eigenmode CST [5] results to validate the adequacy of our measurement setup. Then, we compare two suitable HOM-damping schemes for the 5-cell PERLE cavity based on their beam impedance and HOM power. Finally, we show the RF-heating results of the HOM-damping scheme with higher power absorption.

HOM COUPLER RF MEASUREMENTS

This section shows Q_{ext} measurements for FM, the first monopole (TM₀₁₁) and the first two dipole mode (TE₁₁₁

* carmelo.barbagallo@ijclab.in2p3.fr



(a)



(b)

Figure 1: The Probe, Hook, and DQW HOM couplers (from left to right) (a). HOM coupler on a 2-cell Cu cavity (b).

and TM₁₁₀) passbands, and compare them with simulations. The coupler prototypes were tested at JLab on a 2-cell 801.58 MHz Cu cavity at low power and room temperature (Fig. 1b). The S_{21} transmission is measured from a reference antenna (port 1) at the beam pipe opening to the HOM coupler port (port 2), considering different coupler orientations. The coupler antenna was set to penetrate the cutoff tube by 20 mm. The procedure to measure Q_{ext} for cavity modes involves several steps [6]. The loaded quality factor Q_1 is firstly determined by measuring S_{21} (in dB) transmission. The next step is to measure the coupling factor β , defined for a specific antenna (e.g., reference antenna at port 1) as

$$\beta = \frac{1 \pm |S_{11}|}{1 \mp |S_{11}|}, \quad (1)$$

where the upper sign applies in the case of over-coupling ($\beta > 1$), whereas the lower one stands for under-coupling ($\beta < 1$). In scenarios with weak coupling, the utilization of S_{11} or S_{22} in reflection-type measurements leads to notable errors. Consequently, we distinguish between two types of coupling coefficients for the input or coupler antenna: β_1 for large coupling ($\beta \approx 1$) with the electromagnetic (EM) field inside the cavity, and β_s for small coupling ($\beta \ll 1$). The large-coupling coefficient for a specific HOM is given by

RF CONDITIONING OF MYRRHA COUPLERS AT IJCLAB

N. Elkamchi, C. Joly, C. Magueur, P. Duchesne, S. Berthelot, W. Kaabi, C. Lhomme
Université Paris-Saclay, CNRS/IN2P3, IJCLab, Paris, France

Y. Gomez Martinez, Univ. Grenoble Alpes, CNRS, Grenoble INP, LPSC-IN2P3, Grenoble, France

Abstract

Multi-purpose hYbrid Research Reactor for High-tech Applications (MYRRHA) is an experimental accelerator-driven system in development at SCK-CEN. It will allow fuel developments, material developments for GEN IV systems, material developments for fusion reactors and radioisotope production for medical and industrial applications.

In the framework of the French contribution to MYRRHA project, the IJCLab has in charge the industrial monitoring, the quality control and the RF conditioning of the power couplers up to 80 kW at 352 MHz, to equip spoke cavity cryomodules.

This paper presents the conditioning bench adapted from the successful experience of IJCLAB in the conditioning of the XFEL couplers. The results of the conditioning of prototype couplers are described and discussed.

INTRODUCTION

The MYRRHA project [1] aims to build an Accelerator Driven System (ADS) at MOL (Belgium), driven by a superconducting LINAC (600 MeV, 4 mA proton beam), for irradiation and transmutation experiment purposes. The first section of the superconducting LINAC will consist of 352 MHz single spoke cavities housed in short cryomodules operating at 2K and powered by power couplers designed to support 80 kW CW at 352 MHz

Historically The IJCLab (formerly known as LAL) has acquired within the last fifteen years a large experience in power coupler treatment (mechanical design, RF simulation, vacuum studies, cleaning-assembling procedure and RF conditioning [2]). This experience started with TTF3 couplers that were prepared and conditioned at LAL and installed later at FLASH machine. After this successful experience, the LAL was involved in the industrialisation and the preparation of the 800 XFEL couplers [3].

The MYRRHA project is a part of this continuation; it will take advantage of the knowledge of the lab as well as the human and technical resources inherited from the former experiments.

MYRRHA PROTOTYPE POWER COUPLERS

The couplers series of MYRRHA is preceded by a pre-series of six prototype couplers, which will allow testing several manufacturing technologies to choose the best adapted to the envisaged application, to make modifications and improvements if necessary. The pre-series will also allow validating the preparation and conditioning processes in order to estimate the production rate and to establish a precise production schedule. Finally, the pre-series

will allow our team to get familiar with this type of task in order to make the preparation and conditioning process of the series as smooth as possible.

Two types of couplers will be tested and compared: with and without a TiN coating on the coupler ceramic window.

COUPLERS PREPARATION AND CONDITIONING

The coupler preparation process (cleaning, cavity assembly and baking) takes place in two clean rooms (an ISO5 and ISO4) inherited from the XFEL project. It allows the processing of one pair of couplers at a time over approximately ten days. Improvements will be made to the clean rooms and equipment to reduce this time to half. This limit duration can be improved after a rump up phase.

Coupler Preparation Process

The preparation phase includes several steps: Upon reception at the IJCLab, and after a visual inspection, a particulate cleaning is performed (ISO 5 clean room) and drying (ISO 4 clean room). All the components are then assembled on the conditioning cavity, along with ion pumping units and RGA (Residual gas analyser). A leak test is then carried out (must be less than 10^{-10} mbar/l/s for acceptance) before starting the drying cycle at 150 °C for 72 h to eliminate residual water vapour. The ion pumps are started up as soon as the drying cycle is completed.

The use of the RGA allows investigating the spectral composition of the coupler emissions. The recorded spectrum is compared with a pair of standard couplers to ensure the absence of pollutants.

After all this steps, the coupler pair can be installed on the RF bench and the conditioning can be started.

Couplers RF Conditioning Process

The conditioning bench (see Fig. 1) is composed of a solid-state amplifier delivering a maximum power of 80 kW. The couplers are operated up to this maximum power, above its nominal power (8 kW CW) in order to allow fault-tolerance schema.

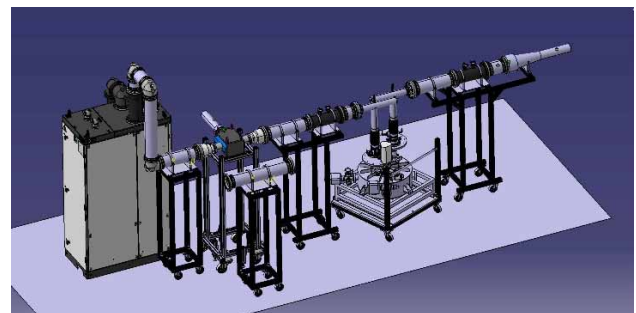


Figure 1: MYRRHA RF Conditioning bench.

IMPROVED STUDY OF THE MULTIPACTOR PHENOMENON FOR THE MYRRHA 80 kW CW RF COUPLERS

Y. Gómez Martínez, P. O. Dumont

Univ. Grenoble Alpes, CNRS, Grenoble INP, LPSC-IN2P3, Grenoble, France

P. Duchesne, N. Elkamchi, C. Joly, W. Kaabi, C. Lhomme¹

Université Paris-Saclay, CNRS/IN2P3, IJCLab, Paris, France

¹also at ACS, Orsay, France

Abstract

MYRRHA (Multi Purpose Hybrid Reactor for High Tech Applications) is an Accelerator Driven System (ADS) project. Its superconducting linac will provide a 600 MeV -4 mA proton beam. The first project phase based on a 100 MeV linac is launched. The Radio-Frequency (RF) couplers have been designed to handle 80 kW CW (Continuous Wave) at 352.2 MHz. This paper describes the multipactor studies on the coupler when it does not work in the nominal configuration without reflected power.

INTRODUCTION

The first section of the superconducting LINAC will be composed of Single Spoke Resonators (SSR) ($\beta_{\text{prototype}} = 0.37$) housed in short cryomodules operating at 2 K [1].

The energy transfer from the RF source to the SSR is made by the RF couplers. The RF coupler also seal the accelerator vacuum thanks to its window and a thermal barrier between air and the SSR while preserving its cleanliness.

As part of an ADS, the LINAC is laid out for the highest achievable reliability. Thus the coupler is studied [2] and tested up to 80 kW CW, well above its nominal power (8 kW CW), to allow the fault-tolerance schema [3] with a study of the multipactor phenomena in all the configurations that coupler can operate.

Multipactor is an undesired phenomenon of resonant electron build up encountered in electromagnetic field regions under vacuum. It appears when an electron is accelerated by the electric field and hits the enclosure's wall. Depending on the secondary electron yield of the wall, more than one electron can be emitted and accelerated by the electric field, creating a self-sustained electron avalanche.

The performance of the couplers can be greatly affected due to multipactor that could in the worst case break the coupler window venting the accelerator.

For the RF coupler of MYRRHA, first multipactor studies [4] have been carried out up to 80 kW CW of two couplers mounted in the conditioning cavity, 50 Ohm loaded.

In this case the coupler handle a traveling wave.

This configuration also corresponds to the coupler mounted to the SSR and matched to the nominal beam or with a $\beta \sim 1$ where β is the ratio of the intrinsic quality factor of the cavity (Q_0) and the external quality factor (Q_{ext}).

$$\beta = \frac{Q_0}{Q_{\text{ext}}}$$

In this paper, we show the multipactor study corresponds to the others situations:

- Case over - bandwidth (OB): for the coupler mounted at the SSR at room temperature over-bandwidth. In this configuration, the cavity behaves as a short-circuit and the coupler handle a standing wave with all the power reflected. This configuration correspond to RF conditioning of the coupler at the SSR.
- Cases slightly mismatched: for the coupler mounted at the SSR operating at 2 K at the resonance frequency with a mismatch. In this configuration the coupler can be undercoupling ($\beta < 1$) or overcoupling ($\beta > 1$) and the coupler handled a mixed wave.
- Case no beam: for the coupler mounted in the SPOKE cavity at 2 K without beam. In this configuration, the cavity is as very over coupling ($\beta \gg 1$) and the coupler handle a standing wave with all the power reflected. We find this configuration while testing the cryomodule to achieve the maximal accelerating field in the cavity or in the accelerator without beam.

HFSS CALCULATIONS

The coupler mounted in the SSR has been modelled and the field maps (see Fig. 1) for each configuration is created with the drivenmode solver of HFSS.

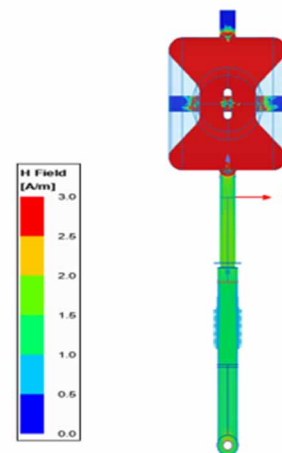


Figure 1: Magnetic field map@1 W for the coupler mounted in the SSR with $\beta \sim 1$.

Content from this work may be used under the terms of the CC BY 4.0 licence (© 2023). Any distribution of this work must maintain attribution to the author(s), title of the work, publisher, and DOI

UPDATE ON CORNELL HIGH PULSED POWER SAMPLE HOST CAVITY*

N. Verboncoeur[†], A. Holic, M. Liepe, T. Oseroff, R. D. Porter¹, J. Sears, L. Shpani
Cornell Laboratory for Accelerator based ScienceS and Education (CLASSE), Ithaca, NY, USA
¹also at SLAC, Menlo Park, California, USA

Abstract

The Cornell High Pulsed Power Sample Host Cavity (CHPPSHC) is designed to measure the temperature-dependent superheating fields of future SRF materials and thereby gain insights into the ultimate limits of their performance. Theoretical estimation of the superheating fields of SRF materials is challenging and mostly has been done for temperatures near the critical temperature or in the infinite kappa limit. Experimental data currently available is incomplete, and often impacted by material defects and their resulting thermal heating, preventing finding the fundamental limits of these materials. The CHPPSHC system allows reaching RF fields in excess of half a Tesla within microseconds on material samples by utilizing high pulsed power, thereby outrunning thermal effects. We are principally interested in the superheating field of Nb₃Sn, a material of interest for the SRF community, and present here the current fabrication and assembly status of the CHPPSHC as well as early results.

INTRODUCTION

One of the major limitations on accelerator technology is improving the efficiency of Radio-Frequency (RF) cavities [1]. For superconducting RF (SRF) cavities, one of the paths of interest is alternative materials such as Nb₃Sn. The current standard niobium (Nb) SRF cavities have a critical temperature of 9 K and typically operate at 2 K in superfluid helium. The ultimate limit of Nb's accelerating gradient is ~ 55 MV/m in TESLA-geometry cavities. This value is determined by the superheating field of Nb, H_{sh} , which is approximately 200 mT at 2 K [2, 3]. In type II superconductors, the superheating field, H_{sh} , is the maximum magnetic field at which the metastable state can exist.

Nb₃Sn, on the other hand, has a critical temperature of 18 K and can operate equivalently at 4.2 K in liquid helium. Operating in liquid helium at 4.2 K instead of in superfluid helium at 2 K would significantly reduce the construction and operational costs of an accelerator due to the reduced requirements in cryoplant facilities. It also opens up the possibility of conduction cooled cavities [4, 5] which would make small-scale accelerators more accessible for medical and industrial applications.

In addition to the exciting implications of a material with a higher critical temperature, Nb₃Sn has a predicted superheating field of ~ 440 mT at 4.2 K [6]. This corresponds

to an accelerating gradient of ~ 100 MV/m – nearly double that of Nb.

The value of H_{sh} quoted for Nb₃Sn has not been confirmed experimentally yet. Previous tests have attempted to measure it before, but have run into various limitations [3, 7]. The Cornell High Pulsed Power Sample Host Cavity (CHPPSHC) is a sample host cavity designed for the specific purpose of probing the superheating fields of different Nb₃Sn recipes and other candidate SRF materials. It utilizes a 1 MW klystron and is geometrically optimized for high magnetic fields on the sample with the ability to reach up to approximately 0.5 T. Design, machining, and assembly of CHPPSHC have been completed and a commissioning test with a Nb sample has been performed.

COMMISSIONING

Design

A sample host cavity presents several benefits over standard single-cell TESLA geometry cavities. Single-cell TESLA cavities have a large surface area and complicated geometries. A sample has a much smaller surface area and a simpler geometry making it easier to test different materials. Another limiting factor is that while single-cell TESLA cavities can reach sufficiently high fields, they require tens of μ s to fill with energy. The longer the filling time, the more likely that thermal effects will cause a premature quench. A custom designed cavity geometry would allow us to optimize for fast filling and high magnetic fields.

In order to ensure that CHPPSHC can reach high enough magnetic fields on the sample, it is optimized for a high ratio between peak magnetic field and the square root of energy stored in the cavity, or $\frac{B_{pk}}{\sqrt{U}}$.

Reaching high fields alone is not enough. The CHPPSHC also needed to be able to reach these fields on a timescale smaller than the spread of thermal effects to ensure that the sample quenches observed were due to fundamental material limits and not heating due to defects. The best way to do this is to ensure that the cavity charges, or "fills", with energy as quickly as possible [8, 9].

These design challenges are achieved through 3 main features: host structure geometry, sample geometry, and strong RF input coupling.

The CHPPSHC operates in a dipole mode. The magnetic field pattern and magnitude can be seen in Fig. 1a and the surface magnetic fields can be seen in Fig. 1b.

The sample is an ellipsoid shape with a sharp knife-edge that is oriented perpendicular to the magnetic fields in the cavity. This knife edge exploits field enhancement, a phenomenon where magnetic fields are magnified at sharp fea-

* This work is supported by the National Science Foundation under Grant No. PHY-1549132 (the Center for Bright Beams) and US Department of Energy grant No. DE-SC0008431

[†] nmv39@cornell.edu

PI LOOP RESONANCE CONTROL FOR THE DARK PHOTON EXPERIMENT AT 2 K USING A 2.6 GHz SRF CAVITY*

C. Contreras-Martinez[†], B. Giaccone, O. Melnychuk, A. Netepenko, Y. Pischalnikov, S. Posen, and V. Yakovlev, Fermilab, Batavia, IL, USA

Abstract

Two 2.6 GHz SRF cavities are being used for a dark photon search at the vertical test stand in FNAL, for the second phase of the Dark SRF experiment. During testing at 2 K the cavities experience frequency detuning caused by microphonics and slow frequency drifts. The experiment requires that the two cavities have the same frequency within the cavity's bandwidth. These two cavities are equipped with frequency tuners consisting of three piezo actuators. The piezo actuators are used for fine-fast frequency tuning. A proportional-integral loop utilizing the three piezos on the emitter was used to stabilize the cavity frequency and match the receiver cavity frequency. The results from this implementation will be discussed. The integration time was also calculated via simulation.

INTRODUCTION

A dark photon is a hypothetical particle that weakly couples to ordinary matter and is an extension of the standard model (SM) of particle physics [1]. The experiment discussed in this paper is one of several which are known as “light-shining-through-wall” experiments [2]. The first phase of the Dark SRF experiment at FNAL was done using two single-cell 1.3 GHz cavities [3]. The next step consists of using two high Q_0 single-cell 2.6 GHz SRF cavities, one of which will be called the emitter cavity and the other the receiver cavity. They will be first tested at vertical test stand (VTS) and later be moved to the dilution refrigerator to improve sensitivity. The emitter will be powered on creating an electromagnetic field (TM_{010}) inside the cavity, the field from this emitter cavity acts as a source of dark photons that can be emitted outside the cavity. The dark photons can penetrate the receiver cavity and be converted to SM photons [3] which have the same frequency as the emitter. This conversion will result in a signal on the receiver. A schematic of this process is shown in Fig. 1. The field excited in the receiver is proportional to the field in the emitter [2, 3].

Resonant enhancement of the receiver signal is achieved when the frequency of the SM photons, that result from the conversion of the dark photons from the emitter cavity, matches the frequency of the receiver cavity. The bandwidth of the cavities is given in Table 1. Note that the receiver cavity has a small bandwidth of 0.56 Hz which puts

a constraint on the peak detuning that the cavity should experience. Additionally, the cavity is extremely sensitive to deformation with a sensitivity of 10 kHz/ μm . Both cavities initially consist of three Physik Instrumente PICMA actuators. The piezos were later changed to stainless-steel rods on the receiver cavity only. The total range of the tuner is ~ 176 kHz (240 V range), more detail on the tuner for these cavities can be found in [4]. During testing microphonics and slow frequency drifts were observed.

During this experimental run, the dark photon search was not conducted. Instead, the feasibility of maintaining the cavity frequencies close to each other was explored. The emitter cavity was powered on and the frequency shift of both cavities was recorded. Once the frequency drift of both cavities was characterized a proportional-integral (PI) loop was implemented only on the emitter cavity to mitigate the cavity frequency mismatch. An estimate of the integration time is given based on the PI loop resonance control of the emitter cavity.

Table 1: Figures of merit of both cavities, the bandwidth is calculated from the loaded Q_L .

Cavity	R/Q [Ω]	Bandwidth [Hz]	$Q_L \times 10^8$
Emitter	104.7	5.84	4.42
Receiver	104.7	0.56	46.4

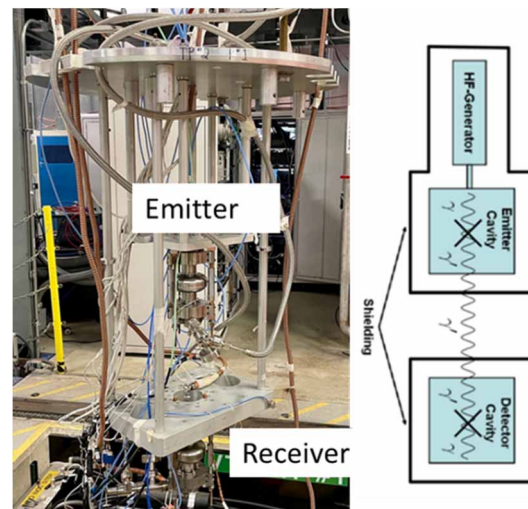


Figure 1: Left picture shows the setup of the experiment. The right picture shows a schematic of the process of dark photon production and detection [5].

*This material is based upon work supported by the U.S. Department of Energy, Office of Science, National Quantum Information Science Research Centers, Superconducting Quantum Materials and Systems Center (SQMS) under contract number DE-AC02-07CH11359

[†] ccontrer@fnal.gov

PREVENTION OF DUAL-MODE EXCITATION IN 9-CELL CAVITIES FOR LCLS II-HE*

P. Owen[†], Jefferson Lab, Newport News, VA, USA

Abstract

Dual-Mode Excitation, also referred to as mode-mixing, is a superposition of two modes in an SRF cavity. In 9-cell TESLA cavities, the π mode of the cavity (1300.2 MHz) is driven with an RF source to determine the gradient and corresponding quality factor. However, above a certain gradient, the $7/9 \pi$ mode (1297.8 MHz) becomes self-excited while the RF is only supplying power at the π mode frequency. In this scenario, the RF power measurement system is unable to differentiate between the superimposed modes on the reflected and probe signals, which invalidates the resulting measurements. This paper demonstrates a new RF control solution which suppresses the $7/9 \pi$ mode during the measurement without impacting the quality measurement itself. The system has been successfully implemented at Jefferson Lab and is now routinely used to test a cavity for the LCLSII-HE project.

BACKGROUND

As part of the LCLSII-HE project, about 200 1.3-GHz 9-cell SRF cavities have to be tested in vertical dewars cooled with liquid helium to about 2 K. Each cavity is tested to determine the maximum achievable gradient and resonant quality factor, and to observe any field emission. In addition to LCLSII, this cavity design is in use at XFEL and ILC research. The phenomenon of mode-mixing begins with multipacting in the cavity at gradients above 17 MV/m [1, 2]. As a consequence, a self-excitation of the $7/9 \pi$ mode in the cavity may appear above this gradient.

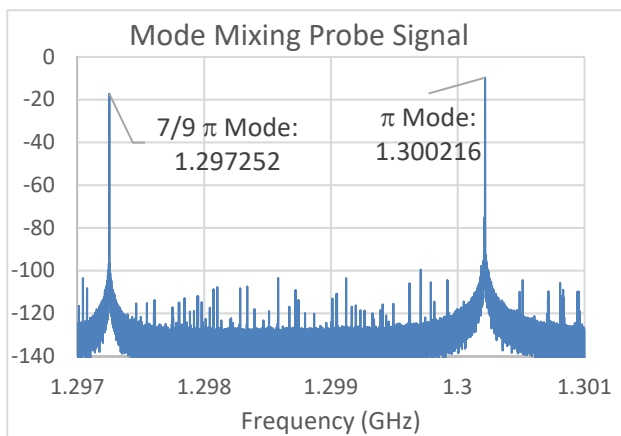


Figure 1: Spectral data from field probe showing mode mixing.

There is a positive feedback loop which allows the mode to grow until it is equal in strength to the π mode, limited by the incident power (Fig. 1). The cavities are equipped with HOM couplers to remove unwanted modes. However, the frequency of the $7/9 \pi$ mode is close enough to the π mode that it is not strongly damped by these notch filters. Mode mixing does increase power in the HOM filters, but it is not sufficiently attenuated to prevent the positive feedback loop.

This behavior is only observed during vertical testing of cavities, not in an assembled cryomodule. This is caused by the significantly lower loaded Q of the fundamental power coupler used in the module compared to the high Q antennas ($1-3 \times 10^{10}$) in the dewar and the correspondingly higher bandwidth.

Mode-Mixing Effects

The RF measurement systems used during vertical test are unable to differentiate between the superimposed modes, making any data recorded during mode-mixing invalid. The presence of mode mixing causes reflected power to increase because of the additional uncontrolled energy in the cavity. Previously, the only way of taking data at high gradients during mode mixing was to power cycle the cavity. As the coupling to the cavity is near critical and the cavity itself has a high Q_0 ($>2.5 \times 10^{10}$), it takes several seconds to let both modes decay. Once both modes have died away, the operator can turn power back on and the cavity returns to the desired gradient. However, there is only a short window of time where the π mode gradient is stable, and/or the $7/9 \pi$ mode has not yet grown enough to interfere with the measurement. This leads to longer testing times and reduces the accuracy of Q_0 measurements. At higher gradients, the superposition of the second mode can cause the cavity to prematurely quench when both fields are present. This prevents RF processing of some high-gradient multipacting barriers.

OFF-RESONANCE POWER

A new RF system layout was designed to prevent the $7/9 \pi$ mode from being self-excited by providing a negative feedback loop specifically at that frequency.

RF System Layout

In the Jefferson Lab Vertical Test Area (VTA), there are five RF systems which are available to test cavities in any one of eight liquid-helium dewars. The exact specifications of the systems vary based on the RF bands in which they operate. Despite this, they all share the same general topology. The control of amplitude, phase, and precise frequency lock are all handled by a field control chassis

* Work supported by the U.S. Department of Energy, Office of Science, Office of Nuclear Physics under contract DE-AC05-06OR23177.

[†] powen@jlab.org

A NEW ULTRA-HIGH VACUUM FURNACE FOR SRF R&D

M. Wenskat^{1,*}, R. Ghanbari¹, C. Bate^{1,2}, C. Martens¹, W. Hillert¹

¹Universität Hamburg, Germany

²Deutsches Elektronen-Synchrotron DESY, Germany

Abstract

A new vacuum furnace has been designed and purchased by the University of Hamburg which is operated in an ISO5 cleanroom. This furnace can anneal single-cell TESLA cavities at temperatures up to 1000 °C and achieves a base pressure of 2×10^{-8} mbar at room temperature after 8 h of pumping. We lay out the underlying design ideas, based on the gained experience from our previous annealing research, and present the commissioning of the furnace itself. Additionally, we will show the first results of sample and cavity tests after annealing in the furnace.

DESIGN CONSIDERATIONS

Based on the experience gained with our vacuum heat treatments and from partner laboratories, we made some layout decisions. All studies indicate that the CO/CO₂ partial pressure levels are crucial for successful treatments [1–4]. Hence, an oil-free vacuum system was designed. Furthermore, a combination of a turbomolecular (TMP) and a cryopump was chosen to achieve the highest pumping speed for hydrogen and water vapor. In addition, to enable a partial pressure operation with the TMP but to avoid a backflow from roughing pumps, a by-pass solution was chosen. This will also allow the operation of a residual gas analyzer (RGA) during partial pressure operation. The furnace itself is vented or operated in partial pressure by bottled 6.0 nitrogen. The whole furnace was planned to be all-metal sealed (except the door) and only molybdenum heaters and heat shields were used. The total gas flow q_{pV} at ultimate pressure was specified to be better than 5×10^{-4} mbarl/s and the overall leak rate Q_L better than 1×10^{-9} mbarl/s. Also, the cooling water can be heated up to 80 °C, which is used prior to opening the furnace to minimize the adsorption of water to the inner furnace walls. The final layout of the furnace is given in Fig. 1. After discussing the specifications with several companies, the company *Xerion Berlin Laboratories® GmbH* had the most convincing concept and built the furnace. The furnace is a bottom loader, capable to fit a 1.3 GHz TESLA single-cell cavity inside, see Fig. 2. The furnace vessel is made out of 1.4301 stainless steel and has electropolished inside surfaces. The maximum achievable temperature is 1100 °C, with a homogeneity of ± 5 °C and is controlled by three heating zones. The furnace is located in a clean room (ISO 5) to minimize particle contamination.

COMMISSIONING

Test runs were carried out at varying temperatures and durations. The ultimate pressure achieved after several days

* marc.wenskat@desy.de

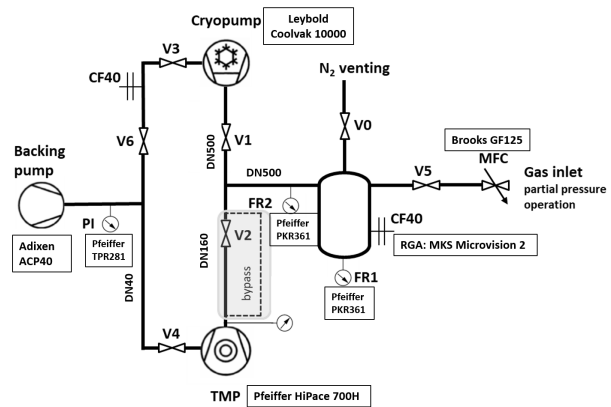


Figure 1: Layout of the vacuum system.

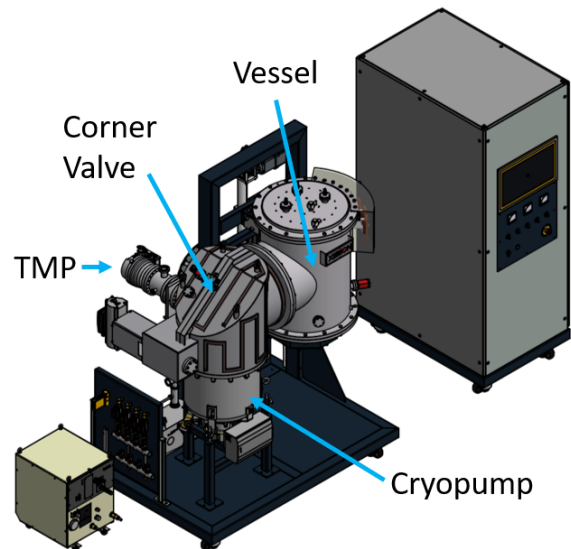


Figure 2: Top: CAD drawing of furnace. Bottom left: Image of the furnace before cleanroom installation. Bottom right: Single-cell cavity 1DE10 installed in the open furnace.

EVALUATION OF PHOTO-CATHODE PORT MULTIPACTING IN THE SRF PHOTO-INJECTOR CRYOMODULE FOR THE LCLS-II HIGH-ENERGY UPGRADE*

Z. Yin[†], W. Hartung, S. Kim, T. Konomi, T. Xu

Facility for Rare Isotope Beams, Michigan State University, East Lansing, MI, USA

Abstract

The high-energy upgrade of the Linac Coherent Light Source will increase the photon energy and brightness. A low-emittance injector (LEI) was proposed to increase the photon flux for high X-ray energies. FRIB, HZDR, Argonne, and SLAC are developing a 185.7 MHz superconducting radio-frequency photo-injector cryomodule for the LEI. The photo-cathode system requirements are challenging, as cathodes must be maintained at the desired temperature, precisely aligned, and operated without multipacting (MP); to avoid field emission, cathode exchange must be particulate-free. A support stalk has been designed to hold the cathode in position under these requirements. A DC bias is used to inhibit MP. We simulated MP for various surface conditions and bias levels. An RF/DC test was developed to evaluate the cathode stalk performance as a subsystem and to identify and correct issues before assembly into the full cryomodule. The RF/DC test makes use of a resonant coaxial line to generate an RF magnetic field similar to that of the cathode-in-SRF-PI-cavity case. High-power test results will be presented and compared to the MP simulations.

INTRODUCTION

The Linac Coherent Light Source (LCLS-II) [1] has been a pioneering facility in the field of X-ray free-electron lasers (XFELs), providing invaluable insights into various scientific disciplines. To further advance the capabilities of LCLS-II and increase the photon energy and brightness, a high-energy upgrade known as LCLS-II-HE is underway. The low-emittance injector (LEI), which aims to enhance the photon flux for high X-ray energies, was proposed. As part of this effort, a collaboration between FRIB, HZDR, Argonne, and SLAC has focused on the development of a 185.7 MHz superconducting radio-frequency photo-injector (SRF-PI) cryomodule for the LEI [2, 3]. A novel support stalk has been designed to securely hold the cathode in position while meeting the stringent requirements of the SRF-PI [4]. This support stalk plays a crucial role in maintaining the desired temperature of the cathode, achieving precise alignment, and inhibiting multipacting (MP)—an important resonance process that can lead to detrimental effects such as elevated temperature and vacuum pressure, thereby impacting photocathode stability and lifetime. To address this, a DC bias is applied.

To evaluate the performance of the cathode stalk as a subsystem and identify any issues before assembly into the full cryomodule, an RF/DC test has been developed as shown in Fig. 1. This test utilizes a resonant coaxial line to generate an RF magnetic field that closely resembles the conditions inside the cathode-in-SRF-PI-cavity case. The desired magnitude of the accelerating field at the photo-cathode is set at 30MV/m. In this paper, we compare the results obtained from the RF/DC test with MP simulations conducted for various surface conditions and bias levels.

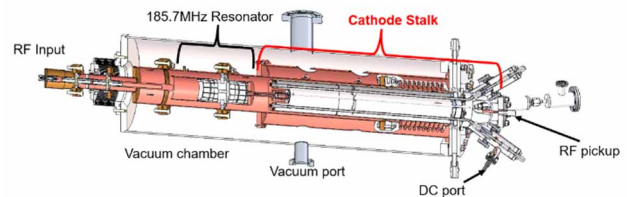


Figure 1: Setup for RF/DC test [4].

MULTIPACTING SIMULATION

CST Microwave Studio (CST) was utilized to conduct simulations of the MP process, and the simulated structure is presented in Fig. 2. To be analogous to real-world scenarios involving cosmic rays, photoemission, or impacting field emissions, initial particles were distributed in a Gaussian manner over time, with a bunch length corresponding to the RF (radio frequency) period. The occurrence of MP in RF structures relies on both the electromagnetic field distribution and the secondary emission yield (SEY) of the materials [5]. We use CST to generate the distributions of RF and DC fields, which were subsequently employed as inputs for the particle simulation. The resulting RF field maps are presented in Fig. 3. Within the cathode stalk, multiple materials were utilized, and their typical SEY values were employed for simulation purposes. The SEY curves for various materials can be observed in Fig. 4 [6-9]. To examine the influence of DC bias and surface conditions, we initially simulated MP without any DC bias and subsequently varied the DC bias to demonstrate its suppressive effect. Additionally, we explored different surface conditions by modifying the SEY values of the various materials.

Without DC Bias

Initially, the simulation is conducted in the absence of DC bias, while altering the RF field distribution. The adjustments made to the field distribution within the cathode

* Work supported by the Department of Energy Contract DE-AC02-76SF00515

[†] yin@frib.msu.edu

THE INFLUENCE OF SAMPLE PREPARATION, SOAK TIME, AND HEATING RATE ON MEASURED RECRYSTALLIZATION OF DEFORMED POLYCRYSTALLINE NIOBIUM*

Z. L. Thune[†], T. R. Bieler[‡], Michigan State University, East Lansing, MI, USA

Abstract

Improving accelerator performance relies on consistent production of high-purity niobium superconducting radio-frequency (SRF) cavities. Current production uses an 800°C 3 hr heat treatment, but 900-1000 °C can improve cavity performance via recrystallization (Rx) and grain growth. As Rx is thermally activated, increasing the temperature and/or the heating rate could facilitate a reduction in geometrically necessary dislocation (GND) density that is associated with the degradation of cavity performance via trapped magnetic flux. Recent work shows that increasing the annealing temperature increased the Rx fraction in cold-rolled polycrystalline niobium. However, the influence of heating rate on the extent of Rx was minimal with a 3 hr soak time. To further assess the influence of heating rate on measured Rx, as well as the effects of sample preparation, electron backscatter diffraction (EBSD) was used to quantify the extent of Rx on samples annealed at a single temperature with different soak times. Comparing samples with different surface preparation shows that removing pinned grain boundaries on the free surface reveals a much larger grain size below the surface.

INTRODUCTION

Improving accelerator performance requires production of niobium superconducting radiofrequency (SRF) cavities with consistent performance. Performance inconsistency may arise from the known variability in microstructures in the as-received Nb polycrystalline sheet. This, as well as locally different strain paths during forming in different parts of the half-cell cause spatially variable dislocation arrangement. Post-cavity formation, the heat treatment used to remove hydrogen causes non-homogeneous rearrangement or removal of dislocations by recovery (Rv) and recrystallization (Rx).

Recovery results in removal of most of the dislocations, but the remaining geometrically necessary dislocations (GNDs) associated with the lattice curvature caused by forming are rearranged into low-angle grain boundaries (LAGBs), which are known to trap magnetic flux [1]. LAGBs are very stable, and not easily removed. Recrystallization, also driven by removing dislocation content, occurs when high-angle grain boundaries (HAGBs) sweep through the material, leaving a nearly perfect crystal in their wake with no GNDs [2], and hence, no LAGBs that trap magnetic flux. As Rx proceeds, grain growth occurs driven by reducing grain boundary area, so HAGBs could sweep through the same volume multiple times.

Furthermore, Rv removes stored strain energy (high dislocation density) that also reduces the driving force for Rx that is necessary to remove LAGBs.

Hence, we hypothesize that the standard 3 hr 800 °C heat treatment facilitates Rv more than Rx, so increasing the holding temperature and/or heating rate should result in more complete Rx that removes the GNDs that degrade cavity performance. Higher temperature anneals between 900 and 1000 °C more effectively remove magnetic flux pinning centers [3, 4], increasing the cavity performance, but at the expense of the strength, as these anneals result in significant grain growth from about 50 to 200 μm in diameter, but the extent of Rx was quite different in samples with different strain path history [5].

Therefore, an ideal heat treatment should exist where Rx occurs nearly completely but is stopped before grains grow significantly. As Rx temperatures are higher than Rv temperatures, it is likely that a hotter but shorter heat treatment may enable Rx without too much grain growth, such that an optimal microstructure can be obtained. Also, a higher heating rate may enable reaching the Rx temperature sooner, so that less Rv occurs. It is likely that this optimal condition will depend on the starting microstructure in the sheet before the cavity is even formed [6].

The present work builds upon prior work [5] to examine the effect of soak time at 940 °C on the extent of Rx after a standard (slow) and a fast heating rate were examined to determine how much the heating rate and soak time influence the Rx process. As the specimen preparation methods varied in these prior investigations and may have affected the measured results, this paper focuses on the effects of methodology on measuring the Rx fraction. Also, the limitations of the analytical method were examined by comparing scans made with the standard Hough transform indexing methods and a spherical indexing method [7] to determine if spatial and angular resolution affected the assessment of the Rx fraction.

EXPERIMENTAL DETAILS

To investigate the effects of the deformation path on microstructure evolution during heat treatment, a proxy for cavities was chosen, by imposing about 30% rolling reduction in coupons in two different directions: the original rolling direction, and the original transverse direction (perpendicular to the rolling direction) [5]. These coupons were carefully polished before heat treatment at different temperatures and heating rates with the same soak time of 3 hr. Samples were heated in evacuated fused quartz ampules to protect the polished characterized surface from oxidation. To assess the fraction Rx in each sample, the same locations on the same surfaces were examined to compare with

* DOE/OHEP (Grant Number: DE-SC0009960)

[†] thunezac@msu.edu

[‡] bieler@msu.edu

STUDY AND IMPROVEMENT OF LIQUID TIN DIFFUSION PROCESS TO SYNTHESIZE Nb₃Sn CYLINDRICAL TARGETS*

D. Ford[†], E. Chyhyrynets, D. Fonnesu, G. Keppel, G. Marconato, C. Pira, A. Salmaso
National Institute of Nuclear Physics (Legnaro National Laboratories), Legnaro, Italy

Abstract

Nb₃Sn films deposited on copper cavities offer significant advantages compared to conventional niobium cavities, particularly regarding the superior thermal conductivity of copper compared to niobium. The enhanced heat exchange provided by copper enables the utilization of cryocoolers, thereby reducing cryogenic costs and minimizing the risk of thermal quench. Coating substrates with complex geometries via DC Magnetron Sputtering, such as elliptical cavities, may necessitate non-planar-shaped targets, which are challenging to produce using traditional powder sintering techniques. The LTD technique, previously developed at LNL for SRF applications, allows the deposition of thick and uniform Nb₃Sn coatings onto Nb substrates, even those with complex geometries. This work presents advancements in the LTD process and improvements in the experimental setup, in order to avoid Cr contaminations previously reported.

INTRODUCTION

Thin film deposition of Nb₃Sn is promising for superconducting radio frequency (SRF) applications, offering higher critical temperature and theoretical accelerating gradient compared to Nb. Nb₃Sn thin films on Nb bulk cavities achieved excellent performance via Vapor Tin Diffusion (VTD). However, there is strong interest in using PVD techniques to grow Nb₃Sn on a Cu substrate due to its higher thermal conductivity [1].

Conventional sintering from powders faces challenges in implementing the required features for cooling the cylindrical cathode due to material fragility. An alternative approach involves producing targets through the growth of thick films of Nb₃Sn directly on a niobium substrate using the Liquid Tin Diffusion (LTD) technique.

Previous work done at LNL showed the feasibility of LTD technique, that allowed the growth of thick layer of Nb₃Sn, even on complex geometries [2]. However, a significant limitation arose from Cr contamination in the samples caused by the Inconel chamber.

Between 2022 and 2023, further experimentation was conducted using the same chamber to enhance the process and achieve increased thickness. Subsequently, in 2023, a complete redesign of the system was implemented to mitigate contamination issues [3].

*This work has received funding from the European Union's Horizon 2020 Research and Innovation pro-gramme under Grant Agreement No 101004730. Work supported by the INFN CSNV experiment SAMARA.

[†] davide.ford@lnl.infn.it

EXPERIMENTALS

Nb₃Sn is synthesized directly on a bulk Nb 1'' circular target by direct immersion in liquid tin (see Fig. 1).

Sample Preparation

The circular target samples are obtained from an RRR300 niobium plate and cut using water jet cutting. The unique shape of the samples is specifically designed to be hung from the niobium wire of the manipulator using a hook, and a protrusion is added on the lower part to prevent the formation of niobium droplets. Both the hook and the lower protrusion are subsequently cut for proper mounting of the target on the magnetron.

The niobium substrates undergo ultrasonic cleaning and subsequent Buffer Chemical Polishing (BCP) using a mixture of HF, HNO₃, and H₃PO₄ in a 1:1:2 ratio for a duration of five to ten minutes. To facilitate pre-nucleation, the substrates are then anodized at 20 V for one minute in a NaOH solution, resulting in the formation of a 70 nm Nb₂O₃ layer.



Figure 1: Nb 1'' circular targets mounted on the sample holder before (a) and after (b) dipping process. The blue colour (a) is due to the anodization process.

The whole process involves the use of two separate UHV systems:

LTD System

The Liquid Tin Diffusion (LTD) system consists of an Inconel chamber as the main component, along with an ultra-high vacuum pumping system, a linear manipulator, a tin-containing crucible furnace, a sample annealing furnace, and a water jacket. The samples are securely fixed to the manipulator using niobium wires. The system is heated and evacuated to achieve a base pressure of 10⁻⁸ mbar.

ADDITIVE MANUFACTURING OF PURE NIOBIUM AND COPPER USING LASER POWDER BED FUSION FOR PARTICLE ACCELERATOR APPLICATIONS*

D. Ford[†], R. Caforio, E. Chyhyrnyets, G. Keppel, C. Pira, National Institute of Nuclear Physics – Legnaro National Laboratories, Legnaro, Italy

S. Candela¹, M. Bonesso, V. Candela¹, R. Dima, G. Favero², A. Pepato, P. Rebesan, M. Romanato, INFN - section of Padova, Padova, Italy

M. Pozzi, Rösler Italiana S.r.l., Concorezzo (MB), Italy

¹also at CRF, University of Padova, Padova, Italy

²also at DTG, University of Padova, Padova, Italy

Abstract

Additive Manufacturing (AM) provides a unique opportunity to produce objects with complex shapes and enables the processing of materials with high melting points and difficulty in machining. This study focuses on the characterization of pure niobium and copper 6 GHz cavities fabricated using Laser Powder Bed Fusion (LPBF) and the optimization of printing parameters. Special attention was given to the development of innovative contactless supporting structures that enhance the quality of downward-facing surfaces with extremely small inclination angles. Through these efforts, a relative density exceeding 99.8% was achieved, demonstrating the effectiveness of the novel supports in enabling the seamless fabrication of SRF cavities. Additionally, surface smoothing treatments were applied, and performance tests were conducted on the additively manufactured cavities.

INTRODUCTION

The traditional subtractive manufacturing processes used to produce RF cavities are often costly due to material requirements and the inability to reuse wasted material. However, Laser Powder Bed Fusion (LPBF) overcomes these issues as the unused metal powder particles can be easily recycled, making it advantageous for processing expensive metals like niobium. Additive Manufacturing allows for the creation of components with complex shapes in a short time. Nonetheless, there are drawbacks associated with these techniques, such as low surface finishing, residual porosity, and impurities in the raw materials used.

In the LPBF process, a powerful laser selectively melts the feedstock powder, which is spread onto a metallic platform. The platform is then lowered, and a new layer of powder is formed. The choice of layer thickness is influenced by factors like Particle Size Distribution of the powder.

* This project has received funding from the European Union's Horizon 2020 Research and Innovation pro-gramme under Grant Agreement No 101004730.

This work has been carried out within the framework of the EUROfusion Consortium, funded by the European Union via the Euratom Research and Training Programme (Grant Agreement No 101052200 - EUROfusion).

[†] davide.ford@lnl.infn.it

To optimize the process, a parameters fine-tuning campaign was conducted to identify the optimum process window for pure niobium. The surface quality of the additively manufactured parts was evaluated, considering the challenge of high surface roughness associated with additive manufacturing techniques. [1, 2] The minimum self-supporting angle of Nb was determined, and the down skin parameters were extensively studied. Additionally, innovative contact-free supporting structures were developed to enhance the quality of the downward-facing surfaces. These supports act as heat sinks, improving heat dissipation and significantly enhancing the quality of the downward surfaces. [3] A total of three Nb cavities were manufactured for this work.

Two pure copper cavities were also produced to test the effectiveness of surface treatments. The future development involves printing 6 GHz copper cavities, performing surface treatments on them, and applying superconducting coatings. The ease and speed of creating these cavities, once the printing processes are optimized, make this alternative highly attractive compared to other, more conventional, manufacturing methods.

EXPERIMENTALS

Niobium Cavities

In this work, AMtrinsic® Niobium spherical powder provided by Taniobis GmbH (Goslar, Germany) was used, with a particle size distribution (PSD) ranging from 18 μm (D10) to 63 μm (D90). The layer thickness was set at 30 μm . The additive manufacturing machine used was an EOS M100 DMLS (Electro-Optical System GmbH, Krailling, Germany), equipped with a Yb:YAG red laser with a maximum power of 200 W. The printing process was conducted in a controlled environment using argon (Ar) as the inert gas to minimize the oxygen level within the printing chamber, maintaining the O₂ content below 0.15%.

To estimate density, cubic samples were produced using different combinations of hatch spacing, laser power, and scanning speed. The relative density of each sample was measured using the Archimedes method, where the mass of each sample was measured multiple times in air and then in distilled water.

FLUX EXPULSION TESTING FOR LCLS-II-HE CAVITY PRODUCTION

J. T. Maniscalco^{1,2,*}, D. Savransky^{2,†}, S. Aderhold¹, T. T. Arkan³, D. Bafia³,
 M. E. Bevins², M. Checchin¹, D. Gonnella¹, A. Grabowski², J. Hogan¹,
 J. Kaluzny³, R. D. Porter¹, S. Posen³, C. E. Reece², J. Vennekate²

¹SLAC National Accelerator Laboratory, Menlo Park, CA, USA

²Thomas Jefferson National Accelerator Facility, Newport News, VA, USA

³Fermi National Accelerator Laboratory, Batavia, IL, USA

Abstract

Nitrogen-doped niobium SRF cavities are sensitive to trapped magnetic flux, which decreases the cavity intrinsic Q_0 . Prior experimental results have shown that heat treatments to 900 °C and higher can result in stronger flux expulsion during cooldown; the precise temperature required tends to vary by vendor lot/ingot of the niobium material used in the cavity cells. For LCLS-II-HE, to ensure sufficient flux expulsion in all cavities, we built and tested single-cell cavities to determine this required temperature for each vendor lot of niobium material to be used in cavity cells. In this report, we present the results of the single-cell flux expulsion testing and the Q_0 of the nine-cell cavities built using the characterized vendor lots. We discuss mixing material from different vendor lots, examine the lessons learned, and finally present an outlook on possible refinements to the single-cell technique.

INTRODUCTION

LCLS-II-HE is an ongoing project to upgrade LCLS-SC, the superconducting part of the X-ray free electron laser at SLAC National Accelerator Laboratory. Among other improvements, the project will extend the linac with 23 additional cryomodules, increasing the target beam energy to 8 GeV. The cavities in the new cryomodules are being prepared with “2N0” nitrogen doping.

Nitrogen-doped cavities exhibit an increase in the residual surface resistance if flux is trapped in the cavity walls during cooldown or quench [1]. For LCLS-SC, a CW machine, it is critical to minimize these losses to keep the heat load within the capacity of the cryoplant. Prior work has shown that high-temperature ($T \geq 900$ °C) heat treatments can improve the flux expulsion efficiency of niobium, but that the precise temperature required for sufficient expulsion can vary between niobium suppliers and even from batch to batch at a given supplier [2]. Generally, higher temperature treatments result in better flux expulsion. On the other hand, treatments at too high of a temperature can soften the niobium, increasing the risk of damage during handling and transport. This is a particular risk for the LCLS-II-HE cavities, which travel thousands of miles by air from the supplier in Europe to Fermilab and Jefferson Lab, and then thousands more by road to SLAC. Therefore, it is desirable to find the minimum heat

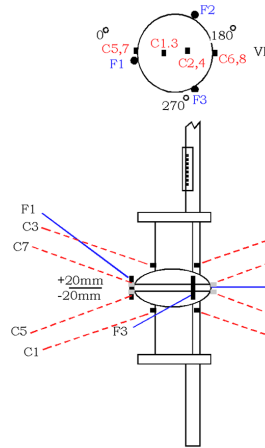


Figure 1: Illustration of the test setup. Left-hand diagram shows the positions of the thermometers (C) and magnetometers (F). Right-hand photo shows the instrumented cavity on the test insert.

treatment temperature required for sufficient flux expulsion for each batch of material.

For LCLS-II-HE, the niobium material was separated into “heat lots” at the supplier, each composed of sheets from two ingots. Each heat lot contains approximately 150 sheets, enough material for eight cavities. One single-cell cavity was constructed from each heat lot, using two non-sequential sheets. These were prepared with the first portion of the LCLS-II-HE cavity recipe, including bulk EP, and treated in the supplier’s furnace at 900 °C. The cavities were then shipped under vacuum and ready for test to Jefferson Lab.

At Jefferson Lab, each single-cell cavity underwent studies to measure its flux expulsion characteristics and determine the appropriate heat treatment temperature for the corresponding material batch. The required temperatures for each material lot were passed along to the cavity supplier to be used in the 9-cell cavity production processes.

SINGLE-CELL TESTING

Procedure

The flux expulsion characteristics of the single-cell cavities were measured using a procedure similar to the one developed for LCLS-II [3]. Each cavity was equipped with a payload of thermometers and flux-gate magnetometers,

* jamesm@slac.stanford.edu

† dsavr@jlab.org

NIOBIUM CHRONICLES: SURFACE QUALITY INVESTIGATION AND RECOVERY DURING MATERIAL PROCUREMENT FOR THE PIP-II HIGH BETA 650 MHz CAVITIES

A. Shabalina[†], ASTeC, STFC, Daresbury Laboratory, Warrington, UK

Abstract

The surface quality of high-purity niobium for superconducting radiofrequency cavities, produced by a reputable manufacturer, experienced a sudden and significant decline in 2021. The recovery process and root cause analysis were challenging due to a variety of factors such as COVID-19 travel restrictions, cultural differences, and bureaucratic processes. Effective open communication was crucial to resolving the issue, especially with direct vendor oversight being impossible.

INTRODUCTION

The United Kingdom Research and Innovation Science and Technology Facilities Council (UKRI-STFC) Daresbury Laboratory is responsible for procuring and testing 20 High Beta 650 MHz cavities for the Proton Improvement Plan II (PIP-II) accelerator project at Fermi National Accelerator Laboratory (FNAL). Niobium stock was ordered from a well-known supplier (a sales representative of The manufacturer) and production started in Spring 2021. Most of the 225 disks for half-cells productions were to be delivered to Deutsches Elektronen-Synchrotron (DESY) for Eddy Current Scanning (ECS). Material for beam tubes, flanges, and the rest of the components was to be delivered to UKRI-STFC Daresbury Lab in the UK.

The production started in May 2021, but delivery was delayed due to an extra layer of difficulty to agree the contract terms following the UK exit from the European Union. The logistical challenges of coordinating this process, particularly during the pandemic, were significant. The first two batches of disks were delivered at DESY by August, but ECS did not start until early September due to staff and equipment availability.

SUDDENLY - DEFECTS

On September 29th, 2021, DESY informed that a major surface quality problem had been observed during Eddy Current Scanning (ECS) of the material provided by the same supplier for a different project. DESY's team randomly sampled our disks – all failed ECS inspection due to the same problem. Both delivered batches — 80% of the disks! — and, potentially, the entire order, were unusable.

The problem manifested as a very high level of noise observed during scanning, indicating an enormous number of irregularities on the surface. The defects appeared as pits, uniformly distributed on both sides of the disks, Fig. 1 most with dimensions ranging from 10 to 40 μm in depth and 40

to 70 μm in width, Fig. 2, and some reaching the depth of 70 μm .

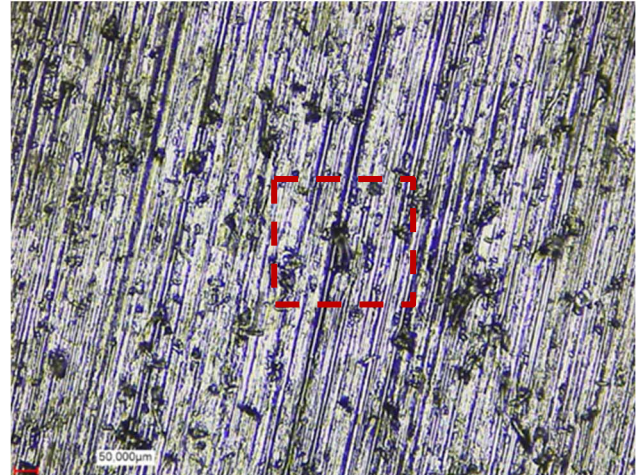


Figure 1: Half-cell material for PIP-II HB650 MHz cavities as received.

By November 2021, at least 500 sheets from various customers had been checked at DESY for surface defects. The results were very concerning - all orders placed with this supplier since May 2021 were affected. Sampling non-cell material at Daresbury supported the findings Fig. 3.

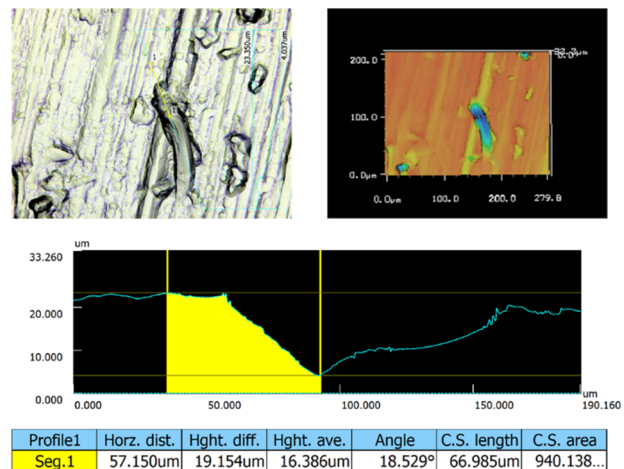


Figure 2: 3D profile of one of the pits shown in Fig. 1.

The defects were not visible by a naked eye, the surface just appeared subjectively rougher, but when compared side-by-side with a known good material, the grinding grooves looked noticeably deeper, Fig. 4.

[†] anna.shabalina@stfc.ac.uk

THERMODYNAMIC PROPERTIES OF SRF NIOBIUM*

P. Dhakal[†], Thomas Jefferson National Accelerator Facility, Newport News, VA, USA
 S. Li, Quantum Design, San Diego, CA, USA

Abstract

Bulk and thin films of niobium are the materials of choice in fabricating superconducting radio frequency (SRF) cavities for modern particle accelerators and quantum computing applications. The thermodynamic properties of Nb are of particular interest in heat management in cryogenic environments. Here, we report the results of measurements of the thermodynamic properties of niobium used in the fabrication of SRF cavities. The temperature and magnetic field dependence of thermal conductivity, Seebeck coefficient, and specific heat capacity was measured on bulk niobium samples.

INTRODUCTION

Modern particle accelerators rely on superconducting radio-frequency (SRF) cavities to accelerate the charged particles as these SRF cavities can store energy with little dissipation [1]. Primarily made of bulk niobium (Nb), the state-of-the-art processing techniques pushed the ultimate performance of these SRF cavities towards the theoretical limit on accelerating gradient set by the superconducting super-heating critical field. In addition, recent advances in the cavity processing technique of surface engineering with material doping led to exceptionally high quality factor resulting in very low RF power dissipation on cavity walls [2-6]. Ideally, the quality factor of SRF cavities is independent of the accelerating gradient until breakdown occurs when the cavity quenches. The quench of SRF cavities refers to the loss of the superconducting state by warming up a part of cavity above the critical temperature or by exceeding the superconducting critical field.

Quench event occurs at weak superconducting regions or at normal conducting defects on the cavity surface. The efficient transfer of the dissipated power to the helium bath is critical in restoring the cavity to the superconducting state and reliable operation of SRF-based accelerators. The thermodynamic properties such as resistivity, thermal conductivity, and thermal diffusivity are material dependent and the characterization of these properties is necessary to understand the performance limitation [7]. In this contribution, we have measured resistivity, thermal conductivity, specific heat capacity, and Seebeck coefficient of SRF Nb. The temperature and magnetic field dependence of thermal conductivity and heat capacity is also measured.

SAMPLE PREPARATIONS AND EXPERIMENTAL SETUP

Rectangular bar sample of $8 \times 1 \times 1 \text{ mm}^3$ for resistivity, thermal conductivity, and Seebeck coefficient and a sample of $\sim 3 \times 3 \times 1 \text{ mm}^3$ weighing 82.4 mg are cut by a wire electro-discharge machining from a large grain niobium ingot sheet. The samples were treated with buffer chemical polishing (BCP) to remove $\sim 50 \mu\text{m}$ from the surface. The measurements were carried out at the Quantum Design facility using the physical properties measurement system [8].

EXPERIMENTAL RESULTS

Resistivity

The dc resistivity of the sample was measured using the 4-probe method with a constant current of 1.5 mA. Figure 1(a) shows the temperature dependence resistivity with transition temperature $\sim 9.3 \text{ K}$. The room temperature resistivity is measured to be $153 \text{ n}\Omega\text{-m}$ with a residual resistivity ratio (RRR) of 154.

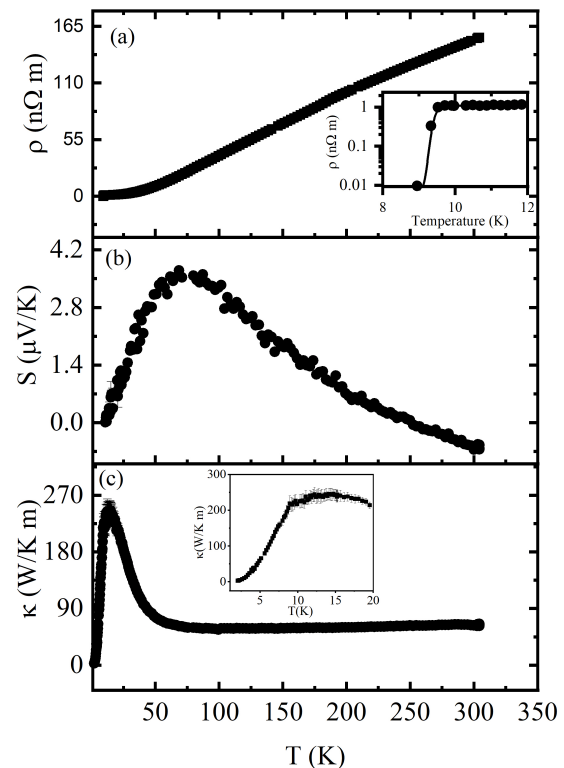


Figure 1: Temperature dependence of (a) resistivity, (b) Seebeck coefficient, and (c) thermal conductivity.

* This manuscript has been authored by Jefferson Science Associates, LLC under U.S. DOE Contract No. DE-AC05-06OR23177.

[†] dhakal@jlab.org

FIRST RESULTS FROM NANOINDENTATION OF VAPOR DIFFUSED Nb₃Sn FILMS ON Nb*

U. Pudasaini[†], Thomas Jefferson National Accelerator Facility, Newport News, VA, USA
G.V. Eremeev, S. Cheban, Fermi National Accelerator Laboratory, Batavia, IL, USA

Abstract

The mechanical vulnerability of the Nb₃Sn-coated cavities is identified as one of the significant technical hurdles toward deploying them in practical accelerator applications in the not-so-distant future. It is crucial to characterize the material's mechanical properties in ways to address such vulnerability. Nanoindentation is a widely used technique for measuring the mechanical properties of thin films that involves indenting the film with a small diamond tip and measuring the force-displacement response to calculate the film's elastic modulus, hardness, and other mechanical properties. The nanoindentation analysis was performed on multiple vapor-diffused Nb₃Sn samples coated at Jefferson Lab and Fermilab coating facilities for the first time. This contribution will discuss the first results obtained from the nanoindentation of Nb₃Sn-coated Nb samples prepared via the Sn vapor diffusion technique.

INTRODUCTION

Nb₃Sn, with a superconducting transition temperature of ~18.2 K and a superheating field of ~400 mT, is a leading alternative material to replace niobium in SRF accelerator cavities [1]. Accordingly, it promises a higher accelerating gradient, quality factor, and operation temperature than traditional bulk Nb. Operating Nb₃Sn SRF cavities at 4.3 K can deliver similar performance to Nb cavities at 2 K, resulting in enormous cost savings for SRF accelerators. That means these cavities can be operated with atmospheric liquid helium or cryocoolers, simplifying and reducing the cost of cryogenic facilities. The successful deployment of Nb₃Sn technology will be transformational, significantly benefiting numerous SRF accelerators and enabling new classes of SRF accelerator applications.

Since Nb₃Sn is a very brittle material with a significantly lower thermal conductivity than Nb, it should be grown as a thin film for application. Several alternate coating techniques are being pursued at multiple labs to grow and optimize Nb₃Sn thin film on metallic structures. Still, the Sn vapor diffusion process is yet the more mature technique for conformality and the only one thus far that has produced rf results for Nb₃Sn-coated Nb cavities. The state-of-the-art single-cell Nb₃Sn cavity frequently attains accelerating gradients of ≥ 15 MV/m with a quality factor ≥ 10¹⁰

[2–5]. Several Nb₃Sn-coated multi-cell cavities have reached ~15 MV with a quality factor of ~10¹⁰ [4, 6]. A significant improvement has been made in the performance of Nb₃Sn-coated cavities over the last decade; these cavities are already suitable for some accelerator applications. Several projects in different laboratories are considering Nb₃Sn-coated cavities for small accelerator applications. The construction of a quarter module using two CEBAF-style C75 cavities is in the final stage at Jefferson Lab. The quarter cryomodule will be installed in the upgraded injector test facility (UITF) to accelerate an electron beam up to 10 MeV [7]. If successful, the facility can use a cryomodule with Nb₃Sn-coated cavities to run low-energy nuclear physics experiments at 4 K. Nb₃Sn cavities have the potential to enable further and significantly simplify widespread use of SRF technology in light-source storage rings, FELs, and other compact accelerators. There have been successful tests of Nb₃Sn cavities operating in conduction-cooled setups as demonstrations suitable for industrial accelerator applications at Fermilab (650 MHz single cell cavity), JLab (1.5 GHz and 952 MHz single cell), and Cornell (2.6 GHz) [8–10]. Detailed plans have been published for a medium-energy, high average-power superconducting e-beam accelerator for environmental applications at Fermilab [11] and a CW, low-energy, high-power superconducting linac for environmental applications by researchers at JLab [12].

Because of the material's brittleness, the mechanical vulnerability is identified as a significant technical challenge in deploying the Nb₃Sn-coated cavities in practical accelerators. The performance degradation of a Nb₃Sn-coated cavity resulting from the tuning of ~300 KHz at room temperatures has been demonstrated [13]. To address this challenge, it is essential to understand the mechanical properties and behavior of vapor-diffused Nb₃Sn thin film. So far, per the authors' knowledge, no such studies have been reported before; we used the nanoindentation technique to obtain fundamental mechanical properties such as elastic modulus, hardness, and yield stress. In this contribution, the first results from nanoindentation of vapor-diffused Nb₃Sn coatings on differently prepared Nb substrates coated in Fermilab and Jefferson Lab coating facilities.

EXPERIMENTAL

Sample Preparation

The substrate samples used here were 30 mm × 30 mm niobium coupons produced by electro-discharge machining (EDM) cutting 3 mm thick, RRR>300 sheet material of the type used for cavity fabrication. These samples received 100-150 μm bulk material removal using buffer

*work supported by the U.S. Department of Energy, Office of Science, Office of Nuclear Physics under contract DE-AC05-06OR23177 with Jefferson Science Associates, including supplemental funding via the DOE Early Career Award to G. Eremeev. The manuscript has been authored by Fermi Research Alliance, LLC, under Contract No. DE-AC02-07CH11359 with the U.S. Department of Energy, Office of Science, Office of High Energy

[†] uttar@jlab.org

INVESTIGATION OF COUPLER BREAKDOWN THRESHOLDS FOR PLASMA PROCESSING OF FRIB QUARTER-WAVE RESONATORS WITH FUNDAMENTAL AND HIGHER-ORDER MODES*

P. Tutt[†], W. Hartung, S. H. Kim, T. Xu

Facility for Rare Isotope Beams, Michigan State University, East Lansing, MI, USA

Abstract

FRIB is developing plasma processing techniques for in-situ recovery of cavity performance in linac cryomodules during long-term user operation. While plasma processing has been shown to be effective for high-frequency (0.8 - 1.5 GHz) elliptical cavities, one of the challenges for FRIB is to avoid plasma breakdown in the fundamental input coupler (FPC), which has relatively weak coupling strength (Q_{ext} ranging from $2E6$ to $1E7$). FRIB cavities are not equipped with higher-order-mode (HOM) couplers; however, in preliminary tests, we found that HOMs are suitable for plasma processing of FRIB Quarter-Wave Resonators (QWRs) driven via the FPC. In this study, we investigated plasma breakdown thresholds in the fundamental and the first 2 HOMs for the FRIB $\beta = 0.085$ QWRs. Electric field distributions in the FPC region and cavity region were calculated for the room-temperature case using CST Microwave Studio's frequency domain solver (FDS). Simulation results will be presented, with a comparison of breakdown thresholds inferred from the RF modeling to the experimental results.

INTRODUCTION

The Facility for Rare Isotope Beams is an accelerator facility that supports a heavy ion linac for nuclear physics research. The linac consists of both quarter-wave resonators (QWR) and half-way resonators (HWR) in its 46 cryomodules. In order to maintain the linac for long-term user operation, mitigation of degrading effects like multipacting and field emission in the superconducting cavities is essential. Plasma processing has been identified as a good technique to reduce field emission at the Spallation Neutron Source (SNS), Fermilab, and others. [1-3]. The technique is advantageous to other surface treatments for Niobium like electropolishing and high-temperature baking because it can be deployed in-situ with the cryomodule.

While plasma processing has been demonstrated to be successful in a wide variety of cavity geometries, there are challenges posed by the potential ignition of the fundamental power coupler (FPC). If ignition occurs within the FPC, the FPC could be damaged or copper from the antenna may be sputtered onto the Niobium surface. Avoidance of this ignition is critical for the implementation of this technique for in-situ use with the cryomodule. In the case of the FRIB

$\beta = 0.085$ QWR, the value of Q_{ext} is on the order of 10^6 to 10^7 which is much greater than the room temperature Q_0 . To improve the coupling of the FPC to the cavity, higher-order modes (HOM) have been investigated as potential candidates for processing which have improved coupling at room temperature.

To investigate the breakdown thresholds for the cavity and coupler volumes of the FRIB $\beta = 0.085$ QWR, CST Microwave Studio (MWS) was used to simulate the electric field distribution inside the cavity and FPC for the fundamental and first two HOMs [4]. Experimental measurements are used to infer the electric field at ignition from the CST model. A theoretical model for the breakdown was adapted from JLab to describe $\beta = 0.085$ QWR for comparison.

CST MWS SIMULATION

To understand the electric field distribution inside the cavity and coupler volumes, CST MWS was used to simulate field distributions at plasma processing conditions. An eigenmode solver was used to assess the cavity fields, but a frequency-driven solver is needed to accurately assess the coupler fields. A mismatch results from room temperature conditions, which were simulated by the inclusion of material with room temperature conductivity of Niobium surrounding the CST model.

A large mismatch between Q_0 and Q_{ext} at the fundamental mode implies that the power delivery to the cavity is poor and reflection is high in the FPC. Not only does this make ignition in the cavity difficult, but a high reflection coefficient can create a standing wave with high electric fields in the FPC that could cause breakdown. HOMs improve the mismatch and have been shown to be effective at FRIB in QWRs and at Fermilab. [5, 6]. Using FDS, the S-parameters were used to identify the first three resonant frequencies which are shown in Table 1. Field distributions were calculated at the resonant frequencies.

Table 1: Resonant Frequencies

Mode	Frequency [MHz]
TEM $\lambda/4$	80.120
TEM $3\lambda/4$	240.92
TEM $5\lambda/4$	402.24

Characterizing E-field for Breakdown

In determining the threshold electric field, several considerations must be made for how breakdown is occurring

* Work supported by the U.S. Department of Energy, Office of Science, Office of Nuclear Physics and used resources of the Facility for Rare Isotope Beams (FRIB) under Award Number DE-SC0000661.

[†] tutt@frib.msu.edu

EXPERIMENTAL STUDY OF MECHANICAL DAMPERS FOR THE FRIB $\beta = 0.041$ QUARTER-WAVE RESONATORS*

J. Brown[†], S. H. Kim, T. Xu, W. Hartung, W. Chang
Facility for Rare Isotope Beams (FRIB), East Lansing, MI, USA

Abstract

The 'pendulum' mechanical mode of superconducting quarter-wave resonators (QWRs) can make them vulnerable to microphonics and/or ponderomotive instabilities. Hence QWRs often make use of stiffening or damping. The FRIB QWRs are equipped with Legaro-style frictional dampers inside the inner conductor along with stiffening elements. In cryomodule tests and linac operation, we observed that the damping efficiency is different for a few $\beta = 0.041$ QWRs. This study aimed to experimentally characterize the damping efficacy as a function of the damper mass and surface roughness. We present damping measurements at room temperature at two different masses and surface roughness as well as discuss future studies for damper re-optimization based on this follow-on study.

INTRODUCTION

Quarter-wave resonators present an effective option for acceleration of charged particles or ions. While the two-gap model of the cavity typically limits the operational speeds to low-beta conditions [1], this means the cavity's effective length is shorter. The shorter axial lengths allows more room for other accelerator elements such as magnets and diagnostic tools. QWRs also have a naturally higher shunt impedance which corresponds to higher accelerating efficiency and lower refrigeration power requirements [2].

Mechanical Modes

FRIB utilizes two variations of QWRs, for $\beta = 0.041$ and $\beta = 0.085$, with both operating at 80.5 MHz in linac segment 1. For both of these QWR types, the electric field is heavily concentrated in the short plane near the bottom of the inner conductor. A map of the electric field for the 0.041 QWR can be seen in Fig. 1. External excitations can cause the inner conductor to swing like a pendulum. In a one dimensional case, the inner conductor can be modeled as a oscillating tube with one end fixed and mode resonant frequencies following [3]:

$$\omega_{mech} = \frac{\alpha^2}{L^2} \sqrt{\frac{E_Y I}{\mu}}, \quad (1)$$

where α is a characteristic mode constant, L is the inner conductor length, E_Y is the Young's modulus of the material

* Work supported by the US Department of Energy, Office of Science, High Energy Physics under Cooperative Agreement award number DE-SC0018362, used resources of the Facility for Rare Isotope Beams (FRIB), which is a DOE Office of Science User Facility, under Award Number DE-SC0000661, and Michigan State University

[†] brownjac@frib.msu.edu

(niobium for SRF applications), I is the tube's moment of inertia, and μ is the linear mass density of the tube. In typical QWR niobium cavities, the pendulum mode frequencies can range from ~ 10 Hz to well over 100 Hz, which can be excited by mechanical pumps, thermo-acoustic oscillation in the cryomodule or cryogenic transfer lines. These modes can have high Q_L , and can persist at high amplitudes for long times if excited on resonance [3].

Microphonics

In QWRs, the RLC circuit model frequency is dependent on the charge (and ultimately, the field) distribution on the two gaps. It is this charge and field that make up the capacitance of the cavity. The total capacitance can be expressed as two plate capacitors:

$$C_{cav} = \frac{2\epsilon A}{d}, \quad (2)$$

where A is the cross sectional area in the short plane, ϵ is the permittivity, and d is the accelerating gap length. As the inner conductor swings, d decreases for one gap and increases for the other by some displacement Δx . This changes the capacitance and thus the resonant frequency of the cavity.

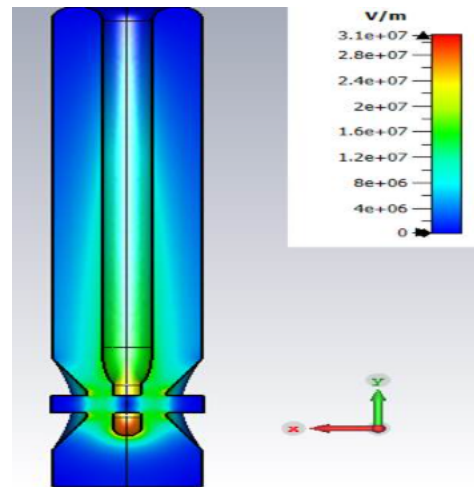


Figure 1: Field map of an FRIB $\beta = 0.041$ QWR from eigenmode simulation in CST Microwave Studio. Field map represents the operational gradient.

Using this lumped circuit model, one can find that $P_f \propto \Delta f^2$, where P_f is the forward power and Δf is the detuning amplitude. The effective length of the $\beta = 0.041$ cavity is 0.160 m, and thus even small displacements of the inner conductor can lead to large detuning amplitudes due to smaller gap sizes. FRIB keeps the detuning within half of

DEMONSTRATION OF MAGNETRON AS AN ALTERNATIVE RF SOURCE FOR SRF ACCELERATORS*

Haipeng Wang[#], Kevin Jordan, Robert A. Rimmer, Jefferson Lab, Newport News, VA, USA
Kyle A. Thackston, James P. Anderson, Charles. P. Moeller, General Atomics,
San Diego, CA, USA
Laurence P. Sadwick, InnoSys, Inc, Salt Lake City, UT, USA

Abstract

Magnetrons have been considered as alternate high-efficiency, low-cost RF sources for linacs and storage rings for national labs and industrial applications. After the demonstration of magnetron power to drive and combine for a radio frequency cavity at 2450 MHz in CW mode, we have used trim coils adding to ferrite magnet and a water-cooled magnetron with a feedback control on coil current amplitude modulation to further suppress the sideband noise to -46.7 dBc level. We have also demonstrated the phase-locking to an industrial grade cooking magnetron transmitter at 915 MHz with a 75 kW CW power delivered to a water load by using a -26.6 dBc injection signal. The sideband noise from the 3-Phase SCRs DC power supply can be reduced to -16.2 dBc level. Further noise reduction and their power combining scheme using magic-tee and cavity type combiners for higher power application (2x50 kW) are to be demonstrated. We intent to use one power station to drive the normal conducting FPC, booster and superconducting RF cavities for the industrial linac.

INTRODUCTION

Magnetrons have been considered as alternative RF sources for superconducting radio frequency (SRF) accelerators since the first demonstration of injection phase lock to an SRF cavity [1]. Comparing to traditional klystrons used in linacs and storage rings, magnetron forms electron bunches in spoke-on-hub process in circular motion in the beam-to-cavity interaction, while klystron only interacts in linear motion. The beam energy can interact with magnetron cavities in multiple circular passes than the single pass in klystron cavities. The spent energy in magnetron is re-used for the cathode heating than being wasted in the beam dump of klystron. To overcome the space-charge force from de-bunching effect, the klystron designs have used lower perveances and longer structures (more cavities) to get higher efficiencies, then higher fabrication cost. Depending on frequency, commercial magnetrons have been operated at 75% to 95% of DC-to-RF efficiency [2]. At Jefferson Lab (JLab), we have first demonstrated injection phase locked magnetron operated at CW, 915 MHz, 75 kW in 2022 [3]. The first installation unit cost was about \$ 1 per Watt. The magnetron tube costs is even less. Current klystrons installed at CEBAF is still at ~\$ 5-8 per Watt.

Solid State Amplifiers (SSAs) are nowadays more popular in SRF applications due to their robust in semiconducting fabrication and utilization in broadcast industries, however application to accelerator is typical at lower frequency (<1.5 GHz), efficiency is around 45-55%, with the cost of \$ 11-15 per watt.

The phase-locked magnetron applications to industrial and medical SRF accelerators [4] could be the first achievable RF sources [5, 6] since the performance of injection phase lock and recent smarter amplitude control progress made will be shown in following sections.

INJECTION PHASE-LOCK DEMONSTRATION OF 915MHZ MAGNETRON

After first demonstrated injection phase lock to a full power of CW 75 kW on the first installed magnetron with a -26.6 dBc injection power, as shown in Fig. 1, we have obtained side band noise reduction from -11.2 dBc to -16.2 dBc at the 360 Hz sideband noise produced by the industrial SCR rectifier type of power supply when the cathode filament current was reduced from the nominal value of 88A to 65 A [3]. Unlike a 2.45 GHz magnetron, the filament power can be complete switched off, further reduction of filament current would affect the magnetron stability performance on the frequency lock.

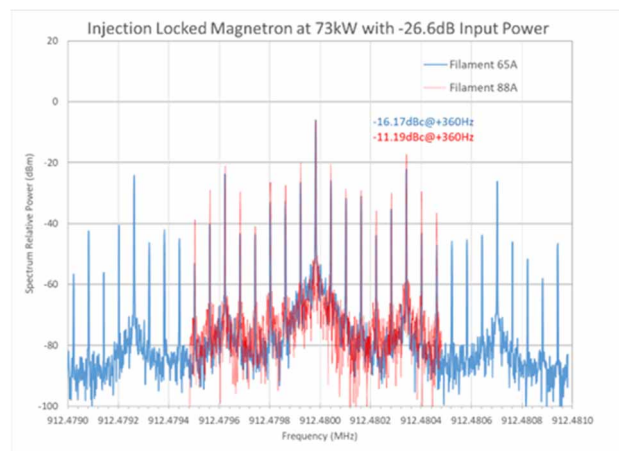


Figure 1: The Injection locked spectrums at 1 Hz of RBW and VBW to compare the noise reductions at 360 Hz on the 1st installed magnetron at 73 kW output power.

The measured anode I-V and I-E curves as shown in Fig. 2 after electrical/RF calibrations have confirmed a negative I-V slope and the DC-to-RF efficiency being

* Authored by Jefferson Science Associates, LLC under U.S. DOE Contract No. DE-AC05-06OR23177, and DOE OS/HEP Accelerator Stewardship award 2019-2023 and FWP2023.
haipeng@jlab.org

TESTING OF THE 2.6 GHz SRF CAVITY TUNER FOR THE DARK PHOTON EXPERIMENT AT 2 K*

C. Contreras-Martinez[†], B. Giaccone, I. Gonin, T. Khabiboulline, O. Melnychuk, Y. Pischalnikov, S. Posen, O. Pronitchev, and J.C. Yun, Fermilab, Batavia, IL, USA

Abstract

At FNAL two single cell 2.6 GHz SRF cavities are being used to search for dark photons, the experiment can be conducted at 2 K or in a dilution refrigerator. Precise frequency tuning is required for these two cavities so they can be matched in frequency. A cooling capacity constraint on the dilution refrigerator only allows piezo actuators to be part of the design of the 2.6 GHz cavity tuner. The tuner is equipped with three encapsulated piezos that deliver long and short-range frequency tuning. Modifications were implemented on the first tuner design due to the low forces on the piezos caused by the cavity. Three brass rods with Belleville washers were added to the design to increase the overall force on the piezos. The testing results at 2 K are presented with the original design tuner and with the modification.

INTRODUCTION

A dark photon is a hypothetical particle that weakly couples to ordinary matter and is an extension of the standard model (SM) of particle physics [1]. At FNAL the search for dark photons consists of two high Q_0 single cell 2.6 GHz SRF cavities, one of which will be called the emitter cavity and the other the receiver cavity. This search is one of several which are known as “light-shining-through-wall” experiments [2]. The emitter will be powered on creating an electromagnetic field (TM_{010}) inside the cavity, the field from this emitter cavity (005) acts as a source of dark photons that can be emitted outside the cavity. The dark photons can penetrate the receiver (006) cavity and be converted to SM photons [2] at the same frequency as the emitter cavity. The receiver cavity thus acts as the sensor. The search for dark photons will take place in the vertical test stand (VTS) at 2 K and inside a dilution refrigerator.

Precise frequency tuning is required for these two cavities so they can be matched in frequency. The 2.6 GHz tuner consists of two titanium (Ti) brackets that attach to the cavity via studs. A cooling capacity constraint on the dilution refrigerator only allows piezo actuators to be part of the tuner system. Three long piezo capsules are used for resonance control. The capsules each contain two $10 \times 10 \times 36$ mm PICMA stacks glued together [3]. The nominal displacement is $38 \mu\text{m}$ per stack when applying a voltage of 0 to 120 V at room temperature and the total stroke

is $76 \mu\text{m}$ per capsule. The piezo capsules are placed in between the two Ti brackets via brass screws that have a ceramic ball (See Fig. 1a). The piezo capsules stretch the cavity increasing the frequency when applying a positive voltage. At temperatures below 77 K, the voltage can go down to -120 V. Applying a negative voltage to the piezo shrinks it with proper piezo preloading, then in this regime the cavity frequency can also be decreased. A schematic of the piezo with different voltages applied to it is shown in Fig. 2.

Before the cavities are placed inside the Dewar for testing the piezos are preloaded by using the screws on the Ti bracket. Since the piezos are stiffer than the cavity and Ti bracket the cavity stretches when the screws are adjusted, the cavity then applies a force on the piezos. The purpose of the preload is to overcome the initial deformation of the Ti bracket and avoid gaps due thermal shrinkage of the different materials once cooled to 2 K. The piezos must have a preload of 1 kN (based on the experimental results from this paper) each to avoid these issues. The preload force applied to the piezos is determined by the 35 kN/mm cavity stiffness and the $10 \text{ kHz}/\mu\text{m}$ longitudinal frequency deformation sensitivity [4]. Once the proper preload has been set the cavity-tuner system has a piezo stroke to cavity deformation efficiency of 70 – 80 % [4]. An estimate of the tuner range can be calculated based on the stroke of the piezo. At 2 K the piezo stroke is 20 % from the room temperature value resulting in a stroke of $15.2 \mu\text{m}$ from 0 to 120 V for the capsule. The efficiency of the tuner is 70 % thus the total range expected is $212 \text{ kHz} \pm 30 \text{ kHz}$ (from -120 V to 120 V).

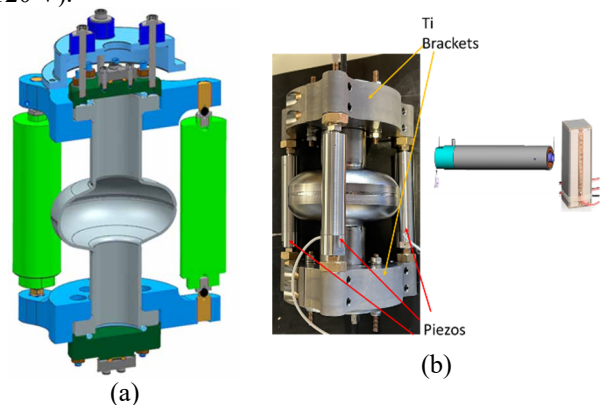


Figure 1: (a) Cross-section view of the cavity. (b) Picture of the cavity with piezos installed. The picture of the actuator with a single stack is also shown.

INITIAL DESIGN

Testing at 2 K requires that the piezo preload set at room temperature is preserved. The different shrink rates of the

*This material is based upon work supported by the U.S. Department of Energy, Office of Science, National Quantum Information Science Research Centers, Superconducting Quantum Materials and Systems Center (SQMS) under contract number DE-AC02-07CH11359.

[†] ccontrer@fnal.gov

STUDY OF DIFFERENT PIEZOELECTRIC MATERIAL STROKE DISPLACEMENT AT DIFFERENT TEMPERATURES USING AN SRF CAVITY*

C. Contreras-Martinez[†], Y. Pischalnikov, JC Yun, Fermilab, Batavia, IL, USA

Abstract

Piezoelectric actuators are used for resonance control in superconducting linacs. The level of frequency compensation depends on the piezoelectric stroke displacement. In this study, the stroke displacement will be measured with a 1.3 GHz SRF cavity by measuring the frequency shift with respect to the voltage applied. The entire system was submerged in liquid helium. This study characterizes the PZT piezoelectric actuator (P-844K093) and a lithium niobate (P-844B0005) piezoelectric actuator. All these actuators were developed at Physik Instrumente (PI). The piezoelectric displacement was measured at different temperatures.

INTRODUCTION

Piezoelectric (piezo) actuators have a wide array of applications such as in resonance control in SRF linacs and various experiments in dilution refrigerators. In a dilution refrigerator the cooling capacity is on the order of μ Ws. In these applications a large stroke and small heat dissipation are crucial, two piezo materials will be compared with these characteristics. Piezo actuators exhibit the piezoelectric effect which occurs below the Curie temperature. Materials exhibiting this effect experience a mechanical deformation when an electric field is applied to the material. The opposite effect is also possible where a mechanical deformation of the material will induce an electric field. Lead zirconate titanate (PZT) is the most widely used material for actuators, it provides larger stroke but it heats up rapidly. Lithium niobate (LiNbO_3) produces 0.3 % of heat dissipation of PZT but has a stroke of 8.3 % of PZT at room temperature. This comparison uses the nominal voltage of each piezo, see Table 1 for properties of both. From the literature, it is known that LiNbO_3 doesn't decrease the displacement stroke as drastically compared to PZT. Thus, when both are at cryogenic temperature the stroke difference won't be as large.

In this experiment, an SRF cavity was used to measure the piezo stroke. The piezo stroke for PZT is cited in the literature as being 10 % of the room temperature value at 4 K [1, 2] and by piezoelectric companies [3, 4]. As reported in [5], LCLS-II cryomodule commissioning showed that the piezo stroke was larger than this value. A more thorough measurement of the piezo stroke is done in this paper to validate the results from the cryomodule commissioning. An SRF cavity was used due to its extreme sensitivity to longitudinal deformation. A 1 nm deformation on

the cavity will result in a 2.3 Hz frequency deviation which can be easily recorded. The PZT piezo actuator used in this experiment (P-844K093) consists of two stacks with dimensions given in Table 1. The LiNbO_3 actuator (P-844B0005) dimensions are also listed in Table 1. The main results from this paper are that the PZT stroke at 4 K is greater than 10 % of the room temperature value and the piezo stroke of the LiNbO_3 actuator is measured with an SRF cavity for the first time. For the PZT piezo actuator the stroke measurements were done from 4 K up to 91 K.

Table 1: Piezoelectric properties of LiNbO_3 and PZT actuators used in this paper. For PZT the voltage to obtain the stroke is 0 V to 100 V and for LiNbO_3 it is from -500 V to 500 V.

	PIC 050	PIC 255/252
Material	LiNbO_3	PZT
Length [mm]	36	18
Cross-section [mm^2]	100	100
Stroke (300 K) [μm]	3	15
Stiffness [$\text{N}/\mu\text{m}$]	195	200
Blocking Force [N]	585	3600
Curie Temperature [K]	1423	623
Density ρ [g/cm^{-3}]	5	7.80
Relative Permittivity	28.7	1750
ϵ_{33}/ϵ_0		

CAVITY FREQUENCY TUNER

The dark-photon search experiment setup [6] was used to conduct the measurements. This setup consists of an LCLS-II tuner that uses a stepper motor and piezos. The cavity-tuner system is supported by an aluminum frame. There are two piezos capsules used to control the frequency, in this case, the PZT and LiNbO_3 capsules were

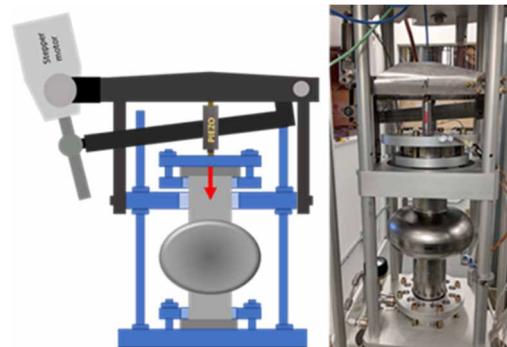


Figure 1: Left: schematic of one cell 1.3 GHz cavity with tuner installed. Right: Picture of the cavity.

*This manuscript has been authored by Fermi Research Alliance, LLC under Contract No. DE-AC02-07CH11359 with the U.S. Department of Energy, Office of Science, Office of High Energy Physics.

[†]ccontrer@fnal.gov

A NOVEL TWIN DRIVE TUNER MECHANISM FOR 1.3 GHz ILC CAVITY

M. Yamanaka[†], KEK, Tsukuba, Ibaraki, Japan

Abstract

We propose a new tuner mechanism for the 1.3 GHz ILC cavity named a twin-drive tuner. A bellow is provided in the central portion of the helium tank in the longitudinal direction, and flanges are provided on both sides of the bellows. A linear motion actuator is mounted to the flange on one side, and the frequency is changed by pushing and pulling the flange on the opposite side. Significantly, two linear motion actuators are placed in circumference and working simultaneously. A prototype tuner was developed, and the frequency tuning was evaluated. The displacement between the flanges and the frequency are proportional, both have good linearity, and the slope is 296 kHz/mm.

INTRODUCTION

A tuner is a device that mechanically deforms a cavity to change the natural frequency. Since the superconducting cavity is cooled by liquid helium, it shrinks from room temperature, and the natural frequency drops. Therefore, expanding the cavity to match the desired operating frequency is necessary. The tuner mechanism for the 1.3 GHz ILC cavity is described in the ILC Technical Design Report (TDR) [1]. Three mechanisms (blade, lever, slide-jack) have been proposed, all expanding and compressing the cavity in the longitudinal direction. Of these, the blade tuner was adopted. E-XFEL in Germany and LCLS-II in the US are large accelerators that use 1.3 GHz TESLA cavities. These accelerators adopted the lever tuner [2, 3]. The E-XFEL and LCLS-II have different helium tank and tuner designs. A lever tuner is located on the pickup side of the cavity and is mounted between the helium tank and a conical flange welded onto the beam tube. The cavity expands and compresses by operating the tuner. The lever tuner was reported as having a low manufacturing cost. Each has a production result of several hundred units.

The author proposes a novel tuner for a 1.3 GHz ILC cavity, which differs from conventional tuners. Here, we explain the mechanism of the proposed twin-drive tuner and show the developed prototype and performance evaluation test results.

PROPOSAL OF A NEW TUNER MECHANISM

An overview of the new tuner mechanism is shown in Fig. 1 [4]. A bellow is equipped so the helium tank can expand and compress in the longitudinal direction. Flanges are provided on both sides of the bellow, and an actuator varies the distance between these flanges. Like the blade and slide-jack tuners, it is placed on the outer circumference of the helium tank. Two actuators are mounted at opposite positions on the circumference. Each actuator comprises a linear motion actuator for coarse

tuning and a piezo actuator for fine tuning. Figure 1 assumes that the cavity is elongated. The specifications required for tuner design are shown in the TDR, some of which are shown in Table 1. The tuning frequency range is 600 kHz. The 9-cell cavity and the helium tank are assembled by welding, and the longitudinal stiffness (spring constant) is 3 kN/mm. Therefore, the required stroke of the tuner is about 2 mm, and the maximum loading force is 6 kN. A twin-drive tuner requires a loading force of 3 kN per unit because two actuators share it. The use of an actuator with a large loading force simplifies the mechanism. The lever tuner uses a double lever mechanism to increase the force by 1:20 [3]. In the proposed scheme, there is no mechanism for power boosting. A piezo actuator for fine movement is arranged in series with the linear actuator. Repeated expansion and compression operation is performed at a high frequency to cancel the cavity's deformation due to the Lorentz force during the pulse operation of the accelerator. Maximum stroke is 3 μ m.

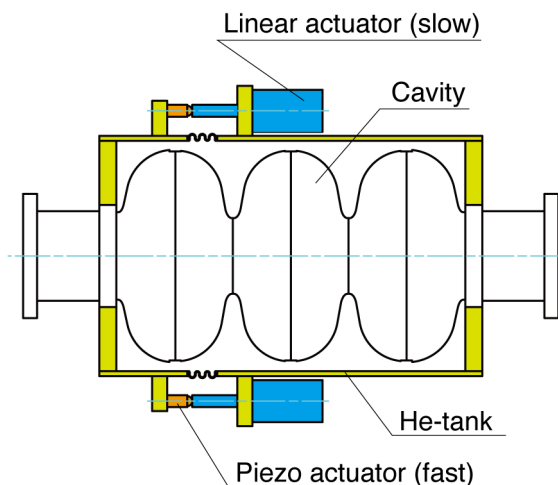


Figure 1: Schematic view of new tuner mechanism.

Table 1: Specifications of ILC Tuner Parameters and Experiment Results

Parameters	Specifications	Experiment results
Cavity elongation tuning $\Delta f/\Delta L$ [kHz/mm]	315	296
Cavity spring constant [kN/mm]	3	2.7
Slow tuner frequency range [kHz]	600	400
Slow tuner dimensional range [mm]	2 (~600/315)	1.3
Required loading force [kN]	6 (3x2)	3.6

[†] masashi.yamanaka@kek.jp

PROTOTYPE SSR2 TUNER PROCUREMENT AND TESTING AT IJCLab FOR PIP-II PROJECT

N. Gandolfo, P. Duchesne, D. Le Dréan, D. Longuevergne, G. Mavilla, T. Pépin-Donat
Université Paris-Saclay, CNRS/IN2P3, IJCLab, Orsay, France
M. Parise, D. Passarelli, Y. Pischalnikov, Fermilab, Batavia, IL, USA

Abstract

IJCLab is involved in the PIP-II project on the design and development of accelerator components for the SSR2 (Single Spoke Resonator type 2) section of the superconducting linac. Five prototype tuners have been built and are being tested at IJCLab. After a short description of the tuner, this paper reports on the procurement strategy and the performance observed at both room and low temperatures in vertical cryostat test with SSR2 prototype cavities. This paper will also share results on accelerated lifetime tests performed in a dedicated nitrogen-cooled cryostat.

INTRODUCTION

The SSR2 tuner (see Fig. 1) for the PIP-II project is based on a mechanical deformation system using a lever arm coupled to an actuator system consisting of a stepper motor and two piezoelectric actuators. It is an adapted version of the SSR1 cavity tuning systems from the same project [1]. The entire system shares all the constraints experienced by the cavity, such as vacuum, low temperatures and radiation. An important feature of this tuner is that every active components are assembled on a plate called “motor cartridge” which is located on the side of the cavity and accessible for replacement in case of maintenance through a service port of the cryomodule.



Figure 1: Prototype SSR2 cavity equipped with its tuner.

PROCUREMENT

Tuners are made up of three types of components: mechanical parts, motor actuators and piezoelectric actuators. They are ordered separately and assembled in laboratory environment.

Mechanical Parts

Due to the risk of magnetic trapping of the cavity during superconducting transition, particular attention is paid to magnetic permeability, so as not to magnetize certain elements of the tuning system. Most mechanical parts (notably the arms) are made from stainless steel AISI 316L (see Fig. 2) to limit magnetization. However, an upgrade to AISI 316LN is planned to further reduce the risk of magnetization. Also, most of the screws are made of silicon bronze C65100.



Figure 2: Every parts of the tuner before first assembling.

Piezoelectric Actuators

The piezoelectric actuators manufactured by PI are low-voltage, multi-layer encapsulated models giving high resistance against risk of mechanical shocks during handling and also against moisture over the storage and installation phases. Individual acceptance tests are carried out for the piezoelectric actuators, with capacitance and stroke measurement. Two piezoelectric actuators are installed for each tuner, sharing force and giving the capability to be used alone or in parallel.

Motor Actuators

Phytron delivered the entire motor actuator which consist of a stepper motor attached to a planetary gearbox and coupled to a screw-nut system as illustrated in Fig. 3. All of these components are dry-lubricated for low-temperature operation under vacuum. Motors are tested immediately after installation.



Figure 3: Motor actuator.

DEVELOPMENT OF 3.9 GHz 9-CELL CAVITIES AT SHINE

Xiaowei Wu, Zhangjiang Lab, Shanghai, China
Jinfang Chen*, Pengcheng Dong, Shenjie Zhao, Xiaohan Ouyang,
Yuefeng Liu, Sen Sun, Yeliang Zhao, Yuxin Zhang, Jiani Wu, Shuai Xing
Shanghai Advanced Research Institute, CAS, Shanghai, China
Zheng Wang, Yue Zong, Xuan Huang
Shanghai Institute of Applied Physics, CAS, Shanghai, China
Runzhi Xia, Yawei Huang, ShanghaiTech University, Shanghai, China

Abstract

The Shanghai high-repetition-rate XFEL and extreme light facility (SHINE) Linac requires two 3.9 GHz cry-modules to linearize energy distribution before the bunch compressor. As a key component to the project, studies of 3.9 GHz cavities were conducted in the past few years. The first 3.9 GHz 9-cell prototype cavity has been fabricated, tested, and qualified. It reached $Q_0=3.5\times 10^9$ at 13.1 MV/m and a maximum accelerating gradient of 25.0 MV/m during the vertical test of the bare cavity. The prototype has been helium tank integrated and reached $Q_0=2.9\times 10^9$ at 13.1 MV/m in the vertical test, with a large margin with respect to the SHINE specification. The second prototype has been fabricated and is planned to be tested in 2023. This paper will cover the fabrication, surface treatment, and RF test of the 3.9 GHz cavities.

INTRODUCTION

The main part of the SHINE Linac is an 8 GeV superconducting accelerator operating in continuous wave (CW) mode. It consists of seventy-five 1.3 GHz cryomodules and two 3.9 GHz cryomodules [1–4]. The third harmonic cavities compensate the nonlinear longitudinal phase space distortion due to the accelerating field curvature in the 1.3 GHz cavities prior to bunch compression [5, 6].

As a key component to maintain low emittance beam for the production of FEL light to the experimental users, 3.9 GHz cryomodules has been successfully applied in the FLASH VUV facility, the European X-ray free electron laser (XFEL), and the Linac coherent light source-II (LCLS-II) [7–15]. The rf design of the 3.9 GHz 9-cell cavity has been optimized for SHINE project [16]. Two prototypes of 3.9 GHz 9-cell cavities have been fabricated and one of them has been vertical tested. Mass production of the 3.9 GHz SHINE cavity series has been started. This paper presents the results of the prototypes achieved so far, and the status of the SHINE 3.9 GHz cavities.

RF DESIGN OF THE CAVITY

The rf design of the SHINE 3.9 GHz 9-cell cavity was optimized based on the design and experience of 3.9 GHz cavities in the XFEL and the LCLS-II projects. Beam pipe and end half-cell of the SHINE 3.9 GHz cavity was

modified compared with the other designs. Inner cell was kept the same. The radius of the beam pipe was decreased to 38.0 mm to shift the lowest dipole mode to 4165 MHz. This is to avoid difficulties for fundamental mode operation and HOM notch tuning [14, 15]. Details of the rf design could be found in Ref. [16].

FABRICATION OF THE PROTOTYPES

The production of two 3.9 GHz 9-cell prototypes was tendered to a domestic company which fabricated several 3.9 GHz single-cell cavities as a starting step [17]. The fabrication of the first prototype started from the beginning of 2021 and the second one started from the end of 2022.

Bare Cavity Fabrication

The production of the SHINE 3.9 GHz prototypes adopted standard fabrication procedures [10]. The components of 3.9 GHz 9-cell cavity including half-cells, dumbbells, and end groups were characterized both in mechanical measurements and rf tests during the processing.

The half-cells were prepared with an additional length at both iris and equator area which accounts for the welding shrinkages and trimming procedures. Inner shape of the half-cells and dumbbells were checked by the coordinate measuring machine. Figure 1 shows all the components of the prototype before final welding.



Figure 1: Components of the prototype before welding.

The dumbbells were trimmed to meet the designed frequency and length at the same time before integrating together. The sensitivity coefficients applied in the trimming

* chenjinfang@sari.ac.cn

RF PERFORMANCE RESULTS OF RF DOUBLE QUARTER WAVE RESONATORS FOR LHC HIGH LUMINOSITY PROJECT

K. Turaj*, J. Bastard[†], R. Calaga, S. J. Calvo, O. Capatina, A. Castilla[‡], M. Chiodini, C. Duval[†], A. Edwards¹, L. M. A. Ferreira, M. Gourragne, P. J. Kohler, E. Montesinos, C. Pasquino, G. Pechaud, N. Stapley, N. Valverde Alonso, and J. D. Walker
CERN, Geneva, Switzerland

¹also at Lancaster University, Lancaster, United Kingdom

Abstract

The LHC High Luminosity (HL-LHC) project includes, among other key items, the installation of superconducting crab cavities in the LHC machine. The Double Quarter Wave (DQW) crab cavity will be utilised to compensate for the effects of the vertical crossing angle. Two bare DQW series cavities were manufactured in Germany by RI Research Instruments and validated successfully at CERN through a cold test at 2 K. Two DQW series cavities were produced in-house at CERN, integrated into a titanium helium tank, and equipped with RF ancillaries. This paper addresses the cavities preparation processes and summarizes the results of cryogenic tests of DQW cavities at CERN.

INTRODUCTION

The HL-LHC project aims to increase the design luminosity by 5-7 times compared to LHC nominal value [1]. This will be achieved in part by using two pairs of RF superconducting crab cavities, both up- and down-stream of the LHC Interaction Points (IPs): 1 (ATLAS) and 5 (CMS), to partially compensate for the geometric reduction in luminosity due to the beam crossing angle at the IPs. The beam crossing angle is necessary to separate bunches immediately before and after the collision point. This leads to a reduction in the geometric overlap of the colliding beams, thereby decreasing the instantaneous luminosity [2]. The crab cavities are designed to impart an appropriate transverse kick to the head and the tail of the bunches to restore the almost head-on collisions at the IP. Due to the difference in the crossing plane at the IPs, two distinct types of crab cavities are required: the Double-Quarter Wave resonator (DQW) at IP5 to provide compensation for the vertical crossing angle and the Radiofrequency Dipole (RFD) crab cavity at IP1 for the horizontal crossing angle. The machine constraints near the IPs limit the cavity transverse dimension therefore the HL-LHC crab cavities are characterized by an unconventional, compact, and complex design. Moreover, they require very precise control of the RF phase so that the rotation of the beam before the collision is precisely cancelled on the other side of the IPs. Each cavity operates at 2 K and is designed to provide a transverse kick voltage of 3.4 MV at 400.79 MHz. They will be assembled in cryomodules, each containing two identical cavities.

DQW cavities (see Fig. 1) are subject to a complex manufacturing procedure [3], as a consequence of their design, requiring rigorous RF inspections to ensure that the cavities are in the appropriate frequency range at each stage of the production process. In addition, RF surface treatment, cold test preparation, and a contamination-free quality control system ensure that the cavities will meet both performance and frequency specifications when operating in the LHC machine. The production of the DQW cavities follows similar procedures as for the RFD cavities [4].



Figure 1: The DQW cavity geometry.

Two DQW series bare cavities were manufactured so far by Research Instruments GmbH (RI) in Germany and tested at 2 K at CERN. The cavities are currently at RI for helium tank assembly. The manufacturing of six additional DQW cavities is ongoing at RI and is expected to be completed by 2024. In addition, two series DQW cavities were produced in-house at CERN, integrated into a titanium helium tank and finally equipped with RF ancillaries. Bare, jacketed and dressed cavity configurations have been validated through cryogenic tests in a vertical cryostat at the CERN SM18 facility. To ensure full control of the process, and thus the comparability of cold test results, the cavities were subjected to the same preparation process. This paper addresses some of the major challenges in preparing, processing and testing the DQW cavities.

FREQUENCY EVOLUTION AND TUNING

During the production of the DQW crab cavities, the fundamental frequency is regularly measured. Furthermore,

* katarzyna.turaj@cern.ch

[†] from consortium AL-40/30

[‡] now at Jefferson Lab, Newport News, USA

COMPLETION OF TESTING SERIES DOUBLE-SPOKE CAVITY CRYOMODULES FOR ESS

R. Santiago Kern*, C. Svanberg, K. Fransson, K. Gajewski, L. Hermansson, H. Li, T. Lofnes,
A. Miyazaki[†], M. Olvegård, I. Profatlova, R. Ruber¹, M. Zhovner
Uppsala University, Uppsala, Sweden

¹also at Thomas Jefferson National Accelerator Facility, Newport News, VA, USA

Abstract

The FREIA Laboratory at Uppsala University, Sweden, has completed the evaluation of 13 double-spoke cavity cryomodules for ESS. This is the first time double-spoke cavities will be deployed in a real machine. This paper summarizes testing procedures and statistics of the results and lessons learned.

THE FREIA LABORATORY

The FREIA Laboratory in Uppsala [1] is a leading laboratory in accelerator R&D in Sweden and currently responsible for testing the 13 double-spoke cryomodules (plus one spare) for the European Spallation Source (ESS) in Lund [2]. These cryomodules have two double-spoke cavities each, are assembled at Laboratoire Irène Joliot-Curie (IJCLab), in Paris (France) and transported to FREIA for testing. In this regards FREIA counts with its own helium liquefaction plant and suitable radio-frequency (RF) power stations.

TESTING TIMELINE AND CAMPAIGN

After the testing of the prototype double-spoke cryomodule finished in October 2019 [3–5], the infrastructure and procedures were updated based on this experience and the instrumentation adapted for the series cryomodule testing. The testing of the 13 series cryomodules started in October 2020 and has ended in May 2023, with just the spare cryomodule left to test at the time of print. From the 13 cryomodules tested, five of them had to be sent to IJCLab for repairs, bringing the total number of tests done at FREIA up to 18. Table 1 gives an overview of the disqualified cryomodules and the reason for the disqualification. There were two reasons that repeated over cryomodules:

- A leak between the double wall tube and the beam vacuum at cold: due to the mechanical polishing of a weld to prepare a perfect surface for copper plating on top, and
- A problem with the stepper motor: became mechanically non responsive after reaching certain position. The stepper motor was exchanged after warming up. The root of the cause is still under investigation by the corresponding parties.

The leaks in the super-critical helium (ScHe) circuit cooling the outer conductor of the coupler, which decouples the 300 K region from the 2 K, were revealed only after the

cryomodules had been cooled with liquid helium. When leak tested in advance at warm there was no leak indication; thus, the cold test at FREIA was the first test identifying this issue. All of these cryomodules were tested once again at FREIA after being repaired, and all were accepted.

Table 1: List of Disqualified Cryomodules (CM) and Their Cause

CM #	Issue
CM02	Stepper motor lack of response
CM03	Stepper motor lack of response
CM04	Stepper motor lack of response
	Vacuum leak in FPC's double wall tube
CM09	Vacuum leak in FPC's double wall tube
CM10	Stepper motor lack of response

Schedule

In average, the time spent testing from arrival of the cryomodule until it is back in the cargo area is ca. six weeks, during which four of those are spent at cold. The cryomodules are shipped with the insulation vacuum and helium circuits filled with dry nitrogen gas while the cavity's beam volume is under vacuum. The cryomodule usually stays a couple of days in the FREIA hall for thermalization before any work is done. The list of tasks and the time they ideally take are, in chronological order, as follows (Fig. 1):

In FREIA's cargo area:

- Reception tests (1 day): to check the electrical continuity of connectors and the beam vacuum's level. Note that the cavities arrive under vacuum (ca. 1×10^{-3} mbar).
- The cryomodule is moved to a frame with wheels and the RF waveguide-coaxial adapters (aka doorknob) are mounted (1 day).
- The cryomodule is then wheeled into the bunker (1 day).

Once in the bunker

- The cryogenic lines of the cryomodule and the valvebox are connected (1/2 day).
- The helium circuit is purged once to check for leaks at vacuum and above atmospheric pressure levels (1/2 day).
- If no leaks are found, the bellow containing all cryogenic connections is closed (1/2 day).

* rocio.santiago_kern@physics.uu.se

[†] now at CNRS/IN2P3/IJCLab, Université Paris-Saclay, Orsay, France

PERFORMANCE ANALYSIS OF SPOKE RESONATORS, STATISTICS FROM CAVITY FABRICATION TO CRYOMODULE TESTING

A. Miyazaki*, P. Duchesne, D. Ledrean, D. Longuevergne, G. Olry
CNRS/IN2P3/IJCLab Université Paris-Saclay, Orsay, France

Abstract

Irène Joliot-Curie Laboratory (IJCLab) has been leading the development of spoke resonators in multiple international SRF projects, from fundamental R&D, prototyping, to series production. The European Spallation Source (ESS) superconducting linac is the first of its kind to put into operation the spoke resonators. After three prototype cavities, 29 ESS production cavities have been processed, tested, assembled into cryomodules at IJCLab, and then shipped to Uppsala for the site acceptance test. Seven prototypes for two other major projects, Multi-purpose hYbrid Research Reactor for High-tech Application (MYRRHA) and Proton Improvement Plan II (PIP-II), designed in collaboration with external institutions, have as well been processed and tested at IJCLab. A new challenge is to fully process series cavities in industry, following the successful implementation of 1.3 GHz elliptical cavities in the other projects. This paper summarises main results obtained from fabrication to final testing, including frequency tuning strategy, performance, limitation in vertical cryostat, and identifies future direction of projects and R&D in the field of spoke cavities.

INTRODUCTION

Superconducting spoke cavities are the choice in a medium- β section of proton drivers. Since the late 1980s [1], spoke cavities have been developed and their technology is matured today [2–6]. However, practical challenges for the deployment of these cavities in real machines need to be identified and overcome. Unlike the 1.3 GHz TESLA-type cavities, spoke cavities are not sufficiently standardised and there are many open questions towards the successful operation of accelerators. Irène Joliot-Curie Laboratory (IJCLab) plays a leading role in this crucial matter in international projects.

IJCLab has been pioneering the development of spoke cavities technology from fundamental studies [7, 8] to design and prototyping work [4, 9] and even deployment in the machines. In this paper, we overview state-of-the-art technology in developing spoke resonators at IJCLab with three international projects as examples. The series production of European Spallation Source (ESS) [10] double-spoke cavities revealed delicate issues in frequency tuning, including fabrication, chemical etching, and heat treatment. We discuss how we overcame these issues with statistics obtained during the production. These ESS cavities have been qualified in cold tests, integrated in cryomodules, and all passed the site-acceptance tests at Uppsala University. The

next challenge of ESS is installation, commissioning, and of course, operation in the machine.

We completed prototyping four single-spoke cavities for the Multi-purpose hYbrid Research Reactor for High-tech Application (MYRRHA) [11]. The next challenge is to industrialise the surface treatment of spoke cavities, whose complicated shape may require special attentions compared to conventional elliptical cavities. We also show preliminary results on heat treatment in prototype MYRRHA cavities, which may be a breakthrough towards 4 K operation of spoke resonators. Finally, we started prototyping Single Spoke Resonator 2 (SSR2) for Proton Improvement Plan II (PIP-II). We discuss preliminary results and trade-off of cavity design between RF performance and cleaning process.

SUPRATECH

IJCLab hosts the SUPRATECH facilities, where one can perform chemical treatments, high-pressure water rinsing (HPR), heat treatment, mechanical frequency tuning, cold tests at 4 K and 2 K, assembly of cavity string and cryomodules, and cryomodule testing. As shown in Fig. 1, two spoke cavities can be tested at a time in a vertical cryostat ($\phi 800$) with a vacuum insert which requires a helium tank welded around the cavity [7]. In SUPRATECH, we do not measure bare cavities today because of the following strategic reasons. First, we can save a huge amount of liquid helium for cold tests, because helium supply is a global issue for the SRF community today. Secondly, the small heat capacitance of the cryostat enables quick cool down and warm up. As a drawback, however, careful frequency tuning is required in fabrication, surface processing, and even cooling down because we skip the cold test of a bare cavity to check the frequency before welding the helium tank. This unique tuning and testing strategy has been successful in the ESS project and the same was adopted for other similar projects (MYRRHA and PIP-II SSR2). Therefore, a global standard of future projects can follow our strategy: accurate frequency tuning and only one cold test in a vertical test-stand.

ESS SERIES CAVITIES

ESS is a proton driver in Sweden for neutron science via nuclear spallation. In the spoke section from 90 MeV to 216 MeV, it deploys 13 cryomodules, each of which accommodates two double-spoke cavities with 352 MHz. The target gradient is $E_{\text{acc}} = 9$ MV/m with an unloaded quality factor $Q_0 = 1.5 \times 10^9$ at 2 K. Since the geometry factor is $G = 133 \Omega$ and the peak field ratio is $6.9 \text{ mT}(\text{MV}/\text{m})^{-1}$, the target surface resistance and peak magnetic field are 89 n Ω and 69 mT, respectively. Compared to state-of-the-art ellip-

* akira.miyazaki@ijclab.in2p3.fr

DEVELOPMENT OF SINGLE-SPOKE CAVITIES FOR ADS AT JAEA

Y. Kondo*, J. Tamura, B. Yee-Rendon, S. Meigo, F. Maekawa, JAEA, Tokai, Naka, Ibaraki, Japan
E. Kako, K. Umemori, H. Sakai, T. Dohmae, KEK, Oho, Tsukuba, Ibaraki, Japan

Abstract

Japan Atomic Energy Agency (JAEA) has been proposing an accelerator-driven system (ADS) as a future nuclear system to efficiently reduce the high-level radioactive waste generated at nuclear power plants. As the first step toward the full-scale CW proton linac for the JAEA-ADS, we are now prototyping a low-beta (around 0.2) single-spoke cavity. Because there is little experience in manufacturing superconducting spoke cavities in Japan, prototyping and performance testing of the cavity are essential to ensure the feasibility of the JAEA-ADS. The dimensional parameters of the prototype spoke cavity were optimized to obtain higher cavity performance. The actual cavity fabrication started in 2020. Most of the cavity parts were fabricated in the fiscal year 2020 by press forming and machining. In 2021, we started welding the cavity parts together. After investigating the optimum welding conditions using mock-up test pieces, each cavity part was joined with smooth welding beads. Currently, the cavity's body section and the beam port sections have been assembled. This paper presents the current status of the JAEA-ADS and its cavity prototyping.

INTRODUCTION

Toward the realization of a sustainable society, nuclear energy has been gathering attention again in recent years, and expectations for new nuclear power systems such as small modular reactors and high temperature gas cooled reactors are increasing. However, the essential problem of generating spent nuclear fuel still exists. In addition, spent fuel that has already been generated must eventually be disposed of, therefore, the disposal of high-level radioactive waste is a common issue to all humankind that must be overcome. In Japan, the OMEGA project has been launched in 1998. Since then, the Japan Atomic Energy Agency (JAEA) has been pursuing the possibility of reducing the volume and toxicity of high-level waste through transmutation using an accelerator-driven subcritical reactor system (ADS) [1]. The purpose of the OMEGA project is the partitioning and transmutation (PT) of long-lived nuclear waste. The JAEA's proposal is, by PT of minor actinoides (MA), to reduce the area needed for geological disposal to 1/200, and to reduce the necessary years to lower the toxicity of the high-level waste below the natural uranium level from 100,000 to 300 years.

Figure 1 shows the schematic view of the JAEA-ADS subcritical reactor, and Table 1 summarizes the specifications of the JAEA-ADS. The transmission rate of 10%/MA / year means that one ADS can transmute the MA from ten units of light water reactor. The essential difference between the

ADS and conventional nuclear systems is that the proton beam from the accelerator controls the criticality of the reactor. The driver linac is the key component of the ADS.

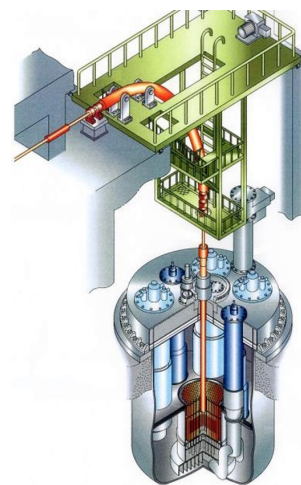


Figure 1: Schematic view of the JAEA-ADS subcritical reactor.

Table 1: Specifications of JAEA-ADS

Spallation target	Pb-Bi eutectic (LBE)
Coolant	LBE
Thermal output	800 MWt
Proton beam power	30 MW
Subcriticality k_{eff}	0.97
MA initial inventory	2.5 t
Transmutation rate	10%/MA / year = 250 kg

During the 1990s, JAEA designed the first ADS linac [2] as a part of the Neutron Science Project (NSP). The NSP was designed to be a multipurpose neutron source that could also be used for ADS research and development. The accelerator had a beam current of 10 mA, a final energy of 1.5 GeV, and used normal conducting (NC) cavities in the low-medium relativistic β range of 0.06 (2 MeV) to 0.42 (100 MeV), as well as superconducting (SC) cavities in the high- β section. Later, the NSP was combined with the Japan Hadron Project (JHP) to become the J-PARC. The J-PARC linac achieves the final energy using NC cavities rather than SC cavities.

Based on the recent progress of low- β SRF technologies, we modernized the linac design from the NSP linac to match the requirement of the ADS dedicated linac listed in Table 2.

We decided to use SRF cavities for low- β region. However, in Japan, there is very little experience in the development of low- β SRF cavities, especially, never completed

* yasuhiko.kondo@j-parc.jp

COMMISSIONING OF THE UHH QUADRUPOLE RESONATOR AT DESY

R. Monroy-Villa*¹, A. Gössel, D. Reschke, M. Röhling, M. Schmökel, J.-H. Thie, M. Wiencek
Deutsches Elektronen-Synchrotron, Hamburg, Germany
W. Hillert, C. Martens, M. Wenskat

Universität Hamburg, Institut für Experimentalphysik, Hamburg, Germany

¹also at Universität Hamburg, Institut für Experimentalphysik, Hamburg, Germany

Abstract

Pushing the limits of the accelerating field or quality factor of SRF cavities beyond pure Nb requires the implementation of specific inner surface treatments, which are yet to be studied and optimized. One of the fundamental challenges in exploring alternative materials is that only samples or cavity cut-outs can be fully characterized from a material science point of view. On the other hand, complete cavities allow for the SRF characterization of the inner surface, while samples can usually only be analysed using DC methods. To overcome this problem, a test resonator for samples, called “Quadrupole Resonator” (QPR), was designed and operated at CERN and a another one later at HZB. In a collaborative project between Universität Hamburg and DESY, a new QPR has been designed, successfully commissioned, and is currently being operated at DESY. It allows for a full RF characterization of samples at frequencies of 0.42 GHz, 0.87 GHz, and 1.3 GHz, within a temperature range of 1.8-20 K and at magnetic fields up to 120 mT. This work presents the design process, which incorporated improvements motivated by mechanical and RF studies and experience. The results from both warm and cold commissioning are discussed as well. More important, the results for the RF tests of a Nb sample after undergoing a series of coarse surface chemistries and an outlook of the further usage of the QPR is presented.

INTRODUCTION

Niobium (Nb) is widely regarded as the optimal material to construct superconducting radio frequency (SRF) cavities for their use in modern particle accelerators. As the accelerating fields within these SRF cavities are approaching their theoretical limit, researchers have explored alternative material and treatments to enhance the cavity performance. Materials such as Nb₃Sn [1, 2], multilayer structures (SIS) [3], and treatments like N-doping [4], N-infusion [5], and mid-T bake [6] of bulk Nb cavities have already demonstrated or have the potential to increase quality factors and maximize achievable fields. However, further investigation is required before cavities manufactures or treated with such recipes can be employed in complete accelerator setups. To expedite alternative material studies, there is a growing interest within the scientific community to characterize small samples of superconducting materials due to the significant cost and time associated with producing and measuring full-scale cavities. Therefore, the development of sample test devices with fast

turn-around times are highly valuable for investigating these materials.

RF Characterization Devices

To satisfy this need, laboratories around the world have developed a variety of setups to measure the surface resistance R_s of samples under controlled conditions, such as frequency, temperature, and peak magnetic field. These devices cover operational frequencies from the ultra-high frequency (UHF) range to the W-band, temperatures ranging from 2 K to 20 K and magnetic fields up to 120 mT. Sample diameters are on the centimetre scale and their shapes consist of flat discs, rods, or thin-films. Examples of these setups include TE Host cavities, Sapphire Loaded cavities, SIC, Hemispherical cavities, and Quadrupole Resonators. An overview of these systems can be found in Ref. [7]. These setups also aid in the development and testing of theoretical models of the surface resistance due to the wide space defined by their parameters.

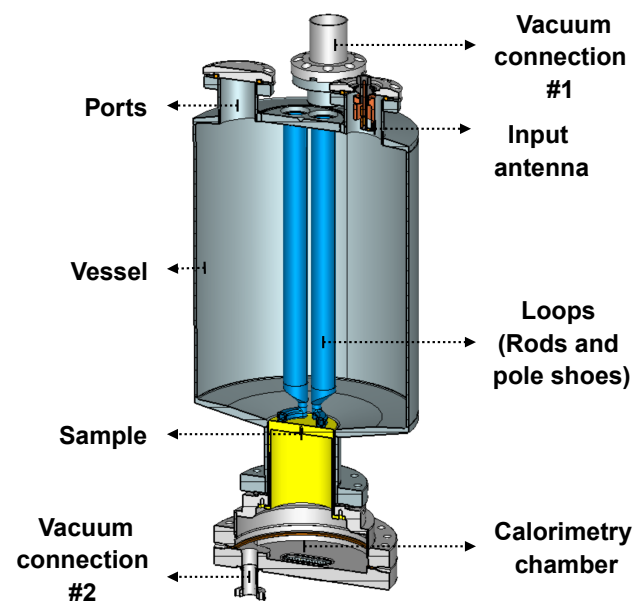


Figure 1: Cross-sectional view of the UHH QPR.

THE QUADRUPOLE RESONATOR

The Quadrupole Resonator was initially developed at CERN (CERN QPR) in 1998 [8, 9]. In the mid-2010s, an optimized version of the QPR (HZB QPR) was reported and brought into operation by Helmholtz-Zentrum Berlin [10, 11]. Subsequently, a redesign of the first CERN QPR (called CERN QPR II) was announced in 2017 [12], and was presented in 2019 [13]. Building upon these advancements, a

* ricardo.monroy-villa@desy.de

INVESTIGATION OF PLASMA PROCESSING FOR COAXIAL RESONATORS*

W. Hartung, W. Chang, K. Elliott, S. Kim, T. Konomi, K. Saito, P. Tutt, T. Xu
Facility for Rare Isotope Beams, Michigan State University, East Lansing, MI, USA

Abstract

Plasma processing has been investigated by several facilities as a method to mitigate degradation of superconducting cavity performance. It provides an alternative to removal and disassembly of cryomodules for refurbishment of each cavity via repeat etching and rinsing. Studies of plasma processing for quarter-wave and half-wave resonators were undertaken at the Facility for Rare Isotope Beams, where a total of 324 such resonators are presently in operation. Plasma cleaning tests were done on several resonators using the fundamental power coupler (FPC) to drive the plasma via the fundamental mode or a higher-order mode (HOM). HOMs allow for less mismatch at the FPC and hence lower field in the coupler relative to the cavity. Before-and-after cold tests showed a significant reduction in field emission X-rays with judicious application of plasma processing.

INTRODUCTION

Particle accelerators for electrons and ions are increasingly making use of superconducting radio-frequency (SRF) cavities to accelerate beams with high accelerating gradients at a high duty cycle. Degradation of cavity performance over time is a concern for long-term SRF accelerator operation. As traditional refurbishment of SRF cryomodules is labor-intensive, costly, and time-consuming, an alternative approach of in-situ plasma processing has been under development by several accelerator-based groups over the past few years. Results so far have been promising, with the first demonstration of plasma processing in an accelerator tunnel having been done at SNS [1]. Plasma processing development work has been done for a number of SRF cavity types, including $\beta = 1$ multi-cell cavities [2], $\beta < 1$ multicells [1], half-wave resonators [3, 4], and spoke cavities [5]. Plasma processing has been applied to several in-tunnel SNS cryomodules [1], an LCLS-II-style cryomodule [6], and a CEBAF cryomodule [7, 8], and has been found to help reduce both field emission (FE) and multipacting.

The Facility for Rare Isotope Beams (FRIB) is a superconducting linac for heavy and light ions. The FRIB driver linac contains 104 quarter-wave resonators (QWRs, 80.5 MHz) and 220 half-wave resonators (HWRs, 322 MHz). The linac began user operations in May 2022 [9, 10]. A pro-active campaign to develop techniques for plasma processing of FRIB cavities was undertaken starting in 2020. Preliminary results have been reported previously [11, 12]. Recent developments in this effort will be described in this paper.

* Work supported by the US Department of Energy Office of Science under Cooperative Agreement DE-SC0000661.

BACKGROUND AND APPROACH

Plasma processing is done at room temperature with a steady flow of process gases. Plasma evaluation and development can be done using a custom-length input antenna with minimal mismatch at room temperature, but in-situ processing must be done by driving the plasma via the fundamental power coupler (FPC) or via a higher-order mode (HOM) coupler. Ignition of coupler plasma is a concern, as this could produce sputtering or damage to the RF window ceramic [7, 13]. The use of HOM couplers has been found to be beneficial for $\beta = 1$ cavities [2, 7].

Features of the FRIB cavities which make plasma processing a challenge include (i) the relatively weak input coupling, which results in a lot of FPC mismatch at room temperature; (ii) the absence of HOM couplers; (iii) the relatively small access ports, which make it difficult to see the cavity's interior and gauge the location of the plasma.

Table 1 provides FRIB FPC coupling information and component counts for the FRIB linac. The FPCs have some adjustability; for plasma processing, we have set the FPC for maximum coupling strength (minimum $Q_{\text{ext},1}$) to minimize the mismatch with the cavity warm. The corresponding coupling factor ($\beta_1 \equiv Q_0/Q_{\text{ext},1}$) ranges from 0.2 to 2%.

The plasma processing development steps planned for the FRIB cavities are outlined in Table 2. Experimental work so far has been for the $\beta = 0.086$ QWRs and the $\beta = 0.54$ HWRs, which are the most numerous.

Plasma processing development was done with FRIB cavities leftover from production or in production as spare cavities. All of the cavities were cold-tested prior to plasma processing. At present, the cavities must be vented between plasma processing and cold tests, with a dedicated setup being used for plasma work. The assembly steps are done in a clean room environment. Either a custom-length input antenna or a spare FPC is used to drive the plasma. A shorter input antenna is used for cold tests.

Table 1: FRIB cavity counts and coupling strengths for a warm cavity. Q_0 = cavity intrinsic quality factor.

Cavity β	0.043	0.086	0.29	0.54
Quantity	12	92	72	148
Nom $Q_{\text{ext},1}$	$2 \cdot 10^6$	$2 \cdot 10^6$	$6 \cdot 10^6$	$1 \cdot 10^7$
Min $Q_{\text{ext},1}$	$1 \cdot 10^6$	$1 \cdot 10^6$	$3 \cdot 10^5$	$8 \cdot 10^5$
Cavity Q_0	$2 \cdot 10^3$	$3 \cdot 10^3$	$6 \cdot 10^3$	$9 \cdot 10^3$
Max β_1	$2 \cdot 10^{-3}$	$3 \cdot 10^{-3}$	$2 \cdot 10^{-2}$	$1 \cdot 10^{-2}$

CRYOCOOLER APPLICATION FOR ACCELERATOR AND DEVELOPMENT STATUS OF POWERFUL CRYOCOOLER AT SHI Ltd.

T. Ikeda[†], S. Sasazaki, Sumitomo Heavy Industries, Ltd., Nishitokyo-shi, Tokyo, Japan

Abstract

Advances in recent Nb₃Sn cavity development makes possible to operate the cavities with $Q_0 \sim 1 \times 10^{10}$ at 4.3 K and to design SRF accelerator in which the cavities are cooled directly with small mechanical cryocoolers instead of using liquid helium. Conduction-cooling with cryocoolers greatly simplify the overall design and also contribute for cost saving of an SRF accelerator, making the SRF technology feasible for industrial accelerators. However, in the case of using current cryocooler systems (like Gifford-McMahon cryocooler, Pulse-Tube cryocooler, etc.) for the conduction-cooling, since the cooling capacity per unit is small, multiple units will be used in combination depending on the required cooling capacity, it will cause problems in terms of power consumption (efficiency), footprint, and maintenance costs. Therefore, SHI have been developing a large-capacity and high-efficiency 4KGM-JT (Gifford-McMahon-Joule-Thomson) cryocooler system in the 10 W class at 4.2 K. This contribution will report the overview of this cryocooler system and its status of development.

INTRODUCTION

Currently, SRF accelerators require liquid helium (LHe) cryopumps, often subcooled to 2 K, to cool the cavities well below the superconducting transition temperature. Whereas niobium (Nb) has been the material of choice for SRF cavities, Nb₃Sn has emerged as a viable alternative in recent years [1]. Since the critical temperature of Nb₃Sn is 4.3 K, instead of 2 K of Nb, it makes possible to design SRF accelerator in which the cavities are cooled directly with small mechanical cryocoolers instead of using LHe cryopumps. Conduction-cooling with cryocoolers greatly simplify the overall design and also contribute for cost saving of an SRF accelerator, making the SRF technology feasible for industrial accelerators.

However, in the case of using current cryocooler systems (like Gifford-McMahon cryocooler, Pulse-Tube cryocooler, etc.) for the conduction-cooling, since the cooling capacity per unit is small (1~2 W at 4.2 K), multiple units will be used in combination depending on the required cooling capacity, it will cause problems in terms of power consumption (efficiency), footprint, and maintenance costs.

Therefore, SHI have been developing a large-capacity and high-efficiency 4KGM-JT (Gifford-McMahon-Joule-Thomson) cryocooler system in the 10 W class at 4.2 K [2]. In this contribution we present the overview of this cryocooler system and its status of development.

OUTLINE OF 4KGM-JT CRYOCOOLER SYSTEM

RJT-100 4KGM-JT Cryocooler

Figure 1 shows the schematic of RJT-100 4KGM-JT cryocooler. RJT-100 is Joule-Thomson (JT) cryocooler using RDE-418D4 two-stage Gifford-McMahon (GM) cryocooler as pre-cooler of gas helium (GHe). Normal temperature and high pressure GHe supplied from JT compressor unit (J117V) is pre-cooled by RDE-418D4 and Four heat exchangers (HEX). The pre-cooled GHe is expanded by fixed orifice (JT expander) and part of GHe is liquified at 4 K cooling interface. Heat exchanged GHe with the customer system at 4 K cooling interface is returned to J117V after heat exchange with the high pressure GHe at HEX. Note that the temperature of the 4 K cooling interface is uniquely determined by saturated vapor pressure of helium, and in this system, the temperature is controlled 4.2 K or less by adjusting the JT return pressure of J117V to a constant.

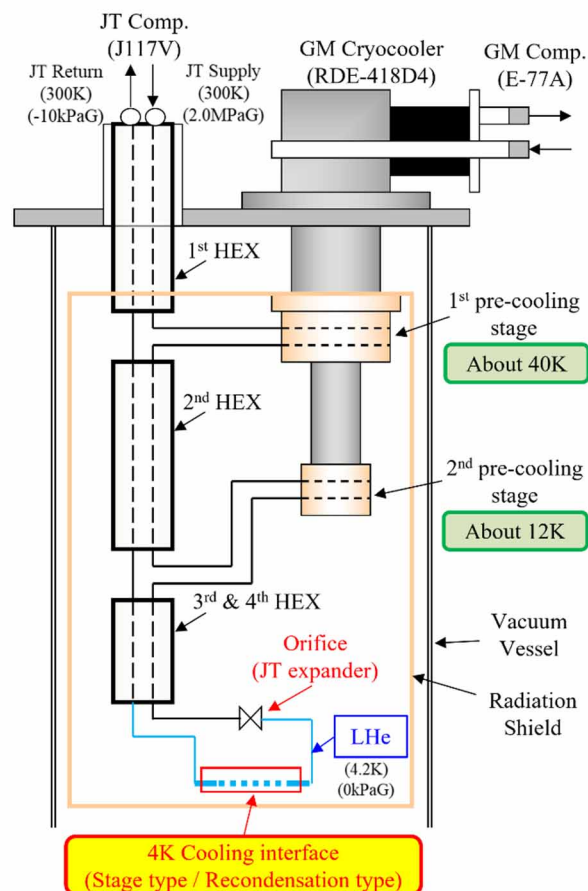


Figure 1: Schematic of RJT-100 4KGM-JT cryocooler.

Content from this work may be used under the terms of the CC BY 4.0 licence (© 2023). Any distribution of this work must maintain attribution to the author(s), title of the work, publisher, and DOI

[†] taiki.ikeda@shi-g.com

CONDUCTION-COOLED SRF CAVITIES: OPPORTUNITIES AND CHALLENGES*

N. A. Stilin[†], H. Conklin, T. Gruber, A. Holic, M. Liepe,
 T. O’Connell, P. Quigley, J. Sears, V. D. Shemelin, J. Turco

Cornell Laboratory for Accelerator-Based ScienceS and Education (CLASSE), Ithaca, NY, USA

Abstract

Thanks to improvements in the performance of both commercial cryocoolers and Nb₃Sn-coated superconducting radio-frequency (SRF) cavities, it is now possible to design and build compact, SRF cryomodules without the need for liquid cryogenics. In addition, these systems offer robust, non-expert, turn-key operation, making SRF technology significantly more accessible for smaller-scale applications in fields such as industry, national security, medicine, environmental sustainability, etc. To fully realize these systems, many technical and operational challenges must be overcome. These include properly cooling the SRF cavity via thermal conduction and designing high-power (~100 kW continuous) RF couplers which dissipate minimal heat (~1 W) at 4.2 K. This paper will discuss these challenges and the solutions which have been developed at Cornell University and elsewhere.

INTRODUCTION

Reports from the U.S. Department of Energy have identified a large number of applications which are ideal for small-scale accelerator operations [1, 2]. These applications represent a range of fields such as energy and environment (wastewater treatment, soil remediation, flue gas treatment), medicine (isotope production, device sterilization), security and defense (scanning), industry (semiconductor production) and more. One advantage of all of these applications is that they fall within a relatively small beam parameter space with moderate energies but high current and power; see Table 1 [1, 2].

Table 1: Typical Beam Parameters

Property	Value	Units
Energy	1 - 10	MeV
Current	100 - 1000	mA
Power	1 - 10	MW

Many of these applications would benefit from the use of SRF technology to increase average power and throughput. However, this would typically require the use of liquid helium for cooling the accelerating cavities. This poses a significant challenge for small operations due to the size and complexity of the infrastructure needed for helium systems.

* This work was supported by U.S. DOE award DE-SC0021038 “Next Steps in the Development of Turn-Key SRF Technology,” which supports the full development of a conduction cooling based cryomodule.

[†] nas97@cornell.edu

This indicates that replacing liquid helium with another cooling source would be a major benefit to the accessibility of SRF technology. This paper explores the use of cryocoolers as a new cooling mechanism for SRF cavities and discusses key aspects of developing new standalone cryomodules in which liquid cryogenics are replaced with cryocoolers.

CONDUCTION COOLED SRF CAVITIES

Two key factors enable SRF cavities to be operated without the use of liquid helium: highly efficient Nb₃Sn cavities and improved commercialized cryocoolers. In recent years, the quality of Nb₃Sn films in SRF cavities has improved dramatically, resulting in cavities which dissipate very low heat even at moderate fields (~10 MV/m) relevant to small-scale operations [3–9]. In addition, commercially available cryocoolers are now able to extract up to 2.5 W at 4.2 K [10]. These developments are represented in Fig. 1, which plots the discussed trends for both Nb₃Sn cavities and cryocooler cooling capacity over time. This highlights how only in the last few years have these technologies matured to the point of enabling the development of conduction-cooled SRF cavities.

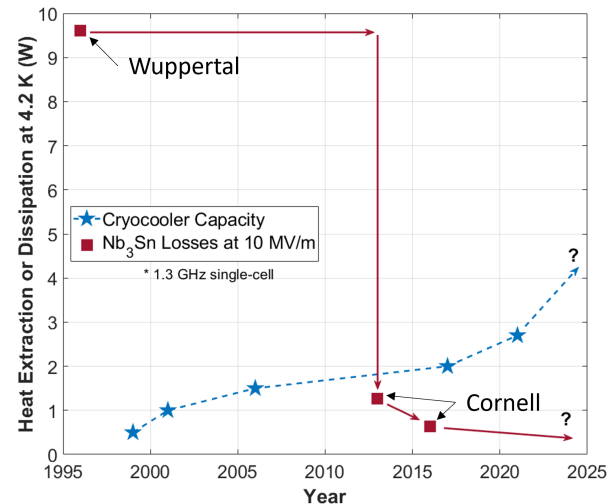


Figure 1: Progress in both Nb₃Sn cavity performance (red squares) and pulse-tube cryocooler capacity at 4.2 K (blue curve) [10].

Multiple labs have already completed proof-of-principle demonstrations of this concept. The cavity assembly used in Cornell’s original studies can be seen in Fig. 2a. Key components indicated include the 2.6 GHz Nb₃Sn cavity,

INSTRUMENTATION FOR HIGH PERFORMANCE CAVITIES AND CRYOMODULE FIELD EMISSION ANALYSIS

G. Devanz, E. Cenni, O. Piquet, M. Baudrier, L. Maurice
CEA Université Paris-Saclay, Gif-sur-Yvette, France

Abstract

Field emission (FE) is one of the main reasons for the degradation of accelerator cryomodules, as field emitted current tends to become more severe during the beam operation. It is essential to better understand how this phenomenon is generated and evolves from the SRF cavity preparation in the clean room, through their assembly in the cryomodule until their final test and operation. Due to the shielding environment of a cavity in its vertical test stand, or the architecture of a cryomodule, the more faint radiation occurring at the FE onset remains undetected. More precise diagnostic and analysis tools are required to gain more information. We present the development of dedicated time-resolved detectors for the FE radiation which aim to improve its coverage in terms of solid angle and lower energy threshold sensitivity. We approach this topic through detailed simulation based on the Geant4 toolkit in order to analyse the interaction of FE radiation with the cavity environment and optimize the detectors with respect to their application in cryomodule or vertical test stands. We illustrate this by analysing recent cryomodule experimental test data.

INTRODUCTION

State of the art cavity preparation and clean room assembly techniques enable individual multi-cell, elliptical cavity field-emission-free performance. Large projects generally choose to minimize the amount of time dedicated to the HPR for a given pass rate on the first RF test of a cavity. Then a new treatment is applied to the field emitting cavity. A high rate of typically 90% is then achieved. The remaining cavities are then dealt with on a case-by-case basis due to diminishing returns.

When the FE-free, vertically tested cavities are assembled into a string, keeping the same level of cleanliness for the assembled cryomodule (CM) is obviously a challenge. First, new parts such as bellows, power couplers and gate valves are now connected to the beam vacuum. Particle counting is the tool of choice to guarantee that the level of cleanliness of the parts will not contaminate the cavity surfaces. Despite all assembly with backflow, evacuation, venting, connections to vacuum pumps and other processes being kept under tight control, the FE threshold is often brought back within the range of cavity operation gradient.

Testing individual cavities within the CM can inform on the possible impact of vacuum equipment connection if end cavities experience a reduction in performance. The test can inform only on a basic level whether the cavity performance is retained or degraded.

Only the absence of FE is a strong proof that the assembly has reached its goal. In the opposite case, one has to

compare two FE measurements done in different contexts and available instrumentation:

- Various shielding situations: The nature and quantity of shielding material between the cavity and the radiation monitors differ from one test infrastructure to the next, and from a vertical test (VT) to a cryomodule test.

- Different radiation monitors,

- Mode of operation: pulsed instead of continuous may introduce an excursion from the linear response of a detector due to its intrinsic dead time. Geiger-Müller (GM) and neutron rem counter are subject to this limitation generating a saturation at higher count rates [1].

A fair comparison between VT and CM tests is possible if one ensures that both situations have used the same measurement equipment. This is one strong motivation to develop a radiation instrumentation that could be used in both cases and installed at the same relative position with respect to the cavity. If the radiation sensitive part of the detection is taking place at cryogenic temperatures, and should be even placed in liquid He directly to be able to cover all the use cases.

A limitation of standard area radiation monitors, GM or ionization chambers is their size which makes it very difficult to imagine a tight coverage in terms of angular distribution around the cavity under test. In a VT test case, they would be installed around the Dewar in room temperature conditions, separated from the source by shielding material. VT setups generally do not include more than two or three monitors, while this number can be increased to more than 10 units in a CM test bunker.

Area radiation monitors, GM or neutron rem-counters measure the ambient dose equivalent $H^*(10)$. The conversion between the equivalent dose and neutron flux requires Monte-Carlo (MC) simulations, since the equivalent dose depends on an energy-dependent weighting factors. Using data from [2] makes evaluating the neutron flux from $H^*(10)$ measurements possible under the hypothesis of a neutron energy spectrum.

Improvements over standard area monitors would be the access to timing information and energy of the radiation. Then combining measurements with MC simulations makes it possible to identify an electron emission scenario and potentially track back to the initial electron current.

During the ESS elliptical cavity CM tests at Saclay [3, 4] and Lund Test Stand (TS2) [5], the false triggering of the power coupler arc detection interlocks with γ radiation occurred multiple times. The time resolved detection of the radiation can provide useful information to inject into the interlock system logic. It can also enable the disambiguation of different origins of the measured radiation in pulsed operation.

HEAVILY DAMPED CRAB CAVITIES FOR HIGH LUMINOSITY COLLISIONS*

Binping Xiao[†], Brookhaven National Laboratory, Upton, NY, USA

Abstract

Next generation colliders require crab cavities to mitigate parasitic collisions caused by finite crossing angle for luminosity leveling and detector data pile up reduction. The Electron Ion Collider (EIC) crab cavity designs will be introduced as an example to fulfill the geometrical constraints, crabbing voltages, multipole components, Higher Order Mode (HOM) power and impedance budgets. Operational challenges such as tuning, high gain low delay control loop, amplitude and phase noises control will be discussed.

INTRODUCTION

Crab cavities are used in modern colliders to compensate the loss of luminosity due to a finite crossing angle at the interaction point (IP). The High-Luminosity Large Hadron Collider (HL-LHC) needs horizontal crabbing for CMS and vertical crabbing for ATLAS [1], the EIC needs horizontal crabbing for IP6, and potentially for IP8 [2]. These two circular machines adopt local crabbing scheme, both bunches need to be crabbed before the IP and uncrabbed after the IP. The International Linear Collider (ILC) needs horizontal crabbing for the IP [3]. Table 1 shows the parameter comparison of these projects. While comparing with the other two projects, EIC has larger crossing angle, lower cavity frequency, higher crabbing voltage and tighter impedance budget. The need of 197 MHz crab cavity for Hadron Storage Ring (HSR) makes it difficult to design (as a pressure vessel), fabricate (fabrication error control, electron beam welding) and surface treatment. HL-LHC uses different types of cavities thus longitudinal and transverse impedance do not overlap. Considering the number of cavities needed to provide the crabbing voltage needed, as well as the need to be upgradable for the second IP, for EIC, the longitudinal impedance budget is two orders of magnitude lower comparing with HL-LHC for 197 MHz and three orders of magnitude lower for 394 MHz, while the transverse impedance budget is one order of magnitude lower for both 197 MHz and 394 MHz. Due to the high current and short bunch length, especially for electron bunch, the HOM power of both 197 MHz and 394 MHz systems are high while comparing with HL-LHC. ILC is a pulsed machine with CW crab cavity operation, thus the average HOM power is low. The longitudinal space allocation of 15 m is tight for EIC since four 197 MHz crab cavities and two 394 MHz crab cavities need to be fitted in. In HL-LHC and

ILC, the adjacent beampipe is included into the crab cryomodule design. While in EIC it is not possible since the crab system can be adjacent to a beampipe, or a superconducting magnet, or beam position monitor, or sometimes, tunnel wall. To follow the Au energy ramp, the 197 MHz system needs ~ 1 MHz tuning range, and the requirement for 394 MHz gets doubled. The preliminary specifications on multipole components require careful design of the cavity, especially on the shape of the capacitive poles. Beyond the cryomodule, the Low Level RF (LLRF) system of EIC crab is also challenging. It needs a high gain low delay control loop, with tight tolerances on phase and amplitude noise.

These requirements are mitigated during the cavity and cryomodule designs. They strongly influence the decisions made during the designs. These will be discussed in detail.

197 MHz HSR CRAB CAVITY

Similar to HL-LHC, two designs were proposed at the beginning, Double Quarter Wave (DQW, Figure 1a) [4] and RF-dipole (RFD, Figure 1b) [5]. Both designs were advanced on RF designs like crabbing voltages and damping, with the RF properties summarized in Table 2. Both designs use two waveguides (one horizontal and one vertical) for HOM damping, with DQW one waveguide absorber and one coaxial absorber (Figure 1a) [4], and RFD two waveguide absorbers (Figure 1b) [5]. Both designs were expected to meet the RF performance requirements, as well as the space allocations. The DQW design is elongated to enhance the crabbing voltage while comparing with HL-LHC design thus is not favored for stress, while RFD remains to be cylindrical thus is favorable as a vacuum vessel and is also easier to be integrated with a helium vessel. RFD with two waveguide absorbers is down selected as the baseline due to its maturity in engineering design.

The RFD 197 MHz was further studied with coaxial absorbers (Figure 1c) instead of waveguide absorbers [4], with its impedance spectrum shown in Figure 2. The advantages of the coaxial absorbers design include lower cost, lighter weighted, using off-the-shelf absorbers instead of further R&D, simpler waveguide structure, simpler engineering and easier transportation, while without degradation on RF performance (peak fields, HOM spectrum, multipacting etc.) [6]. Coaxial absorbers have less power handling capacity compared with waveguide absorbers, but enough for RFD 197 MHz in HSR. There were concerns about the possible impedance enhancement on the coaxial design, detailed error analyses cleared these concerns. RFD 197 MHz with coaxial absorbers is chosen as the current

* Work supported by Brookhaven Science Associates, LLC under Contract No. DE-SC0012704 with the U.S. Department of Energy, and by DOE Contract No. DE-AC02-76SF00515. This work used computer resources at the National Energy Research Scientific Computing Center.

[†] binping@bnl.gov

CRAB CAVITIES FOR ILC

P. A. McIntosh^{†,1}, STFC Daresbury Laboratory, Warrington, UK
 S. Verdú-Andrés, B. Xiao, Brookhaven National Laboratory, Upton, NY, USA
 R. Calaga, CERN, Geneva, Switzerland
 S Belomestnykh, I. Gonin, S. Khabiboulline, A. Lunin, Y. Orlov, V. Yakovlev
 Fermilab, Batavia, IL, USA
 T. Okugi, A. Yamamoto, KEK, Tsukuba, Japan
 G. Burt¹, Lancaster University, Lancaster, UK
 J. Delayen², S. De Silva², Old Dominion University, Norfolk, VA, USA
¹also at Cockcroft Institute, Warrington, UK
²also at Jefferson Laboratory, Newport News, VA, USA

Abstract

For the 14 mrad crossing angle proposed, crab cavity systems are fundamentally anticipated for the viable operation of the International Linear Collider (ILC), in order to maximise its luminosity performance. Since 2021, a specialist development team have been defining optimum crab cavity technologies which can fulfil the operational requirements for ILC, both for its baseline centre-of-mass energy of 250 GeV, but also extending those requirements out to higher beam collision intensities. Five design teams have established crab cavity technology solutions, which have the capability to also operate up to 1 TeV centre-of-mass. This presentation showcases the key performance capabilities of these designs and their associated benefits for both manufacture and integration into the ILC Interaction Point. The recommended outcome of the recently conducted crab cavity technology down-selection, will also be highlighted.

INTRODUCTION

For the ILC's 14-mrad crossing angle, crab cavity systems are a fundamental priority from the reference ILC specifications for 250 GeV and scaling to 1 TeV operations [1] in order to maximise and maintain its luminosity performance. As part of a collective development programme, instigated by the ILC International Development Team (IDT) in 2018, the WP3 Crab Cavity consortium has devoted efforts to develop suitable technology solutions which will comply with ILC operational specifications.

From the associated beam delivery system (BDS) analysis, a minimum beam-pipe aperture of 25 mm is proposed, in order to comply with expected collimation provisions at the interaction point (IP). Figure 1 shows the practical space implementation and the associated cryomodule constraints, providing a longitudinal space availability of 3.85 m and a transverse beam-axis separation of 0.198 m, which dictates transversely, a highly compact ILC crab cavity (ILC-CC) structure design.

A total of five design solutions have been developed, each meeting the stringent specifications, which have been recently reviewed as part of a technology down-selection process. This first stage assessment has been to identify the 2 most effective designs, based on the respective E-M optimisations performed. Such a prioritised selection is also expected to facilitate early-stage procurement of niobium material (sheet or ingot) for the prototype cavity manufacture in conjunction with the associated HOM couplers, but explicitly excluding the forward power coupler (FPC). This prototype qualification will enable a second (and final) technology down-selection for the baseline ILC-CC technology, to be utilised primarily for the 125 GeV beam energy, but also ideally scalable for higher energies.

ILC-CC DESIGN SPECIFICATIONS

The proposed ILC-CC RF parameters have been defined for 3 distinct operating frequencies; 1.3 GHz, 2.6 GHz and 3.9 GHz, thereby identifying the respective total kick voltages required for both operating energy requirements, including a 10 Hz RF repetition rate upgrade for the 250 GeV centre of mass option.

To assist in maximising the operational robustness and to reduce the anticipated breakdown-rate, conservative levels of maximum peak electric (E_p) and peak magnetic (B_p) fields have been adopted as 45 MV/m and 80 mT respectively. Table 1 shows the complete specifications for the ILC-CC system, which also identifies the dimensional space constraints, alignment tolerances, HOM impedance thresholds and kick factor requirements.

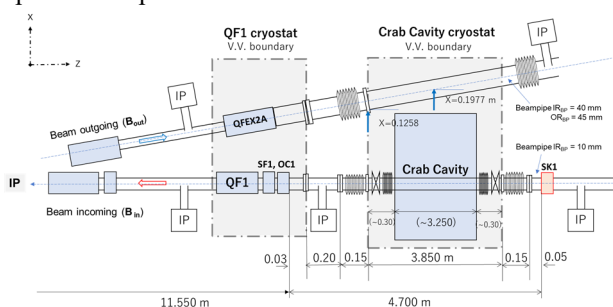


Figure 1: ILC crab cavity IP location.

[†] peter.mcintosh@stfc.ac.uk

AUTOMATION OF FRIB SRF CAVITIES AND SC SOLENOIDS TURN-ON/OFF*

W. Chang[†], Y. Choi, X. Du, W. Hartung, S. Kim, T. Konomi, S. Kunjir,
H. Nguyen, K. Saito, T. Xu, S. Zhao

Facility for Rare Isotope Beams, Michigan State University, East Lansing, MI, USA
A. Facco, INFN - Laboratori Nazionali di Legnaro, Legnaro (Padova), Italy

Abstract

The superconducting driver Linac for the Facility for Rare Isotope Beams (FRIB) is a heavy ion accelerator that accelerates ions to 200 MeV per nucleon. The Linac has 46 cryomodules that contain 324 superconducting radio frequency (SRF) cavities and 69 superconducting (SC) solenoid packages. For operation of all cryomodules with high efficiency and reliability, automation for SRF cavity and SC solenoid fast turn-on/off is essential. Based on cryomodule commissioning results and expert experience, all manual cavity and solenoid turn-on/off procedures and steps have been replaced by automatic programs for FRIB linac operation. This allows the operators to turn the systems on and off without expert-level training. Automation reduces the risk of human error, speeds up beam recovery after user access to experimental areas, and increases beam availability. The cavity turn-on procedure makes sure that the cavity can operate at low field with expected read backs, ramps up the field, and makes sure that the RF amplitude and phase are stable. The design, implementation, and operating experience with automation will be presented.

INTRODUCTION

The Facility for Rare Isotope Beams (FRIB) driver linac is designed to accelerate heavy ion beams from hydrogen to uranium. After commissioning of the FRIB linac, completed with acceleration of heavy ions to energies above 200 MeV/u, the first scientific user experiment was conducted in May 2022 [1].

The FRIB driver linac has a folded layout, as shown in Fig. 1, which consists of three linac segments (LS1, LS2 and LS3) connected with two folding segments (FS1 and FS2). A beamline at the end of LS3 delivers the accelerated beam from LS3 to target hall. Another beam delivery system was built at the end of LS1, dedicated to the FRIB Single Event Effects (FSEE) experimental station to serve industrial users.

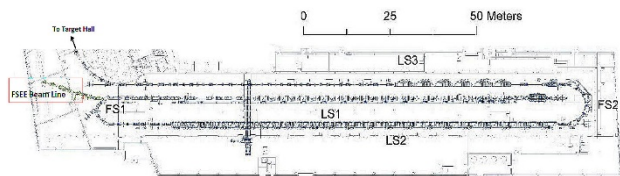


Figure 1: Layout of the FRIB driver linac.

Linac segments and folding segments have 46 cryomodules with a total 324 superconducting radio frequency

* This work is supported by the U.S. Department of Energy Office of Science under Cooperative Agreement DE-SC0000661.

[†] chang@frib.msu.edu

(SRF) cavities and 69 superconducting (SC) solenoid packages [2]. Turn-on and shut-down of this large scale SC device complex with high availability presents a challenge.

EXPERIENCE CONVERTED TO AUTOMATION

The FRIB cryomodules have 104 quarter-wave resonators (QWRs, $\beta = 0.041$ and 0.085), 220 half-wave resonators (HWRs, $\beta = 0.29$ and 0.53) and 69 SC solenoid packages [3]. After commissioning of all cryomodules in the tunnel, all information about optimum control parameters, and each device start-up or shut-down procedures, were well defined and documented. With this information, based on operational experience, all devices can be operated simply by following the correct procedure. However, manual turn-on/off of such large scale and complex system takes a huge cost in terms of time. Moreover, the complexity of these procedures requires expert-level training. To perform this system start-up and shut-down with high efficiency and reliability, the conversion of expert-level experience to automation programs is essential.

In FRIB, all the optimum control parameters for SRF cavities and SC solenoids are saved in files. Automation tools for parameters checks can be used for parameter consistency check before any device is turned on. Once this pre-check is done, the automation procedures for SRF cavities and SC solenoids turn-on can be executed. Automation programs for shut-down of all devices is also important. Once any emergency event happens, a shut-down of all devices through “one button click” allow people to leave the area as fast as possible.

SRF CAVITIES AUTO TURN-ON

Single Cavity Auto Turn-on Logic

All 104 QWRs and 220 HWRs have been manually commissioned one by one. With this commissioning experience, turn-on procedures have been developed, tested and confirmed through specific commissioning tasks and then converted to automatic programs.

For QWR auto turn-on, the logic is:

1. Set field-low interlock to 0 MV/m;
2. Set amplitude as open mode and phase as self-excited mode;
3. RF turn on with initial field set-point 1.5 MV/m to jump through the multipacting low barrier;
4. Tuner lock turn on, tuning the cavity frequency to the centre;

STATUS OF THE SLAC/MSU SRF GUN DEVELOPMENT PROJECT*

S. Miller[†], Y. Al-Mahmoud, W. Chang, Y. Choi, C. Compton, X. Du, K. Elliot, W. Hartung, J. Hulbert, S.-H. Kim, T. Konomi, D. Morris, M. Patil, L. Popielarski, K. Saito, A. Taylor, B. Tousignant, J. Wei, J. Wenstrom, K. Witgen, T. Xu
Facility for Rare Isotope Beams, Michigan State University, East Lansing, MI, USA
C. Adolphsen, R. Coy, F. Ji, M. Murphy, J. Smedley, L. Xiao
SLAC National Accelerator Laboratory, Menlo Park, CA, USA
J. Lewellen, Los Alamos National Laboratory, Los Alamos, NM, USA
M. Kelly, T. Petersen, P. Piot, Argonne National Laboratory, Lemont, IL, USA
A. Arnold, S. Gatzmaga, P. Murcek, R. Xiang, J. Teichert
Helmholtz-Zentrum Dresden-Rossendorf, Dresden, Germany

Abstract

The Linac Coherent Light Source II High Energy project at SLAC includes the construction of a low-emittance injector (LEI) and a superconducting quarter-wave resonator (QWR) at 185.7 MHz. Several alternatives to a superconducting radio frequency (SRF) QWR gun were considered for the LEI, including normal-conducting RF guns evolved from the LCLS-II gun design. Compared to normal-conducting designs, the combination of an intrinsically outstanding vacuum environment (for cathode lifetime), and the potential for a larger ultimate performance envelope, led to the decision to pursue development of the QWR-SRF gun. A prototype gun is currently being designed and fabricated at the Facility for Rare Isotope Beams at Michigan State University. This paper presents performance goals for the new gun design, an overview of the prototype development effort, status, and future plans including fabrication.

INTRODUCTION

In order to increase the electron beam energy to 8 GeV, Linac Coherent Light Source II High Energy (LCLS-II-HE) will construct a low-emittance injector (LEI) in a new tunnel [1, 2]. The beam source for the LEI will utilize a superconducting radio frequency photo-injector (SRF-PI). To mitigate the technical risk in adopting this approach, the LCLS-II-HE project proposed a 4-year R&D program to design, construct, and test a 185.7 MHz QWR SRF gun [3]. The goal of this R&D program is to demonstrate stable continuous wave (CW) operation with a cathode gradient of at least 30 MV/m. For the RF cavity, a major design criterion for the cavity is to achieve a low peak surface to cathode field ratio with consideration to field emission and multipacting. Two versions of the RF cavity are to be manufactured; one with a cathode plug port and one without. The latter will be tested initially to verify the cavity performance independent of the complications arising from the stalk and plug assembly. The Fundamental Power Coupler (FPC) is designed to be multipacting and field emission free, and not produce significant asymmetric fields in the

cavity. The cavity tuner is to be designed to ensure the gun operates at the nominal frequency within the detuning budget. The cathode is to be designed to provide an RF short while minimizing the heat load to the helium bath. The emittance compensation solenoid is designed to be close to the SRF-PI anode and has transverse adjustability to meet alignment specifications. A SRF-PI cryomodule has been developed by Facility for Rare Isotope Beams (FRIB) and its collaborative partners with the aforementioned specifications utilizing a 185.7 MHz quarter-wave resonator (QWR) and a cathode system. Table 1 displays the scope of the collaborators for the project. Table 2 gives the performance parameters associated with the SRF-PI.

Table 1: The Scope of the Collaborative Project Undertaken by FRIB, ANL, HZDR, and SLAC

Scope	FRIB	ANL	HZDR
Project Management	✓		
Cryomodule Design	✓	✓	
Magnet Design and Testing	✓		
Cathode Stalk Design, Fab, Testing	✓	✓	
Load-lock, Insertion/Transport			✓
Cathode Stalk Particulate Testing			✓
Cryomodule Procurement/Assy	✓		
Load-Lock Procurement/ Assy	✓		
Cavity Processing and Cold Testing	✓	✓	
Integrated Cavity Test (Tuner/FPC)			✓
Cavity Bunker Test	✓		

* Work supported by the Department of Energy under Contract DE-AC02-76SF00515

[†] millers@frib.msu.edu